ACTA CHIMICA
ACADEMIAE SCIENTIARUM HUNGARICAE

TOMUS 104 FASCICULUS 1

AKADÉMIAI KIADÓ, BUDAPEST
1980

ACTA CHIM. ACAD. SCI. HUNG. ACASA2 104 (1) 1–106 (1980)

ACTA CHIMICA

A MAGYAR TUDOMÁNYOS AKADÉMIA KÉMIAI TUDOMÁNYOK OSZTÁLYÁNAK IDEGEN NYELVŰ KÖZLEMÉNYEI

Acta Chimica is a journal for the publication of papers on all aspects of chemistry in English, German, French and Russian.

Acta Chimica is published in 3 volumes per year. Each volume consists of 4 issues of varying size.

Manuscripts should be sent to

Acta Chimica
Budapest, P.O. Box 67, H-1450, Hungary

Correspondence with the editors should be sent to the same address. Manuscripts are not returned to the authors.

Hungarian subscribers should order from Akadémiai Kiadó, 1363 Budapest, P.O. Box 24. Account No. 215 11488.

Orders from other countries are to be sent to "Kultura" Foreign Trading Company (H-1389 Budapest 62, P.O. Box 149. Account No. 218 10990) or its representatives abroad.

ACTA CHIMICA
ACADEMIAE SCIENTIARUM HUNGARICAE

REDIGUNT
B. LENGYEL et GY. DEÁK

TOMUS 104

AKADÉMIAI KIADÓ, BUDAPEST
1980

ACTA CHIM. ACAD. SCI. HUNG.

ACTA CHIMICA

TOMUS 104

Fasciculus 1
Fasciculus 2
Fasciculus 3
Fasciculus 4

INDEX

The Editorial Board announces with sorrow that one of its members

Victor BRUCKNER

Member of the Hungarian Academy of Sciences, Honorary Doctor and retired professor of Lóránd Eötvös University, Member of the German Leopoldina Academy of Sciences (Halle), holder of numerous Hungarian and foreign honours and decorations, passed away at the age of 80.

With his death, we have lost a leading personality of organic chemical research, the founder of a school, a scientist of international renown and an active member of the community of Hungarian chemists. We shall keep his memory.

Acta Chimica Academiae Scientiarum Hungaricae, Tomus 104 (1), pp. 1—12 (1980)

ÄQUIDENSITOMETRIE — EINE METHODE ZUR BEURTEILUNG DER STRUKTUR VON PLASMEN, VI*

UNTERSUCHUNG DER PLASMEN VON HOCHSPANNUNGS-IMPULSENTLADUNGEN

A. Petrakiew[1], I. Kolewa[1], S. Wladimirow[1] und K. Dittrich[2]**

(*[1]Physikalische Fakultät der Kliment-Ochridski-Universität, Sofia, VR Bulgarien, [2]Sektion Chemie der Karl-Marx-Universität, Leipzig, DDR*)

Eingegangen am 2. April 1979
Zur Veröffentlichung angenommen am 12. Juni 1979

Es werden die Möglichkeiten der photographischen Äquidensitometrie in Verbindung mit der spektralen Photographie für Untersuchungen an Hochspannungs-Impulsentladungen geprüft.

Verschiedene Methoden für die Gewinnung von Photogrammen und Spektrogrammen werden beschrieben: Zeitliche und räumliche Auflösung, spektrale, zeitliche und räumliche Auflösung.

Zwei Entladungstypen wurden untersucht: Freie (offene) Impulsentladung und örtlich fixierte Kapillarentladung. Im zweiten Fall erhält man ein achsensymmetrisches Plasma guter Reproduzierbarkeit. Im Ergebnis der Untersuchungen werden qualitative Aussagen über die Struktur der Plasmen und halbquantitative Aussagen über die Temperatur und deren Verlauf bei der Kapillarentladung gemacht.

Einführung

Die Grundlagen für die Erzeugung von Äquidensiten bzw. Äquidensitogrammen wurden mehrfach beschrieben [1—3]. Über die Verbesserung des Verfahrens und eine Reihe von Anwendungen wird von **Högner** und **Richter** [4—6] berichtet. Weitere Vervollkommnungen an dieser Methode wurden von **Breido** und **Wilenskaja** [7] und **Wladimirow** [8] hauptsächlich für die Astrophysik vorgenommen. Neben diesem beschriebenen photographischen Verfahren besteht auch die Möglichkeit, Äquidensiten mit Hilfe einer speziellen Elektronik und Fernsehtechnik zu erhalten [21]. Diese Methode hat jedoch einige Unzulänglichkeiten.

Die oben beschriebene photographische Methode wurde zur Plasmadiagnostik in die analytische Atomspektroskopie von **Dittrich**, **Niebergall** und **Rössler** [9] eingeführt. In Kombination mit der spektral auflösenden Photographie mittels eines stigmatisch abbildenden Spektrographen wurde die Methode universell in der analytischen Atomspektroskopie anwendbar [10]. Weitere

---

* Teil V: Zhurn. analit. Khim., XXXIX, 98 (1979).

** Korrespondenzanschrift.

Anwendungen durch **Dittrich** und Mitarbeiter [11, 13], **Dittrich, Petrakiew** und Mitarbeiter [13, 14], **Dittrich, Karjakin** und Mitarbeiter [15] und **Kranz** [16] bestätigten den Nutzen der Methode vor allem für die Diagnostik von Bogenplasmen. Die Anwendung der Äquidensitometrie für die Untersuchung von Hochfrequenz- und Fackelentladungen wurde ebenfalls beschrieben [17–19].

Auf eine ausführliche Darlegung der Grundlagen der photographischen Erzeugung von Äquidensiten spektral aufgelöster Photogramme soll hier verzichtet werden (vgl. dazu [1, 2, 7, 10]). Folgende Kurzinformationen über Probleme und Möglichkeiten werden gegeben:

1. Die Methode dient lediglich der besseren Auflösung eines Photogramms. Sie ermöglicht, die im Photogramm enthaltene Informationen sichtbar zu machen, liefert aber keine neuen Informationen.

2. Die Methode kann auf beliebige Photogramme, die von Lichtquellen oder beleuchteten Objekten erhalten werden, angewendet werden.

3. Für die Erzeugung des Photogramms kann sowohl mono- als auch polychromatisches Licht verwendet werden.

4. Bei der qualitativen oder auch quantitativen Auswertung von Äquidensitogrammen muß folgendes berücksichtigt werden:

a. Oftmals stellen die eingesetzten Photogramme *nur* Flächenprojektionen räumlich ausgedehnter Strahler dar. Dies erfordert vielfach eine zusätzliche mathematische Aufarbeitung der Resultate (z. B. über die bekannte ABELsche Integralgleichung).

b. Die exakte Zuordnung der S-Werte der einzelnen Äquidensiten ist durch einen gut unterteilten und gleichzeitig mit dem Photogramm äquidensitometrierten Graukeil möglich. Man kann das Verfahren auch eichen [20].

c. Relative Intensitäten können aus den S-Werten der Äquidensiten erhalten und diesen zugeordnet werden, wenn man die Schwärzungskurve des Photomaterials des Originalphotogramms kennt oder ermittelt (vgl. *a.* [10]).

In der vorliegenden Arbeit wird auf die Untersuchung von Impulslichtquellen eingegangen, die einige Besonderheiten haben:

1. Die spektrale Zusammensetzung der Strahlung dieser Lichtquellen ändert sich im Verlaufe des Impulses sehr schnell.

2. Diese Änderungen erfolgen in unterschiedlichen Strahlungs- und Raumrichtungen mit unterschiedlicher Geschwindigkeit.

Neben der räumlichen Auflösung benötigt man aus diesen Gründen noch eine zeitliche Auflösung. Es wird in dieser Arbeit der Versuch unternommen, spektral aufgelöste, zeitlich aufgelöste und z. T. spektral und zeitlich aufgelöste Photogramme mit Hilfe der photographischen Äquidensitometrie für die Plasmadiagnostik solcher Impulsentladungen einzusetzen. Auf diesem Wege kann man auch zu entsprechenden Plasmaparametern gelangen.

Experimenteller Teil

Es wurde eine Impulsentladung mit periodischer Löschung, welche in [24] näher beschrieben wurde, eingesetzt: $U = 1{,}6$ kV; $C = 420$ μF. Die verwendeten Impulskondensatoren haben eine minimale Selbstinduktion (Kondensatortypen: IM-5-140 und IM-5-280). Während der ersten Halbperiode der Entladung ergibt sich die maximale Stromamplitude, die 100 μs dauert. Die Gesamtdauer der Entladung beträgt 300 μs. Die Entladung erfolgte bei Atmosphärendruck zwischen Kohleelektroden ($\varnothing = 6$ mm, leicht konisch). Mit dem gleichen Anregungsgerät wurde eine zweite Variante der Entladung realisiert: Die Kapillarentladung.

Die Lokalisierung der Entladung wurde durch zwei planparallele Platten mit entsprechenden Öffnungen, die die Entladungsachse bildeten, erreicht (vgl. Abb. 1). Diese Methode liefert ein sehr gut reproduzierbares, achsensymmetrisches Plasma mit einem großen Tem-

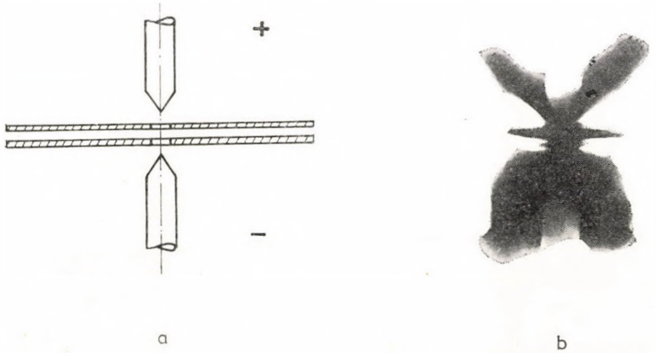

Abb. 1. **Schematische Darstellung der Kapillarentladung und Photogramm einer Kapillarentladung; *a.* Konfiguration der Elektroden und Anordnung der dielektrischen Platten; *b.* Photogramm einer Kapillarentladung**

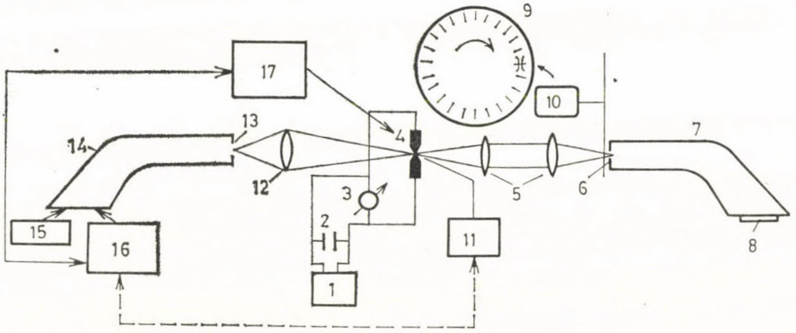

Abb. 2. Optisches und elektrisches Schema für die komplexe, spektral, zeitlich und räumlich auflösende Untersuchung von starken Hochspannungs-Impulsentladungen. 1 — Hochspannungstransformator, 2 — Kondensatorbatterie, 3 — Elektrostatisches Kilovoltmeter, 4 — Entladungszone, 5 — Zwischenabbildungssystem (3 Linsen), 6 — Spektrographenspalt, 7 — Quarzspektrograph für zeitlich aufgelöste Spektren, 8 — Spektralplatte, 9 — rotierende Scheibe für die zeitliche Auflösung der Spektren ohne Synchronisation, 10 — regulierbarer Elektromotor mit Drehzahlmesser, 11 — Hochfrequenzimpulsgenerator zur Initiierung der Entladung (synchronisiert mit 16 und 17), 12 — Spezialabbildungssystem für den spaltlosen Spektrographen 14, 14 — spaltloser Spektrograph, 15 — Photoplatte für die Gewinnung der Spektrogramme, von denen Äquidensiten hergestellt werden, 16 — Hochgeschwindigkeitskamera für die Registrierung einzelner Linien, 17 — Hochgeschwindigkeitskamera für die synchronisierte Registrierung des polychromatischen Lichtes der Entladung

peraturintervall [23]. Es wurden Plexiglasplatten einer Stärke von 1,8 mm im Abstand von 2 mm mit einem Lochdurchmesser von 2,5 mm verwendet.

Für die Aufnahme spektral aufgelöster Photogramme (Spektrogramme) wurde, wie früher beschrieben [10], ein spaltloser Spektrograph benutzt. Mit Hilfe einer Quarzlinse von kurzer Brennweite wurde die Entladung bei starker Verkleinerung (etwa 15 ×) in die ursprüngliche Spaltebene des Spektrographen abgebildet. Infolge der 1 : 1 Abbildung des Spektrographen entsteht an jeder Stelle, wo normalerweise eine Spektrallinie erhalten wird, ein Abbild der Gesamtentladung bezogen auf den jeweiligen Atom- oder Ionenübergang. Wenn nur ein Spektrograph kleiner Dispersion zur Verfügung steht, muß man wegen der möglichen Koinzidenzen linienarme Spektren für die Untersuchung auswählen. Es ist in jedem Falle günstig, einen stigmatisch abbildenden Spektrographen großer Dispersion und ausreichender Lichtstärke zu verwenden. Mit Einschränkungen ist jedoch auch ein Prismenspektrograph einsetzbar. In diesem Falle ist zu berücksichtigen, daß die Abbildung der Entladung in unterschiedlichen Wellenlängengebieten mit unterschiedlicher Dispersion erfolgt. Außerdem kommt es bei den Mikroabbildungen zu kleinen Verzeichnungen.

Wenn man den Verlauf der Impulsentladung in Abhängigkeit von der Zeit untersuchen will, benötigt man eine Hochgeschwindigkeitskamera, mit der die Aufnahme von möglichst monochromatischem Licht möglich ist.

Die Abb. 2 stellt eine Anordnung dar, die die komplexe Untersuchung von Impulsentladungen unter Verwendung von zwei Spektrographen (Typ: Q 24, VEB Carl Zeiss, Jena, DDR) und zwei Hochgeschwindigkeitskameras (Typ: SFR — L) und einer mechanisch betriebenen Zeitauflösung (rotierende Scheibe) ermöglicht. Für die praktische Realisierung solcher Experimente ist eine aufwendige Elektronik für die Synchronisation von 3 Geräten erforderlich, die einige Probleme mit sich bringt. Da auf dem genannten Wege jedoch eine große Informationsmenge über die Entladung erhalten wird, lohnt sich der entsprechende Aufwand.

Tabelle I

Charakteristik der schmalbandigen Interferenzfilter

Wellenlänge in nm	Halbwertsbreite in nm	Durchlässigkeit in %
594	10	50
437	8	45
404	8,5	36
580	6,5	35

Tabelle II

Charakteristik der untersuchten Linien

Linie in nm	Übergang	Angeregte Zustände unterer in eV	Energie oberer in eV	Wellenlänge in nm	rel. Intensität	Normtemperatur K
O I	$3p^3P-6s^3k^0$	10,99	13,04	604,6	12	18 000
C II	$3d^4P^0-4f^4D$	24,65	27,49	437,4	9	33 000
N III	$3s^2S-3p^2P^0$	27,44	30,46	409,7	10	48 000
C IV	$3s^2S-3p^2P^0$	37,55	39,68	580,1	10	60 000

Für die Realisierung der spektralen und sowohl räumlich wie auch zeitlich aufgelösten Strukturuntersuchungen an Plasmen der Kapillar-Impulsentladung wurde ebenfalls eine Hochgeschwindigkeitskamera vom Typ SFR — L verwendet. Für die zeitliche Auflösung des Prozesses wurde ein Doppelrastersystem mit einem ebenen Feld von 10 mm Kantenlänge und dem Aufnahmeobjektiv IM-51 (Brennweite 210 mm) benutzt. Die Drehgeschwindigkeit des Spiegels war 11 500/s. Das entspricht einer Bildaufnahmegeschwindigkeit von 95 000 Bildern/s. Für die spektrale Auflösung verwendeten wir 4 schmalbandige Metallinterferenzfilter, deren Charakteristik in Tabelle I angegeben wurde. Diese Filter wurden für die Untersuchung der in Tabelle II angegebenen Linien benutzt. Es ist auf diesem Wege möglich, eine ziemlich vollständige Information über das Plasma zu erhalten. Allerdings ist es erforderlich, sehr schmalbandige Filter (vgl. [22]) zu verwenden. Diese werden unmittelbar vor dem Spalt der Hochgeschwindigkeitskamera angebracht. Je nach Aufgabenstellung kann man mit dem Doppel- oder Vierfachspalt arbeiten, wodurch das Anbringen von 2 oder 4 Interferenzfiltern möglich ist.

Ergebnisse und Diskussion

Freie (offene) Impulsentladung

Auf der Abbildung 3 wurden 3 Photogramme und die dazugehörigen Äquidensitogramme einer Impulsentladung abgebildet. Die Photogramme wurden mit einem normalen Photoapparat ohne (Teil 1) bzw. mit Interferenzfiltern mit Halbwertsbreiten von 12 nm (Teil 2: 437 nm und Teil 3: 404 nm) aufgenommen.

Die Anwendung eines Spektrographen gab die Möglichkeit für die Untersuchung von Linien unterschiedlich ionisierter Spezies.

In der Abbildung 4 sind die Äquidensitogramme für C I = 247,6 nm, für C II = 251,2, für C II = 283,7 und für C III = 229,7 nm abgebildet.

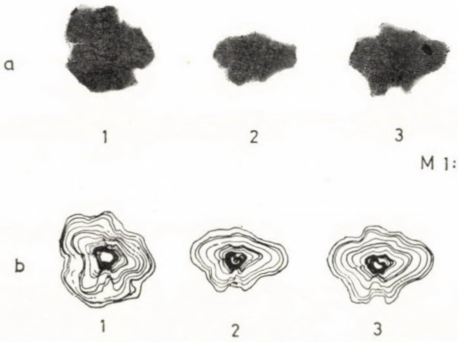

Abb. 3. **Photogramme (Teil *a)* und dazugehörige Äquidensitogramme (Teil *b)* einer freien (offenen) Impulsentladung. 1: Aufnahmen ohne Filter; 2: Aufnahmen mit Interferenzfilter, Wellenlänge: 437 nm; 3: Aufnahmen mit Interferenzfilter, Wellenlänge: 404 nm**

Die Herstellung der Einzeläquidensiten erfolgte nach [5, 6], die der Äquidensitogramme durch 200-fache Vergrößerung. Zeichnen und Photographieren nach [10]. Infolge der Vergrößerung erhält man breitere Äquidensiten.

Da die Temperaturfunktionen und die Normtemperaturen der genannten Übergänge bekannt sind (vgl. [23]), sollte mit den bekannten Näherungsmethoden eine Beurteilung der Temperatur im Plasma vorgenommen werden. Da die

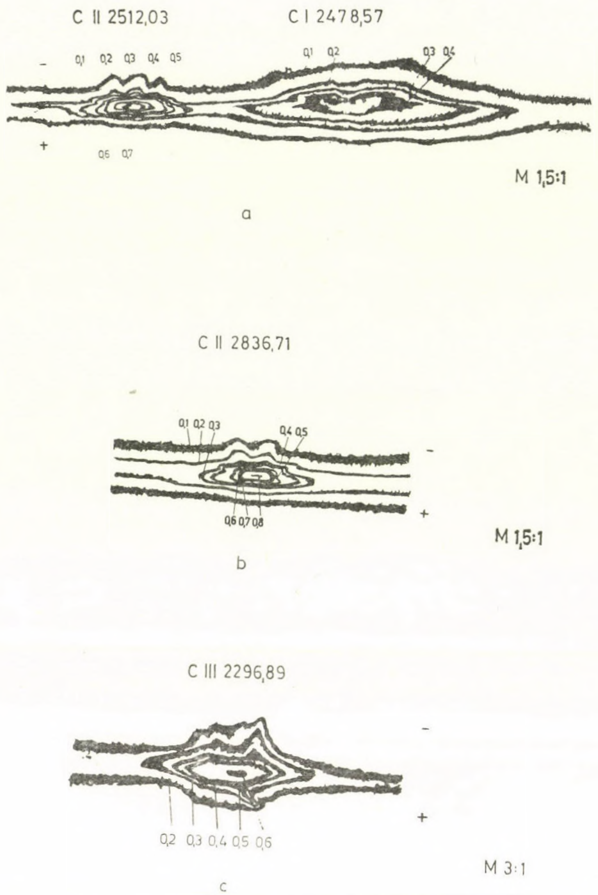

Abb. 4. Spektral aufgelöste Äquidensitogramme (spaltloser Spektrograph) zur Darstellung der Strahlungsverteilung folgender Übergänge: *a.* C II 251,203 nm und C I 247,857 nm, *b.* C II 283,671 nm, *c.* C III 229,689 nm

Abbildungstechnik unter Verwendung des spaltlosen Spektrographen nur ein »integrales« Spektrogramm liefert, kann man für Impulsentladungen nur eine qualitative Beurteilung der Temperatur vornehmen.

Die Äquidensitogramme geben trotzdem die Möglichkeit der Beurteilung der Struktur bzw. der Strukturänderungen der Entladung, wenn man diese bei unterschiedlichen Anregungsbedingungen (Stromstärke, Kapazität, Induktivität) bzw. in einem Magnetfeld oder auch als lokalisierte Entladung durchführt.

Kapillarentladung

In den letzten Jahren wurde das Interesse an lokalisierten Impulsentladungen immer größer. Die Achsensymmetrie und die hohe räumliche Stabilität im lokalisierten Entladungskanal und im Teil zwischen den Platten eröffnet

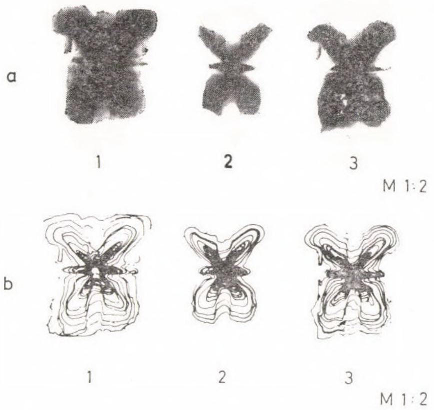

Abb. 5. Photogramme (Teil *a)* und dazugehörige Äquidensitogramme (Teil *b)* einer Kapillar-Impulsentladung. 1: Aufnahmen ohne Filter; 2: Aufnahmen mit Interferenzfilter, Wellenlänge: 437 nm; 3: Aufnahmen mit Interferenzfilter, Wellenlänge: 404 nm

die Möglichkeit der erfolgreichen Anwerdung dieser Entladung für quantitative Plasmauntersuchungen in einem sehr breiten Temperaturgebiet, wie es auf andere Weise im Labor nur schwer zu realisieren ist.

Die spektroskopische Charakteristik dieser Entladung mit dem zwangsweise begrenzten Kanal unterscheidet sich sehr von der freien (offenen) Entladung. Mit Hilfe dieser Entladung ist es z. B. möglich, Informationen über mehrfach ionisierte Ionen, z. B. O VI [25, 26] und deren räumliche Verteilung zu gewinnen. Diese Möglichkeiten sind wiederum interessant für Hochtemperaturlichtquellen in der Spektralanalyse.

Da die chemische Zusammensetzung des Plasmas streng der Zusammensetzung der Kapillarwände entspricht, kann man leicht Plasmen sehr unterschiedlicher Zusammensetzung untersuchen.

Gesetzmäßigkeiten über den Verlauf der Plasmaerzeugung und über die Plasmastruktur kann man gewinnen, wenn man die Äquidensitogramme der Abbildung 5 Teil *b* und die Einzeläquidensiten der Abbildung 6 betrachtet. Zum besseren Vergleich wurden im Teil *a* der Abbildung 5 die Originalphotogrammen dargestellt. Die Aufnahme der Photogramme erfolgte wie bei der offenen Entladung mit einem normalen Photoapparat bei 3 unterschiedlichen Bedingungen [Teil 2 ohne Filter; Teil 2 und 3 mit Interferenzfiltern bei 437 bzw. 404 nm (Abb. 5)].

Es ist deutlich zu erkennen, daß die lokalisierte Entladung achsensymmetrisch ist und daß das Umgebungsgebiet der Elektroden von ihrer Polarität abhängt. In der Anodenzone bildet sich eine leuchtende konische Oberfläche aus, wobei sich der Konuswinkel mit zunehmendem Abstand vom Oberteil vergrößert. Im Kathodengebiet ist die Hauptstrahlung auf der Oberfläche der Elektrode konzentriert, d. h. es wird ein helles Kathodengebiet beobachtet.

Aus den Abbildungen 5 und 6 ist erkennbar, daß ein solches Gebiet auch im achsensymmetrischen Teil, welcher von zwei Platten gebildet bzw. begrenzt wird, beobachtet wird. Dieses entspricht auch den Untersuchungen von **Bondar** und **Kiselewski** [25], welche in diesem Gebiet eine starke Erhöhung der Intensität von Ionenlinien beobachteten. Bei der Herstellung der Äquidensitogramme mußte wegen der großen Zahl der Einzeläquidensiten die Hälfte der Einzeläquidensiten weggelassen werden. Andernfalls hätte man wegen der starken Überlappung der Einzeläquidensiten eine unübersichtliche Darstellung erhalten.

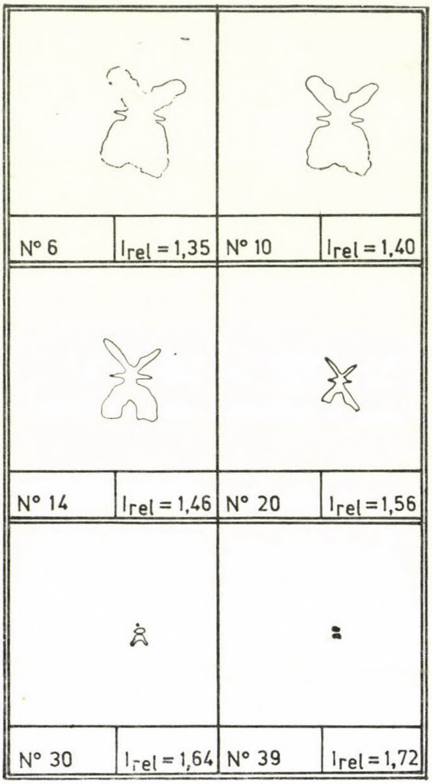

Abb. 6. **Einige charakteristische Einzeläquidensiten der Kapillar-Impulsentladung (diese Äquidensiten wurden der Abb. 5, Teil *b*, 1 (Aufnahme ohne Filter) entnommen)**

Zusätzliche Informationen kann man durch die Betrachtung der Einzeläquidensiten erhalten, wenn man sie, wie es in der Abbildung 6 dargestellt wurde, in einer bestimmten Reihenfolge betrachtet. Von den 40 erhaltenen Einzeläquidensiten wurden in der Abbildung 6 nur die Äquidensiten-Nr. 6, 10, 14, 20, 29 und 39 verwendet. Außerdem wurden die relativen Intensitäten ermittelt und angegeben.

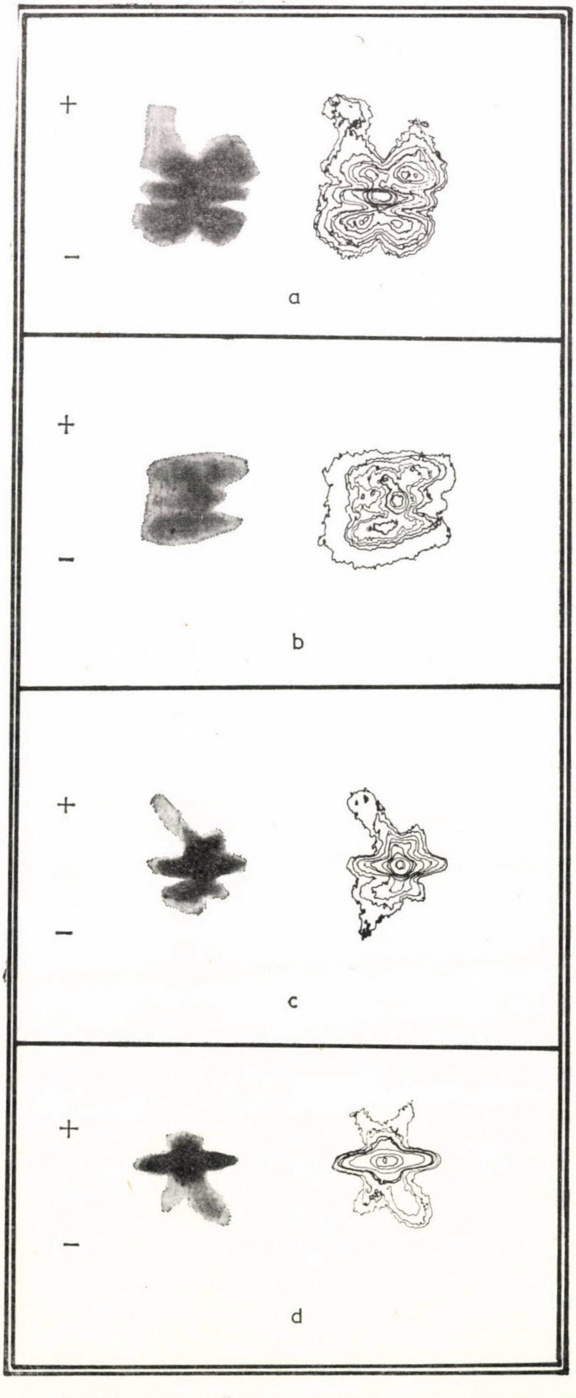

Abb. 7. Photogramme und dazugehörige Äquidensitogramme von Kapillar-Impulsentladungen mit Hilfe der Hochgeschwindigkeitskamera und Filtern. *a.* O I 604,6 nm, Zeitabschnitt: 70—63 μs, *b.* C II 437,4 nm, Zeitabschnitt: 49—42 μs, *c.* N III 409,7 nm, Zeitabschnitt: 35—28 μs, *d.* C IV 580,1 nm, Zeitabschnitt: 21—14 μs

Tabelle III

Schwärzung und Intensitäten von spektral aufgelösten Einzeläquidensiten und für bestimmte Übergänge ermittelte Plasmaparameter

Äquidensiten No.	O I Wellenlänge = 604,6 nm				C II Wellenlänge = 437,4 nm			
	S	$Y_{(r)}$	I/I_{max}	Temperatur in K	S	$Y_{(r)}$	I/I_{max}	Temperatur in K
1	0,70	14,92	1,00	18 000	0,80	25,73	1,00	33 000
2	0,63	8,49	0,6	15 000	0,73	19,57	0,75	22 000
3	0,56	5,22	0,4	14 500	0,67	12,45	0,5	15 000
4	0,49	3,8	0,3	14 000	0,61	8,75	0,35	13 000
5	0,43	2,9	0,2	13 000	0,55	6,1	0,25	12 000
6	0,36	2,13	0,15	12 500	0,48	4,4	0,18	11 000
7	0,29	1,69	0,12	12 300	0,42	3,7	0,15	10 000
8	0,23	1,45	0,1	12 000	0,36	2,5	0,1	9 000
9	0,16	1,2	0,08	11 500	—	—	—	—
10	0,1	1,1	0,07	11 000	0,3	1,8	0,07	8 000

	N III Wellenlänge = 409,7 nm				C IV Wellenlänge = 580 nm			
	S	$Y_{(r)}$	I/I_{max}	Temperatur in K	S	$Y_{(r)}$	I/I_{max}	Temperatur in K
1	0,75	35,19	1,00	48 000	1,00	55,25	1,00	60 000
2	0,69	23,71	0,7	38 000	0,89	37,18	0,6	37 000
3	0,63	16,2	0,75	30 000	0,79	26,41	0,5	34 000
4	0,58	9,17	0,3	27 000	0,69	18,13	0,35	29 000
5	0,53	6,23	0,2	24 000	0,59	14,73	0,3	28 000
6	0,47	4,74	0,15	23 000	0,48	7,8	0,2	27 000
7	0,41	3,71	0,12	22 000	0,38	6,2	0,15	26 000
8	0,36	2,8	0,08	21 500	0,28	4,98	0,1	25 000
9	0,30	2,42	0,06	21 000	—	—	—	—
10	0,25	2,2	0,05	20 000	0,18	2,3	0,05	24 000

Trotz der Tatsache, daß wir bis jetzt nur qualitative Resultate erhielten, wird die Nützlichkeit der Anwendung der Äquidensitometrie auf diese Untersuchungen bestätigt.

Wir machten den Versuch, auf diesem Wege Temperaturen in Plasmen der Kapillarentladungen zu bestimmen. Mit Hilfe der Hochgeschwindigkeitskamera SFR-L wurde der Verlauf der Entladung zeitlich aufgelöst. Mit Hilfe der Interferenzfilter (vgl. Tab. I) wurden jeweils »monochromatische« Abbildungen erhalten. Die auf diesem Wege gewonnene Äquidensitogramme sind in der Abbildung 7 dargestellt worden. Es wurden Übergänge unterschiedlich ionisierter Teilchen ausgewählt. Für die Abbildung 7 wurden jeweils die Äquidensitogramme verwendet, bei denen in Abhängigkeit von der Zeit die maximale Intensität auftrat [23, 27] (vgl. *a.* Tab. II).

Durch diese Versuchsgestaltung wurden nicht nur die Anregungsgebiete für die unterschiedlich ionisierten Teilchen, sondern auch der zeitliche Verlauf ihrer Anregung identifiziert.

Nachdem aus den Schwärzungen die relativen Intensitäten ermittelt worden waren, wurden diese mit Hilfe der ABEL-schen Integralgleichung in räumliche Intensitäten umgerechnet.

Mit Hilfe der bekannten Anregungsfunktionen wurde eine Temperatureichung für alle Äquidensiten des Äquidensitogramms vorgenommen (s. Tabelle III). Auf diese Weise erhielten wir Angaben über den zeitlichen Verlauf der Temperatur im Plasma und auch über deren örtliche Verteilung.

Schlußfolgerungen

Man kann feststellen, daß die photographische Äquidensitometrie in Verbindung mit spektral, zeitlich und räumlich auflösenden Abbildungstechniken erfolgreich für die Plasmadiagnostik und für die Ermittlung von Plasmaparametern von Hochspannungs-Impulsentladungen angewendet werden kann.

*

Die Autoren danken Frau KIROWA und Frau GANEWA für ihre Hilfe bei der Durchführung der Experimente, Frau LASAROWA und Herrn MITOW für ihre Unterstützung bei der Arbeit und Herrn HÖGNER für die Unterstützung bei der technischen Anfertigung der Äquidensiten.

LITERATUR

[1] LAU, B., KRUG, W.: Die Äquidensitometrie — Grundlagen, Verfahren und Anwendungsgebiete, Akademieverlag, Berlin, 1957
[2] KRUG, W., WEIDE, H. G.: Wissenschaftliche Photographie in der Anwendung, Akademische Verlagsgesellschaft, Geest & Portig, Leipzig, 1972, S. 108—132
[3] REKALIĆ, M., NEBE, W.: Experimentelle Technik der Physik, **22**, 467 (1972)
[4] RICHTER, N., HÖGNER, W.: Monatsberichte der DAW **10** (1963), Mitteilung des Karl-Schwarzschild-Observatoriums, Tautenburg
[5] HÖGNER, W.: Jenaer Rdsch., **14**, 340 (1969)
[6] HÖGNER, W., LÖCHEL, N.: DDR-Patent Nr. 110124
[7] BREIDO, I. I., WILENSKAJA, B. G.: Zhurn. nautschn. i prikl. fotograf. i kinematogr., **16**, 374 (1971)
[8] WLADIMIROW, S.: Astronom. Zirkuljar, No. 977, 5 (1977)
[9] DITTRICH, K., NIEBERGALL, K., RÖSSLER, H.: Z. Chem., **13**, 231 (1973)
[10] DITTRICH, K., NIEBERGALL, K., RÖSSLER, H.: Spectrochim. Acta, **31 B**, 331 (1976)
[11] DITTRICH, K., NIEBERGALL, K., RÖSSLER, H.: Acta Chim. Acad. Sci. Hung., **89**, 347 (1976)
[12] DITTRICH, K., NIEBERGALL, K., RÖSSLER, H.: Acta Chim. Acad. Sci. Hung., **89**, 365 (1976)
[13] DITTRICH, K., PETRAKIEW, A., KOLEWA, I., KIROWA, E.: VII. National Conference on Spectroscopy, Burgas, 1976, S. 10
[14] PETRAKIEW, A., DITTRICH, K., GEORGIEWA, L.: XVIII. Colloqu. Spectroscopicum Internationale, Grenoble, 1975, S. 34

[15] DITTRICH, K., KARJAKIN, A. W.: Zhurn. analit. khim., **XXXIV, 98** (1979)
[16] KRANZ, E.: XX. Colloqu. Spectroscopicum Internationale, Prag, 1977, S. 520
[17] KAPIČKA, V., KAPOUN, K., PETRAKIEW, A.: Proceedings of the XIII. International Conference on Phenomena in Ionized Gases, Berlin, 1977, S. 12
[18] KAPIČKA, V., KAPOUN, K., PROTASEWITSCH, E. T., PETRAKIEW, A., WLADIMIROW, S.: Annuaire de L'Université de Sofia, Fac. de Physique, **68,** im Druck (1978)
[19] KAPIČKA, V., LEPKA, K., TALSYK, A., PETRAKIEW, A., KOLEWA, I., PROTAEWITSCH, E.: Annuaire de L'Université de Sofia, Fac. de Physique, **68,** im Druck (1978)
[20] HÖGNER, W.: Privatmitteilung
[21] FISHER, J. F.: Am. J. Roening, **79,** 342 (1958)
[22] SARTOW, G.: Dissertation, Charkower Universität, 1975
[23] PETRAKIEW, A., VÖRÖS, A.: Spectrochim. Acta, **24 B,** 369 (1969)
[24] PETRAKIEW, A., KOLEWA, I., STEFANOWA, D.: Annuaire de L'Université de Sofia, Fac. de Physique, **67,** 221 (1977)
[25] BONDARI, W. A., KISELEWSKI, L. I.: Zhurn. prikladn. Spektrosk., **5,** 568 (1966)
[26] ELJASCHEWITSCH, M. A., BONDARI, W. A., KISELEWSKI, L. I.: Trudy IV. Sibirskowo Soweschtschanija po Spektroskopii, (1969) 310
[27] KREMPL, H.: Zeitschrift für Physik, **167,** 302 (1962)

Asparuch PETRAKIEW
Iwanka KOLEWA
S. WLADIMIROW
Kliment-Ochridski-Universität Sofia, Bulv. Anton Iwanow 5, Physikalische Fakultät, VR Bulgarien

Klaus DITTRICH
Karl-Marx-Universität Leipzig, Sektion Chemie
701 Leipzig, Liebigstr. 18 DDR

Acta Chimica Academiae Scientiarum Hungaricae, Tomus 104 (1), pp. 13–28 (1980)

PREPARATION AND STUDY OF CHELATING RESINS, II

DETERMINATION OF THE PROTONATION CONSTANTS OF A CHELATING RESIN CONTAINING ETHYLENE DIAMINE TRIACETIC ACID FUNCTIONAL GROUPS

Ö. SZABADKA and J. INCZÉDY

(Department of Analytical Chemistry University of Veszprém, Veszprém)

Received March 16, 1979
In revised form June 9, 1979
Accepted for publication June 18, 1979

An equation is derived for the calculation of the protonation constants of ion exchange resins containing weakly acidic functional groups. The protonation is considered as a heterogeneous chemical reaction.

The equation is used for the description of the protonation equilibria of a chelating resin containing ethylene diamine triacetic acid functional groups. From data obtained from the pH titration curve, and measurements of alkali ion and water uptake it was possible to calculate all the three protonation constants of the active groups.

Measurements were carried out at 25 °C in aqueous solution at ionic strengths of 0.01, 0.1, 1.0 and 3.0 mol/dm³. The following values independent of the ionic strength were obtained for the logarithms of the protonation constants:

$$\log K_1 = 10.5 \pm 0.1$$
$$\log K_2 = 5.9 \pm 0.1$$
$$\log K_3 = 3.3 \pm 0.1$$

The constancy of the calculated values of the protonation constants for all the three steps of the dissociation indicates that these data are thermodynamically meaningful constants for the acidic groups of the ethylene-diamine triacetic acid molecule bounded to a styrene-divinyl benzene matrix.

In the first part of this series we reported the preparation of chelating ion exchange resins of well defined and reproducible chemical composition [1]. The resins contain polyamino polycarboxylic acid functional groups on a styrene-divinyl benzene polymer matrix and can be described as follows:

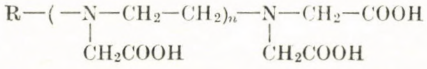

$$\mathrm{R{-}(-\underset{\displaystyle CH_2COOH}{\underset{|}{N}}{-}CH_2{-}CH_2)_{\mathit{n}}{-}\underset{\displaystyle CH_2COOH}{\underset{|}{N}}{-}CH_2{-}COOH}$$

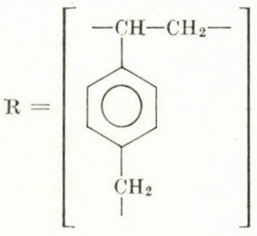

where R is the matrix of the resin and $n = 1$ or 2 according to the table below:

n	Name of functional group
1	ethylene-diamine triacetic acid
2	diethylene-triamine tetraacetic acid

The preparation of the resin containing ethylene-diamine triacetic acid has been developed in our laboratory and now is commercially available, under the trade name Ligandex-E, from the Reanal Fine Chemical Factory (Budapest).

This article deals with the determination of the protonation constants of this Ligandex-E chelating resin.

Introduction

The thermodynamic protonation constants of a chelating resin with acidic functional groups on a styrene divinyl benzene matrix were calculated from water vapor absorption and pH titration data by MARINSKY *et al.* [2, 3]. The protonation constants of Amberlite IRC-50, which contains metacrylic acid functional groups, and the protonation constant of the first dissociation step of Dowex A-1 chelating resin, containing imino-diacetic acid functional groups, were calculated using following equation:

$$\log K = \mathrm{pH} + \log \frac{1-\alpha}{\alpha} + \log \frac{a_{\mathrm{M}}}{a_{\overline{\mathrm{M}}}} - \frac{0.4343}{kT} \left(\frac{\partial G}{\partial \nu} \right)_{\varkappa} \quad (1)$$

where: K is the protonation constant
(MARINSKY *et al.* used the dissociation constant,
K_a in equation (1), which is related to our protonation constant, K, by
$\mathrm{pK_a} = -\log K_a = \log K$);

pH is the equilibrium pH of the solution corresponding to a given degree of dissociation, α (pH and α are in fact the interrelated values of the titration curve);

a_{M} and $a_{\overline{\mathrm{M}}}$ are activities of the counter ions of the negatively charged ligand base, in the solution and in the resin phase respectively;

G is the electrostatic free enthalpy of the polyanion carrying ν negative charges;

$\varkappa$ is the reciprocal Debye radius; its value is controlled by the concentration of the small counter ions;

k is the Boltzmann factor;

T is the absolute temperature.

It should be mentioned here that MARINSKY's original equation contains an additional term which makes allowance for the free enthalpy change caused by the pressure effect of the solvent molecules on the resin matrix. This term, however, is insignificant in comparison to the electrostatic interaction term [2], and has therefore been omitted from equation (1).

To derive an equation suitable for the calculation of the protonation constants we started with the principle of electronneutrality, according to which the resin phase should contain counter ions in an equivalent quantity to the polyelectrolyte. Consequently, the protonation of a monovalent anion base can be represented by the following equation:

$$\overline{R^-} + \overline{M^+} + H^+ \rightleftharpoons \overline{RH} + M^+ \tag{2}$$

where the bars refer to the resin phase components. The thermodynamic equilibrium constant for the above heterogeneous equilibrium is:

$$K = \frac{a_{\overline{RH}}\, a_M}{a_{\overline{R}}\, a_{\overline{M}}\, a_H} \tag{3}$$

which is in fact the protonation constant of the monovalent anion base ($\overline{R}$) in the resin phase.

Expressing the activities in equation (3) by the product of the molal concentrations and activity coefficients and taking logarithms, one obtains the following expression:

$$\log K = \mathrm{pH} + \log \frac{m_{\overline{RH}}}{m_{\overline{R}}} + \log \frac{a_M}{m_{\overline{M}}} + \log \frac{\gamma_{\overline{RH}}}{\gamma_{\overline{R}}} - \log \gamma_{\overline{M}} \tag{4}$$

where $m_{\overline{R}}$, $m_{\overline{RH}}$ and $m_{\overline{M}}$ are the molal concentrations of the base ($\overline{R}$), the protonated base ($\overline{RH}$) and the counter ion ($\overline{M}$) in the resin phase, and $\gamma_{\overline{R}}$, $\gamma_{\overline{RH}}$ and $\gamma_{\overline{M}}$ are the appropriate activity coefficients.

The degree of the dissociation (*i.e.* the neutralisation) of the acid group is defined as follows:

$$\overline{\alpha} = \frac{m_{\overline{R}}}{m_{\overline{RH}} + m_{\overline{R}}}\,. \tag{5}$$

The protonation constant can then be written as:

$$\log K = \mathrm{pH} + \log \frac{1-\overline{\alpha}}{\overline{\alpha}} + \log \frac{a_M}{m_{\overline{M}}} + \log \frac{\gamma_{\overline{RH}}}{\gamma_{\overline{R}}} - \log \gamma_{\overline{M}} \tag{6}$$

A comparison of equations (1) and (6) shows that:

$$\log \frac{\gamma_{\overline{RH}}}{\gamma_{\overline{R}}} = -\frac{0.4343}{kT}\left(\frac{\partial G}{\partial v}\right)_{\varkappa}. \tag{7}$$

In other words, the electrostatic term is in fact the difference in the excess free enthalpy of the unprotonated (ionized) and protonated components.

In equations (1) and (6) the following quantities can be determined experimentally:

- the pH value of the equilibrium solution,
- the degree of dissociation of the acidic groups in the resin phase,
- the activity of the counter ion in the solution phase,
- the concentration of the counter ion in the resin phase.

The activity coefficients $\gamma_{\overline{\mathrm{RH}}}$, $\gamma_{\overline{\mathrm{R}}}$ and $\gamma_{\overline{\mathrm{M}}}$ can only be obtained from a suitable model for the dissociation equilibrium of the acidic group in the resin. The electrostatic term and the activity coefficient in equation (1) were calculated by MARINSKY *et al.* by postulating the validity of the KATCHALSKY model [4, 5, 6] which describes the dissociation equilibria of the linear polyelectrolytes.

The electrostatic free enthalpy is then given by the following equation:

$$\frac{0.4343}{kT}\left(\frac{\partial G}{\partial \nu}\right)_{\varkappa} = \frac{2\alpha e^2}{DbkT}\log\left(1+\frac{6}{\varkappa s b}\right) \tag{8}$$

where α is the degree of dissociation,

e is the unit electronic charge (1.6021 10^{-19}C),
D is the relative permittivity of the equilibrium solution,
k is the Boltzmann factor,
T is the absolute temperature,
b is the hydrodynamic length of a monomer unit (the distance of the functional groups from one another),
s is the number of the monomers in one statistical unit [4],
and $\varkappa$ is the reciprocal Debye-radius, which can be calculated from the Debye-Hückel theory using the following equation:

$$\varkappa^2 = \frac{4\pi e^2}{DkT}\,\frac{\Sigma\, n_i}{V} \tag{9}$$

where n_i is the number of the free ions,
and V is the volume of the monomer unit (*i.e.* molar volume per Avogadro-number).

Equation (8) predicts that the electrostatic interaction (repulsion of the charged cylinders of the macromolecules) is a function of the degree of dissociation.

From the linear polyelectrolyte model an appropriate value of the activity coefficient of the counter ion of the dissociated macromolecule is given by the equation [7]:

$$\log \Phi_p = \log \gamma_{\overline{\mathrm{M}}} \tag{10}$$

where Φ_p is the osmotic coefficient of the polyelectrolyte, which may be calculated from equation (11):

$$\Phi_p = \frac{1-\beta^2}{2\lambda} - \frac{1}{R^2/a^2-1} \,. \tag{11}$$

Here

$$\gamma = \frac{\alpha e^2}{DbkT} = \frac{1-\beta^2}{1+\beta \operatorname{cth}(\delta\beta)} \tag{12}$$

$$\delta = \ln R/a = \frac{1}{2} \ln \frac{1000}{\overline{V} m_{\overline{\mathrm{M}}}} \tag{13}$$

$$R^2 = \frac{1000}{\pi b m_{\overline{\mathrm{M}}} N} \tag{14}$$

$$a^2 = \frac{\overline{V}}{\pi b N} \tag{15}$$

where: R is the average half distance between two neighboring monomer cylinders,

$2a$ is the diameter of the monomer units,

b is the length of the monomer unit,

m is the concentration of the counter ions,

N is the Avogadro's number,

$\overline{V}$ is the partial molar volume of the polymer in the solution,

and β is an integration constant of the differential equation which describes the electrostatic potential of two parallel, cylindrically shaped, polyelectrolyte molecules [4].

From equations (11) and (12) it appears that the activity coefficient of a counter ion decreases with increasing degree of dissociation, α. (For linear polyelectrolytes the validity of the equation, $\Phi\alpha$ = const, can be proved experimentally [8].)

In equations (1) and (6), a comparison of the $\gamma_{\overline{\mathrm{R}}}$ values of the electrostatic free enthalpy term, $\log \frac{\gamma_{\overline{\mathrm{R}}}}{\gamma_{\overline{\mathrm{RH}}}}$ (which becomes more negative with increasing degree of dissociation) with the term containing the logarithm of the activity coefficient of the counter ion in the resin phase, $-\log \gamma_{\overline{\mathrm{M}}}$ (which becomes more positive with the degree of dissociation), shows that these two terms apparently compensate each other over the dissociation range studied. Therefore the omission of these terms from equations (1) and (6) should still give a constant value for the protonation constant:

$$\log K = \mathrm{pH} + \log \frac{1-\overline{\alpha}}{\overline{\alpha}} + \log \frac{a_{\mathrm{M}}}{m_{\overline{\mathrm{M}}}} \,. \tag{16}$$

Experimental

The chelating resin studied is commercially available from Reanal (Budapest) under the trade name Ligandex-E. The ethylene diamine triacetic acid functional groups are bonded covalently to the lightly crosslinked (1.4 DVB%) styrene-divinyl benzene matrix.

The resin, which was obtained as the sodium form, was transformed into the hydrogen form by washing it in a column with 1 mol/dm^3 hydrochloric acid solution.

The hydrogen form resin was washed with deionised water until it was free of chloride, and after drying in air the resin was stored in a dark bottle. The water content of the air dried resin was calculated from the weight loss of the samples after drying in a vacuum desiccator at 105 °C.

Titration curves of the resin

Exactly known quantities (approximately 0.5 g) of the air dried hydrogen form resin samples were weighed into 100 cm^3 glass-stoppered flasks and increasing volumes of 0.1 mol/dm^3 potassium hydroxide solution were then added. The ionic strength and the 100 cm^3 final volume of the suspension was adjusted by the addition of a calculated quantity of water and potassium chloride solution. The pH titration curves were obtained at ionic strengths of 0.01, 0.1, 1 and 3 mol/dm^3. The suspensions were first left to equilibrate under an argon atmosphere in the sealed flasks at a constant temperature, for seven days. The pH of each equilibrated solution was then measured using a calibrated glass electrode. The preparation of the batch samples and the pH measurements were made in a protecting argon gas atmosphere.

The carbonate free potassium hydroxide solution was prepared according to a standard method [9].

The titration curves were obtained by plotting the measured pH values as a function of the quantity of potassium hydroxide per 1 g of the dry resin.

Determination of the water content of the resin phase

When the pH measurements had been made, the resin samples were separated from the solution phase using a centrifuge and dried to constant weight under vacuum at 105 °C [10]. The water content was then calculated with reference to 1 g of the dry hydrogen form resin.

Determination of the potassium uptake

The resin phase absorbs potassium ions:

- in the neutralisation reaction, when the hydrogen ions associated with the acidic groups are exchanged for potassium ions,
- from the potassium chloride solution used for maintaining the ionic strength.

The amounts of potassium ion originating from the first and the second process can be calculated separately as follows. The absorbed potassium ions were eluted from the resin into a 250 cm^3 graduated flask by a known quantity of 0.1 mol/dm^3 nitric acid solution, the resin was then washed free of acid with water, and finally the flask was made up to the mark. The chemically bound potassium was obtained from the decrease of the acidity in the eluent solution. The quantity of potassium ions which had migrated into the resin lattice was determined by titration of the chloride content of the eluent using Mohr's method.

As a check, the potassium uptake was also determined by flame photometry [1]. This latter method gives the total amount of potassium ions in the resin, originating from both the ion exchange and migration processes.

Above pH 11, the quantity of the chemically bound potassium ions was also calculated from the alkalimetric determination of the potassium hydroxide left in the equilibrium solution. These values were in agreement with the values obtained by the elution techniques. The electrolyte migration was negligible in the solution of 0.01 ionic strength (the potassium chloride used for the adjustment of the ionic strength was left practically quantitatively in the solution.) When the protonation constants were calculated for the solutions at high pH values, an allowance had to be made for the fact that residual potassium hydroxide in these solutions caused a slight increase in the ionic strength.

Results and discussion

Interpretation of the potassium uptake

In Fig. 1 the quantity of the chemically bound potassium is plotted as a function of the equilibrium pH of the solutions of ionic strength 0.01, 0.1, 1 and 3 mol/dm^3.

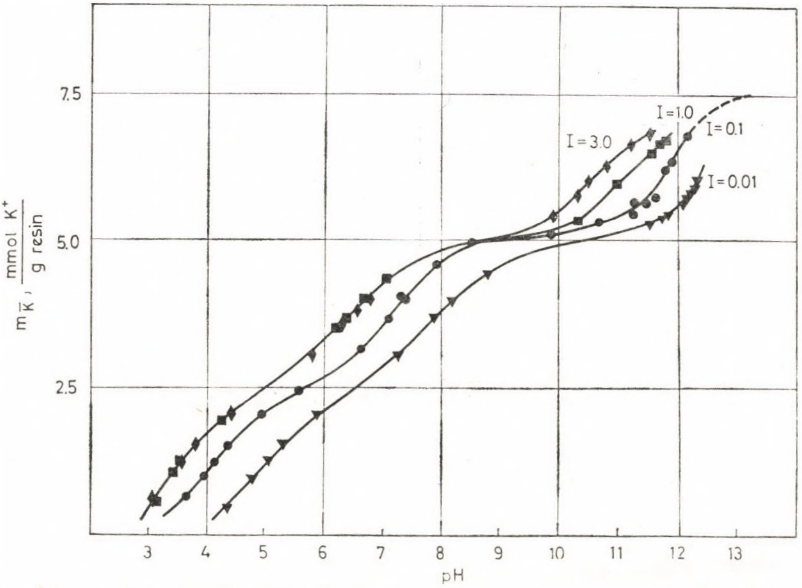

Fig. 1. Quantity of the chemically bound potassium ions as a function of the pH of the equilibrium solution

Three buffer ranges can be observed on these curves, corresponding to the three basic ethylene diamine triacetic acid functional groups of the resin. From the three horizontal inflection points the quantity of the chemically bound potassium ions can be estimated. As can be seen the three ranges are equal to one another.

The exchange capacity corresponding to the stepwise ranges of the neutralisation is:

$$m_{\overline{\mathrm{RH}}} + m_{\overline{\mathrm{R}}} = 2.50 \text{ mmol K}^+/\text{g resin}.$$

Remembering that the functional groups are actually three basic ethylene-diamine triacetic acid molecules the following conclusions are obvious:

— the functional group capacity of the resin *(Q)* is:

$$Q = 2.50, \frac{\text{mmol ethylene diamine triacetic acid}}{\text{g dry hydrogen form resin}}$$

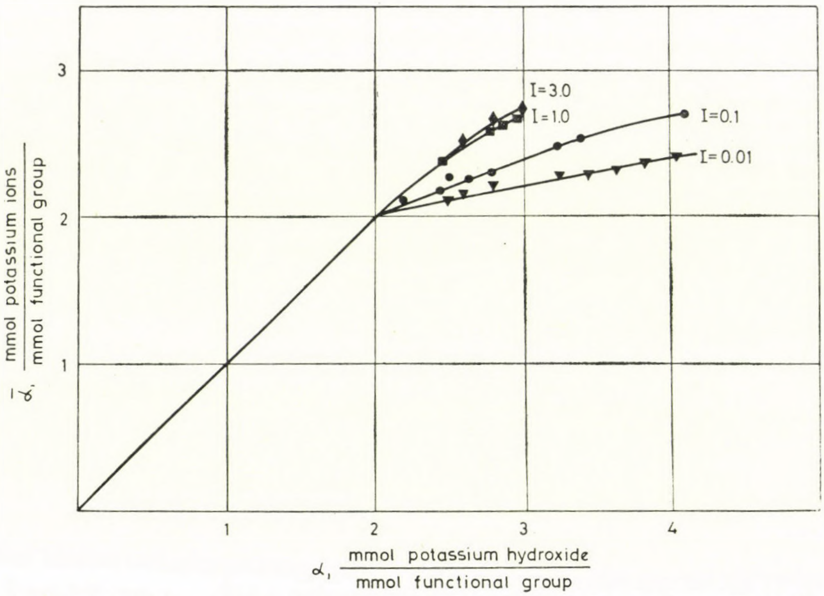

Fig. 2. **The degree of dissociation of the resin phase active groups as a function of the added quantity of the potassium hydroxide**

- the total cation exchange capacity equivalent to the neutralisation of all the three acidic groups is 7.50 mmol M^+/g resin,
- the degree of the dissociation (neutralisation) in the resin phase can be calculated using equation (5a):

$$\bar{\alpha} \equiv \frac{m_{\bar{R}}}{Q} = \frac{m_{\bar{K}}}{Q}, \tag{5a}$$

where: $m_{\bar{K}}$ is the concentration of the chemically bound potassium ions (mmol K^+/gram dry hydrogen form resin),
$\bar{\alpha}$ is the degree of the dissociation (neutralisation) in the resin phase $0 \leq \bar{\alpha} \leq 3$.

The curve in Fig. 2 represents the change of the degree of dissociation of the resin phase as a function of the quantity of the potassium hydroxide used for the neutralisation. This quantity is also referred to the functional groups of the resin:

$$\alpha = \frac{\text{mmol KOH}}{\text{mmol functional groups}} = \frac{\text{mmol KOH}}{Q}.$$

The figure shows that

- the potassium hydroxide is taken up quantitatively by the resin in the first two neutralisation steps, therefore $\bar{\alpha}$ can be calculated from the quantity of the potassium hydroxide used for the neutralisation,

- in the third dissociation step, however, an increasing amount of the potassium will remain behind in the solution, therefore $\bar{\alpha}$ for this dissociation step can only be calculated from the quantity of the chemically bound potassium ($m_{\overline{K}}$).

The quantity of potassium chloride taken up by electrolyte migration ($m_{\overline{KCl}}$) was found to be independent of the degree of titration. The values for $m_{\overline{KCl}}$ are given as a function of the ionic strengths of the solutions in Table I.

Table I

The molal concentration of the potassium chloride in the resin phase, $m_{\overline{KCl}}$ at various values of the ionic strength

Ionic strength	$m_{\overline{KCl}}$
0.01	—
0.1	0.20 ± 0.05
1.0	1.2 ± 0.1
3.0	3.8 ± 0.1

Interpretation of the water uptake

The water uptake of the resin was determined in the titration range 0—3, for all values of the ionic strength (0.01, 0.1, 1.0 and 3.0).

In Fig. 3 the water uptake is shown as a function of the quantity of the chemically bound potassium ion, or in terms of the degree of neutralisation of the resin phase ($\bar{\alpha}$). From this figure it appears that water uptake of the resin phase in the first step of neutralisation is strongly dependent on the ionic strength. For a given value of chemically bound potassium ions, the lower is the ionic strength the larger is the quantity of the absorbed water.

In the second and third steps of neutralisation for a given ionic strength, the water uptake increases proportionally with the quantity of the chemically bound potassium ions, so that the water uptake as a function of neutralisation is represented by a series of parallel straight lines. The slope of these linear plots shows that 5.0 ± 0.5 water molecules are transferred into the resin phase by each potassium ion:

$$\frac{m_{\overline{H_2O}}}{m_{\overline{K^+}}} = 5.0 \pm 0.5 .$$

This is a reasonable value for the solvation number of potasssium ions in moderately concentrated solutions [11], and it seems to corroborate the assumption used in the derivation of equation (2), that the weakly acidic active

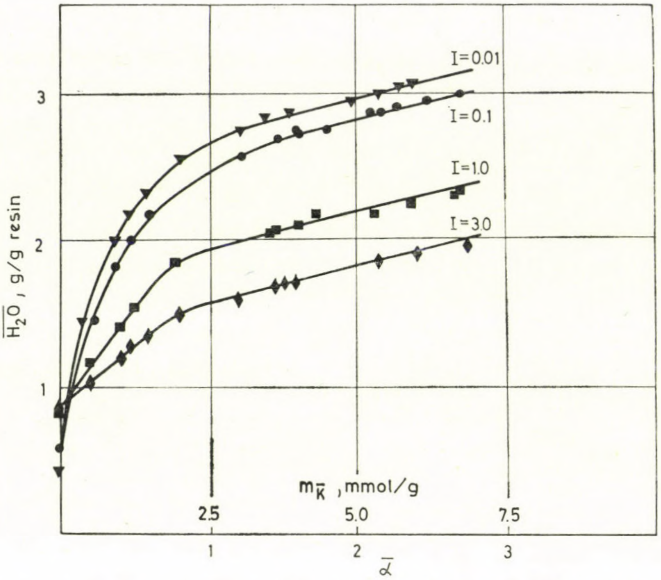

Fig. 3. **The water uptake as a function of the chemically bound potassium ions, as well as the degree of the neutralisation, in the resin phase**

groups in the H-form are strongly associated and permit only a low degree of hydration for the protons ($\overline{RH}$), and that the potassium uptake is accompanied by the dissociation and simultaneous hydration of the active groups ($R^- + K^+$).

Calculation of the protonation constants

The protonation constants were calculated using equation (16). Tables II, III and IV list the experimental data and steps of the calculations for the first, second and third protonation constants respectively.

In the first and the second columns of the tables the quantity of the potassium hydroxide used for the neutralization, and the measured equilibrium pH-values are given. The third and fourth columns represent the chemically bound potassium ions ($m_{\overline{K}}$) and the calculated $\overline{\alpha}$-values ($\overline{\alpha} = m_{\overline{K}}/2.5$). The fifth column gives the log $\frac{1-\overline{\alpha}}{\overline{\alpha}}$ values and the sixth column the water uptake.

The log $m_{\overline{M}}$ values in the seventh column are given by:

$$\log m_{\overline{M}} = \log \frac{m_{\overline{K}} + m_{\overline{KCl}}}{\overline{H_2O}}$$

Column eight lists the logarithms of the counter ion activities in the solution phase. These values, with the exception of the data referring to the 0.01 ionic

Table II

Experimental data and the details of the calculation of the first protonation constant

KOH mmol/g	pH	$m_{\overline{K}}$ mmol/g	$\bar{\alpha}$**	$\log\frac{3-\bar{\alpha}}{\bar{\alpha}-2}$	$\overline{H_2O}$	log $m_{\overline{M}}$	log a_M	log K_1
$I = 0.01$ $m_{\overline{KCl}} = 0$ mmol/g								
6.00	11.34	4.95	2.080	1.06	2.92	0.23	−1.90*	10.27
6.25	11.52	5.23	2.096	0.97	2.98	0.24	−1.87*	10.28
6.50	11.75	5.34	2.117	0.88	3.00	0.25	−1.87*	10.51
7.00	11.83	5.40	2.158	0.73	2.99	0.26	−1.83*	10.47
8.04	12.13	5.62	2.248	0.48	3.00	0.27	−1.96*	10.38
8.54	12.17	5.68	2.274	0.38	3.08	0.27	−1.92*	10.36
9.04	12.22	5.78	2.312	0.34	3.05	0.28	−1.89*	10.46
9.55	12.29	5.87	2.352	0.27	3.10	0.28	−1.82*	10.46
10.12	12.33	5.97	2.396	0.18	3.06	0.29	−1.76*	10.43
$I = 0.1$ $m_{\overline{KCl}}$ 0.2 mmol/g								
5.51	10.64	5.27	2.07	1.12	2.86	0.28	−1.11	10.37
6.13	11.26	5.41	2.17	0.69	2.85	0.29	−1.11	10.57
6.26	11.27	5.65	2.19	0.63	2.82	0.32	−1.11	10.47
6.63	11.49	5.61	2.25	0.48	2.83	0.31	−1.11	10.57
6.97	11.65	5.69	2.30	0.37	2.88	0.31	−1.11	10.60
8.08	11.81	6.20	2.47	0.05	2.93	0.34	−1.11	10.41
8.48	11.90	6.30	2.52	−0.03	2.94	0.34	−1.11	10.42
10.28	12.21	6.75	2.69	−0.35	3.00	0.36	−1.11	10.41
$I = 1.0$ $m_{\overline{KCl}} = 1.2$ mmol/g								
5.43	10.33	5.32	2.128	0.83	2.17	0.48	−0.22	10.44
6.17	10.94	5.94	2.376	0.22	2.24	0.50	−0.22	10.44
6.91	11.52	6.48	2.592	−0.16	2.30	0.52	−0.22	10.62
7.16	11.67	6.66	2.664	−0.30	2.30	0.53	−0.22	10.62
7.40	11.77	6.70	2.680	−0.33	2.32	0.53	−0.22	10.69
$I = 3.0$ $m_{\overline{KCl}} = 3.8$ mmol/g								
5.50	9.93	5.39	2.156	0.74	1.86	0.69	0.23	10.21
6.00	10.32	5.77	2.308	0.35	1.89	0.70	0.23	10.21
6.28	10.51	6.01	2.404	0.17	1.90	0.71	0.23	10.20
6.50	10.78	6.27	2.508	−0.01	1.93	0.72	0.23	10.28
7.00	11.22	6.63	2.652	−0.27	1.92	0.73	0.23	10.45
7.50	11.52	6.86	2.744	−0.46	1.95	0.74	0.23	10.54

*** Values obtained making allowance for the potassium hydroxide remaining in the solution.**

**** Values calculated from the data of Fig. 2.**

Table III

Experimental data and the details of the calculation of the second protonation constant

KOH mmol/g	pH	$m_{\bar{K}}$	$\bar{\alpha}$	$\log \frac{2-\bar{\alpha}}{\bar{\alpha}-1}$	$\overline{H_2O}$ g/g	$\log m_{\bar{M}}$	$\log a_M$	$\log K_2$
$I = 0.01$ $m_{\overline{KCl}} = 0$ mmol/g								
3.00	7.31	3.04	1.216	0.56	2.73	0.05	−2.03	5.79
3.75	7.92	3.71	1.484	0.03	2.99	0.09	−2.03	5.83
4.00	8.22	3.96	1.584	−0.15	2.83	0.15	−2.03	5.89
4.50	8.81	4.38	1.752	−0.49	2.85	0.19	−2.03	6.10
$I = 0.01$ $m_{\overline{KCl}} = 0.2$ mmol/g								
3.14	6.65	3.10	1.240	0.50	2.56	0.11	−1.11	5.93
3.68	7.13	3.66	1.464	0.06	2.67	0.16	−1.11	5.92
3.93	7.31	4.06	1.624	−0.22	2.71	0.20	−1.11	5.78
4.04	7.43	4.01	1.604	−0.18	2.74	0.19	−1.11	5.95
4.56	7.95	4.54	1.816	−0.65	2.76	0.23	−1.11	5.96
$I = 1.0$ $m_{\overline{KCl}}$ 1.20 mmol/g								
3.53	6.22	3.56	1.424	0.13	2.05	0.35	−0.22	5.78
3.71	6.36	3.64	1.456	0.08	2.07	0.35	−0.22	5.85
3.91	6.65	4.01	1.604	−0.18	2.10	0.37	−0.22	5.88
4.37	7.05	4.33	1.732	−0.44	2.18	0.38	−0.22	6.01
$I = 3.0$ $m_{\overline{KCl}} = 3.00$ mmol/g								
3.02	5.80	2.99	1.20	0.61	1.61	0.63	0.23	6.02
3.52	6.30	3.59	1.44	0.11	1.68	0.65	0.23	5.99
3.77	6.57	3.79	1.52	−0.03	1.71	0.66	0.23	6.11
4.00	6.80	4.00	1.60	−0.18	1.72	0.68	0.23	6.07

strength in Table II, are identical with the logarithm of the product of the ionic strength and the mean activity coefficient of the potassium chloride at the given ionic strength. In the first protonation step, however, ($2 \leq \bar{\alpha} \leq 3$) one should bear in mind that a small fraction of the potassium hydroxide remains in the solution phase (see Fig. 2) and contributes slightly to the ionic strength. This effect can be neglected if the ionic strength is equal or higher than 0.1, but it becomes significant in the solution of ionic strength 0.01 when the potassium hydroxide increases the ionic strength up to 0.013−0.015.

The logarithms of the protonation constants calculated by equation (16) are given in the last column of the tables.

Table IV

Experimental data and the details of the calculation of the third protonation constant

KOH mmol/g	pH	$m_{\overline{K}}$ mmol/g	$\bar{\alpha}$	$\log \frac{1-\bar{\alpha}}{\bar{\alpha}}$	$\overline{H_2O}$ g/g	$\log m_{\overline{K}}$	$\log a_M$	$\log K_3$
$I = 0.01$ $m_{\overline{KCl}} = 0$ mmol/g								
0.50	4.37	0.43	0.17	0.68	1.43	−0.52	−2.03	3.54
1.00	4.84	0.98	0.39	0.19	1.98	−0.31	−2.03	3.31
1.25	5.07	1.23	0.49	0.01	2.17	−0.25	−2.03	3.30
1.50	5.34	1.49	0.60	−0.17	2.30	−0.19	−2.03	3.33
2.00	5.94	2.01	0.80	−0.61	2.54	−0.10	−2.03	3.40
$I = 0.1$ $m_{\overline{KCl}} = 0.20$ mmol/g								
0.61	3.67	0.63	0.252	0.47	1.45	−0.24	−1.11	3.27
1.00	3.98	0.96	0.384	0.21	1.81	−0.19	−1.11	3.27
1.25	4.18	1.20	0.480	0.03	1.98	−0.15	−1.11	3.25
1.50	4.41	1.54	0.616	−0.21	2.37	−0.13	−1.11	3.22
2.00	4.96	2.03	0.812	−0.64	2.36	−0.02	−1.11	3.23
$I = 1.0$ $m_{\overline{KCl}} = 1.20$ mmol/g								
0.56	3.16	0.56	0.224	0.54	1.17	0.18	−0.22	3.30
1.02	3.42	1.05	0.420	0.14	1.41	0.20	−0.22	3.12
1.25	3.57	1.27	0.508	−0.01	1.54	0.21	−0.22	3.13
2.00	4.27	1.96	0.784	−0.56	1.86	0.23	−0.22	3.26
$I = 3.0$ $m_{\overline{KCl}}$ 3.8 mmol/g								
0.50	3.10	0.57	0.23	0.53	1.03	0.62	0.23	3.34
1.00	3.42	1.08	0.43	0.12	1.20	0.61	0.23	3.16
1.25	3.60	1.23	0.49	0.02	1.28	0.59	0.23	3.26
1.50	3.82	1.55	0.62	−0.21	1.35	0.60	0.23	3.24
2.00	4.44	2.02	0.81	−0.62	1.49	0.59	0.23	3.46

The titration curves obtained at ionic strengths of 0.01, 0.1 and 1.0 are shown in Fig. 4. Curve 4, based upon the data from curves 1—3, is a plot of ($\mathrm{pH} + \log a_{\overline{M}}/m_{\overline{M}}$) against $\bar{\alpha}$. This shows that the data obtained at different ionic strength lie in fact on the same curve.

The data from Tables II—IV are plotted in Fig. 5 as ($\mathrm{pH} + \log a_{\overline{M}}/m_{\overline{M}}$) against $\log \dfrac{1-\bar{\alpha}}{\bar{\alpha}}$.

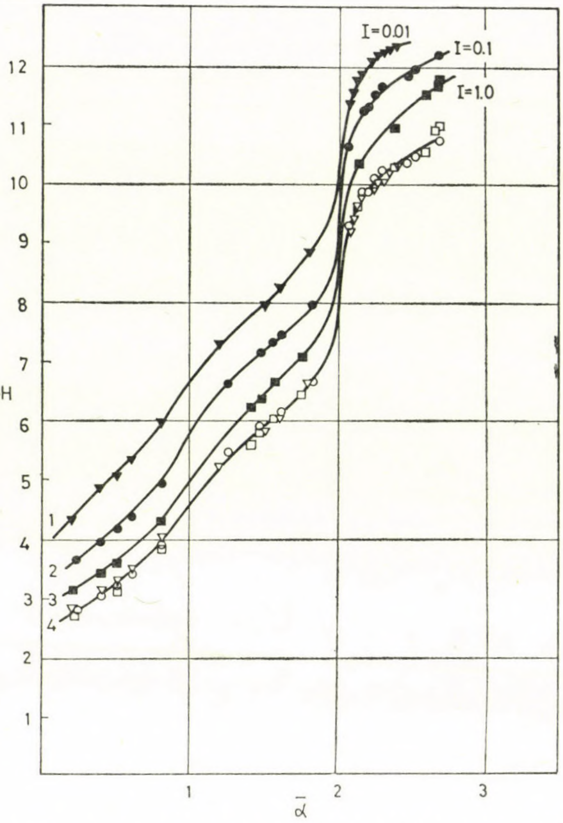

Fig. 4. **The pH of the equilibrium solution as a function of the degree of titration in the resin phase, in solutions of 0.01, 0.1, 1.0 ionic strength.**
Curve 1: $I = 0.01$; Curve 2: $I = 0.1$; Curve 3: $I = 1.0$; Curve 4: ($\mathrm{pH} + \log a_{\mathrm{M}}/m_{\bar{\mathrm{M}}}$) against α

According to equation (16), this plot should give straight lines of unit slope, the intercepts at $\log \frac{1-\bar{\alpha}}{\bar{\alpha}} = 0$ giving the protonation constants.

From the experimental data obtained at the various ionic strengths the following average values for the protonation constants could thus be obtained:

$$\log K_1 = 10.5 \pm 0.1$$
$$\log K_2 = 5.9 \pm 0.1$$
$$\log K_3 = 3.3 \pm 0.1$$

The fact that there is such good agreement between values for the protonation constants obtained from solutions differing in ionic sterength by two orders of magnitude confirms that equation (16) gives an adequate quantitative description of the protonation processes and that the terms describing the molecular interactions in the resin phase do in fact compensate each other over the full dissociation range.

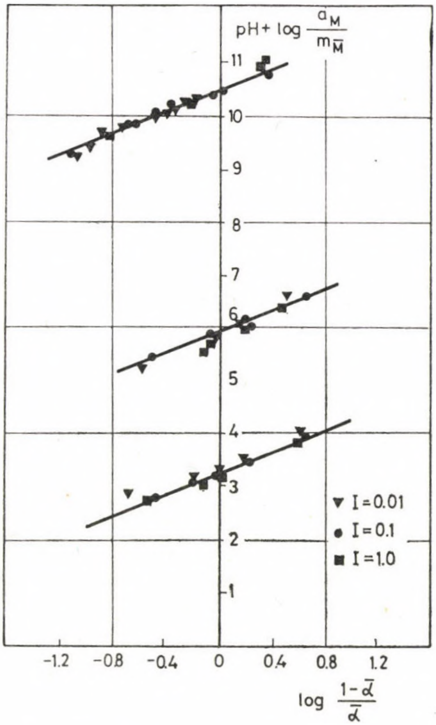

Fig. 5. The plot of the (pH + lg $a_M/m_{\bar{M}}$) values as a function of $\left(\log \frac{1-\bar{\alpha}}{\bar{\alpha}}\right)$ for the determination of the protonation constants

Table V

Calculation and comparison of the electrostatic and the lg Φ_P terms for the first step of neutralisation of the Ligandex-E chelating resin (a)

α	$\frac{0.4343}{kT}\left(\frac{\partial G_e}{\partial \nu}\right)_\varkappa$ (b)	λ (d)	δ (c)	β (d)	$\frac{1}{R^2/a^2-1}$	Φ_P (e)	$-\log \Phi_P$	Δ (f)
0.24	0.12	0.340	0.882	0.50	0.225	0.896	0.05	−0.07
0.40	0.18	0.557	0.825	0.45i	0.238	0.849	0.07	−0.11
0.50	0.20	0.696	0.775	0.71i	0.270	0.879	0.06	−0.11
0.60	0.22	0.835	0.755	0.88i	0.283	0.779	0.11	−0.11
0.80	0.26	1.114	0.629	1.23i	0.394	0.734	0.13	−0.13

(a) The molecular weight of a monomer unit: 400. Data used for the calculation described in [3]: $V = 300$; $b = 0.51$ nm; $s = 10$.
(b) Values calculated by equation (8).
(c) Values calculated by equation (13).
(d) Values calculated by equation (12).
(e) Values calculated by equation (11).
(f) $\Delta = -\frac{0.4343}{kT}\left(\frac{\partial G_e}{\partial \nu}\right)_\varkappa - \log \Phi_P$.

To verify this latter conclusion the KATCHALSKY—LIFSON model was used to calculate the electrostatic interaction and the activity coefficient terms for the first dissociation step in a solution of 0.1 ionic strength.

Table V gives the details of this calculation for the electrostatic interaction term and for the resin phase activity coefficient of the potassium ions.

The last column of the table contains the differences of these terms. Their average value is: -0.11 ± 0.02 in the 0.2—0.8 dissociation range.

The linear polyelectrolyte model cannot be applied to the calculation of the excess free energy term for the second and third ranges of the neutralisation. Due to the wide variety of interactions the elaboration of a new model would be fairly complicated and would probably not have much practical significance because our data in Tables II—IV indicate that the resin phase interaction terms cancel each other in the second and third step of neutralisation as well.

The constancy of the calculated values of the protonation constants for all the three steps of the dissociation indicates that these data are thermodynamically meaningful constants for the active groups of the ethylene-diamine triacetic acid molecule bonded to a styrene-divinyl benzene matrix.

*

The technical assistance of E. VARGA is greatly acknowledged.

REFERENCES

[1] SZABADKA, Ö., INCZÉDY, J.: Acta Chim. Acad. Sci. Hung., **99**, 363 (1979)
[2] CHATTERJEE, A., MARINSKY, A.: J. Phys. Chem., **67**, 41 (1963)
[3] KRASNER, J., MARINSKY, A.: J. Phys. Chem., **67**, 2559 (1963)
[4] KATCHALSKY, A., LIFSON, S.: J. Polymer Sci., **11**, 409 (1953)
[5] LIFSON, S., KATCHALSKY, A.: Polymer Sci., **13**, 43 (1954)
[6] KATCHALSKY, A., SHAVIT, N., EISENBERG, H.: J. Polymer Sci., **13**, 69 (1954)
[7] ALEXANDROWICZ, Z.: J. Polymer Sci., **43**, 325 (1960)
[8] MARINSKY, J.: Ion exchange, Chapter 9. 353 Marcel Decker, New York 1966
[9] ALBERT, A., SERJEANT, E. P.: Ionisation constants John Wiley, London, New York, 1962, Page 24
[10] PEPPER, K. W., REICHENBERG, D., HALE, D. K.: J. Chem. Soc., **1952**, 3129
[11] AMIS, E. S., HINTON, J. F.: Solvent Effects on Chemical Phenomena, Academic Press, New York, London, 1973. Vol. **1**, p. 51

Ödön SZABADKA } H-8201 Veszprém
János INCZÉDY }

Acta Chimica Academiae Scientiarum Hungaricae, Tomus 104 (1), pp. 29—35 (1980)

FIVE-COORDINATE COMPLEXES OF DIVALENT COBALT, NICKEL AND COPPER OF TRIDENTATE PYRIDINE DERIVATIVE

(*SHORT COMMUNICATION*)

S. K. SANGAL and V. B. RANA

(Department of Chemistry, Meerut College, Meerut-250001, *India)*

Received March 16, 1979
Accepted for publication June 18, 1979

In recent years a large number of high-spin five-coordinate complexes of bivalent cobalt, nickel and copper involving pyridine-based tri-, tetra-, and pentadentate ligands have been reported [1—5]. In some cases [6—10], coordination number and stereochemistry of five-coordinate bivalent metal complexes have been based on the metal-ligand (particularly metal-halide) stretching vibrations. However, no examples are known where stereochemistry has been assigned on the basis of 6a (an in-plane pyridine ring deformation) and 16b (an out-of-plane pyridine ring deformation) vibrations [11, 12]. In this paper, we wish to report the synthesis and characterization of high-spin five-coordinate cobalt(II), nickel(II) and copper(II) complexes of 2,6-diacetyldiamino pyridine (DAP) by the help of analyses, magnetic, electronic, conventional and far i.r. spectral studies.

Results and Discussion

The elemental analyses (Table I) indicate 1:1 metal to ligand stoichiometry for all the complexes. The molar conductance measurements reveal that these complexes are non-electrolytes and accordingly the complexes may be represented by a general formula $[M(DAP)X_2]$, where M = Co(II), Ni(II) or Cu(II) and X = Cl, Br, NO_3 or NCS.

The ligand 2,6-diacetyldiamino pyridine is basically a 2,2'-disubstituted pyridine and i.r. studies of such compounds have been reported [13]. The vibrations affected [14] coordination of pyridine-nitrogen to a metal atom are four $\nu(C=C)$, $\nu(C=N)$ bands observed at $\sim$1580, 1530, 1450 and 1420 cm^{-1} the ring-breathing mode $\sim$990 cm^{-1}, an out-of-plane C—H deformation near 800 cm^{-1}, a skeletal mode near 730 cm^{-1}, and an out-of-plane C—C deformation $\sim$400 cm^{-1} in the spectra of the free ligand. The 1580, 1530, 800, and 400 cm^{-1} bands of the free ligand appear at $\sim$1600, 1510, 800—810 and 415 cm^{-1}, respectively, in the spectra of the complexes. The 990 cm^{-1} band splits into two

Table I

Analytical and

Compound	Colour	% Calcd.		
		C	H	N
$C_9H_{11}N_3O_2$	White	55.95	5.69	21.76
$[Co(C_9H_{11}N_3O_2)Cl_2]$	Violet	33.44	3.40	13.00
$[Co(C_9H_{11}N_3O_2)Br_2]$	Light violet	26.22	2.67	10.19
$[Co(C_9H_{11}N_3O_2)(NO_3)_2]$	Pink	28.72	2.92	18.62
$[Co(C_9H_{11}N_3O_2)(NCS)_2]$	Dark Pink	35.87	2.98	19.02
$[Ni(C_9H_{11}N_3O_2)Cl_2]$	Sky blue	33.46	3.40	13.01
$[Ni(C_9H_{11}N_3O_2)Br_2]$	Blue	26.23	2.67	10.20
$[Ni(C_9H_{11}N_3O_2)(NO_3)_2]$	Blue	28.74	2.92	18.62
$[Ni(C_9H_{11}N_3O_2)(NCS)_2]$	Dark blue	35.89	2.99	19.03
$[Cu(C_9H_{11}N_3O_2)Cl_2]$	Apple green	32.97	3.35	12.82
$[Cu(C_9H_{11}N_3O_2)Br_2]$	Light green	25.93	2.64	10.08
$[Cu(C_9H_{11}N_3O_2)(NO_3)_2]$	Green	28.38	2.89	18.39
$[Cu(C_9H_{11}N_3O_2)(NCS)_3]$	Green	35.43	2.95	18.79

components lying between 1020 and 970 cm^{-1}. All these changes indicate [14] the coordination of the pyridine-nitrogen to the metal atom which is confirmed by the appearance of new bands around 265, 270 and 280 cm^{-1} which are assigned to ν(Co-py), ν(Ni-py) and ν(Cu-py) vibrations [11], respectively.

The ligand DAP contains two amide groups and the characteristic bands appear around 1680 cm^{-1} (amide I, due to $\nu C = O$), 1575 cm^{-1} (amide II, $\nu C-N + \delta NH$), 1230 (amide III, due to $\nu C-N + \delta NH$) 650 cm^{-1} (amide IV, $C = O$ out-of-plane deformation), and 450 cm^{-1} (amide VI, $C = O$ in-plane deformation) in the free ligand. The 1680 and 450 cm^{-1} bands appear around 1650 and 475 cm^{-1} in the spectra of the complexes. In the complexes, the 1680 and 450 cm^{-1} bands of the free ligand appear around 1650 and 457 cm^{-1}, respectively. The 1230 cm^{-1} band splits into two components lying between 1220 and 1170 cm^{-1}, while the 650 cm^{-1} band disappears altogether and a new band appears at 560 cm^{-1} in the spectra of the complexes. All these changes are consistent with the amide-oxygen coordination to a metal atom [16]. This coordination is further confirmed by appearance of the new bands in the region (290—315 cm^{-1}) characteristic of metal-oxygen stretching vibrations [17]. Thus, the bands appearing at 290, 298 and 315 cm^{-1} in the spectra of respective metals may be assigned to ν(Co—O), ν(Ni—0) and ν(Cu—O) vibrations, respectively. Another set of new bands appear in the region (415—460 cm^{-1}) and the complexes of cobalt, nickel and copper show these bands, around 425, 440

Magnetic Data

lated		% Found					$\mu_{eff.}$ B. M. (300 °K)
M	X	C	C	N	M	X	
—	—	57.30	5.60	21.90	—	—	—
18.24	21.98	32.65	3.50	12.82	18.98	22.25	4.55
14.30	38.82	26.38	2.70	10.10	14.41	38.70	4.60
15.67	—	28.80	2.95	18.50	15.75	—	4.72
16.01	—	35.75	3.04	18.95	16.10	—	4.60
18.19	22.00	33.58	3.45	12.92	18.22	22.10	3.40
14.26	38.83	26.15	2.65	10.25	14.21	38.75	3.38
15.68	—	28.85	2.90	18.50	15.75	—	3.25
15.96	—	36.00	3.05	18.92	15.88	—	3.32
19.38	21.67	32.85	3.45	12.73	19.50	21.79	1.83
15.25	38.39	26.12	2.75	9.98	15.38	38.30	1.82
16.68	—	28.47	2.80	18.45	16.76	—	1.85
17.04	—	35.60	2.87	18.99	17.15	—	1.82

and 460 cm^{-1}, respectively. These vibrations also appear to have their origin in metal-oxygen stretching modes [18]. Thus the infrared spectra reveal the terdentate nature of the ligand, coordinating through pyridine-nitrogen and amide-oxygen atoms.

Table II records the comparison of the far infrared spectra of each complex and leads to the easy identification of metal-halogen and metal-pseudohalogen stretching vibrations. Such a comparison [19] reveals that metal-chloride vibrations occur at 300, 288, and 230 cm^{-1} for cobalt, nickel and copper complexes, respectively. Similarly, in cobalt, nickel and copper complexes the metal-bromide stretching bands occur at 212, 220 and 210 cm^{-1}, respectively. These values are too low to be assigned to high-spin four-coordinate complexes and too high to be associated with high-spin six-coordinate complexes of these metals [20]. However, these values lie intermediate between those observed for the four, and six-coordinate complexes of the respective metals in the same spin state. A five-coordinate stereochemistry may, therefore, be inferred on the basis of intermediate magnitude of the values of metal-halogen stretching vibrations [20, 21].

The nitrate complexes have strong bands in the range of 1770—1760 cm^{-1} accompanied by another band at 1740—1755 cm^{-1}. These bands indicate that nitrate groups are coordinated to the metal atoms and small splitting (15—20 cm^{-1}) is consistent with the monodentate binding of the nitrate groups

Table II

Reflectance and Far Infrared Spectral Bands

Compound	Reflectance bands mc^{-1}	6a cm^{-1}	16b cm^{-1}	ν(M—Py) cm^{-1}	ν(M—O) cm^{-1}	ν(M—X) cm^{-1}	Unassigned bands cm^{-1}
DAP		600s	400m	—	—	—	650s, 440s and 285m
$[Co(DAP)Cl_2]$	6 800, 12 600, 15 000 and 20 000sh	610s	412s	265m	290m	300m	655m, 450m and 250w
$[Co(DAP)Br_2]$	5 800, 14 000, 15 400 and 19 200sh	608s	410m	260m	300m	212m	660s, 550w and 290w
$[Co(DAP)(NO_3)_2]$	7 200, 13 000, 15 500 and 19 500sh	610s	408m	270m	295m	220w	645s, 450m and 300m
$[Co(DAP)(NCS)_2]$	8 000, 13 500, 15 300 and 19 800	610s	412s	265m	290m	230m	650s, 445s and 315w
$[Ni(DAP)Cl_2]$	7 500, 11 000, 11 600, 16 000 and 23 000sh	615s	415s	255m	300m	288m	640m, 540w, 450m and 275w
$[Ni(DAP)Br_2]$	7 200, 10 900, 12 000, 15 000 and 24 000sh	613s	413s	250m	305m	220m	650s, 440s and 280m
$[Ni(DAP)(NO_3)_2]$	7 000, 11 000, 11 800, 16 000 and 23 500sh	616s	416m	260m	310m	228w	645m, 560m, 450w and 275w
$[Ni(DAP)(NCS)_2]$	7 400, 10 950, 12 000 and 15 000sh	615s	418m	250m	300m	226m	660m, 460m and 280w
$[Cu(DAP)Cl_2]$	10 500, 13 400 and 27 000sh	625s	418s	242m	315m	230m	650s, 450m and 280m
$[Cu(DAP)Br_2]$	9 500, 13 200 and 27 200sh	623s	415s	245m	312w	210m	655m, 460w and 275m
$[Cu(DAP)(NO_3)_2]$	9 200, 13 000 and 27 000sh	625s	415m	240m	315m	230w	655s, 440m and 275m
$[Cu(DAP)(NCS)_2]$	10 000 and 13 800sh	625s	418m	245m	310m	220m	650m, 440s, 285m

[21]. In addition to this, the appearance of bands ~1535, 1395, 995 and 825 cm^{-1} assignable to asymmetric stretching (ν_4), symmetric stretching (ν_3) of NO_2 group, N—O stretching (ν_2) and planar rocking (ν_1), respectively, also indicate the monodentate nature of nitrate. The weak bands appearing at 220, 228, and 230 cm^{-1} may be assigned to ν(Co—O), ν(Ni—O) and ν(Cu—O) of NO_3 group [22]. The thiocyanate complexes show three bands: ~2050, 850, and 460 cm^{-1} assignable [23] to νCN, νCS and δNCS of the N-bonded thiocyanate complexes. The bands observed at 220—230 cm^{-1} are assigned [23] to ν(M—N) (NCS) vibration for the respective metals. In the complexes studied herein, only one band characteristic of ν(M—X) where X = Cl, Br, NO_3 or NCS, is observed indicating that the halides or pseudohalides are arranged in transposition to each other [13, 24].

The stereochemistries of a large number of four- and six-coordinate complexes have been established on the basis of 6a (in-plane pyridine ring deformation) and 16b (out-of-plane pyridine ring deformation) vibrations [11, 12] but no attempt has been made in the case of five-coordinate complexes [25]. In the spectra of the ligand, two bands which appear at 600 and 400 cm^{-1} may be assigned to 6a (in-plane pyridine ring deformation) and 16b (an out-of-plane pyridine ring deformation) vibrations, respectively. In the spectra of cobalt(II), nickel(II) and copper(II) complexes, the 6a vibrations occur around 610, 615 and 625 cm^{-1}. The values of the 'shifts' obtained for the respective metals are intermediate to those obtained for the four- and six-coordinate high-spin complexes of these metals. The changes observed in the case of16b (~400 cm^{-1}) vibrations are inconsistent, and in some cases no shifts are observed at all. This is not surprising, for CLARK *et al.* [11] have reported that the 6a vibration is sensitive to the change of metal atom or stereochemistry. Further, these 'shifts' in the 6a and 16b vibrations depend upon the metallic radii [12] and as the size of the ionic radii decreases, the magnitude of 'shifts' increases. The same pattern has been observed for the present complexes, *i.e.*, the order of 'shifts' is Co:Ni:Cu:10:15:25, which is in the decreasing order of the ionic radii of the metals. Thus, on the basis of ν(M—X), where X = Cl, or Br, and 'shifts' of 6a and 16b vibrations of the pyridine ring, it may be concluded that these complexes have high-spin five-coordinate stereochemistry. These results are further corroborated by electronic spectral and magnetic studies on the complexes.

Magnetic and spectral studies

The magnetic moments at room temperature (300 °K) are in the ranges of 4.55—4.72, 3.25—3.40 and 1.82—1.85 BM for cobalt(II), nickel (II) and copper (II) complexes, respectively. The values observed are well within the ranges postulated for high-spin five-coordinate complexes of the respective metal [25].

The diffuse reflectance spectra of complexes of cobalt, nickel and copper show bands in the following regions: cobalt: 5800—8000, 12 600—14 000, 15 000—15 500, and 19 200—20 000 cm^{-1}; nickel: 7 000—7 500, 10 900—11000, 11 600—12 000, 15 000—16 000 cm^{-1} and 23 000—24 000 cm^{-1}; copper: 9 200—10 500, 13 000—13 800, and $\sim$27 000 cm^{-1}. These spectra cannot be interpreted in terms of a regular or distorted square planar, tetrahedral or octahedral configuration. Instead the spectra resemble to those of five-coordinate complexes whose structures have been determined by X-ray methods [26, 27].

The molecular models of the complexes show that trigonal bipyramidal structure is the most probable structure to result when donor atoms of DAP form an equatorial base and halides or pseudohalides were present on the *trans-axial* positions vide far i.r. Thus assuming D_{3h} symmetry of these complexes, the various bands can be assigned: cobalt [28] 5 800—8 000, 12 600—14 000, 15 000—15 500, and 19 200—20 000 cm^{-1} to $^4A_2' \rightarrow {}^4E''$, $^4A_2' \rightarrow {}^4E'$, $^4A_2' \rightarrow {}^4A_2'(P)$ and $^4A_2' \rightarrow {}^4E''(P)$; nickel [29] 7 000—7 500, 10 900—11 000, 15 000—16 000 and 23 000—24 000 cm^{-1} to $^3E' \rightarrow {}^3E'$, $^3E' \rightarrow {}^3A_1''$, $^3A_2''$, $^3E' \rightarrow {}^3A_2'$ and $^3E' \rightarrow {}^3E'(P) + {}^3A_2'(P)$, respectively. Similarly the bands of copper complexes *viz.*, 9 200—10 500 and 13 000—13 800 cm^{-1} may be assigned [30] to $^2A_1' \rightarrow {}^2E'$ and $^2A_1' \rightarrow {}^2E''$, respectively.

Experimental

The ligand (m.p. 203°) was synthesized by the acetylation of 2,6-diaminopyridine. The stoichiometric amounts of the appropriate metal salt dissolved in acetone or absolute ethanol and ligand in acetone were refluxed on a water bath. The mixture was kept overnight at room temperature ($\sim$ 25°) when crystals of the complex were obtained. The complexes were thoroughly washed with absolute ethanol, acetone and finally dried at 85°. Yield $\sim$ 70%.

Metal contents of the complexes were determined by EDTA titrations and halides by Volhard's method. The infrared spectra were recorded as KBr pellets on a Perkin—Elmer-621 (4000 — 650 cm^{-1}) and in nujol-mull on a Beckman IR-12 (650 — 200 cm^{-1}) spectrophotometers. The diffuse reflectance spectra were taken on a Beckman DK-2A spectrophotometer, and Gouy's method was used for magnetic measurements. The calibrating compound was copper sulphate pentahydrate.

*

The authors are thankful to U.G.C., New Delhi, for financial assistance and R.S.I.C., I.I.T. Madras, for spectral measurements.

REFERENCES

[1] Wood. J. S.: Prog. Inorg. Chem., **16**, 227 (1972)
[2] Morassi, R., Bertini, I., Sacconi, L.: Coord. Chem. Rev., **11**, 351, (1973)
[3] Sahni, S. K., Gupta, S. P., Sangal, S. K., Rana, V. B.: J. Inorg. Nucl. Chem., **39**, 1098 (1977)
[4] Furlani, C.: Coord. Chem. Rev., **3**, 141 (1968)
[5] Sacconi L.: Transition Metal Chem., **4**, 199 (1968)
[6] Keeton, M., Lever, A. B. P.: Inorg. Chem., **10**, 47 (1971)
[7] Keeton, M., Lever, A. B. P., Ramaswamy, B. S.: Can. J. Chem., **48**, 3185 (1970)
[8] Goedken, V. L., Quagliano, J. V., Vallarino, L. M.: Inorg. Chem., **8**, 2331 (1969)

[9] Beecroft, B., Campbell, M. J. M., Grazeskowiak, R.: J. Inorg. Nucl. Chem., Lett., **8,** 1097 (1972)
[10] Sahni, S. K., Gupta, S. P., Sangal, S. K., Rana, V. B.: J. Indian Chem. Soc., **54,** 200 (1977)
[11] Clark, R. J. H., Williams, C. S.: Inorg. Chem., **4,** 350 (1965)
[12] Gill, N. S., Nuttall, R. H., Scaife, D. E., Sharp, D. W. A.: J. Inorg. Nucl. Chem., **18,** 79 (1961)
[13] Dahlhaff, W. V., Nelson, S. M.: J. Chem. Soc. (A), **1971,** 2184
[14] Baldwin, D. A., Lever, A. B. P., Parish, R. V.: Inorg. Chem., **8,** 107 (1969)
[15] Nonoyama, N., Tomita, S., Yamasaki, K.: Inorg. Chim. Acta, **12,** 33 (1975)
[16] Jain, S. C., Gill, M. S., Rao, G. S.: J. Indian Chem. Soc., **53,** 537 (1976)
[17] Reedijk, J.: Inorg. Chim. Acta, **5,** 687 (1971)
[18] Mikami, M., Nakagawa, I., Shimanouchi, T.: Spectrochim. Acta, **23 A,** 1037 (1967); **25 A,** 365 (1969)
[19] Lever, A. B. P., Montovani, E.: Inorg. Chem., **10,** 817 (1971)
[20] Bryson, D. J., Nuttall, R. H.: Inorg. Nucl. Chem. Lett., **5,** 347 (1969)
[21] Postmus, C., Ferraro, J. R., Wozniak, W.: Inorg. Chem., **6,** 2030 (1967)
[22] Lever, A. B. P., Mantovani, E., Ramaswamy, B. S.: Can. J. Chem., **49,** 1957 (1971)
[23] Burmeister, J. L.: Coord. Chem. Rev., **1,** 205 (1966); **3,** 225 (1968)
[24] Adams, D. M.: 'Metal Ligand and Related Vibrations', (E. Arnold, London) (1967)
[25] Barefield, E. K., Busch, D. H., Nelson, S. M.: Quart. Rev., **22,** 457 (1968)
[26] Hall, D., Woulfe, M. D.: Proc. Chem. Soc., **1958,** 346
[27] Ciampolini, M., Nardi, N.: Inorg. Chem., **5,** 41 (1966)
[28] Ciampolini, M., Nardi, N.: Inorg. Chem., **5,** 1150 (1966)
[29] Ciampolini, M.: Inorg. Chem., **5,** 35 (1966)
[30] Hathaway, B. J., Billing, D. E.: Coord. Chem. Rev., **5,** 143 (1970)

S. K. Sangal
V. B. Rana
'Prakashika', 184 Abu Lane, Meerut - 250001, India

Acta Chimica Academiae Scientiarum Hungaricae, Tomus 104 (1), pp. 37–41 (1980)

KINETICS OF THE HYDROLYSIS OF IODINE IN WATER-ETHANOL MEDIA

K. Južnič

(Chemistry Department, "Jožef Stefan" Institute, Ljubljana, Yugoslavia)

Received March 22, 1979

Accepted for publication June 18, 1979

The kinetics of hydrolysis of iodine has been studied in borate buffer solutions and in mixtures of them with ethanol. The rate of reaction was followed potentiometrically by measuring of the voltage of a cell glass electrode //H^+, I_2, I^-, IO_3// Pt-electrode. On the basis of the obtained data a mechanism has been proposed according to which iodine exists in a solution in form of I_x associates, and the slowest step of hydrolysis is the reaction of iodine molecules with water.

Introduction

In the past several studies on the kinetics of hydrolysis of iodine have been performed [1]. Since the experimental conditions were not always the same, the obtained results did not lead to identical conclusions about the rate determinig step and the mechanism. Therefore it seemed worthwhile to elucidate this problem by carrying out some additional experimental work.

In neutral or slightly alkaline media iodine hydrolyses according to $I_2 + H_2O \rightleftharpoons HIO + HI$. The kinetics of this reaction was studied by Eigen and Kustin [2]. They found that the reaction proceeds rather fast and that the overall reaction constant is $3s^{-1}$. Zalkind and Yavorskii [3], who studied the hydrolysis of iodine, in the presence of bromide and iodide, to iodate and iodide claimed that the slowest step of the $3I_2 + 2H_2O = 5I^- + IO_3^- + 6H^+$ reaction is the hydrolysis of iodine to hypoiodus acid, and that the subsequent reactions leading to iodate and iodide are fast. Skrabal suggested a mechanism for the second reaction [4]. In literature also some kinetic studies of the reaction of hypoiodide to iodate can be found which were done by using the stopped flow method.

Experimental

Materials: — Iodine, *p.a.* grade, and the other chemicals of the same purity (produced by Riedel de Haen) were used without further purification. The buffer solutions were prepared by mixing 0.1 N NaOH and 0.1 M H_3BO_3 and by diluting the mixtures to 100 ml [5].

Procedure: — The solutions of iodine were made by adding 1 ml of concentrated solution of iodine in ethanol to the buffer solutions. The concentration changes of iodine were followed potentiometrically by measuring the voltage of a cell glass electrode //H^+, I_2, IO_3^-, I^-//Pt-electrode by a PHM-52 digital pH-meter. The solution was thermostated to the corresponding temperature within ±0.1 °C.

Results and Discussion

The rate of reaction was obtained by comparing the experimental curve of voltage *vs.* time with the calculated curve of voltage *vs.* concentrations for a cell where the reaction:
$3I_2 + 6OH^- = 5I^- + IO_3^- + 3H_2O$ takes place. Since pH was kept constant, voltage was calculated from the following expression:

$$E = E^0 + \frac{RT}{6F} \ln \frac{[IO_3^-][I^-]^5}{[I_2]^3}$$

The initial iodine concentration was 1.06×10^{-3} mol·dm^{-3}. The obtained results are shown in Table I. The rates were evaluated for a moment when half of reaction was accomplished. The rate of reaction is influenced by temperature, pH and concentrations of added iodide and ethanol. The initial iodine concentration and the added iodate have a relatively small effect on the rate of hydroly-

Table I

Rate of hydrolysis of iodine under different conditions

T (°C)	Initial concs. × 10^3 (mol · dm^{-3})			pH	$-d[I_2]/dt \times 10^6 \left(\frac{mol}{dm^3 \cdot min}\right)$
	I_2	I^-	ethanol		
20	1.06	0	0	8.27	3.27
20	1.06	0	0	9.00	6.63
20	1.06	0	0	9.40	7.95
20	1.06	10	0	9.40	5.65
20	1.06	5	0	9.44	7.45
20	1.06	1	0	9.45	7.85
20	3.73	0	0	8.95	6.00
20	2.16	0	0	8.91	5.5
25	1.06	0	0	9.15	8.13
30	1.06	0	0	9.23	17.1
35	1.06	0	0	9.15	25.2
40	1.06	0	0	9.26	60
20	1.06	0	1.3	9.4	22.9
20	1.06	0	2.6	9.6	47.6
30	1.06	0	1.3	9.4	65.5
30	1.06	0	2.6	9.6	135
40	1.06	0	1.3	9.4	199
40	1.06	0	2.6	9.6	399

sis. The temperature dependence of the reaction rate in aqueous media can be expressed by

$$-\frac{\mathrm{d}[\mathrm{I_2}]}{\mathrm{d}t} = 4.23 \times 10^{11} \exp\left(-\frac{22.7\ \mathrm{kcal}}{RT}\right) \mathrm{mol \cdot dm^{-3} \cdot min^{-1}}.$$

The value of activation energy (22.7 kcal/mol) is in a good agreement with that of obtained by ZALKIND [3]. The activation energy of the hydrolysis in a mixture with 2.6 mole · dm^{-3} ethanol is 22.4 kcal/mole, and the preexponential factor is 2 × 10^{12}.

The mechanism of the reaction assumed, includes the following steps:

$$\mathrm{I_{10}} = 5\mathrm{I_2}\,(1)\; K_1 = \frac{[\mathrm{I_2}]^5}{[\mathrm{I_{10}}]} \quad [\mathrm{I_2}] = \sqrt[5]{K_1\,[\mathrm{I_{10}}]}$$

$$\mathrm{I_2 + H_2O} \overset{k_1}{=\!=} \mathrm{I_2OH^- + H^+}(2)$$

$$-\frac{\mathrm{d}[\mathrm{I_2}]}{\mathrm{d}t} = \vec{k}_1\,[\mathrm{I_2}] - \overleftarrow{k}_1[\mathrm{I_2OH^-}][\mathrm{H^+}]$$

$$\mathrm{I_2OH^- + OH^-} \overset{k_2}{=\!=} \mathrm{IO^- + I^- + H_2O}\,(3)$$

$$3\mathrm{IO^-} \overset{k_3}{=\!=} \mathrm{IO_3^-} + 2\mathrm{I}\,(4)\; K_2 = \frac{[\mathrm{IO_2^-}][\mathrm{I^-}]^2}{[\mathrm{IO^-}]^3}\,.$$

Applying the steady state approximation to step (3) we get

$$\frac{\mathrm{d}\,[\mathrm{IO^-}]}{\mathrm{d}t} = \vec{k}_2[\mathrm{I_2OH^-}][\mathrm{OH^-}] - \overleftarrow{k}_2[\mathrm{IO^-}][\mathrm{I^-}] - \vec{k}_3[\mathrm{IO^-}]^3 + \overleftarrow{k}_3[\mathrm{IO_3^-}][\mathrm{I^-}]^2 = 0\,.$$

If we assume that step (2) is the rate determining and by substituting the concentrations of intermediates in eq.2 with the concentrations of reactants and products, respectively, we obtain

$$\frac{-\mathrm{d}\,[\mathrm{I_2}]}{\mathrm{d}t} = \vec{k}_1\,K_1^{0.2}[\mathrm{I_{10}}]^{0.2} -$$

$$-\frac{\overleftarrow{k}_1\,K_w}{\vec{k}_2[\mathrm{OH^-}]^2}\left(\frac{\overleftarrow{k}_2[\mathrm{I^-}]^3\sqrt{[\mathrm{IO_3^-}][\mathrm{I^-}]^2}}{\sqrt{K_2}} + \right.$$

$$\left. + \frac{\vec{k}_3[\mathrm{IO_3^-}][\mathrm{I^-}]}{K_2} - \overleftarrow{k}_3[\mathrm{IO_3^-}][\mathrm{I^-}]^2\right).$$

This equation in a simplified form is

$$-\frac{d[I_2]}{dt} = k[I_2]^{0.2} - \frac{1}{[OH^-]^2}(a[I^-]^{1.66} + b[I^-]^2 + c[I^-])$$

where the constants are $k = 3.21 \times 10^{-5}$,

$a = -7.0 \times 10^{-12}$, $b = 26.7 \times 10^{-12}$ and $c = \pm 1.78 \times 10^{-13}$ $(\text{mol} \cdot \text{dm}^{-2} \cdot \cdot \text{min}^{-1})^z$.

The derived equation includes the variables, the concentrations of iodine, hydroxyl ion, and iodide which influence the rate of hydrolysis.

The low order of iodine in the reaction rate equation can be explained by the association of iodine molecules in the solutions. This is in an agreement with some early assumptions about the nature of the dissolved iodine species in different solvents based on a colour of the solutions. In some cases authors also experimentally confirmed that the dissolved iodine exists in form of $(I_2)_x$ aggregates.

Increasing of OH^- concentration in general increases the reaction rate. In acidic media the reverse reaction takes place. ZALKIND [3] who studied the hydrolysis in the pH range of 6—8 found another expression connecting the rate and OH^- concentration than above, which indicates that the reaction mechanism may change with the pH.

The presence of halide ions decreases the rate of hydrolysis. The inhibitory effect becomes more pronounced in the order Cl^-, Br^- and I^- [3]. The effect is ascribed to the formation of a complex of type XI_2^- the lowest stability constant has been measured for I_3^-.

As seen from Table I the presence of ethanol appreciably enhances the rate of reaction. This is not due to change of dielectric constant, since if the reaction products are ionic the reaction is usually faster in a medium with higher dielectric constant. Also the effect of solubility is different as expected. The solubilities of iodine in water and ethanol at 20 °C are 0.29 and 21.1 g/l, respectively [6]. If the reaction rate is proportional to the inverse value of solubility one would expect that reaction will be slower in mixtures, than in pure water. The activation energy is nearly the same for the hydrolysis in water and in water—ethanol mixtures. This indicates that the mechanism should be the same in both media. The preexponential factor is higher in mixtures, which means that the concentration of species directly involved in the reaction should be higher. It follows that the addition of ethanol to the aqueous solution of iodine changes the extent of association of iodine and its solvation.

REFERENCES

[1] BAMFORD, C. H., TIPPER, C. F. H.: Chemical Kinetics, Vol. **6**, p. 334, Elsevier Publ. Co., N. Y. 1972
[2] EIGEN, M., KUSTIN, K.: J. Am. Chem. Soc., **84**, 1355 (1962)
[3] ZALKIND, G. R., YAVORSKII, S. J.: Izv. Acad. Nauk Turkm. SSR, Ser. Fiz. Tekhn. Khim. Geol. Nauk, **2**, 56 (1962)
[4] SKRABAL, A.: Monatsh. Chem., **32**, 815 (1911)
[5] LANGE, N. A.: Handbook of Chemistry, p. 951, Handbook Pub. Inc., Ohio, 1956
[6] Gmelins Handbuch der Anorganischen Chemie, No. 8, Jod, p. 125, 1939

Karel JUŽNIČ "Jožef Stefan" Institute,
Jamova 39, 61001 Ljubljana,
Yugoslavia

Acta Chimica Academiae Scientiarum Hungaricae, Tomus 104 (1), pp. 43—47 (1980)

ULTRASONIC BEHAVIOUR OF BINARY LIQUID MIXTURES OF BUTYLAMINE WITH AROMATIC HYDROCARBONS

A. KRISHNAIAH and P. R. NAIDU

(Chemical Laboratories, S. V. University, Tirupati 517 502, *India)*

Received April 13, 1979
Accepted for publication June 18, 1979

Sound velocities and densities of mixtures of butylamine with benzene, toluene, *o*-xylene, *m*-xylene and *p*-xylene were determined at 303.15 K as a function of composition. The quantities, isentropic compressibility, available volume and intermolecular free length were computed from the experimental data. The values of isentropic compressibility, excess available volume and excess free length show that the mixtures exhibit small positive deviations from ideal behaviour. The deviations have been ascribed to break-up of hydrogen bonds in self-associated butylamine.

Introduction

A survey of the literature has shown that attempts [1—6] have been made to study ultrasonic behaviour of a large number of binary liquid mixtures. The deviations from ideal behaviour were attributed to the difference in size of the molecules and strength of interaction between them. Some attempts [2, 4, 5] have also been made to calculate the excess free lengths defined by JACOBSON [7]. However, no attempt has been made to study the ultrasonic behaviour of liquid mixtures containing an alkylamine and homologous series of aromatic hydrocarbons. Hence, ultrasonic velocities and densities were measured over the entire range of composition at 303.15 K for the five systems: butylamine + benzene, + toluene, + *o*-xylene, + *m*-xylene, and + *p*-xylene. The common component butylamine exhibits self-association [8] through hydrogen bonding in the pure state. This is likely to influence the ultrasonic behaviour of the mixtures. The quantities, isentropic compressibility, available volume and intermolecular free lengths were computed from the experimental data.

Experimental

Materials

Butylamine was dried over potassium hydroxide for 3 days then refluxed for 2 h and fractionally distilled [9]. The aromatic hydrocarbons were made thiophene-free [10], dried over anhydrous calcium chloride and finally fractionated over metallic sodium. The column used contained 12 theoretical plates. The purity of the samples was checked by comparing the measured densities with those reported in literature [9, 11]. The data are given in Table I.

Table I

Densities of pure component liquids

Component	T/K	Density Present work	ϱ/g cm^{-3} Literature
Benzene	303.15	0.86835	0.86836
Toluene	303.15	0.85762	0.85766
o-Xylene	303.15	0.87157	0.87161
m-Xylene	303.15	0.85566	0.85565
p-Xylene	303.15	0.85224	0.85232
Butylamine	298.15	0.73452	0.73460

Methods

Ultrasonic velocities were measured using a single crystal ultrasonic interferometer at a frequency of 2 MHz and were accurate to $\pm 0.15\%$ [12]. Densities were determined with a bicapillary pycnometer described by NAIDU and KRISHNAN [13]. The values of densities were accurate to $\pm 5\times 10^{-5}$ g cm^{-3}.

Results and Discussion

The isentropic compressibility $(\varkappa_s)$ was calculated using the relation

$$\varkappa_s = \mu^{-2}\,\varrho^{-1} \tag{1}$$

where u and ϱ denote sound velocity and density. The values of $\varkappa_s$ were accurate to $\pm$ 2TPa^{-1} (tera pascals). The quantity K_s was computed using the relation

$$K_s = \varkappa_s - \Phi,\varkappa_{s,1} - \Phi_2\varkappa_{s,2} \tag{2}$$

where $\varkappa_s$, $\varkappa_{s,1}$ and $\varkappa_{s,2}$ stand for isentropic compressibilities of mixture and the pure components. Φ_1 and Φ_2 are volume fractions of butylamine and hydrocarbons, respectively. K_s represents deviation from ideal behaviour.

The available volume, intermolecular free length, excess available volume and excess length were calculated from mole volume (V), sound velocity at any concentration (u), infinite velocity in the molecules $(u_\infty = 1600$ ms$^{-1})$, surface area per mole (Y), mole fractions (x_1, x_2) and surface fractions (S_1, S_2) using the relations [2]

$$V_a = V\left(1 - \frac{u}{u_\infty}\right) \tag{3}$$

$$L_f = \frac{2\,V_a}{Y} \tag{4}$$

$$V_a^E = V_a - x_1\,V_{a,1} - x_2,\,V_{a,,2} \tag{5}$$

$$L_f^E = L_f - S_1 L_{f,1} - S_2 L_{f,2}\ . \tag{6}$$

Table II

Volume fraction Φ_1 of butylamine, density ϱ, sound velocity u, isentropic compressibility $\varkappa_s$, available volume V_a, and free length L_f for butylamine + aromatic hydrocarbons at 303.15 K
ϱ in g cm^{-3}; u in ms^{-1}; $\varkappa_s$ and K_s in TPA^{-1}, V_a in cm^3 mol^{-1} and L_f in Å

Φ	ϱ	u	$\varkappa_s$	K_s	V_a	V_a^E	L_f	L_f^E
Butylamine + benzene								
0.0000	0.86835	1274	710	0	18.33	0.00	0.5221	0.0000
0.1108	0.85226	1266	732	2	18.99	0.24	0.5370	0.0068
0.2067	0.83849	1260	751	4	19.52	0.40	0.5485	0.0112
0.3232	0.82231	1253	775	7	20.17	0.58	0.5621	0.0162
0.4372	0.80402	1250	796	8	20.66	0.42	0.5694	0.0115
0.5506	0.78871	1247	815	6	21.12	0.39	0.5775	0.0107
0.6609	0.77464	1246	832	4	21.32	0.33	0.5803	0.0090
0.7629	0.76109	1244	849	3	21.68	0.25	0.5858	0.0066
0.8898	0.74396	1242	871	2	22.10	0.11	0.5917	0.0029
1.0000	0.73149	1240	889	0	22.50	0.00	0.5974	0.0000
Butylamine + toluene								
0.0000	0.85762	1282	710	0	21.35	0.00	0.5342	0.0000
0.1121	0.84348	1274	731	1	21.71	0.23	0.5468	0.0055
0.2173	0.82827	1267	752	3	22.00	0.39	0.5579	0.0098
0.3129	0.81581	1262	772	6	22.18	0.45	0.5656	0.0114
0.4270	0.80780	1256	785	8	22.30	0.54	0.5749	0.0138
0.5302	0.79098	1250	809	4	22.69	0.63	0.5841	0.0162
0.6780	0.77296	1246	833	2	22.63	0.48	0.5898	0.0125
0.7760	0.76091	1243	851	2	22.66	0.40	0.5940	0.0106
0.8891	0.74651	1241	870	1	22.61	0.23	0.5966	0.0061
1.0000	0.73149	1240	889	0	22.50	0.00	0.5974	0.0000
Butylamine + *o*-xylene								
0.0000	0.87157	1330	649	0	20.56	0.00	0.4671	0.0000
0.1169	0.85482	1313	679	2	21.31	0.48	0.4924	0.0091
0.2100	0.84148	1302	701	4	21.68	0.65	0.5108	0.0154
0.3309	0.82482	1284	735	7	22.43	1.15	0.5391	0.0275
0.4522	0.80723	1272	767	9	22.72	1.17	0.5567	0.0292
0.5506	0.79437	1264	788	7	22.83	1.11	0.5680	0.0276
0.6564	0.77945	1258	811	4	22.77	0.85	0.5756	0.0215
0.7677	0.76453	1251	836	3	22.75	0.64	0.5847	0.0165
0.8832	0.75871	1244	863	2	22.72	0.41	0.5936	0.0108
1.0000	0.73149	1240	889	0	22.50	0.00	0.5974	0.0000

Table II (continued)

Φ	ϱ	u	$\varkappa_s$	K_s	V_a	V_a^E	L_f	L_f^E
Butylamine + *m*-xylene								
0.0000	0.85566	1302	689	0	23.11	0.00	0.5208	0.0000
0.0900	0.84368	1292	710	3	23.37	0.33	0.5356	0.0075
0.2162	0.82824	1280	737	5	23.58	0.63	0.5529	0.0148
0.3171	0.81556	1270	760	8	23.77	0.89	0.5671	0.0211
0.4237	0.80251	1260	785	11	23.92	1.10	0.5811	0.0268
0.5495	0.78691	1256	806	7	23.56	0.82	0.5842	0.0203
0.6676	0.77280	1252	826	3	23.27	0.59	0.5875	0.0149
0.7780	0.75932	1247	847	2	23.05	0.44	0.5924	0.0113
0.8880	0.74596	1243	868	1	22.80	0.27	0.5958	0.0066
1.0000	0.73149	1240	889	0	22.50	0.00	0.5974	0.0000
Butylamine + *p*-xylene								
0.0000	0.85224	1292	703	0	23.98	0.00	0.5391	0.0000
0.1085	0.83954	1280	727	4	24.27	0.48	0.5568	0.0110
0.2217	0.82566	1270	751	6	24.36	0.77	0.5707	0.0181
0.3262	0.81019	1262	775	11	24.36	0.94	0.5812	1.0223
0.4444	0.79664	1252	801	15	24.46	1.23	0.5957	0.0298
0.5526	0.78554	1250	815	9	23.99	0.91	0.5946	0.0224
0.6664	0.77263	1248	827	4	23.56	0.64	0.5945	0.0161
0.7717	0.76013	1244	850	3	23.29	0.51	0.5978	0.0132
0.8869	0.74617	1242	869	1	22.88	0.25	0.5976	0.0660
1.0000	0.73149	1240	889	0	22.50	0.00	0.5974	0.0000

The values of density (ϱ), sound velocity (u), isentropic compressibility $(\varkappa_s)$, the quantity (K_s), available volume (V_a) excess available volume (V_a^E), intermolecular free length (L_f) and excess intermolecular free length (L_f^E) are given in Table II for the five binary mixtures.

The data in Table II show that the mixtures exhibit small positive deviations in isentropic compressibility, available volume and free length over the whole range of composition in all the five mixtures. However, the positive deviations observed in butylamine—*p*-xylene system are greater than those of the other four systems. The deviations may be ascribed to self-association of butylamine through hydrogen bonding. The self-association of butylamine produces non-cyclic trimers as reported by SCHUG and CHANG [8]. These trimers would be reduced to dimers and monomers on the addition of hydrocarbons. Consequently the intermolecular free lengths and available volumes would increase. Also the sound waves would cover smaller distances in solutions contributing to increase in isentropic compressibilities. Hence, the experimental results are in order.

REFERENCES

[1] Prasad, R.: Indian J. Phys., **16**, 307 (1942)
[2] Kaulgud, M. V.: Acustica, **10**, 316 (1960)
[3] Sackmann, H., Bockzek, A.: Z. Physik. Chem., **29**, 329 (1961)
[4] Kaulgud, M. V.: Z. Physik. Chem., **36**, 365 (1963)
[5] Reddy, K. C., Subrahmanyam, S. V., Bhimasenachar, J.: J. Phys. Soc. Japan, **19**, 559 (1964)
[6] Fort, R. J., Moore, W. R.: Trans. Farady Soc., **61**, 2102 (1965)
[7] Jacobson, B.: Acta Chem. Scand., **6**, 1485 (1952)
[8] Schug, J. C., Chang, W. E.: J. Phys. Chem., **75**, 938 (1971)
[9] Reddick, A. J., Bunger, B. W.: Organic Solvents, Wiley, New York 1950
[10] Vogel, A.: Practical Organic Chemistry, Longman, London 1965
[11] Timmermans, J.: Physico-Chemical Constants of Pure Organic Compounds, Elsevier, New York 1950
[12] Rao, M. V. P., Nainu, P. R.: J. Chem. Thermodyn., **8**, 96 (1976)
[13] Naidu, P. R., Krishnan, V. R.: Trans. Faraday Soc., **61**, 1347 (1965)

A. Krishnaiah } Chemical Lab., S. V. University,
P. R. Naidu } Tirupati 517 502, India

Acta Chimica Academiae Scientiarum Hungaricae, Tomus 104 (1), pp. 49–61 (1980)

A SIMPLE AND ACCURATE METHOD FOR THE DETERMINATION OF SOLVENT ACTIVITY IN SWOLLEN GELS

M. NAGY[1] and F. HORKAY[2]

([1]Department of Colloid Science, Loránd Eötvös University, Budapest, [2]National Institute of Occupational Health, Budapest)

Received February 26, 1979

Accepted for publication June 19, 1979

The first part of the paper discusses the fundamental thermodynamical relationships relevant to swelling phenomena, and surveys possible measuring techniques based on these relationships.

According to the experiments, the equilibrium deswelling method developed by the authors makes possible the determination of solvent activity in such wide polymer concentration range, in which earlier this could be achieved only by the measurement of swelling pressure.

A few experimental examples are given for the course in time of the process, the accuracy and reproducibility of the method, and the suitability of the dependence of the overall chemical potential on concentration for studying the structure of networks.

Introduction

The statistical thermodynamical theory of the swelling of cross-linked polymers may furnish fundamental quantitative information on the most important structural parameters of the network (*e.g.* on the density of junction points or on the number of elastically effective network chains), as well as on solvent — polymer interaction, if the mechanical properties of the network, and the dependence of the chemical potential of the solvent on the volume of the swollen gel (or on the concentration of the polymer contained in this volume) are known.

The object of the present work was on the one hand to give a survey on the thermodynamical relationships serving as basis for the measurements, and to review possible measuring techniques closely connected to these relationships, and on the other hand, to report on the new, simple and fruitful experimental method developed by us.

The thermodynamics of semi-open systems

Let us consider a closed system shown in Fig. 1, consisting of the subsystems marked 1 and 2, comprising the pure liquid phase (solvent) of volume $V^{(1)}$ and the two-component mixture (swollen polymer gel) of volume $V^{(2)}$.

The condition of thermodynamical equilibrium between subsystems 1 and 2 is the homogeneous distribution of intensity parameters characteristic of interactions in the whole system. Since subsystem 2 is bicomponent, where one of the components is the same as the pure liquid phase, hence $\mu_1^{(1)} > \mu_1^{(2)}$, where $\mu_1^{(1)}$ and $\mu_1^{(2)}$ is the chemical potential of component 1 (solvent) in subsystem 1 and 2, respectively.

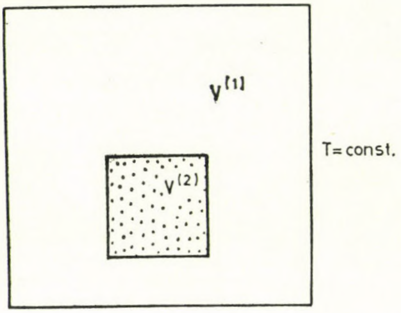

Fig. 1. See text

For such non-equilibrium systems one of the obvious possibilities to attain equilibrium is the equalization of the chemical potentials (and concentrations) by diffusion.

Escaping of component 2 from subsystem 2 can be prevented in two ways: one of these is to surround this subsystem with a membrane permeable only to component 1, the other to produce from component 2 an insoluble, deformable particle network of macroscopic dimension (semi-open subsystem). In both cases thermodynamical equilibrium will be established only if the chemical potential of the solvent, the temperature and the pressure are the same in subsystems 1 and 2. As will be shown below, this means at the same time that the expression of the chemical potential relevant to subsystem 2 must consist at least of two terms.

Let be $V^{(1)} + V^{(2)} =$ constant, and $n_1^{(1)} + n_1^{(2)} = n_1 =$ constant. According to the aforegoing, $n_2^{(1)} = 0$ and $n_2^{(2)} =$ constant (n_1 and n_2 is the number of moles of component 1 and 2, respectively).

Hence

$$\mathrm{d}V^{(1)} = -\,\mathrm{d}V^{(2)} \tag{1}$$

$$\mathrm{d}n_1^{(1)} = -\,\mathrm{d}n_1^{(2)} \tag{2}$$

and

$$\mathrm{d}n_2^{(1)} = \mathrm{d}n_2^{(2)} = 0 \tag{3}$$

The change in Helmholtz energy in the whole system is

$$\mathrm{d}A = \mathrm{d}A^{(1)} + \mathrm{d}A^{(2)} \tag{4}$$

Using at constant temperature the relationship

$$\mathrm{d}A = -p\mathrm{d}V + \sum_i \mu_i \,\mathrm{d}n_i, \tag{5}$$

the equation

$$\mathrm{d}A = p^{(1)}\,\mathrm{d}V^{(2)} - p^{(2)}\,\mathrm{d}V^{(2)} - \mu^{(1)}\,\mathrm{d}n_1^{(2)} + \mu_1^{(2)}\,\mathrm{d}n_1^{(2)} \tag{6}$$

is obtained for the total system under consideration of (1), (2), and (3).

If the system is only in thermal interaction with the environment, then, expressing for equilibrium state ($\mathrm{d}A = 0$) from Eq. (6) the chemical potential of the solvent of subsystem (2), and writing $\mathrm{d}n_1$ instead of $\mathrm{d}n_1^{(2)}$

$$\mu_1^{(2)} = \mu_1^{(1)} + (p^{(2)} - p^{(1)}) \left(\frac{\partial V^{(2)}}{\partial n_1}\right)_{T,n_2} \tag{7}$$

If the chemical potential of the pure solvent is chosen as standard state ($\mu_1^{(1)} = \mu_1^0$), the relationship

$$\mu_1^{(2)} = \mu_1^0 + \Delta p \left(\frac{\partial V^{(2)}}{\partial n_1}\right)_{T,n_2} \tag{8}$$

is obtained.

Finally, writing instead of $\left(\frac{\partial V^{(2)}}{\partial n_1}\right)_{T,n_2}$ the partial molar volume $\overline{V}_1$ of the solvent in subsystem 2,

$$\mu_1^{(2)} = \mu_1^0 + \Delta p\,\overline{V}_1. \tag{9}$$

Naturally, Δp is a function of the volume of subsystem 2, therefore, (9) will suitably be given in the following form:

$$\mu_1^{(2)} = \mu_1^0 + \Delta p\,(V^{(2)})\,\overline{V}_1\,. \tag{10}$$

Since subsystem 2 is in equilibrium with the pure solvent (which has then an a_1 unit activity)

$$\mu_1^{(2)} - \mu_1^0 = \Delta\mu_1 = RT \ln a_1 = 0\ , \tag{11}$$

so that the product $\Delta p(V^{(2)})\overline{V}_1$ must also be zero. Since $\overline{V}_1$ is always positive and of finite magnitude, in Eq. (10) only the term $\Delta p\,(V^{(2)})$ can be zero. In view of the fact that in equilibrium only the negligibly small hydrostatic pressure, corresponding to the vapour pressure of the solvent, acts on both subsystems, $p^{(1)}$ can be considered as zero. Accordingly, in consideration of the nature of the processes in subsystem 2, accompanied by changes in volume, as *e.g.* the deformation of the particle network or the pressure components arising from a change in particle number, the value $p^{(2)}(V^{(2)}) = 0$ can be attributed to the fact that in equilibrium these pressure components always compensate one another.

Let us analyze the processes proceeding in subsystem 2 with the aid of the one-dimensional model shown in Fig. 2.

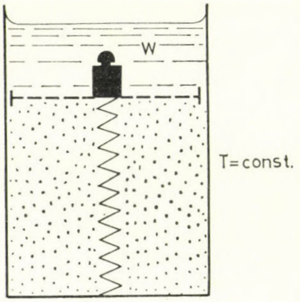

Fig. 2. One-dimensional model of a semi-open system

Subsystems 1 and 2 are separated from each other by a weightless, semipermeable, frictionlessly moving piston, fastened with a spring to the bottom of the cylinder. In the case of equilibrium, the osmotic pressure, π, of the solution in subsystem 2 is exactly compensated by the pressure p_{spring}, exerted by the deformed spring.
Thus:

$$p^{(2)}(V^{(2)}) = p_{\text{spring}} - \pi = 0\,. \tag{12}$$

If the piston is displaced by a hydrostatic pressure p, changeable with weight W, in the new equilibrium state

$$p_{\text{spring}} - \pi = -p. \tag{13}$$

On multiplying both sides of Eq. (13) with the partial molar volume of the solvent:

$$p_{\text{spring}}\overline{V}_1 - \pi\overline{V}_1 = -p\overline{V}_1 \tag{14}$$

and using the relationships $\Delta\mu_{1,\text{osm}} = -\pi\overline{V}_1$ and $p_{,\text{spring}}\ \overline{V}_1 = \Delta\mu_{1,\text{spring}}$, the equation

$$\Delta\mu_{1,\text{spring}} + \Delta\mu_{1,\text{osm}} = -p\overline{V}_1 = \Delta\mu_1 \tag{15}$$

is obtained. In swelling equilibrium with the pure solvent and at zero hydrostatic pressure:

$$\Delta\mu_1 = \Delta\mu_{1,\text{spring}} + \Delta\mu_{1,\text{osm}} = 0 \tag{16}$$

This proves our statement in accordance with the compensation principle, namely that in subsystem 2 of such system the expression representing the chemical potential must consist at least of two terms.

If further interactions affecting local pressure conditions may occur in subsystem 2, the resultant pressure, $p^{(2)}(V^{(2)})$ is given by the expression

$$p^{(2)}(V^{(2)}) = \sum_{i=1}^{m} p_i^{(2)}(V^{(2)}) \quad m \geq 2, \tag{17}$$

and the overall chemical potential in a general form by the equation

$$\mu_1 = \mu_1^0 + \sum_{i=1}^{m} p_i^{(2)}(V^{(2)}) \left(\frac{\partial V^{(2)}}{\partial n_1} \right)_{T, n_2} \quad m \geq 2 \tag{18}$$

where $p_i^{(2)}(V^{(2)})$ is the pressure component belonging to the i-th internal interaction.

In accordance with conditions, Eq. (18) is valid also in the case of an arbitrary number of non-diffusive components.

From the simple model shown in Fig. 2 it becomes also evident that a reference length (in the three-dimensional case a reference volume, $V_0^{(2)}$) belongs to the rest condition of the spring, at which $\Delta\mu_{1,\,\mathrm{spring}} = 0$. Accordingly, Eq. (18) can be written in the following form:

$$\mu_1 = \mu_1^0 + \sum_{i=1}^{m} p_i^{(2)}(V^{(2)}, V_0^{(2)}) \left(\frac{\partial V^{(2)}}{\partial n_1} \right)_{T, n_2} \quad m \geq 2 \tag{19}$$

Since only the resultant pressure (overall chemical potential) can be determined by measurement, the individual pressure (or chemical potential) components can be calculated on the basis of models, taking into consideration also the structure of the given system. From the analysis of the dependence of the overall chemical potential on volume, the change of the resultant pressure with the volume can be obtained, so that an equation of state of type P-V can also be given on the basis of Eqs (17) and (18).

If the discussion is extended to a set of k systems independent from one another, k equations of the form (18) can be written.

By the suitable coupling (*e.g.* mechanical coupling) of semi-open systems of different properties, the overall change in volume can manifest itself in principle in a change in form of discretional orientation or complexity. However, the description of the movement of coupled systems is possible only, if the dependence on place and time of the stresses occurring is exactly known. On the other hand, coupled parts of space with different properties yield a fundamental basis for the thermodynamical description of non-homogenous molecular networks.

Possible measuring techniques

One of the most simple measuring methods can be realized on the basis of Eq. (15) through changing of the volume of subsystem 2 by applying the hydrostatic pressure (swelling pressure) p. In this case, the overall chemical potential can be obtained as a function of the volume of the system (or of the concentration of the particle network). Owing to its relatively difficult technical realization, this method has not been widely used so far [1, 2, 3].

It can be shown that in those simple types of deformation, in which the hydrostatic components of the stress applied are also active (*e.g.* in unidirectional elongation or compression), the overall chemical protential of the solvent can be calculated also from the change in volume produced [4, 5]. However, owing to the relatively low mechanical strength of the swollen polymer networks, on the basis of this process the activity of the solvent can be determined only in a strongly restricted range of volume change.

The other theoretical possibility is to change in subsystem 1 the activity of the solvent. If subsystem 2 is equilibrated instead of the liquid phase pure solvent with its vapour of known pressure p_1, the determination of activity can be traced back through the relationship

$$a_1 = \frac{p_1}{p_0}$$

to the measurement of vapour pressure (p_0 is the saturated vapour pressure of the pure solvent). Practically only the accuracy of vapour pressure measurement limits the applicability of the method. Since with strongly swollen polymer networks the activity is close to $1 (1 > a_1 > 0.9990)$ in the concentration range which yields information on the structure, the measuring of vapour pressure makes possible the reliable calculation of solvent activity mainly for more concentrated systems [6, 7].

The dependence of the chemical potential of the solvent on the volume of the system can be determined also by filling subsystem 1 instead of the pure solvent with a solution, of the components of which only the solvent can penetrate into subsystem 2, and for which the dependence of solvent activity on concentration is exactly known. In the case of polymer networks this can be realized by placing the swollen network into the solution of a polymer of such high molecular mass, which prevents the penetration of its molecules into the gel phase. When the composition of both parts of the space and the activity—polymer concentration function with respect to the polymer solution are known, the change of $\Delta\mu_1$ with concentration can be calculated (equilibrium deswelling method) [8]. It should be emphasized that the precondition of measurement is to know with high accuracy the activity of the solvent in the polymer solution (*e.g.* from osmotic pressure data).

The method has been used by several authors for the investigation of cross-linked polymers [9, 10], but the method did not gain wide application, because of the relatively slow establishment of equilibrium and the rather limited applicable concentration range.

Modified equilibrium deswelling method

According to data available in the literature and our own experiences, one of the main difficulties of the aforesaid method of activity measurement, in principle easy to realize, is the fact that at higher concentrations the viscosity of the polymer solution, of adequate molecular mass for non-penetrating into the network, is already so high that the equilibrium is set in only very slowly. The determination of the composition, the volume of the gel sample taken from the viscous solution causes further considerable difficulties.

To eliminate the difficulties mentioned above, the following method of analysis has been developed. The swollen gel is not placed directly into the polymer solution of known solvent activity, but is contacted with the same through an inserted semi-permeable membrane. In this way, the use of a polymer solution of high molecular mass becomes unnecessary, and moreover, the accuracy of the volume or mass measurement of the gel sample is considerably increased. With this modification, polymers of a few times ten thousand molecular mass can be used for activity measurements. This actually means the extension of the investigations to a wider concentration range, in which so far only swelling pressure measurements were feasible.

Experimental

Materials used for the investigations and their preparation

In the development of the method particular attention was paid to work out a procedure of general applicability, which makes possible measurements in both aqueous and non-aqueous media.

For investigations in aqueous media solutions of known water-activity were prepared dissolving poly(vinyl pyrrolidone) (PVP, K 30, Fluka A. G., Buchs, Switzerland) in cold distilled water. Before use the fraction of low molecular mass was removed by dialysis from the PVP solutions. Dialysis was continued against distilled water, until PVP could not be detected in the equilibrium liquid phase even by interferometry. Main characteristics of the dialyzed sample: $d_{\mathrm{PVP}} = 1.275$ g/cm³, intrinsic viscosity of the aqueous solution at 298 K $[\eta]_{298°} = 0.26 \frac{100\ \mathrm{cm}^3}{g}$, relative molecular mass determined by osmometry $\overline{M}_{\mathrm{n}} = 33.000$.

As an organic solvent toluene or acetone was used. Solvent activity was adjusted in these systems with poly(vinyl acetate) (PVAc, Mowilith M 40, Hoechst, GFR). To remove fractions of low and high molecular mass, the original commercial product was fractionated in acetone—water mixture, and the solution in acetone of the medium fraction was dialyzed. Characteristics of the polymer obtained in this way: $d_{\mathrm{PVAc}} = 1.17$ g/cm³, $\overline{M}_{\mathrm{w}} = 130.000$.

For the toluene systems the equilibrium deswelling tests were carried out also with polystyrene (PS) solutions. PS was prepared by the polymerization of styrene monomer (product Reanal) at 343 K in benzene solution in the presence of benzoyl peroxide initiator. Characteristics of the carefully purified and fractionated PS sample: $d_{PS} = 1.05$ g/cm³, $\overline{M}_w = 37.000$, $\overline{M}_n = 34.000$.

Investigations were carried out on chemically cross-linked poly(vinyl alcohol) (PVA) and poly(vinyl acetate) (PVAc) gels. PVA gels were prepared in aqueous solution by cross-linking with glutaric aldehyde [11]. PVAc gels were prepared from PVA gels by total reacetylation at 363 K in pyridine-glacial acetic acid mixture. After the proceeding of the cross-linking reaction, PVA gels were brought into swelling equilibrium with distilled water, while the medium of the PVAc gels was exchanged after reacetylation for toluene or acetone.

Method of investigation

For the investigation of the equilibrium degree of deswelling the experimental apparatus shown in Fig. 3 was used.

The swollen polymer gel (6) is placed into a narrow dialyzing tube (3) (Kalle A. G., Wiesbaden, GFR) with sealed bottom. The glass capillary (4) arranged above the gel film serves to equalize the pressure difference prevailing between the two sides of the dialyzing membrane with proceeding solvent transport. The dialysis tube with the gel sample is placed into a test tube containing 4—5 cm³ of polymer solution (5). The system is closed with a stopper (1). The small magnetic stirrer (7) at the bottom of the test tube permits the homogenization of the solution.

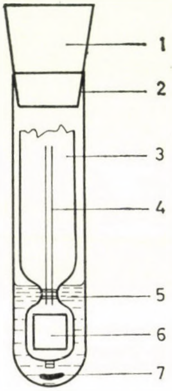

Fig. 3. Apparatus for the determination of solvent activity

Experimental results and their evaluation

The basic condition for the applicability of the method is that the polymer concentration — solvent activity functions shall be known for a wide concentration range of the given polymer. For the polymer—solvent systems used for our experiments osmotic pressure data of high accuracy (± 0.1%) are available in the literature [12, 13]. These measurements were carried out on samples of similar physical characteristics, prepared as described in the aforegoing. Data in the literature have been checked for a few systems by osmotic pressure measurements (Knauer membrane osmometer, and Hewlett—Packard vapour pressure osmometer), and an agreement within 1—2% was found. Solvent activity—polymer concentration functions for different systems are shown in Figs. 4 and 5.

Investigations were carried out on the one hand to determine the time required to attain swelling equilibrium, and on the other hand, to establish the reversibility of the swelling process. Relevant experimental results are shown for a few systems in Figs. 6, 7, 8 and 9. It can be clearly seen from the figures that the time required to attain swelling equilibrium considerably depends on the nature of the solvent and on temperature. It can be considered as reversible; the curves describing the change in volume fraction of the polymer ($v_2 = q_i^{-1}$) with decreasing and increasing solvent activity coincide in the range investigated within the limits of measuring error.

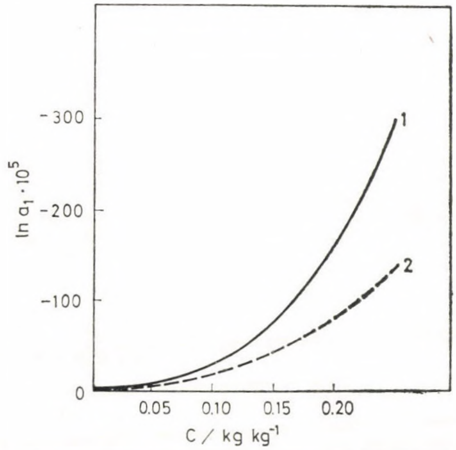

Fig. 4. Dependence of ln a_1 on PVP concentration at various temperatures [PVP—water, $T = 298$ K: (1) [12]; $T = 333$ K: (2)]

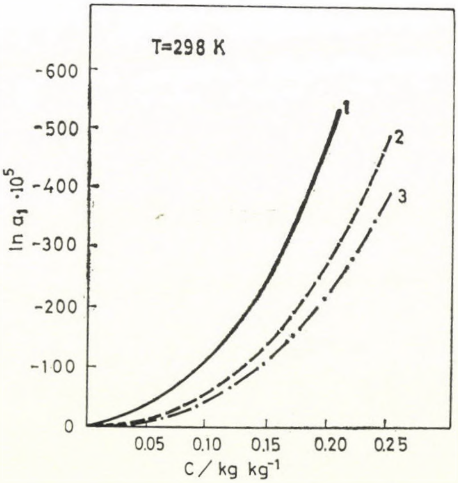

Fig. 5. Dependence of ln a_1 on polymer concentration for various solvent—polymer systems (PS—toluene: (1) PVAc—acetone: (2); PVAc—toluene: (3) [13])

To check the accuracy of solvent activity data of various polymer—solvent systems published in the literature and measured by us, and to investigate the reproducibility of the deswelling process, the solvent activity—polymer volume fraction functions have been determined for the same systems with different polymers (Fig. 10). It can be established on the basis of the figure that the course of the curves is independent of the nature of the polymer, used for

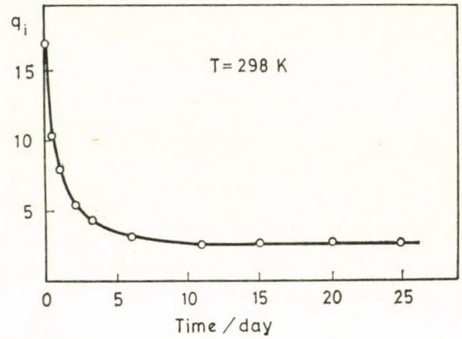

Fig. 6. Dependence of volume degree of swelling on time (PVA hydrogel, degree of cross-linking: 200, starting PVA concentration 6 w%, symbol: 6/200)

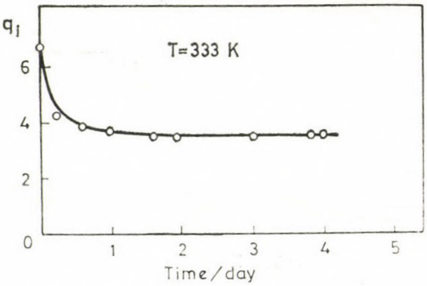

Fig. 7. Dependence of volume degree of swelling on time (PVA hydrogel, 9/100)

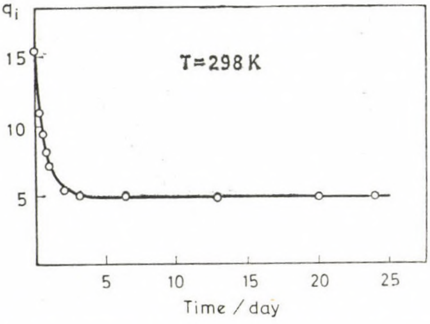

Fig. 8. Dependence of volume degree of swelling on time in PVAc—acetone system (the sample was prepared from 9/200 PVA gel)

the changing of solvent activity. This proves at the same time the reliability of activity data, and the good reproducibility of the measurements.

Since one of the initial conditions of the deduction of the theoretical relationships was the additivity of the volumes, it was thought necessary to check it also experimentally (Table I).

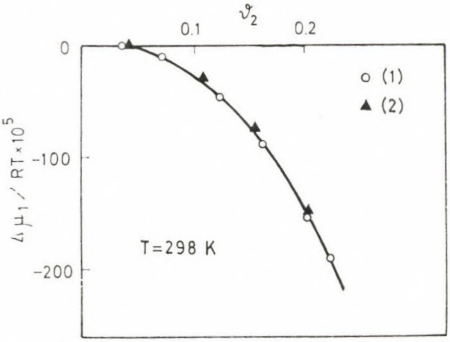

Fig. 9. Investigation of the reversibility of the process accompanied by change in volume (PVA hydrogel, 6/200; curves plotted for decreasing (1) and increasing (2) activity values)

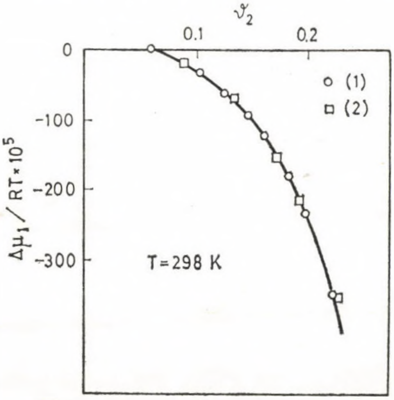

Fig. 10. Dependence of $\Delta\mu_1/RT$ on the volume fraction for PVAc in PVAc—toluene system (polymers changing the activity of the solvent: (1)—PVAc, (2)—PS)

It can be seen from the data in the table that for PVA—water systems the volumes can be considered at good approximation as additive in the range investigated. Similar results were obtained also for the systems PVAc—toluene and PVAc—acetone.

For the application of the new method of investigation a few examples are shown in Figs 11 and 12. Fig. 11 shows functions relevant to PVA gels cross-linked at 6 w% polymer concentration, while Fig. 12 functions relevant to PVAc networks prepared from the same gels by polymer analogue reaction. It can be established on the one part that gels of different degree of cross-link-

Table I

Investigation of the volume additivy of polymer and solvent in PVA—water system

(Polymer concentration at cross-linking: 6w%; degree of cross-linking 200; $V_i = 0.9755$ cm^3, T: 298 K)

Change in volume ΔV/cm^3	Change in mass Δm/g
0.432	0.420
0.501	0.529
0.684	0.680
0.715	0.725
0.721	0.728
0.782	0.790

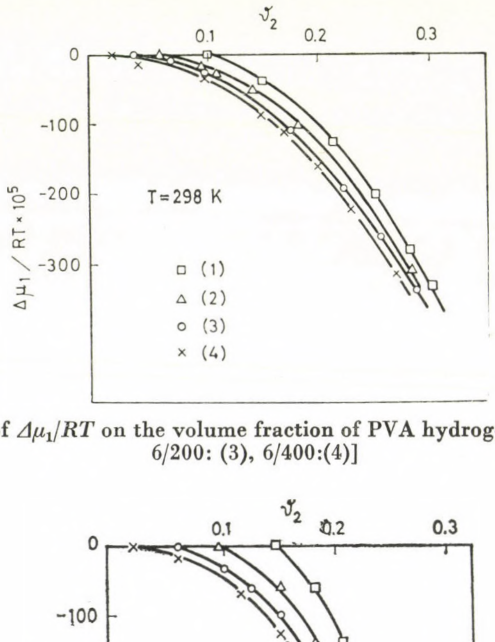

Fig. 11. **Dependence of $\Delta\mu_1/RT$ on the volume fraction of PVA hydrogels [6/50: (1), 6/100: (2), 6/200: (3), 6/400:(4)]**

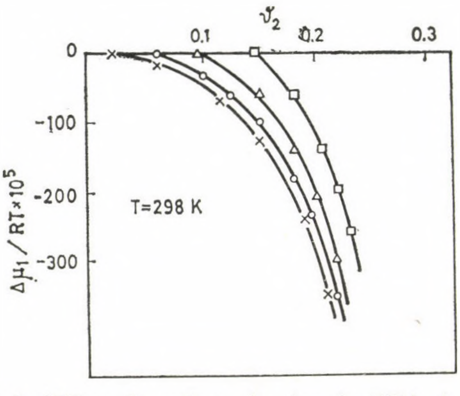

Fig. 12. **Dependence of $\Delta\mu_1/RT$ on the volume fraction for PVAc in PVAc—toluene systems (PVAc gels were prepared from the PVA hydrogels in Fig. 11)**

ing can be easily distinguished from one another, and on the other part that there are no characteristic difference between the curves, that is to say, in all the systems the degree of swelling of the gels decreases according to a monotonic function with the decrease in activity of the solvent. For PVAc—toluene systems the slope of the curves is steeper, than for PVA—water systems, because, toluene being a better solvent for PVAc than water for PVA, the second term of Eq. (15), $\Delta\mu_{1,\mathrm{osm}}$, is larger for these systems (polymer analogue reaction does not affect the number of junction points in the system, so that its effect on $\Delta\mu_{1,\mathrm{spring}}$ is considerably smaller).

It should be mentioned finally that the method can be advantageously used also for the study of biological systems in gel state. By using a membrane of suitable selectivity, not only the solvent, but the chemical potential of other substances (*e.g.* electrolytes) and their thermodynamically well-controlled transport can be investigated.

*

We thank Prof. Ervin Wolfram for his valuable advices during the preparation of the manuscript.

REFERENCES

[1] Pennings, A. J., Prins, W.: J. Polymer Sci., **49**, 507 (1961)
[2] van de Kraats, E. J., Winkelers, M. A. M., Potters, J. M., Prins, W.: Rec. Trav. Chim., **88**, 449 (1969)
[3] Froehlich, D., Crawford, D., Rozek, T., Prins, W.: Macromolecules, **5**, 100 (1972)
[4] Treloar, L. R. G.: Trans. Faraday Soc., **46**, 783 (1950)
[5] Rijke, A. M., Taylor, G. L.: J. Polymer Sci. Pt. A-1, **5**, 1433 (1967)
[6] Gee, G., Orr, W. J. C.: Trans. Faraday Soc., **42**, 507 (1946)
[7] Gee, G., Herbert, J. B. M., Roberts, R. C.: Polymer, **6**, 541 (1965)
[8] Boyer, K. F.: J. Chem. Phys., **13**, 363 (1945)
[9] Rijke, A. M., Prins, W.: J. Polymer Sci., **59**, 171 (1962)
[10] Mukherji, B., Prins, W.: J. Polymer Sci. A-1, **2**, 4367 (1964)
[11] Horkay, F., Nagy, M., Zrínyi, M.: Acta Chim. Acad. Sci. Hung. (in press)
[12] Vink, H.: Europ. Polym. J., **7**, 1411 (1971)
[13] Vink, H.: Europ. Polym. J., **10**, 149 (1973)

Miklós Nagy H-1088 Budapest, Puskin u. 11—13.
Ferenc Horkay H-1096 Budapest, Nagyvárad tér 2.

Acta Chimica Academiae Scientiarum Hungaricae, Tomus 104 (1), pp. 63—67 (1980)

STUDIES ON Pt(IV), Rh(III) AND Co(III) COMPLEXES OF SCHIFF BASES

P. SINGH[1], G. P. POKHARIYAL[1], V. SINGH[2]*, Smt. C. SINGH[2] and G. K. AGRAWAL[2]

([1]Chemistry Department, S. S. V. College, Hapur, Ghaziabad,
[2]J. V. College and D. J. College, Baraut, Meerut, U. P. India)

Received July 25, 1978
In revised form April 28, 1979
Accepted for publication June 26, 1979

Complexes of Pt(IV), Rh(III) and Co(III) with the Schiff bases *N*-4-methyl-7-hydroxy-8-aceto-coumarinylideneanthranilic acid and *N*-4-methyl-7-hydroxy-8-aceto-coumarinylidene-*o*-aminophenol have been isolated and assigned octahedral structures on the basis of analytical, magnetic, conductivity, electronic and IR spectral data. Electronic spectral studies indicate that the ligand field bands observed for Pt(IV) complexes are analogous to those observed in Rh(III) and Co(III) complexes, their positions show the trend $5d^n > 4d^n > 3d^n$. All the complexes are diamagnetic. Relevant ligand field parameters have been evaluated.

Various workers [1—6] have reported the electronic spectra of platinum metal complexes in aqueous solutions but these are subject to question because of the tendency of platinum metal complexes especially those with halide ligands, to undergo hydrolysis [7, 8].

The complexes of platinum metals with amines act as acids in aqueous media and their spectra depend on the pH, due to the presence of conjugate base complexes which have spectra that differ sufficiently from fully protonated complexes [9]. Schiff bases have been reported to be very good chelating agents [10—14]; the above two Schiff bases have been found to form stable complexes of Pt(IV), Rh(III) and Co(III). These complexes have been isolated and characterized on the basis of analytical, magnetic conductance, electronic and IR spectral data. The structural formulae for the two types of complexes, to show their octrahedral structures are displayed below. However, the complexes bear one unit of negative charge in case of Rh(III) and Co(III) whereas they are nonelectrolytes in the cases of Pt(IV).

Experimental

Schiff bases were prepared by refluxing equimolar amounts of 4-methyl-7-hydroxy-8-acetylcoumarin with anthranilic acid/*ortho*-aminophenol in ethanol on a steam bath for 3.5—4 hrs. The reaction mixtures were cooled in a refrigeration and the solid product so obtained were crystallized from ethanol and further purified by TLC using benzene as eluent. Satisfactory elemental analysis were obtained.

---

* To whom correspondence should be addressed.

AR grade samples of metal chlorides (Johnson and Matthey) were used. The organic solvents were of reagent quality and were dried just prior to use.

Carbon, hydrogen and nitrogen analysis were carried out at the Microanalytical Laboratory, I. I. T. Kanpur, India. The magnetic, spectral and conductometric measurements carried out as earlier [13].

Isolation of the complexes

Different colours were found to develop when 200 ml 0.03 *M* ethanolic solutions of the ligands were mixed with 50 ml of equimolar ethanolic solutions of different metal ions at approximate pH (Table I). In the case of the Co(III) complex, a vigorous stream of air was bubbled through the reaction mixture of Co(II) chloride and the corresponding ligand in ethanolic medium at a pH lower than those in other cases. The reaction mixtures were refluxed on a water bath for 2—5 hours, the contents on cooling in a refrigerator yielded crystalline complexes. These were washed thoroughly with water, ethanol, ether and dried in vacuum. The complexes are insoluble in water but soluble in organic solvents like acetone, DMSO, DMF and NM. Analytical data and physical properties of these complexes are given in Table I.

Table I

Analytical data and physical properties of the complexes

Compound	% Analysis; Calcd. (Found)				Colour	pH of Isolation	Conductivity (Ohm^{-1} mole^{-1} cm^{3}) in NM
	C	H	N	Metal			
$[Pt(C_{19}H_{13}NO_5)_2]$	52.60 (51.44)	2.99 (2.84)	3.23 (3.08)	22.54 (22.26)	Red	3.0	25
$[Pt(C_{18}H_{13}NO_4)_2]$	52.11 (51.70)	3.21 (3.10)	3.46 (3.28)	24.09 (23.80)	Red	3.5	32
$H[Rh(C_{19}H_{13}NO_5)_2]$	52.88 (58.00)	3.48 (3.29)	3.61 (3.42)	13.30 (12.75)	Brown	4.8	100
$H[Rh(C_{18}H_{13}NO_4)_2]$	60.11 (59.42)	3.75 (3.58)	3.89 (3.68)	14.32 (13.98)	Blackish Brown	3.5	110
$H[Co(C_{19}H_{13}NO_5)_2]$	62.41 (61.95)	3.69 (3.55)	3.83 (3.78)	8.07 (7.96)	Violet	2.6	120
$H[Co(C_{18}H_{13}NO_4)_2]$	64.09 (63.76)	4.00 (4.20)	4.15 (4.31)	6.95 (7.18)	Violet	2.8	118

Results and Discussions

The ligand field bands (in acetone) observed for Pt(IV) complexes of the Schiff bases (*N*-4-methyl-7-hydroxy-8-acetocoumariny-lidene anthronilic acid and *N*-4-methyl-7-hydroxy-8-acetocoumarinylidene-*o*-aminophenol) are analogous to those observed for the Rh(III) and Co(III) complexes of the same ligand and the band positions follow the order; $5d^n > 4d^n > 3d^n$. All the complexes have been found to be diamagnetic in behaviour [15]. Three d—d transitions have been observed in the absorption spectra of Pt(IV), Rh(III) and

Co(III) complexes out of which two are spin allowed transitions $^1A_{1g} \rightarrow {}^1T_{1g}$ and $^1A_{1g} \rightarrow {}^1T_{2g}$ [16]. The third one is a spin forbidden band involving singlet-triplet transition $^1A_{1g} \rightarrow {}^3T_{1g}$. The energies compared to the ground state have been calculated in terms of splitting energy parameter $10D_q$, Rach parameters B and C. The calculated values of $10D_q$, B, C, and LFSE are listed in Table II and are in good agreement with the expected values for octahedral complexes

Table II

Electronic spectral data of the complexes

Compound	$^1A_{1g} \rightarrow {}^3T_{1g}$ (cm^{-1})	$^1A_{1g} \rightarrow {}^1T_{1g}$ (cm^{-1})	$^1A_{1g} \rightarrow {}^1T_{2g}$ (cm^{-1})	$10D_q$ (cm^{-1})	B (cm^{-1})	C (cm^{-1})	β	C/B	LFSE (kcal/mole)
$[Pt(C_{19}H_{13}NO_5)_2]$	18 500	26 400	34 600	30 350	512	3950	0.71	7.7	208.13
$[Pt(C_{18}H_{13}NO_4)_2]$	18 400	26 500	34 700	30 550	512	4050	0.71	7.9	209.50
$H[Rh(C_{19}H_{13}NO_5)_2]$	15 000	19 600	26 000	21 900	400	2300	0.55	6.0	150.17
$H[Rh(C_{18}H_{13}NO_4)_2]$	14 600	19 300	25 800	21 650	422	2350	0.58	5.6	148.45
$H[Co(C_{19}H_{13}NO_5)_2]$	12 400	18 250	25 500	21 175	453	2925	0.41	6.5	145.20
$H[Co(C_{18}H_{13}NO_4)_2]$	12 500	18 300	25 550	21 200	450	2900	0.62	6.4	145.37

[16] since the complexes are octrahedral and diamagnetic in character, the LFSE in Kcals mole has been evaluated by the equation

$$\mathrm{LFSE} = -24D_q/350.$$

L. F. parameters have been evaluated by using the equations

$$E(^1A_{1g} \rightarrow {}^1T_{1g}) = 10D_q - C$$

$$E(^1A_{1g} \rightarrow {}^1T_{2g}) = 10D_q + 16B - C$$

$$E(^1A_{1g} \rightarrow {}^3T_{1g}) = 10D_q - 3C$$

In addition to the three d—d transitions, one charge transfer band has also been observed in the spectra of the complexes Pt(IV), 38 000, 38 500 cm^{-1}; Rh(III), 39 000, 39 400 cm^{-1}; Co(III), 28 000, 29 100 cm^{-1}, as shown in the Fig. 1. It has been assigned as a ligand to metal charge transfer band because empty ligand orbitals are at energies too high to participate to any extent in the formation of bands.

It is interesting to note that the value of $10D_q$ and thus the stability of these complexes follows the order Pt(IV) $>$ Rh(III) $>$ Co(III). This stability order is in agreement with the spectrochemical series.

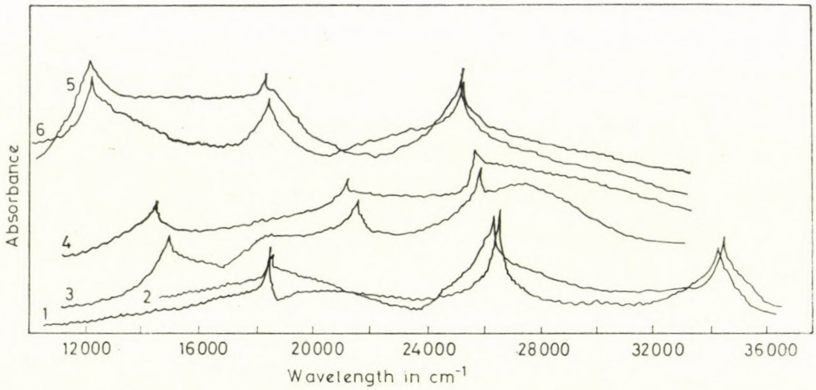

Fig. 1

Infrared spectral studies

A comparison of the IR spectra of the ligands and their Pt(IV), Rh(III) and Co(III) complexes shows that the stretching deformation modes of the phenolic OH groups disappear in the spectra of all the complexes indicating the loss of the phenolic portion on complexation and the formation of M—O bond. The metal—oxygen stretching vibrations appear as weak absorption bands in the region 425—470 cm^{-1}. However, an absorption band appearing at 2770 cm^{-1} due to OH of the carboxylic group [17] in *N*-4-methyl-7-hydroxy-8-acetocoumarinylidene anthranilic acid also disappear on complexation because of the formation of a M—O bond due to the loss of a proton.

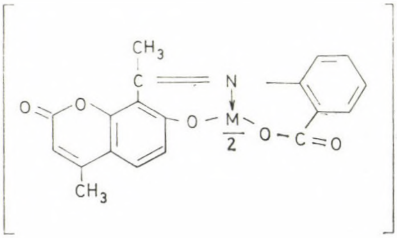

Structure I.

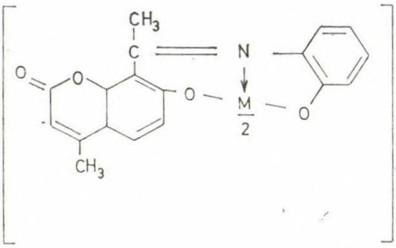

Structure II.

One strong band in the case of each ligand in the region 1600–1610 cm^{-1} has been observed due to the azomethine $CH_3-C=N$ group. This is considerably lowered in the spectra of the complexes and this fact along with changes in deformation, wagging and rocking azomethine vibrations, suggests that the metals are coordinated through the nitrogen atom of the azomethine group. Medium intensity $M-N$ vibrations appear at 510 cm^{-1}, 525 cm^{-1}, for Pt(IV), 515 cm^{-1}, 520 cm^{-1} for Rh(III) and 500 cm^{-1}, 530 cm^{-1} for Co(III).

*

The authors are thankful to Dr. R. P. Mahesh and Dr. R. C. Saxena for encouragement during the course of this work. Thanks are also due to Dr. R. S. Kapil, Scientific Officer, C. D. R. I., Lucknow, for recording the IR spectra and the elemental analysis of the compounds.

REFERENCES

[1] Jørgensen, C. K.: Molec. Phys., **2**, 309 (1959)
[2] Jørgensen, C. K.: Acta Chem. Scand., **10**, 518 (1956)
[3] Schmidtke, H. H.: Ber. Bunsenges. phys. Chem., **71**, 1138 (1967)
[4] Beck, W., Fehlhammer, W. P., Polmann, P., Schuierey, E., Feide, K.: Chem. Ber., **100**, 2335 (1967)
[5] Swihardt, D. L., Mason, W. R.: Inorg. Chem., **9**, 1749 (1970)
[6] Jørgensen, C. K., Brinen, J. S.: Molec. Phys., **5**, 535 (1962)
[7] Nikolaeva, M. M., Pastukhova, E. D.: Russ. J. Inorg. Chem., **12**, 650 (1967)
[8] Dreyer, R., Dreyer, I., Retting, D.: Z. Phys. Chem. (Leipzig), **224**, 199 (1963)
[9] Larsson, R.: Acta Chem. Scand., **21**, 1081 (1967)
[10] Singh, P., Singh, V., Singh, B. P., Goel, R. L.: Acta Chimica Acad. Sci. Hung., **82**, 143 (1977)
[11] Singh, P., Singh, V., Singh, B. P., Mahesh, R. P.: Ind. J. Chem., **13**, 734 (1975)
[12] Singh, P., Singh, V., Goel, R. L., Mahesh, R. P.: Curr. c., **44**, 137 (1976)
[13] Singh, P., Singh, V., Singh, B. P., Saxena, R. C., Mahesh, R. P.: J. Ind. Chem. Soc., **53**, 40 (1976)
[14] Sobhi, K., Adel, S. A.: J. Ind. Chem. Soc., **54**, 678 (1977)
[15] Teotia, M. P., Rastogi, D. K., Malik, W. U.: Inorg. Nucl. Chem., **35**, 3017 (1973)
[16] Teotia, M. P., Rastogi, D. K., Malik, W. U.: Ind. J. Chem., **11**, 1303 (1973)
[17] Ozha, D. D., Kaul, K. N., Mehta, S.: Curr. Sc., **43**, 344 (1975)

P. Singh, G. P. Pokhariyal — Chemistry Department, S. S. V. College, Hapur, (Ghaziabad), India

V. Singh, Smt. C. Singh — J. V. College, Baraut — 250 611 (Meerut), India

G. K. Agrawal — D. J. College, Baraut (Meerut) India

Acta Chimica Academiae Scientiarum Hungaricae, Tomus 104 (1), pp. 69—77 (1980)

CALCULATION OF THE AVERAGE RELATIVE PERMITTIVITY OF ELECTROLYTE SOLUTIONS FROM THE NON-LINEAR DIELECTRIC BEHAVIOUR OF THE SOLVENT

I. Ruff[1], J. Liszi[2] and L. Mészáros[3]

([1]*Institute of Inorganic and Analytical Chemistry, L. Eötvös University, Budapest,* [2]*Department of Analytical Chemistry, The University, Veszprém;* [3]*Research Group for Electrochemistry. Hungarian Academy of Sciences, Veszprém*)

Received May 4, 1979
Accepted for publication June 26, 1979

Comparison is made between the correlations describing the non-linear dielectric behaviour of liquids known so far and the equation taking into account also the field-dependence of the Kirkwood g-factor. A discussion is given on the approximate assumptions leading to the earlier equations from this latter one. It is indirectly confirmed by the application of the lattice model of electrolyte solutions that the equation involving the field dependence of the Kirkwood factor represents correctly the dielectric saturation effects up to field strengths of about 10^4 e.s.u. By comparing the average relative permittivity of several aqueous and non-aqueous electrolyte solutions with the theoretical values, one can conclude that the lattice model can be successfully used for all solutions whose average relative permittivity is higher than about 40. In solutions with lower average relative permittivity the lattice model is a poor approximation because ion pair formation starts to predominate.

1. Introduction

In our previous papers [1, 2] we have concluded that the non-linear dielectric behaviour of water and normal alcohols can be described by the Langevin function only if the field dependence of the Kirkwood factor is supposed. This field dependence originates from the structure-breaking effect of the field on these liquids: it decreases the number and/or size of the chain-like associates, the g-factor decreases, and, thus, the relative permittivity decreases more rapidly with the increase of the field strength. For nitrobenzene the above process is reversed in a certain sense: the pairs of molecules oriented originally with antiparallel dipole moments are separated under the effect of the field, the g-factor increases, and this increase overcompensates the normal dielectric saturation effect at relatively low field strengths, resulting in an anomalous non-linear behaviour.

These conclusions are based on experimental results obtained in the measurement of the so-called differential relative permittivity at a maximum field strength of about 60 kV/cm [3, 4]. Under such conditions the relative permittivity shows a maximum decrease of few tenths of a percent relative to the low-field static value. Such small effects allow the comparison of experimental data with only the cubic term of E of the power series of the Langevin function. For the determination of the terms involving E to the fifth or higher power, the present experimental techniques are insufficient, since even the very low conductivity of the pure liquids causes arc discharges under higher field strengths.

In the vicinity of the ions of electrolyte solutions, however, the solvent molecules are in an electric field stronger by several orders of magnitude than that attainable in macroscopic measurements. Thus, in principle, the effect of higher fields may also be studied, provided that the correlation between the field strength, depending on the position coordinates, and the average macroscopic relative permittivity of the electrolyte solution is known to a sufficient accuracy. In the present paper we intend to utilize the approximations of the lattice-like model of electrolytes [5] with this purpose.

2. Comparison of the various equations approximating non-linear dielectric behaviour

According to the BOOTH—ONSAGER theory [6], the relative permittivity depends on the electric field strength as follows:

$$\varepsilon = n^2 + \frac{4\pi N\mu}{E} L\left(\frac{\mu F}{kT}\right) \tag{1}$$

where N is the number of molecules in unit volume, E the field strength, k the Boltzmann constant, T the temperature, and ε the relative permittivity which is defined by the equation:

$$D = \varepsilon E$$

in which D is the dielectric displacement. The actual dipole moment μ is in the following relationship with the gas phase dipole moment μ_0 and with the internal refraction index n:

$$\mu = \frac{\mu_0(n^2+2)}{3}\sqrt{g} \tag{3}$$

where g is the Kirkwood factor.

The Langevin function denoted by L in Eq. (1) means the following:

$$L(x) = \operatorname{cth} x - 1/x. \tag{4}$$

Finally F represents the so-called cavity field which is proportional to the external field:

$$F = \frac{3\varepsilon}{2\varepsilon + n^2} E \tag{5}$$

Equation (1) is valid if the external field acting on the liquid is homogeneous. If not, an external field such as that of ions would act on the dipole not only by orientating them, but also by attraction which results in electrostriction. This effect can increase ε due to the increase of N and n. Under the effect of high field, the permanent dipole moment of the molecules can also enhance. When the orientation of the molecules of the liquid is not entirely random, the Kirkwood factor may also change with the field strength (it can both increase or decrease).

All these effects can be formally unified into the field dependence of a single quantity, if one assumes that the Kirkwood factor is field dependent, $g = g(E)$, while all the other characteristic quantities are considered independent of the field.

It is seen that Eq. (1) is not an explicit function of the field strength, since F includes the value of ε. Although the relative permittivity can be calculated by a suitable iteration procedure for various field strengths, yet, in equations which would require the handling of ε in conjuction with other variables, this equation is untreatable. In order to avoid this difficulty, let us apply the approximation:

$$2\varepsilon \gg n^2 \tag{6}$$

In this case F becomes equal to $3E/2$ which, when substituted into Eq. (1), yields:

$$\varepsilon = n^2 + 3\,\frac{\varepsilon_0 - n^2}{E\sqrt{3b}}\,L\left(E\sqrt{3b}\right) \tag{7}$$

where

$$b = \frac{3\mu^2}{4k^2T^2} \tag{8}$$

and ε_0 is the low-field static relative permittivity.

As a somewhat cruder approximation, one can assume that the Kirkwood factor does not depend on the field strength:

$$g(E) = g_0 \tag{9}$$

where g_0 is the limiting value of the Kirkwood factor at low fields. Inserting this into Eqs (8) and (7), one obtains the *Booth—Onsager equation*, which has the same form as Eq. (7) but b is independent of the field strength.

However, under the experimental conditions applied usually, not ε but the differential relative permittivity is determined, whose definition is:

$$\varepsilon_{\mathrm{d}} = \frac{\mathrm{d}D}{\mathrm{d}E}\,. \tag{10}$$

If Eq. (9) is valid, one gets from Eq. (7), taking into account Eq. (2) too:

$$\varepsilon_{\mathrm{d}} = n^2 + 3\,(\varepsilon_0 - n^2)\left(\frac{1}{3bE^2} - \frac{1}{sh^2\, E\sqrt{3b}}\right). \tag{11}$$

This equation can be approximated with different accuracies by retaining a different number of terms from the power series of $sh^2\,x$. When, *e.g.*, three terms are retained in the denominator, we have:

$$\varepsilon_{\mathrm{d}} = n^2 + (\varepsilon_0 - n^2)\,\frac{1 + \frac{1}{4}bE^2}{1 + b\,E^2 + \frac{1}{4}b^2\,E^2}\,. \tag{12}$$

From this, the next approximation can be obtained after performating the integration $D = \int \varepsilon_{\mathrm{d}}\,\mathrm{d}E$:

$$\varepsilon = n^2 + \frac{\varepsilon_0 - n^2}{4}\left(\frac{1}{1 + \frac{b}{2}E^2} + \frac{3}{E\sqrt{\frac{b}{2}}}\,\mathrm{arctg}\,E\sqrt{\frac{b}{2}}\right). \tag{13}$$

However, an even cruder approximation can be obtained, when only the first term is retained in the numerator and two in the denominator of Eq. (12). This is the Grahame equation [7], which was published as an intuition prior to Booth's paper [6]:

$$\varepsilon_{\mathrm{d}} = n^2 + \frac{\varepsilon_0 - n^2}{1 + bE^2}\,. \tag{14}$$

The integration of this equation yields the Laidler equation [8]:

$$\varepsilon = n^2 + \frac{\varepsilon_0 - n^2}{E\sqrt{b}}\,\mathrm{arctg}\,E\sqrt{b}\,. \tag{15}$$

On this level of approximation, one can even disregard the difference between ε and ε_{d}, and calculate the field strength from Eq. (15), which, when inserted into Eq. (14), gives:

$$\varepsilon \sim \varepsilon_{\mathrm{d}} = \varepsilon_0 - (\varepsilon_0 - n^2)\,\sin^2\frac{D\sqrt{b}}{\varepsilon_0 - n^2}\,. \tag{16}$$

This equation was used by Ruff [5] in his lattice-like model of electrolyte solutions.

In Table I the relative permittivities of water at 25 °C, as calculated by the different approximations listed above, are compared. The data in the second

Table I

Comparison of the relative permittivity of water at 25 °C as calculated by the different approximations

lg E	Eq. (1) ε	Booth—Onsager		Eq. (13)		Laidler ε	Grahame ε_d	Ruff $\varepsilon_d \sim \varepsilon$
		ε	ε_d	ε	ε_d			
1.0	78.54	78.54	*78.54*	78.54	*78.54*	78.54	***78.54***	78.54
2.0	78.54	78.54	*78.53*	78.54	*78.53*	78.54	***78.53***	78.53
3.0	78.21	78.36	*78.00*	78.32	*77.89*	78.24	***77.65***	77.66
3.5	75.39	76.80	*73.43*	76.44	*72.41*	75.74	***70.48***	71.38
3.7	71.23	74.39	*66.72*	73.60	*64.72*	72.13	***61.14***	64.48
4.0	56.81	65.00	*44.55*	63.26	*41.69*	60.24	***37.11***	49.11
4.3	34.92	46.87	*17.64*	45.14	*16.98*	42.12	***15.27***	32.96
4.5	23.04	34.06	*8.32*	32.90	*8.32*	30.69	***7.81***	24.20
5.0	8.64	13.10	*2.44*	13.06	*2.44*	12.26	***2.43***	10.48
6.0	2.51	3.00	*1.79*	2.98	*1.79*	2.89	***1.79***	2.48
∞	1.78	1.78	*1.78*	1.78	*1.78*	1.78	***1.78***	1.78

column have been obtained by iteration assuming a field dependence of the Kirkwood factor. In our previous paper [2], the assumption was that g can be given as follows:

$$g = g_0 + g_1 E^2 + g_2 E^4 + \ldots \tag{17}$$

Now, we suppose that the coefficients g_2, g_3, . . . are such that Eq. (17) is the power series of the following function:

$$g = 1 + \frac{g_0 - 1}{1 - \frac{g_1}{g_0 - 1} E^2} . \tag{18}$$

Thus we can circumvent the difficulty that the coefficients of the higher terms are unknown from experiments performed under field strengths lower than 10^2 e.s.u. Although the g-factor is assumed to be field independent in all of the remaining equations, the experimental b value was used, which implied a g-factor other than g_0 (see discussion in Ref. [1]).

From Table I it can be concluded that, on one hand, the Grahame and Laidler equation are good approximations of the Booth—Onsager equation, and, on the other, that the data in column *2* calculated by a field-dependent Kirkwood factor are between the ε and ε_d-values. It is also demonstrated that the Ruff equation containing most of the approximations yields also rather good values even above 10^4 e.s.u.

3. Calculation of the average relative permittivity of electrolyte solutions

This latter statement is important from the point of view of the present paper because this approach can be applied with the least difficulty for the calculation of the average relative permittivity of electrolyte solutions, since, on the basis of the theory assuming a lattice-like arrangement of ions in solution, the average value of the dielectric displacement can be determined. This can be inserted into Eq. (16), provided that the relative permittivity calculated with the average value of the dielectric displacement is not too much different

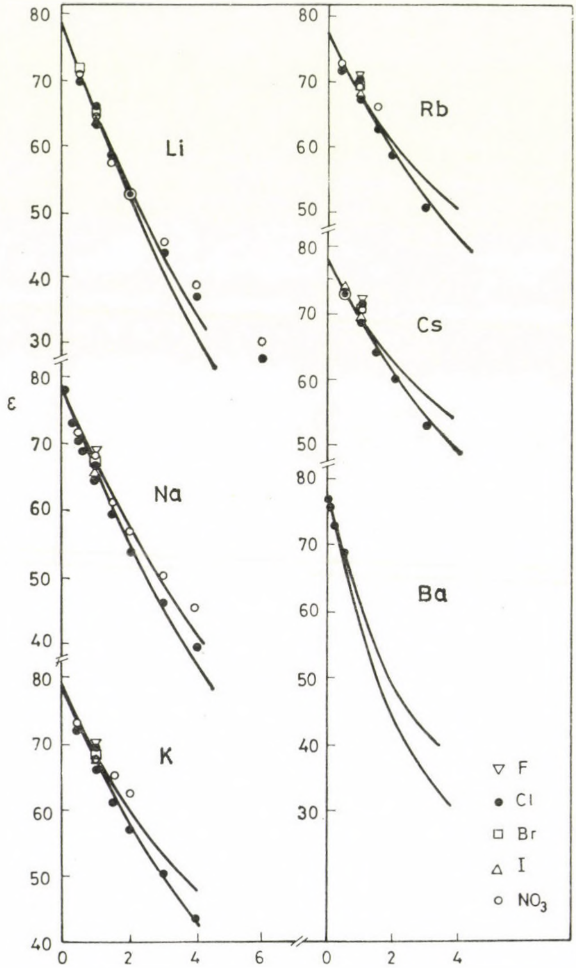

Fig. 1. **Relative permittivity of some aqueous electrolytes as a function of concentration. Of the full curves, the lower corresponds always to the chloride salt, while the upper to the nitrate. The curve of the bromides would fall at about the middle in between the two. The curve of the iodides would practically coincide with that of the nitrates. The experimental points are taken from Refs [9—12]**

from the average of the relative permittivity depending on the space coordinates.

According to the lattice-like model:

$$D = e/f_a^2\, r_0^2 \tag{19}$$

where e is the elementary charge, r_0 is the smallest separation distance between oppositely charged ions in a body-centered cubic lattice:

$$r_0 = \frac{\sqrt{3}}{2}\left(\frac{1000z^2}{z_\mathrm{a}\, z_\mathrm{c}\, Nc}\right)^{1/3} \tag{20}$$

and

$$f_\mathrm{a}^2 = \frac{\frac{2}{9} - 2\pi\,(a_\mathrm{a}^3 + 3_\mathrm{c}^3)/9\, r_0^3}{\left[\frac{\pi}{2\sqrt{2}}\ln\frac{2+\sqrt{2}}{2-\sqrt{2}} + \frac{3\sqrt{2}}{16}\left(1-\frac{\sqrt{2}}{2}\right) - \frac{\pi\,(a_\mathrm{a}+a_\mathrm{c})}{2r_0}\right] z} \tag{21}$$

where z_a and z_c are the charge number of the anion and cation, respectively, z is their highest common factor, a_a and a_c are the crystallographic radii of the anion and cation, respectively, and c the concentration of the electrolyte.

As is seen in Fig. 1, the relative permittivities calculated with these equations and measured [9—12] for aqueous solutions at 25 °C are in very good agreement. The deviations at higher concentrations become significant always in cases when the average field strength, calculated as the ratio of the average dielectric displacement and the average relative permittivity, exceeds the value of 10^4 e.s.u. The errors may be due to ion pair formation which would make the assumption of the lattice-like arrangement inappropriate.

Ion pair formation is known to become predominant at the lower concentration, the lower the relative permittivity of the solvent. This is likely why the above equations describe both aqueous and MFA solutions (see Fig. 2), while for average relative permittivities lower than 40 the lattice-like model breaks down irrespective of being applied to aqueous or non-aqueous solutions. Figure 3 shows the comparison of calculated and measured data for more dilute non-aqueous solutions, which supports also this expectation. The theoretical treatment of such solutions seems to be more successful when not a model of strong electrolytes — one of which is the lattice-like model — but *e.g.* the ONSAGER—PROVENCHER theory [13] is applied.

The success in applying the lattice-like model for the description of solutions with high relative permittivities, however, confirms indirectly the correctness of the equations used for the treatment of the non-linear dielectric behaviour. Thus it can be concluded that insofar as the RUFF approximation in Eq.

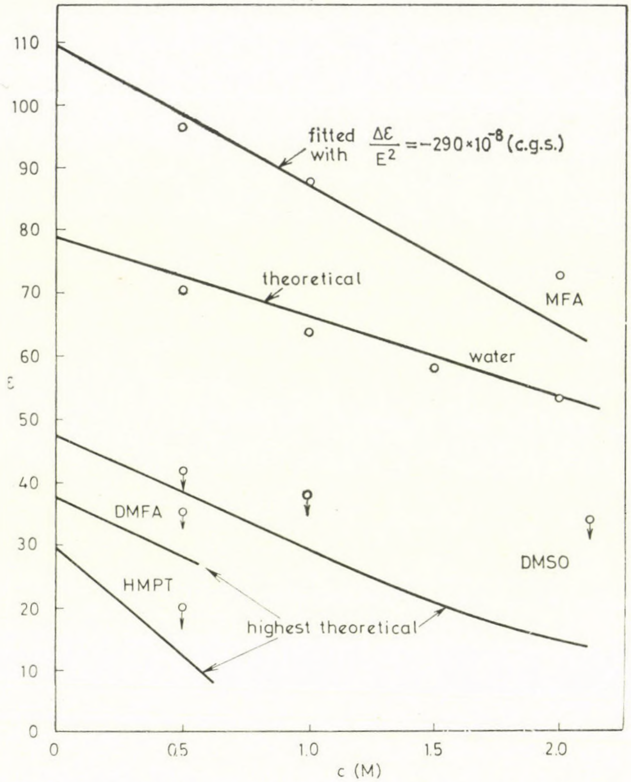

Fig. 2. **Relative permittivity of litium nitrate in various solvents as a function of concentration; (MFA = *N*-methylformamide, DMFA = *N,N'*-dimethylformamide, HMPT = hexamethylphosphoric acid triamide, DMSO = dimethylsulfoxide). With the exception of water, the experimental *b* values of the solvents are unknown. Disregarding the field dependence of the *g*-factor, Eq. (8) can give an estimate for the lower limit of *b*, *i.e.* for the calculation of the highest possible theoretical curve (DMSO, DMFA and HMPT). Such a curve for MFA would lie above that shown, *i.e.* the field dependence of *g* may interpret the fitted curve. The three lower curves, however, would lie higher only when the field had a structure-making effect, which is unlikely in these solvents. The experimental points correspond to data in Ref. [12]**

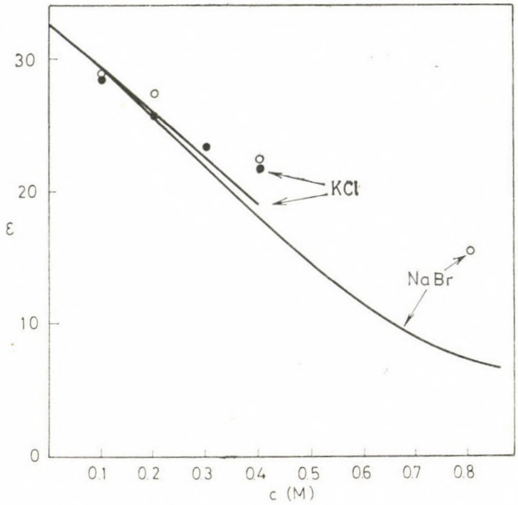

Fig. 3. **The relative permittivity of methanolic KCl and NaBr solutions as a function of concentration. The calculated curves correspond to *b* values determined experimentally. The points are shown according to the data in Ref. [9]**

(16) gives good agreement with Eq. (1) implying the field-dependence of the Kirkwood factor too, non-linear dielectric behaviour follows the theoretical predictions.

REFERENCES

[1] Liszi, J., Mészáros, L., Ruff, I.: Acta Chim. Acad. Sci. Hung., to be published
[2] Liszi, J., Mészáros, L., Ruff, I.: Acta Chim. Acad. Sci. Hung., to be published
[3] Kołodzej, H. A., Parry Jones, G., Davies, M.: J. C. S. Faraday Trans. II., **70**, 269 (1974)
[4] Brown, B. L., Parry Jones, G.: J. C. S. Faraday Trans. II., **70**, 1657 (1974)
[5] Ruff, I.: J. C. S. Faraday Trans. II., **73**, 1858 (1977)
[6] Booth, F.: J. Chem. Phys., **19**, 391, 1327, 1615 (1951)
[7] Grahame, D. C.: J. Chem. Phys., **18**, 903 (1950); **21**, 1054 (1953)
[8] Laidler, K. J.: Canad. J. Chem., **37**, 138 (1959)
[9] Hasted, J. B., Roderick, G. W.: J. Chem. Phys., **29**, 17 (1958)
[10] Barthel, J., Schmithals, F., Behret, H.: Z. phys. Chem., **71**, 115 (1970)
[11] Giese, K., Kaatze, U., Pottel, R.: J. Phys. Chem., **74**, 3718 (1970)
[12] Barthel, J., Behret, H., Schmithals, F.: Ber. Bunsenges., **75**, 305 (1971)
[13] Onsager, L., Provencher, S. W.: J. Am. Chem. Soc., **90**, 3134 (1968)

Imre Ruff H-1088 Budapest, Múzeum krt. 4/B
János Liszi
Lajos Mészáros } H-8200 Veszprém, Schőnherz Z. u. 12.

Acta Chimica Academiae Scientiarum Hungaricae, Tomus 104 (1), pp. 79—83 (1980)

THE SCHMIDT REACTION: SYNTHESIS OF DIENOTETRAZOLES

M. HUSAIN, S. R. HUSAIN and M. S. AHMAD

(*Department of Chemistry,*
Aligarh Muslim University, Aligarh-202001, *India*)

Received April 21, 1979
Accepted for publication June 27, 1979

As reported previously, treatment of the dienone **5** with an excess of hydrazoic acid gave 7-aza-4-oxo-B-homocholest-5-eno[7*a*, 7-d]tetrazole (**17**) instead of the anticipated dienotetrazole (**15**). This observation led to the design of a synthesis of hitherto unexplored dienotetrazoles from the corresponding steroidal dienones. The easily accessible dienones **1—4** were subjected to the Schmidt reaction, using an excess of hydrazoic acid in the presence of boron trifluoride etherate. The dienone **1** afforded 6-aza-B-homocholesta-2,4-dieno[6,7-*d*]tetrazole (**6**) and an oxidation product (**8**). The dienone **2** gave 7a-aza-4-bromo-B-homocholesta-3,5-dieno [7*a*, 7-d]tetrazole (**9**), and **3** yielded 3-aza-acetoxy-A-homocholesta-4a, 6-dieno[3,4-d] tetrazole (**10**). However, **4** provided **11**, **12** and **13** and failed to yield the expected product (**16**). The products were identified on the basis of their spectral properties, chemical transformations and comparison with authentic samples where available.

The reaction of cholesta-3,5-dien-7-one (**5**) with hydrazoic acid has been reported [1] to give an oxidation product, 7-aza-4-oxo-B-homocholest-5-eno [7*a*, 7-*d*] tetrazole (**17**). This compound was formed by virtue of the reaction of the C = C double bond with hydrazoic acid under the conditions of the Schmidt reaction. Our growing interest in this field [1—3] led us to design a synthesis of hitherto unexplored dienotetrazoles from the corresponding steroidal dienones (**1—4**). These dienones were selected in view of preventing the oxidation of a C = C bond. The reaction of cholesta-2,4-dien-6-one (**1**) with an excess of hydrazoic acid gave two compounds with melting points of 165 and 195 °C. The compound melting at 165 °C had correct analysis $C_{27}H_{72}N_4$. This composition indicates the presence of a tetrazole moiety corresponding to structure **6** or its isomer, **7**. The UV absorption maximum at 280 nm (ε 10 200) favours the structure **6**. The assignment of structure **6** was also substantiated by the NMR spectrum which exhibited a doublet *(*$J = 15$ Hz) for one proton at δ 3.24 (C7a—*H)*, a characteristic signal for 6-aza tetrazoles [2]. In the alternative structure a signal would likely be observed at δ4—4.5 for the C7a-protons *(cf.* [4]). The compound with m.p. 195 °C ($C_{27}H_{42}N_4O$) was identified as the oxidation product (**8**) cf. **6**, on the basis of elemental analysis. The UV absorption maximum at 238 nm (ε 12 800) affords clear evidence for the presence of the α,β-enone chromophore. The NMR spectrum also supported this structure, the vinylic proton appearing as a sharp singlet at δ 6.61 (C4—*H)*. Structure **8** was

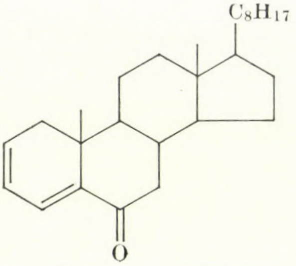

1

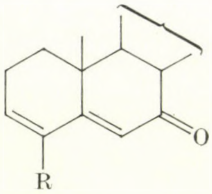

2 R = Br

5 R = H

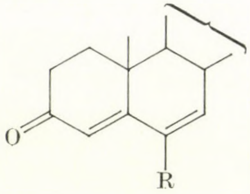

3 R = OAc

4 R = OC_2H_5

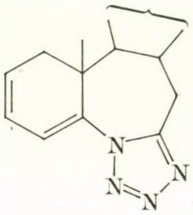

6

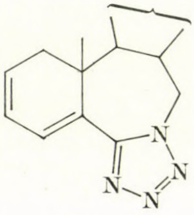

7

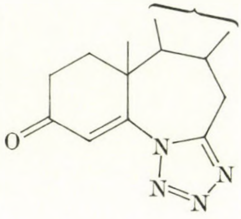

8

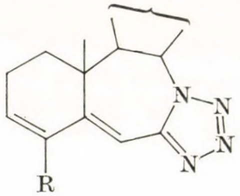

9 R = Br

15 R = H

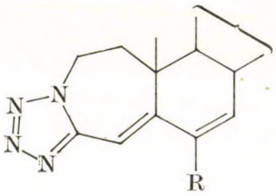

10 R = OAc

16 R = OC_2H_5

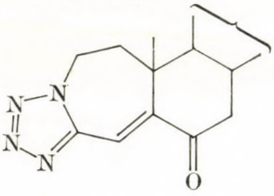

11

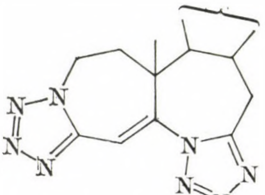

12

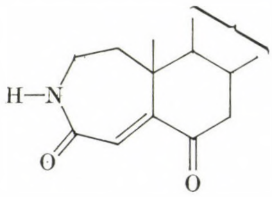

13

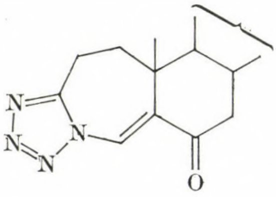

14

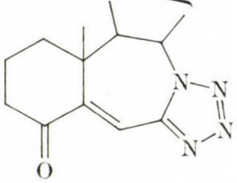

17

further substantiated by treatment of the product with hydrazoic acid to obtain authentic bistetrazole **12** [5].

Upon similar treatment, 4-bromocholesta-3,5-dien-7-one (**2**) gave a compound with m.p. 162 °C ($C_{27}H_{41}N_4Br$), characterized as 7a-aza-4-bromo-B-homocholesta-3,5-dieno [7*a*, 7—*d*] tetrazole (**9**). Its UV spectrum displayed an absorption maximum at 282 nm (ε 16 700), indicating the presence of an extended heterodiene as seen in structure **9**. The notable feature of the NMR spectrum of **9** is the appearance of the C_3-proton as a distorted triplet with $J = 5$ Hz. This distortion may perhaps be due to the long range coupling of the C_3-proton with the C_1-protons. Under similar conditions, 6-acetoxycholesta-4,6-dien-3-one (**3**) provided a single product melting at 213 °C, with correct analysis for $C_{29}H_{44}N_4O_2$. The UV absorption maximum at 293 nm (ε 17 200) accounts for the extended heterodiene system. On the basis of the molecular composition and UV absorption, this compound is considered 3-aza-6-acetoxy-A-homocholesta-4a,6-dieno (3,4-*d*] tetrazole (**10**). Structure **10** is also supported by the NMR spectrum exhibiting a multiplet for 2 protons at δ 4.46, which can be ascribed to C_2-protons (*cf.* [4]). The confirmation of **10** came from the hydrolysis of the product, which furnished the authentic known compound **11** [5].

The reaction of 6-ethoxycholesta-4,6-dien-3-one (**4**) gave three products, **11**, **12** [5] and **13** [6]. These compounds are identical with the products derived from cholest-4-en-3,6-dione under the same conditions. The fact that the reaction of cholest-4-en-3,6-dione with hydrazoic acid afforded both the 3-aza **11** and 4-aza **14** monotetrazoles [3], along with other products, in particular the bis-tetrazole **12**, can be explained by assuming that, on the analogy of the formation of the dienotetrazole **10** from the dienone **3**, ketone **4** was transformed into the 3-azatetrazole **16**, which was then hydrolyzed to the ketone **11**, whose further reaction with hydrazoic acid gave the bis-tetrazole **12**.

Experimental

All m.p.s are uncorrected. IR spectra were determined in KBr with a Perkin—Elmer spectrophotometer and UV spectra were recorded in 95% ethanol with a Beckman DK2 spectrophotometer. NMR spectra were run in $CDCl_3$ on a Varian A60 instrument with TMS as the internal standard. Thin-layer chromatographic plates were coated with silica gel G (BDH, Bombay). A 20% aqueous solution of perchloric acid was used as spraying agent. Silica gel (BDH, Bombay) was used for the column chromatography.

Preparation of hydrazoic acid

Hydrazoic acid solution was prepared according to MOURAL and SYHORA [7]. Sodium azide (4 g) was dissolved in water (20 ml) and to this was added benzene (30 ml) at 0 °C. Sulfuric acid (4 ml) was then added dropwise with shaking over a period of 30 min. at 0—5 °C; shaking was continued for an additional 30 min., the organic layer was then separated, dried (Na_2SO_4) and filtered. This solution of hydrazoic acid (about 30 ml) was made up to 50 ml by the addition of benzene and used in the reactions with the dienones.

Reaction of cholesta-2,4-dien-6-one (1) with hydrazoic acid

A cooled solution of hydrazoic acid in benzene, prepared as above, was mixed with freshly distilled boron trifluoride etherate (1.5 ml) and to this was added a solution of **1** [8] (2 g) in benzene (25 ml) over a period of about 5 h. The reaction mixture was then allowed to stand at room temperature for 30 h. The benzene solution was washed successively with water, sodium bicarbonate solution (5%) and water, and it was dried (Na_2SO_4). Benzene was removed under reduced pressure and the residue *(c.a.* 2.1 g), chromatographed over silica gel (40 g) and eluted in 30 ml portions. Elution with benzene-ether (10 : 1) afforded (850 mg) of **6**, m.p. 165 °C (from light petroleum); λ max 280 nm (ε 10200); ν max 1650, 1590, 1510, 1460, 1375 cm^{-1}; δ 6.05 (m, 3H, C_2H, C_3-H, C_4-H), 3.24 (d, $J = 15$ Hz, 1H, $C_{7a}-H$), 0.9 (S, $C_{10}-CH_3$), 0.7 ppm (S, $C_{13}-CH_3$).

$C_{27}H_{42}N_4$. Calcd. C 76.77; H 9.95; N 13.27. Found C 76.58; H 10.10; N 13.39%.

Further elution with benzene-ether (8 : 1) gave 400 mg of **8**, m.p. 195 °C (from ethanol); λ max 238 nm (ε 12800); ν max 1690, 1640, 1515, 1465, 1380 cm^{-1}; δ 6.16 (S, 1H, C_4-H), 3.48 (d, $J = 15$ Hz, 1H, $C_{7a}-H$), 0.9 (S, $C_{10}-CH_3$), 0.7 ppm (S, $C_{13}-CH_3$).

$C_{27}H_{42}N_4O$. Calcd. C 73.97; H 9.59; N 12.78. Found C 73.73; H 9.60; N 12.93%.

Reaction of 4-bromocholesta-3,5-dien-7-one (2) with hydrazoic acid

The dienone (**2**) [9] (2 g) was treated with hydrazoic acid boron trifluoride etherate in the manner described for **1**. The usual work-up provided a dark brown residue which was subjected to chromatography over silica gel. Elution with benzene-ether (13 : 1) furnished **9** (Positive Beilstein Test), which was crystallized from ethanol; 1.3 g, m.p. 162 °C; λ max 282 nm (ε 16700); ν max 1620, 1500, 1460, 1370, 690 cm^{-1}; δ 7.2 (S, 1H, C_6-H), 6.46 (distorted t, $J = 5$ Hz, 1H, C_3-H), 4.52 (m, 1H, C_8-H), 0.93 (S, $C_{10}-CH_3$), 0.8 ppm (S, $C_{13}-CH_3$).

$C_{27}H_{41}N_4Br$. Calcd. C 64.67; H 8.18; N 11.18. Found C 64.61; H 8.20; N 11.17%.

Reaction of 6-acetoxycholesta-4,6-dien-3-one (3) with hydrazoic acid

Treatment in the usual way of the dienone **3** [10] (prepared by heating cholest-4-ene-3,6-dione with pyridine-acetic anhydride) (2 g) with hydrazoic acid gave (**10**) as an oil which was crystallized from methanol; 1.5 g, m.p. 213 °C; λ max 293 nm (ε 17200), ν max 1760, 1625, 1520, 1465, 1375, 1200 cm^{-1}; δ 6.5 (S, 1H, C_4-H), 5.56 (broad, S, 1H, C_7-H; the Drieding model of **9** shows the dihedral angle between C_7-H and C_8-H to be almost 90°), 4.46 (m, 2H, C_2-H_2), 2.25 (S, 3H, CH_3-COO), 0.9 (S, $C_{10}-CH_3$), 0.76 ppm (S, $C_{13}-CH_3$).

$C_{29}H_{44}N_4O_2$. Calcd. C 72.51; H 9.17; N 11.66. Found C 72.59; H 9.12; N 11.71%.

Reaction of 6-ethoxycholesta-4,6-dien-3-one (4) with hydrazoic acid

The reaction of (**4**) [11] (2 g) was effected in the usual manner and the residue was chromatographed over silica gel. Elution with benzene-ether (11 : 1) yielded **11** (860 mg), m.p. [5] and m.m.p. 220 °C. Further elution with benzene-ether (10 : 1) afforded **12** (330 mg), m.p. [5] and m.m.p. 205 °C. Benzene-ether (4 : 1) gave **13** (65 mg), m.p. [6] and m.m.p. 207 °C.

*

The authors are grateful to Prof. W. Rahman, Head, Department of Chemistry, for providing the necessary facilities and to CSIR (New Delhi) for financial assistance to two of us (MH and SRH).

REFERENCES

[1] Ahmad, M. S., Chaudhry, Z. H., Khan, P. N.: Aust. J. Chem., **29**, 447 (1976)
[2] Ahmad, M. S., Khan, I. A.: Indian J. Chem., **15 B**, 1016 (1977)
[3] Ahmad, M. S., Husain, S. R., Husain, M., Chaudhry, Z. H.: Indian J. Chem., **16 B**, 559 (1978)

[4] SINGH, H., MALHOTRA, R. K., LUHADIYA, N. K.: J. Chem. Soc. Perkin I, **1974**, 1480
[5] SINGH, H., BUTANI, K. K., GUPTA, L. R.: J. Chem. Soc. Perkin I, **1976**, 1210
[6] SINGH, H., PADMANABHAN, S., BOSE, A. K., KUGAJEVSKY, I.: J. Chem. Soc. Perkin I, **1972**, 993
[7] MOURAL, J., SYHORA, K.: Coll. Czechoslov. Chem. Commun., **35**, 2018 (1970)
[8] REICH, H., WALKER, F. E., COLLINS, R. W.: J. Org. Chem., **16**, 1753 (1951)
[9] AKAGI, S., TSUDA, K.: Chem. Pharm. Bull. (Tokyo), **9**, 464 (1961)
[10] KHAN, I. A.: Ph. D. Thesis, Aligarh Muslim University Aligarh (1977)
[11] ROSS, W. C. J.: J. Chem. Soc., **1946**, 737

Mubarak HUSAIN
S. Rafat HUSAIN
M. S. AHMAD
Department of Chemistry, Aligarh Muslim University
Aligarh–202001 India

Acta Chimica Academiae Scientiarum Hungaricae, Tomus 104 (1), pp. 85—87 (1980)

THE BIRCH REDUCTION OF SOME OXYGEN HETEROCYCLES

Á. MAJOR, Z. NAGY and M. NÓGRÁDI*

(Research Group for Alkaloid Chemistry of the Hungarian Academy of Sciences, Budapest)

Received May 2, 1979
Accepted for publication June 27, 1979

On reduction with lithium-ammonia the chromone derivatives **1—5** and the aurone **6** gave by reductive ring opening the corresponding 2-hydroxyacetophenone derivatives **7—11**.

Since there is no satisfactory method available for the transformation of isoflavones to isoflavan-4-ones, further because alkali metal-ammonia is a standard reagent for the reduction of the carbon-carbon double bond in α,β-unsaturated carbonyl compounds [1], we attempted the reduction of 7-methoxyisoflavone to 7-methoxyisoflavan-4-one with lithium-ammonia. This gave, however, the α-methyl ketone **7** in 65% yield, without any chromatographically detectable intermediate. The result was not without precedent since in the reduction of 3-alkoxy-2-cyclohexenones cyclohexanone was detected as a minor by-product [2] and the reduction of 3,3',4',5,7-pentamethoxyflavone with sodium-ammonia yielded 1-(2-hydroxy-4,6-dimethoxyphenyl)-propan-1-one [3].

Subsequently some other typical oxygen heterocycles containing an enone moiety (**2—6**) were subjected to reduction with lithium-ammonia. All of them gave the corresponding acyclic ketone as the only isolable product [**2** → **8** (13%), **3** → **9** (40%), **4** → **10** (21%), **5** → **11** (6%) and **6** → **9** (30%)] except for **5**, where the main product was not **11** but 2'-hydroxybutyrophenone [4] (32%). The latter was presumably obtained by successive Birch reduction and rearomatization of **11**.

Likely intermediates for the described reductive ring cleavage are the corresponding saturated cyclic ketones, which would open by retro-Michael addition to acyclic α,β-unsaturated ketones, the latter being then reduced to the end-product [3]. This proposition, however, could not be confirmed by our experiments: partial reduction of **1** afforded no 7-methoxyisoflavan-4-one [5], further the reduction of pure 7-methoxyisoflavan-4-one gave a complex mixture in which none of the ketone **7** could be detected.

---

* To whom correspondence should be addressed

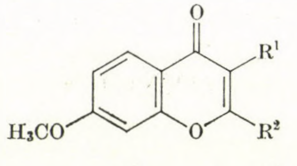

	R^1	R^2
1	Ph	H
2	Ph	CH_3
3	H	Ph
4	H	H
5	H	CH_3

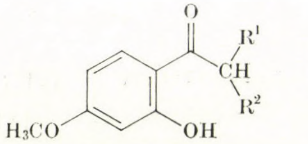

	R^1	R^2
7	Ph	CH_3
8	Ph	CH_2CH_3
9	CH_2Ph	H
10	CH_3	H
11	CH_2CH_3	H

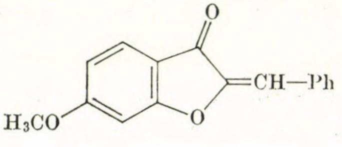

6

Though the yields of the ketones **7—11** were generally low, except for 2'-hydroxybutyrophenone, no well-defined by-product could be isolated from the reaction mixtures. The balance is presumably made up by polymeric products.

Experimental

1 [6], **2** [7], **3** [8], **4** [9], **5** [10], **6** [11], **9** [12], **10** [13], and **11** [14] are known compounds and were identified by their m.p.s. and ^{1}H—NMR spectra.

General method

The substrate (10 mmoles) was dissolved or suspended in dry liquid ammonia (100 ml) and small pieces of clean lithium metal (42—50 mg-atom) were added until persistant blue coloration appeared. After quenching the mixture with ammonium chloride, the ammonia was evaporated and the product extracted with chloroform. Evaporation gave the crude product which was purified by recrystallization or column chromatography on silica gel to give the product in the yields shown above.

1-(2-Hydroxy-4-methoxyphenyl)-2-phenylpropan-1-one (7)

M.p. 108 °C (EtOH);

^{1}H—NMR ($CDCl_3$): $\delta = 1.52$ (d, $J = 6.5$ Hz, 3H, 3-H), 3.74 (s, 3H, OMe), 4.61 (q, $J = 6.5$ Hz, 1H, 2-H), 6.30 (q, $J_0 = 10$ Hz, $J_m = 2.5$ Hz, 1H, 5'-H), 6.47 (s, 1H, 3'-H), 7.25 (s, 5H, Ph), 7.66 (d, $J = 10$ Hz, 1H, 6'-H), 12.97 (s, 1H, OH).

$C_{16}H_{16}O_3$ (256.3). Calcd. C 74.98; H 6.29. Found C 74.76; H 6.24%.

1-(2-Hydroxy-4-methoxyphenyl)-2-phenylbutan-1-one (8)

M.p. 87 °C (EtOH);

^{1}H—NMR ($CDCl_3$): $\delta = 1.89$ (t, $J = 7$ Hz, 3H, 4-H), 2.0 (mc, 2H, 3-H), 3.71 (s, 3H, OMe), 6.32 (t, $J = 7.5$ Hz, 1H, 2-H), 6.15—6.43 (m, 2H, 3',5'-H), 7.20 (s, 5H, Ph), 7.65 (d, $J = 10$ Hz, 1H, 6'-H), 12.70 (s, 1H, OH).

$C_{17}H_{18}O_3$ (270.3). Calcd. C 75.53; H 6.71. Found C 75.67; H 6.50%.

REFERENCES

[1] CAINE, D.: Org. Reactions, **23,** 1 (1976)
[2] SPASSKY—PASTEUR, A.: Bull. Soc. Chim. France, **1969,** 2900
[3] SWEENY, J. G., REDFORD, T., JACOBUCCI, G. A.: Heterocycles, **7,** 57 (1977); J. Org. Chem., **44,** 1494 (1979)
[4] FABBRINI, L.: Ann. Chim. (Roma), **46,** 130 (1956)
[5] INOUE, N.: Nippon Kagaku Zasshi, **79,** 1124 (1958)
[6] BAKER, W., POLLARD, A., ROBINSON, R.: J. Chem. Soc., **1929,** 1473
[7] HEILBRON, J. M., HEY, D. H., LYTHGOE, B.: J. Chem. Soc., **1936,** 295
[8] ROBINSON, R., TURNER, M. R.: J. Chem. Soc., **113,** 876 (1918)
[9] KOSTANECKI, S., DE TUYTER, J. C., DE WILDT, A.: Ber. dtsch. chem. Ges., **35,** 861 (1902)
[10] KOSTANECKI, S., ROZYCKI, A.: Ber. dtsch. chem. Ges., **34,** 108 (1901)
[11] BRÜLL, P., FRIEDLÄNDER, P.: Ber. dtsch. chem. Ges., **30,** 301 (1897)
[12] CRABTREE, H. G., ROBINSON, R.: J. Chem. Soc., **113,** 870 (1918)
[13] TAHARA, Y.: Ber. dtsch., chem. Ges., **25,** 1298 (1892)
[14] ISRAELSTAMM, S. S., STEPHEN, H.: J. S. African. Chem. Inst., **26,** 41 (1943)

Ádám MAJOR
Zoltán NAGY
Mihály NÓGRÁDI
H-1521 Budapest, P. O. B. 91.

Acta Chimica Academiae Scientiarum Hungaricae, Tomus 104 (1), pp. 89—96 (1980)

DIVALENT MANGANESE, COBALT, NICKEL AND COPPER COMPLEXES OF THIO-SCHIFF BASES DERIVED FROM *S*-METHYLDITHIOCARBAZATE AND 2-HYDROXY-1-NAPHTHALDEHYDE AND 2-HYDROXY-(5-BROMO)-ACETOPHENONE

S. K. SENGUPTA, S. K. SAHNI and R. N. KAPOOR*

(*Department of Chemistry, University of Delhi, Delhi-110007, India*)

Received May 11, 1979
Accepted for publication June 27, 1979

Mn(II), Co(II), Ni(II) and Cu(II) complexes of two thio-Schiff bases, *S*-methyl-β-*N*-(2-hydroxynaphthyl)methylenedithiocarbazate (H_2NMT) and *S*-methyl-β-*N*-(2-hydroxy-5-bromophenyl)methylenedithiocarbazate (H_2BMT) have been synthesized and characterized by means of infrared and electronic spectra, electric conductivity and magnetic susceptibility measurements. The manganese(II) complexes are tetrahedral, while nickel(II) and copper(II) complexes have square planar stereochemistry, and cobalt(II) complexes are octahedral. Various ligand field (10 Dq) and nephelauxetic parameters (B, C and β) calculated for the cobalt(II) complexes are consistent with octahedral stereochemistry.

Introduction

In recent years there has been considerable interest in the complexes of thio-Schiff bases containing NS and NSO donor atoms [1—5]. The increased interest in this field may be attributed to the striking structural features and the reported carcinostatic and antiviral activity of SN and SNO donor ligands and the complexes [1, 3] derived therefrom. It has also been observed that a small structural change, such as the change of a substituent, may lead to an enhanced anti-cancer and anti-viral activity of transition metal complexes [4]. With this view, it has been considered worthwhile to investigate the synthetic and structural aspects of transition metal complexes of the thio-Schiff bases derived from *S*-methyldithiocarbazate and 2-hydroxy-1-naphthaldehyde (H_2NMT) and 2-hydroxy (5-bromo)-acetophenone (H_2BMT). The structures of ligands are depicted below:

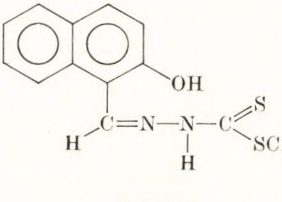

(H_2NMT)

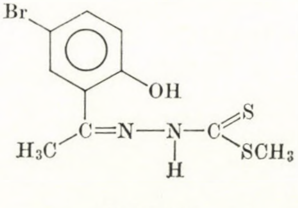

(H_2BMT)

---

* To whom correspondence should be addressed

Experimental

The ligands have been synthesized by the method of LIVINGSTONE *et al.* [4]. All the metal salts used were of analytical grade.

Preparation of the complexes

Two general procedures were adopted to synthesize the complexes.

(a) The complexes of manganese, nickel, copper were obtained by mixing an ethanolic solution of the ligands (0.005 mol) with the appropriate metal salt (0.005 mol) also dissolved in ethanol. The mixture was refluxed from 2 to 3 hrs. The polycrystalline complexes, settled down on cooling or on further concentration of the reaction mixture and subsequent cooling, were throughly washed with ethanol and acetone. Yield ~ 80–85%.

(b) The complexes of cobalt(II) were synthesized by mixing alcoholic solutions of cobalt chloride (0.01 mol) and the ligand (0.02 mol). The mixture was refluxed for about 2 hrs. The mass of the complexes obtained on cooling was washed with ethanol and acetone. Yield ~ 75%.

Elemental analysis and physical measurements

The metal content of the complexes was determined by EDTA titrations employing Eriochrome Black-T and Xylenol Orange as indicators.

The magnetic susceptibilities were measured by the Gouy method using mercury tetrathiocyanocobaltate(II) as calibrant. The infrared spectra were recorded in KBr pellets on a Perkin—Elmer-621 spectrophotometer and the electronic spectra were recorded in nujol mull on a Perkin—Elmer-4000A instrument and a Russian SF-10 (visible range) spectrophotometer. An Elico conductivity bridge type CM.82T was used for conductivity measurements.

Results and Discussion

The elemental analyses (Table I) indicate a 1 : 2 (metal to ligand) stoichiometry for Co(II) and a 1 : 1 stoichiometry for Mn(II), Ni(II) and Cu(II) complexes. These complexes are soluble in solvents such as dimethylformamide, dimethyl sulfoxide and nitrobenzene. The electrical conductance measured in dimethylformamide indicates that all the complexes are nonelectrolytes.

Infrared spectra

The IR spectra (Table II) of the ligands and the complexes are based on the earlier studies of similar compounds [1, 6]. The ligands show bands around 1460, 1240, 1040 and 690 cm^{-1}, which are attributable [7] to thioamide -I, -II, -III and -IV vibrations which indicate the existence of ligands in the thione form. The bands assigned to thioamide vibrations are not pure and have substantial contributions from $\nu C-N$, $\delta C-H$, $\delta N-H$ and $\nu C-S$ vibrations [6]. The band observed at 690 cm^{-1} is found to have maximum $\nu C\overset{\cdots}{=}S$ contribution. In the complexes, the thioamide IV bands shifts to lower frequencies ($\sim$20 cm^{-1}) and its intensity diminishes considerably [8]. The changes in these

Table I

Analytical and magnetic data of divalent metal complexes of thio-Schiff bases

Complex	Colour	Found (calcd.) percentage of					$\mu_{eff.}$ B. M. (300 K)
		C	H	N	S	M	
$[Mn(C_{13}H_{10}N_2S_2O)H_2O]$	Green	44.0 (44.9)	3.2 (3.4)	7.9 (8.0)	18.2 (18.4)	15.2 (15.8)	5.60
$[Mn(C_{10}H_9N_2S_2OBr)H_2O]$	Green	30.5 (30.7)	2.5 (2.8)	7.0 (7.1)	16.3 (16.4)	13.8 (14.0)	5.62
$[Co(C_{13}H_{10}N_2S_2O)(C_{13}H_{11}N_2S_2O)]$	Brown	50.9 (51.3)	3.2 (3.4)	8.9 (9.1)	21.2 (21.0)	9.2 (9.6)	2.20
$[Co(C_{10}H_9N_2S_2OBr)(C_{10}H_{11}N_2S_2OBr)]$	Green	32.5 (33.9)	2.1 (2.7)	7.5 (8.0)	18.1 (18.4)	8.1 (8.4)	4.20
$[Ni(C_{13}H_{10}N_2S_2O)H_2O]$	Red	44.2 (44.4)	3.1 (3.4)	7.3 (7.9)	18.1 (18.2)	16.6 (16.2)	Diamag.
$[Ni(C_{10}H_9N_2S_2OBr)H_2O]$	Dark brown	30.3 (30.7)	2.5 (2.8)	6.9 (7.1)	16.1 (16.3)	14.1 (14.2)	Diamag.
$[Cu(C_{13}H_{10}N_2S_2O)H_2O]$	Dark green	43.7 (43.8)	3.0 (3.8)	7.6 (7.8)	18.0 (18.0)	17.3 (17.8)	1.7
$[Cu(C_{10}H_9N_2S_2OBr)H_2O]$	Dark green	29.7 (30.1)	2.6 (2.7)	7.1 (7.0)	16.2 (16.0)	15.6 (15.9)	2.1

Table II

Important infrared spectral band (cm^{-1}) of ligands and divalent metal complexes

Compound	ν(OH)	ν(C=N)	ν(C—O)	Thioamide I	Thioamide II	δ(C—O)	Thioamide III	Thioamide IV	ν(M—O) phenolic	ν(—MS)	ν(M—N)
H_2NMT	3200s	1635m	1560s	1460m	1240m	1260s	1040s	690w	—	—	—
H_2BMT	3200s	1630m	1560s	1460m	1240m	1260s	1040s	690w	—	—	—
$[Mn(NMT)H_2O]$	3400s	1620m	1565s	1450s	1245s	1265s	1025m	680w	425w	365w	200w
[Co(NMT)(HNMT)]	3200s	1625s	1570s	1455s	1250m	1265s	1030s	1020m	470w	345w	425w
$[Ni(NMT)H_2O]$	3400s	1620s	1565s	1450s	1250w	1270s	1030m	680w	410w	400w	450w
$[Cu(NMT)H_2O]$	3400s	1615s	1565s	1450s	1250m	1265m	1028m	680w	430w	318w	480w
$[Mn(BMT)H_2O]$	3400s	1615s	1565s	1450s	1245s	1270m	1020m	680w	420w	370w	310w
$[Co(BMT)H_2BMT)]$	3200s	1620m	1570s	1455s	1245m	1265s	1020m	675m	480w	330w	445w
$[Ni(BMT)H_2O]$	3400s	1615s	1565m	1455s	1248m	1265s	1020w	670w	415w	395w	490w
$[Cu(BMT)H_2O]$	3400s	1610s	1570s	1445s	1245m	1275m	1020m	680w	430w	318w	520w

bands are consistent with the coordination of sulfur to a metal atom [6, 8]. In the far IR region, the bands appearing at ca. 365—370, 330—345, 395—400 and 318 cm^{-1} may be assigned to ν(Mn—S), ν(Co—S), ν(Ni—S) and ν(Cu—S) vibrations [9], respectively. The value of ν(Co—S) is in the range observed for six-coordinate pseudo-octahedral complexes of these metal ions while the ν(Mn—S), ν(Ni—S) and ν(Cu—S) are consistent with a four-coordinate tetrahedral and square planar geometry [10].

A strong band appearing at *ca.* 1635 cm^{-1} due to ν(C=N) in thio-Schiff bases, occurs at lower frequencies ($\sim$15 cm^{-1}) in the complexes. This lowering indicates coordination of the nitrogen of the azomethine linkage to the metal [11]. The bands appearing at *ca.* 300—310, 425—445, 450—490 and 480—520 cm^{-1} are attributed to ν(Mn—N), ν(Co—N), ν(Ni—N) and ν(Cu—N) vibrations [10], respectively.

The bands appearing at *ca.* 3200 cm^{-1} are assigned to ν(OH) vibrations of the phenolic group. The occurrence of the ν(OH) vibration in a lower region indicates the presence of intramolecular hydrogen bonding [12]. It is also supported by the presence of weak bands at *ca.* 2650—2700 cm^{-1}. In the complexes, these bands disappear, thereby indicating the involvement of a phenolic oxygen in coordination through deprotonation. The weak bands appearing at *ca.* 425, 480, 410 and 430 cm^{-1} may be assigned [13] to ν(Mn—O), ν(Co—O), ν(Ni—O) and ν(Cu—O) vibrations (phenolic), respectively. Two more bands at *ca.* 1560 and 1260 cm^{-1} appear due to ν(C—O) and δ(C—O) vibrations of the phenolic group in the ligands. In the complexes, these bands appear at slightly higher frequencies ($\sim$10 cm^{-1}), thereby indicating the coordination of a phenolic oxygen to metal atom [14]. However, in cobalt(II) complexes a broad band around 3200 cm^{-1}, similar to that in the ligands, is assigned to ν(OH) of the phenolic groups. It appears that the phenolic group of one molecule of the thio-Schiff base coordinates to the metal atom through deprotonation while in the other coordination takes place without deprotonation of the phenolic group. The conclusive evidence for such a mode of coordination of the ligands comes from the appearance of four instead of two bands in the regions of C—O stretching and bending vibrations of the phenolic groups. The cobalt(II) complexes show bands at 1570, 1550, 1265 and 1250 cm^{-1}. If there is considerable shift in the position of ν(C—O) and δ(C—O) bands, it indicates the presence of dimeric or polymeric oxo-bridged structures [15]. However, these complexes appear to be monomeric.

The spectra of manganese(II), nickel(II), copper(II) complexes show additional bands at *ca.* 3400, 1640 and 850 cm^{-1}. These bands indicate the presence of coordinated water 15 and, accordingly, may be assigned to ν(OH), δ(OH) and $\varrho_n(H_2O)$. The weak bands appearing at *ca.* 500 cm^{-1} may be assigned to ν(M—O) vibrations [13].

Magnetic and electronic spectral studies

Manganese(II) complexes. The magnetic moments lie around 5.6 B.M. at room temperature, indicating the high-spin nature of these complexes [6]. Since high-spin manganese(II) complexes have an orbitally non-degenerate ^6S ground term, the spin-only magnetic moments of these complexes are expected to be temperature independent [6, 16].

The electronic spectra of manganese(II) complexes show bands at *ca.* 19 000—21 500, 21 500—22 000, 25 000—25 500 and 27 000—27 500 cm^{-1}. The tetrahedral manganese(II) complexes generally show a number of bands between 19 000—28 000 cm^{-1} while in octahedral complexes, in addition to other bands, one band around 15 000 cm^{-1} is observed [17, 18]. The position of the bands of the present complexes is comparable with those of tetrahedral manganese(II) complexes, whose structure has been established on the basis of X-ray studies [17]. Accordingly, these bands may be assigned [17—19] to $^6A_1 \rightarrow {}^4T_1$ (G), $^6A_1 \rightarrow {}^4T_2$ (G), $^6A_1 \rightarrow {}^4T_2$ (D) and $^6A_1 \rightarrow {}^4E$ (D) transitions in the increasing order of energy.

Cobalt(II) complexes. The room temperature $\mu_{\text{eff.}}$ values of Co(II)—H_2NMT and Co(II)—H_2BMT complexes are 2.2 and 4.2 B.M., respectively. The values are lower than those observed for high-spin tetrahedral or octahedral complexes. This lowering may arise on account of the (i) presence of cobalt(III) species, (ii) covalent nature of the metal-ligand bond, (iii) presence of low symmetry components and (iv) an equilibrium between high-spin and low-spin ($^4A_2 \rightleftharpoons {}^2T_2$) states [20].

The Co(II)—H_2NMT appears to be a mixture of cobalt(II) and cobalt(III) species. In the Co(II)—H_2BMT complex, a slight lowering in $\mu_{\text{eff.}}$ may be attributed to the covalent nature of the metal-sulfur bond and the presence of lower symmetry components.

The electronic spectrum of Co(II)—H_2NMT shows bands at *ca.* 20 400, 21 700, 22 700 and 24 300 cm^{-1}, whereas the Co(II)—H_2BMT complex shows bands around 8000, 17 000 and 20 000 cm^{-1}. The electronic spectra of six-coordinate cobalt(II) complexes generally show three bands due to $^4T_{1g} \rightarrow {}^4T_{2g}$, $^4T_{1g} \rightarrow {}^4A_{2g}$ and $^4T_{1g} \rightarrow {}^4T_{1g}$(P) transitions [21]. The band appearing at 20 400 cm^{-1} in the H_2NMT complex may be due to a $^4T_{1g} \rightarrow {}^4T_{1g}$(P) transitions. The presence of other bands in the vicinity of 20 000 cm^{-1} indicates the presence of cobalt(III) species in this complex, which also absorbs in this region due to $^1A_{1g} \rightarrow {}^1T_{1g}$ and $^1A_{1g} \rightarrow {}^1T_{2g}$ transitions [21]. In view of the uncertain nature of the complex, no attempt has been made to calculate ligand field and nephelauxetic parameters. In the Co(II)—H_2BMT complex, the position of three bands observed are comparable to those observed for other cobalt(II) octahedral complexes involving SNO donor atoms [22]. These bands can be assigned to $^4T_{1g} \rightarrow {}^4T_{2g}$, $^4T_{1g} \rightarrow {}^4A_2$ and $^4T_{1g} \rightarrow {}^4T_{1g}$ (P) transitions in the increasing order of energy. The spectrum of the Co(II)—H_2BMT complex is rationalized in terms of ligand field parameter 10 Dq and nephelauxetic parameters (B, C and β), employing the equations suggested by Lever [21]. The values of 10 Dq, B, C and β come out to be 10 000 cm^{-1}, 955 cm^{-1}, 3820 cm^{-1} and 0.97, respectively. These values are in the range reported for other octahedral cobalt(II) complexes involving SNO donor atoms [22].

Nickel(II) complexes. The thio-Schiff base complexes of nickel(II) are diamagnetic.

The electronic spectra of these complexes show a broad band in the region of 18 000—20 000 cm^{-1}. In the case of the Ni(II)—H_2NMT complex, another band is observed at 10 500 cm^{-1}. The fact that no band is observed below 10 000 cm^{-1} indicates a square planar stereochemistry for these complexes [21], which may also be deduced from their red-brown colour and diamagnetic nature.

In general, the square planar complexes exhibit two strong absorption bands in the visible region between 15 000—25 000 and 23 000—30 000 cm^{-1}. These are referred [21] to as ν_2 and ν_3 bands. The square planar complexes with sulfur ligands generally exhibit an additional well-defined band to lower energies than ν_2 around 11 000 cm^{-1}. This is referred to as ν_1. In the present complexes, the 18 000—20 000 cm^{-1} band (ν_2) may be assigned to ${}^1A_{1g} \rightarrow {}^1A_{2g}$ transition ($b_{2g} \rightarrow b_{1g}$).

Copper(II) complexes. The magnetic moment of Cu(II)—H_2NMT and Cu(II)—H_2BMT are 1.7 and 2.1 B.M. at room temperature, respectively. The values observed for these complexes are in the range for high-spin copper(II) complexes having monomeric structures [23].

The electronic spectra of both complexes show bands around 20 800, 22 000 and 23 000 cm^1. The position of the bands indicates that these complexes have a square planar stereochemistry [21]. A large number of copper(II) complexes possessing a square planar structure are known, but there still exists confusion regarding the ordering of orbitals in square planar copper(II) species. For instance, it has been shown that the highest orbital is ${}^2b_{1g}$ ($d_{x^2-y^2}$) but beyond that there is little agreement [24]. Hatfield and Piper [25] have made crystal field calculations and obtained the ordering $d_{x^2-y^2} > d_{z^2} > d_{xy} > d_{xz}$, d_{yz}. On the other hand, Schuit *et al.* [26] have placed the d_{y^2} orbital lowest on the basis of Wolfsberg—Helmholtz calculations. In the present complexes the band appears to have its origin in d—d transitions, which can be assigned to ${}^2B_{1g} \rightarrow {}^2A_{1g}$ and ${}^2B_{1g} \rightarrow {}^2E_g$ transitions in increasing order of energy. The appearance of a high energy band at *ca.* 23 000 cm^{-1} is a subject of lively discussion in recent years. Some authors have attributed the presence of this band to polymeric structures of the copper complexes [27]. However, in the present case, it appears to be due to charge transfer phenomena.

*

One of the authors (S. K. SENGUPTA) is thankful to the Centre of Advanced Study, University of Delhi, Delhi for financial assistance.

REFERENCES

[1] ALI, M. A., LIVINGSTONE, S. E.: Coord. Chem. Rev., **13**, 101 (1974)
[2] CLEARE, M. J.: Coord. Chem. Rev., **12**, 349 (1974)
[3] WILLIAMS, D. R.: Chem. Rev., **72**, 203 (1972)
[4] DAS, M., LIVINGSTONE, S. E.: Inorg. Chim. Acta, **19**, 5 (1976)
[5] SAHNI, S. K., JAIN, P. C., RANA, V. B.: Indian J. Chem.,**A 16**, 699 (1978)
[6] SAHNI, S. K., RANA, V. B.: Indian J. Chem., **15 A**, 890 (1977)
[7] RAO, C. N. R.: Chemical Applications of Infrared Spectroscopy, 300 p., Academic Press, 1963
[8] SAHNI, S. K., RANA, V. B., JAIN, P. C., SWAMI, M. P., SRIVASTAVA, A. K.: J. Inorg. Nucl. Chem., **38**, 176 (1976)
[9] SAHNI, S. K.: Ph. D. Thesis, Meerut University, Meerut 1975
[10] ADAMS, D. M.: Metal Ligand and Related Vibrations, E. Arnold, London 1967
[11] SAHNI, S. K., RANA, V. B.: J. Inorg. Nucl. Chem., **39**, 2271 (1977)
[12] RASTOGI, D. K., SAHNI, S. K., RANA, V. B., DUA, S. K.: J. Coord. Chem., **8**, 97 (1978)
[13] NAKAMOTO, K.: Infrared Spectra of Inorganic and Coordination Compounds. Wiley Interscience, New York 1970
[14] RASTOGI, D. K., DUA, S. K., RANA, V. B., SAHNI, S. K.: J. Inorg. Nucl. Chem., **40**, 1323 (1978)
[15] JØRGENSEN, C. K.: Inorg. Chim. Acta Rev., **2**, 65 (1968)
[16] FIGGIS, B. N.: Introduction to Ligand Field Theory, 28 p. Interscience, New York 1967
[17] GOODGAME, D. M. L., COTTON, F. A.: J. Chem. Soc., **1961**, 3735; J. Am. Chem. Soc., **83**, 177 (1961)
[18] GOODGAME, D. M. L., COTTON, F. A., GOODGAME, M.: J. Am. Chem. Soc., **83**, 4690 (1961); **84**, 167 (1962)
[19] RASTOGI, D. K., SAHNI, S. K., RANA, B. V., DUA, S. K.: Transition Met. Chem., **3**, 56 (1978)
[20] ALI, M. A., LIVINGSTONE, S. E., PHILLIPS, D. J.: Inorg. Chim. Acta, **5**, 493 (1971)
[21] LEVER, A. B. P.: Inorganic Electronic Spectroscopy, 277 p. Elsevier, Amsterdam 1968
[22] KENNEDY, B. P., LEVER, A. B. P.: Can. J. Chem., **50**, 3488 (1972)
[23] KATO, M., FANNING, J. C., JONASSEN, H. B.: Chem. Rev., **64**, 99 (1969)
[24] WILLETT, R. D., LILES, Jr, O. L., MICHELSON, C.: Inorg. Chem., **6**, 1885 (1967)
[25] HATFIELD, W. E., PIPER, T. S.: Inorg. Chem., **3**, 841 (1964)
[26] ROS, D., SCHUIT, G. C. A.: Theoret. Chim. Acta, **4**, 1 (1966)
[27] PROCTER, I. M., HATHAWAY, B. J., HODGSON, P. G.: J. Inorg. Nucl. Chem., **34**, 3698 (1972); BILLING, D. E., HATHAWAY B. J., NICKOLIS, P.: J. Chem. Soc., (A), **1969**, 316; HATHAWAY, B. J., BILLING, D. E., DUDLEY, R. J.: J. Chem. Soc. (A), **1970**, 1420

S. K. SENGUPTA
S. K. SAHNI
R. N. KAPOOR

Department of Chemistry, University of Delhi
Delhi — 110 007, India

Acta Chimica Academiae Scientiarum Hungaricae, Tomus 104 (1), pp. 97–99 (1980)

SYNTHESIS OF ISONEOPINE

(Preliminary communication)

S. Berényi and S. Makleit*

(Institute of Organic Chemistry, Kossuth Lajos University, Debrecen)

Received October 15, 1979
Accepted for publication December 19, 1979

Isoneopine is a useful starting material for the synthesis of *B/C-trans* morphine derivatives [1], which are important from both the theoretical and pharmacological points of view.

Isoneopine was first prepared by **Okuda** *et al.* [2] by the reduction of 14-bromocodeine with sodium tetrahydridoborate(III), in about 10% yield.

The most commonly used procedure for the preparation of isoneopine is the reduction of neopine. Contrary to earlier literature data [5], **Okuda** *et al.* [2, 4] and **Abe** *et al.* [3] found that the reduction of neopinone with sodium tetrahydridoborate(III) was not stereoselective [6]; neopine and isoneopine were obtained in 1 : 1 ratio.

Wunderly *et al.* [7] succeeded in converting neopinone into neopine by stereoselective reduction. However, when they prepared isoneopine in this way, the selectivity was only 90%, and 10% neopine was obtained as a by-product.

Inconvenience of the above-mentioned methods is that either the yield of isoneopine is low, or the starting material is difficult of access. Namely, the preparation of codeine-free neopinone is quite difficult [1] and the enantiomers must be resolved. For this reason, these procedures cannot be used conveniently for the preparation of substantial amounts of isoneopine.

Procedures worked out for the synthesis of isomorphine, isocodeine and dihydroisocodeine [8, 9] did not give the expected results when applied to 6-*O*-mesylneopine [10].

A simple convenient procedure has now been developed *via* the following reaction steps. The reaction of 6-*O*-mesylneopine (**1**) with sodium azide in dimethylformamide gave the azido derivative (**2**) in 75% yield [10]. Compound (**2**) was reduced with zinc sodium iodide in dimethyl formamide to obtain the amino derivative (**3**) in 65% yield [10].

To our knowledge, the deamination of C-6 and C-8 amino derivatives of morphine alkaloids has not yet been investigated, although this reaction is

---

* To whom correspondence should be addressed.

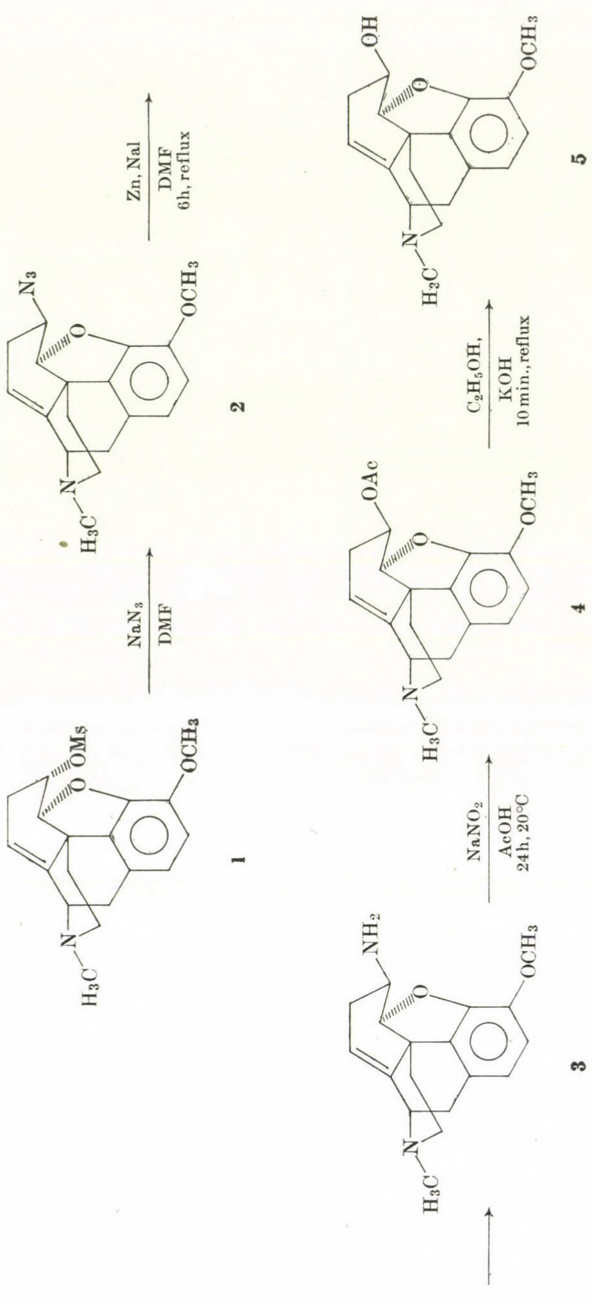
H3C
N
OMs
O
OCH3
1
NaN3
DMF
H3C
N
N3
O
OCH3
2
Zn, NaI
DMF
6h, reflux
H3C
N
NH2
O
OCH3
3
NaNO2
AcOH
24h, 20°C
H3C
N
OAc
O
OCH3
4
C2H5OH,
KOH
10 min., reflux
H3C
N
OH
O
OCH3
5

important from the theoretical point of view, and it was thoroughly studied in other fields [*e.g.* 11, 12, 13].

The amino derivative (**3**) gave the known 6-*O*-acetylisoneopine (**4**) [1, 14] in 90% yield on treatment with sodium nitrite in acetic acid. Neopine, 6-*O*-acetylneopine and demethoxythebaine [10] were not obtained in this way. Saponification of compound (**4**) with alcoholic potassium hydroxide afforded isoneopine (**5**) quantitatively.

Thus, isoneopine was prepared in 44% yield by simple, convenient reaction steps starting from neopine. This procedure makes possible the synthesis of required amounts of isoneopine by optional scale-enlargement.

REFERENCES

[1] INOUE, H., TAKEDA, M., KUGITA, H.: Chem. Pharm. Bull., **18**, 1569 (1970)
[2] OKUDA, S., ONDA, M., YAMAGUCHI, S.: J. Org. Chem., **27**, 4121 (1962)
[3] ABE, K., ONDA, M., OKUDA, S.: Chem. Pharm. Bull., **17**, 1847 (1969)
[4] OKUDA, S., YAMAGUCHI, S., TSUDA, K.: Chem. Pharm. Bull., **13**, 1092 (1965)
[5] CONROY, H.: J. Am. Chem. Soc., **77**, 5960 (1955)
[6] To the definition of selectivity and specificity, see AUALT, A.: J. Chem. Educ., **54**, 614 (1977)
[7] WUNDERLY, S. W., BROCKMANN-HANSSEN, E.: J. Org. Chem., **42**, 4277 (1977)
[8] MAKLEIT, S., BOGNÁR, R.: Acta Chim. Acad. Sci. Hung., **59**, 387 (1969)
[9] MAKLEIT, S., BOGNÁR, R.: Acta Chim. Acad. Sci. Hung., **64**, 281 (1970)
[10] BERÉNYI, S., MAKLEIT, S., BOGNÁR, R., TEGDES, A.: Acta Chim. Acad. Sci. Hung. (in the press)
[11] SCHREIBER, K., RIPPERGER, H.: Ann., **655**, 136 (1962)
[12] SNATZKE, G., VEITHEN, A.: Ann., **703**, 159 (1967)
[13] BACHELOR, F. W., WHITE, E. H.: Can. J. Chem., **50**, 364 (1972)
[14] OKUDA, S., YAMAGUCHI, S., KAWAZOE, Y.: Chem. Pharm. Bull., **12**, 104 (1964)

Sándor BERÉNYI
Sándor MAKLEIT
H-4010 Debrecen, P.O.Box 20

RECENSIONES

Topics in Current Chemistry, Vol. 77

Inorganic and Physical Chemistry

by J. J. Bikerman, H. G. Wiedemann, G. Bayer, M. B. Huglin

edited by Springer Verlag Berlin, Heidelberg, New York, 1978, p. 233

In the present stream of the informations the orientation in the literature and to process its results is impossible in the usual old way — as it was already pointed out several times. Informations provided by the computerized data banks — if they are available — may be of great help, however, even these lack one important feature, namely, the critical selection. This is why I find the *critical* processing of the results of any single field the most useful and indispensable help as compilation of monographies also requires a tremendous effort. Due to some devoted authors and far-seeing editors increasingly great number of such works (progress, review, topics, *etc.)* have recently been published.

The work to be reviewed is the 77. volume of the series "Topics in Current Chemistry" edited by the Springer Verlag. The most important features of this whole series are the critical selection of the results, the outline of the present state and the future trends. To meet the requirements of these three aspects can be only expected from an outstanding author. The volume in question contains three studies which at first glance may seem quite heterogeneous, however, they are interlinked with each other.

The first part is dealing with the surface energy of solids authored by J. J. Bikerman (Dept. of Chemical Engineering, Case Western Reserve University, Cleveland). The idea of surface tension has been well known at liquids since long time, however, its theoretical interpretation, moreover its experimental determination at solids — where the pretreatment of the material has extremely great influence on properties — is quite difficult. Therefore, the importance of the effort to calculate the energy from the interactions operating between the elementary particles cannot be overrated. Unfortunately, it has not yet been cleared up on what model this calculation could be done. The calculation of lattice energy on the basis of atomic parameters is quite accurate, error within 1%, but at surface tension calculations it is not rare that the error amounts to 300%. The semi-empirical calculations yield only average and not surface specific values which refers to its physical meaning, too.

According to Russian researches γ_s is proportional to $T_m/V^{2/3}$ while English authors said γ_s to be proportional to T_m/r^2 what are as a matter of fact identical requirements.

At one of the experimental methods it is considered that the gravity tends to lengthen the test body, while the surface tension tends to shorten it. This simple idea, however, neglects essential factors, not to speak of the influence of the quality of the surrounding gas. To the analogy of capillary pressure of liquids, measurements were performed on crystals of small size. The results obtained are, however, uncertain because of the irregularity (not ideal smoothness) of the surface. For solids, the bubble method, based on electronmicroscopic observation, seems to be a simple technique, but here too, the tensile strength of the block material can hardly be taken into account.

Some ingenious variations of the Thomson (1871) vapour pressure equation have also been introduced, however, doubts here also arised, similarly to the dissolution of materials of different grain size.

The concept stated on the similarity of surfaces of solids and liquids is about to disappear, since just the structures of these two phases are different. A new idea, the cuticular energy has been introduced, but it seems to produce another complicating factor instead of giving solution for the basic problem: for the determination of the surface energy of solids.

Considering the role of surfaces in various processes in general, and especially in the case of catalysts and catalyst carriers, further on in powder metallurgical and ceramic processes, nobody can deny the importance of knowing the surface energy. Thus the author is frank and right even these days, when he says: "No method so far suggested for measuring the surface energy of surface tension of solids is satisfactory". This deficiency originates from a lot of causes of the nature of solid phase. From among these I should like only to point out the follow ings: *a)* the chemical composition of the surface is different from that of bulk substance (*e.g.* oxide layer); *b)* the finer the grain sizes are, the greater is the possibility of crystal defects and of impurity influence. Both of them give grounds for the introduction of a new factor, the cuticular energy.

The paper — outlining these problems — satisfies the aim of the series to direct attention to the future trends.

The second paper of the volume is dealing with the solid phases, too, but in a more familiar and practical way, when summarizing the theory, the means and results of thermal analysis. The temperature changes yield informations regarding such properties of solids which could be gained also in different ways, although not so directly and many-sidedly as by the two main methods of thermal analysis: the thermogravimetry and DTA. These methods have been developed only lately, because instruments of adequate accuracy and sensitivity were lacking. The last three-four decades, however, brought along the construction of such instruments which are able to measure the consequences of temperature changes accurately, reproducibly and sensitively. These new kinds of thermobalances can not only register, but also automatically record, derivate, draw, *etc.* the measured data. Unfortunately, the instrument is sometimes too clever, leaving few opportunity for the research worker to think. Owing to this fact the number of papers published in the field of thermal analysis is growing faster than those of other fields, however, frequently without complete analysis and evaluation of informations obtained by the expensive instrument.

The paper consists of two parts. In the first one the instruments and their accessories, and the experimental techniques are described by the most authentic author, H. G. WIEDEMANN, who constructed the famous Mettler Vacuum Thermobalance. Here not only a simple technical description of the thermobalance is given, but also such details are presented which may serve with new and useful informations even for a practising thermoanalyst. This manual-like paper summarizes valuable points of view when discussing the features of samples and experimental conditions.

The second part of the paper demonstrates examples of application. First of all typical cases are disscussed emphasizing special characteristics. Of course, the selection of these examples is the right of the author and it not always necessarily agrees with that of the reviewer. It is true, however, that beside the experimental results the deeper characteristics of the process are less detailed. (On page 116 there is a striking misprinting on the effect of oxygen pressure). We agree with the author's conclusion that the theoretical background of thermoanalytical methods is already well known, but by this fact we should not be mislead, because the mechanism of thermal reactions is only scarcely understood.

Since the classical molecule concept has been formulated and the physical reality of great molecular weights ($> 10^2 - 10^3$), the importance of their knowledge have become proven, several experimental methods for the determination of high molecular weights have been developed. The chemistry of organic, plastics, polymer and biological reactions required primarily these measurements, however, increasingly often arises the need to know the molecular weight also of inorganic polymers and even to follow polycondensation processes. A significant technological example for the latter is the decomposition of aluminate solutions, the precipitation of aluminium hydrate.

In addition to purely chemical (and radiochemical) processes — due to their wide applicability — the physical methods have spread: vapour pressure and membrane osmometry, various sedimentation processes and methods based on light scattering. From among these, the third part of the book deals with the molecular weight determination based on visible light scattering.

The light scattering on tiny particles has been known already since long, but it is only in this decade that light scattering on molecules in solution has been applied for the determination of molecular weight. A basic condition for this is that a sufficiently great difference should exist between the refractive indices of the solvent and solute and if an instrument of adequate sensitivity is available, then the range of molecular weight determination may reach even 10^{10} order of magnitude.

The basic equations of light scattering were formulated by **Rayleigh**, **Smoluchowski**, **Debye** and others and presently we can classify 3 types of scatterings: *a)* Rayleigh-, *b)* Debye-, *c)* Mie-scattering. The class is dictated by two parameters namely the relative refractive index (n) and the relative size parameter D/λ where D is the greatest particle dimension and λ is the wavelength of the light in the scattering medium:

Rayleigh scattering	$(n-1) \ll 1$	$D/\lambda < 1/20$
Debye scattering	$(n-1) \ll 1$	$1 > D/\lambda > 1/20$
Mie scattering	$(n-1)$ not $\ll 1$	$D/\lambda > 1$.

The theory has developed so far that at various real (not only ideal) solutions the influences of the various shapes can be considered, too.

For measuring the intensity of the scattered light recently we have stable light sources and instruments separating and measuring the incident and scattered light at our disposal. Some photometers include the facility for measuring polarisationg and changing the wavelength. The lasers play a remarkable role in this field, too. These photometers and their data processing suitably are detailed in the paper. The errors of results usually do not exceed 5%, most frequently lie only between 1 and 2%. Especially rich set of examples is given for the polymers.

The determination of the molecular weight based on light scattering is a widely used method, whose main advantage lies in its rapidity, while its drawback is that the sample must be absolutely free of every impurity, *i.e.* scattering contaminations.

The book can be of great help for researchers engaged in one of the above three fields.

Z. G. Szabó

Springer Series in Chemical Physics, 6
Laser induced processes in molecules

Physics and Chemistry

Editors: K. L. Kompa and S. D. Smith

367 pages, 196 figures

The book contains the Proceedings of the European Physical Society Divisional Conference held at the Heriot-Watt University, Edinburgh, Scotland, September 20–22, 1978. The conference was organized by the Quantum Electronics Divisional Board of the European Physical Society, and its aim was to assist the exchange of ideas and results between physicists and chemists active in the field. Divided into five parts, the book gives an account of "the state of the art".

Part I. Study of Lasers and Related Techniques Suitable for Applications in Chemistry and Spectroscopy. Different ways to generate laser radiation in new wavelength regions or with greater efficiencies using new lasing media or mixing techniques is dealt with in 8 papers. Due emphasis is given to the rare gas halide lasers. An interesting method is described for exposing mammalian cells to intense laser radiation.

Part II. Spectroscopic Studies with and Related to Lasers. A vast variety of systems is investigated ranging from diatomic molecules through simple species like HNO or CH_2 to large molecules like phthalocyanines and thio-indigo dyes. Detailed information concerning polarization spectra, energy transfer parameters and spectroscopy of given states in included. Unfortunately the diversity of this new knowledge is not summarized by a main paper. (Apparently, there were no main paper at the conference, but there are review papers in the coming parts.)

Part III. Multiphoton Excitation, Dissociation and Ionisation. Nearly one third of the papers delivered at the conference deals with multiphoton processes. The main aim of these works is isotope separation; most of the researchers intend to clarify different aspects of the underlying photophysical phenomena. A number of papers discuss different properties of

SF_6 upon excitation; nevertheless, even this well studied molecule is not fully understood. As a quantum mechanical treatment of the higher levels of a polyatomic molecule is impossible because huge basis sets would be required, recourse is made to classical and semiclassical methods. Different reactions are studied which could enable isotopic separation of several elements. Multiphoton dissociation is used for the characterization of interesting photofragments — laser induced fluorescence being the most important analytical tool. A few examples are given for multiphoton (mainly two-photon) driven chemical reactions utilizing visible or UV radiation.

Part IV. Laser Control of Chemical Reactions. **There are two important review papers in this chapter; one by R. N. ZARE on reactions with oriented reagents, the other by S. KIMEL on laser specific versus thermal reactions. Advanced experimental techniques make it possible to study state-selective reactions as well as to investigate the effect of the orientation of the reagents. Several papers report on van der Waals molecules, but SF_6 retains its specific role as the most frequently studied molecule. A very interesting paper by MANUCCIA and HSU considers the economical aspects of deuterium enrichment by cw vibrational photochemistry of methane — leading to the surprising conclusion, that the laser chemist should minimize the costs of the connected traditional chemical engineering factors as refrigeration and regeneration of reagents, rather than just striving for the highest enrichment factor. Once again the isotopically selective processes are among the most important topics, resulting in isotopically pure molecules, or based on the same idea, chemically pure isomers.**

Part V. Molecular Relaxation. **Ultrafast relaxation and energy transfer processes give the bulk of the research reported in this chapter. The ingenious method of SCHNEIDER and coworkers to generate time-correlated picosecond laser pulses and their application for rapid sampling of optical relaxation phenomena should be mentioned.**

The conference summarized our knowledge on laser induced processes on a truly international basis. Participation of physicists as well as chemists contributed to the exchange of ideas and better understanding of the processes involved.

The rapid publication of the book enhances the effectiveness of the material and makes it an excellent source of up-to-date information.

T. VIDÓCZY

Topics in Current Physics, Vol. 11
Raman Spectroscopy of Gases and Liquids

Edited by A. WEBER

pp. xi + 318, Springer-Verlag, Berlin, Heidelberg, New York, 1979

This series is designed to give the reader up-to-date information about a very wide variety of modern research fields in physics. This volume, dealing primarily with the fundamental aspects of Raman spectroscopy of gases, seems to be one of the most significant contributions to the line of review books prepared to the 50th anniversary of the discovery of the Raman effect. It certainly succeeds in its aim of bringing together in one volume the results of contemporary research since the appearance of the last review of this subject in 1973.

The volume comprises six comprehensive articles written by recognized authorities in the field of Raman spectroscopy.

Chapter *1* is a short introduction by the editor (with 48 refs.).

Chapter *2*, by S. BRODERSEN, deals with the high-resolution rotation-vibrational Raman spectroscopy (with 123 references). Giving a modern version of the theory of rotational Raman scattering, it assumes a basic knowledge of the treatment of the rotation-vibrational problem. The section on experimental techniques discusses the various units of the standard instrumentation for recording high-resolution Raman spectra, and briefly describes and characterizes the seven best known instruments built in different laboratories. The last section of this article is a fairly complete review of the recently published high-resolution rotation-vibrational Raman spectra. At the end of Chapter *2* it is concluded that, in a number of cases, rotation-vibrational Raman spectroscopy is able to yield more accurate molecular constants than other methods.

In Chapter *3* the pure rotational Raman spectra of gases are discussed by A. WEBER (with 191 references). Emphasis is laid on details of experimental techniques that ensure the required high accuracy of measurements. (At this point there is some overlap between Chapters *2* and *3*, but one may find useful to have information from two different sources.) Again, a complete review is given on rotational Raman studies of different molecules ranging from the simplest diatomics to rather complex polyatomics, and the molecular constants extracted from the works cited are tabulated. It is a real pleasure to look at some of the beautiful spectra appearing in this section (unfortunately, the spectral resolution is not specified anywhere). This chapter illustrates that the interplay between Raman, infrared and microwave studies can lead to highly accurate rotation and centrifugal distortion constants even for asymmetric molecules.

A critical review of the measurements of absolute and relative Raman scattering cross sections of gases and liquids is given by H. W. SCHRÖTTER and H. W. KLÖCKNER in Chapter *4* (with 102 references). The tabulated experimental results, including those obtained with mercury arc excitation, reveal a 5 to 15% accuracy of these measurements. It is hoped that this review will promote further progress in this field, since the methods described in this chapter may have important analytical applications like quantitative analysis of gas and liquid mixtures, air pollution measurements, *etc.* (note that the Raman LIDAR method is mentioned, but not dealt with in this book).

In Chapter *5*, the recent theoretical and experimental developments in the analysis of Raman line shapes, width, and shifts are surveyed by R. P. SRIVASTAVA and H. R. ZAIDI (with 143 references). The impact theory of collision brodening and calculation methods of line widths and shifts are discussed in some detail. It is shown that comparison of theory with experiment permits quantitative (in low pressure gases) and qualitative (in high density gases and liquids) information to be obtained about intermolecular forces.

Chapter *6*, by D. L. ROUSSEAU, J. M. FRIEDMAN and P. F. WILLIAMS, is devoted to resonance Raman scattering, a method promising to be able to investigate different parts independently of even exceedingly large biological molecules (with 83 references). In this chapter, unlike the preceding ones, the authors do not attempt to review all the important works on the application of resonance Raman scattering, which would be quite troublesome in this rapidly expanding field. Instead, the emphasis is laid on the discussion of theory and the presentation of basic mechanisms through which Raman scattering cross sections may be increased *via* resonance enhancement. The general principles and basic phenomena are illustrated in more detail on examples of diatomic molecules (Frank-Condon scattering) and porphyrin compounds (Herzberg-Teller scattering).

The last chapter, by J. W. NIBLER and G. V. KNIGHTEN, is a fair and accurate account of Coherent Anti-Stokes Raman Spectroscopy (CARS), one of the youngest branches of laser Raman spectroscopy (with 139 references). This non-linear optical technique utilizes the coherence and signal strength advantages of stimulated Raman scattering. Besides its indisputable advantages, this technique has numerous inconveniences and shortcomings as compared with spontaneous Raman spectroscopy, and these, too, are properly dealt with in this article. The authors give a detailed discussion of non-linear optical susceptibilities with particular emphasis on their application to CARS and Raman spectroscopy. The apparatus and various procedures used to record CARS spectra are outlined, CARS experimental results accumulated so far in the literature for solids, liquids and gases are surveyed, and some recently suggested improvements to the technique are discussed.

This volume is a very comprehensive description of the state of the art in Raman spectroscopy of gases and liquids. The book is well produced, with 103 clear figures, and is almost error-free (there is some inconsistency in the notation of nonresonant term, χ_{NR}, in the last chapter). Each chapter is concluded by a useful summary, and at the end of the book additional references (including titles), grouped according to the chapters, are given with the aim of completing the list of relevant literature up to 1978.

The authors and the editor are to be congratulated on producing this book in a very short time and also solving one of the usual problems of a multi-authored volume: the maintaining of a uniformly high level of presentation in the different chapters. Definitely, this is a research-oriented volume in an area of molecular spectroscopy that is dealt with in only a few laboratories (with the exception of increasingly popular resonance Raman spectroscopy). It will certainly contribute to the proliferation of these techniques, but the newcomer to the field should read first some basic texts on these aspects of Raman spectroscopy.

G. KERESZTURY

M. Shamma and J. L. Moniot: *Isoquinoline Alkaloids Research 1972–1977*

425 pages, Plenum Press, New York—London, 1978

The name of Professor Shamma, one of the authors of the book, is well known to those working in alkaloid chemistry, on the one hand from his own research results, and on the other, as the author of the book "The Isoquinoline Alkaloids, Chemistry and Pharmacology", published in 1972. Though hardly a few years have passed since the publication of that book, steady advance in this field, the isolation of new alkaloids, and the development of new syntheses have made necessary the publication of a new volume reporting these results. With a few exceptions, new data are to be refound on all those alkaloids which have been already discussed in the book The Isoquinoline Alkaloids. Thus, a separate chapter is devoted to each of the following alkaloids: simple isoquinolines; benzylisoquinolines; isoquinolones; pavines and isopavines; bisbenzylisoquinolines; cularines; dibenzopyrrocolines; proaporphines; aporphines; pakistanamine; aporphine-benzylisoquinoline dimers; phenantrenes; dibenzazonines; protoberberines and retroprotoberberines; secoberberines; benzophenanthridines; protopines; phtalideisoquinolines; spirobenzylisoquinolines; rhoeadines; emetine and related bases; phenethylisoquinolines; homoaporphines and homoproaporphines; 1-phenylisoquinolines; *N*-benzyltetrahydroisoquinolines and cherylline. Completely novel alkaloid types discovered since 1972 are discussed in new chapters. These include baluchistanamine (an isoquinolone-benzylisoquinoline dimer), the aporphine-pavine dimers, the 4,5-dioxoaporphines, secoberbines, 3-arylisoquinolines, eupolauridine, and very recently, imerubrine. Another new chapter discusses the chemistry of the aristolochic acids and aristolactams, a group of substituted phenantrenes. On the other hand, one group of alkaloids which was included in "The Isoquinoline Alkaloids", but deemed not to belong properly in the present work, are the naphthaleneisoquinolines, which include ancistrocladine and its relatives. The chapters begin with structure elucidation and synthesis, followed by a description of typical reactions, and the chapter ends with coverage of biogeneses, pharmacology, and spectroscopy.

The excellently edited book of nice presentation will be of great assistance to those engaged in alkaloid chemistry, and cannot miss from the reference library. The reviewer can only repeat Derek Barton's words: "This new volume will be an essential addition to the libraries of all those interested in the chemistry, biochemistry and biology of alkaloids. It will also become a standard reference work for anyone who wishes to look up known work on isoquinoline alkaloids".

Gy. Deák

INDEX

PHYSICAL AND INORGANIC CHEMISTRY

ORGANIC CHEMISTRY

ANALYTICAL CHEMISTRY

Printed in Hungary

A kiadásért felel az Akadémiai Kiadó igazgatója
Műszaki szerkesztő: Zacsik Annamária
A kézirat nyomdába érkezett: 1979. XI. 14. — Terjedelem: 9,45 (A/5) ív, 34 ábra

80.7705 Akadémiai Nyomda, Budapest — Felelős vezető: Bernát György

Les Acta Chimica paraissent en français, allemand, anglais et russe et publient des mémoires du domaine des sciences chimiques.

Les Acta Chimica sont publiés sous forme de fascicules. Quatre fascicules seront réunis en un volume (3 volumes par an).

On est prié d'envoyer les manuscrits destinés à la rédaction à l'adresse suivante:

Acta Chimica
Budapest, P.O.B. 67, H-1450, Hongrie

Toute correspondance doit être envoyée à cette même adresse.

La rédaction ne rend pas de manuscript.

Abonnement en Hongrie à l'Akadémiai Kiadó (1363 Budapest, P. O. B. 24, C. C. B. 215 11488), à l'étranger à l'Entreprise du Commerce Extérieur « Kultura » (H-1389 Budapest 62, P. O. B. 149 Compte-courant No. 218 10990) ou chez représentants à l'étranger.

Die Acta Chimica veröffentlichen Abhandlungen aus dem Bereich der chemischen Wissenschaften in deutscher, englischer, französischer und russischer Sprache.

Die Acta Chimica erscheinen in Heften wechselnden Umfanges. Vier Hefte bilden einen Band. Jährlich erscheinen 3 Bände.

Die zur Veröffentlichung bestimmten Manuskripte sind an folgende Adresse zu senden

Acta Chimica
Budapest, Postfach 67, H-1450, Ungarn

An die gleiche Anschrift ist jede für die Redaktion bestimmte Korrespondenz zu richten.

Manuskripte werden nicht zurückerstattet.

Bestellbar für das Inland bei Akadémiai Kiadó (1363 Budapest, Postfach 24, Bankkonto Nr. 215 11488), für das Ausland bei »Kultura« Außenhandelsunternehmen (H-1389 Budapest 62, P. O. B. 149. Bankkonto Nr. 218 10990) oder seinen Auslandsvertretungen.

«Acta Chimica» издают статьи по химии на русском, английском, французском и немецком языках.

«Acta Chimica» выходит отдельными выпусками разного объема, 4 выпуска составляют один том и за год выходят 3 тома.

Предназначенные для публикации рукописи следует направлять по адресу:

Acta Chimica
Budapest, P.O.B. 67, H-1450, ВНР

Всякую корреспонденцию в редакцию направляйте по этому же адресу.

Редакция рукописей не возвращает.

Отечественные подписчики направляйте свои заявки по адресу Издательства Академии Наук (1363 Budapest, P.O.B. 24. Текущий счет 215 11488), а иностранные подписчики через организацию по внешней торговле «Kultura» (H-1389 Budapest 62, P.O.B. 149. Текущий счет 218 10990) или через ее заграничные представительства и уполномоченных.

Reviews of the Hungarian Academy of Sciences are obtainable at the following addresses:

AUSTRALIA
C.B.D. LIBRARY AND SUBSCRIPTION SERVICE. Box 4886, G.P.O., *Sydney N.S.W. 2001*
COSMOS BOOKSHOP, 145 Ackland Street, *St. Kilda (Melbourne), Victoria 3182*

AUSTRIA
GLOBUS, Höchstädtplatz 3, *1200 Wien XX*

BELGIUM
OFFICE INTERNATIONAL DE LIBRAIRIE, 30 Avenue Marnix, *1050 Bruxelles*
LIBRARIE DU MONDE ENTIER, 162 Rue du Midi, *1000 Bruxelles*

BULGARIA
HEMUS, Bulvar Ruski 6, *Sofia*

CANADA
PANNONIA BOOKS, P.O. Box 1017, Postal Station "B", *Toronto, Ontario M5T 2T8*

CHINA
CNPICOR, Periodical Department, P.O. Box 50, *Peking*

CZECHOSLOVAKIA
MAD'ARSKÁ KULTURA, Národni třida 22, *115 33 Praha*
PNS DOVOZ TISKU, Vinohradská 46, *Praha 2*
PNS DOVOZ TLAČE, *Bratislava 2*

DENMARK
EJNAR MUNKSGAARD, Norregade 6, *1165 Copenhagen*

FINLAND
AKATEEMINEN KIRJAKAUPPA, P.O. Box 128, *SF-00101 Helsinki 10*

FRANCE
EUROPERIODIQUES S.A., 31 Avenue de Versailles, *78170 La Celle St. Cloud*
LIBRAIRIE LAVOISIER, 11 rue Lavoisier, *75008 Paris*
OFFICE INTERNATIONAL DE DOCUMENTATION ET LIBRAIRIE, 48 rue Gay-Lussac, *75240 Paris Cedex 05*

GERMAN DEMOCRATIC REPUBLIC
HAUS DER UNGARISCHEN KULTUR, Karl-Liebknecht-Strasse, 9, *DDR-102 Berlin*
DEUTSCHE POST ZEITUNGSVERTRIEBSAMT, Strasse der Pariser Kommüne 3—4, *DDR-104 Berlin*

GERMAN FEDERAL REPUBLIC
KUNST UND WISSEN ERICH BIEBER, Postfach 46, *7000 Stuttgart 1*

GREAT BRITAIN
BLACKWELL'S PERIODICALS DIVISION, Hythe Bridge Street, *Oxford OX1 2ET*
BUMPUS, HALDANE AND MAXWELL LTD., Cower Works, *Olney, Bucks MK46 4BN*
COLLET'S HOLDINGS LTD., Denington Estate, *Wellingborough, Northants NN8 2QT*
WM. DAWSON AND SONS LTD., Cannon House, *Folkestone, Kent CT19 5EE*
H. K. LEWIS AND CO., 136 Gower Street, *London WC1E 3BS*

GREECE
KOSTARAKIS BROTHERS, International Booksellers, 2 Hippokratous Street, *Athens-143*

HOLLAND
MEULENHOFF-BRUNA B.V., Beulingstraat 2, *Amsterdam*
MARTINUS NIJHOFF B.V., Lange Voorhout 9—11, *Den Haag*
SWETS SUBSCRIPTION SERVICE 347b Heereweg, *Lisse*

INDIA
ALLIED PUBLISHING PRIVATE LTD., 13/14 Asaf Ali Road, *New Delhi 110001*
150 B-6 Mount Road, *Madras 600002*
INTERNATIONAL BOOK HOUSE PVT. LTD., Madame Cama Road, *Bombay 400069*
THE STATE TRADING CORPORATION OF INDIA LTD., Books Import Division, Chandralok, 36 Janpath, *New Delhi 110001*

ITALY
EUGENIO CARLUCCI, P.O. Box 252, *70100 Bari*
INTERSCIENTIA, Via Mazzé 28, *10149 Torino*
LIBERIA COMMISSIONARIA SANSONI, Via Lamarmora 45, *50121 Firenze*
SANTO VANASIA, Via M. Macchi 58, *20124 Milano*
D. E. A., Via Lima 28, *00198 Roma*

JAPAN
KINOKUNIYA BOOK-STORE CO. LTD., 17-7 Shinjuku-ku 3 chome, Shinjuku-ku, *Tokyo 160-01*
MARUZEN COMPANY LTD., Book Department, P.O. Box 5050 Tokyo International, *Tokyo 100-61*
NAUKA LTD. IMPORT DEPARTMENT, 2-40-19 Minami Ikebukuro, Toshima-ku, *Tokyo 171*

KOREA
CHULPANMUL, *Phenjan*

NORWAY
TANUM-CAMMERMEYER, Karl Johansgatan 41—43, *1000 Oslo*

POLAND
WEGIERSKI INSTYTUT KULTURY, Marszalkowska 80, *Warszawa*
CKP I W ul. Towarowa 28 *00-958 Warszawa*

ROUMANIA
D. E. P., *Bucureşti*
ROMLIBRI, Str. Biserica Amzei 7, *Bucureşti*

SOVIET UNION
SOJUZPETCHATJ — IMPORT, *Moscow*
and the post offices in each town
MEZHDUNARODNAYA KNIGA, *Moscow G-200*

SPAIN
DIAZ DE SANTOS, Lagasca 95, *Madrid 6*

SWEDEN
ALMQVIST AND WIÓSELL, Gamla Brogatan 26, *101 20 Stockholm*
GUMPERTS UNIVERSITETSBOKHANDEL AB, Box 346, *401 25 Göteborg 1*

SWITZERLAND
KARGER LIBRI AG, Petersgraben 31, *4011 Basel*

USA
EBSCO SUBSCRIPTION SERVICES, P.O. Box 1943, *Birmingham, Alabama 35201*
F. W. FAXON COMPANY, INC., 15 Southwest Park, *Westwood Mass. 02090*
THE MOORE-COTTRELL SUBSCRIPTION AGENCIES, *North Cohocton, N. Y. 14868*
READ-MORE PUBLICATIONS, INC., 140 Cedar Street, *New York, N. Y. 10006*
STECHERT-MACMILLAN, INC., 7250 Westfield Avenue, *Pennsauken N. J. 08110*

VIETNAM
XUNHASABA, 42, Hai Ba Trung, *Hanoi*

YUGOSLAVIA
JUGOSLAVENSKA KNJIGA, Terazije 27, *Beograd*
FORUM, Vojvode Mišića 1, *21000 Novi Sad*

27. VI. 1980   HU ISSN 0001—5407   Index: 26.007

ACTA CHIMICA
ACADEMIAE SCIENTIARUM HUNGARICAE

TOMUS 104 FASCICULUS 2

AKADÉMIAI KIADÓ, BUDAPEST
1980

ACTA CHIM. ACAD. SCI. HUNG. ACASA2 104 (2) 107—199 (1980)

ACTA CHIMICA

A MAGYAR TUDOMÁNYOS AKADÉMIA KÉMIAI TUDOMÁNYOK OSZTÁLYÁNAK IDEGEN NYELVŰ KÖZLEMÉNYEI

Acta Chimica is a journal for the publication of papers on all aspects of chemistry in English, German, French and Russian.

Acta Chimica is published in 3 volumes per year. Each volume consists of 4 issues of varying size.

Manuscripts should be sent to

Acta Chimica
Budapest, P.O. Box 67, H-1450, Hungary

Correspondence with the editors should be sent to the same address. Manuscripts are not returned to the authors.

Hungarian subscribers should order from Akadémiai Kiadó, 1363 Budapest, P.O. Box 24. Account No. 215 11488.

Orders from other countries are to be sent to "Kultura" Foreign Trading Company (H-1389 Budapest 62, P.O. Box 149. Account No. 218 10990) or its representatives abroad.

Acta Chimica Academiae Scientiarum Hungaricae, Tomus 104 (2), pp. 107–112 (1980)

1,2,4-TRIAZINE DERIVATIVES, XXII*

A NOVEL SYNTHESIS OF 5-SUBSTITUTED 3-ALKYLAMINO-5*H*-[1,2,4]TRIAZINO[5,6-*b*]INDOLE DERIVATIVES

G. Doleschall and K. Simon-Ormai

(Department for Organic Chemistry, Technical University, Budapest)

Received April 20, 1979

Accepted for publication June 28, 1979

A novel synthesis of 5-substituted 3-alkylamino-5*H*-[1,2,4]triazino[5,6-*b*]indole derivatives, starting with primary amines and 6-(2-aminophenyl-3-methylthio-1,2,4-triazin-5-(2*H*)-one or 6,6-dimethyl-3-methylthio-6,7-dihydro-[1,2,4]triazino[1,6-*c*]quinazolin-5-ium-1-olate, has been devised.

3-Alkylamino-5-methyl-5*H*-[1,2,4]triazino[5,6-*b*]-indole derivatives are specific virus RNA inhibitors [1]. According to the investigation of researchers at Allen and Hanbury Ltd. [2] and at Smith, Kline and French Laboratories [3], 3-(3-hydroxypropyl)-5-methyl-5*H*-[1,2,4]triazino[5,6-*b*]indole (**7**) and its derivatives alkylated in the propyl side chain proved to be efficient in *in vitro* experiments against rhinovirus, herpes and smallpox viruses. Moreover, they were effective prophylactics also in animal experiments (mice, chimpanzee), and at present clinical tests are already in progress [4].

So far, two routes have been known for the synthesis of 3-alkylamino-5*H*-[1,2,4]triazino[5,6-*b*]indoles: condensation of isatin (**1**) with aminoguanidines (non-structure-proving synthesis) [5], and aminolysis of the respective 3-thioxo, 3-methylthio or 3-chloro derivatives [4]. The present communication reports on an advantageous and convenient alternative synthesis route.

It has been found earlier [6] that on reacting salts of isatinic acid, formed from isatin in alkaline medium, with thiosemicarbazide, 6-(2-aminophenyl)-3-thioxo-3,4-dihydro-1,2,4-triazin-5(2*H*)-one (**2**) is obtained. The 3-methylthio derivative **3**, formed by methylation of **2**, appeared to be a useful potential starting material for the synthesis of 5-substituted 3-alkylamino-5*H*-[1,2,4]-triazino[5,6-*b*]indole derivatives. The advantage of this new synthesis is that the methylthio group is attached to a non-aromatic ring, and is thus more reactive.

We found that when **3** is refluxed in water with primary amines, the corresponding 3-alkylamino-6-(2-aminophenyl)-1,2,4-triazin-5(2*H*)-ones (**5**) are indeed obtained, with the elimination of methanethiol.

6,6-Dimethyl-3-methylthio-6,7-dihydro-[1,2,4]triazino[1,6-*c*]quinazolin-5-ium-1-olate (**4**), formed on the addition of acetone, and subsequently of acetic

---

* Part XXI: Voustas, G. P., Venotopoulos, Cl. C., Kálmán, A., Párkányi, L., Hornyák, Gy., Lempert, K.: Tetrahedron Letters, **1978**, 4431

acid to the reaction mixture obtained after methylation of **2** in alkaline medium, can be isolated more easily and in better yields, than compound **3** [7, 8]. In water **4** can be aminolyzed to yield type **5** derivatives, since it is hydrolyzed in aqueous alkaline medium to **3** [7].

Moreover, it seemed suitable to condense also the resulting 3-alkylamino derivatives with acetone to the respective compounds **6** and to isolate them in this form. The structures of the condensation products obtained, at least in the crystalline state, were proved on the basis of analogy with the 3-methylthio derivative **4** of known structure [8] and also by the fact that the characteristic $\nu C=O$ band of 1,2,4-triazol-5(2*H*)-ones is lacking from their IR spectra.

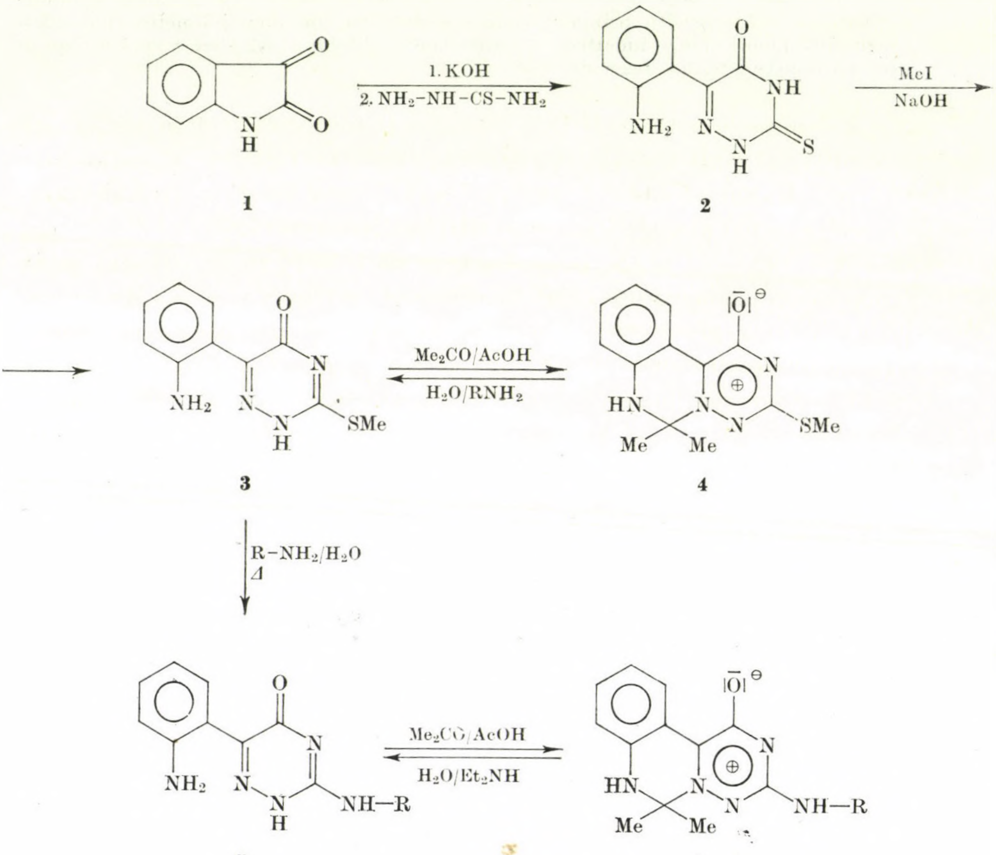

a: $R = PhCH_2—$

b: $R = HO—CH_2CH_2—$

c: $R = HO—CH_2CH_2CH_2—$

Fig. 1

3-Alkyl-amino-6,7-dihydro-6,6-dimethyl-[1,2,4]triazino[1,6-*c*]quinazolin-5-ium-1-olates **6** are hydrolyzed with aqueous diethylamine to the 1,2,4-triazin-5(2*H*)-ones **5**.

Since **2** and **3** may be cyclized both by simple heating and by refluxing with acetic acid to yield [1,2,4]triazino-[5,6-*b*]indoles [7], it could be expected that compound **5** can as well be converted by *amino-N*-alkylation and ring closure into 5-substituted 3-alkylamino-5*H*-[1,2,4]triazino [5,6-*b*]indoles. On treatment with dimethyl sulfate in dimethyl-formamide, 6-(2-aminophenyl)-3-(3-hydroxy-propylamino)-1,2,4-triazin-5(2*H*)-one (**5c**) was indeed converted, already under the conditions of work-up (steam distillation), into 3-(3-hydroxy-propylamino)-5-methyl-5*H*-[1,2,4]-triazino[5,6-*b*]indole (**7**). With ethyl bromoacetate, ethyl 2-[3-(-hydroxypropylamino)-5-oxo-2,5-dihydro-1,2,4-triazin-6-yl]-phenylglycinate (**8**) was similarly obtained. By refluxing with acetic acid **8** is converted into the [1,2,4]triazino[5,6-*b*]indole **9**.

In addition to its preparative convenience, the synthetic method devised by us has the advantage over those known so far that it allows introduction of the substituent to position 5 in the last step.

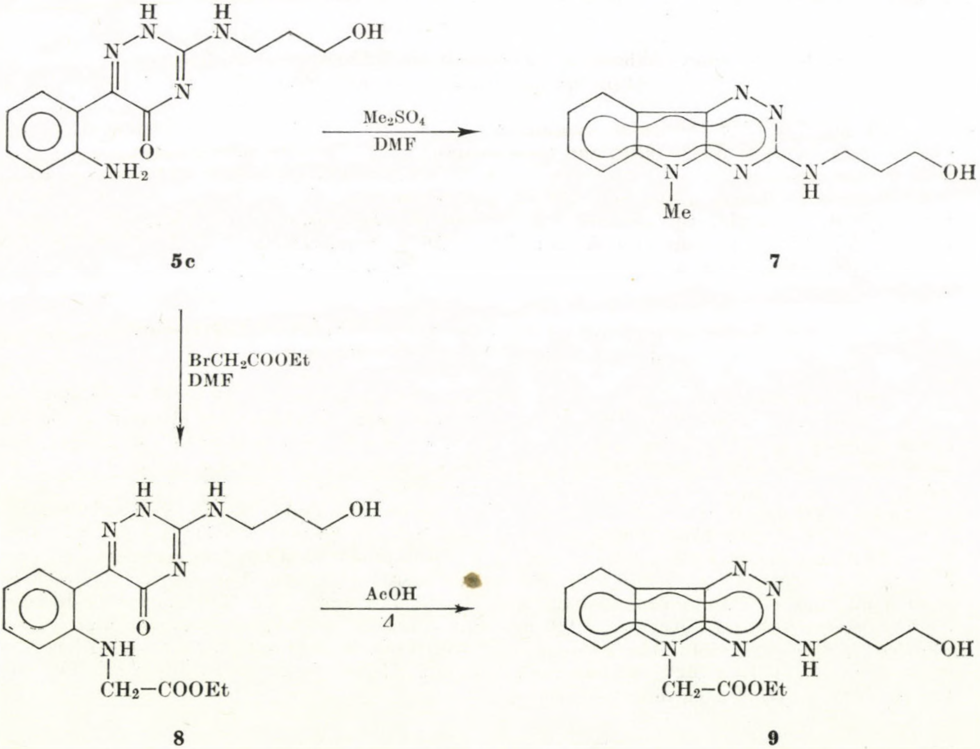

Fig. 2

Experimental

6,6-Dimethyl-3-methylthio-6,7-dihydro-[1,2,4]triazino-[1,6-*c*]quinazolin-5-ium-1-olate (4)*

Isatin (40 g; 272 mmoles) was dissolved in a boiling aqueous (400 ml) solution of potassium hydroxide (40 g; 720 mmoles). The yellowish-brown solution was cooled to 80—90 °C and thiosemicarbazide (28 g; 309 mmoles) was added. The mixture was refluxed for 30 min, cooled to 0 °C, and vigorously stirred with methyl iodide (22 ml; 320 mmoles) first for 1 h under cooling with ice-water, and for 2 h at room temperature. To the yellowish-brown solution acetone (100 ml) and acetic acid (60 ml) were added, and the mixture was stirred for 30 min. The red solution containing a precipitate was then allowed to stand for 2 h, the orange-coloured crystals were filtered off, washed with hot DMF (150 ml) and with acetone (2 × 100 ml) and dried in air to obtain 58.2 g (78%) of the title compound, m.p. 226—228 °C (decomp.).

6-(2-Aminophenyl)-3-(benzylamino)-1,2,4-triazin-5(2*H*)-one (5a)

(*a*) A mixture of **3** (5 g; 21.3 mmoles), benzylamine (5 ml; 46 mmoles) and water (5 ml) was refluxed for 10 h; after cooling, the two phases were separated. The lower phase was washed with water (2 × 10 ml), dissolved in hot ethyl alcohol (15 ml), acidified with acetic acid and allowed to stand overnight. The precipitate was filtered off, washed with water and dried over phosphorus pentoxide to obtain 3.2 g (48%), of compound **5a,** m.p. 242—244 °C (from a 2 : 1 pyridine–water mixture).

IR: νNH and νOH: 3400—2700 cm^{-1}, νC=O: 1650 cm^{-1}.

$C_{16}H_{15}N_5O$ (293.32). Calcd, C 65.51; H 5.16; N 23.88. Found C 64.96; H 5.19; N 22.93%.

(*b*) A mixture of **4** (10 g; 36.5 mmoles), benzylamine (6 ml; 55 mmoles) and water (60 ml) was refluxed for 15 min. The resulting solution was evaporated in vacuum, and the residue refluxed with a mixture of benzylamine (7 ml; 64 mmoles) and water (10 ml) for 10 h. Work-up as described under (*a*) furnished 3.5 g (33%) of compound **5a**.

3-(2-Hydroxyethylamino)-6,6-dimethyl-6,7-dihydro-[1,2,4]-triazino-[1,6-*c*]quinazolin-5-ium-1-olate (6b)

A mixture of **4** (10 g; 36.5 mmoles), 2-aminoethanol (4 ml; 66 mmoles) and water (40 ml) was refluxed for 15 min, and then evaporated in vacuum. The residue was refluxed with 2-aminoethanol (10 ml; 166 mmoles) and water (10 ml) for 10 h and, after cooling, a mixture of acetone (20 ml), acetic acid (20 ml) and water (120 ml) was added. The mixture was kept at 0 °C overnight, the product was filtered off and washed with water (2 × 30 ml) to obtain 7.1 g (68%) of compound **6b**, m.p. 218—219 °C (from DMF).

$C_{15}H_{17}N_5O_2$ (287.31). Calcd. C 58.35; H 5.81 Found C 58.54; H 6.14%.

3-(3-Hydroxypropylamino)-6,6-dimethyl-6,7-dihydro-[1,2,4]triazino-[1,6-*c*]quinazolin-5-ium-1-olate (6c)

(*a*) A mixture of **3** [7] (10 g; 42.7 mmoles), 3-aminopropanol (10 g; 66.6 mmoles) and water (10 ml) was refluxed for 10 h. After cooling, a mixture of acetone (10 ml), acetic acid (10 ml) and water (120 ml) was added, and the mixture was allowed to stand overnight. The resulting crystals were filtered off, washed with acetone and dried in air at 80 °C to obtain 9.4 g (73%) of compound **6c**, m.p. 212 °C (from DMF).

IR: νNH and νOH: 3350—2800 cm^{-1}, first band in the double bond region at 1600 cm^{-1}.

$C_{15}H_{19}N_5O_2$ (301.34). Calcd. C 59.78; H 6.36; N 23.24. Found C 59.71; H 6.81; N 23.45%.

(*b*) A mixture of **4** (20 g; 72.8 mmoles), 3-amino-propanol (10 g; 133 mmoles) and water (75 ml) was refluxed for 15 min and then evaporated in vacuum. The residue was refluxed with a mixture of 3-aminopropanol (20 g; 266 mmoles) and water (20 ml) for 10 h. After cooling, acetone (30 ml), acetic acid (30 ml) and water (20 ml) were added. The mixture was allowed to stand overnight. The product was filtered off, washed with water, and dried in air at 80 °C to obtain 18 g (82%) of compound **6c**, m.p. 212 °C (from DMF), identical (IR) with the product prepared according to (*a*).

---

* Modification of the method published in Ref. [7].

6-(2-Aminophenyl)-3-(2-hydroxyethylamino)-1,2,4-triazin-5(2*H*)-one (5b)

A mixture of **6b** (2 g; 7 mmoles), diethylamine (2 ml; 19.3 mmoles) and water (20 ml) was heated to the boiling point and then evaporated to dryness in vacuum. The residue was dissolved in water (20 ml), the solution was acidified at 0 °C with acetic acid, the product was filtered off, washed with cold water (2 × 5ml) and dried in vacuum over phosphorus pentoxide to obtain 1.6 g (86%) of compound **5b**, m.p. 228—229 °C (from water).

IR: νNH and νOH: 3400—3600 cm^{-1}; νC=O: 1650 cm^{-1}.

$C_{11}H_{13}N_5O_2 \cdot H_2O$ (265.27). Calcd. C 49.80; H 5.70; N 26.40. Found C. 49.63; H. 6.20; N 26.20%.

6-(2-Aminophenyl)-3-(3-hydroxypropylamino)-1,2,4-triazin-5(2*H*)-one (5c)

A mixture of **6c** (8 g; 26.5 mmoles), diethylamine (16 ml; 155 mmoles) and water (160 ml) was heated to the boiling point and then evaporated to dryness in vacuum. The residue was dissolved in hot water (30 ml), the solution was cooled to 0 °C and acidified with acetic acid. The product was filtered off, washed with cold water and dried in vacuum over phosphorus pentoxide, to obtain 6.5 g of the crude product. Recrystallization from ethanol (130 ml) gave 5.2 g (76%) of compound **5c**, m.p. 198—199 °C.

IR: νNH and νOH: 3400—2600 cm^{-1}; νC=O: 1640 cm^{-1}.

$C_{12}H_{15}N_5O_2$ (261.29). Calcd. C 55.16; H 5.79; N 26.81. Found C 55.01; H. 5.99; N 26.08%.

3-(3-Hydroxypropylamino)-5-methyl-5*H*-[1,2,4]triazino-[5,6-*b*]indole (7)

A mixture of **5c** (6 g; 23.1 mmoles), dimethyl sulfate (2.6 ml; 27.3 mmoles) and anhydrous DMF (10 ml) was allowed to stand overnight. The resulting red solution was diluted with water (50 ml), and then evaporated to dryness in vacuum on a steam bath. The residue was dissolved in water (50 ml) and the solution was made alkaline (pH 12—13) with 40% sodium hydroxide solution. The mixture was cooled to 0 °C, the product was filtered off, washed with water (2 × 10 ml), and dried in air to obtain 2.9 g (49%) of compound **7**, m.p. 164 °C (from water), indentical by m.p., mixed m.p. and IR with the product described in the literature [2].

Ethyl 2-[3-(3-hydroxypropylamino)-5-oxo-2,5-dihydro-1,2,4-triazin-6-yl]-phenylglycinate (8)

A mixture of **5c** (7 g; 27 mmoles), ethyl bromoacetate (3.5 ml; 32 mmoles) and anhydrous DMF (10 ml) was allowed to stand overnight. Water (75 ml) was added to the mixture which was then neutralized with 5% $NaHCO_3$ solution. The resulting precipitate was washed with water (2 × 15 ml), dried in vacuum over phosphorus pentoxide, and recrystallized from ethanol (30 ml) to obtain 2.5 g (27%) of compound **8**, m.p. 139 °C.

IR: νNH and νOH: 3450—2800 cm^{-1}; νC=O (ester): 1730 cm^{-1}; νC=O (triazinone): 1650 cm^{-1}.

$C_{16}H_{21}N_5O_2$ (437.36). Calcd. C 55.31; H 6.09; N 20.16. Found C 56.08; H 6.24; N 19.34%.

Ethyl [3-(3-hydroxypropylamino)-5*H*-[1,2,4]triazolo-[5,6-*b*]-indol-5-yl]-acetate (9)

A mixture of **5c** (3 g; 11.6 mmoles) ethyl bromo-acetate (1.5 ml; 15.5 mmoles) and anhydrous DMF (5 ml) was allowed to stand for 48 h at room temperature. Water (30 ml) was added, and the mixture was neutralized with 5% $NaHCO_3$ solution. The product which precipitated was filtered off, refluxed in acetic acid (30 ml) for 1 h, evaporated to dryness in vacuum, and the residue was triturated with 5% $NaHCO_3$ solution (70 ml). The resulting product was dissolved in chloroform (3 × 70 ml), and the chloroform solution was washed with 5% $NaHCO_3$ solution (2 × 25 ml), and with water (2 × 40 ml), dried over calcium chloride, evaporated to dryness in vacuum, and recrystallized from ethanol (20 ml) to obtain 1.6 g (42% of compound **9**, m.p. 153—154 °C.

IR: νNH and νOH: 3300—2800 cm^{-1}; νC=O: 1745 cm^{-1}.

$C_{16}H_{19}N_5O_3$ (329.35). Calcd. C 58.35; H 5.81; N 21.27. Found C. 58.51; H 6.14; N 20.41%.

*

The authors thank Miss A. LÁSZLÓ and Mrs. F. SENKEI for technical assistance, Miss K. ÓFALVI, Mrs. S. VISZT-SIMON and Mrs. I. ZAUER-CSÜLLÖG for the microanalyses and Miss M. CSIRKE for the IR spectra.

REFERENCES

[1] MATSUMOTO, S., STANDFIELD, F. J., BOORE, M. Y., HAFF, R. F.: Proc. Soc. Exp. Biol. Med., **139**, 455 (1972)

[2] ALLEN and HANBURYS Ltd.: Neth. Appl. 6410823 (18. 3. 1965); CA, **63**, 13295 (1965)

[3] GLADYCH, M. Z., HORNLY, R., HUNT, J. H., JACK, D., BOYLE, J. J., FERKUTS, R. J., HAFF, R. F., KÖRMENDY, CH., G., STANFIELD, F. J., STEVARTI, R. C.: J. Med. Chem., **15**, 277 (1972); CA, **74**, 149493f (1972)

[4] ROMANCHICK, W. A., JOULLIE, M. M.: Heterocycles, **9**, 1631 (1978)

[5] KING, H., WRIGHT, J.: J. Chem. Soc., **1948**, 2314

[6] DOLESCHALL, G., LEMPERT, K.: Acta Chim. Acad. Sci. Hung., **64**, 369 (1970)

[7] DOLESCHALL, G., LEMPERT, K.: Tetrahedron, **29**, 639 (1973)

[8] DUISENBERG, A. J. M., KÁLMÁN, A., DOLESCHALL, G., LEMPERT, K.: Cryst. Struct. Comm., **4**, 295 (1974)

Gábor DOLESCHALL
Klára SIMON-ORMAI
H-1521 Budapest, Gellért tér 4.

Acta Chimica Academiae Scientiarum Hungaricae, Tomus 104 (2), pp. 113—115 (1980)

SYNTHESIS AND EVALUATION OF THE ANTIBACTERIAL ACTIVITY OF ETHYL 2,3-DIOXOBUTYRATE-2-(SUBSTITUTED SULFONAMIDOPHENYL)HYDRAZONES

C. P. SINGH and A. C. OJHA
(Chemical Laboratories, Sahu Jain College, Najibabad, India)

Received May 13, 1979
Accepted for publication June 29, 1979

Eight new ethyl 2,3-dioxobutyrate-2-(substituted *p*-sulfonamidophenyl)hydrazones have been synthesized by the interaction of substituted sulfonamidobenzenediazonium chlorides and ethyl 2,3-dioxobutyrate. Four compounds were tested for their antibacterial activity *in vitro:*

Ethyl 2,3-dioxobutyrate [1] has been coupled with diazotized sulfanilamide, N^1-2-pyrimidylsulfanilamide, N^1-2-thiazolylsulfanilamide, N^1-2-(4,6-dimethyl)pyrimidyl-sulfanilamide, N^1-4-pyridylsulfanilamide, sulfguanidine, N^1-4-acetylsulfanilamide and N^1-2-quinoxalylsulfanilamide, respectively, to obtain the corresponding ethyl 2,3-dioxobutyrate-2-(substituted *p*-sulfonamidophenyl)hydrazones. The products were purified and screened against ten

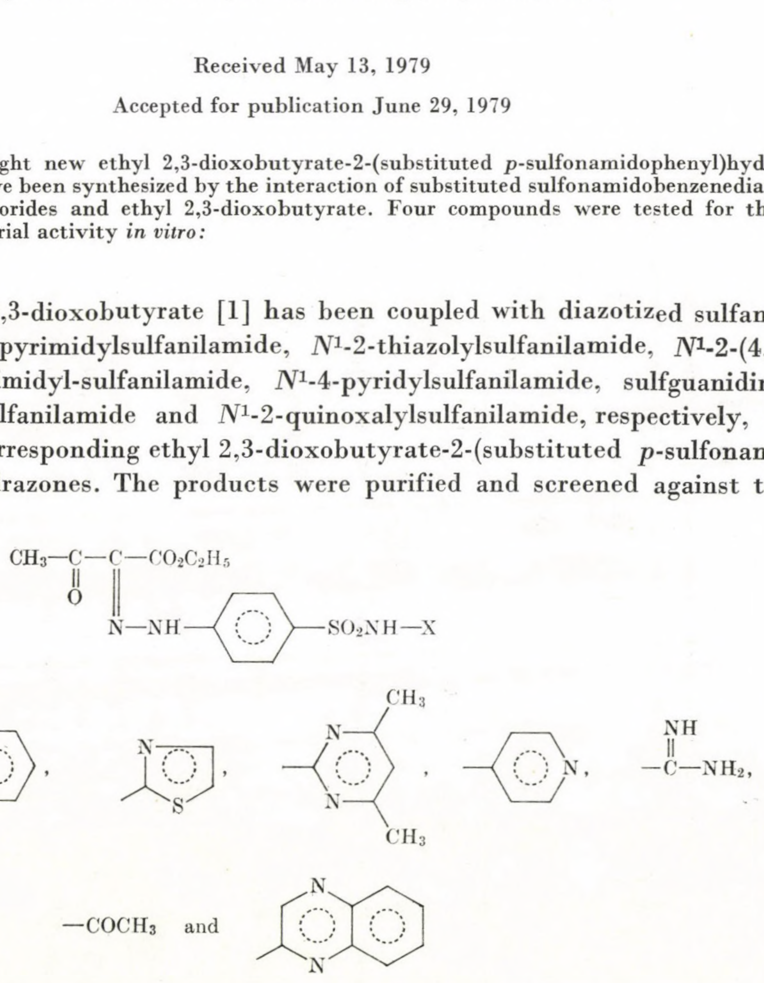

pathogenic organisms for their *in vitro* antibacterial activity. The homogeneity and purity of the compounds were checked by TLC. The structures of the compounds were assigned on the basis of elemental analyses and spectral studies.

Table I

Characteristics of ethyl 2,3-dioxobutyrate-2-(substituted sulfonamidophenyl) hydrazones

Ethyl 2,3-dioxobutyrate-2-[(X)-sulfonamidophenyl]hydrazones

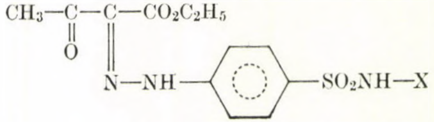

Sl.No.	X	M.P., °C	Colour	Yield, %	Molecular formula	N, %		S, %		R*
						Found	Calcd.	Found	Calcd.	
1	*N*¹-2-pyrimidyl	166	Light yellow	80	$C_{16}H_{17}N_5O_5S$	17.32	17.42	7.76	7.89	0.7454
2	*N*¹-2-thiazolyl	173	Shining organe yellow	90	$C_{15}H_{16}N_4O_5S_2$	14.07	14.15	16.05	16.16	0.8061
3	*N*¹-2-(4,6-dimethyl)-pyrimidyl	172	Light pale yellow	78	$C_{18}H_{21}N_5O_5S$	16.65	16.70	6.97	7.03	0.8685
4	*N*¹-4-pyridyl	175	Pale yellow	82	$C_{17}H_{18}N_4O_5S$	14.21	14.36	8.04	8.21	0.9915
5	*N*¹-4-guanidyl	182	Shining dark yellow	85	$C_{13}H_{17}N_5O_5S$	19.46	19.72	8.96	9.02	0.9026
6	*N*¹-4-acetyl	200	Light yellow	80	$C_{14}H_{17}N_3O_6S$	11.78	11.83	8.76	8.98	0.8260
7	*N*¹-2-quinoxalyl	170	Greyish brown	75	$C_{20}H_{19}N_5O_5S$	15.86	15.91	7.02	7.11	0.4906

* The R_f values for all the compounds on silica gel plates (thickness 0.5 mm) with developer as acetone/dimethylformamide (2 : 1) in saturated chambers at room temp. (20 ± 1 °C)

Experimental

All chemical used were BDH or E. Merck products.

Ethyl 2,3-dioxobutyrate-2-(*p*-sulfonamidophenyl)hydrazone

Sulfanilamide (0.05 mole) was dissolved in a mixture of hydrochloric acid (12.5 ml) and water (12.5 ml), and cooled to 0 °C. Sodium nitrite (0.05 mole) was then gradually added to the hydrochloride solution. The diazotized solution of sulfanilamide thus obtained was filtered into a well cooled and stirred mixture of sodium acetate (30.0 g) and ethyl 2,3-dioxobutyrate (0.05 mole) in ethanol (100 ml). Ethyl 2,3-dioxobutyrate-2-(sulfonamidophenyl) hydrazone separated as pale yellow solid. It was filtered off, washed with water and recrystallized from ethanol to obtain shining pale yellow crystals, m.p. 128 °C.

$C_{12}H_{15}N_3O_5S$. Calcd. N 13.42; S 10.22. Found N 13.26; S 10.12%.

By analogous procedures, several ethyl 2,3-dioxobutyrate-2-(substituted sulfonamidophenyl)hydrazones have been synthesized, their characteristics are recorded in Table I.

IR spectra

IR spectra were recorded in KBr pellets. The spectra had characteristic peaks at 1650 cm^{-1} ($>C=O$), 1510 to 1550 cm^{-1} ($>C=NH-N$) and 1380 cm^{-1} (sulfonamido group).

NMR spectra

In the NMR spectra, the peak at δ 12.8 to 14.9 ppm (relative to TMS) gave evidence of the —NH proton. Further peaks at δ 6.8 to 8.3 ppm, δ 2.4 to 2.5 ppm and δ 4.4 to 5.2 ppm corresponded to the presence of the aromatic ring, the CH_3 protons of the $COCH_3$ and the OCH_2CH_3 groups, respectively.

Biological assay

Ethyl 2,3-dioxobutyrate-2-(sulfonamidophenyl)hydrazone was found to be active against *E. coli*, *A. hydrophilis*, *P. mirabilis*, *K. pneumoniae*, *S. typhi*, *P. schigelloids*, *Citrobacter* and *C. ovis*. Ethyl 2,3-dioxobutyrate-2-N^1-2-(pyrimidylsulfonamidophenyl)hydrazone was active against *V. cholerae*, *P. hydrophilis*, *P. schigelloids* and *P. vulgaris*. Ethyl 2,3-dioxobutylrate-2-N^1-2-(thiazolylsulfonamidophenyl) hydrazone had activity against *E. coli*, *A. hydrophilis*, *P. mirabilis*, *P. schigelloids* and *Citrobacter*. Ethyl 2,3-dioxobutyrate--2-N^1-2-[(4,6-dimethyl)pyrimidylsulfonamidophenyl]hydrazone was active against *A. hydrophilis*, *P. mirabilis*, *K. pneumoniae*, *P. vulgaris*, *Citrobacter* and *C. ovis*.

*

The authors wish to express their sincere thanks to Prof. M. K. JAIN (Principal), Sahu Jain College, Najibabad, for laboratory facilities and to CDRI, Lucknow, for the spectral data and elemental analyses. The authors also express their gratitude to C.S.I.R., New Delhi (India), for financial assistance.

REFERENCES

[1] VOGEL, A. I.: A Text Book of Practical Organic Chemistry, pp. 477—478, Longmans, Green and Co. Ltd., London 1968

C. P. SINGH
A. C. OJHA
Chemical Laboratories, Sahu Jain College, Najibabad
246763, U.P., India

Acta Chimica Academiae Scientiarum Hungaricae, Tomus 104 (2), pp. 117—122 (1980)

INFRARED ABSORPTION INTENSITIES OF STEROIDS

G. ARULDHAS,* G. JALSOVSZKY and S. HOLLY

(Central Research Institute for Chemistry, Hungarian Academy of Sciences, Budapest)

Received April 16, 1979
Accepted for publication July 6, 1979

The IR absorption intensities of the $\nu C{=}O$ and $\nu C{=}C$ bands of seven steroid derivatives have been determined. In acetoxysteroids different $\nu C{=}O$ intensities were obtained for the primary, secondary and tertiary acetoxy groups. The $\nu C{=}O$ intensity of the 20-oxo group was found to depend on the substituents.

Introduction

This paper deals with the $\nu C{=}O$ and $\nu C{=}C$ band intensities of pregn-4-ene-3,20-dione derivatives. These compounds have at least three, more or less overlapping bands in the 1750—1600 cm^{-1} region, which makes the individual band intensities difficult to determine by methods used so far.

Intensity measurements of fundamental importance were made by JONES *et al.* [1] on 55 steroid derivatives. They measured the $\nu C{=}O$ intensities of 41 steroid monoketones, which were found to be fairly independent of the position of the keto group (except when conjugated with $C{=}C$ bonds). Significantly different intensities were obtained, however, for the 20-oxo group in the pregnane side chain. For compounds with more carbonyl groups, only the total intensities of the overlapping bands were determined, and no attempt was made to estimate individual intensities.

In contrast with these results, no significant difference was found between the $\nu C{=}O$ intensities of cyclic and acyclic keto groups by DVORJANTSEVA and SHEINKER [2].

For compounds with more carbonyl groups the graphic resolution of overlapping bands is known to cause large and unpredictable errors, and thus this method cannot be used to obtain reliable intensities. Therefore, the measurements reported so far were restricted to the determination of total band areas.

However, overlapping bands may be resolved by means of iterative least-squares fitting methods [3]. Assuming that the shapes of isolated IR absorption bands may be described to good approximation by analytical functions (Gauss, Cauchy, or their product or sum functions), the resolution of overlapping bands into the sum of such functions may lead to a unique solu-

---

* On leave from Kerala University, India.

tion, and the integrals of the components can be regarded as the individual band intensities. The aim of our work was to determine intensities by this method.

Experimental

Chloroform solutions of 0.2, 0.1 and 0.05 mole/l concentration were prepared. The solutions and the solvent were filled into matched pairs of sodium chloride liquid cells, the accurate path lengths of which were determined by the method of interference fringes.

The spectra in the region 1850—1550 cm^{-1} were recorded on a Perkin–Elmer 225 spectrophotometer using a scale expansion of 2 mm/cm^{-1}. With slit program 6, the spectral band width varied between 1.70 and 1.75 cm^{-1} over the region studied. Transmittances were read from the chart at 2 cm^{-1} intervals, and the data were punched on Hollerith cards for computer processing.

For all solutions two spectra were recorded with different instrument settings (gain, scan speed, pen response time), and the spectra were digitized and evaluated separately.

Calculation methods

The spectra were resolved into Gauss–Cauchy product functions by Method V of PITHA and JONES [3]. The integrals of the component functions were calculated by Simpson's rule in each cycle, and iteration was terminated when the integrals changed less than 1% between two cycles. From a plot of the component bands the apparent half-band widths were determined graphically, and they were used to determine the true half-band widths by means of the correction factors given by RAMSAY [4]. Since in most cases the ratio of spectral band width to half-band widths was below 0.1, the corrections were small.

The bands were integrated between the limits set by the beginning and the end of recording, and wing corrections were performed according to the method of RAMSAY [4]. They were found to be between 1 and 7%.*

Intensities were calculated in the form of integrated absorption coefficients

$$A = \frac{0.02303}{c \cdot d} \int \log_{10} \left(\frac{T_0}{T} \right) \mathrm{d}\nu$$

where c is the concentration in mole $\cdot$ l^{-1}, d is the path length in cm, T is percentage transmittance, and ν is the wavenumber in cm^{-1}. The value of A is obtained in km $\cdot$ $\text{mole}^{-1} = 100\ \text{l} \cdot \text{mole}^{-1} \cdot \text{cm}^{-2}$. Mean values and variances were calculated from the results of six parallel measurements.

Results and Discussion

The compounds investigated are listed in Table I, together with the absorption maxima and intensities obtained from the band fitting calculation. For compounds **1—6** the spectra could be resolved unambiguously into the

---

* In some calculations, the integrals were evaluated more precisely, beyond the above limits. The results were practically equal to those obtained over the region of 1850—1550 cm^{-1}, indicating that RAMSAY's wing corrections are overestimated for the band shapes actually recorded.

Table I

Absorption maxima and intensities obtained by the band fitting calculation

No.	Compound	ν cm^{-1}	A km · mol^{-1}
1	21-Hydroxypregn-4-ene-3,20-dione 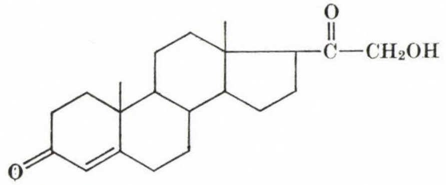	1616	62 ± 9
		1665	421 ± 10
		1707	152 ± 14
2	21-Acetoxypregn-4-ene-3,20-dione 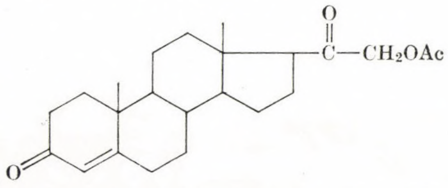	1616	42 ± 1
		1665	434 ± 8
		1725	272 ± 5
		1750	193 ± 4
3	16α-Methyl-17α,21-dihydroxypregn-4-ene--3,20-dione 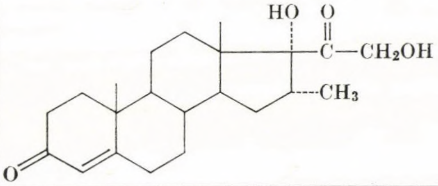	1614	62 ± 19
		1665	433 ± 10
		1709	148 ± 17
4	17α-Hydroxy-21-acetoxypregn-4-ene-3,20-dione 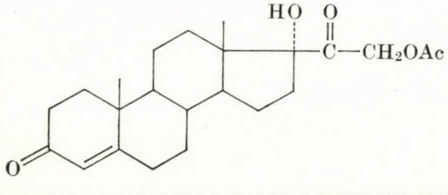	1615	79 ± 20
		1664	447 ± 19
		1727	257 ± 7
		1748	171 ± 13
5	17α-Acetoxy-21-hydroxypregn-4-ene-3,20-dione 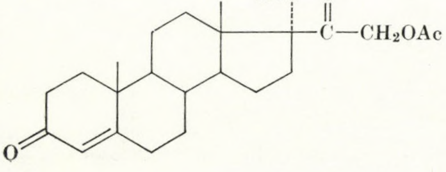	1616	66 ± 11
		1665	451 ± 17
		1712	68 ± 12
		1733	347 ± 16

Table 1 (continued)

No.	Compound	ν cm^{-1}	A $km \cdot mol^{-1}$
6	17α,21-Diacetoxypregn-4-ene-3,20-dione 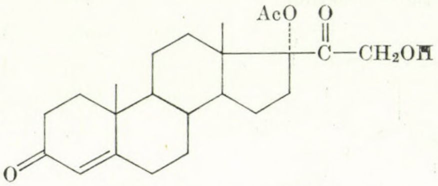 	1616 1665 1732 1736 1751	60 ± 15 467 ± 21 302 ± 21 179 ± 15 200 ± 8
7	11β,17α,21-Triacetoxypregn-4-ene-3,20-dione 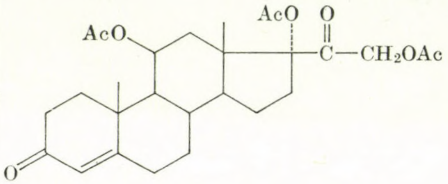 	1619 1668 1720 1750*	37 ± 5 381 ± 18 — 921 ± 25

* Four bands in this region

required number of bands, but for compound **7** our attempts failed owing to the strong overlap in the region 1750—1720 cm^{-1}, and therefore only the intensity sum of four bands is given.

On the basis of previous experiences concerning the absorption frequencies of primary and tertiary acetoxysteroids, the resolved absorption bands could be assigned to the functional groups. Table II shows the intensities as grouped on the basis of these assignments.

Table II

Characteristic group intensities

No. of compound	Intensity km · mole⁻¹					
	4-C=C	3-oxo	20-oxo	11β-Ac	17α-Ac	21-Ac
1	62	421	152	—	—	—
2	42	434	272	—	—	193
3	62	433	148	—	—	—
4	79	447	257	—	—	171
5	66	451	68	—	347	—
6	60	467	179	—	302	200
7	37	381	(179)	240*	(302)	(200)

* Estimated from the total intensity, using data of compound **6**

Although the small number of compounds studied so far does not allow general conclusions to be drawn, some interesting tendencies can be read from the results. As could be expected, the highest absorption intensity is always due to the $\nu C{=}O$ vibration of the 3-oxo group, which is conjugated with the double bond in position 4. The next highest intensity can be assigned to $\nu C{=}O$ of the 17-acetoxy group.

The behaviour of the absorption of the 20-oxo group is very interesting. If there are hydroxyl groups in positions 17α and 21, the intensity of the above absorption is about 150 km · mole^{-1}. This intensity is substantially increased by 21-acetylation, but *decreased* by acetylation in position 17α. The opposite effects of the 17α- and 21-substituents are also shown by the medium intensity of the 20-oxo band in the 17α,21-diacetoxy derivative, compound **6**. In connection with this behaviour of intensity, it is worth noting that the frequency of the 20-oxo band is *increased* by both acetoxy substitutions.

Since the only difference between compound **6** and compound **7** is one acetoxy group in the 11β position, one can estimate the intensity of its absorption, although the corresponding band cannot be separated unambiguously. If it is assumed that the 11β-acetoxy group in compound **7** has no significant effect on the intensities of the 17α,21-diacetoxy-20-one system, the difference between the intensity sum measured for compound **7** and the sum of three band intensities corresponding to the 17α-acetoxy, 20-one and 21-acetoxy groups of compound **6** can be regarded as the intensity corresponding to the 11β-acetoxy group. The result of calculation, 240 km · mole^{-1}, is between the intensities of primary and tertiary acetoxy groups, *i.e.* the intensities of ester carbonyl absorptions increase in the primary, secondary, tertiary direction. Note that the corresponding frequencies show opposite behaviour.

The intensities of the bands arising from the conjugated $C{=}C{-}C{=}O$ system also show interesting features. As the bands are relatively separated from the other bands in the spectra, these intensities could be determined unambiguously for compound **7**, too. Therefore, it may be considered significant that the intensities of both the $\nu C{=}O$ and $\nu C{=}C$ bands are lower for compound **7** than for any of the other derivatives. Taking into account that the corresponding frequencies are slightly higher, it can be concluded that the extent of conjugation between the $C{=}O$ and $C{=}C$ bonds is smaller for this compound. It can therefore be assumed that a steric hindrance between the 11β-acetoxy group and the 19-methyl group causes some distortion in the A ring of the steroid ring system, which decreases the overlap between the p_z orbitals of C_4 and C_5 and possibly also decreases the coupling between the $C{=}C$ and $C{=}O$ stretching modes.

*

The authors feel indebted to Dr. J. Tóth (Gedeon Richter Pharmaceutical Works) for the samples, and to Mrs. V. Molnár for her assistance in the measurements.

REFERENCES

[1] JONES, R. N., RAMSAY, D. A., KEIR, D. S., DOBRINER, K.: J. Am. Chem. Soc., **74**, 80 (1952)
[2] DVORJANTSEVA, G. G., SHEINKER, YU. N.: Izv. Akad. Nauk. Ser. Fis., **26**, 1290 (1962)
[3] PITHA, J., JONES, R. N.: Can. J. Chem., **44**, 3031 (1966)
[4] RAMSAY, D. A.: J. Am. Chem. Soc., **74**, 72 (1952)

G. ARULDHAS University of Kerala — Trivandrum, India
György JALSOVSZKY
Sándor HOLLY } H-1025 Budapest, Pusztaszeri út 59–67.

Acta Chimica Academiae Scientiarum Hungaricae, Tomus 104 (2), pp. 123–140 (1980)

FLUORINATED STEROIDS, II*

POLYHALOGEN DERIVATIVES

Á. Néder, A. Uskert,** Zs. Méhesfalvi and J. Kuszmann
(Institue for Drug Research, Budapest)

Received June 1, 1979

Accepted for publication July 6, 1979

Addition of Br—F to 3-acetoxy-5,6-unsaturated steroids (**1**) yielded 5α-bromo-6β-fluoro derivatives **3** as the main components and the sterically less favoured 5α-fluoro-6β-bromo (**6**) and 5β-fluoro-6α-bromo isomers (**4**) as by-products. Formation of the theoretically possible fourth *trans* isomer, the 5β-bromo-6α-fluoro derivative (**7**) was not observed. Elimination of HBr from **3**-type steroids could only be achieved after oxidizing the 3-hydroxyl group to an oxo group. The 3-hydroxyl group in **14** and **25** could not be replaced by fluorine with FAR, as elimination of water took place to give 2,3-unsaturated derivatives. The same reaction was observed in the case of 5α-fluoro derivatives, which were obtained by addition of HF to 5,6-unsaturated steroids.

Addition of HF or Br—F to 3-fluoro-5,6-unsaturated steroids resulted in polyhalogenated derivatives. In one case the migration of the Me-19 group from C-10 to C-5 was also observed (**31**). Elimination of HBr from $3\beta,6\beta$-difluoro-5α-bromopregnan-20-one (**41**) could be achieved by treatment with a base, but isomerization of the 17-acetyl group took place.

The structures of all compounds, including their stereochemistry were unambiguously established by spectroscopy, using IR, ^{1}H- and ^{13}C-NMR methods.

In our previous paper [1] the synthesis of 3-fluoro-5,6-unsaturated steroids, starting from the corresponding 3-hydroxy derivatives was described. For investigating the structure–activity relationship of these biologically interesting compounds [2], the synthesis of 3,6-difluoro-4,5-unsaturated derivatives was decided. A conceivable synthesis of these compounds starts from 3-hydroxy- or -acetoxy-5-ene steroids which by addition of Br—F can be converted into 5-bromo-6-fluoro derivatives. The latter might give on treatment with a base the 3-hydroxy-4-en-6-fluoro compounds, the hydroxyl group of which may be exchanged with FAR [1] into fluorine.

Because of its instability [3], Br—F is usually prepared *in situ* in the reaction mixture according to the method of Olah *et al.* [4] using NBS or Br$_2$—AgNO$_3$ and (HF)$_x$-pyridine complex. Another possibility is to use *N*-bromoacetamide and anhydrous hydrogen fluoride [5] in a mixture of dichloromethane and tetrahydrofuran. Tetrahydrofuran is necessary to enhance the low ionisation of hydrogen fluroide. According to Bowers *et al.* [6] the addition

---

* For Part I, see Ref. [1].

** Present address: Institute of Agricultural Chemical Technology, University of Technical Sciences, Budapest.

reaction proceeds *via* a bromonium cation, similarly to the electrophilic addition of halogens to an olefinic double bond and, due to the prevailing anti-Markovnikov rule, the *trans*-5-bromo-6-fluoro derivatives are formed. The addition of J—F does not obey this rule, as exclusively the 5-fluoro-6-iodo isomer is obtained [7]; some years later a similar anomaly was found even in the case of F—Br [8].

Starting from an 5,6-unsaturated steroid (**1**) theoretically two bromonium cations (**2** and **5**) can be formed. Because of steric reasons, formation of the 5α,6α-isomer **2** is more probable than that of the 5α,6α-isomer **5** in which the 19-methyl group is in steric compression with the bromonium cation. Therefore the **2**⇌**5** equilibrium is shifted towards **2**. Attack of fluoride on the bridge atoms C-5 or C-6 will lead in the case of **2** to **3** and **4**. The same reactions yield the isomers **6** and **7** in the case of **5**. Of the so formed four dihalogen isomers, **3** and **6** are sterically more stable than **4** and **7**, as the A/B rings are *trans*-fused in the former two derivatives, and *cis*-fused in the latter ones. For all these reasons the most stable isomer **3** which is formed *via* the more stable intermediate **2** should be the predominant product. Nevertheless, in a dynamically controlled process the other isomers can also be formed; *e.g.* in the case of 13-ethyl-gonan-5-ene derivatives compound **6** was the main product [8].

In our experiments first 3β-acetoxy-5-androsten-17-one (**8**) was treated with Br—F, which had been generated according to WIESKE [9] using 70% aqueous hydrogen fluoride and NBS. Four compounds were isolated from the reaction mixture. Besides the 5α-bromo-6β-fluoro derivative **9**, which was formed as the main product (58%), the 5β-fluoro-6α-bromo isomer **10** (17%) and the 5α-fluoro-6β-bromo isomer **11** (9%) were found. The fourth component **12** was the deacetylated main product **9**.

The structures of the isomers **9**, **10** and **11** were established by NMR spectroscopy. As there is no H—F coupling in the spectra of **10** and **11**, the fluorine must be in position 5. According to the half-band width of H-3 ($\Delta\nu \sim$ 6Hz), being geminal to the β-hydroxyl group, this proton is equatorially arranged in **10**, indicating an A/B *cis* anellation. On the contrary, in **11** the same proton is axially arranged ($\Delta\nu \sim$ 24 Hz), consequently the A/B rings are *trans*-fused. Accordingly, the fluorine atom must be 5β in **10** and 5α in **11**. Owing to the *trans* addition of the halogen atoms, the bromine should be in 6α- and 6β-position, respectively, in these two isomers. This is in full agreement with the spectra, as the 6β situated bromine atom causes a strong paramagnetic shift of the Me-19 signal in compound **11** (1.40 ppm) compared with **10** (1.05 ppm). On the other hand, the half-band width of the geminal 6-H proton proves its *axial* (β) arrangement in compound **10** ($\Delta\nu \sim$26 Hz) and *equatorial* (α) in compound **11** ($\Delta\nu \sim$10 Hz). (For spectral data see Table I.)

The spectrum of the main component **9** shows the presence of the characteristic H—F coupling of 48 Hz; splitting of the Me-19 signal to a doublet

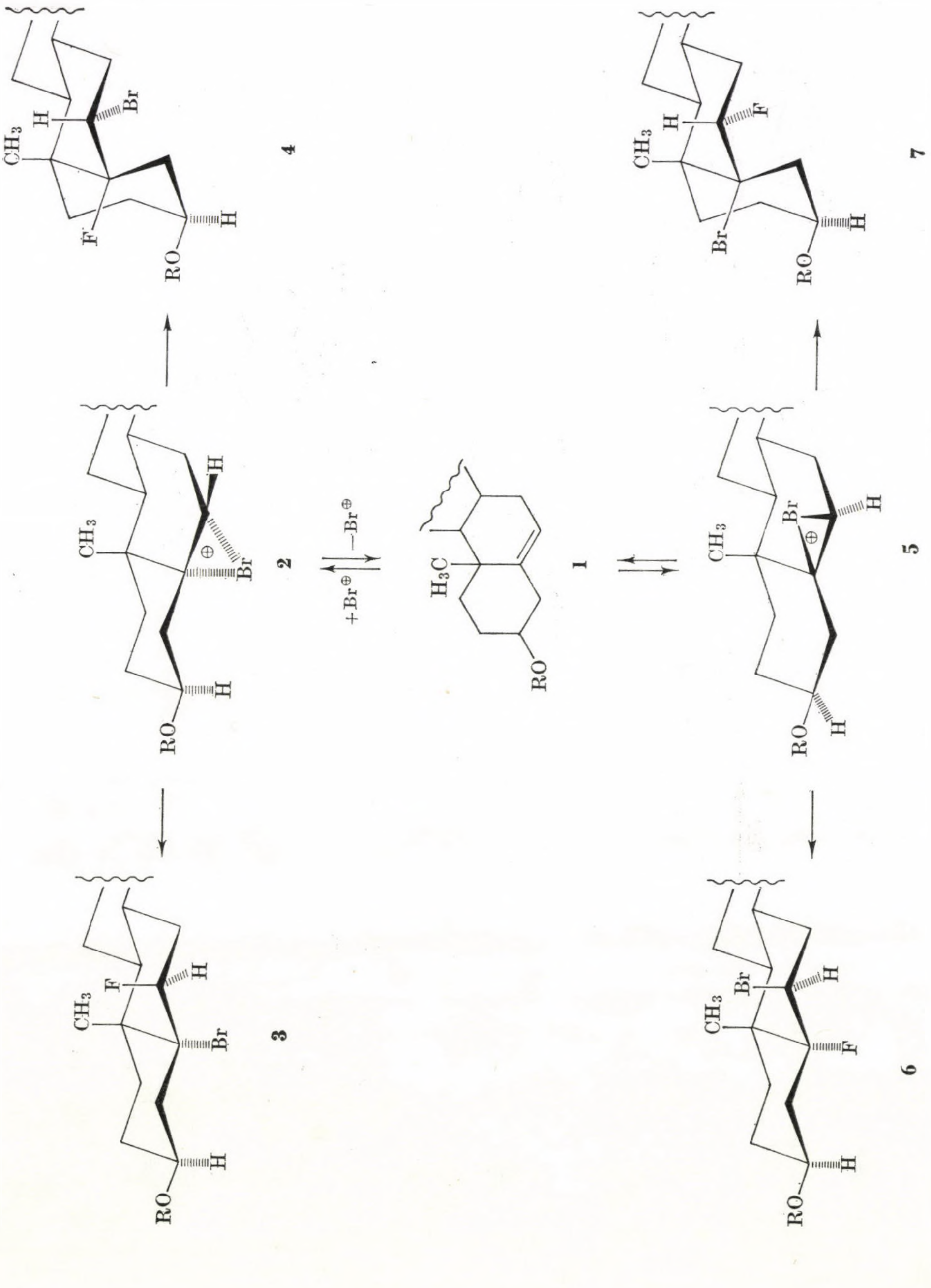
1
2
3
4
5
6
7
RO
H
CH₃
H₃C
F
Br
⊕
+Br⊕
−Br⊕

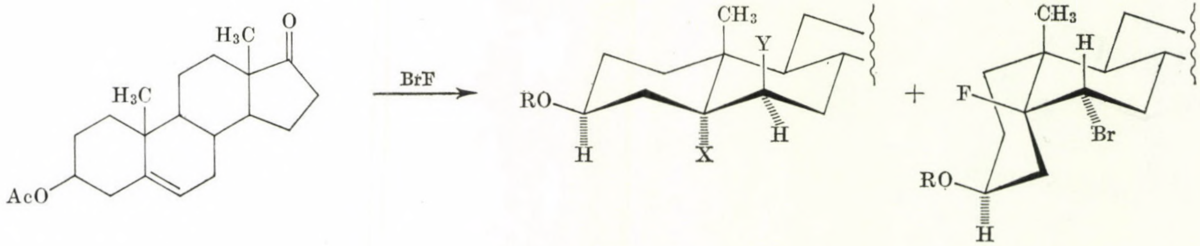

8

9 R=Ac, X=Br, Y=F
11 R=Ac, X=F, Y=Br
12 R=H, X=Br, Y=F

10 R=Ac
13 R=H

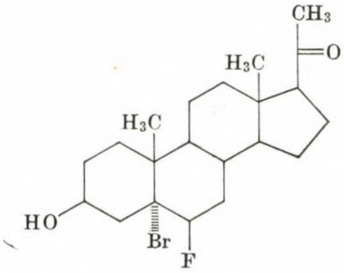

14

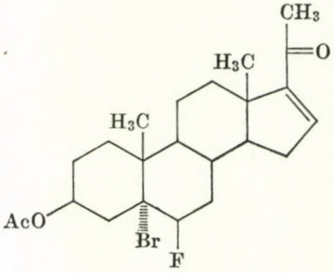

15

Table I

^{1}H-NMR data of compound* **9—15, 17, 19, 22** *and* **25—27**

Compound	Substituents at			Chemical shifts				
	C-3	C-5	C-6	H-3	H-6	Me-18	Me-19	Other signals
9	βAcO	αBr	βF	5.35 (24)	4.40; 5.22 (6)	0.88	1.27 (*d* $J = 4.5$)	2.02 AcO
10	βAcO	βF	αBr	5.10 (10)	4.60 (26)	0.85	1.05	2.05 AcO
11	βAcO	αF	βBr	5.10 (24)	4.08; 4.28 (10) ($J_{FH} = 10$)	0.90	1.40	2.05 AcO
12	βHO	αBr	βF	4.30 (25)	4.40; 5.22 (7)	0.87	1.27 (*d* $J = 4$)	—
13	βHO	βF	αBr	4.10 (10)	4.65 (26)	0.85	1.05	—
14	βHO	αBr	βF	5.30 (22)	4.40; 5.22 (8)	0.65	1.25 (*d* $J = 4$)	2.05 Me-21
15	βAcO	αBr	βF	5.40 (26)	4.45; 5.25 (6)	0.90	1.30 (*d* $J = 4$)	2.05 AcO; 2.25 Me-21; 6.7 H-16
17	βHO	β-epoxy		3.70 (25)	3.12 ($J = 3$)	0.87	1.05	—
19	=O	en	αF	—	4.70; 5.50 (22)	0.90	1.20	6.08 H-4
22	en	αBr	βF	5.62 (5)	4.45; 5.52 (6)	0.68	1.12 (*d* $J = 3$)	5.62 5 H-2
25	βHO	αF	H	4.0 (30)	—	0.62	0.98	2.12 Me-21
26	en	αF	H	5.55 (8)	—	0.62	0.88	2.07 Me-21
27	αF	αF	H	4.35; 5.15 (8)	—	0.62	0.83	2.09 Me-21

* δ scale, half-band width in Hz is given in brackets

($J = 4.5$ Hz), due to long range coupling with the *axial* fluorine atom [10], as well as the *equatorial* (α) arrangement ($\Delta\nu \sim 6$ Hz) of the geminal H-6 prove the β arrangement of the fluorine atom. The half-band width ($\Delta\nu \sim 24$ Hz) of H-3 proves its *axial* arrangement, consequently rings A/B are *trans*-fused and the bromine must be in 5α position.

The addition of Br—F to unsaturated steroids was further studied on 3-acetoxypregn-5-en-20-one and 3-acetoxy-pregna-5,16-dien-20-one, but in both cases only the corresponding 5α-bromo-6β-fluoro isomers **14** and **15** could be isolated, which had been already briefly mentioned in the literature [9, 10, 11].

The elimination of HBr from the above mentioned bromo-fluoro isomers was studied in detail in the androstane series. Treatment of the 3β-acetoxy-5α-bromo-6β-fluoro derivative **9** with K_2CO_3 in methanol gave only the deacetylated product **12**, whose further treatment with zinc in ethanol resulted in the elimination of both halogen atoms, affording, after acetylation, the 5,6-unsaturated starting material **8**.

No reaction occurred when **12** was treated with potassium *t*-butoxide in *t*-butanol, with diaminobicyclo-octane (DABCO) in methanol, or with hydrogen chloride in ethyl acetate. Under more drastic conditions (ethanol–potassium hydroxide, reflux temperature) only halogen-free products, *i.e.* androst-4-en-3,17-dione (**16**) [12] and the corresponding 5,6β-epoxide **17** [13] were formed. The structure of the latter was further proved by converting it into its known acetate [14].

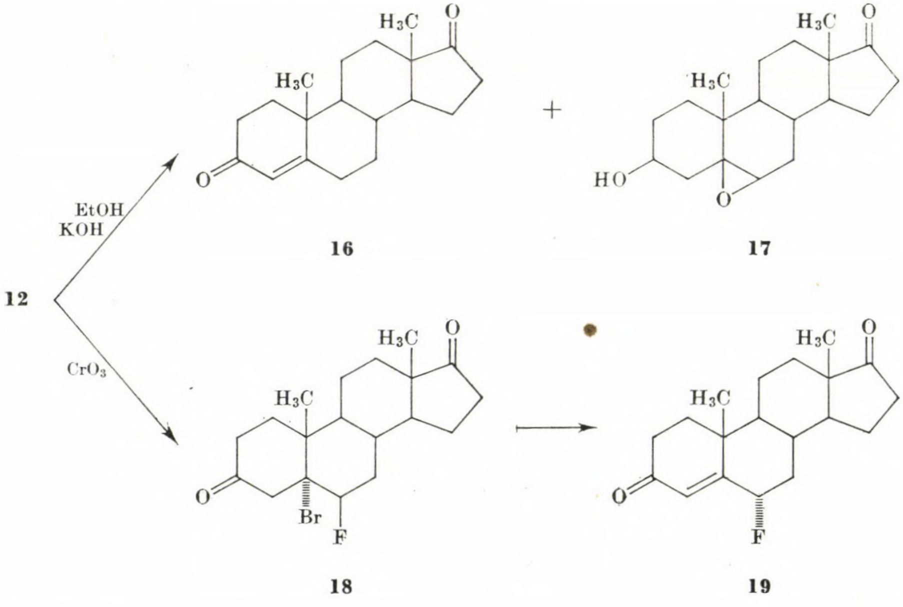

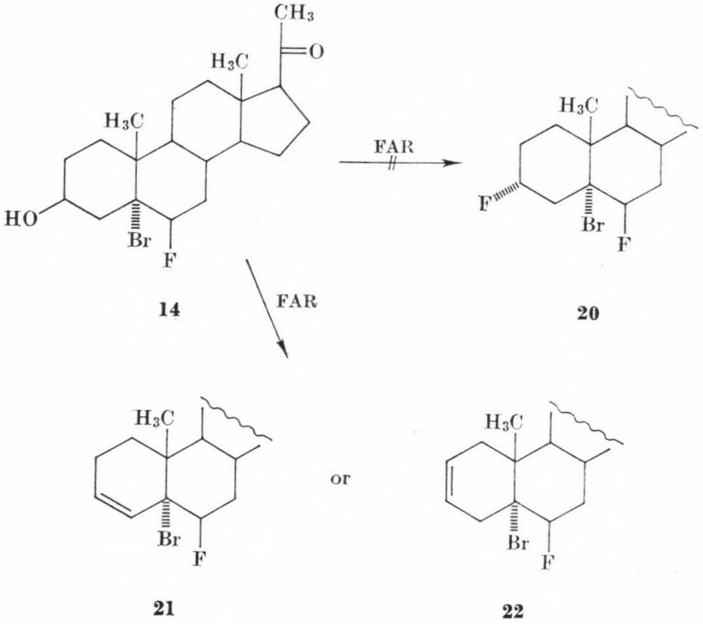

Contrary to **12**, the 5β-fluoro-6α-bromo isomer **10** resisted even the drastic reaction condition mentioned above, and only deacetylation took place affording compound **13**, which could be reacetylated to **10**.

When the hydroxyl group of **12** was oxidized with CrO_3 [15], the bromine in position 5 became labile, and treatment of the resulting 3-oxo derivative **18** with hydrogen chloride in ethyl acetate afforded, in accordance with the literature [16], the expected 4,5-unsaturated compound **19**. The driving force of this elimination reaction is clearly the formation of a conjugated double bond, as in the absence of the 3-oxo group no reaction took place.

To check the influence of the presence of the halogen atom in the steroid on the OH—F exchange reaction, the 3β-hydroxy-5α-bromo-6β-fluoro derivative **14** was treated with FAR as described previously [1]. Instead of the expected 3α-fluoro compound* **20**, however, an elimination reaction took place, leading to an unsaturated compound the structure of which could be either **21** or **22**. In the ^{1}H-NMR spectrum of the obtained compound the two protons of the double bond gave an overlapped multiplet at 5.62 ppm with a half-band width of ~8 Hz. That means that their chemical shifts must be very similar, suggesting the more symmetric 2,3-unsaturated structure **22** in which the double bond is flanked by two methylene groups, rather than a 3,4-unsaturated one (**21**).

---

* The OH—F exchange reaction should take place with inversion of configuration, according to the described mechanism [19].

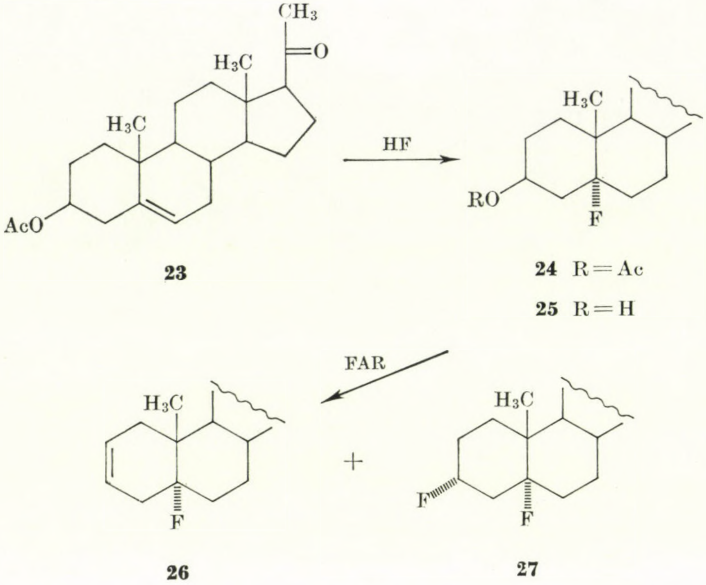

23

24 R = Ac

25 R = H

26

27

Complete shift of the fluorination reaction towards the unsaturated derivative means that stabilization of the formed carbonium intermediate by deprotonation [18] is in this case a much faster process than the attack of the fluoride anion. For investigating the role and influence of the bromine atom on the elimination process, the synthesis of a bromine-free model compound was carried out. Treatment of 3β-acetoxypregn-5-en-20-one (**23**) with anhydrous hydrogen fluoride [17] afforded the corresponding 5α-fluoro derivative **24** [25] which was deacetylated to **25**. Treatment of the latter with FAR yielded in this case, too, the unsaturated compound **26** as the main product, besides traces of the 3α,5α-difluoro derivative **27**. Thus the deprotonation reaction is practically unaffected by the electronegativity of the substituent in position 5, which is quite different in the cases of bromine and fluorine.

The location of the double bond in compound **26** could be proved unambiguously by ^{1}H- and ^{13}C-NMR investigation. In the proton spectrum the signal of the protons belonging to the double bond appeared at 5.55 ppm as a narrow multiplet ($\Delta\nu \sim 8$ Hz), similar to that of compound **22**. In the decoupled ^{13}C-spectrum the corresponding two unsaturated carbon atoms appeared at 126.0 and 121.9 ppm, respectively. The 5α-fluoro atom caused a doublet splitting of the C-5 signal (99.9 and 93.1 ppm) due to a geminal coupling of $J_{CF} = 171.5$ Hz. The similar shifts of the two protons and two carbon atoms, respectively, as well as the absence of any H—F or C—F coupling with the H and C atoms of the double bond excluded an allylic fluorine atom, consequently the double bond must be located in 2,3-position.

As the synthesis of the required 3,6-difluoro-4,5-unsaturated steroids could not be effected according to the original strategy because of the failure of the OH—F exchange reaction, another synthetic approach was needed. As model compound 3β-fluoroandrost-5-one (**28**) [1] was used, which was treated first with anhydrous hydrogen fluoride applying the method described for the analogous cholesterol derivatives [17]. Three compounds were isolated from the reaction mixture; the 5α-fluoro isomer **29** was the main product (57%), accompanied by the thermodynamically less favoured 5β-fluoro isomer **30** (5%) containing an A/B *cis*-fused system. Both structures were proved by ^{1}H-NMR spectroscopy (see Table II). The third compound, which was obtained in a yield of 3.7% contained, according to the analytical data, two fluorine atoms, but its ^{1}H-NMR spectrum had only the signal of one proton being geminal to fluorine, that of H-3, at δ 4.45 and 5.25 ppm, respectively. As the half-band width (10 Hz) proved its *equatorial* arrangement, the A/B rings must be *cis*-fused. The lack of a second proton with a geminal H—F coupling shows that the second fluorine must be attached to one of the bridge atoms. The paramagnetic shift of the Me-19 group (1.20 ppm) compared with the similarly *cis*-fused 5β-fluoro derivative **30** (1.03 ppm) suggested the 19-nor structure **31**, in which migration of the Me-19 group from C-10 to C-5 took place and the fluorine is attached to C-10, in β-position. A similar rearrangement reaction has been described in the case of other steroids [20].

When 3β-fluoropregn-5-en-20-one (**32**) was treated under similar conditions with H—F, the corresponding 5α-fluoro isomer **33** was obtained as the

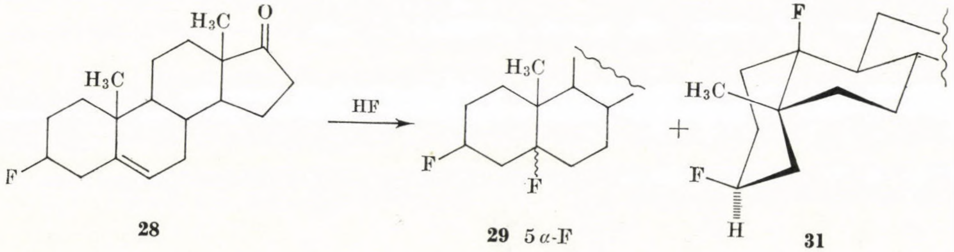

28

29 5α-F

30 5β-F

31

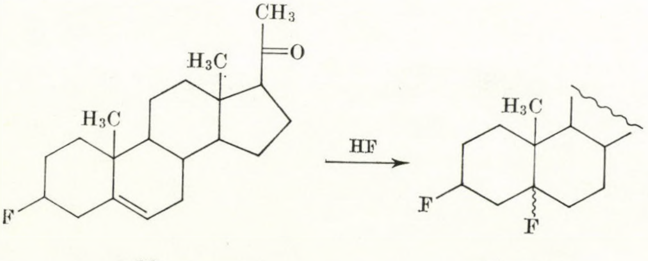

32

33 5α-F

34 5β-F

Table II

^{1}*H-NMR data* of 3β-fluoro-substituted steroids* **28–31**, **33–45** *and* **47–50**

Compound	Substituents at		Chemical shifts				
	C-5	C-6	H-3	H-6	Me-18	Me-19	Other signals
28	en	en	3.95; 4.80 (25)	5.45 (10)	0.90	1.08	—
29	αF	H	4.40; 5.25 (25)	—	0.85	1.05	—
30	βF	H	4.50; 5.30 (10)	—	0.87	1.05	—
31	βMe	H	4.45; 5.25 (10)	—	0.90	—	1.20 C_5—Me
33	αF	H	4.30; 5.20 (26)	—	0.65	1.05	2.10 Me-21
34	βF	H	4.50; 5.30 (10)	—	0.62	1.05	2.10 Me-21
35	αBr	βF	4.70▽; 5.55● (22)	4.40▽; 5.25● (10)	0.90	1.30 (*d* $J = 4$)	—
36	βF	αBr	4.45▽; 5.25 (10)	4.60▽ (24)	0.87	1.07	—
37	αMeO	βHO	4.30; 5.15 (22)	4.00 (10)	0.90	1.25	3.15 MeO
38	αMeO	βAcO	4.25; 5.15▽ (30)	5.15▽ (8)	0.90	1.22	3.25 MeO
39	αBr	βF	4.80; 5.70 (22)	4.60; 5.35 (5)	0.95	1.32 (*d* $J = 4$)	4.60 8 H-4
40	en	βF	4.70▽; 5.55● (20)	4.55▽; 5.35● (10)	0.95	1.25 (*d* $J=1.5$)	5.65; 5.85 ($J_{HH} = 4.5$; $J_{FH} = 11$) H-4
41	αBr	βF	5.00; 5.50 (30)	4.60; 5.08 (8)	0.64	1.27 (*d* $J = 4$)	2.10 Me-21
42	βF	αBr	4.55; 5.30 (12)	4.55 (26)	0.62	1.05	2.10 Me-21
43	en	βF	4.75▽; 5.30● (30)	4.55▽; 5.35● (*t* $J = 5$)	0.68	1.20 (*d* $J = 2$)	2.10 Me-21; 2.50 H-17; 5.65; 5.74 ($J_{HH}=5$; $J_{FH}=12$) H-4
44	en	βF	4.65▽; 5.30● (26)	4.55▽; 5.25● (7)	0.96	1.20 (*d* $J = 2$)	2.10 Me-21; 2.80 H-17; 5.65; 5.75 ($J_{HH}=5$; $J_{FH}= 12$) H-4
45	β-epoxy		4.40; 5.00 (32)	3.05 ($J = 2$)	0.62	1.05	2.10 Me-21
47	en	βF	4.75; 5.30 (30)	4.55; 5.35 (*t* $J = 5$)	0.66	1.20 (*d* $J = 2$)	5.65; 575 ($J_{HH} = 5$; $J_{FH} = 12$) H-4
48	en	en	3.95; 4.78 (26)	5.45 (10)	0.77	1.05	3.25 ≡CH; 3.95 OH
49	αF	H	3.30; 5.20 (26)	—	0.78	1.02	3.25 ≡CH
50	en	βF	4.45; 5.30 (20)	4.45; 5.30 (10)	—	1.25 (*d* $J = 2$)	2.55 ≡CH; 5.75 ($J_{HH} = 6$; $J_{FH} = 12$) H-4

* δ scale, half-band width in Hz is given in brackets

▽, ● overlapped multiplets

main component (69%) and the corresponding 5β-isomer **34** as a by-product (9.4%).

In our further experiments the addition reaction of Br—F was investigated according to WIESKE [9]. Starting from the unsaturated androstane derivative **28**, the reaction afforded the expected 5α-bromo-6β-fluoro isomer **35** as the main component (62%) and the less favoured, A/B *cis*-fused 5β-fluoro-6α-bromo isomer **36** as a by-product (15%). Besides these two isomers two further compounds were isolated. One proved to be a further brominated derivative **39** (1.6%), which could have been formed from **35** by oxidative bromination at C-4, whereas the other was formed probably during the work-up of the reaction mixture as the halogen atoms at C-5 and C-6 were substituted by an α-methoxyl and β-hydroxyl group, respectively (**37**). The structure of the latter derivative, which was isolated in a yield of 1.3%, was proved by acetylation (**38**) and the ^{1}H-NMR spectrum. The half-band width of H—3 proved its *axial* arrangement, consequently the A/B rings are *trans*-fused. The signal of the methoxyl group appears at 3.20 ppm, but no corresponding geminal partner proton can be detected. The signal of H-6 being geminal to the hydroxyl group appears at 4.00 ppm with a half-band width of 10 Hz, proving its *equatorial* arrangement and thereby the β-arrangement of the hydroxyl group. This is in good agreement with the observed paramagnetic shift of the Me-19 group (1.25 ppm).

To obtain chemical proof for the structure of the dibromo compound **39**, the bromine atoms were removed by reduction with zinc in ethanol. Under these conditions, however, the fluorine at C-6 was also eliminated and the original starting material, the 3β-fluoro-5,6-unsaturated derivative (**28**) was

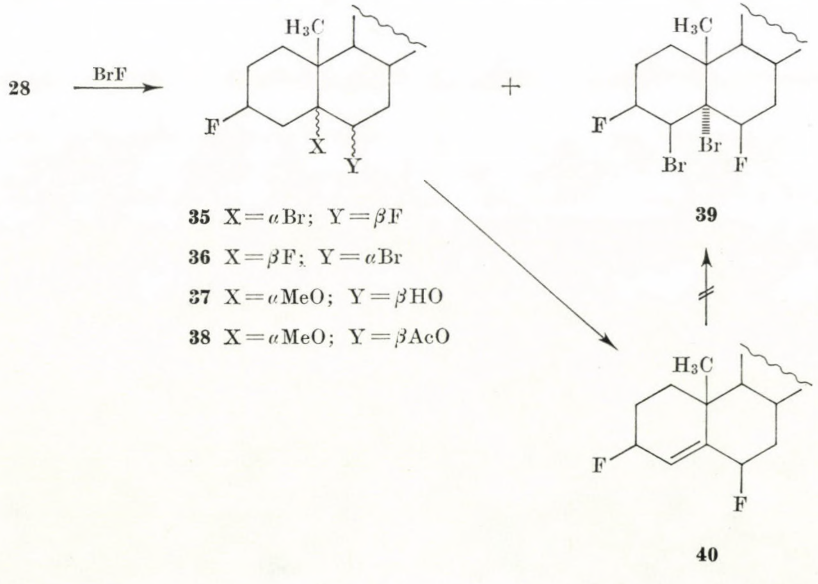

35 X=αBr; Y=βF

36 X=βF; Y=αBr

37 X=αMeO; Y=βHO

38 X=αMeO; Y=βAcO

39

40

formed. Another synthetic approach to prepare compound **39** started with the 5α-bromo derivative **35**, which on treatment with potassium *t*-butoxide could be converted into the 3β,6β-difluoro-4-ene derivative **40**. This is in sharp contrast with the corresponding 3-hydroxy derivative **12**, mentioned earlier, where no elimination of HBr took place under similar conditions. The different behaviour of these two compounds shows that fluorine in position 3 resembles much more the presence of an oxo group (**18**) promoting the elimination of HBr, even under acidic conditions. The 5-bromo compound **35** remains, however, unchanged when treated with acid, consequently the driving force of the base-catalyzed elimination reaction is the easy deprotonation of the methylene group at position 4, being flanked by two strong electron-withdrawing halogen atoms.

Addition of bromine to compound **40** should give either **39**, or the less stable, A/B *cis*-fused 4α,5β-dibromo isomer. The double bond proved, however,

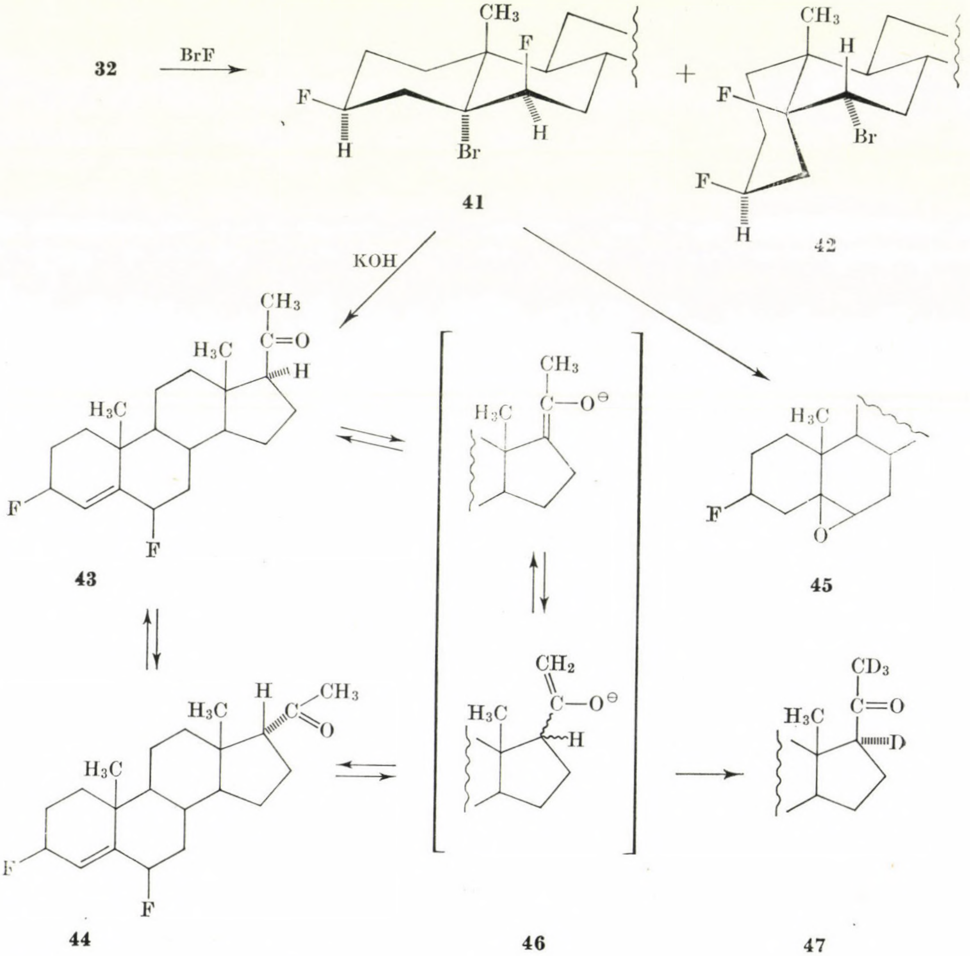

to be completely unreactive, which is probably due to the presence of two fluorine atoms in allylic position.

When the 3,5-difluoro-6-bromo derivative **36** was treated with potassium *t*-butoxide in *t*-butanol, with DABCO in methanol, or with potassium hydroxide in ethanol, no elimination of HBr took place. The different behaviour of this compound compared with the isomer **35** can be explained by the different positions of the methylene group, deprotonation at which is the critical step in the elimination reaction of HBr. As mentioned above, this methylene group is activated in **35**, but in isomer **36** it is the H-7 proton which should be removed, and this is not activated enough.

Addition of Br—F to the pregnene derivative **32** yielded the expected 5α-bromo-6β-fluoro compound **41** as the main product (59%) and the 5β-fluoro-6α-bromo isomer **42** as a by-product (3%). The structures of the isomers could be established unambiguously by ^{1}H-NMR, following the same reasoning as described for the isomeric pair **9** and **10**. Compound **41** gave on treatment with potassium hydroxide in ethanol three derivatives. Two of them, **43** and **44**, proved to be isomers, differing only in the steric arrangement of the 17-acetyl group. Epimerization of this group in the presence of a strong base is well known and was described first in 1937 [21]. The epimerization proceeds *via* an enolate **46**. This could be proved by the proton spectrum after treating compound **43** in the presence of a catalytic amount of potassium hydroxide in D_2O. During this reaction the H-17 as well as the protons of the Me-21 group are exchanged by deuterium, affording the deuterated derivative **47**.

The third derivative, which was isolated from the reaction mixture on treating **41** with base, contained only one fluorine atom and an epoxide at C-5,6. The steric arrangement of the latter could not be proved unambiguously by ^{1}H-NMR, as the corresponding α- and β-epoxides give very similar chemical shifts [22]. The positive optical rotation suggests, however, 5β,6β-structure for **45**.

To increase the biological activity of the different fluorinated androstane derivatives (**28**, **29**, **40**) an ethynyl group was introduced into position 17, using potassium acetylide reagent [23].

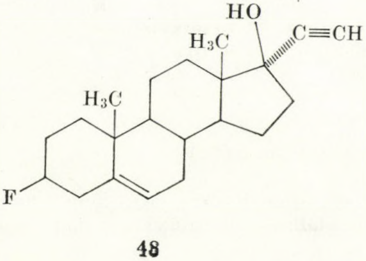

48

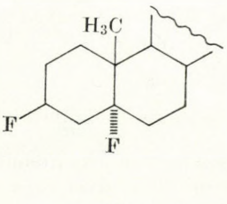

49

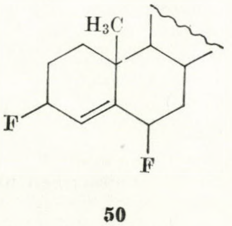

50

The so obtained derivatives **48**, **49** and **50** proved to be more active compared with the starting materials. For instance, compound **48** revealed a significant androgenic activity at a dose of 2 mg/day (170%), whereas **50** showed an uterotropic activity at a dose of 1 mg/day (180%).

Experimental

M.p.'s were determined with a Boetius apparatus and are uncorrected. TLC was effected on Kieselgel HF_{254} with benzene–tetrahydrofuran 40:3 (*A*) and 4 : 1 (*B*). For detection a 20% solution of $SbCl_5$ in chloroform was used with subsequent heating at 110 °C. Column chromatography was carried out on Woelm Silica Gel (63—200 μm) using benzene–tetrahydrofuran 25 : 1 (*C*) and 6 : 1(*D*) for elution. The ^{1}H-NMR spectra were recorded at 60 MHz with a JEOL-60-HL spectrometer and the ^{13}C-NMR spectra with a VARIAN XL-100 spectrometer for solutions in chloroform-*d*, using tetramethylsilane as internal standard. IR spectra were recorded in KBr pellets with a Perkin–Elmer 577 spectrometer. Mass spectra were obtained with a Varian MAT SM-1 instrument.

All evaporations were performed in a rotary evaporator under diminished pressure after having dried the organic solutions over sodium sulfate. Reactions with hydrogen fluoride were carried out in polyethylene bottles. Optical rotations were determined in chloroform ($c = 1$).

Reaction of 3β-acetoxyandrost-5-en-17-one (8) with Br—F

To a stirred solution of **8** (30 g) in methylene dichloride (300 ml) aqueous HF (70%; 28.5 ml; sp.gr. 1.27) and subsequently NBS (20.4 g) were added at 0 °C. The reaction mixture was stirred at 0 °C for 30 min and then poured into a solution of potassium hydrogen carbonate (133.5 g) in water (700 ml). The separated organic solution was washed with water, dried and evaporated. The residue (40.4 g) was separated by column chromatography, using solvent *C* for elution. The corresponding fractions were evaporated and the residue was recrystallized from methanol to give the following four components:

3β-Acetoxy-5α-bromo-6β-fluoroandrostan-17-one (**9**, 22.50 g; 58%), m.p. 183—186 °C, $[\alpha]^{20}_{D}-3°$; R_f 0.70 (*A*); 3β-acetoxy-5α-fluoro-6β-bromoandrostan-17-one (**11**, 3.51 g; 9%), m.p. 218—220 °C, $[\alpha]^{20}_{D}+6°$; R_f 0.55 (*A*); 3β-acetoxy-5β-fluoro-6α-bromoandrostan-17-one (**10**, 6.60 g; 17%), m.p. 186—189 °C, $[\alpha]^{20}_{D}+55°$; R_f 0.40 (*A*).

$C_{21}H_{30}O_3BrF$ (429.41). Calcd. Br 18.60; F 4.45. Found for **9**: Br 18.98; F 5.16; for **11**: Br 17.90; F 5.12 and for **10**: Br 18.60; F 4.45%.

3β-Hydroxy-5α-bromo-6β-fluoroandrostan-17-one (**12**, 1.76 g; 5%), m.p. 175—177 °C, $[\alpha]^{20}_{D}+3.5°$, R_f 0.20 (*A*).

$C_{19}H_{28}O_2BrF$ (387.32). Calcd. Br 20.60; F 4.90. Found Br 20.42; F 5.17%.

Reaction of 9 with ethanolic KOH

Compound **9** (14.7 g) was boiled with a solution of potassium hydroxide (10 g) in ethanol (400 ml) for 1.5 h. The solution was then diluted with water (500 ml) and the alcohol was evaporated. The obtained crude syrup was separated by column chromatography using solvent *D* for elution. The proper fractions were evaporated and the residue was recrystallized from methanol to yield the following two components:

Androst-4-en-3,17-dione (**16**, 4.2 g; 43%), m.p. 171—173 °C, $[\alpha]^{20}_{D}+192°$, R_f 0.60 (*B*), *Lit.* [12] m.p. 171—173 °C, $[\alpha]^{20}_{D}+196°$ (c 1.61); and 3β-hydroxy-5,6β-epoxyandrostan-17-one (**17**, 0.98 g; 9.8%), R_f 0.30 (*B*), which was converted by treatment with pyridine–acetic anhydride into its acetate (1.09 g; 97.5%), m.p. 185—186 °C, $[\alpha]^{20}_{D}+39°$, R_f 0.80 (*B*). *Lit.* [14] m.p. 186—187 °C, $[\alpha]^{20}_{D}+40.3°$ (c 1.595).

3β-Hydroxy-5β-fluoro-6α-bromoandrostan-17-one (13)

Compound **10** (5 g) was treated with a solution of potassium hydroxide (3 g) in ethanol (100 ml) as described for compound **9**, to give, after recrystallization from ethanol, pure **13** (2.65 g; 58.5%), m.p. 194—196 °C, $[\alpha]^{20}_{D}+70°$, R_f 0.6 (*B*).

$C_{19}H_{28}O_2BrF$ (387.32). Calcd. Br 20.6; F 4.9. Found Br 19.82; F 5.35%.

3β-Hydroxy-5α-bromo-6β-fluoropregnan-20-one (14)

A stirred solution of 3β-acetoxypregn-5-en-20-one (10 g) in methylene dichloride (75 ml) was treated at 0 °C with a 7 : 3 mixture of HF–pyridine (12.3 g) and subsequently with NBS (6.8 g). The reaction mixture was stirred for 30 min at 0 °C and was then poured onto ice. The mixture was neutralized with sodium carbonate and the separated organic solution was washed with water, dried and evaporated. Recrystallization of the residue from methanol gave 3β-acetoxy-5α-bromo-6β-fluoropregnan-20-one (7.8 g), R_f 0.72 (*A*), m.p. 180—184 °C. This was dissolved in methanol (500 ml) and a solution of potassium carbonate (5 g) in water (30 ml) was added. The reaction mixture was boiled for 15 min, then water (200 ml) was added and the methanol was evaporated. The remaining slurry was cooled, filtered and the crystals were washed with water to yield pure **14** (6.7 g; 57.5%), m.p. 184—187 °C, $[\alpha]_D^{20}$ 0°, R_f 0.2 (*A*) *Lit.* [9] m.p. 168—170 °C, $[\alpha]_D^{20}+4.8°$.

3β-Acetoxy-5α-bromo-6β-fluoropregn-16-en-20-one (15)

To a solution of 3β-acetoxypregn-5,16-dien-20-one (5 g) in methylene chloride (50 ml a 7 : 3 mixture of HF–pyridine (6.5 g) and subsequently NBS (3.4 g) were added. The reaction mixture was processed as described for the Br—F addition of compound **8**, to give, after column chromatography (*C*) and recrystallization from methanol, pure **15** (3.6 g; 50.8%), m.p. 181—184 °C, $[\alpha]_D^{20}-45°$. *Lit.* [11] m.p. 183—185 °C, $[\alpha]_D^{20}-47.6$ °C.

6α-Fluoroandrost-4-en-3,17-dione (19)

A solution of the 5α-bromo-6β-fluoro derivative **12** (2.4 g) in acetone (260 ml) was oxidized at 0 °C as described in the literature [15], by adding gradually a solution (3 ml) prepared by dissolving CrO_3 (26.72 g) in conc. H_2SO_4 (23 ml) and diluting the mixture with water to 100 ml. The reaction mixture was stirred at 0 °C for 10 min, and was then poured into 5 volumes of ice-water. The precipitate was filtered off after 1 h and was washed with water till neutral, to give crude 5α-bromo-6β-fluoroandrostan-3,17-dione (**18**). This was treated without purification with HCl-saturated ethyl acetate (50 ml) according to the literature [16]. After 2 h at 5 °C the reaction mixture was diluted with two volumes of ethyl acetate and was washed with water, 5% aqueous sodium hydrogen carbonate and water. The dried solution was evaporated and the residue recrystallized from ethyl acetate–ether to give pure **19** (1.09 g; 58.5%), m.p. 228—231 °C, $[\alpha]_D^{20}+184°$. *Lit.* [24] m.p. 229—231°, $[\alpha]_D^{20}+185°$.

5α-Bromo-6β-fluoropregn-2-en-20-one (22)

A solution of compound **14** in dry chloroform (80 ml) was treated with FAR [1] (8.5 ml) as described for compound **25**. The crude product was purified by column chromatography (*C*) to give, after evaporation and recrystallization of the residue from methanol, pure **22** (4.9 g; 60%), m.p. 145—147'°C, R_f 0.85 (*A*).

$C_{21}H_{32}OBrF$ (397.4). Calcd. Br 20.20; F 4.80. Found Br 20.50; F 5.15%.

3β-Acetoxy-5α-fluoropregnan-20-one (24)

Dry HF (15.8 g) was added to methylene chloride (100 ml) at −60 °C. To the stirred mixture a solution of compound **23** (10 g) in methylene dichloride (100 ml) was added during 5 min. The reaction mixture was stirred at −60 °C for 1 h, and was then poured into saturated aqueous sodium hydrogen carbonate solution. The organic layer was washed with water, dried, evaporated, and the residue was recrystallized from methanol to yield pure **24** (5.82 g; 53.5%), m.p. 192—195 °C, $[\alpha]_D^{20}+85°$. *Lit.* [25] m.p. 194—196 °C, $[\alpha]_D^{20}+86°$.

3β-Hydroxy-5α-fluoropregnan-20-one (25)

Compound **24** (5.75 g) was deacetylated as described for **14** to give pure **25** (4.8 g; 93.5%), m.p. 187—189 °C, $[\alpha]_D^{20}+105°$. *Lit.* [25] m.p. 188—189 °C, $[\alpha]_D^{20}+109°$.

Reaction of compound 25 with FAR

A solution of compound **25** (4.5 g) in dry chloroform (30 ml) was treated at 0 °C with FAR [1] (4.5 ml). Stirring was continued for 2 h at 0 °C and then for 1 h at room temperature. Sodium fluoride (22.5 g) was added, and after 1 h the reaction mixture was cooled to 0 °C and the excess of FAR destroyed by the addition of methanol (2.25 ml). The precipitated salts were filtered off and the filtrate evaporated. The solid residue was recrystallized from methanol to yield a crude mixture (3.15 g) which was separated by column chromatography using solvent *C* for elution.

The fractions having R_f 0.85 (*A*) gave, after evaporation and recrystallization from methanol, pure 5α-fluoropregn-2-en-20-one (**26**, 2.46 g; 58.2%), m.p. 166—168 °C, $[\alpha]^{20}_{D}+125°$.

$C_{21}H_{31}OF$ (318.46). Calcd. F 5.97. Found F 6.12%.

The fractions of R_f 0.70 (*A*) gave after similar treatment 3α,5α-difluoropregnan-20-one (**27**, 0.15 g; 3.3%), m.p. 198—201 °C, $[\alpha]^{20}_{D}+92$ °C.

$C_{21}H_{32}OF_2$ (338.47). Calcd. F 11.20. Found F 11.25%.

Reaction of compound 28 with dry HF

Addition of HF to **28** (10 g) was carried out as described for compound **24** to yield, after evaporation, a crude mixture (9.12 g), which was separated by column chromatography (*C*). The fractions gave, after evaporation and recrystallization from methanol, the following components: 3β,5α-difluoroandrostan-17-one (**29**, 6.1 g; 57.1%), m.p. 165—166 °C, $[\alpha]^{20}_{D}+79$ °C, R_f 0.77 (*A*); 3β,10β-difluoro-5β-methyl-nor-androstan-17-one (**31**, 0.4 g; 3.75%), m.p. 187—190 °C, $[\alpha]^{20}_{D}+87°$, R_f 0.65 (*A*) and 3β,5β-difluoroandrostan-17-one (**30**, 0.52 g; 4.85%), m.p. 181—184 °C, $[\alpha]^{20}_{D}+87°$, R_f 0.55 (*A*).

$C_{19}H_{28}OF_2$ (320.41). Calcd. F 12.20. Found for **29**: F 12.30; for **31**: F 12.25; for **30**: F 12.31%.

Reaction of compound 32 with dry HF

Addition of HF to **32** (5.24 g) was carried out as described for compound **28** to give the following derivatives: 3β,5α-difluoropregnan-20-one (**33**, 2.2 g; 68.9%), m.p. 162—164 °C, $[\alpha]^{20}_{D}+81°$, R_f 0.90 (*A*) and the 3β,5β-difluoro isomer **34** (0.30 g; 9.35%), m.p. 160—162 °C, $[\alpha]^{20}_{D}+76°$, R_f 0.30 (*A*).

$C_{21}H_{32}OF_2$ (338.47). Calcd. F 11.25. Found for **33**: F 11.19; for **34**: F 11.18%.

Reaction of compound 28 with Br—F

Addition of Br—F to compound **28** (20 g) was carried out as described for **8** to give, after column chromatography (*C*) and recrystallization from methanol, the following four compounds: 3β,6β-difluoro-4β,5α-dibromoandrostan-17-one (**39**, 0.5 g; 1.5%), m.p. 193—196 °C, $[\alpha]^{20}_{D}-12°$, R_f 0.85 (*A*).

$C_{19}H_{26}OBr_2F_2$ (468.23). Calcd. Br 34.10; F 8.15. Found Br 33.89; F 8.30%.

3β,6β-Difluoro-5α-bromoandrostan-17-one (**35**, 16.6 g; 61.8%), m.p. 179—181 °C, $[\alpha]^{20}_{D}$ 0°, R_f 0.66 (*A*) and 3β,5β-difluoro-6α-bromoandrostan-17-one (**36**, 3.9 g; 14.6%), m.p. 233—235 °C, (subl.), R_f 0.47 (*A*), $[\alpha]^{20}_{D}+67.3°$.

$C_{19}H_{27}OBrF_2$ (389.62). Calcd. Br 20.50; F 8.80. Found for **35**: Br 20.86; F 9.85, for **36**: Br 20.92; F 9.82%.

3β-Fluoro-5α-methoxy-6β-hydroxyandrostan-17-one (**37**, 0.3 g; 1.3%), m.p. 215—217 °C, R_f 0.20 (*A*).

$C_{20}H_{31}O_3F$ (338.45). Calcd. F 5.65. Found F 6.63%.

Acetylation of **37** (0.2 g) with pyridine–acetic anhydride afforded the corresponding 6β-acetoxy derivative **38** (0.22 g; 98.2%), m.p. 142—145 °C, $[\alpha]^{20}_{D}+8°$.

$C_{22}H_{33}O_4F$ (380.45). Calcd. F 4.98. Found F 4.85%.

3β,6β-Difluoroandrost-4-en-17-one (40)

To a solution of **35** (5 g) in *t*-butanol (250 ml) 1*M* potassium *t*-butoxide (20 ml) was added, and the reaction mixture was refluxed for 1.5 h. Water (200 ml) was then added and the butanol removed by distillation. The remaining slurry was filtered, the crude product was washed with water, dried, and recrystallized from methanol to yield **40** (3.72 g; 93.5%), m.p. 119—121 °C, $[\alpha]_D^{20}$+79°, R_f 0.60 (*A*).

$C_{19}H_{26}OF_2$ (308.40). Calcd. F 12.30. Found F 12.60%.

Reaction of compound 32 with Br—F

Addition of Br—F to compound **32** (12 g) was carried out as described for compound **28** to give the following two isomers: 3β,6β-difluoro-5α-bromopregnan-20-one (**41**, 9.35 g; 58.9%), m.p. 163—165 °C, $[\alpha]_D^{20}$+83°, R_f 0.75 (*A*) and 3β,5β-difluoro-6α-bromopregnan-20-one (**42**, 0.45 g; 2.85%), m.p. 189—191°, R_f 0.55 (*A*).

$C_{21}H_{31}OBrF$ (417.38). Calcd. Br 19.10; F 9.15. Found for **41**: Br 19.35; F 9.14, for **42**: Br 19.51; F 8.88%.

Reaction of compound 41 with ethanolic KOH

Treatment of **41** (5 g) with ethanolic KOH was carried out as described for **9** and the mixture of the reaction products was separated by column chromatography (*C*) to yield, after recrystallization from methanol, the following three components: 3β,6β-difluoro-17α-acetyl-androszt-4-ene (**44**, 0.24 g; 5.95%), m.p. 131—134 °C, $[\alpha]_D^{20}$—74°, R_f 0.84 (*A*) and 3β,6β-difluoropregn-4-en-20-one (**43**, 2.20 g; 54.5%), m.p. 171—173°, $[\alpha]_D^{20}$+80°, R_f 0.70 (*A*).

$C_{21}H_{30}OF_2$ (336.45). Calcd. F 11.30. Found for **44**: F 11.65; for **43**: F 11.62%.

3β-Fluoro-5,6β-epoxypregnan-20-one (**45**, 0.1 g; 2.5%), m.p. 170—171°C, $[\alpha]_D^{20}$+44°, R_f 0.52 (*A*).

$C_{21}H_{31}O_2F$ (334.46). Calcd. F 5.70. Found F 5.91%.

Deuteration of compound 41

Potassium (0.4 g) was dissolved in deuterated methanol (10 ml), then D_2O (0.2 ml) and compound **41** (0.6 g) were added. The solution was boiled for 1.5 h, cooled, neutralized with carbon dioxide and diluted with water (20 ml). Methanol was removed by evaporation, the precipitated material was filtered off, dried and purified by column chromatography (*C*) to obtain **47** (0.26 g; 53.5%), m.p. 164—166 °C, $[\alpha]_D^{20}$+70°, R_f 0.72 (*A*).

3β-Fluoro-17α-ethynylandrost-5-en-17β-ol (48)

A stream of dried acetylene was passed into a slurry of potassium *t*-butoxide (5.9 g) in tetrahydrofuran (120 ml) for 1 h. A solution of compound **28** (5 g) in dry tetrahydrofuran (120 ml) was then added and the bubbling of acetylene through the reaction mixture was continued for 3 h, until the starting material had been consumed (checked by TLC). The excess of acetylene was expelled by nitrogen, the reaction mixture was poured into ice-water and saturated with ammonium chloride. The organic layer was separated, dried and the solvent evaporated. The residue gave on recrystallization from methanol pure **48** (4 .38 g; 80.5%) m.p. 201—203 °C, $[\alpha]_D^{20}$—129°, R_f 0.48 (*A*).

$C_{21}H_{29}FO$ (316.44). Calcd. F 6.00. Found F 5.96%.

3β,5α-Difluoro-17α-ethynylandrostan-17β-ol (49)

Compound **29** (4.5 g) was treated with acetylene as described above, but the reaction was complete in 1.5 h. Recrystallization of the residue from methanol afforded pure **49** (4.16 g; 86.2%), m.p. 208—210 °C, $[\alpha]_D^{20}$—37°, R_f 0.66 (*A*).

$C_{21}H_{30}F_2.O$ (336.45). Calcd. F 11.30. Found F 11.35%.

3β,6β-Difluoro-17α-ethynylandrost-4-en-17β-ol (50)

Compound **40** (4.5 g) was treated with acetylene as described above, but the reaction was complete in 30 min. The reaction mixture was processed in the usual way to yield **50** (4.25 g; 87.5%), m.p. 117—119 °C, $[\alpha]_D^{20}$—39°, R_f 0.51 (*A*).

$C_{21}H_{28}F_2O$ (334.40). Calcd. F 11.41. Found F 11.58%.

REFERENCES

[1] Néder, Á., Uskert, A., Nagy, É., Méhesfalvi, Zs., Kuszmann, J.: Acta Chim. Acad. Sci. Hung. **103**, 231 (1980)
[2] Ciba Foundation Symposium: Carbon-Fluorine Compounds. Ass. Sci. Publ. Amsterdam—London—New York, 1972
[3] Ruff, O., Braida, A.: Z. Anorg. Allgem. Chem. **214**, 81 (1933)
[4] Olah, G. A., Nojima, M., Kerekes, I.: Synthesis, **1973**, 780
[5] Bowers, A.: J. Am. Chem. Soc., **81**, 4107 (1959)
[6] Bowers, A., Ibánez, L. C., Denot, E., Becerra, R.: J. Am. Chem. Soc. **82**, 4001 (1960)
[7] Bowers, A., Denot, E., Becerra, R.: J. Am. Chem. Soc., **82**, 4007 (1960)
[8] Kreb, U., Wiechert, R.: Ann., **572**, 78 (1971)
[9] Wieske, R.: German Pat. 19 16 923.1 (1969)
[10] Cross, A. D.: J. Am. Chem. Soc., **86**, 4011 (1964)
[11] Samsonova, N. V., Grinenko, G. S., Alekseeva, L. M., Skeinker, Yu. N.: Zh. Chem. Pharm., **10** (2), 106 (1976)
[12] Brooks, C. J. W., Norymberski, J. K.: Biochem. J., **55**, 371 (1953)
[13] Borgna, J. L., Mousseron-Canet, M.: Bull. Soc. Chim. France, **1970**, 2218
[14] Ruzicka, L., Muhr, A. C.: Helv. Chim. Acta, **27**, 503 (1944)
[15] Ahrem, A. A., Kamernickij, A. V., Kulikova, L. E., Levina, I. S., Terehina, A. J., Lisica, L. I., Ganina, I. V.: Zh. Chem. Pharm., **11** (8), 24 (1977)
[16] Carpio, H., Crabbé, P., Fried, J. H.: J. Chem. Soc. Perkin I, **1973**, 227
[17] Jacquesy, R.-C., Jacquesy, R., Levisalles, J.: Bull. Soc. Chim. France, **1967**, 1649
[18] Mousseron-Canet, M., Borgna, J.-L.: Bull. Soc. Chim. France, **2**, 613 (1969)
[19] Knox, L. H., Velarde, E., Berger, S., Cuadriello, D., Cross, A. D.: J. Org. Chem., **29**, 2187 (1964)
[20] Jacquesy, J.-C., Jacquesy, R., Petit, M.: Tetrahedron Lett., **1970**, 2595
[21] Butenandt, A.: Ber., **70**, 96 (1937)
[22] Borgna, J.-L., Mousseron-Canet, M.: Bull. Soc. Chim. France, **6**, 2210 (1970)
[23] Bite, P., Moravcsik, I., Schäfer, I., Horváth, Gy., Méhesfalvi, Zs., Borvendég, J., Hermann, I.: Brit. Pat. 1,507,103 (1976)
[24] Bowers, A., Ringold, H. J.: Tetrahedron, **3**, 14 (1958)
[25] Bowers, A., Denot, E., Urquiza, R.: Tetrahedron Lett., **1960**, 34

Ágnes Néder
Andor Uskert
Zsuzsa Méhesfalvi
János Kuszmann
H-135 Budapest, P.O. Box 82

Acta Chimica Academiae Scientiarum Hungaricae, Tomus 104 (2), pp. 141–146 (1980)

EXPLOSION METHOD FOR THE SYNTHESIS OF PEROVSKITE-TYPE BINARY OXIDES

L. Wachowski, S. Zieliński* and A. Burewicz

(Laboratory of General Chemistry and Synthesis of Catalysts,
A. Mickiewicz University, Poznań, Poland)

Received March 2, 1979

Accepted for publication July 9, 1979

A new explosion method has been proposed for the synthesis of perovskite-type binary oxides and compared with the methods already described in the literature. The synthesis of $LaCoO_3$ was taken as an example. The proposed method enables the preparation of X-ray pure final product of a large surface area due to relatively low temperature of calcination.

Introduction

The perovskite-type binary oxides with the general formula ABO_3 are extensively studied for a long time. The reason for this fact is the technological importance of their physical properties such as magnetic, ferro-, pyro-, and piezoelectric ones as well as their electro-optical effects [1, 2]. Recently the perovskites, mainly binary oxides of rare earth elements and transition metal elements, have aroused interest in their applications as catalysts of redox reactions [3]. It has been found that perovskites can be used as electrodes for fuel cells instead of noble metals [4] and as catalysts for automative exhaust gases [5] and these facts gave an impulse to study the catalytic properties of perovskites. The perovskite samples used in the catalytic studies were synthesized most often by ceramic [6], coprecipitation [7], spray-drying [8] and freeze-drying [9, 10] methods. As results from the critical review of perovskite methods given by Voorhoeve *et al.* [11], the freeze-drying method enables to obtain samples with good chemical homogeneity at lower temperatures compared to the other methods. The samples prepared by the above method distinguish also by higher surface area than the ones obtained by other techniques.

Our paper is aimed at presenting a new and simple method elaborated by us for perovskite synthesis. The method proposed by us takes an advantage of the explosive properties of ammonium nitrate present in the reaction medium. The above salt is formed as a result of the nitrate ions of the reaction sub-

---

* To whom correspondence should be addressed.

strates and ammonium ions introduced to the reaction medium in form of ammonium carbonate. The application of ammonium nitrate as an agent for explosive reaction initiation has been known for a long time, *e.g.* in the synthesis of magnetic materials with spinel structure [12, 13]. However, it was applied for the first time for preparation of ABO_3-type compounds in our study.

The ceramic, coprecipitation and freeze-drying techniques were also used in this study for comparison purposes.

Experimental

$LaCoO_3$ was synthesized by explosion, coprecipitation, freeze-drying and ceramic methods. In the case of the first three mentioned techniques 0.2 *M* aqueous solutions of lanthanum(III) and cobalt(II) nitrates were used as substrates. The solution of lanthanum(III) nitrate was obtained by dissolving when heated an appropriate amount of La_2O_3 (99.99% purity) in 2 *N* HNO_3. In the prepared solutions, lanthanum was determined gravimetrically as La_2O_3 and cobalt electrogravimetrically [14].

In the case of the explosion method the aqueous solution of a mixture of lanthanum(III) and cobalt(II) nitrates with the stoichiometry of La : Co = 1 : 1 was treated with saturated ammonium hydrogen carbonate solution until pH 7.0 was reached. The amounts of the above nitrates taken to prepare the solution were aimed at obtaining about 20 g of the final product. The resulted precipitate of carbonates was dissolved in glacial acetic and then concentrated in a vacuum evaporator to about 300 cm^3 what makes about 30 cm^3 of the starting volume. Further evaporation of the solution was carried out in a quartz vessel until a spontaneous explosive reaction was initiated. A dark-brown powder was obtained as a result of the explosion. We divided it into portions which were calcinated at 773 and 973 K, respectively, for 5—30 hours (in the range of every 5 h) in an oxygen stream (flow rate of 20 dm^3/h). In another series of experiments, the product obtained after the explosion was placed into a reaction tube (made of quartz glass) connected to a vacuum system and heated to 573 K. The heating time was 2 h and the pressure 1.33 Pa (10^{-2} mm Hg). Further thermal treatment was carried out at 773 K for 10 h in an oxygen stream (20 dm^3/h).

While using the coprecipitation technique, an aqueous solution of a mixture of lanthanum(III) and cobalt(II) nitrates with an appropriate stoichiometry was treated with 10% solution of oxalic acid (100% excess of the acid used). The resulted precipitate was filtered, washed and dried at 393 K for 3 h. After a thorough grinding in a mortar, the product was calcinated at 1173 K for 15 h in an oxygen stream (20 dm^3/h).

The preparation of $LaCoO_3$ by the freeze-drying technique was performed by spraying a mixture of La(III) and Co(II) nitrates with an appropriate stoichiometry onto the surface of liquid nitrogen and then the frozen mixture of nitrates was introduced into a reaction tube connected to a vacuum system. After lyophilization, the reaction tube filled with anhydrous nitrates was attached to a vacuum evaporator, the temperature was gradually raised to 523K which was maintained for 2 h while the pressure was 1.33 Pa. Then the reaction tube content was transferred into a platinum crucible and calcinated at 773 K for 10 h in a stream of oxygen (20 dm^3/h).

For the ceramic method lanthanum(III) oxalate dihydrate was used. This was prepared by adding a saturated solution of oxalic acid to a lanthanum(III) nitrate solution. The precipitate $[La_2(C_2O_4)_3 \cdot 2\ H_2O]$ was filtered, washed, and dryed at 388 K for 24 h. Cobalt(II) carbonate — used as the other starting material — was obtained in the reaction between saturated solution of ammonium carbonate and a solution of cobalt(II) nitrate. The resulted precipitate was filtered, washed and then dried at 388 K for 10 h. The substrates prepared in such a way were analyzed for lanthanum and cobalt contents using the same methods as described above. The mechanical mixture of substrates (La : Co = 1) was pelletized and then calcinated at 1523 K for 48 h.

In order to improve the homogeneity, the calcination was interrupted every 10 hours and the product was ground in a mortar. Then the pelletizing was repeated and the calcination continued. During the thermal treatments the temperature was kept constant within ±5 K.

The samples of lanthanum cobaltate prepared by the above described methods were analyzed for La and Co. Cobalt was determined electrogravimetrically [12] whereas the determination of lanthanum was carried out colorimetrically measuring the absorption of the lanthanum-arsenazo(III) [15] complex after the electrodeposition of cobalt. A similar analytical procedure has been applied by us earlier [16] for the determination of nickel in the presence of lanthanum and neodymium.

The surface area of the samples was measured by gas chromatographic method using a Perkin–Elmer Sorptometer Model 212 C. Helium was used as a carrier gas, nitrogen as an adsorbate. The X-ray analysis was performed on a diffractometer TUR-M-62 with a goniometer HZG-3 made in GDR. Nickel-filtered Cu K_α radiation was used.

Results and Discussion

A series of $LaCO_3$ synthesis was carried out by us using the above described techniques but only those results are presented in the paper which led to products of the highest surface area and were crystallographically homogeneous. The application of ammonium bicarbonate as a precipitating agent was aimed, among others, to add ammonium ions to the reaction mixture. On the other hand, the introduction of glacial acetic acid enabled to obtain a homogeneous solution of lanthanum and cobalt ions again as well as to remove carbonate ions. The above procedure made possible to introduce into the reaction mixture the amount of NH_4^+ ions necessary to combine with NO_3^- ions present in the solution. The solution of lanthanum and cobalt acetates, concentrated in vacuum evaporator, became syrupy liquids during the further evaporation in a quartz vessel. The explosion occurred when "the syrup" attained the temperature of 533 K. The presence of ammonium nitrate is responsible for the explosion. On the ground of numerous tests, a good reproducibility of the process was established. The dark-brown powder obtained after the explosion was subjected to X-ray analysis. The crystallographic structure of substrates was already undetectable whereas it was possible to

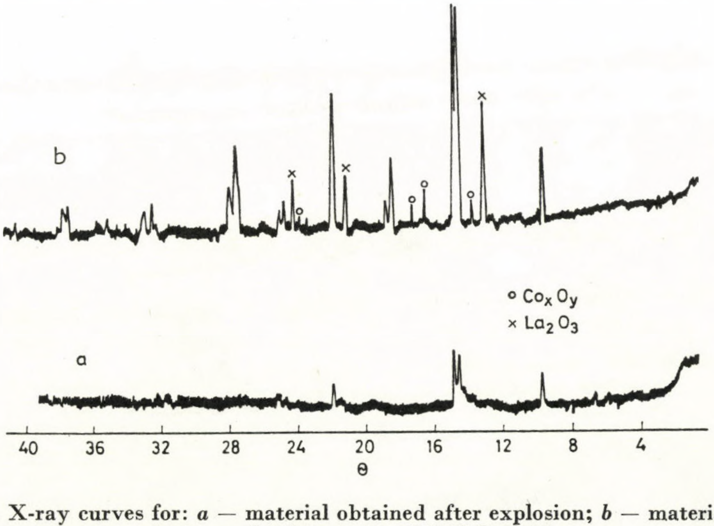

Fig. 1. X-ray curves for: *a* — material obtained after explosion; *b* — material after explosion and calcinated at 773 K for 30 hours

identify clearly the fundamental reflections of the crystallographic structure R_3^{-} *m* in the trigonal system with parameters of $\alpha = 60° 48'$, $a = 5.436$ Å or pseudocubic one with $\alpha = 90° 42'$ $a = 3.83$ Å [17, 18] (Fig. 1a). The calcination at 773 K for 30 h of the explosive reaction product does not lead to X-ray pure $LaCoO_3$. In such a case, small amounts of La_2O_3 ($d = 2.98$ Å) and Co_xO_y ($d = 2.87$ Å corresponding to Co_2O_3 and $d = 2.49$ Å corresponding to Co_3O_4) occured in addition to the predominant phase of $LaCoO_3$ (Fig. 1b). Only calcination at 973 K resulted in final product of high crystallographic purity. It is worth to mention the changes in phase composition during calcination. After 5 hours of calcination, a principally monophase product (with some relics of other phases) is obtained (Fig. 2a). A positive test for the presence of nitrate in the sample (the reaction with diphenylamine) forced us to extend the calcination time in order to remove them completely. After 10 h calcination, a growth of the concomitant phases (La_2O_3 and Co_xO_y) have been observed (Fig. 2b). They transformed into the phase of $LaCoO_3$ as a longer calcination time (Fig. 2c). The X-ray pure $LaCoO_3$ was obtained under these conditions after 30 h calcination (Fig. 2d). The surface area of $LaCoO_3$ sample

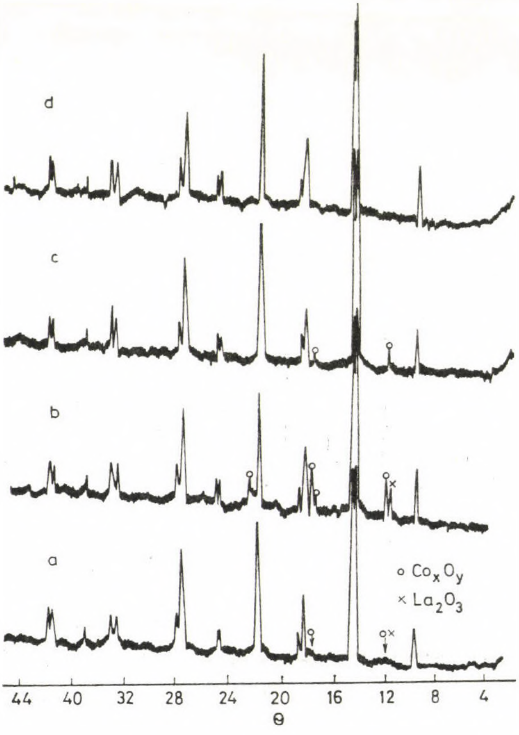

Fig. 2. X-ray curves for the material obtained after explosion and calcinated at 973 K for: *a* — 5 h; *b* — 10 h; *c* — 25 h; *d* — 30 h

Table I

Description of $LaCoO_3$

Method of preparation		Calcination temperature, K	Time of calcination, h	Surface area, m^2/g	Composition		
					%La	%Co	Co/La ratio
Ceramic		1523	48	1.7	56.12	24.76	1.04
Coprecipitation		1173	15	4.5	56.04	24.57	1.03
Freeze-drying		773	10	36.2	56.18	24.11	1.01
Explosion	without preliminary calcination	973	30	16.8	56.01	24.17	1.06
	with preliminary calcination at 573 °K, p = 1.33 Pa	773	10	34.6	56.10	24.66	1.04

prepared in such a way was 16.8 m^2/g. Though this value is considerably higher than the ones for samples obtained by ceramic and coprecipitation methods (Table I), nevertheless it is much below the value of surface area of the sample prepared by TSEUNG [10] (38 m^2/g) by the freeze-drying technique. In order to prepare $LaCoO_3$ sample with the highest possible surface area, the material obtained after the explosion was preliminary heated at 573 K for 2 h under p = 1.33 Pa and then calcinated at 773 K for 10 h in an oxygen stream (20 dm^3/h). The above procedure made possible to obtain $LaCoO_3$ sample with a surface area of 34.6 m^2/g.

The diffraction pattern of the above sample shows the same maxima and their intensities as the one given in Fig. 2d.

Conclusions

It results from the data on different techniques of $LaCoO_3$ preparation (presented in Table I) that the required temperature of calcination depends on the degree of homogeneity of substrates provided by a given method. The explosion method, developed by us, enables to maintain in the moment of the explosion, the homogeneity existing in the glacial acetic acid solution of the substrates. However, a small part of nitrates does not react during the explosion. It decomposes at higher temperatures under atmospheric pressure or at lower ones under reduced pressure. The optimal parameters for thermal treatment of the explosive reaction products are 973 K and 30 h whereas in the case of preliminary vacuum calcination they are 773 K and 10 h.

The obtained results lead to the conclusion that a decrease in the calcination temperature enables to obtain by the explosion method final product with a relatively high surface area comparable with that of the product prepared by the freeze-drying technique. The juxtaposition of the explosion method and the other techniques show such advantages of our method as its relative simplicity, relatively low expenditure of work (*e.g.* when compared with the freeze-drying technique) and the possibility of obtaining X-ray pure $LaCoO_3$ of rather large surface area. The explosion method can be easily adapted for the synthesis of other perovskite-type binary oxides.

REFERENCES

[1] Galasso, F. S.: Structure, Properties and Preparation of Perovskite-type Compounds, Pergamon Press, New York 1969

[2] Goodenough, J. B., Longo, J. M.: Landolt-Börnstein Numerical Data and Functional Relationship in Science and Technology, Springer-Verlag, New York 1970, vol. **4a**, pp. 126—314

[3] Meadowcraft, D. B.: Nature (London), **226**, 847 (1970)

[4] Libby, W. F.: Science, **171**, 499 (1975)

[5] Voorhoeve, R. J. H.: Advanced Materials in Catalysis, Academic Press, New York 1977, p. 129 Ir.

[6] Johnson, D. W., Gallagher, P. K., Shrey, F., Rhodes, W. W.: Am. Ceram. Soc. Bull., **55**, 520 (1976)

[7] Gallagher, P. K., Johnson, D. W. Jr., Shrey, F.: Mat. Res. Bull., **9**, 1345 (1974)

[8] De Lau, F. M.: Am. Ceram. Soc. Bull., **49**, 572 (1970)

[9] Schnettler, F. J., Monforte, F. R., Rhodes, W. W.: Sciences in Ceramics, Academic Press, New York 1968, vol. **4**, p. 79

[10] Tseung, A. C. C.: German Patent, 2.119.702 (1971) 4 Nov.

[11] Voorhoeve, R. J. H., Johnson, D. W. Jr., Remeika, J. P., Gallagher, P. K.: Science, **195**, 827 (1977)

[12] Proell, W., Stanley, W.: US Patent No. 3,137,598 (1964), US Patent No. 2,987,389 (1961), US Patent No. 2,955, 033 (1960)

[13] Burewicz, A.: Acta Chim. (Budapest) **77**, 45 (1973)

[14] Minczewski, J., Marczenko, Z.: Chemia analityczna, PWN, Warszawa 1965

[15] Marczenko, Z.: Kolorymetryczne oznaczanie pierwiastków, WNT, Warszawa 1968

[16] Zieliński, S., Wachowski, L.: Roczniki Chem., **45**, 1701 (1971), **50**, 1023 (1976)

[17] Raccah, P. M., Goodenough, J. B.: Phys. Rev., **155**, 932 (1966)

[18] Wold, A., Post, B., Banks, E.: J. Amer. Chem. Soc., **79**, 6365 (1957)

Leszek Wachowski
Stanisław Zieliński
Andrzej Burewicz
60—780 Poznań, Grunwaldzka 6, Poland

Acta Chimica Academiae Scientiarum Hungaricae, Tomus 104 (2), pp. 147—160 (1980)

REACTIONS OF MONO- AND DIARYLIDENECYCLOALKANONES WITH THIOUREA AND AMMONIUM THIOCYANATE, III*, **

ACYLATION AND ALKYLATION OF 3,4,5,6,7,8-HEXAHYDRO-2(1*H*)-QUINAZOLINETHIONES

T. LÓRÁND,[1] D. SZABÓ[1] and A. FÖLDESI[2]
([1]*Chemical Department of the Medical University, Pécs and*
[2]*Central Research Laboratory of the Medical University, Pécs*)

Received December 22, 1976
In revised form May 23, 1979
Accepted for publication July 11, 1979

4-Phenyl-3,4,5,6,7,8-hexahydro-2(1*H*)-quinazolinone (**B**), -quinazolinethione (**A**) and their 8-benzylidene derivatives (**C, D**) were acylated in position 3. With alkyl halides **A** and **C** gave 2-alkylmercapto derivatives (**Vc**, **VIa**—**Xa**). The tautomerism of **VIb**—**IXb** is discussed in detail.

Previously we reported the synthesis of some 3,4,5,6,7,8-hexahydro-2(1*H*)-quinazolinethiones and -quinazolinones (**A**—**D**) [2]. The present paper deals with the acyl and alkyl derivatives of these compounds.

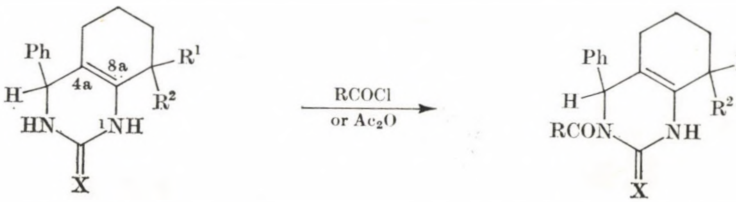

A ($X = S$, $R^1 = R^2 = H$)
B ($X = O$, $R^1 = R^2 = H$)
C ($X = S$, $R^1, R^2 = {=}CH{-}Ph$)
D ($X = O$, $R^1, R^2 = {=}CH{-}Ph$)

Ia ($X = S$, $R = CH_3{-}$, $R^1 = R^2 = H$)
Ib ($X = S$, $R = C_2H_5{-}$, $R^1 = R^2 = H$)
Ic ($X = S$, $R = C_6H_5{-}$, $R^1 = R^2 = H$)
IIa ($X = O$, $R = CH_3{-}$, $R^1 = R^2 = H$)
IIb ($X = O$, $R = C_2H_5{-}$, $R^1 = R^2 = H$)
IIIa ($X = S$, $R = CH_3{-}$, $R^1, R^2 = {=}CH{-}Ph$)
IIIb ($X = S$, $R = C_2H_5{-}$, $R^1, R^2 = {=}CH{-}Ph$)
IIIc ($X = S$, $R = C_6H_5{-}$, $R^1, R^2 = {=}CH{-}Ph$)
IVa ($X = O$, $R = CH_3{-}$, $R^1, R^2 = {=}CH{-}Ph$)
IVb ($X = O$, $R = C_2H_5{-}$, $R^1, R^2 = {=}CH{-}Ph$)

$Ac = CH_3CO{-}$

Fig. 1

---

* Part II, see Ref. [1].

** This research was presented in part at the Conference of the Hungarian Chemical Society, Veszprém, 1975.

Table I

Compound			M.p., °C	Formula, M.w. Yield, %	UV (ethanol) λ_{max}, nm (log ε)	IR, cm^{-1} (KBr)	^{1}H-NMR δppm, (CDCl$_3$)
	R	X					
Ia	CH$_3$	S	148–149	$C_{16}H_{18}N_2OS$ 286.41 41	276 (3.74) 332 (4.06)	νNH 3100–3370[d] νC=C 1720 amide I 1695 thioamide II 1220	1.4–2.3 *m* 8H CH_2 2.8 s 3H CH_3CO 5.9 s 1H CH 7.4 s 1H Ar 9.3 s 1H NH[a]
Ib	C_2H_5	S	166–170	$C_{17}H_{20}N_2OS$ 300.43 74	277 (3.93) 330 (4.15)	νNH 3100–3330[d] νC=C 1710 amide I 1670 thioamide II 1220	1.2 t 3H CH_3 1.4–2.3 m 8H CH_2 2.8–3.7 m 2H CH_2CO 5.7 s 1H CH 7.1–7.4 m 5H Ar 8.5 s 1H NH[a,b]
Ic	C_6H_5	S	155–162	$C_{21}H_{20}N_2OS$ 348.47 72	237 (4.08) 280 (4.01) 347 (3.81)	νNH $\begin{cases}3235 \text{ (sh.)}\\3170\end{cases}$ νC=C 1710 amide I 1690 thioamide II 1215	1.2–2.3 m 8H CH_2 5.3 s 1H CH 7.2–7.7 m 10H Ar, ArCO 10.9 s 1H NH[a,c]
IIa	CH$_3$	O	203–205	$C_{16}H_{18}N_2O_2$ 270.26 11	263 (3.69)	νNH 3160–3420[d] νC=O $\begin{cases}1725\\1685\end{cases}$ νC=C 1710 (sh.)	1.0–2.5 m 8H CH_2 2.6 s 3H CH_3CO 5.9 s 1H CH 7.2–7.6 m 5H Ar 8.1 s 1H NH[d]
IIb	C_2H_5	O	186 (d.)	$C_{17}H_{20}N_2O_2$ 284.37 43	264 (3.48)	νNH 3160–3380[d] νC=O $\begin{cases}1730\\1690\end{cases}$ νC=C 1715 (sh.)	1.1 t 3H CH_3 1.4–2.3 m 8H CH_2 2.6–3.3 m 2H CH_2CO 5.8 s 1H CH 7.0–7.4 m 5H Ar 7.5 s 1H NH[d,b,e]

[a] Disappears on the effect of D_2O

[b] ^{1}H-NMR data obtained with a 100-MHz instrument

[e] Recorded in $(CD_3)_2SO$

[c] Broad band with partial maxima

[d] All analyses of the new compounds were within accepted limits for C, H, N and S

Table II

Compound		M.p., °C	Formula, M.w. Yield, %	UV ethanol λ_{max}, nm (log ε)	IR, cm^{-1} (KBr)	^{1}H—NMR δppm, (CDCl$_3$)
R	X					
IIIa CH$_3$	S	190—194	$C_{23}H_{22}N_2OS$ 374.51 83	269 (4.32) 293 (4.28) 339 (3.9α)	νNH 3130—3370 amide I 1665 thioamide II 1210	1.6—3.0 m 6H CH$_2$ 2.8 s 3H CH$_3$CO[a] 6.1 s 1H CH 6.7 s 1H =CH 7.2—7.6 m 10H Ar 8.8 s 1H NH[b]
IIIb C$_2$H$_5$	S	164—166	$C_{24}H_{24}N_2OS$ 388.53 51	269 (4.51) 298 (4.42) 339 (4.12)	νNH 3150—3330 amide I 1665 thioamide II 1190	1.2 t 3H CH$_3$ 1.4—2.8 m 6H CH$_2$ 2.8—3.7 m 2H CH$_2$CO 5.9 s 1H CH 6.6 s 1H =CH 7.1—7.5 m 10H Ar 8.4 s 1H NH[b,c]
IIIc C$_6$H$_5$	S	210—215	$C_{28}H_{24}N_2OS$ 436.58 77	233 (4.53) 277 (4.61) 350 (3.95)	νNH 3170—3370 amide I 1695 thioamide II 1210	1.4—2.9 m 6H CH$_2$ 5.5 s 1H CH 7.0 s 1H =CH 7.1—7.7 m 15H Ar, ArCO 10.1 s 1H NH[b,d]
IVa CH$_3$	O	168—170	$C_{23}H_{22}N_2O_2$ 358.44 49	262 (4.38) 296 (4.37)	νNH 3150—3400[e] νC=O 1690 1665 (sh.)	1.4—2.8 m 6H CH$_2$ 2.4 s 3H CH$_3$CO[a] 5.9 s 1H CH 6.8 s 1H =CH 7.0—7.6 m 10H Ar 8.5 s 1H NH[b]
IVb C$_2$H$_5$	O	161 (d.)	$C_{24}H_{24}N_2O_2$ 372.47 50	262 (4.24) 298 (4.23)	νNH 3185—3400[e] νC=O 1695 1660	0.9 t 3H CH$_3$ 1.4—3.2 m 8H CH$_2$, CH$_2$CO 5.9 s 1H CH 6.8 s 1H =CH 7.1—7.5 m 10H Ar 8.2 s 1H NH[b,c,f]

[a] The CH$_3$CO signal overlaps the CH$_2$ signals

[b] Disappears on the effect of D$_2$O

[c] ^{1}H-NMR data obtained with a 100-MHz instrument

[d] Recorded in (CD$_3$)$_2$SO

[e] Broad band with partial maxima

[f] All analyses of the new compounds were within accepted limits for C, H, N and S

On acylating 2-oxo-tetrahydropyrimidines, ZIGEUNER *et al.* found that only one of the two NH groups was acylated [3].

The IR spectrum of **Ia** (Table I), prepared by acetylating **A**, has both the ν NH band (3100—3370 cm^{-1}) and the amide I band (1695 cm^{-1}). The signal of the ^1H-NMR spectrum at δ 2.8 ppm is assigned to the methyl of an acetyl group, and the signal at δ 9.2 ppm, disappearing on the effect of D_2O, is assigned to an NH group. Simple acetylation was concluded from the previous observations. The position of the acetyl group was determined by comparing the ^1H-NMR spectrum of **Ia** with that of **A**. As the shift at δ 4.8 ppm assigned to the C-4 methine proton of **A** increased to δ 5.9 ppm after acetylation, we came to the conclusion that the acetyl group attached to the nitrogen atom in the 3-position and the anisotropy effect of the CO group is responsible for the increase of the shift by 1.1 ppm.

We attempted to work with higher homologues of carboxylic acid derivatives, with sulfonic acid chlorides, and with aromatic carboxylic acid chlorides. In the aliphatic homologous series only the reaction with propionyl chloride was successful. With the higher homologues, the relatively great steric requirement of the reagent hinders the reaction. In the ^1H-NMR spectrum of the 3-propionyl derivatives of **A**—**D** (**Ib**—**IVb**; Tables I—II) the methylene protons of the propionyl group did not present the expected quartet (A_2X_3 spin system), but they gave a complicated multiplet.

We succeeded in preparing the 3-benzoyl derivatives of **A** and **C** (**Ic**, **IIIc**; Tables I—II); isonicotinic acid chloride, 3,5-dinitrobenzoyl chloride, *p*-toluenesulfonyl chloride and benzenesulfonyl chloride did not react with **A**. Compounds **B** and **D** afforded similarly the 3-acetyl and 3-propionyl derivatives (**IIa**, **IVa**, **IIb**, **IVb**; Tables I—II). In the IR spectrum of these compounds

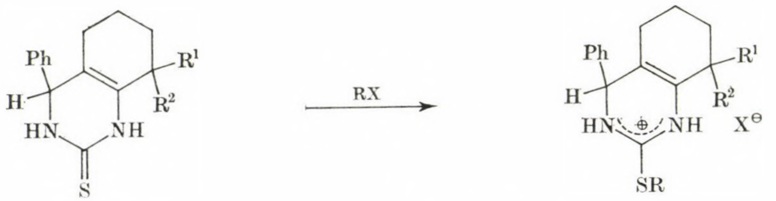

A ($R^1 = R^2 = H$)

C ($R^1, R^2 = =CH—Ph$)

[**Va** ($R = CH_3—$, $X=I$, $R^1=R^2= H$)]

VIa ($R = CH_3—$, $X=I$, $R^1,R^2= =CH—Ph$)

VIIa ($R = C_2H_5—$, $X = Br$, $R^1,R^2= =CH—Ph$)

VIIIa ($R = C_3H_7—$, $X = I$, $R^1,R^2= =CH—Ph$)

IXa ($R = C_4H_9—$, $X = Br$, $R^1,R^2 = =CH—Ph$)

Xa ($R = CH_2=CH—CH_2—$, $X= Br$, $R^1,R^2= =CH—Ph$)

Fig. 2

the νCO band appears as a doublet (1730—1660 cm^{-1}) due to the coupled vibration of "diacylamide" CO groups [4].

Our acylations always occurred at the nitrogen atom in the 3-position. The nitrogen atom in the 1-position is less reactive because it is probably more conjugated.

The alkylation of 2-quinazolinethiones and pyrimidines affords *S*-alkyl compounds [5—6].

In the IR spectrum of **Vc** (Table III), made by methylating **A** and subsequently treating it with perchloric acid, there is a broad band (2400—3460 cm^{-1}) which is characteristic of ionic NH groups, while the NH band of **A** was found at 3220 cm^{-1}. The strong thioamide II band, characteristic of **A**, has disappeared, pointing to an *S*-alkyl derivative. In the ^{1}H-NMR spectrum of **Vc** the methyl signal is found at δ 2.7 ppm, in agreement with the chemical shifts published by TÓTH and TOLDY for *S*-methylisothiuronium salts [7], and with the shifts of the *S*-methyl signals of condensed pyrimidine derivatives reported by others [8]. These facts suggest an *S*-methyl derivative.

Similar alkylations were made with **C**. The IR spectra of **VIa—Xa**, isolated as hydrobromide and hydroiodide salts, were similar to that of **Vc** (broad νNH band, lack of the thioamide II band), in addition there was a νC=N band (1650—1600 cm^{-1}). In the ^{1}H-NMR spectrum of **VIIa** the SCH_2 group gives a complicated multiplet (δ 2.8—3.7) instead of the expected quartet (A_2X_3). A similar phenomenon was observed with the *S*-propyl and *S*-butyl analogues (**VIIIa—IXa**).

From the salts **VIa—IXa** the corresponding bases (**VIb—IXb**; Table III) were liberated. In the IR spectrum of the bases the shape of the νNH band changed, the broad system of bands disappeared, being replaced by a sharp band between 3360 and 3380 cm^{-1} (free NH), and the wavenumber of the νC=N band decreased (1635—1620 cm^{-1}). In the ^{1}H-NMR spectrum of the bases **VIb—IXb** the SCH_2 signal was similar to that of the salts, but the multiplet became simpler. The profound NMR examination of the *N*-propionyl (**Ib—IVb**) and *S*-alkyl (**VIa, b—IXa, b**) compounds will be discussed in a later publication.

Alkylation at the sulfur atom is also supported by the comparison of the UV spectrum of **C** [2] and **VIb—IXb**. In the UV spectrum of the *S*-alkyl derivatives a new band was observed at 234—237 nm, and the absorption at the highest wavelength exhibited a small bathochromic shift (from 315 to 322—326 nm). On the basis of the UV spectra of the bases (**VIb—IXb**) it can be stated that in these compounds a new chromophor appeared as compared with **C**, which is only possible for the *S*-alkyl derivatives.

Besides the spectroscopic evidence, we attempted to prove chemically that alkylation had occurred at the sulfur atom. Acid hydrolysis of 2-methylmercaptopyrimidines yields 2-oxo derivatives [9]. On hydrolyzing **VIa** with

Table III

Compound		M.p., °C	Formula, M.w. Yield, %	UV (ethanol) λ_{max}, nm (log ε)	IR, cm^{-1} (KBr)	^{1}H-NMR δppm, (CDCl$_3$)
R	X					
Vc CH_3	ClO_4	171–173	$C_{15}H_{94}ClO_4N_2S$ 358.87 33	218 (4.09) 297 (3.53)	$\nu = \overset{|}{N}H^+$ 2400–3460 νClO_4^- 1050–1160	1.3–2.6 m 8H CH_2 2.7 s 3H CH_3S 5.3 s 1H CH 7.5 s 5H Ar 7.8; 8.4 s 2H $=\overset{|}{N}H^{+a,b}$
VIa CH_3	I	167–170	$C_{22}H_{23}IN_2S$ 474.41 86	274 (4.51) 322 (4.62)	$\nu = \overset{|}{N}H^+$ 2400–3300 $\nu C{=}N$ 1650	1.3–2.4 m 6H CH_2 2.8 s 3H CH_3S 5.5 s 1H CH 7.1 s 1H =CH 7.2–7.7 m 10H Ar 11.0 s 2H $=\overset{|}{N}H^{+c,f}$
VIb CH_3	—	121–123	$C_{22}H_{22}N_2S$ 346.50 82	234 (4.39) 275 (4.64) 326 (4.17)	νNH 3360 $\nu C{=}N$ 1635	1.0–3.0 m 6H CH_2 2.5 s 3H CH_3S^d 4.9 s 1H CH 4.2–5.5 s 1H NH^e 7.2–7.7 m 11H Ar, =CH
VIIa C_2H_5	Br	215–218	$C_{23}H_{25}BrN_2S$ 441.44 40	236 (4.38) 276 (4.61) 323 (4.18)	$\nu = \overset{|}{N}H^+$ 2400–3300 $\nu C{=}N$ 1655	1.0 t 3H CH_3 1.3–2.9 m 6H CH_2 2.9–3.7 m 2H SCH_2 5.3 s 1H CH 7.1–7.8 m 11H Ar, =CH 10.7 s 2H $=\overset{|}{N}H^{+f}$

VIIb C_2H_5	—	126–130	$C_{23}H_{24}N_2S$ 360.52 82	234 275 326	(4.39) (4.59) (4.18)	νNH νC=N	3370 1635	1.4 t 3H CH_3 1.5–2.9 m 6H CH_2 2.9–3.4 m 2H SCH_2 4.9 s 1H CH 7.0–7.7 m 11H Ar, =CH 4.5–5.2 s 1H $NH^{e,f,g}$
VIIIa $CH_3(CH_2)_2$	I	205–208	$C_{24}H_{27}IN_2S$ 502.46 93	276 325	(4.40) (4.00)	$\nu{=}\overset{\mid}{N}H^+$ νC=N	2400–3300 1600	0.9 t 3H CH_3 1.4–2.9 m 8H CH_2 2.9–3.8 m 2H SCH_2 5.5 s 1H CH 7.2–7.6 m 11H Ar, =CH 9.0–10.0 s 2H $=\overset{\mid}{N}H^{+f,g}$
VIIIb $CH_3(CH_2)_2$	—	95–104	$C_{24}H_{26}N_2S$ 374.55 85	237 276 322	(4.20) (4.44) (4.04)	νNH νC=N	3380 1620	1.0 t 3H CH_3 1.4–2.9 m 8H CH_2 2.9–3.4 m 2H SCH_2 4.8 s 1H CH 4.6–5.2 s 1H $NH^{e,f}$ 7.1–7.5 m 11H Ar, =CH
IXa $CH_3(CH_2)_3$	Br	179–181	$C_{25}H_{29}BrN_2S$ 469.50 92	237 277 324	(4.15) (4.40) (3.95)	$\nu{=}\overset{\mid}{N}H^+$ νC=N	2400–3240 1660	0.4–3.8 m 15H CH_3, CH_2, SCH_2 5.3 s 1H CH 7.1–7.5 m 10H Ar 7.6 s 1H =CH 10.6 s 2H $=\overset{\mid}{N}H^{+f}$
IXb $CH_3(CH_2)_3$	—	85–90	$C_{25}H_{28}N_2S$ 388.59 71	237 276 325	(4.13) (4.38) (3.93)	νNH νC=N	3380 1620	0.9 t 3H CH_3 1.1–2.9 m 10H CH_2 2.9–3.4 m 2H SCH_2 4.9 s 1H CH 4.7–5.2 s 1H $NH^{e,f}$ 7.2–7.5 m 11H Ar, $=CH^g$

Table III (continued)

Compound		M.p., °C	Formula, M.w. Yield, %	UV (ethanol) λ_{max}, nm (log ε)	IR, cm^{-1} (KBr)	^{1}H-NMR δppm, (CDCl$_3$)
R	X					
X $CH_2{=}CH{-}CH_2$	Br	189–192	$C_{24}H_{25}BrN_2S$ 453.45 80	234 (4.13) 277 (4.41) 324 (3.95)	$\nu{=}\overset{\vert}{N}H^+$ 2400–3220 $\nu C{=}C$ 1655 $\nu C{=}N$ 1640	1.1–2.3 m 6H CH_2 3.4–6.0 m 6H $CH_2{=}CH{-}CH_2S$, CH 6.8–7.6 m 11H $=CH$, Ar 11.2 s 2H $=\overset{\vert}{N}H^{+c,f}$
XIV CH_3	—	148–150	$C_{24}H_{24}N_2OS$ 388.53 57	230 (4.31) 284 (4.66)	amide I 1670 $\nu C{=}N$ 1625	1.2–3.1 m 6H CH_2 2.4; 2.5 s 6H CH_3S^d, CH_3CO^d 5.9 s 1H CH 7.0–7.6 m 11H Ar, $=CH$
XV C_2H_5	—	130–133	$C_{25}H_{26}N_2OS$ 402.57 61	230 (4.46) 284 (4.83)	amide I 1680 $\nu C{=}N$ 1625	1.4 t 3H CH_3 1.5–3.5 m 8H CH_2, CH_2S 2.5 s 3H CH_3CO^d 5.9 s 1H CH 7.0–7.5 m 11H Ar, $=CH^g$
XVI $CH_3(CH_2)_3$	—	73–76	$C_{27}H_{30}N_2OS$ 430.62 53	229 (4.13) 285 (4.47)	amide I 1685 $\nu C{=}N$ 1620	0.7–3.4 m 15H CH_3, CH_2, SCH_2 2.5 s 3H CH_3CO^d 5.9 s 1H CH 7.1–7.5 m 11H Ar, $=CH^g$
XVII $CH_2{=}CH{-}CH_2$	—	130–133	$C_{26}H_{26}N_2OS$ 414.58 28	230 (4.07) 285 (4.45)	amide I 1685 $\nu C{=}C$ 1640 $\nu C{=}N$ 1635 (sh.)	1.5–3.2 m 6H CH_2 2.4 s 3H CH_3CO^d 3.3–4.2 m 2H CH_2S 5.0–6.3 m 4H $CH{=}CH_2$, CH 7.0–7.5 m 11H Ar, $=CH^h$

[a] Disappears on the effect of D_2O

[b] Recorded in trifluoroacetic acid

[c] Recorded in $(CD_3)_2SO$

[d] The methyl signal overlaps the signal of methylenes

[e] The methine signal overlaps the broad NH signal, it became sharp on the effect of D_2O

[f] Disappears on the effect of D_2O

[g] ^{1}H-NMR data obtained with a 100 MHz instrument

[h] All analyses of the new compounds were within accepted limits for C, H, N and S

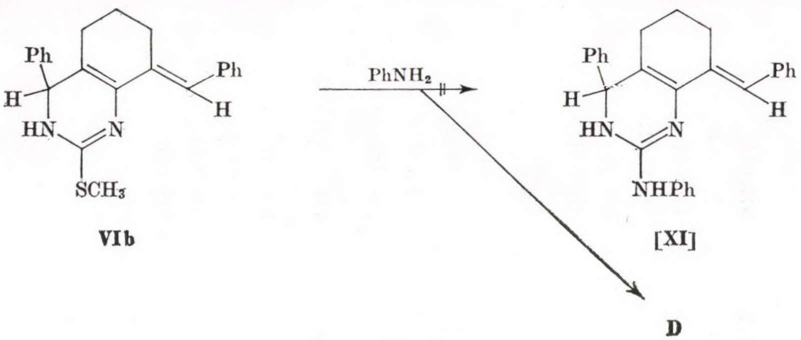

Fig. 3

hydrochloric acid we did not obtain the expected **D**, the reaction mixture became a tar. The aminolysis of 2-methylmercaptopyrimidines which gives 2-aminopyrimidin derivatives [9] can prove the structure of **VIa**—**IXa** and **Xa**. This reaction was tried with **VIb** applying aniline and *p*-nitroaniline as the amine, but the attempts remained unsuccessful. Applying the results of LEMPERT and BREUER [10], we carried out the reaction in *n*-butanol with aniline and acetic acid. To our great surprise it was not the 8-benzylidene-4-phenyl-2-phenylamino-3,4,5,6,7,8-hexahydro-2(1*H*)-quinazoline (**XI**) that was isolated, but the known **D**, which is explained by subsequent hydrolysis.

To prove the structure of the **VIb**—**IXb** tautomers, starting from 2,6-dibenzylidenecyclohexanone and *N*-methylthiourea we synthesized the *N*-methyl derivative of **C**, 8-benzylidene-3-methyl-4-phenyl-3,4,5,6,7,8-hexahydro-2(1*H*)-quinazolinethione (**XIIa**; Table IV). The structure of **XIIa** is in accordance with its spectroscopic data. The position of the methyl group should be proved chemically, too, as this can give rise to two isomers. As the compound could not be acylated, the conclusion can be drawn that the structure is **XIIa**. This is in accordance with the results of SAMMOUR *et al.* who allowed *N*-substituted thioureas to react with 2,6-diarylidenecyclohexanones and obtained 3,4,5,6,7,8-hexahydro-2(1*H*)-quinazolinethiones substituted in the position 3 [11].

The structure of **XIIa** was confirmed by the ^{1}H-NMR spectra of its derivatives (**XIIIa**, **b**); **XIIa** was treated with methyl iodide, and from the salt

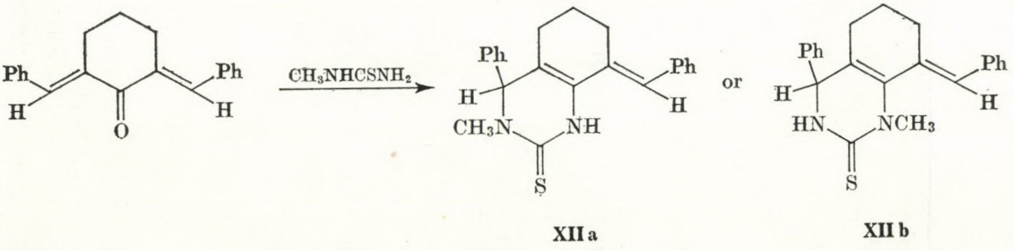

Fig. 4

Table IV

Compound		M.p., °C	Formula, M.w. Yield, %	UV ethanol λ_{max}, nm (log ε)	IR, cm^{-1} (KBr)	^{1}H-NMR δppm, (CDCl$_3$)
R	X					
XIIa		195 (d.)	$C_{22}H_{22}N_2S$ 346.50 66	267 (4.41) 319 (4.07)	νNH 3260 thioamide II 1280	1.2—2.9 m 6H CH_2 3.2 s 3H NCH_3 4.7 s 1H CH 6.5 s 1H =CH 6.8—7.5 m 10H Ar 7.7 s 1H NH^a
XIIIa		142 (d.)	$C_{23}H_{25}IN_2S$ 488.44	280 (4.43) 340 (3.84)	$\nu\!=\!\overset{|}{N}H^+$ 2700—3200	1.3—2.9 m 6H CH_2 3.1 s 3H SCH_3 3.3 s 3H NCH_3 5·4 s 1H CH 7.0—7.7 m 11H Ar, =CH 9.4—10·0 s 1H $=\overset{|}{N}H^{+a,b}$
XIIIb		123—126	$C_{23}H_{24}N_2S$ 360.52 90	235 (4.15) 279 (4.45) 334 (3.86)	$\nu_{as}CH_3$ 2950 ν_sCH_3 2865 νC=N 1620	1.4—2.8 m 6H CH_2 2.5 s 3H SCH_3 2.8 s 3H NCH_3 4.6 s 1H CH 7.1—7.4 m 10H Ar 7.5 s 1H =CH^d

[a] Disappears on the effect of D_2O

[b] Broad band

[c] The methyl signal overlaps the signal of methylenes

[d] All analyses of the new compounds were within accepted limits for C, H, N and S

(**XIIIa**, Table IV) the base (**XIIIb**; Table IV) was liberated, thus an analogue of **VIa—Xa** was synthetised.

In the IR spectrum of **XIIIb** there is no νNH band; sharp methyl bands are found at 2950 and 2865 cm^{-1}, and the νC=N band is at a similar wavenumber (1620 cm^{-1}) as in the *S*-methyl derivative (**VIb**). In the ^1H-NMR spectrum of **XIIIb** two sharp singlets appear (δ 2.5 ppm SCH_3, δ 2.8 ppm NCH_3) the former chemical shift is in agreement with the value found for **VIb**

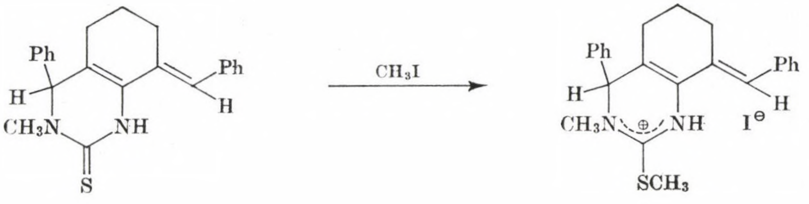

XII a **XIII a**

Fig. 5

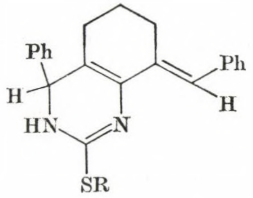

VIb ($R= CH_3—$)

VIIb ($R= C_2H_5—$)

VIIIb ($R= C_3H_7—$)

IXb ($R= C_4H_9—$)

Fig. 6

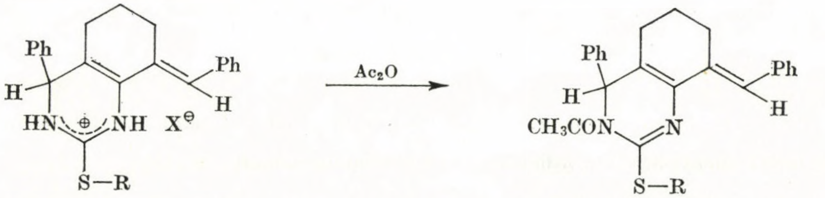

VI a ($R=CH_3—$, $X = I$)

VII a ($R=C_2H_5—$, $X = Br$)

IX a ($R=C_4H_9—$, $X = Br$)

X a ($R=CH_2{=}CH—CH_2—$, $X = Br$)

XIV ($R=CH_3—$)

XV ($R=C_2H_5—$)

XVI ($R=C_4H_9—$)

XVII ($R=CH_2{=}CH—CH_2—$)

Fig. 7

(see Table III). The C-4 methine proton can be recognized at δ 4.6 ppm, while the corresponding signal of **VIb** is at δ 4.9 ppm. The diamagnetic shift is explained by the $+I$ effect of the neighbouring methyl group.

The ^{1}H-NMR spectrum of **XIIIb** was also recorded in the presence of a shift reagent [Eu(fod$_3$)—d_{27}, CDCl$_3$, molar proportion of reagent to **XIIIb**; 2/3] to determine the position of the NCH$_3$ group. By comparing the chemical shift of the singlets with shift reagent and without it ($\Delta\delta$SCH$_3$: 0.24, $\Delta\delta$NCH$_3$: 0.08, $\Delta\delta$CH: 0.07, $\Delta\delta$=CH: 0.15) one can state that the sulfur atom and the nitrogen atom in position 1 have the highest complexing inclination, which certifies the 3-position of the NCH$_3$ group and precludes the possibility of structure **XIIb**.

Comparing the UV spectrum of **XIIIb** with that of **VIb**—**IXb** (Tables III—IV) one can establish that the spectrum of the *N*, *S*-dimethyl derivative is in essentially good agreement with the spectra of *S*-alkyl compounds. Thus the tautomeric structures supposed for the bases **VIb**—**IXb** were proved on the basis of their UV spectra, and their acetylation provided further data.

In the IR spectrum of the products (**XIV**—**XVII**; Table III) the amide I vibration is found between 1670 and 1685 cm^{-1}. As to the ^{1}H-NMR spectrum of **XIV**—**XVI**, it is the C-4 methine proton again which is the clue to the structure: its chemical shift (owing to the reasons mentioned earlier) increased from δ 4.9 ppm (**VIb**—**VIIb**, **IXb**) to δ 5.9 ppm. This is possible only in the case of the 3-acetyl derivative, which further proves the suggested tautomeric structures for all the *S*-alkylquinazolines. (From **Xa** the corresponding base could not be prepared, treatment with sodium hydroxide caused decomposition.)

Experimental

The IR spectra were recorded with a Zeiss UR-10 spectrophotometer (KBr pellet), the majority of the ^{1}H-NMR spectra was obtained with a Perkin–Elmer R-12 (60 MHz) spectrometer (CDCl$_3$, TMS internal standard, except otherwise noted). Some of the NMR spectra were taken with a Varian XL-100-15 FT instrument. The UV spectra were recorded with a Perkin–Elmer 402 spectrophotometer (solvent: ethanol). The analysis data of the products agreed with the calculated values.

For the preparation of **A**—**D** see Ref. [2].

Acetylation of 4-phenyl-3,4,5,6,7,8-hexahydro-2(1*H*)-quinazolinethione (A)

3-Acetyl-4-phenyl-3,4,5,6,7,8-hexahydro-2(1*H*)-quinazolinethione (Ia)

To a solution of **A** (2.00 g; 0.008 mole) in dry pyridine (100 ml) acetic anhydride (8.64 g; 0.086 mole) was added, and the reaction mixture was refluxed for 9 h. The hot solution was poured into water. After standing for 24 h, the oily substance crystallized. The precipitate was filtered off, washed with water until neutral and crystallized from a small amount of acetone.

The synthesis of 3-acetyl-4-phenyl-3,4,5,6,7,8-hexahydro-2(1*H*)-quinazolinone (**IIa**) was accomplished in a similar way by acetylating **B**.

Ib, c, IIb were prepared by acetylation with the corresponding acid chloride. The solvent of recrystallization was methanol for **Ib** and **IIb**, ethanol for **IIa**, and benzene for **Ic**.

Ia—**c**, **IIa**—**b** were colourless substances, their other data are shown in Table I.

Acetylation of 8-benzylidene-4-phenyl-3,4,5,6,7,8-hexahydro-2(1*H*)-quinazolinethione (C)

3-Acetyl-8-benzylidene-4-phenyl-3,4,5,6,7,8-hexahydro-2(1*H*)-quinazolinethione (IIIa)

The synthesis of **IIIa** was carried out in a manner similar to that of **Ia**, by means of acetic anhydride.

Compounds **IIIb, c** and **IVb** were prepared by reactions with acid chloride. **IIIa** was recrystallized from a mixture of acetone and water, **IIIb, IVa, b** from methanol, and **IIIc** from benzene.

IIIa—c, IVa—b were colourless crystals, their other data are listed in Table II.

Reaction of 4-phenyl-3,4,5,6,7,8-hexahydro-2(1*H*)-quinazolinethione (A) with methyl iodide

2-Methylmercapto-4-phenyl-3,4,5,6,7,8-hexahydroquinazoline perchlorate (Vc)

To a solution of **A** (3 g; 0.013 mole) in anhydrous ethanol (140 ml) methyl iodide (10.8 g; 0.076 mole) was added and the reaction mixture was refluxed for 2 h. The solution was then evaporated to dryness. The hydroiodide of the product (**Va**) could not be crystallized, therefore it was converted to the perchlorate: the red oil obtained after the evaporation was dissolved in hot water and 36% perchloric acid (2 ml) was added to the colourless solution. Compound **Vc** precipitated as colourless crystals which were recrystallized from water.

Reaction of 8-benzylidene-4-phenyl-3,4,5,6,7,8-hexahydro-2(1*H*)-quinazolinethione (C) with methyl iodide

8-Benzylidene-2-methylmercapto-4-phenyl-3,4,5,6,7,8-hexahydroquinazoline hydroiodide (VIa)

The preparation of **VIa** was similar to that of **Vc**. The hydroiodide of the product was isolated and crystallized from acetone.

The analogous compound **VIIa** was prepared with ethyl bromide, **VIIIa** with propyl iodide, **IXa** with butyl bromide and **Xa** with allyl bromide; the products were crystallized from acetone.

8-Benzylidene-2-methylmercapto-4-phenyl-3,4,5,6,7,8-hexahydroquinazoline (VIb)

To a hot solution of **VIa** (4.74 g; 0.01 mole) in methanol (100 ml) a 0.06 *N* methanolic solution of KOH (25 ml) was added and the solution was concentrated in vacuum. It was cooled, the crystals which deposited were filtered off and washed with methanol and water until neutral. The product was recrystallized from methanol.

VIIb—IXb were prepared in a manner similar to the synthesis of **VIb**; the products were recrystallized from methanol.

Reaction of 8-benzylidene-2-methylmercapto-4-phenyl-3,4,5,6,7,8-hexahydroquinazoline (VIb) with aniline

VIb (4.46 g; 0.01 mole), aniline (4.65 g; 0.05 mole) and acetic acid (1.5 g; 0.025 mole) were dissolved in *n*-butanol (10 ml), and the reaction mixture was refluxed for 2.5 h. The solution was then evaporated in vacuum and the brown oily residue was crystallized from acetone. The colourless crystals which separated on cooling were identical with **D** [2] in every respect.

Reaction of 2,6-dibenzylidenecyclohexanone with *N*-methylthiourea

8-Benzylidene-3-methyl-4-phenyl-3,4,5,6,7,8-hexahydro-2-(1*H*)-quinazolinethione XIIa

The synthesis of **XIIa** was effected in a manner similar to that of **C** [2]. The colourless product was crystallized from methanol.

8-Benzylidene-3-methyl-2-methylmercapto-4-phenyl-3,4,5,6,7,8-hexahydroquinazoline hydroiodide (**XIIIa**) and the corresponding base (**XIIIb**) were prepared in the same way as **VIa** and **VIb**; the colourless substances were crystallized from methanol.

Other data for **XIIa** and **XIIIa, b** are shown in Table IV.

Reaction of 8-benzylidene-2-methylmercapto-4-phenyl-3,4,5,6,7,8-hexahydroquinazoline hydroiodide (VIa) with acetic anhydride

3-Acetyl-8-benzylidene-2-methylmercapto-4-phenyl-3,4,5,6,7,8-hexahydroquinazoline (XIV)

To a solution of **VIa** (7.11 g; 0.015 mole) in dry pyridine (100 ml) acetic anhydride (15.3 g; 0.15 mole) was added and the reaction mixture was refluxed for 30 min. The hot solution was poured into water. After standing for 1 h, the precipitate was filtered off, and washed with water until neutral. The product was crystallized from methanol.

The preparation of **XV–XVII** was carried out similarly. The products were crystallized from methanol.

Vc, **VIa, b–IXa, b**, **Xa** and **XIV–XVII** are colourless crystals; their other data are listed in Table III.

*

The authors' thanks are due to Mr. A. NESZMÉLYI for the PMR spectra recorded at 100 MHz, to Mr. R. OHMACHT for the IR spectra and the analyses, to Mr. P. MOLNÁR for the UV spectra and to Mrs. L. ZUBOR and Miss Cs. SZEGVÁRI for their technical assistance.

REFERENCES

[1] LÓRÁND, T., SZABÓ, D.: Acta Chim. (Budapest) **94**, 363 (1977)
[2] LÓRÁND, T., SZABÓ, D., NESZMÉLYI, A.: Acta Chim. (Budapest) **93**, 51 (1977)
[3] ZIGEUNER, G., FUCHS, E., GALATIK, W.: Monatsh. Chem., **97**, 43 (1966)
[4] HOLLY, S., SOHÁR, P.: Infravörös spektroszkópia. p. 98, Műszaki Kiadó, Budapest 1968
[5] STÁJER, G. KOTTKE, K., POHLOUDEK-FABINI, R.: Pharmazie, **28**, 433 (1973)
[6] HARTMANN, H., MEYER, R.: J. Prakt. Chem., **30**, 87 (1965)
[7] TÓTH, G., TOLDY, L.: Acta Chim. (Budapest) **80**, 349 (1974)
[8] ZIGEUNER, G., HAMBERGER, H., PINTER, E., ECKER, R.: Monatsh. Chem., **104**, 585 (1973)
[9] LEMPERT, K.: Szerves kémia. p. 819., Műszaki Kiadó, Budapest 1976
[10] LEMPERT, K., BREUER, J.: Magyar Kém. Folyóirat, **68**, 452 (1962)
[11] SAMMOUR, A., MAREI, A., HUSSEIN, M.H.M.: U.A.R. J. Chem., **12**, 451 (1969); Chem. Abstr., **74**, 53702 (1971)

Tamás LÓRÁND
Dezső SZABÓ
András FÖLDESI
H-7643 Pécs, Szigeti út 12.

Acta Chimica Academiae Scientiarum Hungaricae, Tomus 104 (2), pp. 161—168 (1980)

DETERMINATION OF 1,2-ETHANEDIAMINE, *N,N'*-DIMETHYL-1,2-ETHANEDIAMINE AND *N,N'*-DIETHYL-1,2-ETHANEDIAMINE BY PERIODATE OXIDATION

L. Maros, I. Molnár-Perl and M. Molnár

(*Institute of Inorganic and Analytical Chemistry, Eötvös L. University, Budapest*)

Received April 13, 1979

Accepted for publication July 18, 1979

A titrimetric method has been developed for the determination of 1,2-ethane diamine containing primary and secondary amino groups, based on periodate oxidation.

Stoichiometric oxidation with periodate of these compounds is hindered by formaldehyde which forms in the reaction. This difficulty can be eliminated by performing the oxidation in the presence of 1,3-propanediamine, which does not react with periodate, however, binds formaldehyde. The methods are based on the iodometric determination of the excess periodate and the formaldehyde produced in the reaction. Determinations can be carried out with an accuracy of $\pm 0.5\%$ on $0.1N$ and $0.02N$ scale. The iodometric determination of formaldehyde as aldehyde bisulfite has a negative error of 4—6%.

Introduction

The oxidation of α-amino alcohols containing primary and secondary amino groups with periodate in alkaline solutions at room temperature is a fast, stoichiometric process, thus being suitable for the quantitative determination of these compounds [1, 2, 3]. No success has been reached up to the present with the stoichiometric periodate oxidation of 1,2-diamines. Upon investigating the oxidation of 1,2-ethanediamine Fleury *et al.* [2] established that formaldehyde produced by oxidation reacts with the unoxidized 1,2-ethanediamine, thus giving supposedly diethylenetetramethyltetramine [4], which further on does not react or only very slowly with periodate.

$$H_2N{-}CH_2{-}CH_2{-}NH_2 + IO_4^- + H_2O = 2\,CH_2O + 2\,NH_3 + IO_3^- \qquad (1)$$

$$2\,H_2N{-}CH_2{-}CH_2{-}NH_2 + 4\,CH_2O =$$

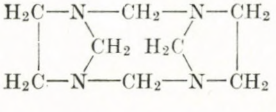

$$+ \; 4\,H_2O \qquad (2)$$

We have reported earlier [3] that 1,2-ethanediamine reacts rapidly with periodate in alkaline solution at boiling temperature, and distillation and measuring of ammonia formed stoichiometrically during oxidation is suitable for the determination of this compound. Under such conditions, however, formal-

Table I

Time dependence of periodate oxidation of 1,2-ethanediamine, N,N′-dimethyl-1,2-ethanediamine and N,N′-diethyl-1,2-ethanediamine in an unbuffered pH = 9.6 solution at 20 °C

Duration of oxidation (min)	Reduced periodate/1,2-diamine (mol/mol)		
	1,2-ethanediamine	*N,N′*-dimethyl-1,2-ethanediamine	*N,N′*-diethyl-1,2-ethanediamine
10	0.42	0.33	0.29
30	0.45	0.38	0.32
60	0.50	0.48	0.38
120	0.60	0.54	0.46

dehyde is also oxidized and thus there is no possibility to determine the excess periodate and formaldehyde produced during the reaction.

Room temperature periodate oxidation of *N,N′*-dimethyl-1,2-ethanediamine and *N,N′*-diethyl-1,2-ethanediamine containing secondary amino groups — similarly to the oxidation of 1,2-ethanediamine — is first fast, then slow, according to our results (Table I)

The fast and stoichiometric oxidation of secondary 1,2-diamines with periodate is also hindered by the reaction between formaldehyde evolved in the reaction and unoxidized 1,2-diamine.

$$\mathrm{R{-}NH{-}CH_2{-}CH_2{-}NH{-}R + IO_4^- + H_2O = 2CH_2O + 2R{-}NH_2 + IO_3^-} \qquad (3)$$

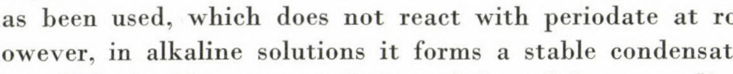

(4)

The stoichiometric oxidation of 1,2-ethanediamines containing primary and secondary amino groups with periodate can be carried out if the formaldehyde formed in the reaction is removed. For this purpose 1,3-propanediamine has been used, which does not react with periodate at room temperature, however, in alkaline solutions it forms a stable condensation product with formaldehyde. The compound formed from 1,3-propanediamine and formaldehyde decomposes in acidic solution thus the formaldehyde originating from the oxidation of 1,2-ethanediamine can be determined iodometrically as aldehyde bisulfite [3, 5] after the reduction of excess periodate with sulfite.

On the basis of the periodate oxidation in presence of 1,3-propanediamine it became possible to determine the primary and secondary 1,2-ethanediamines by measuring the excess periodate and the formaldehyde evolved in the reaction.

The rate of reactions [1] and [3] is optimal in the pH range of 9—11 [6].

The pH of the solution and the binding of formaldehyde during the oxidation is ensured by adding 1,3-propanediamine adjusted to pH = 10.5 with sulfuric acid to the solution. The determination based on measuring the excess periodate is performable on 0.1 and 0.02*N* scale. The formaldehyde produced in the course of oxidation can be determined on a 0.1*N* scale as aldehyde bisulfite. The analyses gave identical results under the above conditions for 20—60 min oxidation on 0.1*N* scale and 40—100 min on 0.02*N* scale.

The mixing sequence of solutions should be kept in mind; the right way is to add the periodate to the mixture of 1,2-ethanediamine and 1,3-propanediamine. In the case, namely, if 1,3-propanediamine is added to the mixture of periodate and 1,2-ethanediamine the rate of oxidation becomes slower. This can be explained by the fact that 1,2-ethanediamines react fast with periodate, but the reaction between formaldehyde and 1,2-ethanediamines is even faster. The subsequently introduced 1,3-propanediamine reacts slowly with the condensation product of formaldehyde and 1,2-ethanediamine.

The amount of 1,3-propanediamine is identical for determinations on 0.1 and 0.2*N* scales: 2 cm^3 2*M* 1,3-propanediamine solution (4 mmol). This corresponds to a 4—5 fold excess compared to the highest amounts of 1,2-ethanediamine determined on 0.1*N* scale. More 1,3-propanediamine does not increase significantly the oxidation rate. According to our investigation, the rate of periodate oxidation of 1,2-ethanediamine is also increased in the presence of ammonia or aliphatic monoamines (butylamine) under the optimum pH conditions. Their accelerating effect is, however, significantly smaller than that of 1,3-propanediamine thus we do not propose their use.

We note that under the above conditions the *N*,*N*-diethyl-1,2-ethanediamine and the *N*,*N*,*N*′,*N*′-tetramethyl-1,2-ethanediamine containing tertiary amino groups do not react with periodate: thus their comparable amounts do not interfere the determination of primary and secondary 1,2-ethanediamine.

In the determination based on measuring the excess periodate, the generally used iodometric method of MÜLLER and FRIEDBERGER [7] is applied: in a solution buffered with sodium hydrogen carbonate the iodine liberated after adding potassium iodide to the solution is titrated with a sodium arsenite solution. Formaldehyde formed in periodate oxidation is determined as formaldehyde bisulfite: after oxidation the solution is acidified, and the iodate and periodate are reduced with sodium sulfite. By further addition of sodium sulfite formaldehyde bisulfite is formed. After a suitable waiting period the excess sulfite is oxidized with a iodine solution. After that the solution is alkalified with sodium hydroxide in the presence of phenolphthalein indicator until the appearence of a pink colour, and the sulfite released from the formaldehyde bisulfite is titrated with iodine.

Determinations based on the analysis of formaldehyde produced in the course of oxidation can be carried out with an accuracy of about −5%.

Procedures

1. Determination of 1,2-ethanediamine, N,N'-dimethyl-1,2-ethanediamine and N,N'-diethyl-1,2-ethanediamine based on measuring the excess periodate iodometrically

Reagents:

0.1 and 0.02M sodium periodate solution,

0.1*N* sodium arsenite solution (4.945 gr arsenic trioxide is dissolved in 40 cm^3 20% sodium hydroxide solution. After dilution, the solution is neutralized with 20% sulfuric acid in the presence of methyl red indicator, washed into a 1000 cm^3 volumetric flask and after introducing 10 gr sodium hydrogen carbonate, filled up to the mark with distilled water).

0.02*N* sodium arsenite solution (prepared from the 0.1*N* solution with accurate dilution), 15% 1,3-propanediamine solution (15 cm^3 distilled 1,3-propanediamine diluted with distilled water to 50 cm^3, the pH of the solution adjusted to 10.5 with 20% sulfuric acid, and the volume filled up to 100 cm^3 with distilled water),

20% sulfuric acid solution,
0.1% alcoholic methyl red solution,
1% indicator starch solution,
sodium hydrogen carbonate (solid),
potassium iodide (solid).

Samples measured with analytical precision (0.28—0.32 gr 1,2-ethanediamine, 0.42—0.46 gr *N,N'*-dimethyl-1,2-ethanediamine or 0.56—0.60 gr *N,N'*-diethyl-1,2-ethanediamine) are washed into a 100 cm^3 volumetric flask with distilled water, and filled up. A 10.00 cm^3 portion of the solution is pipetted into a 200 cm^3 glass-stoppered Erlenmeyer flask and mixed with 2.0 cm^3 1,3-propanediamine. After that 10.00 cm^3 0.1M sodium periodate solution is

Table II

Determination of 1,2-ethanediamine by measuring excess periodate

Measured 1,2-ethanediamine hydrate gr/500 cm^3	Solution volume for the determination cm^3	0.1*N* periodate solution consumed, cm^3		1,2-ethanediamine found*	
		individually	mean	mg	%
	15.01	12.82 12.87	12.85	38.6	78.5
1.6400	10.00	8.65 8.70	8.67	26.1	79.4
	5.01	4.30 4.28	4.29	12.9	78.4
		0.02*N* periodate solution consumed, cm^3			
	15.01		12.82	7.70	78.3
0.3280	10.00		8.61	5.17	78.9
	5.01		4.32	2.60	79.2

* The 1,2-ethanediamine content of 1,2-ethanediamine hydrate measured acidimetrically is 78.5%

Confidence limit $|\bar{X} \pm tsn^{1/2}| = 78.7 \pm 0.7\%$, where $t = 4.27$; $s = \pm 0.5$ and $n = 9$. (Student test)

Table III

Determination of N,N′-dimethy-1,2-ethanediamine by measuring excess periodate

Measured N,N′-dimethyl-1,2-ethanediamine gr/500 cm³	Solution volume used for the determination cm³	0.1N periodate solution consumed, cm³		N,N′-dimethyl-1,2-ethanediamine found*	
		individually	mean	mg	%
2.1822	10.00	9.70 9.69	9.70	42.75	97.9
	5.01	4.85 4.80	4.83	21.29	97.5
		0.02N periodate solution consumed, cm³			
		individually	mean		
0.4364	10.00	9.68 9.66 9.68 9.68	9.68	8.53	97.8
	5.01	4.83 4.81 4.86	4.83	4.26	97.6

* The N,N′-dimethyl-1,2-ethanediamine content of the sample measured acidimetrically is 97.8%

Confidence limit $|X \pm tsn^{1/2}| = 97.6 \pm 0.4\%$, where $t = 3.58$; $s = \pm 0.4$ and $n = 11$ (Student test)

added to the flask, and filled up to 40—50 cm³ with distilled water. The stoppered flask is shaken and after a waiting time of 30—40 min the solution is neutralized by adding sulfuric acid dropwise to the solution in the presence of one drop of methyl red, then 2 gr sodium hydrogen carbonate is added to the solution. The content of the flask is shaken, the glass stopper is lifted several times to let the solution adhering to the ground joint to be neutralized. After this the solution is diluted with distilled water to 100 cm³, 0.2—0.3 gr potassium iodide is introduced into the flask, and the evolved iodine titrated with sodium arsenite standard solution. The end point is detected with starch indicator. Blank measurements are also performed using all the reagents, and calculations made with the differences in the consumptions.

The equivalent weight of 1,2-ethanediamine is one half of the molecular weight in this process. Thus 3.005 mg 1,2-ethanediamine, 4.407 mg N,N′-dimethyl-1,2-ethanediamine or 5.810 mg N,N′-diethyl-1,2-ethanediamine corresponds to 1 cm³ 0.1N sodium arsenite solution.

The procedure is the same for determination on the 0.02N scale with the exceptions that the time of oxidation is 60 min, and the solution is not diluted before titration.

Table IV

Determination of N,N′-diethyl-1,2-ethanediamine by measuring excess periodate

Measured N,N'-diethyl-1,2-ethanediamine gr/500 cm^3	Solution volume used for the determination cm^3	$0.1N$ periodate consumed, cm^3		N,N'-diethyl-1,2-ethanediamine found*	
		individually	mean	mg	%
2.2324	15.01	10.65 10.69	10.67	62.0	92.6
	10.00	7.25 7.24	7.23	42.0	94.0
	5.01	3.59 3.60	3.60	20.9	93.5
		$0.02N$ periodate consumed, cm^3			
		individually	mean		
0.4448	15.01	10.77 10.90	10.84	12.60	94.4
	10.00	7.20 7.20	7.20	8.37	94.0
	5.01	3.60 3.55	3.58	4.16	93.5

* The N,N'-dietyl-1,2-ethanediamine content of the sample is 94.9 %, measured acidimetrically

Confidence limit $|\bar{X} \pm tsn^{1/2}| = 93.6 \pm 0{,}6\ \%$, where $t = 3.53$; $s = \pm 0.6$ and $n = 12$ (Student test)

2. *Determination of 1,2-ethanediamine, N,N'-dimethyl-1,2-ethanediamine and N,N'-diethyl-1,2-ethanediamine as formaldehyde produced in the course of periodate oxidation*

Reagents:

as in the above determination further on
$0.1N$ iodine solution,
5% iodine solution,
$1.5M$ sodium sulfite solution,
10% acetic acid solution,
20% sodium hydroxide solution,
0.1% alcoholic phenolphthalein solution

5.00 cm^3 of the stock solution prepared by the above procedure is pipetted into a 200 cm^3 Erlenmeyer flask and mixed with 2 cm^3 1,3-propanediamine. After adding 10 cm^3 0.1M sodium periodate solution the mixture is made up to 40—50 cm^3. After 30—40 min waiting time the solution is neutralized with sulfuric acid added from a calibrated pipette in the presence of 1 drop methyl red, and acidified with a further 1 cm^3 of sulfuric acid. Sodium sulfite solution is added dropwise under strirring to the mixture until the disappearance of the initially formed iodine, and further 1 cm^3 of sodium sulfite is added. The stoppered flask is shaken several times. This is followed by neutralization with sodium hydroxide and acidification with 1 cm^3 of acetic acid. After this 10 cm^3 pentane is poured to the solution in order to form a protective layer. After 60 min waiting time most of the excess sulfite is oxidized with a 5% iodine solution added from a calibrated pipette in the presence of 0.5 cm^3 starch solution, and titrated with $0.1N$ iodine solution until the appearance of a blue colour. The content of the stoppered flask is shaken several times, lifting the stopper in order to oxidize the sulfite adhering to the ground joint. (The solution retains its blue colour from 1 drop excess $0.1N$ iodine solution for 10—15 sec.)

The following steps are to alkalify the solution by adding sodium hydroxide dropwise from a calibrated pipette until incipient pink colour, and to titrate the sulfite produced by the decomposition of formaldehyde bisulfite with $0.1N$ iodine solution. The initial iodine consumption is fast, near the end of the titration it becomes slow. Meanwhile the pH of the solution also decreases, and sodium hydroxide solution should be added until the appearance of the pink colour; then the titration is carried on. At the end point the violet colour originating from 1 drop of excess $0.1N$ iodine solution remains unchanged for at least 1 min.

Table V

Determination of 1,2-ethanediamine, N,N′-dimethyl-1,2-ethanediamine and N,N′-diethyl-1,2-ethanediamine by measuring formaldehyde formed during the periodate oxidation

Measured mgs of 1,2-ethanediamine	$0.1N$ iodine consumed, cm^3		Found amounts of 1,2-ethanediamine		Deviation
	individually	mean	mg	%	%
25.75	16.37 16.33	16.35	24.57	95.4	—4.6
12.87	8.12 8.25	8.19	12.31	95.6	—4.4
N,N′-dimethyl-1,2-ethanediamine			*N,N′*-dimethyl-1,2-ethanediamine		
42.68	18.25 18.25	18.25	40.21	94.2	—5.8
21.34	9.15 9.10	9.13	20.12	94.3	—5.7
N,N′-diethyl-1,2-ethanediamine			*N,N′*-diethyl-1,2-ethanediamine		
42.37	13.95 13.90	13.93	40.47	95.5	—4.5
21.19	6.90 7.00	6.95	20.19	95.3	—4.7

The equivalent weight of 1,2-ethanediamine in this reaction is 1/4 of its molecular weight. 1 cm^3 of the $0.1N$ iodine solution corresponds to 1.503 mg 1,2-ethanediamine, 2.204 mg *N,N'*-dimethyl-1,2-ethanediamine or 2.905 mg *N,N'*-diethyl-1,2-ethanediamine.

REFERENCES

[1] Nicolet, B. H., Shinn, L. A.: J. Amer. Chem. Soc., **61**, 1615 (1939)
[2] Fleury, P., Courtois, J., Grandchamp, M.: Bull. Soc. Chim. France, **1949**, 88
[3] Maros, L., Molnár-Perl, I., Schulek, E.: Acta Chim. Acad. Sci. Hung., **30**, 119 (1962)
[4] Bischoff, C. A.: Ber. Dtsch. Chem. Ges., **31**, 3248 (1898)
[5] Mitchell, J. Jr., Kolthoff, I. M., Proskauer, E. S., Weisberger, A.: Organic Analysis Vol. I, Intersci. Publ. Inc. New York, 260 1953
[6] Maros, L., Molnár-Perl, I., Schissel, E., Szerdahelyi, V.: J. Chem. Soc. Perk. II. **1980**, 39
[7] Müller, E., Friedberger, O.: Ber. Dtsch. Chem. Ges., **35**, 2652 (1902)

László Maros
Ibolya Molnár-Perl
Margit Molnár
H-1088 Budapest, Múzeum krt. 4/B

Acta Chimica Academiae Scientiarum Hungaricae, Tomus 104 (2), pp. 169–181 (1980)

NORMAL COORDINATE ANALYSIS AND MEAN AMPLITUDES OF VIBRATION OF TRIMETHYLMETHOXYSILANE

B. N. Cyvin,[1] S. J. Cyvin[1] and I. Hargittai[2]

(*[1]Division of Physical Chemistry, The University of Trondheim, Trondheim-NTH, Norway,*
[2]Central Research Institute for Chemistry, Hungarian Academy of Sciences, Budapest, Hungary)

Received May 23, 1979

Accepted for publication July 19, 1979

A normal coordinate analysis is performed for the staggered and eclipsed conformations of $(CH_3)_3SiOCH_3$. The symmetry coordinates of molecular vibrations are constructed with account for the correlations between local C_{3v} symmetries of the methyl groups and the overall C_s symmetry. The mean amplitudes of vibration are computed and compared with data from electron diffraction. Different rotational isomers are studied under the approximation of a point-mass model and with special emphasis on the mean amplitudes for the long C...C distances separated by Si and O.

Introduction

Extensive gas electron diffraction studies have been made for the series of methylmethoxysilanes: tetramethoxysilane [1], methyltrimethoxysilane [2], trimethylmethoxysilane [3, 4] and hexamethyldisiloxane [4], while the corresponding work on dimethyldimethoxysilane is in progress. Mean amplitudes of vibration [5] are part of the structural data obtained by these modern methods [6]. It is of great interest to supplement these studies with mean amplitudes computed from spectroscopic analysis. Such data are reported here for the first time for one of the molecules in question: trimethylmethoxysilane.

A few works on normal coordinate analysis of trimethylmethoxysilane are available [7–9]. Another work [10] contains calculated frequencies of trimethylmethoxysilane among a series of trimethylalkoxysilanes, but does not give much detail of the normal coordinate analysis. The other normal coordinate analyses [7–9] are based on experimental vibrational frequencies for $(CH_3)_3SiOCD_3$ [7] in addition to $(CH_3)_3SiOCH_3$, and also $(CD_3)_3SiOCH_3$ [11] and $(CD_3)_3SiOCD_3$ [9]. The latter work [9] includes a reinvestigation in infrared and Raman of all practically accessible isotopic species of the molecule in question. Nevertheless, we give the references to earlier experimental works on the vibrational spectra of trimethylmethoxysilane and its isotopic species [7, 9, 11–14]. The list may be supplemented further by means of the bibliographies of the works cited here.

It seems not justified to report many details of the present normal coordinate analysis on the background of the already existing works. Neither have we aimed at the production of a most accurate force field based on several isotopic molecules. We have produced a fairly simple force field, which gives satisfactory agreement with the experimental frequencies for $(CH_3)_3SiOCH_3$, and is supposed to be accurate enough for the purpose of calculating the mean amplitudes of vibration.

Symmetry coordinates

The normal coordinate analysis was primarily based on a staggered model of C_s symmetry: the gauche structure is assumed for the skeleton, all methyl groups are in the staggered positions, and the $O-CH_3$ group in particular is staggered to the $Si-O$ bond (see Figs 1 and 2).

Figure 1 shows the numbering of atoms and the notation adopted for the stretching coordinates. The bending coordinates are specified in Fig. 2. In addition, the following five torsional coordinates were introduced.

τ' (7-1-4-5)
τ_1 (10-2-4-5)
τ_2 (11-3-4-5)
θ (16-6-5-4)
π (6-5-4-1)

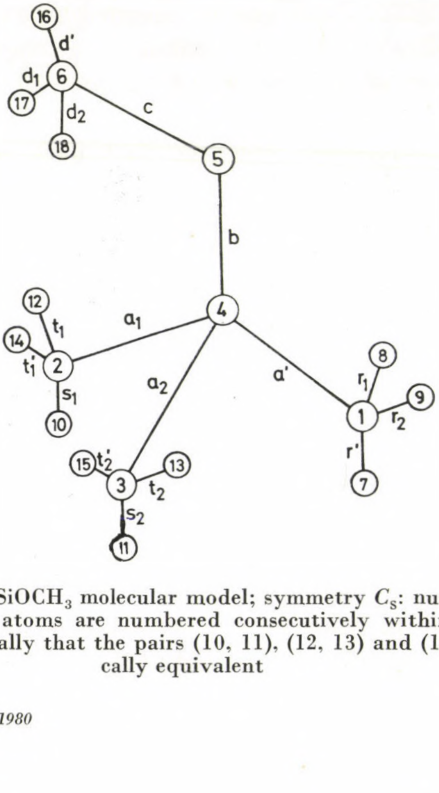

Fig. 1. The staggered $(CH_3)_3SiOCH_3$ molecular model; symmetry C_s: numbering of atoms and stretching coordinates. The atoms are numbered consecutively within each symmetrically equivalent set. Notice especially that the pairs (10, 11), (12, 13) and (14, 15) are symmetrically equivalent

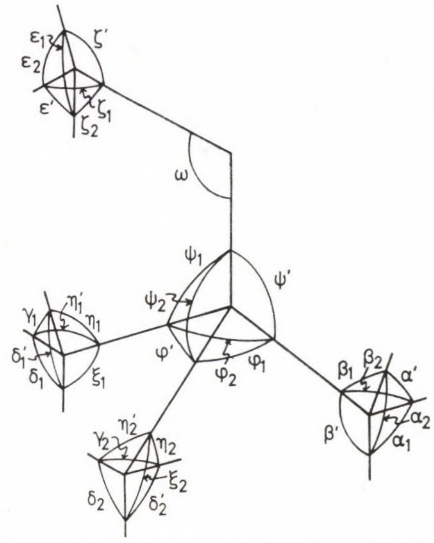

Fig. 2. The staggered $(CH_3)_3SiOCH_3$ model; bending coordinates

The normal modes of vibration are distributed in the two symmetry species of the C_s group according to

$$\Gamma_{\text{vib}} = 27\,A' + 21\,A''$$

We have constructed a complete set of independent symmetry coordinates by taking into consideration local trigonal symmetries of the methyl groups. The local symmetry-adapted combinations of valence coordinates for each methyl group are distributed under the C_{3v} group according to

$$\Gamma_{\text{methyl}} = 2\,a_1 + 3\,e$$

The methyl groups are designated M_1, M_2, M_3 and M_4, pertaining to the carbon atoms number 1, 2, 3 and 6, respectively.

The symmetry coordinates are summarized in Table I, which contains the correlations between the symmetry species of the two groups (C_s and C_{3v}) considered. Normalization and scaling factors are omitted for the sake of brevity. In general, every bending, say α_{ikj}, is scaled in the usual way by $(r_{ik}r_{jk})^{1/2}$, while every torsion say τ_{ijmn}, is scaled by $(r_{ij}r_{mn})^{1/2}$; the scaling factors have the dimension of length.

Force field

The form of the constructed symmetry coordinates (Table I) suggests the type of approximation we have employed. In the initial force field we assumed a block-diagonal **F** matrix in accord with the correlation scheme

Table I

Symmetry coordinates

Methyl group	Species of C_s (capital letters) and of C_{3v} (small letters)			
	A'		A''	
M_1	$r' + r_1 + r_2$	a_1		
	$\alpha' + \alpha_1 + \alpha_2$			
M_1	$2r' - r_1 - r_2$	e_a	$r_1 - r_2$	e_b
	$2\alpha' - \alpha_1 - \alpha_2$		$\alpha_1 - \alpha_2$	
	$2\beta' - \beta_1 - \beta_2$		$\beta_1 - \beta_2$	
M_2/M_3	$(s_1 + t_1 + t_1') + (s_2 + t_2 + t_2')$	$a_1(+)$	$(s_1 + t_1 + t_1') - (s_2 + s_2 + t_2')$	$a_1(-)$
	$(\gamma_1 + \delta_1 + \delta_1') + (\gamma_2 + \delta_2 + \delta_2')$		$(\gamma_1 + \delta_1 + \delta_1') - (\gamma_2 + \delta_2 + \delta_2')$	
M_2/M_3	$(2s_1 - t_1 - t_1') + (2s_2 - t_2 - t_2')$	$e_a(+)$	$(2s_1 - t_1 - t_1') - (2s_2 - t_2 - t_2')$	$e_a(-)$
	$(2\gamma_1 - \delta_1 - \delta_1') + (2\gamma_2 - \delta_2 - \delta_2')$		$(2\gamma_1 - \delta_1 - \delta_1') - (2\gamma_2 - \delta_2 - \delta_2')$	
	$(2\xi_1 - \eta_1 - \eta_1') + (2\xi_2 - \eta_2 - \eta_2')$		$(2\xi_1 - \eta_1 - \eta_1') - (2\xi_2 - \eta_2 - \eta_2')$	
M_2/M_3	$(t_1 - t_1') + (t_2 - t_2')$	$e_b(+)$	$(t_1 - t_1')) - (t_2 - t_2')$	$e_b(-)$
	$(\delta_1 - \delta_1') + (\delta_2 - \delta_2')$		$(\delta_1 - \delta_1') - (\delta_2 - \delta_2')$	
	$(\eta_1 - \eta_1') + (\eta_2 - \eta_2')$		$(\eta_1 - \eta_1') - (\eta_2 - \eta_2')$	
M_4	$d' + d_1 + d_2$	a_1		
	$\varepsilon' + \varepsilon_1 + \varepsilon_2$			
M_4	$2d' - d_1 - d_2$	e_a	$d_1 - d_2$	e_b
	$2\varepsilon' - \varepsilon_1 - \varepsilon_2$		$\varepsilon_1 - \varepsilon_2$	
	$2\zeta' - \zeta_1 - \zeta_2$		$\zeta_1 - \zeta_2$	
	$a' + a_1 + a_2$	a_1		
	$\varphi' + \varphi_1 + \varphi_2$			
	$2a' - a_1 - a_2$	e_a	$a_1 - a_2$	e_b
	$2\varphi' - \varphi_1 - \varphi_2$		$\varphi_1 - \varphi_2$	
	$2\psi' - \psi_1 - \psi_2$		$\psi_1 - \psi_2$	
	b			
	c			
	ω		τ'	
	$\tau_1 - \tau_2$		$\tau_1 + \tau_2$	
			θ	
			π	

between the symmetry species of the C_s and C_{3v} groups. The same approach has previously been applied to methyl borate [15] and different complexed molecules with trigonal ligands [16].

The initial force field was refined in order to improve the fit with experimental vibrational frequencies [9], but all the time it was attempted to preserve the main features of the approximation. The force constants of the preliminary refined force field are given in Table II in terms of the symmetry coordinates. The part of the **F** matrix pertaining to the methyl coordinates is almost completely block-diagonal; only two interaction terms, *viz.* $\mathbf{F}_{15,24}$ and

Table II

Symmetry force constants (N/m)

Methyl group	Species A' and A''								
M_1	a_1	475		e	470				
M_2		0	65		0	43			
M_3					0	0	20		
M_4	a_1	475		e	470				
		0	100		0	44			
					0	−2	60		
	Rest of A'								
	346.2							$\mathbf{F}_{15,24}$ = 30.5	
	−0.5	27.8						$\mathbf{F}_{15,25}$ = −31.7	
	−0.8	−0.9	320.1						
	0.1	0.3	−0.2	18.8					
	−0.6	−2.0	−0.8	0.4	15.1				
	−1.7	4.7	−1.3	−0.2	4.3	456.7			
	12.4	−3.2	−0.1	0.3	0.2	−28.9	431.7		
	−0.9	1.8	0.9	−0.1	3.9	−4.1	−0.8	9.6	
	−0.2	0.2	−0.2	0.2	−0.2	−0.2	−0.2	−0.2	4.9
	Rest of A''								
	328.2								
	−2.0	21.1							
	0.7	0	19.8						
	-0.0_4	0.2	0.3	5.0					
	0.0_1	−0.1	−0.2	−0.1	5.0				
	−0.2	0.1	−0.4	0.1_1	-0.0_1	5.0			
	0.8	−0.3	0.4	−0.1	0.1	0.2	5.0		

$\mathbf{F}_{15,25}$, were introduced (see Table II). The blocks for the methyl groups M_1, M_2 and M_3 (attached to the Si atom) are identical, while the M_4 group (attached to the O atom) has slightly different force constant values. In all cases the corresponding A' and A'' blocks are identical. The rest of the **F** matrix (*i.e.* not pertaining to the methyl coordinates) is seen to contain reasonably small and mostly negligible interaction terms.

The final force field was produced by adjusting the force constants of Table II to a chosen assignment of vibrational frequencies (see Table III). Under this adjustment the normal coordinate transformation matrix (**L**) from the preliminary refinement (Table II) was maintained. The final assignment was chosen with the aid of observed frequencies from TENISHEVA *et al.* [9] as well as the preliminary calculated ones. All the time it was attempted to preserve the main features of the force field approximation. The estimated lowest frequencies are the most uncertain ones; some of them are not reported either as observed or calculated by TENISHEVA *et al.* [9]. Table III includes an approximate description of the normal modes. It was set up with the aid of the calculated potential energy distribution, which is not given here for the sake of brevity.

Calculated vibrational frequencies

The preliminary force field (Table II) was used to calculate the vibrational frequencies for the staggered and eclipsed models. The latter model emerges by a rotation of 180° around the Si—O bond (4—5; *cf.* Fig. 1); hence it belongs to C_s symmetry with the symmetry plane through the atoms 1-4-5-6 exactly as in the case of the staggered model considered. The same symmetry coordinate scheme (*cf.* Table I) was employed for both of these models. The calculated frequencies are shown in Table III. The most pronunced shifts (>10 cm^{-1}) are found for the following five frequency pairs (staggered/eclipsed in cm^{-1}): 293/268, 197/166, 89/122, 314/368 and 273/257.

The last column of figures in Table III shows the final assignment of frequencies. The final force fields were produced for both models (staggered and eclipsed) individually in order to fit the same assignment.

Mean amplitudes of vibration

The final force fields produced individually for the staggered and eclipsed structures of $(CH_3)_3SiOCH_3$ were used to calculate the mean amplitudes [5] for all the types of interatomic distances. Mean amplitude values at different temperatures (0, 298, 323 and 373 K) were produced, but for the sake of brevity only those at room temperature (298 K) are discussed in the following.

Table III

Calculated vibrational frequencies (cm^{-1})

Species	Preliminary force field*		Final force field	Approximate description**
	Staggered	Eclipsed		
A'	2977	2977	2977	ν_{as} $M_{1,2,3,4}$
	2970	2970	2970	
	2970	2970	2970	
	2969	2969	2969	
	2876	2876	2876	ν_s $M_{1,2,3,4}$
	2876	2876	2876	
	2868	2868	2868	
	1456	1456	1456	δ_{as} M_4
	1433	1433	1433	δ_{as} $M_{1,2,3}$
	1402	1402	1401	
	1401	1401	1401	
	1377	1377	1400	δ_s M_4
	1248	1248	1248	δ_s $M_{1,2,3}$
	1247	1247	1246	
	1218	1217	1215	ϱ M_4
	1095	1090	1079	ν CO
	833	830	829	ϱ $M_{1,2,3}$
	825	824	823	
	765	765	765	
	732	732	721	ν_{as} SiC
	716	715	690	ν SiO
	603	602	606	ν_s SiC
	293	268	327	$\delta_s + \delta_{as}$ SiC_3
	241	232	241	
	209	207	209	τ SiC
	197	166	170	ϱ SiC_3
	89	122	122	δ SiOC
A''	2976	2976	2976	ν_{as} $M_{1,2,3,4}$
	2971	2971	2971	
	2969	2969	2969	
	2969	2969	2969	
	2876	2876	2876	ν_s $M_{2,3}$
	1474	1474	1469	δ_{as} $M_{1,2,3,4}$
	1434	1434	1434	
	1432	1432	1432	
	1401	1401	1401	
	1250	1250	1248	δ_a $M_{2,3}$
	1161	1162	1160	ϱ $M_{1,2,3,4}$
	832	835	835	
	771	771	771	
	766	766	766	
	734	735	683	ν_{as} SiC
	314	368	293	ϱ SiC_3
	273	257	209	δ_{as} SiC_3
	208	208	208	τ SiC
	208	207	207	
	190	190	190	τ CO
	115	105	105	τ SiO

* Table II

** s = symmetric, as = antisymmetric, ν = stretching, δ = bending, ϱ = rocking, τ = torsion, M = methyl group

Table IV

Calculated and observed mean amplitudes (pm units) for selected interatomic distances in staggered $(CH_3)_3SiOCH_3$ *at 298 K*

Distance type	Atom numbers	(r/pm)	Mean amplitude	
			Calculated	Observed [3]
Si—O	4—5	(163.9)	4.4	4.5 ± 0.2
Si—C	1—4, 2—4	(186.4)	5.0	6.2 ± 0.2
C—O	5—6	(142.3)	4.9	8.2 ± 0.4
C—H	1—7, 1—8 2—10, 2—12 2—14, 6—16 6—17	(111.4)	7.9	7.9 ± 0.2
C...C *anti*	1—6	(421.8)	9.9	12 ± 3
C...C *gauche*	2—6	(338.1)	20.5	13 ± 1
Si...C	4—6	(268.7)	10.1	7.9 ± 0.8
C...C	1—2, 2—3	(306.0)	10.0—10.5	10.2 ± 0.7
Si...H	4—7, 4—8 4—10, 4—12 4—14	(248.4)	12.2—12.3	12.5 ± 0.6
O...C	1—5, 2—5	(284.8)	9.9—10.0	8.7 ± 0.5

Table IV shows the calculated mean amplitudes for selected interatomic distances in staggered $(CH_3)_3SiOCH_3$ compared with the values obtained from the gas electron diffraction experiment [3]. The parenthesized values (*r*/pm) are the interatomic distances calculated from the adopted structural parameters [3]. Many groups of distances are listed together. They are not symmetrically equivalent in the strict mathematical sense, but are supposed to be nearly equivalent chemically. The mean amplitudes for such distances are in most cases, as a gratyfying fact, found to be practically identical (within 0.1 pm), the maximal deviation being 0.5 pm. Table V shows the calculated mean amplitudes for some additional distances, for which no electron diffraction data have been reported. In some instances the deviations for chemically nearly equivalent distances are larger than in Table IV (maximum 0.8 pm). Tables IV and V together contain all the types of interatomic distances in the molecule, except: (*a*) H...H distances other than the shortest ones (within the same methyl group); 29 types, and (*b*) long C...H distances whose length depends on the Si—O torsion; 10 types. These 39 types of mean amplitudes are omitted here for the sake of brevity and because they are not supposed to be of prime interest for the electron diffraction investigations.

In general, the agreement between calculated and observed mean amplitudes (see Table IV) is satisfactory. In five cases (Si—O, C—H, C...C *anti*, $C_1 \ldots C_2$ and Si...H) it is excellent. Only in two cases, *viz.* C—O and C...C *gauche*, are very large discrepancies found. The electron diffraction C—O value is undoubtedly bad. More puzzling is the *gauche*-C...C mean amplitude, because the agreement on the radial distribution of the electron diffraction experiment [3] was very good in the region where the contribution from the *gauche* interaction occurs. However, the results calculated here with the *anti*-C...C mean amplitude significantly smaller than *gauche*-C...C reflect the expected feature.

Many of the calculated mean amplitudes for the eclipsed $(CH_3)_3SiOCH_3$ model came out with practically the same values as in the staggered model and need no further comments. Also, differences up to about 0.8 pm may be considered as insignificant. A definitely significant difference was found for the Si...H (4—17) distance, for which the mean amplitude of the eclipsed model amounts to 21.5 pm. In this connection, however, the C...C 1—6

Table V

Calculated mean amplitudes (pm units) for additional interatomic distances in staggered $(CH_3)_3SiOCH_3$ *at 298 K*

Distance type	Atom numbers	(r/pm)	Mean amplitude
O...H	5—16, 5—17	(206.7)	10.4—10.5
H...H	7—8, 8—9 10—12, 10—14 12—14	(180.7)	13.0
H...H	16—17, 17—18	(183.0)	12.7
O...H	5—8, 5—12 5—14	(309.7)	19.7—20.0
O...H	5—7, 5—10	(380.2)	12.4—12.5
Si...H	4—17	(293.7)	19.4
Si...H	4—16	(360.7)	11.2
C...H	1—12, 2—8 2—15	(326.8)	21.9—22.7
C...H	1—10, 2—7 2—11	(328.6)	20.3—21.1
C...H	1—14, 2—9 2—13	(402.6)	12.4—12.7

Table VI

Calculated mean amplitudes (pm units) for the C. . .C distances separated by Si and O in staggered and eclipsed $(CH_3)_3SiOCH_3$ *at 298 K*

Type	r/pm	Mean amplitude	Model
syn	305.1	21.6	eclipsed
gauche	338.1	20.5	staggered
gauche	395.8	17.0	eclipsed
anti	421.8	9.9	staggered

and 2—6 types of distances, which change their equilibrium values on passing from the staggered to the eclipsed model, are the most interesting ones. Table VI shows the calculated results in these two models (*cf.* also Table IV).

Point-mass model and rotational isomers

In modern gas electron diffraction investigations it is often of interest to know the approximate variation of certain mean amplitudes with angles of internal rotation. In the present case the C. . . C distances listed in Table VI are of special interest. A more extensive list of this type of C. . . C mean amplitudes as a function of the rotational angle around Si—O or the interatomic distance is a formidable computational task. When the C_s symmetry is destroyed, this problem involves the solution of a secular equation in the 48-dimensional case with subsequent calculation of mean amplitudes. This task is beyond the capacity of the usually available computers or UNIVAC-1108 in our case.

Table VII

Calculated mean amplitudes (pm units) for the rotation-independent interatomic distances of the point-mass model at 298 K

Distance type	Atom numbers	Mean amplitude
Si—O	4—5	4.4
Si—C	1—4, 2—4 3—4	4.9
C—O	5—6	4.8
Si. . .C	4—6	12.2
C. . .C	1—2, 2—3 1—3	9.7—9.8
C. . .C	1—5, 2—5 3—5	10.3

We have therefore considered the point-mass model of $(CH_3)_3SiOCH_3$, *i.e.*, the six-particle model, where all the methyl groups are taken as point masses. The relevant part of the symmetry coordinates (Table I) was adapted to this model. Also the appropriate force constant values from Table II were transferred to the point-mass model. All interactions between two coordinates originally belonging to the A' and A'' species, respectively, were neglected. The mean amplitudes of vibration were computed for the different angles of rotation $\Theta = 0°$ (staggered), 20°, 30°, 40°, 50°, 60° (corresponding to atoms 6 and 2 in the *syn* position), and finally 180° (eclipsed).

Table VII shows the calculated mean amplitudes at 298 K for the distances which do not depend on the angle Θ. Also the mean amplitudes appeared to be practically independent of Θ (within <0.1 pm). Furthermore it is seen on comparison with Table IV that the rigorously calculated mean amplitudes are approached very well; the largest difference, ~ 2 pm, occurs for Si...C, while the agreement is much better for the other distances.

Table VIII shows the calculated mean amplitudes for the longest (Θ-dependent) C...C distance. For $\Theta = 0°$ (staggered) and $\Theta = 180°$ (eclipsed)

Table VIII

***Calculated** mean amplitudes (pm units) for the C...C distances separated by Si and O in the point-mass model at 298 K*

r/pm	Mean amplitude	Θ/°
305.1	21.6	180
305.1	27.1	60
306.2	27.0	50
309.3	26.6	40
314.3	26.0	30
320.9	25.2	20
338.1	23.2	0
358.0	20.7	20
368.1	19.4	30
378.0	18.1	40
387.3	16.9	50
395.8	15.8	180
395.8	15.7 12.9	60
403.4	12.0	50
409.9	11.3	40
415.0	10.7	30
418.7	10.2	20
421.8	9.8	0

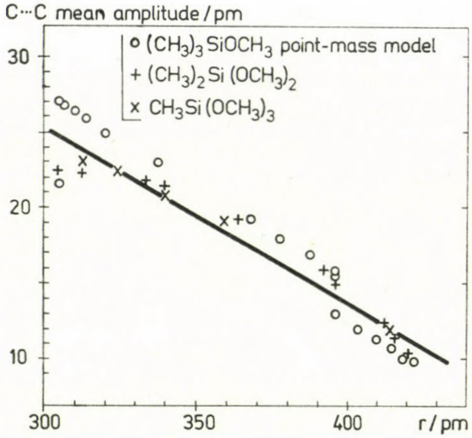

Fig. 3. Mean amplitudes of the C. . . C distances separated by Si and O *vs.* the interatomic distances

the results may again be compared with those from the rigorous calculations (Table VI). The largest difference is about 3 pm, which may be taken as the limit of reliability of the present approximation. When the C. . . C mean amplitudes are plotted against the interatomic distances (Fig. 3) rather than the rotational angle (Θ) the curve appears to be roughly linear. The apparent discontinuity of the plotted points at $r = 396$ pm (see Fig. 3) may be well understood. The reason is that the adopted force field does not preserve the condition for chemical equivalence of the Si—C bond stretchings and similar coordinates. Hence, for instance, at $\Theta = 60°$, which actually is an eclipsed conformation the two C. . . C distances ($r = 395.8$ pm), *viz.* 1—6 and 3—6, are not considered as equivalent. This feature is of course not real physically, and the force field could be repaired in order to remove these effects. We have not found it worth while to undertake this work because the effects are hardly significant within 3 pm, which is the tolerated inaccuracy of the point-mass model approximation.

Actually we performed several computations with different versions of force constant refinements on the point-mass model. In particular, some versions with various estimated torsional frequencies were tested. None of these computations gave significant improvements of the calculated mean amplitudes.

Computations for $CH_3Si(OCH_3)_3$ and $(CH_3)_2Si(OCH_3)_2$

Normal coordinate analyses with computations of mean amplitudes were also performed for $CH_3Si(OCH_3)_3$ and $(CH_3)_2Si(OCH_3)_2$ along with several rotational isomers of these molecules. No details of this unpublished work are to be reported here. We have ony plotted the calculated mean amplitudes at 298 K for the long C...C distances also for these molecules in Fig. 3. It is gratifying to notice how closely they follow the trend deduced from the present investigation of $(CH_3)_3SiOCH_3$.

*

Financial support to BNC from The Norwegian Research Council for Science and Humanities is gratefully acknowledged.

REFERENCES

[1] Boonstra, L. H., Mijlhoff, F. C., Renes, G., Spelbos, A., Hargittai, I.: J. Mol. Struct., **28,** 129 (1975)
[2] Gergő, É., Hargittai, I., Schultz, Gy.: J. Organometal. Chem., **112,** 29 (1976)
[3] Csákvári, B., Wagner, Zs., Gömöry, P., Hargittai, I., Rozsondai, B., Mijlhoff, F. C.: Acta Chim. (Budapest) **90,** 149 (1976)
[4] Csákvári, B., Golubinszkij, A. V., Gömöry, P., Hargittai, I., Masztrjukov, V. Sz., Mijlhoff, F. C., Rozsondai, B., Vilkov, L. V., Wagner, Zs.: Kémiai Közlemények, **46,** 473 (1976)
[5] Cyvin, S. J.: Molecular Vibrations and Mean Square Amplitudes. Elsevier, Amsterdam 1968
[6] Rymer, T. B.: Electron Diffraction. Methuen, London 1970; Davis, M. I.: Electron Diffraction in Gases. Dekker, New York 1971
[7] Lazarev, A. N., Peuker, Chr., Kukharskaya, E. V.: Neorg. Materialy, **3,** 2029 (1967)
[8] Marchand, A., Forel, M. T.: Bull. Soc. Chim. France, **1975,** 72
[9] Tenisheva, T. F., Lazarev, A. N., Uspenskaya, R. I.: J. Mol. Struct., **37,** 173 (1977)
[10] Kozlova, N. V., Kovalev, I. F., Voronkov, M. G.: Dokl. Akad. Nauk SSSR, **236,** 383 (1977)
[11] Kozlova, N. V., Bazov, V. P., Kovalev, I. F., Voronkov, M. G.: Izv. Akad. Nauk Latv. SSR, Ser. Chem., **1971,** 604
[12] Forneris, R., Funck, E.: Z. Elektrochem., **62,** 1130 (1958)
[13] Marchand, A., Valade, J., Forel, M. T., Josien, M. L., Calas, R.: J. Chim. Phys., **59,** 1142 (1962)
[14] Dedier, J., Marchand, A., Forel, M. T., Frainnet, E.: J. Organometal. Chem., **81,** 161 (1974)
[15] Rogstad, A., Cyvin, B. N., Cyvin, S. J., Brunvoll, J.: J. Mol. Struct., **35,** 121 (1976)
[16] Cyvin, S. J., Cyvin, B. N., Hargittai, I.: J. Mol. Struct., **23,** 385 (1974); Cyvin, S. J., Cyvin, B. N., Andreassen, R., Müller, A.: J. Mol. Struct., **25,** 141 (1975); Cyvin, S. J., Lyhamn, L.: J. Mol. Struct., **25,** 151 (1975); Andreassen, R., Cyvin, S. J., Lyhamn, L.: J. Mol. Struct., **25,** 155 (1975); Cyvin, S. J.: Mol. J. Struct., **30,** 311 (1976); Cyvin, B. N., Cyvin, S. J., Schmidt, K. H., Wiegeler, W., Müller, A., Brunvoll, J.: J. Mol. Struct. **30,** 315 (1976); Cyvin, B. N., Cyvin, S. J., Schmidt, K. H., Müller, A., Brunvoll, J.: J. Mol. Struct., **32,** 269 (1976); Whitmer, J. C., Cyvin, S. J.: J. Mol. Struct., **38,** 277 (1977)

B. N. Cyvin
S. J. Cyvin } N-7000 Trondheim-NTH, Norway

István Hargittai H-1431 Budapest, P.O.B. 117.

Acta Chimica Academiae Scientiarum Hungaricae, Tomus 104 (2), pp. 183–191 (1980)

APPLICATION OF DUBININ-RADUSHKEVICH TYPE EQUATION FOR DESCRIBING THE ADSORPTION FROM NON-IDEAL SOLUTIONS ON REAL SOLID SURFACES

A. DABROWSKI and M. JARONIEC
(*Institute of Chemistry, M. Curie-Skłodowska University, Lublin, Poland*)

Received March 23, 1979
In revised from June 28, 1979
Accepted for publication July 26, 1979

It has been shown in work [1] that application of Dubinin–Radushkevich (DR)-type equation for describing adsorption from binary regular liquid mixtures gives good results. In the present paper, the DR equation has been applied to describe the IAP (ideal adsorbed phase/non-ideal bulk phase) and NBP (non-ideal both phases) adsorption models. The adsorption parameters, appearing in DR equation for IAP model, have been evaluated for many experimental systems available from literature. A great utility of DR equation for characterizing the liquid/solid systems has been shown.

Introduction

The majority of papers dealing with the adsorption from binary liquid mixtures on solid surfaces are based on the assumption that the adsorbent surface is energetically homogeneous and solution is ideal in both surface and bulk phase. However, the use of these assumptions is in variance with the experimental studies of COLTHARP and HACKERMAN [2], DÉKÁNY, *et al.* [3], as well as other authors [4]. On the other hand, the theoretical description of adsorption on solid surfaces, involving energetic heterogeneity of the adsorbent and non-ideality of the solution in both phases is very complex [5].

In our previous paper [1] the Freundlich (F) and Dubinin–Radushkevich (DR)-type equations have been used to describe the experimental adsorption isotherms from binary liquid mixtures on solid. These studies have been made for two adsorption models: ideal behaviour in both phases (IBP model), and regular bulk phase/ideal adsorbed phase (IAP-r model). It has been shown that for these models the DR equation gives considerably better agreement with experimental data than the F equation and the IAP-r model works better than the IBP one.

In this paper the DR equation for NBP adsorption model (non-ideal behaviour in both phases) will be discussed. The simpler form of this equation is that for IAP model, which will be used to characterize the experimental adsorption systems available from literature.

Theoretical

The integral equation, discussed in Reference [1], may be easily generalized to adsorption from non-ideal liquid mixtures on heterogeneous solid surfaces (NBP adsorption model); this extension gives:

$$\vartheta_1(x) = \int_{\Delta} \Theta_1(x, \beta, E) \cdot \mathrm{F}(E)\,\mathrm{d}E \tag{1}$$

where $x = x_1/x_2$ is the ratio of the mole fractions of both components in the bulk phase, and $x_1 + x_2 = 1$; ϑ_1 and Θ_1 are mole fractions of the 1-st component in surface phase on heterogeneous and homogeneous surfaces, respectively; $\beta = (f_1^s/f_2^s)/(f_1/f_2)$ is the ratio of the activity coefficients in both surface (superscript s) and bulk phases, respectively; $E = E_1 - E_2$ is the difference of adsorption energies of both components; $\mathrm{F}(E)$ is the distribution function normalized to unity; and Δ is the integration region. Integral (1) is formally identical with that derived for IBP model [6], but in the case of the NBP model the activity coefficients f_i^s and f_i $(i = 1, 2)$ should be taken into account.

Now, we shall discuss more exactly the integral equation (1). In the case of the IAP model $f_1^s = f_2^s = 1$; f_1 and f_2 are functions of x_1 only. Then Eq. (1) is valid for different models of heterogeneous surfaces, *i.e.*, the topography of sites on the adsorbent surface does not change on adsorption. However, in the case of the NBP model, f_1^s and f_2^s are functions of mole fraction of the 1-st component in the surface phase; it means that expressions for mole fractions in the surface phase depend on the topography of adsorption sites on the surface. According to papers [7, 8] we consider two models of heterogeneous adsorbent surface; in the first model the adsorption sites of equal E are grouped in patches on the surface, however, in the second model the adsorption sites are distributed randomly on the surface. For patchwise model f_1^s and f_2^s are functions of Θ_1, whereas in the case of model of "random surface" f_1 and f_2 are functions of ϑ_1. Since ϑ_1 is the mole fraction of the 1-st component calculated with regard to the whole surface phase, the activity coefficients f_1^s and f_2^s for "random surfaces" are independent on E. Then, β is also independent on E, *i.e.*, β is constant which may be included to the constant appearing in the expression on Θ_1.

It means that solution of Eq. (1) are formally identical for IBP, IAP and NBP models; the final equations have this same form. They differ in parameters only. Thus, the solutions of Eq. (1) for IBP model may be easily generalized for both IAP and NBP models; in the case of NBP model we also assume a random distribution of adsorption sites on the surface. In this way the DR equation for IBP model [6] will be extended to the NBP model and "random surfaces". Namely, assuming for mole fraction Θ_1 the following equation [5]

$$\Theta_1(x, \beta, E) = [1 + (\beta/x) \exp(-E/RT)]^{-1} \tag{2}$$

and using the procedure described in references [5, 6], we obtain the following form for the DR equation:

$$\vartheta_1 = \exp\left[-B\left(RT\ln\frac{a\cdot f^s}{A}\right)^2\right] \text{for } a\cdot f^s \leqslant A \tag{3}$$

where $a = a_1/a_2$ is the ratio of the activities of both components in the bulk phase, $a_i = x_i f_i$; $f^s = f_1^s/f_2^s$ is the ratio of the activity coefficients in the surface phase; B is the heterogeneity parameter; A is the constant connected with the maximum value of E. The relationship between ϑ_1 and the excess adsorption $n_1^{\sigma(n)}$ is following:

$$\vartheta_1 = n_1^{\sigma(n)}/n^s + x_1 \tag{4}$$

where n^s is the total number of moles of both components in the surface phase and it is independent of the composition of the bulk phase for ideal and regular solutions. For IAP model the parameters B, A and n^s may be determined from excess adsorption data $n_1^{\sigma(n)}$ *vs.* x_1 by means of the following linear form of Eq. (3):

$$(-\ln\vartheta_1)^{1/2} = RTB^{1/2}\cdot\ln a - RTB^{1/2}\cdot\ln A \tag{5}$$

In the previous work [1], concerning the adsorption from regular solutions, for n^s the values calculated by assuming the homogeneity of the adsorbent surface were used. In this paper, the parameters A, B and n^s will be determined from experimental excess adsorption isotherms by using the best-fit procedure to Eqs (4) and (5). The knowledge of the parameters B and A makes possible the calculation of the distribution function F(E) according to the expression from reference [6], which characterizes the energetic heterogeneity of the adsorbent surfaces with respect to the adsorbing components.

Results and Discussion

The aim of the numerical calculations was to show the utility of the linear form of the DR equation (3) for the description of experimental data concerning the adsorption from binary non-ideal liquid mixtures on solid surfaces. For this purpose 37 experimental adsorption systems, available from the literature, were investigated. These systems are summarized in Table I, simultaneously provided with reference numbers of original papers. The parameters B, A and n^s were determined from experimental data $n_1^{\sigma(n)}$ *vs.* x_1 using the following procedure:

(i) calculation of the activity coefficients f_i ($i = 1, 2$) and next the activities a_i; the activity coefficients for systems investigated are available in literature (see Table I),

Table I

Information concerning the adsorption systems investigated

No. of ad. system	Liquid mixture		Adsorbent	Temp. °C	Ref. to ad. system	Ref. to act. coefficient
	component "1"	component "2"				
1	ethylene dichloride	benzene	titania gel	20	[12]	$f_1=f_2=1$
2	ethyl alcohol	benzene	titania gel	20	[12]	[13]
3	methyl alcohol	benzene	boehmite	20	[14]	[15]
4	ethyl alcohol	benzene	boehmite	20	[14]	[13]
5	benzene	cyclohexane	boehmite	20	[14]	[16]
6	chloroform	benzene	boehmite	20	[14]	[17]
7	methyl acetate	benzene	boehmite	20	[14]	[16]
8	ethyl alcohol	benzene	Bi oxide + Mo oxide catalyst I	45	[18]	[19]
9	ethyl alcohol	benzene	Bi oxide + Mo oxide catalyst II	45	[18]	[19]
10	methyl alcohol	benzene	Bi oxide + Mo oxide catalyst I	45	[18]	[15]
11	benzene	*n*-heptane	silica gel	25	[20]	[15]
12	benzene	ethylene dichloride	silica gel	30	[22]	$f_1=f_2=1$
13	*n*-hexane	benzene	tin oxide gel	35	[23]	[13]
14	*n*-hexane	benzene	tin oxide ppt	35	[23]	[13]
15	benzene	ethyl alcohol	activated carbon	30	[22]	[13]
16	benzene	ethylene dichloride	activated carbon	30	[22]	$f_1=f_2=1$
17	benzene	cyclohexane	graphit	20	[16]	[16]
18	benzene	cyclohexane	spheron	20	[16]	[16]
19	ethylene dichloride	benzene	charcoal	20	[16]	$f_1=f_2=1$
20	chloroform	carbon tetrachloride	charcoal	20	[16]	[16]
21	trichloroethane	butyl chloride	charcoal	20	[16]	[16]
22	trichloroethane	carbon tetrachloride	charcoal	20	[16]	[16]
23	propyl chloride	carbon tetrachloride	charcoal	20	[16]	[16]
24	methyl acetate	benzene	charcoal	20	[16]	[16]
25	benzene	cyclohexane	charcoal	20	[16]	[16]
26	pyridine	ethyl alcohol	charcoal	20	[16]	[16]
27	butyloamine	benzene	charcoal	20	[16]	[16]
28	ethyl alcohol	benzene	charcoal	20	[16]	[16]
29	chloroform	acetone	charcoal	20	[16]	[16]
30	benzene	cyclohexane	silica gel	0	[24]	[25]
31	benzene	cyclohexane	silica gel	30	[24]	[25]
32	benzene	cyclohexane	silica gel	60	[24]	[25]
33	benzene	ethyl alcohol	graphon	20	[26]	[13]
34	benzene	ethyl alcohol	graphon	25	[26]	[13]
35	benzene	ethyl alcohol	graphon	30	[26]	[13]
36	benzene	ethyl alcohol	graphon	40	[26]	[27]
37	benzene	ethyl alcohol	graphon	50	[26]	[27]

(ii) calculation of ϑ_1 *vs.* a for a given value of n^s,

(iii) calculation of the best-fit parameters B and A for $\vartheta_1(a)$ and standard deviation SD, where

$$\mathrm{SD} = [S/(k-2)]^{0.5} = \left\{ \sum_{i=1}^{k} [(-\ln \vartheta_{1,i})^{0.5} - RTB^{0.5} \ln a - RTB^{0.5} \ln A]^2/(k-2) \right\}^{0.5} \tag{6}$$

and S is sum of square deviations, k is the number of experimental points, the subscript i refers to the i-th experimental point,

(iv) determination of $n^s = N^s$ for which the dependence S *vs.* n^s reaches a minimum.

Parameter N^s, and parameters B and A evaluated by means of Eqs (5) and (4) for $n^s = N^s$, characterize a given adsorption system. These parameters are summarized in Table II.

Table II

Adsorption parameters of the linear form of the Dubinin–Radushkevich equation (5)

No. of ad. system	N^s mmole/g	n_h^s mmole/g	Method* of calculation of n_h^s	Parameter B		Parameter A		Standard deviation SD	
				for N^s	for n_h^s	for N^s	for n_h^s	for N^s	for n_h^s
1	0.70	2.66	E	0.078	0.070	5.89	18.46	0.0249	0.0727
2	1.20	1.08	E	0.007	0.011	5.47	6.04	0.0430	0.1045
3	1.88	2.41	E	0.105	0.307	2.11	1.88	0.2202	0.2580
4	3.05	2.68	SN	0.038	0.013	8.34	21.67	0.0087	0.0324
5	1.14	1.09	SE	0.054	0.046	5.89	6.40	0.0414	0.0486
6	1.40	1.88	E	0.054	0.050	7.92	14.16	0.0598	0.0754
7	1.27	1.43	E	0.040	0.036	3.94	6.70	0.0357	0.0396
8	0.62	0.59	E	0.207	0.173	2.02	2.03	0.0259	0.0294
9	0.64	0.72	SE	0.215	0.181	1.72	2.23	0.0416	0.0460
10	0.95	3.37	E	0.801	0.908	1.63	2.24	0.1151	0.4274
11	2.57	2.04	E	0.013	0.014	18.15	2.41	0.0101	0.0412
12	1.05	1.44	L	0.078	0.073	61.68	52.52	0.0298	0.0328
13	0.42	0.37	SE	0.075	0.072	4.41	6.82	0.0274	0.0303
14	0.31	0.36	E	0.063	0.060	4.47	6.52	0.0148	0.0164
15	3.97	4.50	L	0.099	0.105	3.67	4.13	0.1206	0.1371
16	1.69	0.79	SE	0.023	0.007	42.83	11.90	0.0238	0.0419
17	0.45	0.34	SN	0.035	0.026	26.60	21.28	0.0342	0.0352
18	0.37	0.42	E	0.055	0.052	4.77	7.06	0.0157	0.0179
19	1.57	1.05	SN	0.019	0.008	835.26	$5.5 \cdot 10^4$	0.0393	0.0563
20	1.32	1.46	SE	0.038	0.035	5.56	8.52	0.0298	0.0334
21	1.68	2.39	E	0.059	0.051	4.51	11.31	0.0795	0.0971
22	1.16	0.51	SN	0.034	0.007	55.30	$1.7 \cdot 10^3$	0.0163	0.0234
23	2.98	1.50	SN	0.059	0.030	63.50	930.02	0.0707	0.1491
24	2.92	1.52	SN	0.054	0.035	91.14	792.01	0.0355	0.1009
25	4.02	1.92	E	0.044	0.026	17.75	5.70	0.1030	0.1499
26	3.56	1.58	SN	0.023	0.011	50.57	214.97	0.0744	0.5942
27	2.37	1.57	E	0.018	0.009	28.64	7.18	0.0323	0.0536
28	3.77	3.03	SN	0.093	0.070	40.45	90.66	0.0227	0.1216
29	0.60	0.63	SN	0.011	0.012	55.62	63.95	0.0639	0.0645
30	5.28	3.61	E	0.049	0.043	12.11	5.97	0.0538	0.0749
31	5.22	3.34	E	0.052	0.045	11.07	6.69	0.0678	0.0823
32	2.70	3.12	E	0.053	0.048	4.67	7.56	0.0744	0.0860
33	0.52	1.06	E	0.770	0.584	1.55	2.41	0.0196	0.0439
34	0.50	0.88	E	0.543	0.456	1.69	2.53	0.0244	0.0381
35	0.48	0.90	E	0.757	0.578	1.53	2.36	0.0173	0.0332
36	0.46	0.83	E	0.995	0.795	1.24	1.76	0.0365	0.0532
37	0.42	0.66	E	0.734	0.626	1.26	1.80	0.0383	0.0473

*E — EVERET's method [10]
SN — method of SCHAY and NAGY [9]
SE — method of SISKOVA and ERDŐS [11]
L — taken from Ref. [17]

For comparative investigations, in Table II the parameters B and A, evaluated from Eqs (4) and (5) by assuming that $n^s = n_h^s$, where n_h^s was determined by SCHAY and NAGY [9], EVERETT [10] or ŜISKOVA and ERDŐS [11] methods. For both groups of parameters the standard deviation has been calculated according to Eq. (6). All parameters are summarized in Table II. For illustrative purposes, in Figures 1—4 the numerical results are shown for four adsorption systems. Figures 1,2 present the excess isotherms of 2-nd type according to SCHAY and NAGY classification [9], and Figs 3, 4 show the excess isotherms of 4-th type. In part (a) of each figure the experimental excess (white circles) isotherms are compared with the theoretical curves calculated for parameters from Table II; solid line was calculated for B and A corresponding to N^s, whereas, dashed line was obtained for B and A relating to n_h^s. The part (b) of each figure presents straight lines (5) for N^s (solid line with white circles) and n_h^s (dashed line with black circles). The part

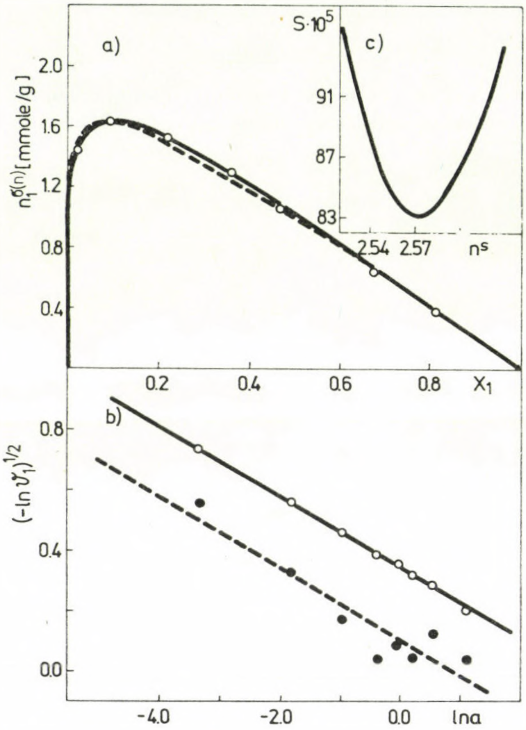

Fig. 1. Adsorption of benzene(1)-n-heptane(2) mixture on silica gel at 25 °C; (a) — experimental excess adsorption isotherm (white circles) in comparison to the theoretical curves calculated according to Eqs (3) and (4) for N^s (the solid line) and n_h^s (the dashed line), (b) — linear dependences, Eq. (5), calculated for N^s (the solid line with white circles) and n_h^s (the dashed line with black circles), (c) — the dependence S *vs.* n^s

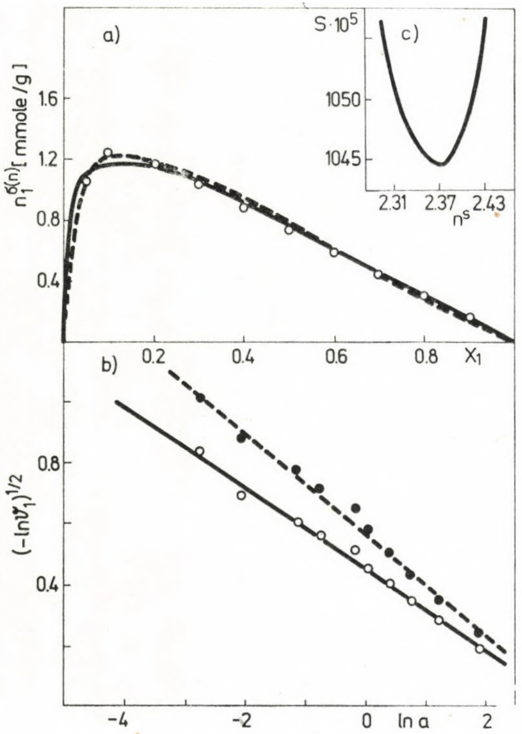

Fig. 2. Adsorption of butylamine(1)-benzene(2) mixture on charcoal at 20 °C; labelling as in Fig 1

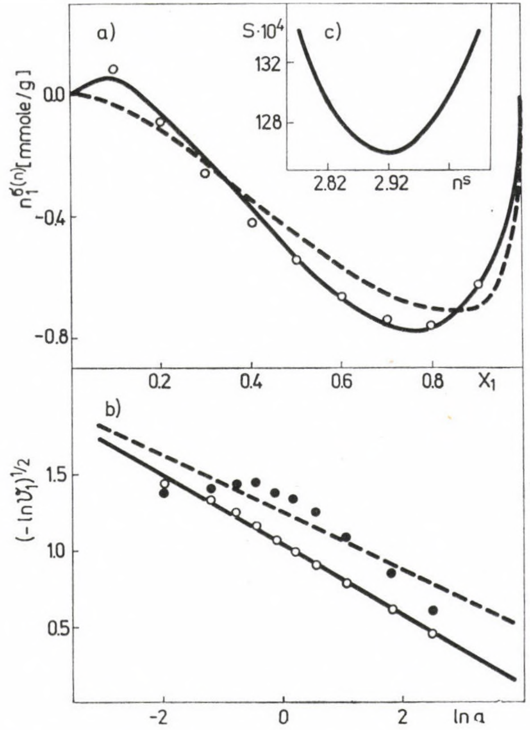

Fig. 3. Adsorption of methyl acetate(1)-benzene(2) mixture on charcoal at 20 °C; labelling as in Fig. 1

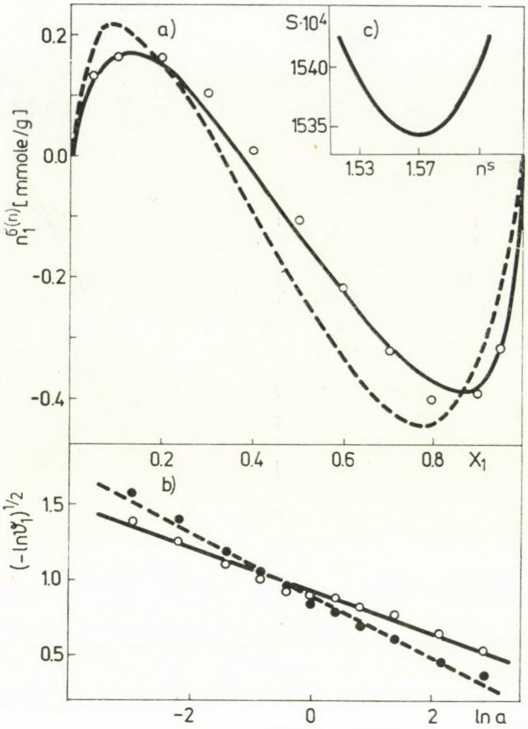

Fig. 4. Adsorption of ethylene dichloride(1)-benzene (2) mixture on charcoal at 20 °C; labelling as in Fig. 1

c) of each figure shows the dependence S *vs.* n^s. From the numerical results, summarized in Table II, and Figs 1—4 the following conclusions can be drawn:

(i) DR equation (3) can be applied for characterizing all types of experimental excess adsorption isotherms,

(ii) the parameters B, A corresponding to the minimalized value N^s predict better excess adsorption data than that relating to n_h^s,

(iii) the dependence S *vs.* n^s shows a distinct minimum and it may be used to evaluate parameter N^s.

REFERENCES

[1] Dabrowski, A., Jaroniec, M.: Acta Chim. Acad. Sci. Hung. **99**, 255 (1979)
[2] Coltharp, M. T., Hackerman, N. J.: J. Colloid Interface Sci. **43**, 185 (1973)
[3] Dékány, I., Szántó, F., Nagy, L. G.: Colloid Polymer Sci., **256**, 150 (1978)
[4] Puri, B. R., Kumar, S., Sandle, N. K.: Indian J. Chem., **1**, 418 (1963)
[5] Dabrowski, A., Oscik, J., Rudzinski, W., Jaroniec, M.: J. Colloid Interface Sci., **69**, 287 (1979)

[6] Oscik, J., Dabrowski, A., Jaroniec, M., Rudzinski, W.: J. Colloid Interface Sci., **56,** 403 (1976)
[7] Jaroniec, M.: Thin Solid Films, **50,** 163 (1978)
[8] Jaroniec, M., Borowko, M., Patrykiejew, A.: Surface Sci., **78,** L501 (1978)
[9] Schay, G., Nagy, L. G.: J. Chim. Phys., **58,** 149 (1961)
[10] Everett, D. H.: Trans. Faraday Soc., **60,** 1803 (1964)
[11] Siskova, M., Erdős, E.: Coll. Czech. Chem. Commun., **25,** 2599 (1960)
[12] Kipling, J. J., Peakall, D. B.: J. Chem. Soc., **1957,** 4054
[13] Smith, V. C., Robinson, R. L.: J. Chem. Eng., Data, **15,** 391 (1970)
[14] Kipling, J. J., Peakall, D. B.: J. Chem. Soc., **1956,** 4828
[15] Scatchard, G., Wood, S. E., Mochel, J. M.: J. Am. Chem. Soc., **68** 1957 (1946)
[16] Blackburn, A.,Kipling, J. J., Tester, D. A.: J. Chem. Soc., **1957,** 2373
[17] Kipling, J. J., Pekall, D. B.: J. Chem. Soc., **1958,** 3899
[18] Chopra, B., Ramakrishna, V.: Indian J. Chem., **10,** 187 (1972)
[19] Hwang, S. Ch., Robinson, R. L.: J. Chem. Eng. Data, **22,** 319 (1977)
[20] Fóti, G., Nagy, L. G., Schay, G.: Acta Chim. Acad. Sci. Hung., **76,** 269 (1973)
[21] Brown, I., Fock, W., Smith, F.: Aust. J. Sci. Res. **4,** 198 (1951)
[22] Sircar, S., Myers, A. L.: J. Phys. Chem., **74,** 2828 (1970)
[23] Madan, R. L., Sandle, N. K., Tyagi, J. S.: Curr. Sci., **44,** 879 (1975)
[24] Sircar, S., Novosad, J., Myers, A. L.: Ind. Chem. Eng. Fundamen., **11,** 249 (1972)
[25] Scatchard, G., Wood, S. E., Mochel, J. M.: J. Phys. Chem., **43,** 119 (199
[26] Brown, Ch. E., Everett, D. H., Morgan, Ch. J.: Trans. Faraday Soc., **71,** 883 (1975)
[27] Brown, J., Smith, F.: Aust. J. Chem., **7,** 264 (1954)

A. Dabrowski
M. Jaroniec

Department of Theoretical Chemistry, Institute of Chemistry, M. Curie-Skłodowska University, 20031 Lublin, Poland

RECENSIONES

A. YEHASKEL: *Fire and Flame Retardant Polymers. Recent Developments*

Noyes Data Corporation, New Jersey, USA, 1979

Is it possible that in the torrent of technical and scientific information of our age the time is not far, when the most useful technical books will be written by computers? Indeed, even the raising of this question may rightly elicit the aversion of somebody who is used to a broad view, to detailed expounding of thoughts, abstractions and conclusions, who can distinguish on the merit of arguments, technical and scientific solutions, can weigh these — thus the aversion of the thinking man, scientist, or engineer.

Well, the book published recently by the Noyes Data Corporation on fire and flame retardant polymers can be regarded as such a "computer" book, although the name of A. YEHASKEL is given as author. The book of 482 pages, published by one of the largest data banks of America, is essentially a collection of patents. It gives a very thorough and detailed description of the 261 U.S. patents published during the two years between July 1976 and June 1978, on the subject of fire retardant polymers. In consideration of the closing date of editing and the fact that this book, its excellent typography also being on world level, was available as early as April 1979 on the European book market, the rapidity of information flow in itself is praiseworthy.

This book is neither a monograph, nor a handbook or textbook, nevertheless it is of great value. It surveys recent patents relevant to fire retarding, grouped from the point of view of the polymers. The book is divided into chapters on polyurethans, polyesters, epoxy and silicone resins, phenolic resins and other thermosetting resins, polypropylene and polyethylene, polystyrene and ABS, polycarbonates, PVC and other thermoplastic polymers, natural polymers, additives of general purpose and mixed processes.

The character of the book becomes evident when compared with an excellent work of KURYLA and PAPA, considered today as the text-book on the flame retardancy of polymers [W. C. KURYLA and A. J. PAPA (editors) Flame Retardancy of Polymeric Materials, M. Dekker Inc. New York, 1973]. This earlier book discusses *e.g.* the inflammability of polyethylene and polypropylene in a chapter of 50 pages. After a detailed discussion of the combustion of polyolefins and the mechanism of flame retardancy, the book of KURYLA first describes, according to concepts accepted earlier, halogen-containing fire retardant additives, proceeding to discuss the interaction of additives containing halogens and antimony, and this is followed by fire retardants containing phosphorus.

The chapter of the new book by A. YEHASKEL dealing with polypropylene and polyethylene gives a detailed description of only 16 new U.S. patents, on 33 pages. However, these recent patents contain everything promised by the sub-title of the book *(Recent Developments)*; thus one may even speak of a change in attitude in achieving fire retardancy of polyolefins. Here, not only additives evolving HCl and HBr gases or additives of similar action are concerned, but also multicomponent, possibly cross-linked systems, which, though burning, do not pour, but carbonize with occasional foaming, and scarcely give off corrosive gases or vapours during this process. An example of this kind is U.S. Pat. No. 4,072,643 of Phillips Petroleum Co. (February 1978), according to which polyethylene or polypropylene is mixed with an elastic ethylene-propylene copolymer, then cross-linked in the presence of the following components: pentaerythritol, melamine and phosphorus pentoxide. Another example is U.S. Pat. No. 4,085,162 of General Electric Co., filed in April 1978, according to which polyethylene is cross-linked with a phosphorylated phenol-formaldehyde resin of novolak type and triallyl cyanurate. From the detailed examples of this latter patent it becomes evident that the polyethylene cross-linked with dicumyl peroxide contains, in addition to carbon black, antioxidant and 10% w/w of phosphorylated phenol-formaldehyde resin of novolak type, also 50% w/w of calcinated and siliconized clay as filling material. In this way, excellent flame-retarded cable sheathing, not pouring even in fire, has been prepared.

Though the book does not give an evaluation and no conclusions are drawn, the collection of patents nevertheless permits to recognize the trends prevailing in the field of the fire and flame retardation of polymers. In recent patents, additives retarding flame propagation as regarded a chain reaction, substances of complex action producing foaming and coking, and additives preventing the pouring of polymers into the fire have gained prominence.

Very good results can be achieved with high-molecular fire retardants built into the polymer. A good example in U.S. Pat. No. 4,081,598 of W.R. Grace Co. (March 1978), dealing with halogenated polythiols. The *bis* (2-hydroxyethyl ether) derivative of tetrabromodiphenylol propane is allowed to react with mercaptopropionic acid and the resulting polythiol is cross-linked with triallyl cyanurate by the action of light, to give an elastic sealing material, whose reduced inflammability is well characterized by its relatively high (30.2%) oxygen index.

Most plastics, the synthetic structural materials of our age, are of organic origin, and thus cannot be made absolutely fire resistant. However, the industrial manufacture of polymers not propagating the flame and fire, and thus the fire protection of plastics structures will undergo further important development, as testified by this useful book. It is only regretable that the greatest merit of the volume, its up-to-date character, will soon expire.

T. CZVIKOVSZKY

M. GUTCHI: *Edible Oils and Fats. Recent Development*

Noyes Data Corporation, New York, 1979 (402 pages, 33 illustrations)

Based upon patents registered in the USA since 1973, this book acquaints its readers with the latest developments in the manufacture of edible oils and fats. This book is a long-needed one because it shows the complete collection of the pertinent patents issued in the USA in the last five years.

The essential of the new patent specifications are presented to the specialists in this field. Here we have a comprehensive review which provides concise and professional information with expressions concerning the aspects of patent law kept in the background.

Since not scientific but patent literature is the basis of this book, a very great number of up-to-date and recent technologies are included and many newly marketed products are described.

To achieve timeliness, the text passed very rapidly through the stages of publication: about 250 of the patents discussed were registered before June 1978.

The subject matter is divided into fourteen parts which deal with
— the extraction of edible oils
— the refining of edible oils
— the improvement of the stability of fats and oils in the presence of oxidative agents
— the modification of the properties of fats and oils
— margarines and similar edible fats
— salad oils, mayonnaise and various emulsions
— oils for frying and cooking
— fats for confectionery or sweets industry
— aromatic substances
— emulsifiers
— peanut butter
— additive fats and other additives used in food processing
— fatty substances used in other fields of application
— indexes, according to registration number, applicant, and patentee of the U.S. patents involved.

The manufacturing technologies as well as the new products embody very much new ideas. To give few examples of new technologies, extraction by means of aqueous solutions of sulfonates, filtration of crude oils through press-cakes, extraction of oil from yeast, extraction with a mixture of hexane and acetic acid, refining with an alkali and xylene sulfonate, clarification on a silica gel column, refining by removal of waxes, hydrogenation coupled to treatment with steam, stabilization with novel antioxidants like polyphenols and thiodipropionic with novel antioxidants like polyphenols and thiodipropionic acid, thiodialkane esters together with metal desactivators, chroman compounds, 3-*tert*-butyl-4-hydroxy-5-methylphenyl stearate *i.e.* methional, methods for the prevention of the autooxidation of water-in-oil emulsions, straight-chain aliphatic 1,3-diols for the conservation of cosmetic products, inhibition of the poisoning of catalysts used in hardening processes, acceleration of transesterification with help of ketones, the dispersion of alkali metals in fats for transesterification may be mentioned.

In the group of new products we find formulas for new, so-called soft margarines, rapidly crystallizing margarine fat base with much palm oil in it, margarine for frying, fatty acid sugar esters as emulsifiers, stable margarine with low caloric value, frying oils, non-hardened stable soybean oil, liquid oil made from palm oil, fats for substituting cocoa butter, coffee oil, monoglycerides, polyglycerol esters of dimerized fatty acids, non-deteriorating stable peanut butter, full-milk powder well dispersible in cold water, crystalline stable fat powder, cream powders, fat concentrates, edible emulsions, emulsified fats suitable for intravenous injection.

Illustrations render this work very expressive and the quoting of examples from the specifications makes it easily comprehensible: all in all, this book is a well ordered and serviceable collection of much novel, useful informations.

É. KURUCZ

RANNEY, W. R.: *Crude Oil Drilling Fluids*

Noyes Data Corp., Park Ridge, New Jersey, USA, 1979, 348 pages

The book presents in clear technological wording 250 USA patents issued in the years from 1974 to 1978 for crude oil drilling fluids, particularly for drilling mud, but also for other fluids of crude oil production, omitting "legal jargon and juristic phraseology", as stated in the preface of the book.

In accordance with the title of the book, chapters discussing patents of crude oil drilling fluids in the stricter sense, of drilling mud and cement slurry, are the most extensive.

The first large chapter on drilling muds deals with patents on additives affecting colloidal and rheological properties, to discuss then among others *e.g.* reagents providing for salt resistance and preventing the heaving of shale, forming the bore hole wall or additives forming stable drilling foams, further additives influencing the characteristics of the drilling fluids of drilling in permafrost area.

Another chapter relative to drilling muds discusses patents of additives and methods, providing for lubrication, corrosion prevention, increase in density, and other drilling fluid functions.

In addition to chapters describing the patents on crude oil drilling fluids in the stricter sense, separate chapters are devoted to formation fracturing fluids, to patents covering various additives of fluids for reservoir formation stimulations, sand consolidation, secondary and tertiary crude oil production processes, and to patents concerning procedures furthering these aims.

A separate chapter deals with the patents of the processes of steadily increasing actuality for the recovery of heavy oil from tar sand and oil shale.

The collection of patents discussed will be useful for project engineers planning drilling, well completion, well workover operations, or secondary and tertiary production processes, as well as for researchers of the fluids for these operations.

Indexes of the inventors, patent holders and patent numbers help in the utilization of the book.

Ö. ALLIQUANDER

A. KNOP and W. SCHEIB: *Chemistry and Application of Phenolic Resins*

Springer Verlag, Berlin—Heidelberg,—New York, 1979. 269 pages, 111 figures and 89 tables

This book is the third member of the series "Polymers — Properties and Applications" which is the continuation of the old series entitled "Chemie, Physik und Technologie der Kunststoffe in Einzeldarstellungen".

The volume contains the following chapters:
Historical and economic development of phenolic resins
Raw materials

Reaction mechanisms
Resin production
Physiology and enviromental protection
Analytical methods
Degradation of phenolic resins by heat, oxygen and high energy radiation
Modified and thermal-resistant resins
Composite wood materials
Molding compounds
Heat and sound insulation materials
Industrial laminates and paper impregnation
Coatings
Foundry resins
Abrasive materials
Friction materials
Phenolic resins in rubbers and adhesives
Phenolic antioxidants
Other applications

The first eight chapters (101 pages) deal with the chemistry of phenolic resins, while the remaining part (155 pages) with the different technological applications. The book gives a good survey of our present-day knowledge of the current theory in phenolic resin chemistry and the technical applications of phenolic resins based on day-to-day experiences in research, production and marketing, with a background of economic relevance.

The book is equally modern in the selection of the topics, the way of their treatment, and in the arrangement of the subject-matter. All chapters are up-to-date, especially the one referring to the chemistry of phenolic resins.

A somewhat more critical selection of material of the technological part and thus some restriction would have been advantageous.

Reference at the end of each chapter help the reader in finding further information. The literature is covered up to July 1978; the authors selected mainly the most recent references.

According to the impression of the reviewer, the literature references are not as complete as desirable. The way of quoting the references frequently seems somewhat unusual.

The short time between the writing and publication of the book is remarkable and should be appreciated; on the other hand, it is regrettable that the book contains many misprints, which could have been eliminated by more careful proof-reading. It is hoped that these disturbing errors will be eliminated in a later edition.

The lucidity and usability of the book is somewhat reduced by a rather great number of inaccuracies throughout the volume, such as incomplete figures without explanation of the different curves (Fig. 3.4); missing of the meaning of abbreviations: BHF (p. 16), BPA (pp. 19,189), RP (pp. 23, 83), BOD (p. 68), MSA (= *m*aleic *a*cid *a*nhydride, p. 193: (13.4) chemical formula); RT (p. 218), SBR (p. 241), AO (pp. 243, 244, 245); omission of the meaning of symbols (WZ: Fig. 9.7, p. 114; DM, MS: Fig. 9.12, p. 117); inexact citations: references 4, 17, 23, 34 (Chapt. 10), 16 (Chapt. 11), 17, 21 (Chapt. 12), 3 (Chapt. 13), 6, 7, 8, 9 (Chapt. 14) and 11, 12, 26, 35, 37 (Chapt. 19) are only in the list of references but nowhere mentioned in the text; in turn, reference 49 (Chapt. 10) is mentioned in the text but not to be found in the list of references; a great number of the figures and tables given are not referred too in the context.

In spite of the incompleteness mentioned above, the book gives useful information of the present state of knowledge of phenolic resins and can be recommended to the wide circle of chemists, engineers, marketing professionals and students.

I. GÉCZY

Springer Series in Chemical Physics, Vol. 1
I. I. SOBELMAN (Lebedev Institute of Physics, USSR Academy of Sciences): *Atomic Spectra and Radiative Transitions*

Springer Verlag, Berlin—Heidelberg—New York, 1979

The present volume is a suitably shortened and partly updated version of a book by the same author, first published fifteen years ago. Although it can be regarded as the first part of a monograph planned to appear in two volumes, also on its own it provides a complete and applicable set of methods and knowledge. The aim of the book is to sum up the information which makes atomic spectroscopy applicable in the description of plasma, in astrophysics, layer physics and other rapidly developing fields. The volume of 306 pages consists of two parts. The *first part, Elementary Information on Atomic Spectra*, occupies 53 pages. It can be taken as an introduction, a guide to the reader. In this part the atomic spectra of the elements of the periodic table are described, starting with hydrogen and hydrogen-like atoms, and the basic physical principles of atomic spectra are summarized. Theoretical resuts are compared to experimental data in order to judge the validity of the approximations involved *e.g.* in the application of self-consistent field or in the various coupling schemes of angular momentum. The first part of the volume contains three chapters. *1.* The chapter "The Hydrogen Spectrum" presents the analytical solutions of the Schrödinger and Dirac equations for the hydrogen atom and the approximate solutions for hydrogen-like atoms, used as a basic method in the interpretation of atomic spectra. *2.* The chapter "Systematics of the Spectra of Multielectron Atoms" describes the application of self-consistent field concept for the two limting cases of angular momentum coupling, *i.e.* LS and jj type coupling. *3.* The chapter "Spectra of Multielectron Atoms" briefly discusses the most important features of the spectra, as a function of the occupation of electron shells varying over the periodic system.

The *second part, Theory of Atomic Spectra*, consists of 250 pages. The systematic treatment applies the Racah techniques and the method of fractional parentage coefficients for the calculation of angular moments. The use of these very efficient methods for the problems of atomic spectroscopy is illustrated by several examples and tables. This is followed by a very detailed discussion of radiation phenomena, such as multipole radiation, Bremsstrahlung, photorecombination and photoionization. Particular attention is devoted to the approximate calculation of transition probabilities and cross sections. The oscillator strengths of electric dipole and quadrupole transitions and the cross sections of photorecombination are given in tabular form. The choice was governed by the aspects of applicability in other branches of atomic spectroscopy and physics. The second part is divided into five chapters. *4* The chapter "Angular Momenta" discusses the Racah technique in the calculation of the matrix elements of spherical tensor operators, which can be applied in many problems of atomic spectroscopy. The required tables and equations are also given. The importance of the Racah method is illustrated by the fact that it enables several, formerly very tedious calculations to be performed almost instantaneously using ready-made results represented by the coefficients taken from the tables. *5.* The chapter "Systematics of the Levels of Multielectron Atoms" applies again the Racah method for the calculation of term schemes and fine splitting, with the use of fractional parentage coefficient. Again, several examples are given for testing the method. *6.* The chapter "Hyperfine Structure of Spectral Lines" is concerned with the effect of the magnetic moments and electric quadrupole moments of the nuclei. The isotope shift of lines is also discussed. *7.* The chapter "The Atom in an External Electric Field" is devoted primarily to the effect of the plasma microfields on the atomic levels and transition probabilities. It deals not only with the linear and quadratic Stark effect in homogeneous and static electric field, but also takes into account the effect of inhomogeneous and variable fields. *8.* The chapter "Atom in an External Magnetic Field" discusses the effect of weak and strong magnetic fields equally, including the splitting of hyperfine components. *9.* The last chapter, "Radiative Transitions" occupies 103 pages in itself. It discusses in detail the various radiation phenomena (electric dipole, multipole, Bremsstrahlung, photorecombination, photoionization), together with transition probabilities and approximate methods for the calculation of cross sections. Approximation formulas are given, and the results of numerical calculations are summarized in several tables.

The volume contains 20 line diagrams and 46 tables. The formulas and results are given in CGS system.

GY. VARSÁNYI

A. F. WILLIAMS: *A Theoretical Approach to Inorganic Chemistry*

Springer Verlag, Berlin—Heidelberg—New York, 1979, 316 pages

This work by A. F. WILLIAMS reviews the up-to-date fundamental theories of inorganic chemistry and chemical physics. Eight chapters, an appendix in two parts, and a subject index constitute this volume of 316 pages, 144 illustrations and 17 tables help comprehension. Bibliographies at the end of each chapter comprise 231 items all together, and 135 examples distributed after the chapters facilitate to get the mastery and to arrive at a practical application of this theoretical matter.

The composition of this book is excellent. Every part is completed by a summary; the bibliographies refer to the most important books and to concise reviews. Special mention must be made of the fact that most recent works, those which appeared in 1978, are also included in these bibliographies. The examples at the end of each chapter help to make use of imparted knowledge in practice.

The theoretical foundation and the most important notions of quantum mechanics, atomic theory and simple molecular orbitals are treated in the first two chapters. In the third, the applications of molecular orbital theory to problems of structure are dealt with; in the fourth, the author describes the most important features of electronic spectra and magnetic properties of inorganic compounds. The title of the fifth chapter refers to alternative methods and notions. Here important theoretical matter like electronegativity, oxidation state, theories of acids and bases are discussed. The sixth chapter is concerned with mechanisms and reactivity. The main group elements, the transition elements, the lanthanides and the actinides are characterized in the seventh chapter. The eighth is a brief survey of the various physical and spectroscopic methods. The appendix contains tables of group theory abbreviations, symbols and units of energy.

The outstanding feature of this book is that its author has found an excellent pedagogical and critical way of discussing various quantumchemical models, various types of chemical bonding as well as molecular orbital theories, valence vibrations and ligand field theory. In order to present and interpret the structures, bondings and geometries in inorganic compounds, the author utilizes group theory and spectroscopic methods.

This book is equally useful to university students and to research workers engaged in problems of inorganic chemistry or chemical physics.

J. **Nagy**

Coulometric Analysis

Edited by E. **Pungor** and I. **Buzás**

Akadémiai Kiadó, Budapest 1979

This book is the collection of papers presented at the First International Conference on Coulometry, held at Mátrafüred (Hungary), October 17—19, 1978. 301 pages bring the subject matter and the discussion of the eight plenary lectuses of the fourteen papers read in the sections.

The plenary lectures offer very good reviews of the various fields of the coulometric methods.

Two of these lectures deal with theoretical aspects.

E. **Bishop** (UK) discusses the possibility of a quantitative prediction in respect of the optimum experimental conditions of a coulometric titration, by means of a function derived for the titration curve.

L. **Meites** (USA) deals with computerized data processing applicable in CPC methods, partly from the analyst's point of view, partly with reference to reaction mechanisms.

In another paper L. **Meites** summarizes the theoretical directives or the application of CPC methods for the elucidation of electrode processes and as one of the most experienced experts in this field, offers a critical review of the indispensable conditions of successful experimental work.

The other five plenary lectures summarize some recent methods and the new results of applications of coulometric techniques.

A paper presented by E. **Pungor** *et al.* (Hungary) is concerned with the theoretical bases and the latest results of their method of current programmed coulometric titration in flowing solutions.

Z. **Galus** (Poland) summerizes the chrono-coulometric method and presents new results of the application of this method.

P. **Agasyan** (USSR) deals with the new possibilities of the reagent generation methods of coulometry.

A. **Hulanicki** (Poland) discusses the possibilities of coulometric titrations in non-aqueous media and gives a critical review of latest results.

Gy. **Farsang** (Hungary) discusses possibilities for combining the CPC method with other electroanalytical techniques, aiming at the elucidation of the mechanism of redox reactions and cites his results in the explication of the colour-change mechanism of diphenylamine type indicators.

Among the fourteen discussion papers one deals with theoretical subject.

J. MOCAK *et al.* (Czechoslovakia) treat the application of numerical methods for the evaluation of current *vs.* time and of charge *vs.* time curves when reaction mechanisms are studied by the CPC method with the aim to detect coupled chemical reactions and the mechanism of the electrode reaction.

The CPC study of the mechanism of the electrode reaction of chromium complexes is the subject of the paper by D. BUSTIN *et al.* (Czechoslovakia).

J. BERCIK *et al.* (Czechoslovakia) report on their results of coulometric titration as a high precision analytical tool, while, P. GRÜNDLER (GDR) considers the method of amperometric end-point indication from the same point of view.

Four of the lectures on novel applications of coulometric titration treat new methods of acid-base titration in non-aqueous media, three others report on new titration methods in aqueous media.

Two lectures deal with the application of coulometric titration for clinical and pharmaceutical analyses.

Finally, a comprehensive review is given by T. DAMOKOS and J. HAVAS (Hungary) of the research, manufacture and development of coulometric instrumentation in Hungary.

The concise reproduction of the discussions which followed the lectures conveys an adequate impression of the active participation in the sessions which dealt with well defined topics; these sessions offered abundant opportunity for workers in this field to gather up-to-date information concerning the actual problems which emerge in connection with the methods discussed.

The plenary lectures are good, up-to-date summaries of the present state of this field, completed in some cases with directives of future trends. Several important and recent results of internationally acknowledged research is summarized. Useful and important references are collected by the authors: thus readers who wish to get a general view of this field may use this as a source book.

Unfortunately, only one paper deals with automated techniques of coulometry. Similarly are lacking the modern principles of the instrumentation of coulometric methods and the review of available intsruments. Even references to this part of the literature are scarce.

The discussion papers mainly present new results, new methods in comprehensive and informative form. Though the number of papers are relatively small, a complete cross section of the field of coulometry is given. References to the literature are sufficient to facilitate rapid orientation. It took hardly more than half a year to have this book issued from the press, thus items in it are up-to-date indeed. Due to great editorial care, and in spite of the manuscripts not having been submitted to referees in order to save time, this book offers professionally valuable and up-to-date information.

This is a book useful for analysts who apply, or are interested in coulometry: orderly arranged items of latest knowledge make it a book well worth to purchase.

GY. FARSANG

INDEX

PHYSICAL AND INORGANIC CHEMISTRY

ORGANIC CHEMISTRY

ANALYTICAL CHEMISTRY

Printed in Hungary

A kiadásért felel az Akadémiai Kiadó igazgatója. Műszaki szerkesztő: Zacsik Annamária
A kézirat nyomdába érkezett: 1979. XII. 14. — Terjedelem: 8,40 (A/5) ív, 38 ábra

---

80.7805 Akadémiai Nyomda, Budapest — Felelős vezető: Bernát György

Les Acta Chimica paraissent en français, allemand, anglais et russe et publient de mémoires du domaine des sciences chimiques.

Les Acta Chimica sont publiés sous forme de fascicules. Quatre fascicules seront réunis en un volume (3 volumes par an).

On est prié d'envoyer les manuscrits destinés à la rédaction à l'adresse suivante:

Acta Chimica
Budapest, P.O. Box 67, H-1450, Hongrie

Toute correspondance doit être envoyée à cette même adresse.

La rédaction ne rend pas de manuscript.

Abonnement en Hongrie à l'Akadémiai Kiadó (1363 Budapest, P.O.B. 24, C. C. B. 215 11488), à l'étranger à l'Entreprise du Commerce Extérieur « Kultura » (H-1389 Budapest 62, P. O. B. 149 Compte-courant No. 218 10990) ou chez représentants à l'étranger.

Die Acta Chimica veröffentlichen Abhandlungen aus dem Bereich der chemischen Wissenschaften in deutscher, englischer, französischer und russischer Sprache.

Die Acta Chimica erscheinen in Heften wechselnden Umfanges. Vier Hefte bilden einen Band. Jährlich erscheinen 3 Bände.

Die zur Veröffentlichung bestimmten Manuskripte sind an folgende Adresse zu senden

Acta Chimica
Budapest, Postfach 67, H-1450, Ungarn

An die gleiche Anschrift ist jede für die Redaktion bestimmte Korrespondenz zu richten.

Manuskripte werden nicht zurückerstattet.

Bestellbar für das Inland bei Akadémiai Kiadó (1363 Budapest, Postfach 24, Bankkonto Nr. 215 11488), für das Ausland bei »Kultura« Außenhandelsunternehmen (H-1389 Budapest 62, P.O.B. 149. Bankkonto Nr. 218 10990) oder seinen Auslandsvertretungen.

«Acta Chimeca» издают стильи по химии на русском, английском, французском и немецком языках.

«Acta Chimica» выходит отдельными выпусками разного объекта, 4 выпуска составхяют одинтом и за год выходят 3 тома.

Предназначенные для публикации рукописи следует направлять по адресу:

Acta Chimica
Budapest, P.O. Box 67, H-1450, ВНР

Всякую корреспонданцию в редакцию направляйте по этому же адресу.

Редакция рукописе не возвращает.

Отечественные подписчики направляйте свои заявки по адресу Издательства Академии Наук (1363 Budapest, P.O.B. 24. Текущий счет 215 11 488), а иностранные подписчики через организацию по внешней торговле «Kultura» (H-1389 Budapest 62, P.O.B. 149. Текущий счет 218 10990) или через ее заграничные представительства и уполномеченных.

Reviews of the Hungarian Academy of Sciences are obtainable at the following addresses:

AUSTRALIA
C.B.D. LIBRARY AND SUBSCRIPTION SERVICE, Box 4886, G.P.O., *Sydney N.S.W. 2001*
COSMOS BOOKSHOP, 145 Ackland Street, *St. Kilda (Melbourne), Victoria 3182*

AUSTRIA
GLOBUS, Höchstädtplatz 3, *1200 Wien XX*

BELGIUM
OFFICE INTERNATIONAL DE LIBRAIRIE, 30 Avenue Marnix, *1050 Bruxelles*
LIBRAIRIE DU MONDE ENTIER, 162 Rue du Midi, *1000 Bruxelles*

BULGARIA
HEMUS, Bulvar Ruski 6, *Sofia*

CANADA
PANNONIA BOOKS, P.O. Box 1017, Postal Station "B", *Toronto, Ontario M5T 2T8*

CHINA
CNPICOR, Periodical Department, P.O Box 50, *Peking*

CZECHOSLOVAKIA
MAD'ARSKÁ KULTURA, Národni třida 22, *115 66 Praha*
PNS DOVOZ TISKU, Vinohradská 46, *Praha 2*
PNS DOVOZ TLAČE, *Bratislava 2*

DENMARK
EJNAR MUNKSGAARD, Norregade 6, *1165 Copenhagen*

FINLAND
AKATEEMINEN KIRJAKAUPPA, P.O. Box 128, *SF-00101 Helsinki 10*

FRANCE
EUROPERIODIQUES S. A., 31 Avenue de Versailles, *78170 La Celle St.-Cloud*
LIBRAIRIE LAVOISIER, 11 rue Lavoisier, *75008 Paris*
OFFICE INTERNATIONAL DE DOCUMENTATION ET LIBRAIRIE, 48 rue Gay-Lussac, *75240 Paris Cedex 05*

GERMAN DEMOCRATIC REPUBLIC
HAUS DER UNGARISCHEN KULTUR, Karl-Liebknecht-Strasse 9, *DDR-102 Berlin*
DEUTSCHE POST ZEITUNGSVERTRIEBSAMT, Strasse der Pariser Kommüne 3—4, *DDR-104 Berlin*

GERMAN FEDERAL REPUBLIC
KUNST UND WISSEN ERICH BIEBER, Postfach 46, *7000 Stuttgart 1*

GREAT BRITAIN
BLACKWELL'S PERIODICALS DIVISION, Hythe Bridge Street, *Oxford OX1 2ET*
BUMPUS, HALDANE AND MAXWELL LTD., Cowper Works, *Olney, Bucks MK46 4BN*
COLLET'S HOLDINGS LTD., Denington Estate, *Wellingborough, Northants NN8 2QT*
WM. DAWSON AND SONS LTD., Cannon House, *Folkestone, Kent CT19 5EE*
H. K. LEWIS AND CO., 136 Gower Street, *London. WC1E 6BS*

GREECE
KOSTARAKIS BROTHERS, International Booksellers, 2 Hippokratous Street, *Athens-143*

HOLLAND
MEULENHOFF-BRUNA B.V., Beulingstraat 2, *Amsterdam*
MARTINUS NIJHOFF B.V., Lange Voorhout 9—11, *Den Haag*
SWETS SUBSCRIPTION SERVICE, 347b Heereweg, *Lisse*

INDIA
ALLIED PUBLISHING PRIVATE LTD., 13/14 Asaf Ali Road, *New Delhi 110001*
150 B-6 Mount Road, *Madras 600002*
INTERNATIONAL BOOK HOUSE PVT. LTD., Madame Cama Road, *Bombay 400039*
THE STATE TRADING CORPORATION OF INDIA LTD., Books Import Division, Chandralok, 36 Janpath, *New Delhi 110001*

ITALY
EUGENIO CARLUCCI, P.O. Box 252, *70100 Bari*
INTERSCIENTIA, Via Mazzé 28, *10149 Torino*
LIBRERIA COMMISSIONARIA SANSONI, Via Lamarmora 45, *50121 Firenze*
SANTO VANASIA, Via M. Macchi 58, *20124 Milano*
D. E. A., Via Lima 28, *00198 Roma*

JAPAN
KINOKUNIYA BOOK-STORE CO. LTD., 17-7 Shinjuku-ku 3 chome, Shinjuku-ku, *Tokyo 160-91*
MARUZEN COMPANY LTD., Book Department, P.O. Box 5050 Tokyo International, *Tokyo 100-31*
NAUKA LTD. IMPORT DEPARTMENT, 2-30-19 Minami Ikebukuro, Toshima-ku, *Tokyo 171*

KOREA
CHULPANMUL, *Phenjan*

NORWAY
TANUM-CAMMERMEYER, Karl Johansgatan 41—43, *1000 Oslo*

POLAND
WĘGIERSKI INSTYTUT KULTURY, Marszalkowska 80, *Warszawa*
CKP 1 W ul. Towarowa 28 *00-958 Warszawa*

ROUMANIA
D. E. P., *Bucureşti*
ROMLIBRI, Str. Biserica Amzei 7, *Bucureşti*

SOVIET UNION
SOJUZPETCHATJ — IMPORT, *Moscow*
and the post offices in each town
MEZHDUNARODNAYA KNIGA, *Moscow G-200*

SPAIN
DIAZ DE SANTOS, Lagasca 95, *Madrid 6*

SWEDEN
ALMQVIST AND WIKSELL, Gamla Brogatan 26, *S-101 20 Stockholm*
GUMPERTS UNIVERSITETSBOKHANDEL AB, Box 346, *401 25 Göteborg 1*

SWITZERLAND
KARGER LIBRI AG, Petersgraben 31, *4011 Basel*

USA
EBSCO SUBSCRIPTION SERVICES, P.O. Box 1943, *Birmingham, Alabama 35201*
F. W. FAXON COMPANY, INC., 15 Southwest Park, *Westwood, Mass, 02090*
THE MOORE-COTTRELL SUBSCRIPTION AGENCIES, *North Cohocton, N. Y. 14868*
READ-MORE PUBLICATIONS, INC., 140 Cedar Street, *New York, N. Y. 10006*
STECHERT-MACMILLAN, INC., 7250 Westfield Avenue, *Pennsauken N. J. 08110*

VIETNAM
XUNHASABA, 32, Hai Ba Trung, *Hanoi*

YUGOSLAVIA
JUGOSLAVENSKA KNJIGA, Terazije 27, *Beograd*
FORUM, Vojvode Mišića 1, *21000 Novi Sad*

21. VIII. 1980 HU ISSN 0001—5407 Index: 26.007

ACTA CHIMICA
ACADEMIAE SCIENTIARUM HUNGARICAE

TOMUS 104 FASCICULUS 3

AKADÉMIAI KIADÓ, BUDAPEST
1980

ACTA CHIM. ACAD. SCI. HUNG. ACASA2 104 (3) 201–319 (1980)

ACTA CHIMICA

A MAGYAR TUDOMÁNYOS AKADÉMIA KÉMIAI TUDOMÁNYOK OSZTÁLYÁNAK IDEGEN NYELVŰ KÖZLEMÉNYEI

Acta Chimica is a journal for the publication of papers on all aspects of chemistry in English, German, French and Russian.

Acta Chimica is published in 3 volumes per year. Each volume consists of 4 issues of varying size.

Manuscripts should be sent to

Acta Chimica
Budapest, P.O. Box 67, H-1450, Hungary

Correspondence with the editors should be sent to the same address. Manuscripts are not returned to the authors.

Hungarian subscribers should order from Akadémiai Kiadó, 1363 Budapest, P.O. Box 24. Account No. 215 11488.

Orders from other countries are to be sent to "Kultura" Foreign Trading Company (H-1389 Budapest 62, P.O. Box 149. Account No. 218 10990) or its representatives abroad.

Acta Chimica Academiae Scientiarum Hungaricae, Tomus 104 (3), pp. 201—209 (1980)

COPPER(I) COMPLEXES WITH 3-ACETYL- AND 3-PROPIONYLPYRIDINE DERIVATIVES

M. A. S. Goher and A. Attia*

(*Department of Chemistry, Faculty of Science, Alexandria University, Alexandria, Egypt*)

Received May 8, 1978

Accepted for publication August 2, 1979

The copper(I) complexes of 3-acetylpyridine (3-AcP) and 3-propionylpyridine (3-PrP) have been prepared and characterized. Stirring of a mixture of copper(II) halides (chloride and bromide) and 3-propionylpyridine in alcoholic media led to the formation of the corresponding 1 : 1 copper(I) halide complexes of the parent ligand. Those of 3-acetylpyridine of the formula $(3\text{-AcP})_n$. CuX, where $n = 1, 2$ for X = Cl, Br, I; $n = 1$, for X = CN and SCN and $n = 2$ or 3 for $X = ClO_4$, have been prepared by reduction of copper(II) salts in aqueous ethanolic media by ascorbic acid in the presence of the ligand, or by direct interaction between the components. The infrared spectra and other physical data are discussed in correlation with the structure of the isolated complexes.

Introduction

Copper(I) complexes with 3-R-pyridine derivatives have been reported [1, 2]. Complexes with copper to ligand ratios of 1 : 1 and 1 : 2 have been isolated when R was a carboxylic or carbomethoxy group. On the other hand, when R was a carboethoxy group complexes of only 1 : 1 stoichiometric ratio have been isolated. In this latter case the steric requirement of the carboethoxy group was considered to be the only factor which prevents the formation of copper(I) halide complexes with ligand contents higher than 1 : 1.

In order to verify the different factors with affect the apparent overall coordination number around copper(I) in its complexes with pyridine derivatives, we tried to prepare those of 3-carbonyl derivatives. Since copper(I) complexes of these latter ligand have not yet been mentioned in the literature, we now reported the synthesis and characterization of those with 3-acetyl- and 3-propionylpyridines.

Experimental

The ligands were GLC purified and the other chemicals were of analytical grade and commercially available.

Magnetic measurements were made by Gouy's method at room temperature. Reflectance, electronic and infrared spectra, conductivity measurements and elemental analyses were done as described previously [1, 2].

---

* Present address: National Research Centre, Dokki, Cairo, Egyp.

Preparation of the complexes

1 : 1 copper(I) complexes of 3-AcP, except with thiocyanate, have been prepared according to the method described previously [1, 2] by addition of ascorbic acid to an aqueous solution of $CuSO_4 \cdot 5\,H_2O$ and the ligand (in a 1 : 1 molar ratio), followed by addition of a solution of KX. The thiocyanate complex was conveniently prepared as follows. After precipitation of the canary yellow 1 : 3 copper(I) perchlorate complex, an aqueous solution of potassium thiocyanate (1 : 1 molar ratio to copper ion) was added dropwise under vigorous stirring until the yellow colour disappeared and a faint yellow precipitate was obtained. The IR spectrum of the isolated powder shows that it is completely free from perchlorate ion.

The 1 : 2 complexes of 3-AcP were prepared by stirring a suspension of copper(I) halides in the smallest amount of water or ethanol with a 4-fold excess of the ligand. The mixture was boiled for several minutes and allowed to cool.

Copper(I) chloride complex of 3-propionylpyridine was prepared by stirring a mixture of the ligand and copper(II) chloride dihydrate in methanol until a pale yellow precipitate was obtained. Stirring for a few minutes produced a yellowish-green precipitate. The 1 : 1 bromide complex was prepared by the addition of KBr to an ethanolic solution of copper(II) nitrate with continuous stirring until complete dissolution, followed by the ligand, until a pale brown powder was obtained.

The complexes were washed with alcohol and dried, except tris(3-AcP)copper(I) perchlorate which was filtered off, washed and dried in vacuum.

Results and Discussion

While 3-AcP did not affect copper(II) ion in aqueous or alcoholic media and the formation of its copper(I) complexes required the addition of ascorbic acid as a reducing agent, stirring of a 3-PrP–copper(II) halide mixture in alcoholic medium led to the isolation of pale yellow or pale brown copper(I) halide complexes. Their elemental analysis (Table I) reveals a CuX to PrP ratio of 1 : 1. These complexes are diamagnetic and do not show the d–d transitions characteristic of copper(II) ion. Thus copper(II) is reduced in alcoholic media in the presence of 3-PrP. In aqueous solution no reduction took place. When we tried to reduce copper(II) ion in the presence of 3-PrP in aqueous or aqueous–ethanolic media by ascorbic acid, we obtained only a milky solution possibly because of the immediate dissociation of the complex in water. When the reduction by ascorbic acid was carried out in ethanol, a yellow resinous material solidifying after several minutes was formed.

It has been found [3] that 1-methylpyrimidine-2-thione reduces copper(II) to a dark red cluster compound with a parent ligand to copper(I) perchlorate ratio of 3 : 2. On the other hand, 1,4,6-trimethylpyrimidine-2-thione did not reduce copper(II) ion [4]. Similarly, while thiosemicarbazide produced copper (II) complexes with no sign of copper(II) reduction, thiosemicarbazones reduced copper(II) and only copper(I) chelates of the parent ligands isolated [5, 6]. It was pointed out [7] that the reduction of copper(II) with aldehyde or ketone thiosemicarbazones depends upon the nature of the substituent group of the thiosemicarbazone as well as the copper(II) salt used. For these latter reactions, the reduction of copper(II) has been assumed to proceed through the formation of an intermediate copper (II) chelate of the parent ligand. The cationic

Table I

Analytical data

Formula	Colour and appearance	Analysis: % found/required				
		Cu	X	C	H	N
(3-AcP)CuCl	yellow	28.63	16.01	38.36	3.14	6.25
	needles	28.85	16.13	38.15	3.20	6.36
(3-AcP)CuBr	yellow	23.85	30.01	31.69	2.50	5.22
	needles	24.01	30.21	31.78	2.60	5.20
(3-AcP)CuI	yellow	20.23	40.17	27.17	2.30	4.52
	powder	20.33	40.73	26.98	2.26	4.48
(3-AcP)CuCN	pale yellow	30.25		45.26	3.42	13.40
	powder	30.15		45.62	3.34	13.30
(3-AcP)CuSCN	yellow	26.05		39.72	2.97	11.48
	powder	26.18		39.60	2.90	11.54
(3-AcP)$_2$CuCl	orange-red	18.89	10.52	49.45	4.00	8.20
	needles	18.62	10.39	49.27	4.13	8.20
(3-AcP)$_2$CuBr	orange-red	16.62	20.34	43.32	3.73	7.10
	needles	16.47	20.72	43.60	3.65	7.25
(3-AcP)$_2$CuI	orange	14.78	29.74	38.50	3.34	6.31
	powder	14.68	29.33	38.85	3.37	6.47
(3-AcP)$_2$CuClO$_4$	white microcryst.	15.42		41.87	3.37	7.01
	powder	15.68		41.50	3.48	6.91
(3-AcP)$_3$CuClO$_4$	canary yellow	12.23		47.50	4.01	7.92
	cryst. powder	12.07		47.92	4.02	8.12
(3-PrP)CuCl	pale yellow	27.43	15.02	41.43	3.99	5.73
	cryst. powder	27.22	15.20	41.04	3.88	5.89
(3-PrP)CuBr	pale brown	23.00	28.81	34.60	3.35	4.87
	powder	22.81	28.69	34.49	3.25	5.02

chelates undergo electron transfer giving rise to a free radical cation. The abstraction of a hydrogen atom by the generated cationic radical from the solvent molecule finally gives the copper(I) compounds [6, 7].

Thin layer chromatographic investigations of the reaction mixture of copper(II) chloride and 3-PrP after filtration of the yellow product, did not reveal the presence of any material other than the parent ligand. Thus the reduction of copper(II) in the presence of 3-PrP may take place through an intermediate, or 3-PrP may lower the potential of the Cu(II)/Cu(I) couple, that the alcohol reduces its copper(II) complex. However, a thorough investigation of this reaction and similar reactions is in progress.

Since the steric requirements of the $-COOCH_3$ and $-COCH_3$ groups in the β-position of the pyridine ring are more or less identical, 3-AcP forms 1 : 1 and 1 : 2 copper(I) halide complexes similar to those of methyl nicotinate [2]. 3-PrP, on the other hand, forms only 1 : 1 copper(I) halide complexes similarly to ethyl nicotinate [1].

The isolated complexes are stable in air when well-dried, except tris (3-AcP)copper(I) perchlorate. The 1 : 2 complexes transform to 1 : 1 complexes when left in normal atmosphere for several days. In solvents like alcohols, acetone, *etc.*, they are either insolube or dissociate (when very dilute) to 1 : 1 complexes or simple copper(I) salts and the ligand. Similarly to copper(I) complexes of other ligands [8, 9], their stability against air oxidation increases from chloride to iodide.

All the isolated complexes are diamagnetic at room temperature. They are coloured, except the *bis*(3-AcP) copper(I) perchlorate complex.

As seen from Table II, the copper(I) perchlorate compounds of 3-AcP behave as uni-univalent electrolytes in nitrobenzene [10] and acetone [11]. On the other hand, the copper(I) halide complexes gave non-conducting solutions in these solvents. In acetone, however, the measured conductivity values are very small compared to those of 1 : 1 electrolytes [11].

(i) *Electronic spectra*

Table II summarizes the reflectance spectral data. In the UV region of the spectra of solutions of the free ligands, their complexes as well as in the spectra of the solid samples, an absorption band is observed around 270—280 nm. This band is attributed to transitions due solely to the ligands [12].

Intense absorption bands are observed in the visible spectral region of the reflectance spectra of copper(I)–3-AcP complexes, except the 1 : 2 copper(I) perchlorate compound. These bands are assigned as M → L charge transfer transitions from the completely filled d^{10} orbitals of the copper(I) ion to an empty π^*-orbital on the ligands. Similar M → L bands are observed in the visible spectra of complexes between copper(I) and similar ligands [13, 14].

The electron attracting power of the acetyl group causes the electron density to migrate from the delocalized system on the pyridine ring to the substituent and thus lowers the electron density on the nitrogen atom. Therefore, increasing the number of ligands per copper(I) ion in the complex molecule enhances the reduction. *i.e.* its tendency to accept electrons, of the acceptor part in the complex molecule, and hence the M → L charge transfer bands shift to lower energies as the number of ligands increase [15], as seen from Table II.

Copper(I) halide complexes dissociate below 10^{-3} *M* concentration in solvents like alcohol, chloroform, *etc.*, to the free ligand and complexes of lower

Table II

Reflectance spectra and conductivities[a]

Compound	$\pi-\pi^*$	$M \rightarrow L$	Molar conductivity[b] Ω^{-1} cm^2 mol^{-1}	
			NB	A
3-AcP	270[c]			
(3-AcP)CuCl	270	410	insoluble	insoluble
(3-AcP)CuBr	270—280	410	insoluble	insoluble
(3-AcP)CuI	270—280	410	insoluble	insoluble
(3-AcP)CuCN	280	410	insoluble	insoluble
(3-AcP)CuSCN	270	410	insoluble	insoluble
(3-AcP)$_2$CuCl	280	460—470	2.6	23
(3-AcP)$_2$CuBr	270	460—470	1.7	yellow ppte[d]
(3-AcP)$_2$CuI	270	440	turbid	yellow ppte[d]
(3-AcP)$_2$CuClO$_4$	270		30.5	133.0
(3-AcP)$_3$CuClO$_4$	270	420	28.5	137.0
3-PrP	270[c]			
(3-PrP)	275	410	insoluble	insoluble

[a] λ is given in nm; [b] the conductivities given are based on the formula weights; [c] from the electronic spectra of 10^{-4} M solutions in chloroform; [d] the filtrate solutions are conducting, NB = nitrobenzene, A = acetone

ligand contents or simple copper(I) salts. This dissociation was indicated by the change of the intense red colour of 10^{-2}—10^{-3} M solutions of the 1 : 2 chloride complex to a faint yellow upon dilution; the spectra did not show the M → L charge transfer bands which were observed in the reflectance spectra of solid samples.

(ii) *Infrared spectra*

Tables III and IV summarize the infrared spectral data of the ligands and their copper(I) complexes. The assignments of the bands are given according to earlier works [16, 17] or by comparison with other 3-substituted pyridines [18, 19]. Table V contains the vibrational frequencies of the cyanide, thiocyanate and perchlorate anions which are diagnostic of their bonding modes.

Examination of Tables III and IV shows that the carbonyl stretching vibration frequencies are not influenced by complexation of either ligand. 3-AcP and 3-PrP therefore do not coordinate *via* the carbonyl groups.

Table III

IR spectra of free and coordinated 3-acetylpyridine (3-AcP)

3-AcP	1 : 1 iodide	1 : 1 cyanide	1 : 2 chloride	1 : 3 perchlorate	Assignments
1700 vs	1705 vs	1700 vs	1700 vs	1705 vs	νC=O st.
1590 vs	1600 s	1605 s	1605 s	1600 m	ν8a, ν(C–C)
1575 m	1580 w		1575 sh	1580 w	ν8b, ν(C–C)
1490 m	1500 w	1500 w	1500 w	1500 w	
1480 m	1475 m	1480 m	1480 m	1480 m	ν19a, ν(C–C, C–N)
1430 vs	1440 s	1440 s	1440 s	1435 m	ν19b, ν(C–C, C–N)
1370 s	1380 m	1380 m	1380 m	1380 m	CH_3
1320 wm	1325 m	1320 m	1320 m	1320 m	ν14, ν(C–C, C–N)
1280 vs	1280 w	1280 w	1280 w	1280 m	
1255 m	1265 s	1260 s	1260 s	1260 s	νCCO
	1245 m	1245 m	1245 m	1240 m	
1190 m	1200 m	1195 m	1200 m	1200 m	ν9a, β(C–H)
1110 m	1120 m	1110 m	1115 m	(++)	ν18a, β(C–H)
1095 m	1100 m	1095 m	1100 m	(++)	ν3, β(C–H)
1030 sh	1040 ms	1040 ms	1040 m	1040 m	ν1, ring, β(C–H)
1010 s	1020 m	1020 m	1030 m	1025 m	ν12, ring
			1020		
960 vs	960 vs	955 s	970 s	965 s	ν5, γ(C–H)
930 sh	940 w	940 w	940 w	940 w	
820 vs	810 vs	810 vs	815 vs	815 vs	ν10b, γ(C–H)
750 m	750 m	750 m	750 m	750 m	
700 vs	700 vs	695 vs	700 vs	700 vs	ν4, Φ(CC)
640 wm	660 w	655 m	655 w	660 m	ν6b, α(CCC)
580 w	595 m	595 ms	595 m	595 m	ν16a, R-sens.
470 w	480 w	480 w	480 w	480 w	ν6a, ring
	418 w	420 w	420 w	420 w	ν11, Φ(CC)

v = very, w = weak, m = medium, s = strong, sh = shoulder, st. = stretching, R-sens. = substituent sensitive, (++) masked by perchlorate absorption

Comparison of the vibrational frequencies of the free ligands with those of the coordinated ones show marked changes upon complexation. Major blue shifts are observed for the bands attributed to ring C—C, C—N stretching vibrations, ring C—H in-plane, and out-of-plane and ring breathing vibration frequencies. Similar blue shifts are observed for coordinated pyridine [20] and other pyridine derivatives [21]; a result which is indicative of the coordination

Table IV

IR spectra of free and coordinated 3-propionylpyridine (3-PrP)

3-PrP	(3-PrP)CuCl	(3-PrP)CuBr	Assignments
1700 vs, sp	1705 vs, sp	1705 vs	νC=O st.
1575 m	1595 m	1590 m	ν8a, ν(C—C)
	1575 wm	1575 wm	ν8b, ν(C—C)
1450 s	1465 m	1465 m	ν19a, ν(C—C, C—N)
1410 ms	1420 s	1420 vs	ν19b, ν(C—C, C—N)
1380 sh	1380 w	1380 w	νCH_3
1350 m	1350 m	1350 ms	
1310 s	1320 m	1315 wm	ν14, ν(C—C, C—N)
1270 s	1280 vs	1275 s	νCCO
1220 wm	1230 w	1225 w	ν9a, β(C—H)
1170 s	1180 m	1180 ms	ν18a, β(C—H), β(C—R)
1150 m	1150 w	1150 sh	
1095 s	1115 m	1120 m	ν3, β(C—H)
	1090 ms	1090 m	
1070 s	1080 w	1080 w	ν18b, β(C—H)
1020 sh	1045 m	1045 m	ν1, ring
1010 s	1020 w	1020 m	ν12, ring
950 wm	955 m	955 m	ν5, γ(C—H)
835 wm	845 w	840 w	ν10b, γ(C—H)
790 ms	790 m	790 m	
730 vs	730 vs	730 s	
700 vs	690 vs	690 vs	ν4, Φ(CC)
625 m, b	650 wm	645 m, b	ν6b, α(CCC)
510 m	560 m, b	525 m, b	ν6a, ring, R-sens.
	410 w	405 w	ν16a, ring

See Table III.

of both ligands *via* the nitrogen atoms. This conclusion is confirmed by the blue shifts of the ring deformation frequencies below 700 cm^{-1}, which are the most influenced frequencies upon coordination through the nitrogen atom of the pyridine ring [22].

Examination of Table V shows that *tris*(3-AcP)copper(I) perchlorate is ionic [23], and hence a trigonal geometry may be assigned for the cation $[(3\text{-AcP})_3\text{Cu}]^+$. X-ray crystallographic analysis [24] has revealed the existence of a similar structure for the *tris*(3-picoline)copper(I) perchlorate complex.

Table V

Vibration frequencies (cm^{-1}) of the cyanide,thiocyanate and perchlorate groups in complexes

Complex	ClO_4			νCN	δSCN
	ν1	ν3	ν4		
(3-AcP)CuCN				2138 vs	
(3-AcP)CuSCN				2135 vs, 2090 m	455, 435
$(3\text{-AcP})_3CuClO_4$	930 w	1110 s	525 m		
$(3\text{-AcP})_2CuClO_4$	930 w	1125 vs	625 s		
		1090 s	620 s		
		1060 m	615 m		

For the *bis*(3-AcP)copper(I) perchlorate splitting of the ν_3 and ν_4 modes of the perchlorate group is consistent with bidentate perchlorate groups [23]. The formally dicoordinated complex may thus be formulated as $[(3\text{-AcP})_2CuClO_4]$ in which copper(I) is tetrahedrally coordinated.

Table V also shows that the 1 : 1 copper(I) cyanide complex of 3-AcP has only one cyanide stretching frequency around 2140 cm^{-1}. As has been indicated previously [25], the appearance of only one cyanide stretching band above 2100 cm^{-1} in the case of copper(I) complexes indicates a bridging cyanide group for this complex. A bridging thiocyanate group is also proposed for the 1 : 1 copper(I) thiocyanate complex of 3-AcP due to the appearance of two cyanide stretching bands below and above 2100 cm^{-1}, and two other bands below 450 cm^{-1} in the region of the δ SCN bending vibration frequency [26].

The terminal copper-chloride stretching vibration bands given in the literature for copper(I) complexes are observed above 200 cm^{-1} [27—30]. Since no bands above 200 cm^{-1}, to be attributed to copper(I)-chloride stretching frequencies, are observed in the spectra of the 1 : 1 and 1 : 2 copper(I) chloride complexes, one may assign bridging halogen atoms for these complexes. For the 1 : 2 halide complexes, it is more reasonable to propose a tetrahedral geometry around the copper(I) ion through the bridging halogen in the dimer $[(3\text{-AcP})CuX]_2$.

Very recently, the structure of the pyridine-copper(I) iodide adduct was studied by means of X-ray crystallography [31]. In this 1 : 1 adduct the asymmetric unit is $Cu_4I_4Py_4$, based on the well-known tetrahedral tetrameric Cu_4I_4. Since no bands above 200 cm^{-1} could be attributed to the copper(I)-chloride complex of 3-AcP, it is most probable to propose a structure similar to that of the copper(I) iodide–pyridine adduct, in which copper(I) ion is tetrahedrally coordinated.

REFERENCES

[1] Goher, M. A. S., Dratovsky, M.: Coll. Czech. Chem. Commun., **40**, 26 (1975)
[2] Goher, M. A. S.: Coll. Czech. Chem. Commun., **42**, 2080 (1977)
[3] Goodgame, D. M. L., Leach, G. A., Skapski, A. C., Woode, K. E.: Inorg. Chim. Acta, **31**, 1375 (1978)
[4] Goodgame, D. M. L., Leach, G. A.: Inorg. Chim. Acta, **25**, 1127 (1977)
[5] Campbpell, M. J., Grzeskawaik, R.: J. Chem. Soc. (A), **1967**, 496
[6] Gingras, B. A., Hornal, R. W., Bayley, C. H.: Can. J. Chem., **38**, 712 (1960); Gingras B. A., Somorjai, R. L., Bayley, C. H.: Can. J. Chem., **39**, 973 (1961); *ibid.*, **42**, 17 (1964)
[7] Iskander, M. F., El-Sayed, K., El-Toukhy, A.: J. Inorg. Nucl. Chem. (in press)
[8] Marsich, N., Camus, A., Cebules, E.: J. Inorg. Nucl. Chem., **34**, 933 (1972)
[9] Goher, M. A. S.: Can. J. Chem., **53**, 2657 (1975)
[10] Ainscough, E. W., Plowman, R. A.: Austral. J. Chem., **23**, 699 (1970)
[11] Fergusson, J. E., Hickford, J.: Austral, J. Chem., **23**, 543 (1970)
[12] Tong, M., Brewer, D. G.: Can. J. Chem., **49**, 102 (1961)
[13] Lever, A. B. P.: Inorganic Electronic Spectroscopy, p. 299, Elsevier, Amsterdam 1968
[14] Goher, M. A. S., Dratovsky, M.: J. Inorg. Nucl. Chem., **38**, 1269 (1976)
[15] Williams, R. J. P.: J. Chem. Soc., **1955**, 137
[16] Katritzky, A. R., Hands, A. R., Jones, R. A.: J. Chem. Soc., **1958**, 3165
[17] Katritzky, A. R., Hands, A. R., Beard, J. A. T., Dearnaley, D. P., Earl, N. S.: J. Chem. Soc., **1958**, 2182
[18] Katritzky, A. R.: Quart. Rev. Chem. Soc., **13**, 353 (1959)
[19] Green, J. H. S., Kynaston, W., Paisley, H. M.: Spectrochim. Acta **19**, 549 (1963)
[20] Gill, N. S., Kingdon, H. J.: Austral. J. Chem., **19**, 2197 (1966)
[21] Clark, R. J. H., Williams, H. J.: Inorg. Chem., **4**, 350 (1965)
[22] Gill, N. S., Nuttall, R. H., Scaife, D. E., Sharp, R. W. A.: J. Inorg. Nucl. Chem., **18**, 79 (1961)
[23] Nakamoto, K.: Infrared Spectra of Inorganic and Coordination Compounds, p. 170. Wiley, London 1970 and references therein
[24] Lewin, A. H., Michl, R. J., Ganis, P., Lepore, U.: Chem. Commun., **1972** 661
[25] Goher, M. A. S., Dratovsky, M.: Coll. Czech. Chem. Commun., **41**, 3213 (1976)
[26] Goher, M. A. S.: Coll. Czech. Chem. Commun., **42**, 1478 (1977)
[27] Baldwin, P. D. A., Lever, A. B. P., Parish, R. V.: Inorg. Chem., **8**, 107 (1976)
[28] Petillon, F., Guinchais J. E.: J. Chem. Soc., **1973**, 1209
[29] Goher, M. A. S.: Naturwissenschaften, **62**, 237 (1975)
[30] Goher, M. A. S., Dratovsky, M.: J. Inorg. Nucl. Chem. (in press)
[31] Raston, C. L., White, A. H.: J. Chem. Soc., **1976**, 2153

Mohamed A. S. Goher
Abdel-Hamid Attia
Chemistry Department, Faculty of Science,
Alexandria University, Alexandria, Egypt

Acta Chimica Academiae Scientiarum Hungaricae, Tomus 104 (3), pp. 211—221 (1980)

DETERMINATION OF THE OXYGEN INDEX OF NON-STOICHIOMETRIC TUNGSTEN OXIDES AND COMPOUNDS OF BRONZE TYPE

B. A. Kiss and F. Tisza

(*United Incandescent Lamp and Electric Corporation, Research Institute, Budapest*)

Received April 27, 1979

Accepted for publication August 2, 1979

The value of y for non-stoichiometric tungsten compounds described by the formulas WO_{3-y} and $(M_2O)_{x/2} \cdot WO_{3-y} \cdot z(H_2O)$, *i.e.* The O/W ratio depending on the measure of reduction is known in most cases only with uncertainty or not at all. Therefore, a method was developed for the determination of the oxygen index.

The principle of the method is the dissolution of the reduced tungsten oxide or polytungstate in $K_3[Fe(CN)_6]$ — KOH mixture and the permanganometric titration of the hexacyano ferrate (II) ions formed in the oxidation-reduction reaction. For the calibration of the analytical procedure and for the determination of the error of the method, WO_2 has been used as standard substance. Results can be given at a confidence level of 99.7% in the form of O/W = measured oxygen index ± 0.00169, thus *e.g.* in the case of WO_2 O/W $= 1.99_9 \pm 0.00169$ has been obtained.

The oxygen indexes of the non-stoichiometric tungsten compounds formed in the reduction of ammonium paratungstate have been determined by the method and conclusions were drawn from the data on some characteristics of the reduction process.

Introduction

In the reduction of WO_3 or $WO_3 \cdot H_2O$ in H_2 stream, several intermediates as *e.g.* $W_{20}O_{58}$, $W_{18}O_{49}$ and WO_2 are formed prior to the formation of tungsten powder. In a certain period of the reduction preceding the formation of α-tungsten, β-tungsten is also formed in the system, which, as is well known, is not actually a pure metal, but tungsten oxide of low oxygen content, *e.g.* W_3O [1] or $W_{20}O$ [2]. On interrupting the reaction at an arbitrarily selected temperature of the laboratory or technological reduction process, systems of rather complicated phase composition are met. Crystallographically pure phases are found only as exception, mostly mixed phases of different oxides are present. Neither does usually the composition of the β- and γ-phases correspond to the ideal formulas $W_{20}O_{58}$ and $W_{18}O_{49}$, as the crystal structure corresponding to them can be realized within wider limits of composition [1]. It can be seen already from this brief discussion that the prevailing reduction state between WO_3 and W, *i.e.* the information obtained by the determination of the O/W ratio of the intermediates, is an important characteristic of the process.

The situation is still more complicated in the partial reduction of ammonium paratungstate $[(NH_4)_{10}(W_{12}O_{40}/OH/_2) \cdot 4\ H_2O]$ in $H_2 + N_2$ mixtures, because the products formed in the initial stage of the process (the so-called blue oxides) cannot be considered either in the chemical or in the crystallographical sense as oxides, but as a mixture of changing ratio of polytungstates reduced to different extents, of ammonium and hydrogen tungsten bronzes and of the oxide species $W_{20}O_{58}$ [3].

It should be mentioned that according to the classical concept, bronzes in the case of tungsten can be characterized by the formula M_xWO_3, where according to Dickens and Whittigham [4], the quantity of electropositive metal atom can change within the limits $0 < X < 1$.

However, as the phase conditions of the NH_4—W—O system are still unknown, the exact formulas of the reduced ammonium tungstates cannot be given, because in addition to the simultaneous presence of NH_4^+ and H^+ ions [3] the compounds may contain bound water molecules [5] and probably also structural OH groups. We think that the general composition of this group of compounds is best approximated by the formula $(M_2O)_{x/2} \cdot WO_{3-y} \cdot z(H_2O)$, where M is NH_4^+ and/or H^+ ions. If $y<x/2$, the compound can be considered as a reduced polytungstate, if $y=x/2$, then as a bronze, while if $y>x/2$, as an oxide containing impurity. As a knowledge of the value of y is one of the preconditions of a more intensive study of this group of compounds, the filling of this gap in the literature motivated the development of our method.

Experimental

a) Principle of determination

Oxide of polytungstate reduced to an unknown extent is dissolved in a $K_3[Fe(CN)_6]$ — KOH mixture of suitable concentration and the quantity of hexacyanoferrate (II) ions formed in the oxidation-reduction reaction is measured. Provisions must be made in the determination that both oxidant and KOH shall be present in an adequate excess for the conversion of the reduced tungsten compound into K_2WO_4.

b) *Procedure*

The air-dry tungsten compound placed into a weighing bottle is washed with 2.0×10^{-5} m^3 distilled water into a titration flask of 1.0×10^{-4} m^3, then 1.0×10^{-5} m^3 $K_3[Fe(CN_6)]$ solution of 2.5×10^2 $molm^{-3}$ concentration and 1.0×10^{-5} m^3 of 10% KOH solution are added. Under stirring, the substance is quantitatively dissolved in 15—20 min at room temperature.

Next, to avoid the precipitation of tungstic acid, 1.0×10^{-5} m^3 concentrated phosphoric acid, then 4.0×10^{-6} m^3 of 5×10^3 $molm^{-3}$ sulfuric acid are added to the mixture. The solution warmed up by neutralization is cooled to room temperature and the quantity of hexacyanoferrate(II) ions in the solution is titrated without delay with a 50 $molm^{-3}$ $KMnO_4$ solution.

Depending on the oxygen index to be expected, the weight of the sample will be selected as follows:

y	Weight of sample (g)	Nature of the substance
0 —0.1	0.5	Bronzes and reduced polytungstates,
0.1—0.4	0.4	$W_{20}O_{58}$, $W_{18}O_{49}$ and closely similar compositions,
0.4—1.0	0.1	WO_2 and closely similar compositions,
1.0—3.0	<0.1	Average compositions between WO_2 and W.

For the determination of the WO_3 content of the sample to be tested, one part of the substance is heated at 700 °C in air for 30 min to convert it into WO_3.

The formula used for the calculation of the oxygen index is:

$$O_{(I)} = O/W = 3 - \frac{A \cdot f \cdot 4 \times 10^{-4} \cdot M_{(WO_3)}}{M_{(Ox.)} \cdot m_{(WO_3)}} \tag{1}$$

where:

A is the volume of the $KMnO_4$ solution consumed (in 10^{-6} m^3),
f is the titer of the titrating solution,
$M_{(WO_3)}$ is the molecular weight of WO_3,
$M_{(Ox.)}$ is the atomic weight of oxygen and
$m_{(WO_3)}$ is the weight (in g) of WO_3 equivalent to the sample weighed in for titration.

With the process described various reduced tungsten compounds have been analyzed, thus β-and δ-tungsten oxides and a product called "blue oxide". The first two proved to be $W_{20}O_{58}$ and WO_2 of X-ray purity. Moreover "blue oxide" samples have been investigated, the oxygen index of which has been determined already earlier by other methods.

Results

a) *Tungsten dioxide* ($y = 1$)

Since in the series of reduced tungsten oxides the only oxide species stable with respect to both composition and structure is WO_2, this is the most suitable substance for the calibration of our method. Naturally, metallic tungsten proper ($y = 3$) could also be used for this purpose, but as the method has a practical importance mainly in the range of $y = 0 - 1$, it is more suitable to choose WO_2 as the standard substance. The WO_2 used proved, also on the basis of gravimetric determination discussed later in conjunction with Eqs (2) and (3), to have the theoretical composition ($O/W = 2.000$), which supported its selection as reference substance.

Analytical results obtained by the method described are shown in Table I which illustrates that the oxygen index can be determined with a very high accuracy by this method. This is proved also by the error calculations in Table II, from which it can be seen that the oxygen index measured differs from the true value only in the third decimal.

b) *β-Tungsten oxide* ($y \sim 0.1$)

Analysis results obtained for β-tungsten samples of exactly 0.400 g are contained in Table III. The error is also in this case within the limits given in Table II, the standard deviation of the oxygen index actually being $\delta\% = \pm 0.011$. The low standard deviation in the range of $y \sim 0.1$ values proves also the reliability of the method.

Though in the present case the exact oxygen index of our β-tungsten oxide is not known, so that there is no possibility for the characterization of the deviation of the measured and true values, the reality of the oxygen obtained is supported by the fact that it falls within the composition limits valid for

Table I

Analytical results obtained for the oxygen index of WO_2

Ser. No.	Weight of sample (g)	Consumption of titrating solution (cm^3)	Actual consumption (cm^3)	O/W
0	—	0.28	(blank)	—
1.	0.100	16.99	16.71	2.0011
2.	0.100	17.04	16.76	1.9981
3.	0.100	17.08	16.80	1.9957
4.	0.100	16.99	16.71	2.0011
5.	0.100	17.02	16.74	1.9993
6.	0.100	17.01	16.73	1.9999
7.	0.100	17.01	16.73	1.9999
8.	0.100	17.00	16.72	2.0005
9.	0.1024	17.46	17.18	1.9970
10.	0.0932	15.89	15.61	1.9988
11.	0.0871	14.87	14.59	2.0000
				1.99_{92}

Titer: 1.1074, $m_{(WO_3)} = 0.10741$ (from 1—8)

Table II

Error calculations relevant to WO_2

Type of error	Formula	Result
Standard deviation of the oxygen index	$\delta = \pm \sqrt{\dfrac{\sum\limits_{n=1}^{n} (\bar{x} - x_n)^2}{(n-1)}}$	± 0.00187
Variation coefficient	$\delta\% = \pm \dfrac{\delta \cdot 100}{\bar{x}}$	± 0.0935
Standard error of the mean	$\delta_k = \pm \dfrac{\delta}{\sqrt{N}}$	$\pm 5.638 \cdot 10^{-4}$
% relative deviation of the mean	$\delta_k\% = \pm \dfrac{\delta_k \cdot 100}{\bar{x}}$	± 0.0282
Characterization of the deviation of true and measured values	$K = \dfrac{2.00 - \bar{x}}{\delta} \sqrt{N}$	$1.48 < 1.96$
Result at 99.7% confidence level	$\bar{x} \pm \dfrac{3.0 \cdot \delta}{N}$	$1.99_9 \pm 0.00169$

Table III

Measured oxygen index of β-tungsten oxide ($W_{28}O_{58}$)

No.	Corrected consumption of titrating solution (cm^3)	O/W
1.	5.50	2.9118
2.	5.47	2.9124
3.	5.46	2.9125
4.	5.51	2.9117
5.	5.47	2.9124
6.	5.45	2.9127
7.	5.45	2.9127
8.	5.45	2.9127
9.	5.46	2.9125
10.	5.47	2.9124
11.	5.46	2.9125
		2.91_{23}

Titer: 1.108, $m_{(WO_3)} = 0.40204$
Weight of sample: 0.400 g

Table IV

Measured oxygen index of a reduced polytungstate ("blue oxide")

No.	Corrected consumption of titrating solution (cm^3)	O/W
1.	5.07	2.9373
2.	5.08	2.9372
3.	5.13	2.9366
4.	5.00	2.9382
5.	5.04	2.9377
6.	5.05	2.9376
7.	5.07	2.9373
8.	5.00	2.9382
9.	4.98	2.9384
10.	5.01	2.9380
		2.93_{76}

Titer: 1.065, $m_{(WO_3)} = 0.4995_2$
Weight of sample: 0.500 g

β-tungsten oxides. As characteristic of the tungsten oxides with oxygen deficiency, the composition of β-tungsten oxide usually never corresponds to the ideal formula $W_{20}O_{58}$ or $WO_{2\cdot90}$, the crystal structure characteristic of β-tungsten oxide being realized between the limits $WO_{2\cdot88}$ to $WO_{2\cdot94}$ [1, 6]. Thus, our method serves for the determination of the true oxygen index within these limits.

c) "*Blue oxide*" $(y < 0.1)$

It can be clearly seen from Table IV that the method desribed yields also in the case of this substance results of the same accuracy as in the preceding cases ($\delta\% = \pm 0.019$).

d) *Results of comparative tests*

Seven "blue oxide" samples were available, the oxygen index of which had been determined earlier [8], by the method of Choain and Marion [7]. The oxygen index of the samples became known to us only after performing our own determinations. The scheme of the said method is the following:

$$\mathrm{WO}_x + (6-2x)\,\mathrm{Ag}^+ \dashrightarrow \mathrm{W}^{6+} + x\mathrm{O}^{2-} + (6-2x)\,\mathrm{Ag}^0$$

↑	↑	↑
in KOH+KCN solution	in the form of $K_3[Ag(SCN)_4](KSCN)$	Silver precipitated is filtered and titrated in HNO_3 with KSCN solution

As can be seen from Table V, the results obtained by the two methods show a better agreement than expected. With the exception of one sample, values deviate only in the third decimal.

Table V

Comparison of the results of the two methods for oxygen index determination

No.	O/W		Deviation
	Choain and Marion	This work	
1.	2.988	2.990	±0.002
2.	2.950	2.954	±0.004
3.	2.911	2.910	±0.001
4.	2.893	2.894	±0.001
5.	2.877	2.881	±0.004
6.	2.835	2.863	±0.028
7.	2.787	2.782	±0.005

Discussion

a) *Fundamental principles of the method*

In the case of reduced oxides the oxygen index is often determined by the oxidation of the sample to WO_3. However, it is evident on the basis of the formula given for bronzes and other reduced polytungstates that *e.g.* in the case of "blue oxides" the change in weight obtained by oxidation into WO_3 cannot be directly correlated to the measure of reduction because the change in weight is the resultant of two opposite processes, namely of the oxygen uptake of the WO_{3-y}-part and of the loss of NH_3 and H_2O. Therefore, another method had to be found for the determination of the oxygen index.

It has been known since a long time that metallic tungsten can be dissolved in strong alkalies in the presence of the oxidizing component potassium ferricyanide [9—13]. The reaction was used first in metallography for the etching of metal surfaces in microscopic investigations [9]. We found later that the dissolution process can have under certain conditions an opposite effect so that the solvent can be made suitable also for the polishing of the metal surface [14—18]. This reaction applied in technology [19] has been further developed into an analytical method.

Under consideration of LATIMER's conception [20], at that time the mechanism of the oxidation reaction has been built up from the following steps [15]:

$$W + 4\,OH^- = WO_2 + 2H_2O + 4\,e^- \tag{a}$$

$$WO_2 + OH^- = 1/2\,W_2O_5 + 1/2\,H_2O + e^- \tag{b}$$

$$1/2\,W_2O_5 + OH^- = WO_3 + 1/2\,H_2O + e^- \tag{c}$$

Electrons remaining in the metal during the oxidation steps are taken up by the hexacyanoferrate(III) ions,

$$6[Fe(CN_6)]^{3-} + 6e^- = 6[Fe(CN)_6]^{4-} \tag{d}$$

while WO_3 formed is dissolved in the excess KOH.

$$WO_3 + 2OH^- = WO_4^{2-} + H_2O \tag{e}$$

Summarizing the reaction steps, the overall reaction is:

$$W + 6[Fe(CN)_6]^{3-} + 8OH^- = WO_4^{2-} + 6[Fe(CN)_6]^{4-} + 4H_2O \tag{f}$$

The oxidation steps had to be modified only in so far as, according to our present knowledge, there is no oxide phase of W_2O_5 composition having a separate crystal structure, so that presumably the steps of the process must be modified to the intermediate states involving the series

$$W \dashrightarrow WO_2 \dashrightarrow W_{18}O_{49} \dashrightarrow W_{20}O_{58} \dashrightarrow WO_3 \tag{g}$$

It seemed obvious to use the reaction for the determination of the composition of phases of unknown reduction state because the general equation of the oxidation–reduction reaction for any of the reduced products is the following:

$$\begin{aligned} WO_{3-y} + 2y[Fe(CN)_6]^{3-} + (2y+2)OH^- &= WO_4^{2-} + \\ + 2y[Fe(CN)_6]^{4-} + (y+1)H_2O & \end{aligned} \tag{h}$$

where y is any number between 0 and 3.

b) *Gravimetric determination of the oxygen index of oxide phases*

In the reduction step in which the solid phase consists only of oxides, it would seem evident to determine the oxygen index by ignition in air according to the following equation:

$$WO_{3-y} + \frac{y}{2}O_2 = WO_3 \tag{2}$$

From two weights the oxygen index can be calculated as follows:

$$O/W = \frac{1}{M_{(Ox.)}}\left[\frac{M_{(WO_3)} \cdot m_1}{m_2} - M_{(W)}\right] \tag{3}$$

where:

$M_{(WO_3)}$ is the molecular weight of WO_3 (231.92),

$M_{(Ox.)}$ is the atomic weight of oxygen,

$M_{(W)}$ is the atomic weight of tungsten (183.92),

m_1 is the weight of the tungsten oxide sample (g),

m_2 is the weight after ignition, measured as WO_3 (g).

This mode of determination naturally presumes that our WO_{3-y} oxide to be determined does not contain any more bound water. However, this does not hold true in the predominant part of the cases and consequently, oxygen indexes calculated in this way are not reliable. Though determination can be made exact by thermoanalytical recording, this method is time-consuming and thus, less suitable for plant control measurements.

Related to this, by the help of the described method, it is possible to do some interesting and useful calculations. Thus, for example, among others the contribution of the loss of ($NH_3 + H_2O$) and of H_2O to the resulting weight change on ignition and the oxygen uptake of the reduced oxide can be given. The resulting weight change, Δm, can be given by the following equation:

$$\Delta m\% = -m\%_{(NH_3+H_2O)} + m\%_{(WO_{3-y} \to WO_3)} \tag{4}$$

The increase in weight caused by oxidation can be calculated from the relationship

$$+m\% = (3.00 - O_{(I)})\mathrm{Ox.}\ \% \tag{5}$$

and the decrease in weight due to the loss of gases from the relationship

$$-m\% = [100 - (\mathrm{W}\% + \mathrm{Ox.}\ \%)] \tag{6}$$

The expanded equation suitable also for calculation will be of the following form:

$$\Delta m\% = -100\left[1 - \frac{m_2}{m_1}\left(\frac{M_{(W)} + O_{(I)} \cdot M_{(Ox.)}}{M_{(WO_3)}}\right)\right] + \\ + \left[100\,\frac{m_2}{m_1}\left(\frac{3.00 - O_{(I)} \cdot M_{(Ox.)}}{M_{(WO_3)}}\right)\right] \tag{7}$$

where

m_1	is the weighed sample used for titration (g),
m_2	is the WO_3 content corresponding to m_1 (g),
$O_{(I)}$	the oxygen index, O/W,
$M_{(W)}$	the atomic weight of tungsten,
$M_{(Ox.)}$	the atomic weight of oxygen and
$M_{(WO_3)}$	the molecular weight of WO_3.

Analyzing the sample series investigated in an earlier communication [3] and applying relationship (7), the changes in the percentage of Δm, $+m$ and $-m$ are plotted in Fig. 1 as a function of the oxygen index. The samples have been prepared by the reduction of ammonium paratungstate at gradually increasing temperatures in a gas mixture of 4 l H_2 + 30 l N_2/hour [3].

In the resultant change in weight Δm, the increase in weight due to oxidation obviously increases linearly with decreasing oxygen index, as contrary to the decrease in weight caused by the loss of volatile products. It can be seen from Fig. 1 that up to an oxygen index of 2.95 the departure of $NH_3 + H_2O$ gases predominates and the function presents a minimum in this region. From this point the volatile content of the phases increases again and passing through a maximum, approaches $m = 0$. The curves of the figure are consistent with our earlier X-ray and IR spectrophotometric phase analysis results, according

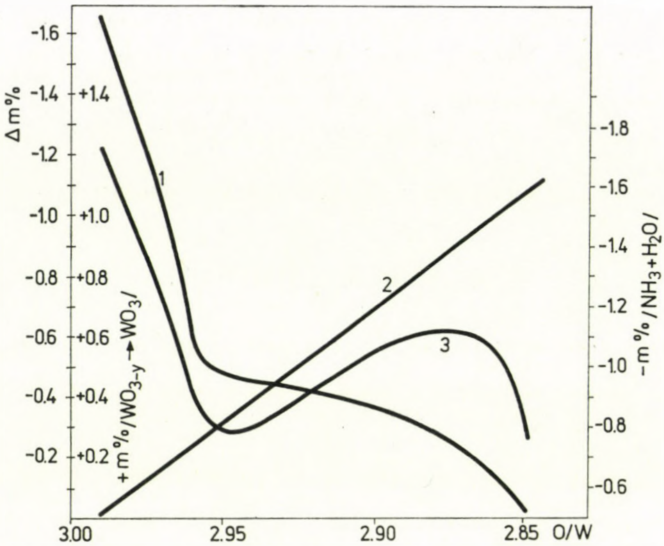

Fig. 1. Loss in weight on ignition of the intermediate phases formed during the reduction of ammonium paratungstate and change of the components of the resultant loss in weight as a function of the oxygen index; 1. $\Delta m\%$, 2. $+m\%$ ($WO_{3-y} \rightarrow WO_3$), 3. $-m\%$ ($NH_3 + H_2O$)

to which, the system consists up to about 2.96 predominantly of ammonium bronze, from 2.96 to 2.91 of hydrogen bronze, and below this value of β- and γ-tungsten oxides. Moreover, it is evident from the figure that in the case of oxide phases, *e.g.* in the cases $O/W < 2.90$, from data available by the determination of the oxygen index, conclusions can be drawn also on the bound volatile content of the oxides utilizing Eq. (7), *i.e.* the chemically and adsorptively bound water content of the oxides can be determined.

c) *Evaluation of the method*

The advantages of our method can be summarized as follows.

1. The method is very simple and at the same time it demands less work than the method of CHOAIN and MARION, and is thus quicker.

2. It furnishes results of high accuracy, so that it can be used in addition to plant control also for the solving of more exacting research tasks.

3. The method can be used up to $y = 0-3$, *i.e.* within the whole reduction range. This is an important advantage over the method of CHOAIN and MARION, because the latter method gives good results only within the limits $y = 0-0.15$, while according to experience, in the case of $y > 0.15$ the sample is not dissolved completely in the KOH—KCN system, whereby the solution will be turbid or will contain a sediment [21].

Finally it should be mentioned that the method described can be used according to our experiments without any modifications also in the case of reduced molybdenum compounds and can be presumably extended to all those non-stoichiometric oxides which are dissolved under oxidation in the $K_3[Fe(CN)_6]$ – KOH system.

We hope that in addition to being useful in practical work, the method described will also help in the research of non-stoichiometric tungsten compounds.

REFERENCES

[1] Rieck, G. D.: Tungsten and its Compounds, p. 94. Pergamon Press, Oxford 1967

[2] Neugebauer, J.: A Magyar Tudományos Akadémia Műszaki Fizikai Kutató Intézetének Közleményei **0–15**, 23 (1974)

[3] Bartha, L., Gyarmathy, Gy., Kiss, B. A., Németh, T., Salamon, A., Szalay, T.: Acta Chim. Acad. Sci. Hung. **101**, 127 (1979)

[4] Dickens, P. G., Whittingham, M. S.: Quart. Rev., **22**, 30 (1968)

[5] Neugebauer, J., Millner, T., Hegedüs, A.: MTA Kém. Tud. Tud. Oszt. Közleményei, **12**, 37 (1959)

[6] Gadó, P.: C. Sc. Dissertation, 1970

[7] Choain, Ch., Marion, I.: Bull. Soc. Chim., **1963**, 212

[8] Samples were prepared and analyzed at the Techn. Phys. Research Institute of the Hung. Acad. Sci.

[9] van Liempt, J. A. M.: Rec. Trav. Chim., **52**, 425 (1923)

[10] Schröter, K.: Z. Metallkunde, **20**, 31 (1928)

[11] Agta, K., Becker-Rose, H., Heyne, G.: Z. Anorg. Chem., **38**, 1121 (1925)

[12] Smithells, I. E.: Metal Reference Book., p. 265. Butten Wonth London 1949

[13] Smithells, I. E.: Tungsten, p. 67. Chapan and Hall Limited London 1945

[14] Neugebauer, J., Kiss, A.: Acta Chim. Acad. Sci. Hung., **44**, 241 (1965)

[15] Kiss, A., Neugebauer, J.: *ibid.*, **44**, 253 (1965)

[16] Kiss, A.: *ibid.*, **45**, 1 (1965)

[17] Kiss, A.: *ibid.*, **45**, 267 (1965)

[18] Kiss, A.: *ibid.*, **48**, 279 (1966)

[19] Neugebauer, J., Kiss, A.: Hung. Pat. 151. 573 (1964)

[20] Latimer, W. M.: The Oxidation State of Elements and their Potentials in Aqueous Solution, p. 264. New York 1952

[21] Salamon, A.: Private communication

András B. Kiss
Ferenc Tisza
H-1044 Budapest, Váci út 77.

Acta Chimica Academiae Scientiarum Hungaricae, Tomus 104 (3), pp. 223—226 (1980)

MEASUREMENT OF ZEOLITE ACIDITY BY ISOTOPE EXCHANGE METHOD

Gy. Kárpáti, I. Kiricsi and P. Fejes

(*Applied Chemistry Department, József Attila University, Szeged*)

Received May 28, 1979

Accepted for publication August 2, 1979

The fast isotope exchange reaction between H^+ and T^+ ions (present in the zeolitic framework and water, respectively) followed by radioactive assay of the water, using liquid scintillation technique can be used for the quantitative determination of acidity in zeolite samples.

After "activation" (heating and evacuation at the respective temperature) between 473 and 723 K the acidity of CaY and REY samples decreased linearly with temperature. Acidity values obtained under different experimental conditions on *similar* zeolitic samples are in good agreement.

Introduction

The nature of acid centres in zeolites, their strength, number and distribution in the zeolite framework are intriguing questions of zeolite research. About the recent advances in this field, a detailed review has been published by Jacobs [1].

Emmett and Haldeman [2] used an isotopic dilution technique for the determination of the number of OH groups in different acid catalysts (*e.g.* silica, aluminium oxide, silica alumina *etc.*). This paper is concerned with the further development of the isotopic dilution method making use of the progress in the field of liquid scintillation counting in the last two decades.

Experimental

For the experiments, binder containing commercial samples of CaY (Lot No. 30—511) and REY (Lot No. 9685—30007) supplied by the Union Carbide Co. have been used (their composition in mass per cent is given in Table I). The cylindrical pellets were crushed and sized. The sieve fraction between 0.8—1.0 mm was separated. Pretreatment was carried out at 473 K for 24 hrs in air.

Table I

Composition of zeolites used

Type of zeolite	Components (m%)				
	SiO_2	Al_2O_3	Na_2O	CaO	La_2O_3
CaY	62.81	23.02	2.45	9.95	—
REY	65.0	22.7	1.6	—	10.7

The specific activity of water labelled with T was 0.2953 TBq mol^{-1}.

The exchange equipment consisted of two communicating cylindrical glass vessels (one for the zeolite sample the other for water) which, if necessary, could be separated from each other by a valve and evacuated either together or separately. In each case 10^{-3} kg zeolite was equilibrated with 1×10^{-7} m^3 THO. The water was degassed by the "freeze and thaw" technique under vacuum and kept frozen in liquid nitrogen until commencing the measurement. The other vessel was evacuated for 3 hrs at the relevant "activation" temperature. At the beginning of the experiment the two evacuated vessels were connected, the water was allowed to melt and at the same time the solid sample was cooled to accelerate condensation. Short periods of repeated cooling and heating were used to attain isotopic equilibrium as soon as possible. Finally, the water (or part of it) was condensed out again.

The isotope exchange between the (OH) groups of the zeolite sample and water consists in the exchange of protium and tritium ions until isotopic equilibrium (*i.e.* equal probability of occurrence of both ions in all exchangeable OH groups) is reached:

$$(OH)_z + TOH \rightleftharpoons (OT)_z + HOH \tag{1}$$

The activity of the initial and the equilibrated water sample has been determined by the TRI-CARB technique, using the liquid scintillation cocktail described by BRAY [3]. The 0.2953 TBq mol^{-1} activity of the water sample was too high, therefore, it had to be reduced by dilution in such a way that after equilibration with the zeolite sample the remaining activity be low enough to produce experimental intensities somewhere between $1\times10^4 - 2\times10^4$ cpm.

If the following symbols are used

n_z (mmol): amount of $(OH)_z$ groups in the zeolite sample;

n_{H_2O} (mmol): the same for water;

A_0 (cpm $mmol^{-1}$): initial intensity of water;

A (cpm $mmol^{-1}$): intensity after equilibration then, using the well known equation of isotopic dilution analysis, the amount of zeolitic $(OH)_z$ groups can be determined from

$$n_z = n_{H_2O}\left(\frac{A_0}{A} - 1\right) \tag{2}$$

Results and Discussion

The results of isotopic equilibration using different reaction times and temperatures are shown in Table II. Isotopic equilibrium is attained within short periods of reaction time, therefore, 30 minutes as the time of equilibration was chosen following this set of experiments.

Table II

Effect of temperature and reaction time on isotope exchange

Reaction time (ks)	Amount of exchanged H+ ions in CaY [mmol H+ g^{-1}]		
	473 K	573 K	673 K
1.8	2.94	2.07	0.84
3.6	2.65	1.9	0.91
5.4	2.95	2.09	0.84
7.2	2.83	1.76	0.85
16.2	2.94	1.88	0.87

The amount of exchangeable H^+ ions in the CaY and REY samples after "activation" at different temperatures is shown in Fig. 1.

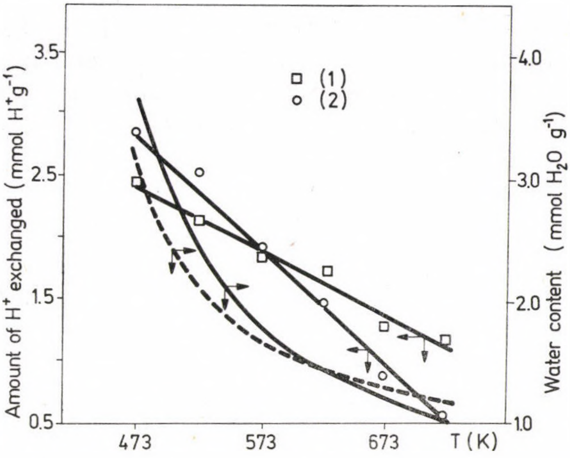

Fig. 1. Amount of exchangeable H^+ ions for CaY (1) and REY (2) zeolites as a function of the activation temperature

Every OH group in the zeolite structure undergoes H—T exchange with tritiated water, although the rate, depending on acid strength, may be different.

The decrease of the number of OH groups upon heat treatment is a consequence of dehydration, which can be traced back to several causes:

— up to about 520—570 K, sorbed water is removed (this is the water interacting with O^{2-} ions of the framework and that present in the hydration sphere of cations);

— above 570 K, the "structural" water is released from the OH groups of the framework and the cations as a direct consequence of increased proton mobility above 500 K.

Figure 1 contains data also about thermogravimetric investigations carried out on the same "activated" samples. (The dashed line refers to the REY sample, the full one to CaY.)

If the water content of the samples after a heat treatment at 1220 K is arbitrarily taken as zero* (the mass of *this* sample be denoted by m_∞) then the difference of the actual mass, $m(T)$, and m_∞, *i.e.* $[m(T) - m_\infty]$ is proportional to the number of OH groups in the structure (provided the activation temperature is high enough: $570\ \mathrm{K} < T < 1220\ \mathrm{K}$). These values can be seen on the ordinate to the right. The order of magnitude is *similar*, though, $\frac{[m(T) - m_\infty]}{18.01} \cdot 2 = M(T)$, corresponding to the stoichiometry

$$(\mathrm{OH})_z \rightarrow \mathrm{O}_z + (\mathrm{H}^+)_z$$

$$(\mathrm{OH})_z + (\mathrm{H}^+)_z \rightarrow \square + \mathrm{H_2O}$$

---

* The marked decrease in the rate of water release around this temperature is due to the very low concentration of OH groups and, consequently of mobile H^+ ions in the structure.

(where □ stands for an anion vacancy in the framework) is unmistakably greater than $n_z(T)$. Now it should not be forgotten that T ***has a different meaning in the two cases***: in the first case T in $n_z(T)$ corresponds to a 3-hour "activation" (including evacuation) at T, while in the last case it is a temperature reached and passed by during a temperature-programmed heating of the sample. Nevertheless, it is interesting to note that the curves $M(T)$ and those for the $(OH)_z$ content cross each other at similar temperatures.

From what has been said before, it follows that after the desorption of "sorbed" water, *i.e.* above *ca.* 550 K, the H—T exchange method measures the amount of acidic $(OH)_z$ groups and that belonging to di- or trivalent cations, therefore, these data can be compared with acidity values obtained by other methods. Such a comparison is shown in Table III using data by OEHME [4] and MOSCOU [5]. According to Table III, the acidity data of the samples are in good agreement regardless of whether they have been determined by NMR spectroscopy, titration or, as in our case, by isotope exchange.

Table III

Comparison of the acidity of CaY and REY samples determined by different methods

Activation temperature (K)	Acidity of CaY (mmol OH g^{-1})		Acidity of REY (mmol OH g^{-1})		
	This work	OEHME [4]	This work	OEHME [4]	MOSCOU [5]
473	2.86	—	2.46	—	2.3
523	2.52	—	2.12	—	—
573	1.94	1.17	1.85	1.65	1.8
623	1.45	—	1.74	—	2.05
673	0.86	0.58	1.28	1.94	1.2
723	0.53	—	1.16	—	—

REFERENCES

[1] JACOBS, P. A.: Carboniogenic Activity of Zeolites, Elsevier, Amsterdam 1977
[2] EMMETT, P. H., HALDEMAN, R. G.: J. Am. Chem. Soc., **78**, 2917(1956)
[3] BRAY, G. A.: Analytical Biochemistry, **1**, 279 (1960)
[4] OEHME, W.: Dissertation, Leipzig, 1973
[5] MOSCOU, L.: Advances in Chemistry Series, **102**, 337 (1971)

György KÁRPÁTI
Imre KIRICSI
Pál FEJES
H-6720 Szeged, Rerrich Béla tér 1.

Acta Chimica Academiae Scientiarum Hungaricae, Tomus 104 (3), pp. 227–233 (1980)

SYNTHESIS OF BRADYKININ LABELLED WITH TRITIUM*

J. Seprődi,[1] I. Teplán,[1+] M. Magócsi[2] and K. Medzihradszky[2]

([1] *First Institute of Biochemistry, Semmelweis University Medical School, Budapest, and*
[2] *Central Research Institute for Chemistry, Hungarian Academy of Sciences, Budapest)*

Received February 23, 1979

Accepted for publication August 7, 1979

A bradykinin analogue containing 4-chlorophenylalanine in position 5 has been synthesized by the classical solution methods of peptide synthesis. Catalytic tritiation of this compound gave the tritium-labelled hormone, with a specific radioactivity of 18 Ci/mmole.

Bradykinin is a polypeptide hormone consisting of nine amino acids with the sequence given in Fig. 1.**

Arg–Pro–Pro–Gly–Phe–Ser–Pro–Phe–Arg

Fig. 1

This peptide is formed in the blood stream from the serum protein bradykininogen by specific enzymic cleavage, thus it belongs to the group called tissue hormones. Its main biological activities are causing the contraction of smooth muscles and dilatation of blood vessels, simultaneously decreasing the blood pressure.

Like other polypeptide hormones, bradykinin exerts its biological effects in extremely small amounts. As low as 0.1 ng/ml concentration is effective *in vitro*, and its 0.1 μg/kg dose effects the pressure of different species *in vivo*. It is obvious that such small amounts cannot be measured quantitatively by simple chemical means, and a meaningful picture of the mechanism of action can only be obtained either by measuring biological activities, or by using hormone derivatives labelled with radioisotopes of high specific activity. As biological effects are strongly influenced by the experimental conditions, labelling, with tritium, seems to be the best approach.

+ To whom correspondence should be addressed.

* This work was presented, without experimental details, at the Gasteiner International Symposium of "Radioactive Isotope in Klinik und Forschung", Bad Gastein, January, 1976.

** Symbols and abbreviations are used according to the rules adapted by the IUPAC IUB Commission on Biochemical Nomenclature, J. Biol. Chem., **247,** 977 (1972). Further abbreviations: Cpa = 4-chloro-L-phenylalanine, NB- = 4-nitrobenzyl-, PCP- = pentachlorophenyl-, Z- = benzyloxycarbonyl-, BOC- = *t*-butyloxycarbonyl-. All amino acid derivatives mentioned in this paper are of the L-configuration.

For the tritiation of polypeptide hormones numerous methods have been elaborated and reported in the last decade. Among them those procedures proved to be the most useful, where peptide derivatives containing such precursor amino acids were synthesized which made the compound suitable for the introduction of tritium atoms in the last step of the synthesis. One of the advantages of this procedure lies in the fact that a sufficient amount of the labelled peptide can be prepared in a simple operation immediately before application, avoiding the danger of autoradiolysis during long storage. An example of the application of 3,5-dibromotyrosine as the precursor amino acid is the synthesis of α-melanotropin labelled with tritium in the tyrosine residue [1, 2].

As bradykinin does not contain tyrosine, another approach had to be elaborated for the labelling. Earlier experiments above shown [3] that 4-chlorophenylalanine can be converted into phenylalanine by catalytic hydrogenation or tritiation without difficulty. By this means a suitable label with high specific radioactivity can be introduced into polypeptides containing a phenylalanine residue, in cases when radioiodination or tritiation *via* the iodinated product is impossible because of the absence of the necessary reactive amino acids.

The steps leading to the synthesis of the precursor hormone are shown in Fig. 2.

α-Benzyloxycarbonyl-nitroarginyl-prolyl-proline pentachlorophenyl ester (peptide 1—3) and prolyl-phenylalanyl-nitroarginine 4-nitrobenzyl ester (peptide 7—9) were synthesized according to Bajusz *et al.* [4], with slight modi-

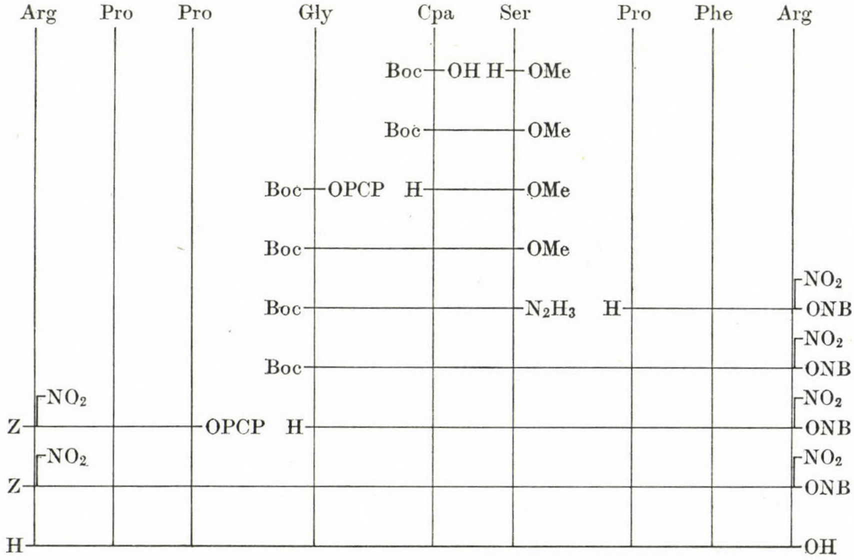

Fig. 2

fications. For the preparation of the *t*-butyloxycarbonyl-glycyl-4-chlorophenylalanyl-serine hydrazide (peptide 4—6) *t*-butyloxycarbonyl-4-chlorophenylalanine was coupled with serine methyl ester by using the dicyclohexylcarbodiimide procedure. Removal of the *N*-terminal protecting group and acylating the resulting dipeptide ester with *t*-butyloxycarbonyl-glycine pentachlorophenyl ester gave the pure, crystalline tripeptide ester. Treatment of this compound with hydrazine hydrate at 50 °C yielded the pure hydrazide.

Coupling between peptides 4—6 and 7—9 was effected without isolating the intermediary azide; the crude hexapeptide ester was purified by chromatography on a silica gel column. Deprotection of this product by trifluoroacetic acid yielded the hexapeptide ester with a free terminal amino group. This compound proved to be pure enough for the last coupling which was accomplished using the pentachlorophenyl ester of the protected *N*-terminal tripeptide in pyridine as solvent. Fractionation on silica gel gave the pure protected nonapeptide ester, which, in turn, was deblocked by treatment with liquid hydrogen fluoride in the presence of anisole. This procedure was used instead of catalytic hydrogenolysis to avoid premature removal of the chlorine substituent from the phenylalanine residue. The deblocking step afforded chromatographically pure Cpa^5-bradykinin hydrogen fluoride, possessing the correct amino acid composition.

Tritiation was performed in an equipment developed earlier [5], in the presence of a large excess of palladium-on-aluminium oxide catalyst saturated with tritium, in water containing triethylamine. Pure tritiated bradykinin with the theoretical amino acid composition was obtained after chromatography on carboxymethyl cellulose, using an ammonium acetate buffer system with increasing pH and molarity. The labelled hormone emerged at about pH 6.5 at a 0.75 molar buffer concentration.

It is worth mentioning that, while the chromatographic properties of the protected intermediates containing 4-chlorophenylalanine were similar to those of compounds derived from unsubstituted phenylalanine, Cpa^5-bradykinin could easily be distinguished from the native hormone both by thin-layer chromatography and paper electrophoresis. On this basis the quantitative transformation of the chloro-substituted compound into the hormone containing the natural sequence could be established.

The specific radioactivity of the product was about 18 Ci/mmole. The biological activity, measured on rat uterus pretreated with Syntestrin corresponded to that of pure synthetic bradykinin. When stored at —20 °C as a lyophilisate for 3 months, the biological activity decreased by about 30%. On storage in methanol solution at —20 °C no change in radiochemical purity could be detected after one year.

Cpa^5-baradykinin has 1% the biological activity of the natural hormone.

Experimental

M.p.'s were determined on a hot-stage Boetius Mikroheiztisch and are uncorrected. R_f values refer to thin-layer chromatograms which were run on Merck-DC Alufolien Kieselgel 60 layer in the following solvent systems (proportions given in volumes):

(1) Acetone–toluene 1 : 1
(2) Ethyl acetate–pyridine–acetic acid–water 240 : 20 : 6 : 11
(3) Ethyl acetate–pyridine–acetic acid–water 120 : 20 : 6 : 11
(4) Ethyl acetate–pyridine–acetic acid–water 60 : 20 : 6 : 11
(5) Ethyl acetate–pyridine–acetic acid–water 30 : 20 : 6 : 11

For the paper electrophoresis Whatman No. 3 paper was used at 1200 V in a 0.1 molar pyridine–acetic acid buffer (pH 5). Radiochromatograms were evaluated by a Berthold Dünnschicht Scanner (Model LB 27) or a Packard Scanner (Model 7201). Radioactivities were determined on a Packard Tri-Carb M 3375 liquid scintillation spectrometer. Amino acid analyses were made, after hydrolysis of the peptide (105 °C, 6*N* hydrochloric acid, 24 h, evacuated tubes), on a JEOL JLC-5, and a Chinoin LYS-75 amino acid analyzer.

t-**Butyloxycarbonyl-4-chlorophenylalanine** (BOC-Cpa-OH)

4-Chlorophenylalanine [3] (21 g; 105 mmoles) was suspended in a 1 : 1 mixture of dioxane–water (420 ml) and freshly prepared BOC azide (28 ml) was added. The solution was made alkaline (pH 10) and stirred for 48 h at room temperature, maintaining the pH at 10 by repeated additions of 2 *N* sodium hydroxide solution. The excess BOC azide was removed by extraction with ether, the aqueous phase acidified at 0 °C to pH 3 with ice-cold 2 *N* hydrochloric acid solution, and extracted four times with 200 ml portions of ethyl acetate. The organic phase was collected, washed with 50 ml water, dried and evaporated. To the remaining oil petroleum ether (100 ml) was added, and the resulting white crystalline substance was, after standing in a refrigerator overnight, filtered off.

The yield was 25.6 g (81%), m.p. 106–108 °C, R_f^3: 0.85, R_f^1: 0.45. To prepare analytically pure compound, 20.0 g of the crude product was dissolved in acetone (60 ml) and, under vigorous stirring, water (200 ml) was added. The separated crystals were collected and dried to obtain 18.1 g of the substance, m.p. of 110–111 °C, $[\alpha]_D^{25} = +14° \pm 1°$ ($c = 1.0$, methanol).

$C_{14}H_{18}O_4NCl$ (299.7). Calcd. C 56.09; H 6.05; N 4.67; Cl 11.83. Found C 55.92; H 6.06; N 4.62; Cl 11.91%.

t-**Butyloxycarbonyl-4-chlorophenylalanyl-serine methyl ester** (BOC-Cpa-Ser-OMe)

BOC-Cpa-OH (2.40 g; 8 mmoles) and serine methyl ester hydrochloride (1.24 g; 8 mmoles) were dissolved in a mixture of tetrahydrofuran (10 ml) and acetonitrile (10 ml). To the chilled (−10 °C) solution 1.11 ml of triethylamine and dicyclohexylcarbodiimide (1.74 g; 8.5 mmoles) were added, and the mixture was stirred at −5 °C for 1 h, at 0° C for 5 h and at room temperature overnight. Dicyclohexylurea was filtered off, the solution evaporated in vacuum, the residue dissolved in ethyl acetate (100 ml) and washed successively with 5% ice-cold citric acid, saturated sodium bicarbonate and saturated sodium chloride solutions, dried and evaporated. The resulting oil was dissolved in 30 ml of warm dioxan; on the addition of a few ml of water a small additional amount of dicyclohexylurea separated. This was removed by filtration and the dipeptide ester was precipitated by the addition of further 100 ml of water, to obtain 2.75 g (86%) of the product, m.p. 144–146 °C, R_f^1: 0.6.

$C_{18}H_{25}O_6N_2Cl$ (400.8). Calcd. C 53.93; H 6.28; N 6.98; Cl 8.85. Found C 53.80; H 6.25; N 7.10; Cl 8.75%.

4-Chlorophenylalanyl-serine methyl ester hydrochloride (H-Cpa-Ser-OMe. HCl)

BOC-Cpa-Ser-OMe (3.50 g; 8.75 mmoles) was dissolved in 4 *N* methanolic hydrochloric acid (40 ml), stirred for 2 h at room temperature, and evaporated in vacuum. The residue was dissolved in methanol, evaporated again and mixed with anhydrous ether, filtered off and dried in desiccator.

Yield 2.70 g (91%), m.p. 202–203 °C, R_f^3: 0.2, R_f^4: 0.5.

$C_{13}H_{18}O_4N_2Cl_2$ (337.2). Calcd. C 46.30; H 5.38; N 8.30; Cl 21.03. Found C 45.90; H 5.40; N 8.25; Cl 20.65%.

t-Butyloxycarbonyl-glycyl-4-chlorophenylalanyl-serine methyl ester (BOC-Gly-Cpa-Ser-OMe)

H-Cpa-Ser-OMe hydrochloride (3.2 g; 9.5 mmoles) was dissolved in dimethylformamide (30 ml) and to the clear solution 4.0 g (9.5 mmoles) of *t*-butyloxycarbonyl-glycine pentachlorophenyl ester was added, followed by the addition of 1.33 ml triethylamine. The mixture was allowed to stand at room temperature overnight, the triethylamine hydrochloride was filtered off and the solution evaporated in vacuum (bath temperature max. 45 °C). The residue was powdered under ether, filtered off and dissolved in 50 ml of warm ethanol. Crystallization started on the addition of 50 ml water, seeding or scratching. The mixture was allowed to stand in a refrigerator overnight, filtered and dried in air.

The yield was 3.5 g (80.3%), m.p. 188—190 °C, R_f^2: 0.85.

$C_{20}H_{28}O_7N_3Cl$ (457.9) Calcd. C 52.46; H 6.16; N 9.17; Cl 5.77 Found C 52.41; H 6.10; N 9.15%.

Amino acid analysis: Ser, 0.98; Gly, 1.0; Cpa, 1.02.

t-Butyloxycabonyl-glycyl-4-chlorophenylalanyl-serine hydrazide (BOC-Gly-Cpa-Ser-N_2H_3)

The protected tripeptide ester (1.20 g; 2.6 mmoles) was dissolved in methanol (50 ml), 98% hydrazine hydrate (15 ml) was added, and the reaction mixture was allowed to proceed at 50 °C for 4 h. After evaporation of the solvent, the residue was dried in vacuum over conc. sulfuric acid for 24 h, and the resulting solid crystallized from 60 ml of hot methanol, to obtain 0.99 g (83%) of the product, m.p. 163—166 °C, R_f^2: 0.25.

$C_{19}H_{28}O_6N_5Cl$ (457.9). Calcd. C 49.84; H 6.16; N 15.29; Cl 7.74. Found C 29.63; H 6.19; N 15.24; Cl 7.69%.

t-Butyloxycarbonyl-glycyl-4-chlorophenylalanyl-seryl-prolyl–phenylalanyl-nitroarginine 4-nitrobenzyl ester [BOC-Gly-Cpa-Ser-Pro-Phe-Arg(NO_2)-ONB]

BOC-Gly-Cpa-Ser-N_2H_3 (458 mg; 1 mmole) was dissolved in dimethylformamide (2.0 ml), the solution chilled to —20 °C, and slowly an ice-cold mixture of dimethylformamide (0.3 ml) and 6 *N* hydrochloric acid (0.36 ml) was added under stirring, followed by the addition of a conc. aqueous solution of sodium nitrite (75.9). After 10 min at —10 °C, a chilled (—10 °C) solution of H-Pro-Phe-Arg(NO_2)-ONB (710 mg; 1.2 mmoles) and triethylamine (0.47 ml) in 2 ml of dimethylformamide was added. Stirring was continued for 1 h, then for 2 h at 0 °C, and the mixture was allowed to stand in a refrigerator overnight. The solvents were evaporated in vacuum (40 °C), the residue was dissolved in 50 ml of ethyl acetate, washed with cold 10% citric acid, saturated sodium bicarbonate and saturated sodium chloride solutions, dried and evaporated. The residue was powdered under ether, filtered off and air-dried. The slightly yellow colored material was dissolved in the minimum amount of Solvent 3, applied onto a silica gel column (20 × 500 mm) and eluted with Solvent 2. The fractions containing the pure product were collected, evaporated in vacuum, the residue was powdered under ether, filtered, washed and dried in air.

The yield was 0.52 g (51%), R_f^2: 0.6, R_f^1: 0.25.

$C_{46}H_{58}O_{14}N_{11}Cl$ (1024.5). Calcd. N 15.04; Cl 3.46. Found N 14.78; Cl. 3.40%.

Amino acid analysis: Ser, 0.95; Cpa, 1.04; Gly, 1.00; Pro, 0.85; Phe, 1.04; Arg, 0.91.

Benzyloxycarbonyl-nitroarginyl-prolyl-proline [Z-Arg(NO_2)-Pro-Pro-OH]

To a cold suspension of 49.4 g (0.1 mole) of benzyloxycarbonylnitroarginine pentachlorophenyl ester and 21.2 g (0.1 mole) of prolyl-proline in dimethylformamide (200 ml) there was added 14.0 ml (0.1 mole) of triethylamine, and the mixture was stirred for 1 h at 0 °C, then at room temperature overnight. The solvent was evaporated in vacuum (bath temperature 45 °C), the remaining oil was dissolved in a mixture of ethyl acetate (200 ml) and water (200 ml), the aqueous phase was washed with ethyl acetate and acidified with 6 *N* hydrochloric acid to pH 2. The oily substance which separated was extracted three times 200 ml portions of chloroform, the combined solutions were washed with 0.1 *N* hydrochloric acid, water, dried and evaporated. The remaining solid was powdered under ether, filtered off and dried over sulfuric acid in a desiccator to obtain 39.4 g (72%) of the product, R_f^3: 0.15.

$C_{24}H_{33}O_8N_7$ (547.6). Calcd. N 17.91. Found N 17.60%.

Benzyloxycarbonyl-nitroarginyl-prolyl-proline pentachlorophenyl ester [Z-Arg(NO_2)-Pro-Pro-OPCP]

Benzyloxycarbonyl-nitroarginyl-prolyl-proline (27.4 g; 50 mmoles) and pentachlorophenol (14.5 g; 55 mmoles) were dissolved in methylene chloride (140 ml) and, under stirring and cooling (0 °C), dicyclohexylcarbodiimide (11.3 g; 55 mmoles) was added in small portions. Stirring was continued for 2 h at 0 °C, then 3 h at room temperature. The mixture was then allowed to stand overnight. Dicyclohexylurea was filtered off and washed on the filter with methylene chloride. The combined solutions were evaporated in vacuum. The resulting product was powdered under anhydrous ether, decanted and washed with the same solvent, collected and dried. The white microcrystalline substance weighed 28.0 g (70%); it contained a small amount of dicyclohexylurea, but could be used for coupling with the C-terminal hexapeptide ester without further purification; R_f^3: 0.9.

Benzyloxycarbonyl-nitroarginyl-prolyl-prolyl-glycyl-4-chlorophenylalanyl-seryl-prolyl-phenylalanyl-nitroarginine 4-nitrobenzyl ester [Z-Arg(NO_2)-Pro-Pro-Gly-Cpa-Ser-Pro-Phe-Arg(NO_2)-ONB]

(*a*) The protected hexapeptide ester (150 mg; 0.146 mmoles) was dissolved in trifluoroacetic acid (1 ml) chilled to 5 °C. The clear solution was allowed to stand at room temperature for 30 min, and the hexapeptide trifluoroacetate was precipitated by the addition of 5 ml anhydrous ether, filtered, washed with ether and dried in a desiccator over conc. sulfuric acid and sodium hydroxide pellets, to obtain 144 mg (93%) of the hexapeptide trifluoroacetate.

Amino acid analysis: Ser, 0.91; Pro, 1.03; Gly, 1.03; Phe, 1.00; Arg, 0.95; Cpa, 0.98.

(*b*) The hexapeptide trifluoroacetate (140 mg; 0.135 mmoles) was dissolved in pyridine (0.6 ml) and triethylamine (0.02 ml) and Z-Arg(NO_2)-Pro-Pro-OPCP (122 mg; 0.15 mmoles) were added to the solution. After stirring at room temperature for 24 h, the pyridine was removed in vacuum, the residue powdered under ether, filtered and dried in air.

The crude product was purified by column chromatography on silica gel, using Solvent 3 for elution, and isolated as described for the protected hexapeptide.

The yield was 155 mg (79%), R_f^3: 0.3, R_f^2: 0.1.

$C_{65}H_{81}O_{19}N_{18}Cl$ (1453.9). Calcd. N 17.34; Cl 2.44. Found N 17.10; Cl 2.38%.

Amino acid analysis: Ser, 0.83; Pro, 3.38; Gly, 1.00; Phe, 0.91; Cpa, 0.96; Arg, 1.88.

Arginyl-prolyl-prolyl-glycyl-4-chlorophenylalanyl-seryl-prolyl-phenylalanyl-arginine hydrogen fluoride (H-Arg-Pro-Pro-Gly-Cpa-Ser-Pro-Phe-Arg-OH · 3 HF; Cpa^5-bradykinin)

The protected nonapeptide ester (64 mg; 44 μmoles) was mixed with 0.15 ml of anisole, placed into the TEFLON flask of the deprotecting equipment, and 10 ml of hydrogen fluoride was condensed into the solution. The mixture was stirred at 0 °C for 1 h, and the hydrogen fluoride removed by evaporation. The residual oil was rubbed with anhydrous ether, the resulting powder washed with ether and dried in a desiccator over conc, sulfuric acid and sodium hydroxide pellets.

The yield was almost quantitative. R_f^5: 0.3; E_{Brad}: 1.25.

Amino acid analysis: Ser, 0.95; Pro, 2.89; Gly, 1.00; Phe, 1.11; Arg, 2.29; Cpa, 1.07.

Arginyl-prolyl-prolyl-glycyl-phenylalanyl [4-^{3}H]-seryl-prolyl-phenylalanyl-arginine (H-Arg-Pro-Pro-Gly-Phe [4-^{3}H]-Ser-Pro-Phe-Arg-OH; Phe [4-^{3}H]^{5}bradykinin)

Cpa^{5}bradykinin hydrogen fluoride (11.5 mg; 10 μmoles) was dissolved in 0.1 molar aqueous triethylamine(0.62ml), water (0.2 ml) was added and, after freezing by immersion into liquid nitrogen, 10% Pd-on-Al_2O_3 catalyst (100 mg) was layered into the frozen mixture. The reaction vessel was connected with the vacuum manifold, evacuated, and saturated with carrier-free tritium at a pressure of 540 Hg-mm. After thawing, the tritiation was started with magnetic stirring, and stopped after 20 min, at the uptake of 0.87 ml normal tritium gas. The reaction mixture was diluted with 1% acetic acid (25 ml), the catalyst was filtered off and washed with 25 ml of 1% acetic acid. The solution was evaporated in vacuum, the residue dissolved in 10 ml of water and evaporated again. The tritiated peptide was taken up in 0.01 molar ammonium acetate buffer (2.0 ml; pH 4.8) and fractionated on carboxymethyl cellulose (10 × 100 mm), first with the same buffer (30 ml per h), then, after 90 min, with a gradient prepared from the above buffer (150 ml) and 0.15 molar ammonium acetate (150 ml; pH 8.5). The fraction containing the main peak which emerged after 7 h (radioactivity and UV absorption) was collected, evaporated in vacuum and lyophilized to yield 5.8 mg (46%) of pure tritiated bradykinin. R_f^5: 0.15–0.20. Radiochemical purity: over 98%. Specific radioactivity: 18.5 ± 1.5 Ci/mmole. (The quantity was measured by spectrophotometry.)

Amino acid analysis: Ser, 0.93; Pro, 2.80; Gly, 1.00; Phe, 1.95; Arg, 2.11.

REFERENCES

[1] Nikolics, K., Teplán, I., Medzihradszky, K.: in "Radioaktive Isotope in Klinik und Forschung", Band 11. Proc. of the Gasteiner International Symposium, 1974, p. 282. (Ed. R. Hőfer), Urban and Schwaarzenberg, 1975
[2] Nikolics, K., Teplán, I., Medzihradszky, K.: J. Label. Comp. Radiopharm., **12**, 163 (1976)
[3] Kovács, J., Teplán, I., Mező, I.: Acta Chim. (Budapest) **84**, 109 (1975)
[4] Bajusz, S., Fauszt, I., Borsay, J.: Hung. Pat. 161 475; Chem. Abstr., **77**, 20027 (1972)
[5] Mező, I., Teplán, I., Seprődi, J., Morgat, J. L., Fromageot, P., Tóth, G., Sirokmán, F.: J. Label. Comp. Radiopharm., **14**, 557 (1978)

János Seprődi
István Teplán
H-1088 Budapest, Puskin u. 9.

Mária Magócsi
Kálmán Medzihradszky
H-1025 Budapest, Pusztaszeri út 59/67.

Acta Chimica Academiae Scientiarum Hungaricae, Tomus 104 (3), pp. 235—242 (1980)

SYNTHESIS AND STEREOCHEMISTRY OF EPIMERIC 3-BENZOYLTROPANES

P. NEMES, P. SCHEIBER, G. KRAISS and K. NÁDOR*

(Department of Chemistry, Veterinary University, Budapest)

Received April 20, 1979
In revised form July 23, 1979
Accepted for publication August 7, 1979

Possible synthetic routes to prepare the epimeric 3-benzoyltropanes were investigated. Despite the use of 3α-substituted tropane derivatives as key precursors in attempts to obtain 3α-benzoyltropane (**VIII**), the formation of 3β-benzoyltropane (**I**) was mostly observed. However, a reasonable synthetic route was worked out for the preparation of the α-epimer (**VIII**) *via* 3-benzoyltropene-2 (**VII**). The configurations of the C-3 epimeric ketones were established on spectroscopic evidence. Furthermore, dipole moment measurements were carried out to determine their probable conformations.

Introduction

ARCHER *et al.* described earlier that both 3α-cyanotropane [1] and 3β-cyanotropane [2] gave the same product when made to react with phenylmagnesium bromide and phenyllithium, respectively. This product was identified as 3β-benzoyltropane (I), the formation of which from 3α-cyanotropane was explained by its substantially greater thermodynamic stability; it was proposed that the inversion of the C(3) relative configuration had occurred either during the Grignard reaction, or during the subsequent acid hydrolysis of the intermediate iminoketone.

Results and Discussion

Synthesis of 3-*benzoyltropanes*

Known examples of the 3α $\rightleftharpoons$ 3β epimerization in the tropane series [1, 3] prompted our first investigations to reveal the stage at which the inversion at the C(3) atom in the reaction of 3α-cyanotropane takes place. Accordingly we studied the reaction of 3α-cyanotropane with phenylmagnesium bromide and phenyllithium. GLC analysis indicated the prompt formation of 3β-cyanotropane in the reaction mixture examined just after starting the reaction. Therefore, epimerization is faster than addition to the cyano group attached

---

* To whom correspondence should be addressed

to the tropane skeleton in 3α position, which explains the formation of 3β-benzoyl-tropane.

The synthesis was also attempted by the Friedel-Craft acylation of tropene-2 with benzoyl chloride and, in view of the easy elimination of hydrochloric acid [4] from β-haloketones, the formation of an α,β-unsaturated ketone was anticipated. However, only tropene-2 could be isolated although various solvents and Lewis acids were tried at different temperatures.

Similarly, tropene-2 did not undergo acylation with benzoic acid in the presence of polyphosphoric acid [5] even at high temperatures.

A successful synthesis of 3α-benzoyltropane was realized using tropene-(2)-3-carboxylic acid (**V**) as the starting material. The methyl ester of this compound (**III**) was prepared by ZIRKLE *et al.* [6] through pyrolysis of *O*-acetyl-α-ecgonine methyl ester (**II**) (Scheme 1). As this step gave **III** only in a poor yield in our experiments, we tried to prepare the compound by dehydration of α-ecgonine methyl ester (**IV**). Using polyphosphoric acid at 150 °C, **IV** afforded the ester olefin **III** in 60% yield. Hydrolysis of **III** resulted in the unsaturated amino acid **V**, whose structure was proved by NMR (δ 2.30 ppm, 3H, s, $N-CH_3$; δ 6.75–6.50 ppm, 1H, m —CH=). Compound **V** was then converted to the acid chloride **VI** in the usual manner, and this was made to react with benzene in the presence of aluminium chloride to give the unsaturated ketone **VII** (Scheme 2) (NMR: δ 2.36 ppm, 3H, s, $N-CH_3$; δ 6.62–6.42 ppm, 1H, m, =CH—; δ 7.68–7.20 ppm, m, 5H, Ar—H).

The hydrogenation of **VII** over Adams PtO_2 catalyst at atmospheric pressure gave stereospecifically 3α-benzoyltropane, **VIII**. When the reduction

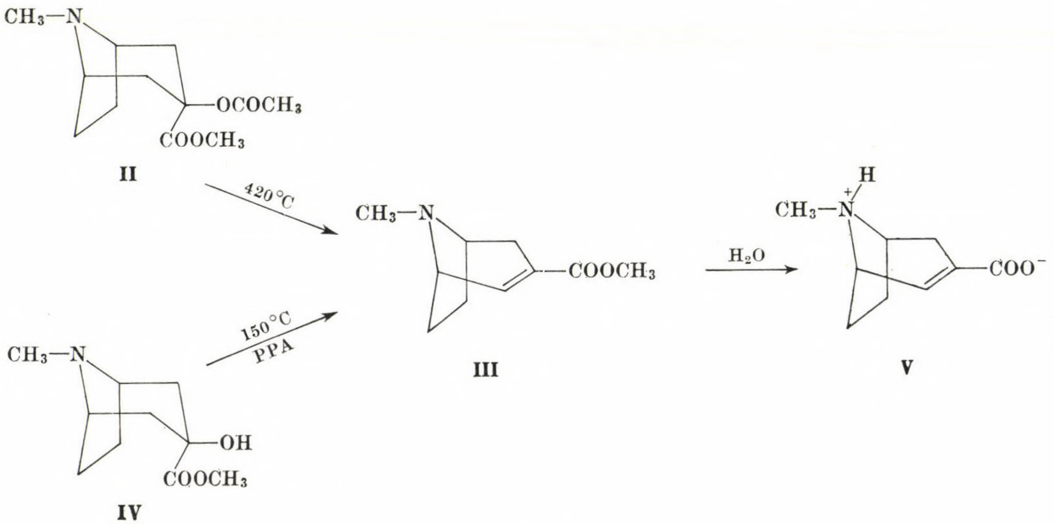

Scheme 1

was carried out with rhodium-platinum catalyst, the predominant formation of the β-epimer (**I**) was observed. The infrared spectrum of **VIII** shows significant differences in the fingerprint region when compared with **I**. Similarly, the hydrochloride salt derived from **VIII** was identified as the hydrochloride of **I** (**I**. HCl).

Catalytic reduction of **V** with Adams PtO_2 catalyst led to tropan-3α-carboxylic acid **IX**, which on subsequent treatment with thionyl chloride and benzene, nevertheless, afforded **I** again. The inversion at C(3) was obviously caused by the reaction conditions during the formation of the acid chloride, or the Friedel—Crafts acylation.

The structure of **VIII** was proved by IR and NMR spectroscopy.

In the ^{1}H-NMR spectrum the C(3)—H proton of **VIII** shows a relatively narrow (24 Hz) triplet-like signal at δ 3.26 ppm, with further fine splitting of the lines. This is due to a hydrogen atom attached equatorially to the six-membered ring with chair form. The benzoyl group is, therefore, an α *(axial)* substituent. The C(3)—H proton of **I** has, on the contrary, a heptet at δ 3.53 ppm with a band width of 36 Hz. The line shapes of the C(3)—H signals in

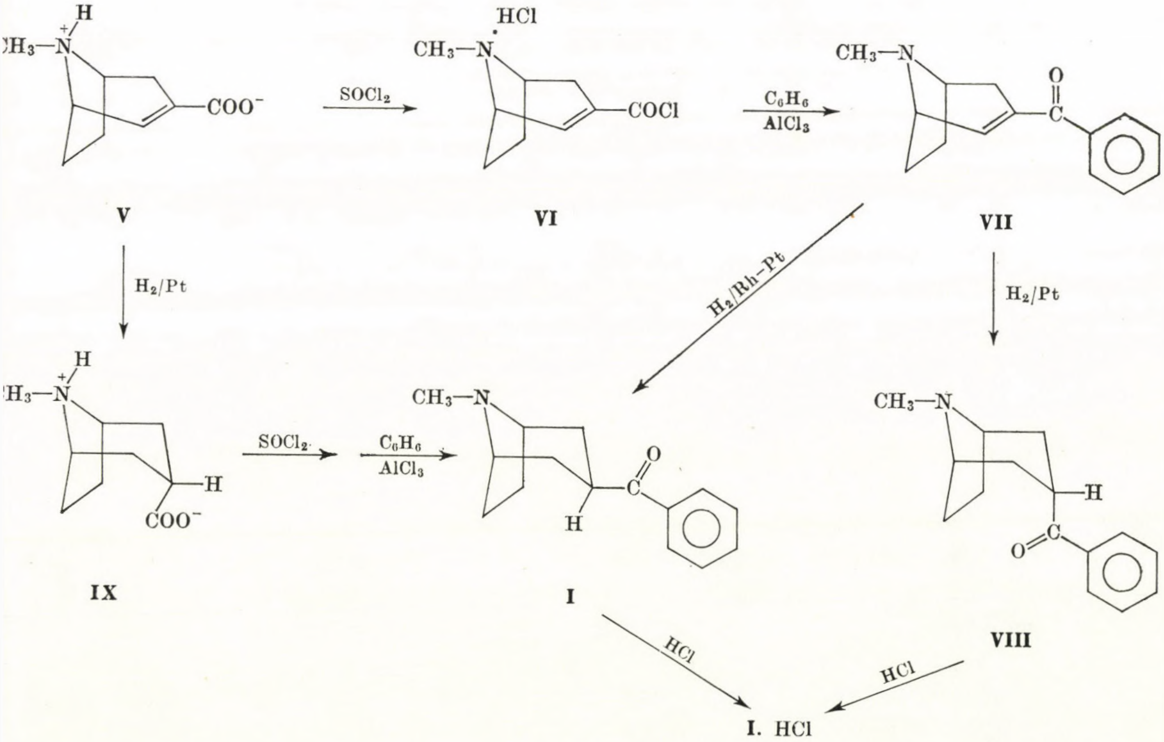

Scheme 2

the spectra of the epimeric ketones **I** and **VIII** are in good accordance with the numerous NMR results obtained earlier [7, 8] in determining the C(3) configuration.

The ^{13}C-NMR shifts of the epimeric ketones **I** and **VIII** (Table I) show the differences usually observed in 3α–3β pairs. Though the change of the C(3) substituent stereochemistry had no striking influence on the chemical shifts of C(3) and C(6), C(7) [9], in a ^{13}C-NMR study of several C(3) pairs we have observed that 3α-substituted tropanes show a stronger upfield shift for C(6), C(7) than the 3β derivatives do [10]. The chemical shifts found for C(6), C(7) (δ 25.18 ppm and δ 26.88 ppm for **VIII** and **I**, respectively) also prove the C(3) configurations deduced from the ^{1}H-NMR spectra.

Table I

^{13}C chemical shifts[a] of epimeric 3-benzoyltropanes

	C(3)	C(2), C(4)	C(1), C(5)	C(6), C(7)	N–CH$_3$	C=O	C$_{Ar}$	
3α-Benzoyltropane,	36.27	31.49	60.51	25.18	39.95	196.68	128.43	132.12
VIII							128.53	136.85
3β-Benzoyltropane,	36.76	32.94	60.56	26.88	39.35	198.28	128.23	132.66
I							128.63	136.73

[a] ppm units in δ scale; CDCl$_3$ solution

Epimerization of 3α-*benzoyltropane*

3α-Benzoyltropane (**VIII**) has little stability at room temperature. The epimerization takes place both in the crystalline state producing a viscous oil, and in solution under acidic or basic conditions.

The transition into the β-epimer was monitored by NMR spectroscopy. In the presence of a catalytic amount of sodium methoxide-d_3, 3α-benzoyltropane in methanol-d_4 underwent a 100% epimerization within one hour and a half at 25 °C. During this process no deuterium incorporation took place. This observation invalidates the possible mechanism of isomerization assuming a route *via* the enol form of **VIII**.

The ability to rapid isomerization can be attributed to the repulsion forces acting between the C(6), C(7) bridge and the bulky 3α-benzoyl group (see below).

The conformation of 3-*benzoyltropanes*

In addition to the NMR studies, dipole moments of the epimeric ketones were also measured to establish their probable conformation (Table II).

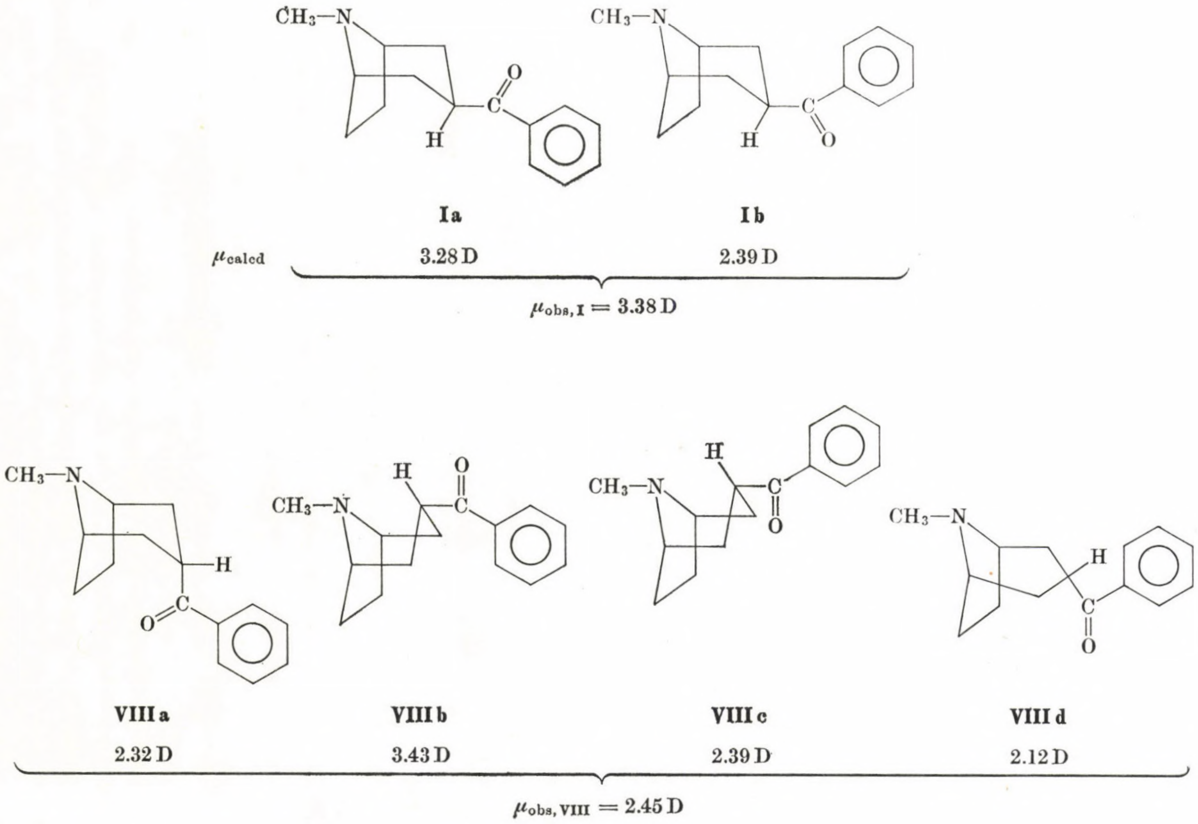

Ia **Ib**

μ_{calcd} 3.28 D 2.39 D

$\mu_{\text{obs,I}} = 3.38$ D

VIII a **VIII b** **VIII c** **VIII d**

2.32 D 3.43 D 2.39 D 2.12 D

$\mu_{\text{obs,VIII}} = 2.45$ D

Scheme 3

Table II

Experimental data of dipole moment measurements

	a_ε*	a_n+	μ++
3α-Benzoyltropane, **VIII**	2.98	0.14	2.45 D
3β-Benzoyltropane, **I**	5.54	0.12	3.38 D
Benzoylcyclohexane	4.58	0.12	2.78 D

* a_ε is defined as the slope of the straight line function of the dielectric constant increments of benzene solutions *versus* the concentration expressed in weight fraction of solute, w_2 $(\Delta\varepsilon = a_\varepsilon \cdot w_2)$

\+ a_n is defined similarly as a_ε for increments in quadratic refractive indices, $n^2(\Delta n^2 = a_n \cdot w_2)$

\+\+ Calculated from the equation $\mu^2 = \frac{27\,kT}{4\pi N} \cdot \frac{M}{(\varepsilon_1 + 2)^2 \cdot d} \cdot (a_\varepsilon - a_n)$ [8]

Some possible conformations of **I** and **VIII** considered in this study are depicted in Scheme 3. Their dipole moments were calculated by adding the moments of the individual dipolar bonds, in the usual way. The bond angles in the conformations studied were derived from Dreiding stereomodels. In our calculations the following group moments were applied: $\mu_{NR_3} = 0.80D$, found for *N*-methylpiperidine by KATRITZKY *et al.* [11] and $\mu_{C=O} = 2.78D$, found for benzoylcyclohexane by us. The *axial* ⇌ *equatorial* equilibrium of the *N*-methyl group was also taken into consideration favouring the *equatorial* orientation in 90% [12].

In the conformations drawn in Scheme 3 the phenyl ring lies in the plane of the sheet of paper. However, its perpendicular position may be more favourable. This rotational isomerism was not studied in detail, as it does not influence the magnitudes of the calculated dipole moments.

The comparison of the calculated and measured dipole moments in the case of **I** clearly shows that this compound adopts the conformation **Ia**.

As the conformation **VIIIa** can be hardly constructed with Stuart—Briegleb models, the boat conformations **VIIIb** and **VIIIc** should also be considered. The ^{1}H-NMR pattern due to the C(3)-H proton, the almost identical ^{13}C-NMR chemical shifts, and, in part, the dipole moment data, all together, render these, in turn, unlikely. As the C(3)-H proton of **VIII** shows essentially a triplet similar to the case of most 3α-substituted tropanes, one may suppose that **VIII** exists in a flattened chair conformation, **VIIId**. Nevertheless, the dipole moment calculated for **VIIId** differs from the measured value; this may by due to an alternate $N-CH_3$ population by which the calculated moment is considerably influenced (*e.g.* with a ratio *equ*/*ax* = 70/30, the calculated moment is 2.35 D instead of 2.12 D, calculated with ratio 90/10).

Recently HAMOR [13] established a considerable ring flattening in benzoyltropine hydrochloride by X-ray diffraction, and estimated the repulsive interaction energies between the C(3)-oxygen and C(6), C(7) atoms to be about 10 kJmole^{-1} for the undistorted model. Owing to ring flattening, this value decreases to about -0.3 kJmole^{-1}. Accordingly, a similar distortion can be presumed in the 3α-benzoyltropane **VIII**, in which the tricoordinated carbon atom in the 3α-position seems still bulkier than the bivalent oxygen atom in benzoyltropine.

Experimental

M.p.'s were determined in capillary tubes on a Büchi apparatus, type SMP 20, and are uncorrected. The IR spectra were recorded on a Spektromom 2000 type instrument. The ^{1}H-NMR spectra were taken at 80 MHz with a Tesla BS 487A spectrometer in $CDCl_3$, D_2O or CD_3OD solutions, using HMDS or DSS as internal references. The ^{13}C-NMR spectra were run on a Varian XL-100-15 PFT instrument in $CDCl_3$ solutions (TMS).

Tropen-(2)-3-carboxylic acid methyl ester (III)

P_2O_5 (40 g) was added to 85% phosphoric acid (20 g) in small portions, with vigorous stirring. The polyphosphoric acid thus prepared was allowed to cool to 50 °C and α-ecgonine methyl ester (20 g) was added. The mixture was stirred and heated slowly to 150 °C. After cooling the reaction mixture to room temperature, 200 cm^3 of water was added. The solution was made strongly alkaline with sodium hydroxide solution. The mixture was then extracted with four 50 cm^3 portions of chloroform. The combined extracts were dried (Na_2SO_4) and the solvent evaporated. The residue was fractionated to give 8.0 g (44%) of **III**; b.p. 125–127 °C/ 12 mm-Hg.

IR (film on KBr pellet): 1720 cm^{-1} (νC=O); 1640 cm^{-1} (νC=C); 1250 cm^{-1}, 1085 cm^{-1}.

NMR ($CDCl_3$): δ (ppm) 6.91 (*d*, =CH); 3.65 (s, OCH_3); 3.50–3.12 (m, C(1)–H, C(5)–H); 2.81–1.37 (*m*, CH_2 groups); 2.30 (s, N–CH_3).

Tropen-(2)-3-carboxylic acid (V)

Compound **III** (20.0 g) was dissolved in water (100 cm^3), and the solution was refluxed for 3 h. The solvent was then removed in vacuum and the residue crystallized from ethanol-acetone to give **V** (17.0 g; 92%); m.p. 350 °C (d).

IR (KBr pellet): 3350 cm^{-1}; 2600–2000 cm^{-1}; 1645 cm^{-1} (νC=C); 1580 cm^{-1} (COO$^-$).

NMR (D_2O/DSS): δ (ppm) 6.75–6.50 (m, =CH); 4.37–3.87 (m, C(1)–H, C(5)–H); 2.82 (d, $J = 2$ Hz, N–CH_3); 2.62–1.50 (m, CH_2 groups).

3-Benzoyltropene-2 (VII)

Compound **V** (16.0 g) was refluxed with thionyl chloride (100 cm^3) for 1 h. The excess of thionyl chloride was removed in vacuum. The residue was dissolved in benzene (400 cm^3), and to the stirred mixture $AlCl_3$ (64 g) was added at the temperature of an ice bath, during a period of 30 min. The reaction mixture was slowly warmed to reflux temperature, and after refluxing for 3.5 h it was poured into a mixture of ice and hydrochloric acid. The organic phase was removed and discarded. The aqueous layer was made strongly alkaline with solid potassium carbonate, and extracted three times with chloroform. The combined extracts were dried (Na_2SO_4) and concentrated in vacuum. A yellow oil (13.0 g; 60%) was obtained which was identified as **VII**.

IR (film on KBr pellet): 3000 cm^{-1} (νAr–H); 1720 cm^{-1} (νC=O); 1640 cm^{-1} (νC=C); 1600 cm^{-1}, 1580 cm^{-1} (νAr).

NMR ($CDCl_3$): δ (ppm) 7.68–7.20 (m, Ar–H); 6.62–6.42 (m, =CH); 3.50–3.25 (m, C(1)–H, C(5)–H); 2.92–1.37 (m, CH_2 groups); 2.36 (s, N–CH_3).

The hydrochloride of **VII** was crystallized from ethanol-ether, m.p. 221–222 °C.

$C_{15}H_{17}NO \cdot HCl$ (263.76). Calcd. C 68.30; H 6.87; N 5.31; Cl$^-$ 13.44. Found C 68.39; H 7.16; N 5.05; Cl$^-$ 13.78%.

3β-Benzoyltropane (VIII)

A solution of **VII** (2.0 g) in ethanol (50 cm^3) was hydrogenated in the presence of platinum(IV) oxide (0.2 g) for 5 h. After absorption of one mole equivalent of hydrogen, the catalyst and the solvent were removed to leave an oily material (2.0 g of crude product), which was crystallized under petroleum ether (b.p. 40 – 70 °C). After several recrystallizations from petroleum ether a white crystalline material (0.8 g) was obtained, m.p. 61 – 62 °C.

$C_{15}H_{19}NO$ (229.31). Calcd. 78.56; H 8.38; N 6.10; Found C 78.35; H 8.52; N 5.96%.

IR (KBr pellet): 3000 cm C^{-1} (ν – H); 1680 cm^{-1} (νC=O); 1590 cm^{-1} (νAr); 760 cm^{-1}; 700 cm^{-1}.

NMR ($CDCl_3$): δ (ppm)7.78 – 7.17 (m, Ar – H); 3.26 (t, C(3) – H, band width $W = 24$ Hz); 3.12 – 2.82 (bs, C(1) – H, C(5) – H); 2.30 (s, N – CH_3); 2.37 – 1.30 (m, CH_2 groups).

Hydrogenation of **VII** over Rh/Pt catalyst gave mainly 3β-benzoyltropane, which was contaminated with 3α-benzoyltropane. Crystallization from petroleum ether gave a white solid, m.p. 58 – 59 °C.

IR (KBr-pellet): 3000 cm^{-1} (νAr – H); 1680 cm^{-1} (νC=O); 1600 cm^{-1}, 1580 cm^{-1} (νAr); 780 cm^{-1}, 700 cm^{-1}.

NMR ($CDCl_3$): δ (ppm) 7.92 – 7.25 (m, Ar – H); 3.53 (h, C(3) – H, band width $W = 36$ Hz); 3.28 – 3.03 (bs, C(1) – H, C(5) – H); 2.40 (s, N – CH_3); 2.37 – 1.32 (m, CH_2 groups).

Dipole moment measurements. The dipole moments of **I**, **VIII** and benzoylcyclohexane were determined by the measurement of the dielectric constant and refractive index of dilute benzene solutions at 25.0 °C, at 2 MHz and 589 nm, respectively. The evaluation of the experimental data and the instruments used were described in detail previously [8]. The a_ε and the a_n values, *i.e.* the slopes of the straight line function of the dielectric constants (ε) and quadratic refrective indices (n^2) *versus* concentration of the benzene solutions are summarized in Table II.

REFERENCES

[1] Archer, S., Bell, M. R., Lewis, T. R., Schulenberg, J. W., Unser, M. J.: J. Am. Chem. Soc., **80,** 4677 (1958)

[2] Bell, M. R., Archer, S.: J. Am. Chem. Soc., **82,** 151 (1960)

[3] Beckett, A. H., Harper, N. J., Balon, A. D. J., Watts, T. H. E.: Tetrahedron, **6,** 319 (1959)

[4] Houben-Weyl: Methoden der Organischen Chemie, Band VII/2a, p. 427. G. Thieme, Stuttgart 1973

[5] Dev, S.: J. Indian Chem. Soc., **33,** 703 (1956)

[6] Zirkle, C. L., Geissman, T. A., Bloom, M., Craig, P. N., Gerns, F. R., Indik, Z. K., Pavloff, A. M.: J. Org. Chem., **27,** 1269 (1962)

[7a] Chen, C. Y., Le Févre, R. J. W.: J. Chem. Soc., **1965,** 3473

[7b] Bishop, R. J., Fodor, G., Katrizky, A. R., Sóti, F., Sutton, L. E., Swinbourne, F. J.: J. Chem. Soc. (C), **1966,** 74

[8] Scheiber, P., Kraiss, G., Nádor, K., Neszmélyi, A.: J. Chem. Soc. (B), **1971,** 2149

[9] Wenkert, E., Bindra, J. S., Ching-jer Chang, Cochran, D. W., Schell, F. M.: Acc. Chem. Res., **7,** 46 (1974)

[10] Scheiber, P., Neszmélyi, A.: Unpublished results

[11] Bishop, R. J., Deneen, D., Jones, R. A. Y., Katritzky, A. R., Sutton, L. E., Wyatt, R. J.: J. Chem. Soc., **1967,** 493

[12] Scheiber, P., Kraiss, G., Nádor, K.: J. Chem. Soc., (B), **1970,** 1366

[13] Hamor, T. A.: J. Chem. Soc. Perkin II, **1976,** 1359

Péter Nemes
Pál Scheiber
Gábor Kraiss
Károly Nádor

H-1400 Budapest, P.O.Box 2.

Acta Chimica Academiae Scientiarum Hungaricae, Tomus 104 (3), pp. 243—252 (1980)

VARIOUS OPTICAL METHODS FOR INVESTIGATION OF FLAME CHARACTERISTICS IN FLAME SPECTROMETRIC DETERMINATION

L. I. Kiss,[1] K. Szivós[2] and E. Pungor[2]

*([1] Institute for Engineering Thermodynamics and Energy Systems,
[2] Institute for General and Analytical Chemistry, Technical University, Budapest)*

Received March 21, 1979
Accepted for publication August 12, 1979

The authors examined the possibilities of quantitative and qualitative optical projection of flames. They studied with different schlieren methods (Toepler, "grid" and coloured stripe methods) the temperature distribution of acetylene-air flames and the changes in geometry due to the applied organic solvents. The observed distribution of temperature was controlled with the help of the indium two-line technique. It was found, that in the presence of organic aerosols the position of the flame contour is nearly unchanged, while the inner blue cone becomes longer. This latter plays an important role from the aspect of sensitivity of flame spectrometric analysis. The authors studied also the turbulence of the fuel-rich flame by high speed photography.

Introduction

The knowledge of flame characteristics is very important for flame spectroscopy. The temperature of flame, the optimal position of the light beam, the stability of flame all are strongly affecting the power of detection in spectrometric determinations. As an example we refer to the problem of application organic solvents. Their use increases the sensitivity in comparison to that in aqueous solutions. Mechanism of the increase is complex,organic solvents cause changes in nebulization parameters and also in the structure of flame.

In recent work we present various optical techniques for structural investigation of flame. Investigation of geometrical changes and temperature distribution will be shown as examples.

Theory

Flame as an optical object

The most simple method to examine a flame — to observe it by naked eyes, or to take an ordinary photo of it. These methods utilize the light emitted by the flame itself, but self-radiation of flame in the visible region is often very weak. Except the inner blue cone, the flame has significant self-radiation only in the case of a fuel-rich one, when soot particles emit light. By visual observation even the boundary of the flame cannot be determined exactly.

However, a flame can be studied also in transparent light as its refractive index changes from point to point. Refractive index of a gas is the function of other properties, namely the temperature, the pressure and the composition. In the practice LORENTZ—LORENZ and GLADSTONE—DALE formulas are commonly used. [1—2]. Either in the first or in the second, refractive index is the function of density as the only variable. The equation of state gives further information. The GLADSTONE—DALE formula has the next form [1]: (it can be derived from the LORENTZ—LORENZ equation considering $n \approx 1$)

$$n - 1 = k\varrho \tag{1}$$

where

n refractive index (dimensionless)

k proportionality factor (m^3/kg)

ϱ density (kg/m^3)

Dependence of refractive index on wave-length is given by the dispersion formula of CAUCHY [1—2]:

$$n - 1 = A\left(1 + \frac{B}{\lambda^2}\right) \tag{2}$$

where

λ wave-length (nm)

A, B constants

The equation of state of a perfect gas:

$$\frac{p}{\varrho} = RT \tag{3}$$

where

P pressure (N/m^2)

T absolute temperature (K)

R gas constant (Nm/kgK)

In a free jet — as flame is while shock waves do not appear — the pressure change can be neglected. Difficulties arise at calculation of the influence of composition and dissociation. Several authors examined this problem. Calculations showed the average density (computed from equation of state for mixture of perfect gases) to be proportional to refractive index even in the case of large concentrations of oxygen atoms and electrons. DIXON-LEWIS and WILSON [3] calculated the effect of composition change upon refractive index not to be more than 10% of temperature effects.

So the GLADSTONE—DALE relation between density and refractive index is valid even in the presence of large concentrations of oxygen atoms and electrons. On the other hand, the presence of nitrogen atoms seriously disturbs the previous relation, and the optical methods become composition sensitive [4]. So quantitative study is possible only up to 5000 Kelvin.

Consequently we can consider the flame as an inhomogeneous optical object, refractive index of which varies along the space coordinates mainly due to temperature differences.

Optical methods for investigation of refractive index fields

An optically inhomogeneous object distorts the wave front of light passed through it. Measurement of distortion of an originally regular (plane, sphere) wave front is the basic principle of each optical methods applied in flame research.

Distortion of wave front can be measured by the radius of curvature r of light ray going through a given point (Fig. 1) [1—2]:

$$\frac{1}{r}=\frac{grad\, n}{n}\sin\alpha \tag{4}$$

or

$$\frac{1}{r}=\nu\cdot grad\,(\ln n). \tag{5}$$

where

r radius of curvature

ν unit vector of ray

α angle between the unit vector of ray and gradient of refractive index. Generally (4) is the basic relation for evaluation of optical records, but depending on different methods it is preferable to express it in terms of other, easily measurable quantities.

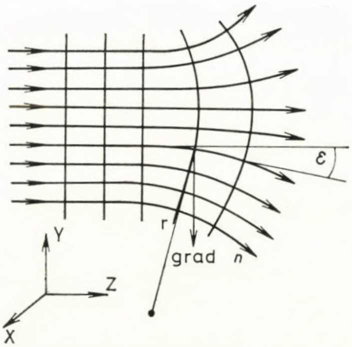

Fig. 1. Distortion of wave front of light

In the case of small distortions the characteristics of light beam can be given as follows:

$$\left.\begin{aligned} \varepsilon_x &\cong \frac{1}{n_0}\left(\frac{\partial n}{\partial x}\right)\cdot L \\ \varepsilon_y &\cong \frac{1}{n_0}\left(\frac{\partial n}{\partial y}\right)\cdot L \end{aligned}\right\} \tag{6}$$

$$\varphi(x, y) \cong [n(x, y) - n_0]\cdot L \tag{7}$$

where

n_0 refractive index of non-disturbed flow

L length of inhomogeneity along optical axis

ε_x, ε_y deflection angle

φ phase of light wave

If a screen is placed behind the object, light intensity on it will not be uniform because of optical inhomogeneity. The change of intensity

$$\Delta I \sim \left(\frac{\partial^2 n}{\partial x^2} + \frac{\partial^2 n}{\partial y^2}\right) \tag{8}$$

Optical methods can be classified by the different quantities (6) (7) or (8) that they measure.

1. Shadowgraph methods have the most simple optical arrangement. It is based on Eq. (8). The resulting picture depends on the distance between object and screen, and gives only few information. The quality of pictures are not of a high level.

2. Schlieren methods determine the deflection angle over the field of vision. For evaluation (6) or — in the case of greater deflections — successive approximation procedure can be applied [1].

3. Interferometry is the only method which gives directly the value of refractive index, by measuring the phase shift between the distorted and original wave.

In our investigations we applied different modifications of schlieren technique for flames having two dimensional plane distribution of refractive index $n(x, y)$. Optical methods can be applied also for cylindrically symmetrical flames, only the computational work needed for quantitative analysis grows significantly.

Simplest method is the so-called Toepler one. Array of optical elements can be seen in Fig. 2. Light source is placed into the focus of first objective,

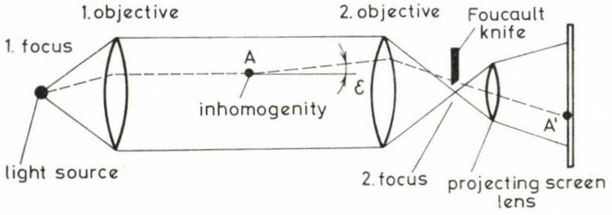

Fig. 2. Principle of the Toepler–method

which produces a parallel light beam through the object. If the object is homogeneous, all the rays are collected in the second focus, and due to the non-transparent Foucault-knife the screen will be dark. In case of optical inhomogeneity in point A, deflected ray will pass out of second focus, and corresponding point A' on screen becomes bright. Measuring position of edge of Foucault-knife one can compute deflection angle on basis of geometric relations. A fixed position of Foucault-knife gives a line of constant deflection angle in x or y direction $\left(\text{approximately } \frac{\partial n}{\partial x} = \text{const, or } \frac{\partial n}{\partial y} = \text{const}\right)$ on the picture, as it is shown in Figs 3a and 3b. These figures show pictures of air—acetylene flame taken in a plane perpendicular to the burner outlet. Water or methyl acetate

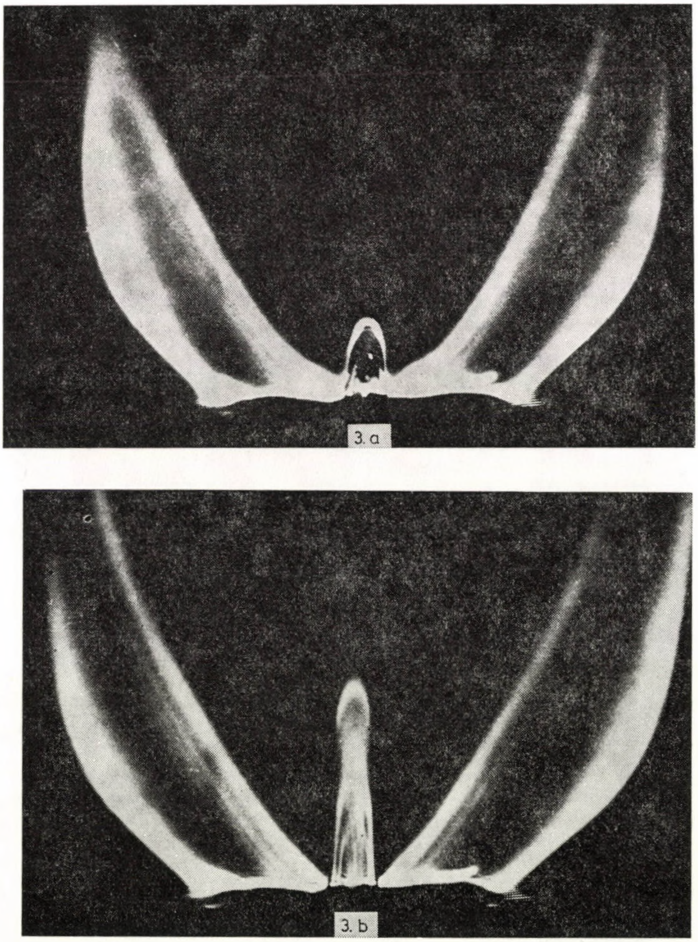

Fig. 3. Schlieren picture of stoichiometric acetylene–air flame. Nebulized solvents: a) water, b) methyl-acetate

was nebulized into the flame. An interpretation of the phenomena observed will be given later.

One can get more detailed information applying the so-called coloured stripe method. In that technique light rays of different deflection are dyed for different colours. In a colour picture one can get a series of constant gradient lines serving quantitative and qualitative evaluation.

Third technique often used by us is the "grid" method. A regular grid is placed into the path of light beam, the displacement of a grid element is proportional to the refractive index gradient in that point. Figure 4 shows a schlieren–picture of a stoichiometric acetylene–air flame, made by the application of a grid of stripes. Distortion of the originally straight lines shows the structure of flame. Where the distortion of refractive index is uniform, distortion does not occur.

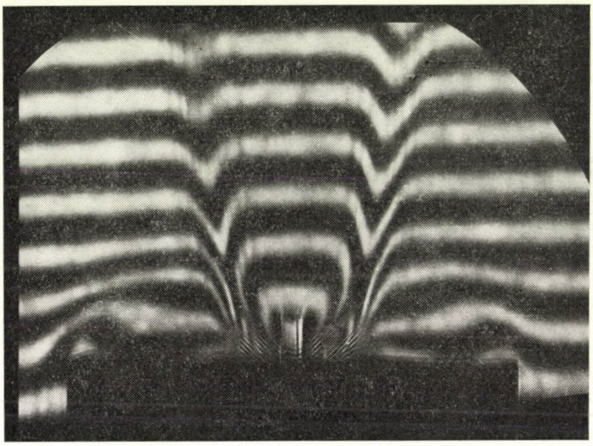

Fig. 4. Stoichiometric acetylene–air flame, by "grid" method

Experimental

Apparatus

As base for optical research a Zeiss-80 schlieren apparatus served. Nebulizer, cloud chamber and burner system were from UNICAM type Sp 90 A spectrophotometer. Size of the one-slit air–acetylene burner was ten centimeters long and 0.45 mm wide.

As light source a high pressure mercury lamp (*max.* 500 W) with monochromatic filter for 546 nm, or a General Radio 1538-A "Strobotac" stroboscope was used. In connection with the latter a Hungarian Optical Works Photorecorder with continuous film moving was used as a camera. For high speed photography we also used a Pentazet–camera with rotating prism.

For black-and white pictures ORWO NP 20 negative film, for colour slides ORWO UT-18 reversal film was used.

Nebulized solvents

Water, ethanol, *n*-propyl alcohol, ethyl acetate, methyl acetate, acetone.

Results

Qualitative and quantitative evaluation of schlieren pictures is possible. For the first look at a schlieren picture one can determine easily homogeneous parts of the object, boundary or volume of a flame. Going along fixed coordinates, by numerical or graphical integration the refractive index field can be determined. If numerical values of constants in Eqs (1) and (2) are known the temperature field can be calculated, too. As a constant of integra-

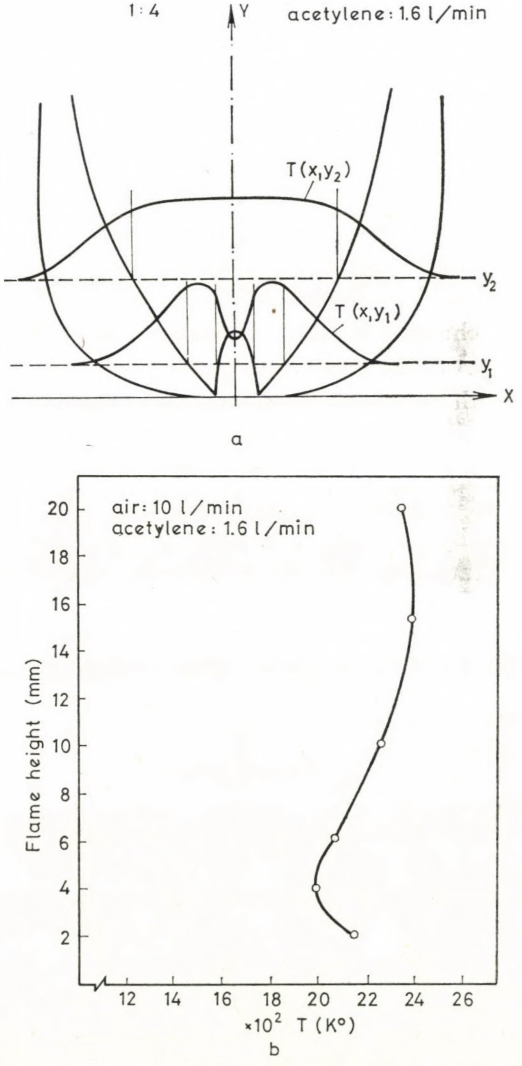

Fig. 5. a) Dimensionless temperature distribution of stoichiometric acetylene–air flame by schlieren method; b) temperature of stoichiometric acetylene–air flame in center line along *y* axis by indium two-line method

tion we should measure the temperature in one point by other way as it can be found in [5] and [6]. By measuring the temperature in several points, we can "calibrate" the optical method. As a first step, dimensionless temperature distribution can be determined. In Fig. 5a the dimensionless temperature plotted against x, for different heights y_1, y_2 over the burner can be seen. (Maximum value of dimensionless temperature in each cross section being equal one.) This plot can be coupled with a flame temperature measurement along the y axis by indium two-line method [5].

Schlieren-measured dimensionless temperature distribution along x-axis of stoichiometric flame is shown in Fig. 5a. In Fig. 5b the values from the two-line method are plotted. In the preheating zone temperatures are low, the height of preheating zone is approximately 4 mm. The highest value was measured in height approximately 16 mm above burner top. In that equilibrium zone the temperature distribution along y axis is nearly uniform.

The "boundary layer" behaviour at the edge of flame can be observed in Fig. 5a, illustrated by temperature plots along x axis. Our measurements and calculations are in good accordance with the results of atomic fluorescence measurements in cylindrical flames [8].

Morphological changes in flame structure due to application of organic solvents can be shown easily constructing boundaries of different flames into one plot (Fig. 6). Both schematic plots belong to the same stoichiometric air–acetylene flame, but one of them with water sprayed in, the other with organic solvent (see in Fig. 3a-b). The inner zone suffers the biggest change in case of methyl acetate, other organic solvents cause gradually smaller effect in the following series: methyl acetate > acetone > ethyl acetate > ethanol > n-propanol > water. Naturally, the effect depends on the mass rate of solvent [9]. Previous series is related to the same volumetric rate. Situation is physically analogous to that with fuel rich flames. The height of inner cone is increased, so optimal position of light beam of hollow cathode lamp is shifted.

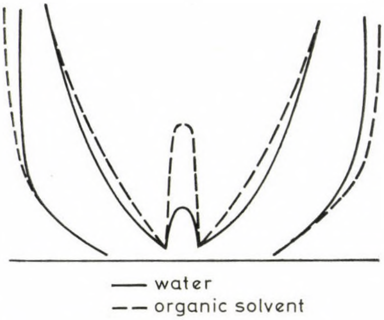

Fig. 6. Structure of flames in case of water and methyl acetate

Time-dependent phenomena

In case of turbulent, or laminar but oscillating flames the appropriate exposure time has an important role. Fuel-rich flames with high recirculation rate are strongly oscillating. The frequency of oscillations cover a range from ten to hundred cycles per second. For getting sharp pictures exposure time generally was one millisecond in our experiments. This value can be reached by the mechanical shutter of Zeiss 80 schlieren apparatus. For shorter exposure times we used Pentazet high-speed film camera giving movie pictures up to 5000 frames per second, or GR Strobota type stroboscope (shortest flash duration, 0.8 microsecond) for single pictures. By high-speed schlieren photography we studied also other transient phenomena of flames, for example separation, structure of turbulent premixed flame *etc.*

These investigations give better information about the physical background of signal-to-noise ratio in spectrophotometric determinations.

As an illustration we present an originally coloured schlieren picture in black and white of an unstable, separating acetylene–air flame (Fig. 7).

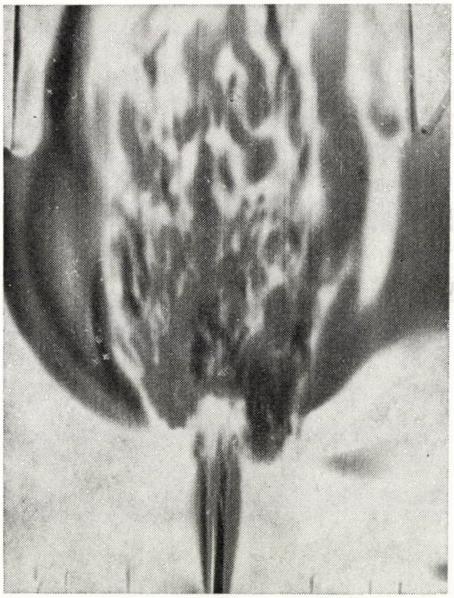

Fig. 7. High-speed photography of the reductive, separated acetylene–air flame

Discussion

Structural changes caused by organic solvents fed into flame are known from earlier works [6]. It was also pointed out in [7], that expansion of a reductive flame can be an important influencing factor in the flame spectrometric sensitivity.

Optical methods for study of flames have multiple advantages: they do not disturb flame, and give general and detailed information about the whole flame [10—11].

Step by step we developed our experimental technique, computational methods for evaluation to have an effective tool for flame research [12—13]. Grid and coloured schlieren methods proved to be most convenient for numerical evaluation. Combining them with high-speed photography, the investigation of transient phenomena becomes possible.

REFERENCES

[1] Grigull, U., Hauf, W.: Optical Methods in Heat Transfer, Academic Press, New York—London 1970
[2] Born, M., Wolf, E.: Principles of Optics, Pergamon Press, Oxford 1970
[3] Dixon-Lewis, G., Wilson, M. J. G.: Trans. Faraday Soc., **47**, 1106 (1951)
[4] Fristrom, R. M., Westernberg, A. A.: Flame Structure, McGraw-Hill, New York 1965
[5] Browner, R. F., Winefordner, J. D.: Anal. Chem., **44**, 247 (1972)
[6] Gaydon, A. G., Wolfhard, H. G.: Flames, their Structure, Radiation and Temperature, Chapman and Hall Ltd. New York 1970
[7] De Galan, L., Winefordner, J. D.: J. Quant. Spectrosc. Radiat. Transfer, **7**, 251 (1967)
[8] Haraguchi, H., Winefordner, J. D.: Appl. Spectrosc., **31**, 195 (1977)
[9] Szivós, K., Pólos, L., Pungor, E.: Spectrochim. Acta, **31B**, 289 (1976)
[10] Weinberg, F. J.: Optics of Flames, Buttervorths, London 1963
[11] Aldous, K. J., Browner, R. F., Clark, D., Dagnall, R. M., West, T. S.: Talanta, **19**, 927 (1972)
[12] Kiss, L. I., Szivós, K., Pungor, E.: Second European Conference on Analytical Chemistry Budapest, Paper No. 1.b-22 (1975)
[13] Kiss, L. I. Szivós, K., Pungor, E.: VII. Nat. Conf. on Spectroscopy, Slanchev Bryag, Bulgaria (1976)

László I. Kiss — H-1502 Budapest, Műegyetem rkp. 3/9, D épület

Klára Szivós
Ernő Pungor
H-1502 Budapest, Gellért tér 4.

Acta Chimica Academiae Scientiarum Hungaricae, Tomus 104 (3), pp. 253—265 (1980)

ELECTRON DEFICIENT HETEROAROMATIC AMMONIOAMIDATES, XIX[+]

N-(3-QUINAZOLINIO)AMIDATES, VII[++]

THE PHOTOCHEMISTRY OF *N*-(3-QUINAZOLINIO)AMIDATES IN THE PRESENCE OF AMINES AND OF ACETAMIDE

G. BARTA-SZALAI,[+++] J. FETTER, K. LEMPERT* and J. MØLLER[1]

(Department of Organic Chemistry, Technical University Budapest,
[1]Department of Chemistry, Odense University, Odense, Denmark)

Received July 11, 1979

Accepted for publication August 23, 1979

Irradiation by Pyrex-filtered light of the quinazolinioamidates **1c—1f** and of the dimers **2a** and **2b** in butylamine, of compound **2b** in benzylamine and morpholine, and in the presence of acetamide in dioxane or dichloromethane, as well as of the adducts **5a** and **5b** in dichloromethane leads to complex mixtures of Type **6—16** products. While the compounds **6—9** are the products of Type II cleavage processes of the Type **3—5** adducts, the parent quinazolines **12** are formed from the amidates **1** themselves, amides **14** being the co-products in both cases. Compound **10a** is formed by deacetylation of **9a** during work-up, while compound **11b** is a secondary photosubstitution product of **12b** by the solvent dioxane. At least part of the compounds **13**, **15** and **16** is the result of dark reactions.

The photochemistry of *N*-(3-quinazolinio)amidates of Type **1** and/or their Type **2** dimers in alcohols and α-toluenethiol–chloroform mixtures has been studied recently [1, 2]. In continuation of this work we here report on the photochemistry of these compounds in amine solutions and in the presence of acetamide as a further nucleophile.

By analogy with the behaviour of these quinazolinioamidates in alcohols and in the presence of α-toluenethiol, their photochemistry in the presence of *N*-nucleophiles was expected to depend mainly on whether they exist under irradiation conditions as the free amidates or as their adducts (*e.g.* **3—5**) with the nucleophile. Therefore, the propensity for adduct formation of selected Type **1** and **2** compounds with selected *N*-nucleophiles was first studied.

[+] For Part XVIII, see LEMPERT—SRÉTER, M., LEMPERT, K., TAMÁS, J., VÉKEY, K.: Acta Chim. Acad. Sci. Hung., **103**, 259 (1980).

[++] For Part VI, see Ref. [1].

[+++] Chinoin Pharmaceutical Works, Budapest, research fellow, 1975—1979.

* To whom correspondence should be addressed.

Results and Discussion

According to ^{1}H-NMR experiments, addition of increasing amounts of benzylamine to a $CDCl_3$ solution of compound **1c** (which is known [3] to exist in pure $CDCl_3$ solution almost entirely as such) results in gradual conversion into the adduct **3c**. Consequently, **1c** is assumed to exist entirely in form of the adducts **3c** and **4c** in pure benzylamine and butylamine, respectively. On the other hand, compounds **1a** and **1b** exist in $CDCl_3$ as equilibrium mixtures with their Type **2** dimers [3], *i.e.* the stabilities of the dimers **2** relative to the amidate forms **1** are greater in the **a** and **b** than in the **c** series. Since both adduct formation and dimerization involve nucleophilic attack of C-4 of the quinazoline ring, and electrophile attack at the amidate nitrogen, it is assumed that also the stabilities of the adducts **4** relative to the amidate forms are greater in the **a** and **b** than in the **c** series. Compounds **1a** and **1b**, too, may therefore be assumed to exist entirely as the corresponding adducts **4a** and **4b** in butylamine solutions, irrespective of whether they have been introduced as such or as the dimers **2a** and **2b**. Compound **2b** probably exists as a similar adduct also in morpholine solution, and similar adducts (**5a** and **5b**) were obtained from compounds **2a** and **2b**, respectively, with acetamide. The adducts **5a** and **5b** were shown (^{1}H NMR) to dissociate partially into their components (**1a** and **1b**, respectively, and acetamide) in DMSO solutions.

No adduct formation was noticed in solutions of compound **1f** in $CDCl_3$–benzylamine mixtures, nor could Type **5** adducts be obtain in the **d**—**f** Series ($R^4 = Me$). In view of similar differences between the quinazolinioamidates with $R^4 = H$ and $R^4 = Me$ concerning their abilities of adduct formation with *O*- and *S*-nucleophiles [1, 3], it is reasonable to assume that no Type **4** adducts are present in butylamine solutions of **1d**—**1f**, either.

Compounds **2a**, **2b** and **1c**—**1f** were irradiated in butylamine, and compound **2b** in benzylamine and morpholine as well. The acetamide adducts **5a** and **5b** were irradiated in CH_2Cl_2 solutions containing (in order to improve the solubilities of the starting compounds) a small amount of acetic acid; for comparison, irradiation of **2b** was performed in the presence of acetamide in the same solvent, as well as in dioxane. The conditions and results of these experiments are presented in Table I.

As expected, the reactions of the adducts give rise to products different from those obtained from the amidates themselves. In all cases the main photoproducts obtained from the adducts may be rationalized by assuming Norrish Type II cleavages of the adducts to yield compounds **6**—**9**, with imidic acids as the co-products which subsequently tautomerize into the more stable amides **14**. By irradiation of the adduct **5a** (experiment No. 18) only traces of the expected Type II cleavage product **9a** were isolated, the main product being compound **10a**. The latter is formed, as shown by separate

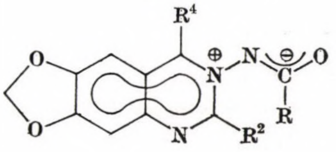

1

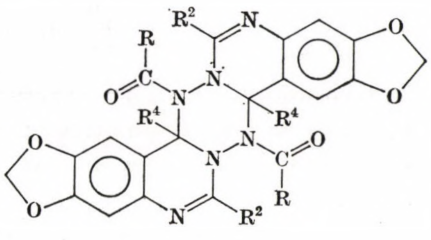

2

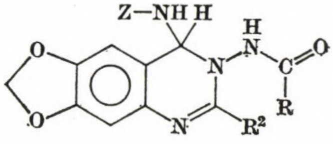

3: Z = PhCH$_2$—

4: Z = Bu—

5: Z = Ac—

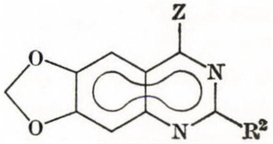

6: Z = BuNH—

7: Z = PhCH$_2$NH—

8: Z = morpholino

9: Z = AcNH—

10: Z = H$_2$N—

11: Z = 2-dioxanyl

11A: Z = MeS—

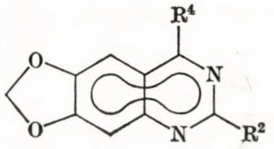

12

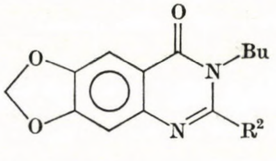

13

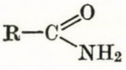

$R-C(=O)NH_2$

14

1–15

	R^2	R^4	R
a	H	H	OEt
b	Me	H	OEt
c	Me	H	Ph
d	H	Me	OEt
e	Me	Me	OEt
f	Me	Me	Ph

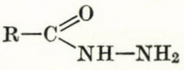

$R-C(=O)NH-NH_2$

15

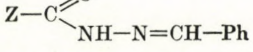

$Z-C(=O)NH-N=CH-Ph$

16: Z = Ph

17: Z = OEt

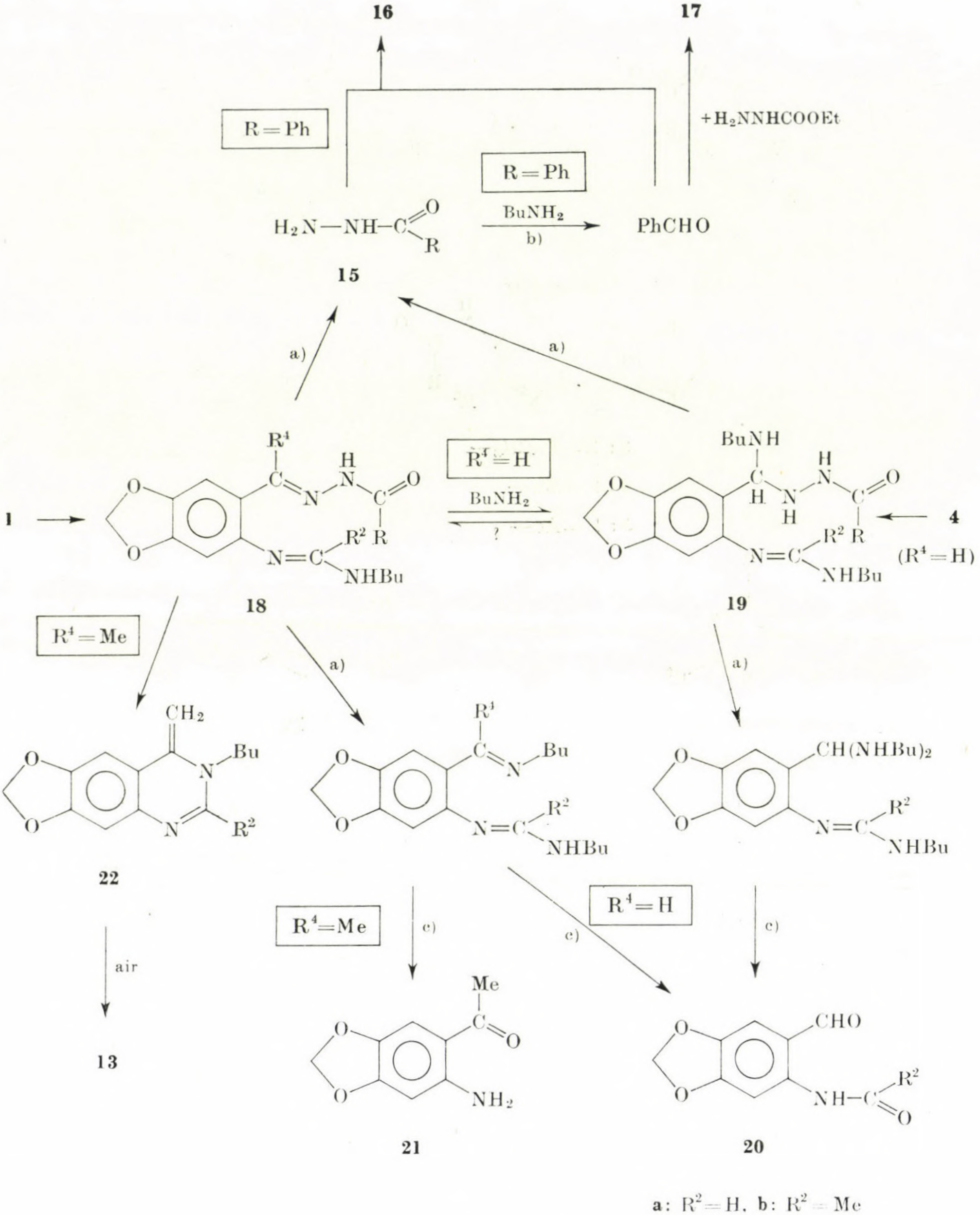

Scheme 1

[a] $BuNH_2$, amine exchange. [b] α-Elimination. [c] Hydrolysis during work-up

experiments, by methanol-induced* deacetylation of **9a** during work-up, rather than by photo-deacetylation of **9a**.

---

* Methanol was used as the solvent for chromatographic work-up.

The results of the irradiation of compound **2a** in butylamine, *i.e.* of the adduct **4a** (experiments 1 and 2), are exceptional. In contrast with the case of compound **2b**, no appreciable amount of the expected Type II product **6a** was obtained. Instead, substantial amounts of compound **13a** (which has been shown [6] to be a non-photochemical oxidation product of **2a** in the presence of butylamine and air) were formed. In order to achieve complete disappearance of the starting compound, **2a** had to be irradiated for a longer period than the other compounds studied (*cf.* Table I). This suggests that the Type II photocleavage of **4a** is too slow to compete effectively with the dark reaction leading to **13a**.

An important photoreaction of the amidates **1e** and **1f** ($R^4 = Me$) is the elimination of an acyl nitrene to furnish the parent quinazoline **12** and the amides **14**. (The amides are in this case formed *via* hydrogen abstraction from the solvent by the acyl nitrenes.) Interestingly, this process was not noticed in the case of the amidate **1d**. Moreover, this type of reaction is not possible for those quinazolinioamidates which exist exclusively in the form of adducts under the conditions of irradiation, and no compounds **12** could be detected among the photoproducts in these cases, except for experiment No. 16. The decreased stabilities of the acetamide adducts **5** as compared with the stabilities of the amine adducts (*e.g.* **3** and **4**) may possibly account for this discrepancy.

Compound **11b** is probably a secondary photoproduct, formed by reaction of compound **12b** with the solvent dioxane, as shown by irradiation of separately prepared **12b** in dioxane. Similar reactions are known from the literature, see *e.g.* Ref. [5].

At least parts of compounds **13**, **15** and **16** are the result of dark reactions of the quinazolinioamidates. This has been established earlier for the formation of compound **13** in the **a** and **b** Series, and for the formation of compound **15** in the **b** Series [6]. Further experiments are listed in Table II for the **c** and **d** Series.

The most striking observations were (1) the formation of Type **13** products in the **d** and **f** Series, *i.e.* demethylation at position 4 of the quinazoline ring even in the absence of irradiation; and (2) the formation of compounds **16** and **17**, which shows that at least part of the benzoylhydrazine incorporated into compounds **1c** (or **4c**) and **1f** is converted in the presense of butylamine to benzaldehyde. As shown by the last run listed in Table II, and in agreement with expectation, no similar transformation of ethyl carbazate takes place.

Likely precursors of compounds **15**—**17**, **20**, **21** as well as of the demethylation products **13** are the compounds **18** and, in the case R = H, **19** which both could be easily formed *via* ring opening of **1** and **4**, respectively, initiated by attack at C-2 of one molecule of the solvent butylamine. An additional pathway of formation of **19** from **18**, as well as possible pathways leading from

Table I

Irradiation products of some N-(3-quinazolinio)amidates **1** *(or their dimers* **2***) in amines*[a] *or in the presence of acetamide, and of some acetamide adducts* **5** *in the absence of added N-nucleophiles*[b]

Experiment No.	Starting compound (mmole)	Solvent (ml)	Irradiation time (h)	Products and yields ,%					
				6—9[e]	**12**	**13**[f]	**14**	**15**[f,g]	**16**[f]
1.	**2a** (2.9)	BuNH$_2$ (150)	100	0[h]	0	22 (**C**)	10 (**B**)[i]	7 (**C**)	—[j]
2.	**2a** (1.0)	BuNH$_2$ (150)	50	+[h]	0	33 (**D**)	13 (**D**)	10 (**D**)	—[k]
3.	**2b** (2.7)	BuNH$_2$ (150)	15	36 (**B**+**C**)	0	0	21 (**B**)	0	—
4.	**2b** (2.7)	PhCH$_2$NH$_2$ (150)	20	40 (**B**+**C**)	0	—[l]	14 (**B**)	0	—
5.	**2b** (2.7)	morpholine (150)	20	36 (**B**+**C**)	0	—	16 (**B**)	0	—
6.	**1c** (0.4)	BuNH$_2$ (100)	7	58 (**D**)	0	0	43 (**D**)	0	0
7.	**1c** (2.0)	BuNH$_2$ (100)	8	32 (**B**)	0	0	81 (**B**)	0	9 (**B**)
8.	**1c** (4.9)	BuNH$_2$ (150)	16	26 (**B**+**C**)	0	8 (**C**)	27 (**B**)	10 (**C**)	15 (**B**)
9.	**1c** (9.8)	BuNH$_2$ (300)	16	23 (**B**+**C**)	0	11 (**C**)	27 (**C**)	13 (**C**)	18 (**C**)[m]
10.	**1d** (5.5)	BuNH$_2$ (150)	25	—	0	56 (**B**+**C**)	0	33 (**C**)	—[n]
11.	**1e** (5.2)	BuNH$_2$ (150)	25	—	40 (**B**+**C**)	0	+	0	—
12.	**1e** (1.7)	BuNH$_2$ (100)	4	—	90 (**C**)	?	?	?	—
13.	**1e** (1.9)	BuNH$_2$ (150)	20	—	69 (**D**)	6 (**D**)	21 (**D**)	3.5 (**D**)	—

14.	**1f** (4.7)	BuNH$_2$ (150)	25	—	+	20 (**C**)	12 (**C**)	+	5 (**C**)
15.	**1f** (1.6)	BuNH$_2$ (100)	7	—	7 (**D**)	52 (**D**)	35 (**D**)	+	+
16.	**2b**[o] (1.8)	dioxane (100)	30	20 (**A**+**C**)	4 (**C**)	—	5 (**B**)	0	—[p]
17.	**2b**[o] (1.8)	CH$_2$Cl$_2$[q] (200)	30	26 (**B**+**C**)	0	—	5 (**B**)	0	—
18.	**5a** (1.6)	CH$_2$Cl$_2$[q] (100)	12	36 (**C**)[r]	0	—	+	0	—
19.	**5b** (1.5)	CH$_2$Cl$_2$[q] (100)	8	87 (**C**)	0	—	+	0	—

[a] The quinazolinioamidates **1a**—**1c** exist in benzylamine solutions exclusively as the Type **3** adducts (irrespectively of whether they have been introduced as such or as their Type **2** dimers) and, presumably, similar adducts are formed with butylamine (**4**) and morpholine; the amidates **1b**—**1f**, in contrast, exist under the same conditions practically exclusively as such. The adducts **5** partially decompose, at least in DMSO solutions, into their components **1** and acetamide

[b] HPK-125 (Philips) high-pressure mercury immersion lamps, Pyrex filter, argon-flushed solutions

[c] +: Traces detected by TLC and identified by the IR spectrum; 0: nothing detectable by TLC; —: in principle impossible products, not detected by TLC; ?: no search was made for this product

[d] The letters **A**—**D** behind the yield data refer to the methods of isolation, see Experimental

[e] **6**, **7**, **8** and **9**, respectively, for the irradiations performed in butylamine, benzylamine, morpholine, and in the presence of acetamide

[f] Product of dark reaction of the amidate with the solvent amine

[g] Isolated in form of the acetone condensation product

[h] The negligible yield of formation of compound **6a** is *not* the result of its subsequent photo-oxidation into **13a**, since **6a**, when irradiated in the presence of an equimolecular amount of **14a** for 50 h in butylamine, proved photostable

[i] In one of several runs

[j] 5% (**C**)[d] of 2-formylamino-4,5-methylenedioxybenzaldehyde (**20a**) was also isolated

[k] 5% (**D**)[d] of 2-formylamino-4,5-methylenedioxybenzaldehyde (**20a**) was also isolated

[l] No search was made for the analogue of compound **13b** with an *N*-benzyl replacing the *N*-butyl group

[m] 4% (**C**)[d] of 2-acetylamino-4,5-methylenedioxybenzaldehyde (**20b**) [4] was also isolated

[n] 8% (**B**+**C**)[d] of 2-amino-4,5-methylenedioxyacetophenone (**21**) was also isolated

[o] In the presence of added acetamide (23 mmoles/mmole of **2b**)

[p] 3% (**C**)[d] of compound **11b** was also isolated

[q] With 1 vol.% of acetic acid added

[r] Almost pure **10a**, formed during work-up by deacetylation of **9a**, and containing only traces of **9a**, detected by TLC

Table II

*Dark reactions of some N-(***3***-quinazolinio)amidates* (**1**) *and butylamine at room temperature*

Starting compound (mmole)	$BuNH_2$ (ml)	Reaction time (h)	Products and yields, %[a,b]		
			13	15[c]	16
1c (1)	30	100	80 (**D**)	+	80 (**D**)
1c (1)	30[d]	100	67 (**D**)	+	+[e]
1d (1.1)	30	100	64 (**D**)	53 (**D**)	—[f]

[a] +: Traces detected by TLC and identified by the IR spectrum
0: Nothing detectable by TLC
—: In principle impossible product, not detected by TLC

[b] The letter **D** in parentheses after the yield data refers to the method of preparation, see Experimental

[c] Isolated in form of the acetone condensation products

[d] With 3 mmoles of ethyl carbazate added

[e] 57% of compound **17** was also isolated

[f] 2% of 2-amino-4,5-methylenedioxyacetophenone (**21**) was also isolated

18 and **19** to compounds **15**—**17**, **20**, **21** and, *via* **22**, to **13** are shown in Scheme 1. Thus, formation of the demethylation products **13** is thought to be an oxidative process related to the oxidative *C*-debenzylation of certain 1,2-dibenzylisoquinolinium salts under mild alkaline conditions, *cf.* Ref. [11].

The structures of all products have been derived from their ^1H NMR, IR, mass and UV spectra. Most of them have been substantiated by comparison with authentic samples.

Experimental

IR, ^1H NMR and UV spectra were recorded with Spektromom 2000 IR (Hungarian Optical Works, Budapest), Perkin-Elmer R-12 60 MHz NMR, Varian XL-100A 100 MHz FT-NMR, Specord (Carl Zeiss, Jena, GDR) and Unicam SP-700 UV spectrometers, respectively. The mass spectra were obtained on a Varian MAT 311A (Grant No. 511—3809 from the Danish Natural Science Research Council) by electron impact (70 eV) and using the direct insertion system.

^{1}H NMR study of adduct formation of compounds 1c and 1f with benzylamine in $CDCl_3$ solution

(*a*) Gradually increasing amounts of benzylamine were added to a $CDCl_3$ solution of compound **1c**, and the changes in the ^1H NMR spectrum were studied. The characteristic signals of the initial spectrum (δ 3.0 s, 2-Me; 6.3 s, OCH_2O; 9.65 s, 4-H [3]) gradually disappeared and became replaced by new signals which could be assigned to the adduct **3c** (δ 2.0 s, 2-Me; 5.8 s, OCH_2O; *no* signal above δ 8.6 ppm) and to the added amine (δ 1.3 s, 3.7 s, 7.25 s), respectively.

(*b*) No similar changes in the ^1H NMR spectrum of a $CDCl_3$ solution of compound **1f** were brought about by the addition of benzylamine.

Synthesis of the acetamide adducts 5

(*a*) Acetamide (0.52 g; 8.8 mmoles) was added to the hot solution of compound **2a** (2.0 g; 3.8 mmoles) in anhydrous benzene (20 ml). The mixture was heated to the boiling point and allowed to cool to obtain colorless crystals (2.2 g; 90%) of the adduct **5a**, which were purified by extraction with boiling methanol; mp. 188—190 °C.

$C_{14}H_{16}N_4O_5$ (320.3). Calcd. C 52.49; H 5.04; N 17.49. Found C 52.31; H 5.29; N 17.45%. IR (KBr): 3400, 3250, 2950, 1740, 1665 cm^{-1}.

FT ^1H NMR (DMSO-d_6 + $CDCl_3$; TMS): δ 1.25 t + 4.16 qu, $J = 7$ Hz, COOEt; 1.82 s, Ac of $AcNH_2$; 1.84 s, Ac of **5a**; 5.96 s, OCH_2O of **5a**; 6.38 s, OCH_2O of **1a**; 6.45 d, $J = 9$ Hz (collapses into a s on addition of D_2O), 4-H of **5a**; 6.56 s + 6.61 s, 5-H + 8-H of **5a**; 7.04 s, 2-H of **5a**; 7.36 s + 7.58 s, 5-H- + 8-H of **1a**; 8.4 d, exchangeable, N**H**Ac of **5a**; 9.02 s, 2-H of **1a**; 9.48 s, exchangeable, N**H**COOEt of **5a**; 9.89 s, 4-H of **1a**. As shown by the relative intensity of the corresponding signals, the ratio of **5a** and **1a** was approximately 3 : 1.

(*b*) Acetamide (0.45 g; 7.6 mmoles) was added to the hot solution of compound **2b** (2.0 g; 3.6 mmoles) in anhydrous dioxane. The mixture was treated as described above to obtain colourless crystals (2.3 g; 95%) of the adduct **5b**, which were purified by extraction with boiling methanol; mp. 185—187 °C.

$C_{15}H_{18}N_4O_5$ (334.3). Calcd. C 53.89; H 5.43; N 16.76. Found C 54.14; H 5.66; N 16.81%. IR (KBr): 3400, 3180, 2980, 1750, 1650 cm^{-1}.

FT ^1H NMR (DMSO-d_6 + $CDCl_3$; TMS): δ 1.23 t + 4.13 qu, $J = 7$ Hz, COOEt; 1.79 s, Ac of $AcNH_2$; 1.84 s, Ac of **5b**; 2.00 s, 2-Me of **5b**; 2.77 s, 2-Me of **1b**; 5.94 s, OCH_2O of **5b**; 6.36 s, OCH_2O of **1b**; 6.36 d, $J = 9$ Hz (collapses into a s on addition of D_2O), 4-H of **5b**; 6.52 s + 6.56 s, 5-H + 8-H of **5b**; 7.39 s + 7.53 s, 5-H + 8-H of **1b**; 8.43 d, $J = 9$ Hz, exchangeable, N**H**Ac of **5b**; 9.45 bs, exchangeable, N**H**COOEt of **5b**; 9.68 s, 4-H of **1b**. The ratio of **5b** and **1b** was approximately 5 : 2.

MS (160 °C), m/z (% rel. int.): 334 (3.3 $M^{+\cdot}$), 276 (6.8), 275 (15), 246 (15), 230 (12), 204 (9.5), 203 (15), 189 (18), 188 (100), 187 (23), 161 (9.5), 120 (30).

Irradiations and work-up of the irradiation mixtures

The starting compounds **1**, **2** and **5** were dissolved at room temperature with stirring in the solvents indicated in Table I and containing already the added reagents (if any). The solutions were flushed with argon and irradiated with HPH-125 high-pressure mercury immersion lamps (Philips) until, according to TLC (Kieselgel G; benzene–MeOH, 10 : 1, or benzene–acetone, 1 : 1; detection: iodine vapour or UV light), the starting substances were completely used up. A slow stream of argon was introduced into the gradually darkening solutions throughout the whole irradiation period.

The resulting mixtures were evaporated to dryness in vacuum. The residues resulting from the irradiations performed in solvent amines were taken up in benzene or xylene, and the mixtures were evaporated again; in order to remove traces of the amines, this procedure was repeated several times. The dry residue resulting from the irradiation of compound **2b** and acetamide in dioxane was triturated with water to obtain the crystalline fraction **A**. The aqueous filtrate of the latter was extracted with chloroform, the organic layer dried ($MgSO_4$) and evaporated to dryness; the aqueous layer which contained only acetamide was discarded.

The dry residues obtained after removal of the excess amines, and of the excess acetamide and fraction **A**, respectively, were dissolved in benzene or methanol. Kieselgel 60 (Merck, 0.063—0.200 mm, 3 g) was added, and the mixtures were evaporated to dryness. The residues were transferred onto columns (prepared from 60 g of Kieselgel 60 with benzene) and chromatographed first with pure benzene and then with benzene–acetone mixtures in which the amount of the polar component was gradually increased so as to end up with 1 : 1 (vol/vol) benzene–acetone mixtures. Fractions of about 10 ml of the eluate were collected and examined by TLC. Those containing the same products were combined and evaporated to dryness in vacuum. The residues were, in general, recrystallized (ethyl carbamate was purified by sublimation at 2670 Pa = 20 Torr/100 °C, bath temperature) to yield the fractions **B**.

In those cases where the attempts at obtaining crystalline fractions **B** failed, the residues were worked up by preparative TLC (Kieselgel $PF_{254+366}$; solvents: benzene–acetone or benzene–dioxane, 5 : 1—1 : 1, benzene–MeOH, 5 : 1, or acetonitrile; detection: UV light or iodine vapour) to obtain the fractions **C**; the filtrates of the crystalline fractions **B** were worked up by the same method.

The smaller runs (where the crude mixture of products was not more than 0.5 g) were worked up, without previous column chromatography, directly by preparative TLC (as above) to obtain the fractions **D**.

For the yields, see Table I.

R_f values (adsorbent Kieselgel; solvent benzene–acetone, 1 : 1): **6a**: 0.6; **6b** = **6c**: 0.6; **7b**: 0.6; **8b**: 0.7; **9a**: 0.3; **9b**: 0.6; **11b**: 0.7; **12b** = **12c**: 0.5; **12e** = **12f**: 0.45; **13a** = **13d**: 0.6; **13b** = **13c** = **13f**: 0.7; **14a** = **14b** = **14d** = **14e**: 0.9; **14c** = **14f**: 0.7; acetone condensation product of benzohydrazide (**15c** = **15f**): 0.5; acetone condensation product of ethyl carbazate (**15a** = **15b** = **15d** = **15e**): 0.4; **16**: 0.95; **17**: 0.8; **20a**: 0.8; **20b**: 0.8; **21**: 0.8

The known compounds **12b** = **12c** [3], **12e** = **12f** [2], **13a** = **13d** [6], **13b** = **13c** = **13e** = **13f** [6], ethyl carbamate (**14a**, *etc.*), benzamide (**14c** = **14f**), the acetone condensation products of benzohydrazide (**15c** = **15f**) [7] and of ethyl carbazate (**15a**, *etc.*) [8], **16** [9], **17** [8], and **20b** [4] were identified by comparison (mp., mixed mp., TLC, IR spectrum) with authentic samples obtained as described in the literature.

13a (= **13d**), MS (120 °C), *m/z* (% rel. int.): 246 (56, $M^{+\cdot}$), 229 (24), 217 (7), 204 (48), 203 (7), 191 (16), 190 (100), 189 (27), 173 (16), 163 (8).

13b (*etc.*), MS (90 °C), *m/z* (% rel. int.): 260 (52, $M^{+\cdot}$), 245 (22), 243 (29), 231 (5), 218 (22), 217 (4), 205 (15), 204 (100), 203 (15), 187 (15).

Authentic samples of the new compounds **6a**, **6b** = **6c**, **7b**, **8b**, **9a**, **9b**, **10a**, **10b**, **20a** and **21** were obtained as described below; the photoproducts proved in all cases identical (m.p., mixed m.p., TLC, IR spectrum) with the corresponding samples. No authentic sample of the new compound **11b** has been obtained; however, this compound was formed also on irradiation of 2-methyl-6,7-methylene-dioxyquinazoline (**12b**) in dioxane as described below.

Irradiation of 2-methyl-6,7-methylenedioxyquinazoline (12b) in dioxane

A solution of compound **12b** (56 mg; 0.35 mmoles) in anhydrous dioxane (100 ml) was irradiated with a HPK-125 lamp under argon until the starting substance was completely used up (25 h). The resulting mixture was worked up by preparative TLC (solvent: benzene–acetone, 1 : 1), to obtain 5% of compound **11b**, m.p. 228 °C (benzene).

$C_{14}H_{14}N_2O_4$ (274.3). Calcd. C 61.31; H 5.15; N 10.21 Found C 61.43; H 5.45; N 10.49%.

UV (EtOH): 224 (4.33), sh; 236 (4.38); 290 (3.58), sh; 307 (3.67), sh; 316 (3.88); 333 (3.91).

^1H NMR ($CDCl_3$, TMS): δ 2.8 s, 3H, 2-Me; 3.8—4.15 m, 6H, and 5.15 dd, J = 8.5 and 4.5 Hz, 1H, dioxanyl group; 6.1 s, 2H, OCH_2O; 7.2 s, 1H, and 7.55 s, 1H, 5-H + 8-H.

MS (90 °C), *m/z* (% rel. int.): 274 (14, $M^{+\cdot}$), 273 (4.5), 246 (7.2), 244 (5.0), 243 (6.5), 229 (6.0), 217 (30), 216 (35), 215 (100), 188 (8.5), 187 (17), 147 (7.0).

No attempt was made to elucidate the structures of the other products of irradiation.

Dark reactions of the amidates 1c and 1d with butylamine

The amidates were dissolved in butylamine (for the relative amounts of the reagents see Table II) as described for the photoreactions, and allowed to stand for 100 h at room temperature. Work-up of the resulting mixtures was identical with that used in the irradiation experiments. For the yields, see Table II.

6,7-Methylenedioxy-4-methylthioquinazoline (11Aa) and its 2-methyl derivative (11Ab)

(*a*) 1*N* NaOH (14.5 ml) was added to a suspension of 6,7-methylenedioxy-4(3*H*)-quinazolinethione [1] (3.0 g; 14.5 mmoles) in methanol (90 ml), and the resulting yellow solution treated with methyl iodide (1.15 ml; 18 mmoles). The crystals of the *S*-methyl derivative **11Aa** soon started to precipitate. The mixture was stirred for an additional 30 min, the product was separated, washed, dried and recrystallized from ethanol (150 ml) to obtain 1.7 g (53%) of **11Aa** as colourless needles, m.p. 190—191 °C.

$C_{10}H_8N_2O_2S$ (220.3). Calcd. N 12.72; S 14.56. Found N 12.53; S. 14.54%.

UV (EtOH): 217 (4.23); 236 (4.28); 250 (4.24), sh; 282 (3.88), sh: 325 (4.08); 340 (4.15).

^1H NMR ($CDCl_3$; TMS): δ 2.7 s, 3H, *S*-Me; 6.1 s, 2H, OCH_2O; 7.17 s, 1H, and 7.25 s, 1H, 5-H + 8-H; 8.82 s, 1H, 2-H.

(*b*) The 2-methyl derivative (**11Ab**) of the above compound, m.p. 205—206 °C, was similarly obtained in 51% yield starting with 2-methyl-6,7-methylenedioxy-4(3*H*)-quinazolinethione [1] (4.4. g; 20 mmoles), 1*N* NaOH (20 ml), methanol (120 ml) and methyl iodide (1.6 ml; 25 mmoles).

$C_{11}H_{10}N_2O_2S$ (234.3). Calcd. C 56.39; H 4.30; N 11.96. Found C 56.44; H 4.35; N 12.14%.

UV (EtOH): 205 (4.18), sh; 213 (4.28); 233 (4.32); 245 (4.32); 308 (3.79), sh; 314 (3.81), sh; 330 (4.07); 344 (4.13), in agreement with the spectra of model compounds described in Ref. [1].

Synthesis of authentic samples of compounds 6a, 6b = 6c, 7b, 8b, 10a and 10b

(*a*) A mixture of compound **11Aa** (0.44 g; 2 mmoles) and butylamine (20 ml) was refluxed for 70 h and evaporated to dryness in vacuum. The residue was recrystallized from benzene (10 ml) to obtain 0.32 g (65%) of compound **6a**, m.p. 206 °C.

$C_{13}H_{15}N_3O_2$ (245.3). Calcd. C 63.66; H 6.16; N 17.13. Found C 63.63; H 6.35; N 17.39%.

UV (EtOH): 210 (4.34); 222 (4.20), sh; 242 (4.40); 278 (3.79); 290 (3.82); 306 (3.86), sh; 3.18 (4.05); 328 (3.92), sh; 333 (4.03).

^1H NMR ($CDCl_3$; TMS): δ 1.9 distorted t, + 1.35—1.9 m, + 3.6 m, *n*-Bu; 5.35 bs, NH; 6.05 s, OCH_2O; 6.95 s and 7.15 s, 5-H and 8-H; 8.55 s, 2-H.

(*b*) A mixture of compound **11Ab** (0.23 g; 1 mmole) and butylamine (10 ml) was refluxed for 30 h and evaporated to dryness in vacuum. The residue was recrystallized from benzene (3 ml) to obtain 0.15 g (58%) of compound **6b** (= **6c**), m.p. 193 °C.

$C_{14}H_{17}N_3O_2$ (259.3). Calcd. C 64.65; H 6.61; N 16.21. Found C 64.59; H 6.50; N 16.03%.

UV (EtOH): 212 (4.40); 224 (4.22), sh; 246 (4.42); 281 (3.78); 292 (3.77); 326 (4.02); 340 (3.98).

^1H NMR ($CDCl_3$; TMS): δ 0.97 distorted t, 3H, + 1.4—1.8 m, 4H, + 3.7 m, 3H, *n*-Bu; 2.6 s, 3H, 2-Me; 5.6 bs, 1H, NH; 6.05 s, 2H, OCH_2O; 7.05 s, 1H, and 7.10 s, 1H, 5-H + 8-H.

MS (85 °C), *m/z* (% rel. int.): 259 (45, $M^{+\cdot}$), 258 (7.3), 244 (4.5), 230 (45), 217 (23), 216 (24), 203 (100), 202 (2.0), 188 (18), 187 (39), 163 (3.9), 147 (7.7), 120 (2.9).

(*c*) A mixture of compound **11Ab** (0.23 g; 1 mmoles) and benzylamine (10 ml) was kept for 10 h at 130 °C, and evaporated to dryness in vacuum. The residue was triturated with ether to obtain 0.08 g (27%) of compound **7b**, m.p. 198—200 °C (benzene).

$C_{17}H_{15}N_3O_2$ (293.3). Calcd. C 69.61; H 5.15; N 14.33. Found C 69.72; H 5.19; N 14.25%.

UV (EtOH): 213 (4.45); 222 (4.26), sh; 245 (4.47); 280 (3.77); 288 (3.77); 324 (4.01); 336 (3.94).

^1H NMR ($CDCl_3$; TMS): δ 2.64 s, 3H, 2-Me; 4.9 d, 2H, CH_2NH; 6.1 s, 2H, OCH_2O; 7.0 s, 1H, and 7.2 s, 1H, 5-H + 8-H; ~7.4, 1H (partly covered by the Ph signal), NH; 7.48 s, 5H, Ph.

MS (135 °C), *m/z* (% rel. int.): 293 (100, $M^{+\cdot}$), 292 (23), 216 (5.2), 188 (57), 187 (17), 147 (22), 120 (6.6), 106 (72), 91 (27).

(*d*) A mixture of compound **11Ab** (0.23 g; 1 mmole) and morpholine (10 ml) was refluxed for 10 h and evaporated to dryness. The residue was recrystallized from benzene to obtain 0.1 g (37%) of compound **8b**, m.p. 187 °C.

$C_{14}H_{15}N_3O_3$ (273.3). Calcd. C 61.53; H 5.53; N 15.38. Found C 61.61; H 5.45; N 15.43%.

UV (EtOH): 218 (4.38); 230 (4.27), sh; 250 (4.32); 285 (3.78); 294 (3.72); 339 (4.01).

^1H NMR ($CDCl_3$; TMS): δ 2.65 s, 3H, 2-Me; 3.57 t, 4H, and 3.94 t, 4H, J = 4.5 Hz, morpholino group; 6.10 s, 2H, OCH_2O; 7.15 s, 1H, and 7.20 s, 1H, 5-H + 8-H.

MS (110 °C), *m/z* (% rel. int.): 273 (100, $M^{+\cdot}$), 272 (43), 242 (27), 228 (32), 216 (95), 215 (60), 203 (4.2), 202 (7.3), 188 (98), 187 (57), 147 (49), 120 (9.7).

(*e*) A mixture of compound **11Aa** (1.0 g; 4.5 mmoles) and ammonium acetate (10 g) was kept for 20 min at 180 °C. The resulting melt solidified when allowed to cool. The solid was triturated with water and made alkaline with 10% aqueous NaOH to obtain 0.64 g (74%) of compound **10a**, m.p. above 320 °C (dec).

$C_9H_7N_3O_2$ (189.2). Calcd. C 57.14; H 3.73; N 22.21. Found C 57.19; H 3.43; N 22.31%.

UV (EtOH): 210 (3.98); 223 (3.98), sh; 243 (4.26); 253 (4.11), sh; 278 (3.66); 298 (3.60), sh; 320 (3.73); 333 (3.72).

(*f*) A mixture of compound **11Ab** (1.5 g; 6.4 mmoles) and ammonium acetate (15 g) was kept for 20 min at 190 °C. The resulting melt solidified when allowed to cool, and was triturated with water to obtain 1.0 g (76%) of compound **10b**, m.p. 304 °C (BuOH).

$C_{10}H_9N_3O_2$ (203.2). Calcd, C 59.10; H 5.32; N 20.72. Found C 59.27; H 4.94; N 20.51%.

MS (120 °C), *m/z* (% rel. int.): 203 (100, $M^{+\cdot}$), 202 (6.5), 188 (3.0), 187 (5.5), 186 (3.5), 163 (16), 162 (7.8), 161 (4.8), 145 (3.0), 104 (9.3), 101 (6.9).

The same compound was obtained in about 10% yield when 2-cyano-4,5-methylenedioxyacetanilide [4] was treated with ethanolic ammonia for 20 h at 190 °C.

Acetylation of 4-amino-6,7-methylenedioxyquinazoline 10a and of its 2-methyl derivative 10b

(*a*) A mixture of compound **10a** (0.30 g; 1.6 mmoles), acetic anhydride (0.4 ml; 3.6 mmoles) and anhydrous dioxane (25 ml) was refluxed for 8 h and treated with Norite to obtain on cooling 0.28 g (76%) of compound **9a**, m.p. 227 °C.

$C_{11}H_9N_3O_3$ (231.2). Calcd. C 57.14; H 3.92; N 18.17. Found C 57.07; H 3.93; N 18.10%.

IR (KBr): 3400—2700 b, 1690 with sh at 1700 cm^{-1}.

UV (EtOH): 204 (3.95); 227 (4.28), sh; 244 (4.48); 278 (3.74), sh; 309 (3.81), sh; 320 (3.99); 333 (4.05).

^1H NMR (DMSO-d_6; DMSO-d_5 = 2.50 ppm): δ 2.3 s, 3H Ac; 6.3 s, 2H, OCH_2O; 7.33 s, 1H, and 7.55 s, 1H, 5-H + 8-H; 8.87 s, 1H, 2-H.

(*b*) A mixture of compound **10b** (70 mg; 0.34 mmole), acetic anhydride (0.04 ml; 0.38 mmole) and anhydrous dioxane (5 ml) was refluxed for 1 h to obtain 60 mg (72%) of compound **9b**, colourless needles, m.p. 282 °C (dioxane), which were washed with ether.

$C_{12}H_{11}N_3O_3$ (245.2). Calcd. C 58.77; H 4.52; N 17.13. Found C 58.88; H 4.41; N 17.26%.

IR (KBr): 3400, 1690 cm^{-1}.

UV (EtOH): 206 (4.12); 224 (4.38), sh; 243 (4.55); 280 (3.65), sh; 323 (3.96); 337 (3.97), sh; 339 (3.99).

^1H NMR (DMSO-d_6; DMSO-d_5 = 2.50 ppm): δ 2.2 s, 3H, Ac; 2.5 s, 3H, 2-Me; 6.15 s, 2H, OCH_2O; 7.15 s, 1H, and 7.35 s, 1H, 5-H + 8-H.

MS (135 °C), *m/z* (% rel. int.): 245 (62, $M^{+\cdot}$), 244 (23), 230 (54), 203 (100), 202 (6.5), 188 (6.3), 187 (29), 163 (22), 162 (11), 161 (8.0), 104 (10).

Deacetylation of 4-acetylamino-6,7-methylenedioxyquinazoline 9a and its 2-methyl derivative 9b by methanol

(*a*) A methanolic solution of compound **9a** was allowed to stand at room temperature overnight. The deacetylated product **10a** was detected by TLC. After 2 weeks **9a** was almost completely converted (TLC) into **10a**, which could be recovered in 90% yield, based on the amount of compound **9a** introduced.

(*b*) When a methanolic solution of compound **9b** was treated similarly, **10b** could be detected (TLC) only after 3 days; and after two weeks part of compound **9b** was still unchanged. Preparative work-up of the solution at this point furnished 60% of unchanged **9b** and 30% of **10b**, based on the amount of compound **9b** introduced.

Attempted photochemical deacetylation of 4-acetylamino-6,7-methylenedioxyquinazoline 9a

A solution of compound **9a** (0.13 g) in a mixture of CH_2Cl_2 (100 ml) and acetic acid (0.5 ml) was allowed to stand for 12 h at room temperature. No traces of the deacetylated product **10a** could be detected by TLC. Subsequently the solution was irradiated (HPK-125 lamp) for 15 h, and evaporated to dryness. The residue was triturated with ether to obtain 94% of unchanged starting material.

2-Formylamino-4,5-methylenedioxybenzaldehyde (20a)

Acetic formic anhydride (0.15 ml) was added to a mixture of 2-amino-4,5-methylenedioxybenzaldehyde [4] (0.16 g; 1 mmole) and dry CH_2Cl_2 (5 ml). The mixture was stirred for 1 h at room temperature during which time a clear solution formed, from which subsequently the title compound, 0.12 g (62%), yellow needles, m.p. 194—195 °C (EtOH), started to separate.

$C_9H_7NO_4$ (193.1). Calcd. C 55.97; H 3.65; N 7.25. Found C 55.86; H 4.21; N 7.47%.

2-Amino-4,5-methylenedioxyacetophenone (21)

A slurry of the 2-nitro analogue [10] (10.5 g; 50 mmoles) in ethanol (250 ml) was reduced in the presence of a 8% Pd—C catalyst at room temperature. After the calculated amount of hydrogen had been adsorbed, the mixture was heated up to its b.p. and filtered hot. The filtrate was concentrated to about 1/5 of its original volume to obtain 6.0 g (67%) of the title compound, m.p. 170—171 °C (EtOH).

$C_9H_9NO_3$ (179.2). Calcd. C 60.33; H 5.10; N 7.82. Found C 60.02; H 4.91; N 8.08%. IR (KBr): 3380, 3280, 1625 cm^{-1}.

*

The authors are grateful to Mrs. I. Balogh-Batta and staff for the microanalyses, to Dr. P. Kolonits and staff for the IR and ^1H NMR spectra, to Dr. L. Radics for the FT ^1H NMR spectra and to Mrs. I. Balogh-Batta and Dr. F. Ruff for the UV spectra.

REFERENCES

[1] Barta-Szalai, G., Fekete, J., Fetter, J., Lempert, K., Møller, J.: Acta Chem. Scand., **B33**, 79 (1979)
[2] Fetter, J., Lempert, K., Barta-Szalai, G., Møller, J., Párkányi, L.: Acta Chim. (Budapest) **94**, 233 (1977)
[3] Fetter, J., Lempert, K., Møller, J.: Tetrahedron, **31**, 2559 (1975)
[4] Bogert, M. T., Elder, F. R.: J. Am. Chem. Soc., **51**, 537 (1929)
[5] Castellano, A., Catteau, J. P., Lablache-Combier, A., Planckaert, B.: Tetrahedron Letters, **1973**, 4185; and earlier references cited therein
[6] Fetter, J., Barta-Szalai, G., Jaber, A., Bertha, F.: Periodica Polytechn. Budapest, Ser. Chem. Engng., **22**, 143 (1978)
[7] Grammaticakis, P.: Bull. chim. soc. France, **1950**, 690
[8] de Graaf, H.: Diss., Leiden, 1930; Chem. Abstr. **24**, 5724 (1930)
[9] Bergmann, M.: Ber., **53**, 979 (1920)
[10] Mosettig, E., Czadek, K.: Monatsh. Chem., **57**, 291 (1931)
[11] Beaumont, D., Waigh, R. D.: Chem. and Ind., **1978**, 808

Gizella Barta-Szalai
József Fetter
Károly Lempert
H-1111 Budapest, Gellért tér 4.

Jørgen Møller
Campusvej 55, DK-5230 Odense M, Denmark

Acta Chimica Academiae Scientiarum Hungaricae, Tomus 104 (3), pp. 267—271 (1980)

SYNTHESIS OF THE TRIETHYL ESTERS OF 1-HALOGENOBUTANE-1,4,4-TRICARBOXYLIC ACIDS

M. INCZE, F. SÓTI and CS. SZÁNTAY

(Central Research Institute for Chemistry of the Hungarian Academy of Sciences, Budapest)

Received July 25, 1979

Accepted for publication August 23, 1979

A method of preparation of triethyl 1-chloro- and 1-bromobutane-1,4,4-tricarboxylate is described.

The triethylester **1**, not yet described in the literature, was needed in our laboratory for syntheses of natural organic compounds.

The synthetic route attempted was the alkylation of diethyl malonate with ethyl α, γ-dihalogenobutyrate (**2**).

Of the esters of α,γ-dihalogenobutyric acids, the dibromo- and the dichloro derivatives have been reported in the literature; the former can be synthesized from γ-butyrolactone [1] or from cyclopropanecarboxylic acid [2], the latter from γ-butyrolactone [3]. Compounds **2a** and **2b** were prepared in our laboratory in a way even simpler than that described in the literature.

However, we did not succeed in our attempts of isolating **1a** from the product of the reaction between the sodium salt of diethyl malonate and **2a**. Even a wide variation of the experimental conditions afforded only the cyclobutane derivative **3**, a new compound, whose structure was evident from the NMR spectrum.

The intramolecular alkylation of the primary product **1a** is probably much more rapid than the reaction leading to its formation, thus the isolation of **1a** is very difficult under the experimental conditions used. Neither did the situation change when a solution of the sodium salt of diethyl malonate was added to **2a** present in great excess, nor when a solution of sodium ethoxide was slowly added to the common solution of diethyl malonate and **2a**.

A similar result was obtained when the less reactive **2b** was used instead of **2a**. The former was prepared by the chlorination of butyrolactone and subsequent esterification of the resulting α,γ-dichlorobutyric acid by means of ethanol containing hydrogen chloride.

The reaction could be effected, however, when the alkylating agent was ethyl α-chloro-γ-bromobutyrate (**2c**): the required derivative **1b** formed in a yield of 17.5%.

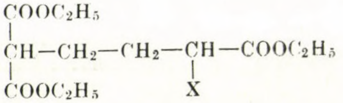

$$\underset{COOC_2H_5}{\overset{COOC_2H_5}{CH}}-CH_2-CH_2-\underset{X}{CH}-COOC_2H_5$$

1a,b

1a X = Br

b X = Cl

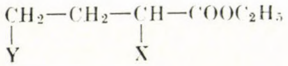

$$\underset{Y}{CH_2}-CH_2-\underset{X}{CH}-COOC_2H_5$$

2a—c

2a X = Y = Br

b X = Y = Cl

c X = Cl, Y = Br

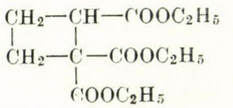

3

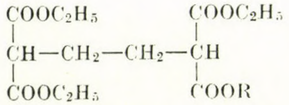

$$\underset{COOC_2H_5}{\overset{COOC_2H_5}{CH}}-CH_2-CH_2-\underset{COOR}{\overset{COOC_2H_5}{CH}}$$

4a,b

4a R = C_2H_5

b R = H

Compound **2c** was prepared by converting butyrolactone with hydrogen bromide into γ-bromobutyric acid, making its acid chloride by means of thionyl chloride, subsequent chlorination with sulfuryl chloride and, finally, esterification with ethanol.

The bromo-derivative **1a** was yet prepared in a different way. The tetraethyl ester **4a** is readily obtained [4] from ethyl malonate and ethylene dibromide, and can then be selectively hydrolyzed to **4b**. This product was converted into the desired compound by Hunsdiecker reaction (HgO, and treatment with bromine; yield 61%).

Experimental

M.p.'s and b.p.'s are uncorrected. The former were determined on a Koffler apparatus. NMR spectra were recorded with a Varian XL-100 instrument using TMS as internal standard.

Ethyl α,γ-dibromobutyrate (2a)

Below the surface of a vigorously agitated and ice-cooled mixture of γ-butyrolactone (21.5 g; 0.25 mole) and red phosphorus (2.95 g; 0.095 mole), bromine (13.3 ml, 0.26 mole) was introduced dropwise (20 min) at 20—30 °C internal temperature. The mixture was warmed to 70 °C and a further portion (13.3 ml; 0.26 mole) of bromine was introduced below the surface during 30 min, with stirring. After stirring at 70 °C for 3h more, the mixture was cooled to room temperature, and anhydrous ethanol (58.5 ml; 1.0 mole) was very carefully introduced below the surface; the mixture was then allowed to stand overnight. The volatile components were removed in a rotary evaporator, the residue was diluted with ether (50 ml), washed with six 20-ml portions of 3% sodium hydrogen carbonate solution, and dried over magnesium sulfate. After evaporating the solvent, the residue was repeatedly distilled under reduced pressure, b.p. 62—63 °C at 3 mm-Hg; yield: 49.3 g (72%); n_D^{25} 1.4942.

Triethyl cyclobutane-1,1,2-tricarboxylate (3)

Sodium metal (1.15 g; 0.05 mole) was dissolved in anhydrous ethanol (25 ml). At 50 °C diethyl malonate (8.25 g; 7.8 ml; 0.0515 mole), and then, at 50—55 °C ethyl 2,4-dibromobutyrate were added dropwise during 15 min, with stirring. The resulting mixture was refluxed until it became neutral (about 1.5 h). The alcohol was removed in a rotary evaporator, the residue diluted with water (20 ml) and the liquid layer was separated. The lower, organic, layer was taken up in ether (50 ml) and washed with three 30-ml portions of water. The ethereal solution was dried ($MgSO_4$), and the solvent evaporated to leave a thick, viscous oil (15.3 g) which was studied by gas chromatography. The chromatograms revealed the presence of a third substance besides the two starting materials; this (5.9 g; 43.4%) was separated by means of fractional distillation (b.p. 148—150 °C at 11 mm-Hg). Analyses and NMR spectra proved this substance to be the triethyl ester of cyclobutane-1,1,2-tricarboxylic acid.

^{1}H NMR ($CDCl_3$): δ (ppm) 1.24 (t, $J = 7$ Hz, 6H, 2 $-CH_3$); 1.27 (t, $J = 7$ Hz, 3H, $-CH_3$); 2.05—2.8 (m, 4H, 2 $-CH_2-$); 3.65—3.85 (m, 1H, $-\overset{|}{C}H-$); 4.15 (q, $J = 7$ Hz, 2H, $-OCH_2-$); 4.20 (q, $J = 7$ Hz, 2H, $-OCH_2-$); 4.25 (q, $J = 7$ Hz, 2H, $-OCH_2-$).

^{13}C NMR ($CDCl_3$): δ (ppm) 14.02, 14.02, and 14.14(q, 3 $-CH_3$); 19.97 (t, C-3); 26.73 (t, C-2); 43.56 (d, C-4); 55.55 (s, C-1); 60.76, 61.55 and 61.66 (q, 3 $-OCH_2-$); 169.57, 170.66, and 171.90 (s, 3 $-CO-$).

$C_{13}H_{20}O_6$ (272.29). Calcd. C 57.34; H 7.40. Found C 57.02; H 7.37%.

α,γ-Dichlorobutyric acid

Chlorine gas was passed, with stirring, into γ-butyrolactone (285 gr; 3.0 moles) maintained between 125 and 150 °C, for 6 h. The reaction mixture was allowed to cool, then it was washed twice with water (100 ml portions), dried ($MgSO_4$) and finally distilled under reduced pressure. Unchanged γ-butyrolactone was the first fraction followed by the product (b.p. 88—90 °C at 3 mm-Hg; 120.4 g; 33.3%).

^{1}H NMR ($CDCl_3$): δ (ppm) 2.3—2.6 (m, 2H, $-CH_2-$); 3.76 (dd, $J_{3,2A} = 6$ Hz, $J_{3,2B} = 7$ Hz, 2H, $-CH_2Cl$); 4.63 (dd, $J_{1,2A} = 6$ Hz, $J_{1,2B} = 8$ Hz, 1H, $-CHCl-$); 8.7 (s, 1H, exchangeable, OH).

$C_4H_6O_2Cl_2$ (157.00). Cacld. C 31.59; H 3.94; Cl 42.46. Found C 31.68; H 4.02; Cl 42.50%.

Ethyl α,γ-dichlorobutyrate (2b)

A solution of hydrogen chloride in ethanol (100 ml) was added to α,γ-dichlorobutyric acid (13 g; 0.083 mole) and the mixture was allowed to stand for 2 days at room temperature. The solvent was then removed in a rotary evaporator. The residue was taken up in ether (50 ml) and washed with water (six 50 ml portions) until neutral. The ethereal solution was dried ($MgSO_4$), the solvent evaporated and the residue distilled under reduced pressure, b.p. 58—60 °C at 3 mm-Hg. The yield was 10.2 g (66.7%).

$C_6H_{10}O_2Cl_2$ (185.05). Calcd. C 38.94; H 5.45; Cl 38.32. Found C 38.79; H 4.98; Cl 38.37%.

γ-Bromobutyric acid

γ-Butyrolactone (86 g; 1.0 mole) was refluxed (120—130°) in 48% aqueous hydrogen bromide solution (300 ml) for 24 h. After cooling, the reaction mixture was diluted with water (150 ml) and extracted with ether (5 portions, 150 ml each). The ethereal solution was dried ($MgSO_4$), and the ether was evaporated. The residual γ-bromobutyric acid (60.8 g; 36.4%) was used directly in the synthesis of its chloride.

γ-Bromobutyric acid chloride

At strict exclusion of moisture, crude γ-bromobutyric acid (52.5 g) was refluxed at 70 °C in distilled thionyl chloride (30 ml) until the evolution of gas had stopped (3 h). The excess thionyl chloride was distilled off in a rotary evaporator and the residue distilled under reduced pressure; b.p. 97—98 °C at 36 mm-Hg; yield 46.1 g (79%).

Ethyl α-chloro-γ-bromobutyrate (2c)

γ-Bromobutyric acid chloride (46.1 g; 0.25 mole) was refluxed at 70 °C for 24 h, in an atmosphere of nitrogen, in distilled sulfuryl chloride (160 ml) to which iodine (1 g) had been added. The excess sulfuryl chloride was removed in a rotary evaporator and from the crude α-chloro-γ-bromobutyric acid chloride its ethyl ester was prepared directly.

The crude acid chloride was added by drops into anhydrous ethanol (80 ml) which was stirred and cooled in an ice-bath. Stirring was continued for 1 h after the admixture of the acid chloride. The excess alcohol was then evaporated, the residue taken up in ether (100 ml) and washed subsequently with a 10% solution of sodium thiosulfate, water, 3% sodium hydrogen carbonate, and with water again. The ethereal solution was dried ($MgSO_4$), the ether evaporated, and the residue distilled under reduced pressure to give 10 g (17%) of the product b.p. 64—66 °C at 2 mm-Hg.

$C_6H_{10}O_2ClBr$ (229.51). Calcd. C 31.40; H 4.39; Br 34.80; Cl 15.45. Found C 31.22; H 4.61; Br 35.15; Cl 15.40%.

Triethyl 1-chlorobutane-1,4,4-tricarboxylate (1b)

To an agitated mixture of diethyl malonate (48.0 g; 0.3 mole) and ethyl α-chloro-γ-bromobutyrate (22.95 g; 0.1 mole) there was added by drops a solution of sodium ethoxide prepared from pure ethanol (120 ml) and sodium metal (2.3 g; 0.1 mole); the temperature was maintained between 5 and 10 °C. Stirring, first at 15 °C for 7 h, then at room temperature was continued until the reaction mixture became neutral (2 days). The solvent was then removed under reduced pressure; the lower, organic, layer was diluted with ether (150 ml), washed with three 100-ml portions of water-dried ($MgSO_4$), the solvent evaporated, and the product re-distilled in vacuum on a 40 cm Vigreux column to yield 5.4 g (17.5%) of **1b**, b.p. 150—155 °C at 3 mm-Hg.

^1H NMR ($CDCl_3$): δ (ppm) 1.27 (t, $J = 7$ Hz, 6H, 2 $-CH_3$); 1.30 (t, $J = 7$ Hz, 3H, $-CH_3$); 1.95—2.15 (m, 4H, 2 $-CH_2-$); 3.25—3.45 (m, 1H, $-\overset{|}{C}H-$); 4.22 (q, $J = 7$ Hz, 4H, 2 $-OCH_2-$); 4.25 (q, $J = 7$ Hz, 2H, $-OCH_2-$); 4.25 (in overlap, 1H, $-CHCl-$).

$C_{13}H_{21}O_6Cl$ (308.76). Calcd. C 50.57; H 6.86; Cl 11.48. Found C 50.49; H 6.78; Cl 11.51%.

Tetraethyl butane-1,1,4,4-tetracarboxylate (4a)

A solution of diethyl malonate (120 g; 0.75 mole) and carbon tetrachloride (1.25 ml) in anhydrous ethanol (140 ml) was slowly added to magnesium chips (9 g), keeping the mixture in gentle boiling. To the resulting solution dibromoethane (70.5 g; 0.375 mole) was added, and the mixture was refluxed for 10 h. After cooling, 20% H_2SO_4 (110 ml) was added. The two phases were separated, the aqueous part was washed with two 50 ml portions of ether then the combined organic phase was washed with a solution of sodium chloride and with water, dried ($MgSO_4$), and the solvent was removed under reduced pressure. The residue was distilled in vacuum; b.p. 167 °C at 3 mm-Hg; the yield was 33.2 g (25.5%).

^1H NMR ($CDCl_3$): δ (ppm) 1.27 (t, $J = 7$ Hz, 12H, 4 $-CH_3$); 1.85—2.00 (m, 4H, 2 $-CH_2-$); 3.25—3.45 (m, 2H, 2 $-\overset{|}{C}H-$); 4.22 (q, $J = 7$ Hz, 8H, 4 $-OCH_2-$).

Triethyl ester of butane-1,1,4,4-tetracarboxylic acid (4b)

To an agitated and ice-cooled solution of **4a** (17.3 g; 0.05 mole) a solution of potassium hydroxide (2.8 g; 0.05 mole) in anhydrous ethanol (100 ml) was added dropwise in about 1.5 h. The ice-bath was allowed to attain room temperature and allowed to stand overnight. Next day the mixture was poured on ice (50 g) (pH 8) and the alcohol was removed in a rotary evaporator. The residue was diluted with water (50 ml), the pH adjusted to 8.5 with 1*N* NaOH, and the mixture was extracted with 3×25 ml of ether. The ether extract was dried ($MgSO_4$) and the solvent evaporated; in this way 5 g of unchanged, initial tetraethyl ester was recovered. The aqueous phase was cooled to −5 °C, mixed with ether (50 ml) and the acidity was adjusted, while stirring, to pH 2 with *conc.* phosphoric acid. After separation, the aqueous phase was washed with three 50 ml portions of ether, the combined organic solution was washed with two 50 ml portions of water and dried ($MgSO_4$); the product was finally dried to constant weight at 50 °C under reduced pressure. The desired compound was separated from the contaminant diethyl ester by means of column chromatography (SiO_2, with a 4 : 5 : 1 mixture of $CHCl_3$, cyclohexane and AcOH as the eluant) to yield 6.8 g (42.8%) of **4b**, m.p. 36–39 °C.

^1H NMR ($CDCl_3$): δ (ppm) 1.26 (t, $J = 7$ Hz, 6H, 2 $-CH_3$); 1.28 (t, $J = 7$ Hz, 3H, $-CH_3$); 1.85–2.05 (m, 4H, 2 $-CH_2-$); 3.3–3.5 (m, 2H, 2 $-CH-$); 4.22 (q, $J = 7$ Hz, 4H, 2$-OCH_2-$); 4.24 (q, $J = 7$ Hz, 2 H, $-OCH_2-$); 8.24 (s, 1H, exchangeable, OH).

$C_{14}H_{22}O_8$ (318,32). Calcd. C 52.82; H 6.97. Found C 52.85, H 6.84%.

Triethyl 1-bromobutane-1,4,4-tricarboxylate (1a)

Red mercuric oxide (2.74 g; 0.0125 mole) and the triethyl ester of butane-1,1,4,4-tetracarboxylic acid (3.98 g; 0.0125 mole) were heated together with dibromoethane (6 ml) at 160 °C. In the course of this treatment first the mercuric oxide dissolved; the heating was continued until about 6 ml of a mixture of water and solvent had been removed. After cooling to 70 °C, bromine (1.29 ml; 0.025 mole) in dibromoethane (2 ml) was added dropwise to the reaction mixture. Stirring during the nigth and next morning dilution with ether (20 ml) followed. The mercury(II) bromide which separated was filtered off, the filtrate washed with water, dried over magnesium sulfate, and the ether was evaporated. The product was purified by chromatography (SiO_2 column, 93 : 7 mixture of benzene and ethanol) and distilled, b.p. 152–155 °C at 3 mm-Hg; the yield was 5.4 g (61.62%).

^1H NMR ($CDCl_3$): δ (ppm) 1.27 (t, $J = 7$ Hz, 6H, 2 $-CH_3$); 1.30 (t, $J = 7$ Hz, 3H, $-CH_3$); 1.85–2.4 (m, 4H, 2 $-CH_2-$); 3.25–3.45 (m, 1H, $-CH-$); 4.2 (overlap, 1H, $-CHBr-$); 4.22 (q, $J = 7$ Hz, 4H, 2 $-OCH_2-$); 4.25 (q, $J = 7$ Hz, 2H, $-OCH_2-$).

$C_{13}H_{21}O_6Br$ (353.22). Calcd. C 44.20; H 5.99; Br 22.62. Found C 44.16; H 5.99; Br 22.56%.

*

The authors wish to thank the REANAL Factory of Fine Chemicals, Budapest, for financial support of this work; the Microanalytical Laboratory of this Institute for the analyses; the Spectroscopy Group under the leadership of Dr. L. Radics for help in the recording and interpretation of the NMR spectra; Mr. P. Schrammel for gas chromatography; and Mrs. J. Bischof for technical assistance.

REFERENCES

[1] Wladislaw, B.: J. Org. Chem., **26**, 711 (1961)
[2] Kizhner, N.: J. Russ. Phys.-Chem. Soc., **41**, 660 (1909); Beilstein, **2**, 285
[3] Reppe, W.: Ann., **596**, 190 (1955)
[4] Golmov, V. P., Malevannaya, Z. P.: Zh. Obshch. Khim., **31**, 665 (1961); Chem. Abstr., **55**, 22162b (1961)

Mária Incze
Ferenc Sóti
Csaba Szántay
H-1025 Budapest, Pusztaszeri út 59–67.

Acta Chimica Academiae Scientiarum Hungaricae, Tomus 104 (3), pp. 273—278 (1980)

NON-LINEAR DIELECTRIC BEHAVIOUR IN NORMAL ALCOHOLS AND WATER

J. LISZI,[1] L. MÉSZÁROS[2] and I. RUFF[3]

([1]*Department of Analytical Chemistry, The University, Veszprém,* [2]*Research Group for Electrochemistry, Hungarian Academy of Sciences, Veszprém,* [3]*Institute of Inorganic and Analytical Chemistry, Eötvös L. University, Budapest*)

Received March 2, 1979

Accepted for publication August 31, 1979

Theoretical calculations are reported on the non-linear dielectric behaviour of liquids. The differential relative permittivity and the $\Delta\varepsilon/E^2$ ratio have been calculated on the basis of the BOOTH—ONSAGER theory. For normal alcohols and water, the equation deduced yields results within the order of magnitude of the experimental data only if correction is made with respect to the KIRKWOOD *g*-factor. The experimental results indicate that the low-field static relative permittivity and the $\Delta\varepsilon/E^2$ value characterizing the non-linear behaviour of water and normal alcohols can be calculated theoretically with two different KIRKWOOD factors.

Introduction

The linear correlation between dielectric polarization and electric field becomes invalid for fields higher than 10^4 V/cm. Under such conditions the dielectric behaves non-linearly or — as this phenomenon is frequently called — dielectric saturation takes place. If the polarization is not a linear function of the field, then the **D** vector of dielectric displacement is not such either, and the field-dependence of **D** is to a first approximation [1]:

$$\mathbf{D} = \mathbf{E} + 4\pi\mathbf{P} = \varepsilon_0\mathbf{E} + 4\pi\xi E^2\mathbf{E} \tag{1}$$

Here **E** is the external (Maxwell) field, **P** the polarization, ε_0 the static relative permittivity under weak fields ($E \ll 10^4$ V/cm), and ξ the dielectric saturation factor.* Equation (1) is a heuristic relationship based on the equality $\mathbf{P(E)} = -\mathbf{P}(-\mathbf{E})$, *i.e.* on the fact that **D** is an odd function of **E**. In this approximation ξ is a phenomenological constant. Depending on whether $\xi < 0$ or $\xi > 0$, the dielectric saturation is called normal or anomalous. In this paper only liquids with normal dielectric saturation are treated.

---

* The equations in this paper correspond to the electrostatic (Gauss) convention of units common in the literature of dielectrics.

The non-linear effect is usually measured in such a way [2—6] that a weak alternating field is superimposed on a strong static one, and the differential relative permittivity,

$$\varepsilon_{\mathrm{d}} = \frac{\mathrm{d}D}{\mathrm{d}E} \tag{2}$$

is determined with this alternating field. In the approximation represented by Eq. (1), this means that

$$\varepsilon_{\mathrm{d}} = \varepsilon_0 + 12\pi\xi E^2 \tag{3}$$

The non-linear behaviour is usually characterized by the quantity [1—5]:

$$\frac{\Delta\varepsilon}{E^2} = \frac{\varepsilon_d - \varepsilon_0}{E^2} \tag{4}$$

The non-linear dielectric behaviour may be the result of several effects. Such an effect can be the anisotropy of polarization, hyperpolarization or electrostriction [1]. When special intermolecular interactions produce components with different polarizations — *e.g.* due to assocation of dipoles or hydrogen bonding —, it may be that the high field favours the form with greater polarity, and the relative permittivity of the liquid increases with increasing field. This sort of anomalous dielectric saturation has been studied in detail by PIEKARA and MAŁECKI [7—13].

The difficulties in the description of non-linear dielectric saturation arise from the fact that the $\Delta\varphi = 0$ Laplace equation cannot be applied for the determination of the cavity field (φ is the electric potential). To overcome this obstacle, THIÉBAUT *et al.* [14, 15] assumed that no large errors are introduced into the calculation of the orientation and internal field if the D/E ratio is taken as constant over the entire dielectric. With this approximation, the obtain:

$$\frac{\Delta\varepsilon}{E^2} = \frac{\varepsilon_{\mathrm{d}} - \varepsilon_0}{E^2} = \frac{4\pi N\mu_g^4}{45(kT)^3} \cdot \frac{\varepsilon_0^4(n^2+2)^4}{(2\varepsilon_0+n^2)^2\,(2\varepsilon_0^2+n^4)} \tag{5}$$

where N is the number of molecules in unit volume, μ_{g} the permanent dipole moment of the polar molecule in the gas phase, k the Boltzmann constant, T the temperature, and n the internal refraction index of the liquid. Equation (5) is however, unsuitable for the calculation of the differential relative permittivity of normal alcohols and water in agreement with experimental data. This is unequivocally shown by the comparison in Table II, in which the data were calculated using the values in Table I, where n_{D} is the refraction index for the $\mathrm{Na_D}$-line, g the KIRKWOOD-factor [16] and V is the molar volume.

Table I

Liquid	n_D^2	ε_0	μ_g/D	g	V (cm^3/mol)
Water	1.79	78.36	1.85	2.8	18.07
Methanol	1.77	32.64	1.71	2.83	40.48
Ethanol	1.85	24.3	1.70	3.10	58.37
1-Propanol	1.92	20.1	1.69	3.10	75.13
1-Butanol	1.96	17.8	1.67	3.10	91.52
1-Pentanol	1.99	13.9	1.65*	3.1*	108.69
1-Hexanol	2.01	13.3	1.63*	3.1*	125.58

* Estimated value

Table II

Dielectric saturation data at 298 K

Liquid	ε_0 (exp.)	ε_0 (calc.)	$\frac{\Delta\varepsilon}{E^2} \times 10^8$ (e.s.u.)$^{-2}$ (exp.)	$\frac{\Delta\varepsilon}{E^2} \times 10^8$ (e.s.u.)$^{-2}$ (THIÉBAUT)*	$\frac{\Delta\varepsilon}{E^2} \times 10^8$ (e.s.u.)$^{-2}$ (calc.)**
Water	78.36	79.7	−90 [4]	−4.2	−39
Methanol	32.64	31.5	−54 [5]	−1.3	−14
Ethanol	24.3	25.5	−36 [5]	−0.9	−11
1-Propanol	20.1	20.4	−27 [5]	−0.7	− 9
1-Butanol	17.8	17.1	−20 [5, 2]	−0.6	− 7
1-Pentanol	13.9	14.6	−17 [2]	−0.5	− 6
1-Hexanol	13.3	12.8	−15 [2]	−0.4	− 5

* Calculated from Eq. (5)
** Calculated from Eq. (14)

Non-linear dielectric behaviour and the Booth—Onsager equation

Based on the ONSAGER model [18], BOOTH [17] has deduced the following equation for the field dependence of the static relative permittivity ε:

$$\varepsilon = \frac{4\pi N \mu_g (n^2+2)}{3E} L \cdot \left\{ \frac{\mu_g (n^2+2) E}{2kT} \right\} \tag{6}$$

in which the simplifying assumption $\varepsilon \gg n^2$ has been exploited, and $L(x) = \operatorname{cth} x - 1/x$ is the Langevin function.

Equation (6) involves the relationship:

$$\mu = \frac{n^2 + 2}{3} \mu_g \tag{7}$$

where μ is the actual dipole moment in the liquid phase. The dielectric displacement vector can be obtained from Eqs (6) and (7):

$$\mathbf{D} = n^2 E + 4\pi N \mu L \left(\frac{3\mu E}{2kT}\right) \tag{8}$$

from which the differential relative permittivity is:

$$\varepsilon_{\mathrm{d}} = \frac{\mathrm{d}D}{\mathrm{d}E} = n^2 + 4\pi N \mu \frac{2kT}{3\mu E^2} - \left\{\frac{3\mu}{2kT \operatorname{sh}^2 \left(\frac{3\mu E}{2kT}\right)}\right\} \tag{9}$$

This equation gives, in priciple, the correct value of the differential relative permittivity for all liquids for which the ONSAGER equation is valid under low fields. Unfortunately, no experimental ε_d data are available to test the validity of Eq. (9), whereas the $\Delta\varepsilon/E^2$ ratio, which can be determined experimentally, cannot be expressed explicitly from Eq. (9). Thus, the comparison with experimental data will be made using the approximate form of this equation, which could be deduced by expanding the Langevin function in Eq. (8) and retaining only the first two terms:

$$\varepsilon_{\mathrm{d}} = n^2 + \frac{2\pi N \mu^2}{kT} \left\{1 - \frac{9}{20} \left(\frac{\mu}{kT}\right) E^2\right\} \tag{10}$$

The deduction of the Langevin function was carried out only with respect to space coordinates as independent variables for a given permanent dipole moment and local field strength [18, 13]. Considering that the latter quantities were taken as parameters, the effect of intermolecular interactions on these two quantities can be accounted for in an independent way.

For associating liquids, the following correlation is valid between the actual dipole moment in the liquid state and that in the gas phase:

$$\mu = \frac{n^2 + 2}{3} g^{1/2} \mu_g, \tag{11}$$

where g is the KIRKWOOD factor [16]. From Eqs (10) and (11) we have:

$$\varepsilon_{\mathrm{d}} = n^2 + \frac{2\pi N g \mu_{\mathrm{g}}^2 (n^2 + 2)^2}{9kT} - \frac{\pi N g^2 \mu_{\mathrm{g}}^4 (n^2 + 2)^4}{90 (kT)^3} E^2 \tag{12}$$

The first two terms of this equation yield the static low-field relative permittivity:

$$\varepsilon_0 = n^2 + \frac{2\pi N g \mu_g^2 (n^2+2)^2}{9kT} \tag{13}$$

while from Eqs (12) and (13), we obtain:

$$\frac{\Delta\varepsilon}{E^2} = -\frac{\pi N g^2 \mu_g^4 (n^2+2)^4}{90(kT)^3} \tag{14}$$

If $g = 1$ Eq. (14) and BOOTH's approximation of $\varepsilon \gg n^2$ is introduced into Eq. (5), then Eqs (5) and (14) become the same.

Equations (13) and (14) can be directly tested against experimental data. The comparison made in Table II indicates that, while Eq. (13) is good description of the low-field static relative permittivity, Eq. (14) — although giving an agreement better by an order of magnitude than the THIÉBAUT equation — yields approximately only one third of the measured $\Delta\varepsilon/E^2$ values.

In order to assess these results, it must be noted that it is very difficult to judge the reliability of the experimental data. Both KOŁODZIEJ, PARRY JONES and DAVIES [4], and MAŁECKI [2] give approximately 10% as the reproducibility of the $\Delta\varepsilon/E^2$ data, and their results are in agreement with one another. On the other hand MALSCH [19] and GUNDERMANN [20] measured some $\Delta\varepsilon/E^2$ values which were higher by one order of magnitude. This shows that the experimental data decreased by a factor of 10 over 30—40 years. This decrease can be attributed unequivocally to the development of experimental techniques, and the results of MAŁECKI and PARRY JONES *et al.* are by all means closer to reality. However, one must be aware of the likeliness that measured and calculated data can become closer not only by the improvement of the theory but by that of experiments, too.

Table III

Kirkwood factors in the non-linear term of Eq. (14), which reproduce the experimental $\Delta\varepsilon/E^2$ data

Liquid	g_E
Water	4.25
Methanol	5.50
Ethanol	5.6
1-Propanol	5.4
1-Butanol	5.2
1-Pentanol	5.2
1-Hexanol	5.4

One of the quantities in Eq. (14) is likely to change under the effect of high field: this is the KIRKWOOD g-factor. In Table III, those KIRKWOOD factors are shown which, when substituted into the non-linear term, would reproduce the experimental $\Delta\varepsilon/E^2$ data. It is seen that this g_E is approximately $\sqrt{3}$ times the low-field g in Table I. One of the possible reasons for this difference will be discussed in our next paper.

REFERENCES

[1] BÖTTCHER, C. J. F.: Theory of Electric Polarization, 2nd Ed., Completly revised by O. C. van BELLE, P. BORDEWIJK and A. RIP, Elsevier, Amsterdam 1973
[2] MAŁECKI, J.: Acta Phys. Polon., **XXI**, 13 (1962)
[3] BRADLEY, P. A., PARRY JONES, G.: J. Phys. E, **7**, 449 (1974)
[4] KOŁODZIEJ, H. A., PARRY JONES, G., FAVIES, M.: J. C. S. Faraday II, **72**, 269 (1974)
[5] BROWN, B. L., PARRY JONES, G.: J. C. S. Faraday II. **72**, 1657 (1974)
[6] MAŁECKI, J.: J. Chem. Phys., **36**, 2144 (1962)
[7] MAŁECKI, J.: Acta Phys. Polon., **XXVIII**, 891 (1965)
[8] PIEKARA, A.: J. Chem. Phys., **36**, 2145 (1962)
[9] MAŁECKI, J.: Acta Phys. Polon., **XXIX**, 45 (1966)
[10] MAŁECKI, J., JADZIN, J.: J. Phys. Chem., **78**, 1203 (1974)
[11] PIEKARA, A., NOWAK, J., MALECKI, J.: Chem. Phys. Lett., **19**, 453 (1973)
[12] MAŁECKI, J., DOPIERAŁA, Z.: Acta Phys. Polon, **XXXVI**, 409 (1969)
[13] MAŁECKI, J.: Acta Phys. Polon., **46**, 125, 133 (1974)
[14] THIÉBAUT, J. M.: Thesis, Nancy, 1968
[15] THIÉBAUT, J. M., WEISBECKER, A., GINET, C.: Compte Rendu, **267**, 661 (1968)
[16] KIRKWOOD, J. G.: J. Chem. Phys., **7**, 911 (1939)
[17] BOOTH, F.: J. Chem. Phys., **19**, 391 (1951)
[18] ONSAGER, L.: J. Am. Chem. Soc., **58**, 1486 (1936)
[19] MALSCH, J.: Phys. Z., **30**, 837 (1929)
[20] GUNDERMANN, H.: Ann. Phys. (Leipzig), **6**, 545 (1930)

János LISZI
Lajos MÉSZÁROS } H-8200 Veszprém, Schönherz Z. u. 12.

Imre RUFF H-1088 Budapest, Múzeum krt. 4/b.

Acta Chimica Academiae Scientiarum Hungaricae, Tomus 104 (3), pp. 279—285 (1980)

NON-LINEAR DIELECTRIC BEHAVIOUR AND THE FIELD-DEPENDENCE OF THE KIRKWOOD FACTOR

J. LISZI,[1] L. MÉSZÁROS[2] and I. RUFF[3]

([1]*Department of Analytical Chemistry, The University, Veszprém,* [2]*Research Group for Electrochemistry, Hungarian Academy of Sciences, Veszprém,* [3]*Institute of Inorganic and Analytical Chemistry, Eötvös L. University, Budapest*)

Received March 2, 1979

Accepted for publication August 31, 1979

An equation has been deduced for the description of non-linear dielectric behaviour, taking into account the field-dependence of the KIRKWOOD g-factor. The equation gives predictions for both normal and anomalous dielectric saturation as well as information on the structure-breaking and structure-making effect of the electric field. The comparison with experimental results indicates that it is very difficult to detect the field-dependence of g in permittivity measurements by the present techniques, although it plays an important role in the value of $\Delta\varepsilon/E^2$ as well as in the thermodynamic parameters of ionic solvation.

Introduction

In our previous paper [1] we concluded that the low-field static relative permittivity and the $\Delta\varepsilon/E^2$ ratio, characterizing the non-linear behaviour, can only be calculated in agreement with experimental data if two different KIRKWOOD factors are applied in the terms linear and non-linear in E. This difference is reflected also in the method which corrects the first two terms of the power series of the Langevin function with two different factors R_p and R_s [2, 3]. According to this method, the average of the dipole moment component in the direction of **E** is:

$$\langle m\rangle_E = -\frac{\mu_g^2 F}{3kT} R_p - \frac{\mu_g^4 F^3}{45(kT)^3} R_s, \tag{1}$$

where μ_g is the permanent dipole moment in the gas phase, k the Boltzmann constant, T the temperature, F the local field strength acting on the molecule in liquid phase, R_p the correlation factor of the orientational polarization and R_s is the correlation factor of dielectric saturation. R_p and R_s are independent of the electric field, R_p is a quantity corresponding to the KIRKWOOD g-factor, and for liquids "with no special interactions" $R_p^3 = g^3 = R_s$. Experiments indicate that $R_s > g^3$ for normal alcohols which is in qualitative agreement with that has been written in our previous paper.

Taking into account that in the deduction of the Langevin function the permanent dipole moment and the local field appeared as constant parameters, the correction of the first two terms of the power series by two different factors cannot be objected to in principle. It seems, however, more logical to use a single quantity which is allowed to vary with the field and its field-dependence reflects the changes occurring in the liquid under the effect of electric field.

Field-dependent Kirkwood factor

The KIRKWOOD g-factor accounts for the non-random orientation of molecules (structure) brought about by special intermolecular interactions in liquids. If $g > 1$ the molecular dipoles are, partially, oriented parallel in the liquid phase, some chain-like structures are formed, and the liquid phase dipole moment becomes greater than that measurable in the gas phase. If $g < 1$, the molecules are partly in antiparallel orientation, some ring-like structures are formed and the liquid phase average dipole moment becomes lower than that in the gas phase. If the electric field is suitable to change such liquid structures, this change should be reflected in the KIRKWOOD factor, too, *i.e.* the g-factor must depend on the field strength.

With a simple numerical example the possibility of such structural changes can be confirmed. Let the example be the case of water. According to the ONSAGER theory [4], the reactive field is:

$$\mathbf{R} = \frac{4\pi}{3}\frac{N_A}{V}\frac{2\varepsilon_0 - 2}{2\varepsilon_0 + n^2}\frac{n^2+2}{3}\mu_g \tag{2}$$

where $\mathbf{R}$ is the reactive field, N_A the Avogardo number, V the molar volume, ε_0 the low-field static relative permittivity of the liquid, and n its internal refraction index. At 298 K, $V = 18.07$ cm^3/mol, $\varepsilon_0 = 78.36$, $n_D^2 = 1.79$ (where subscript D indicates the sodium D-line) for water. From these data the reactive field can be calculated to be $\mathbf{R} = 3.25 \times 10^5$ e.s.u. ($= 9.75 \times 10^7$ V/cm).* The potential energy corresponding to the interaction between the permanent dipole and the reactive field is:

$$W = \frac{1}{2}\mu\mathbf{R} = -\frac{4\pi N_A^2}{3V}\frac{(\varepsilon_0 - 1)(n^2+2)}{3(2\varepsilon_0 + n^2)}\mu_g^2 \tag{3}$$

---

* According to the ONSAGER theory, the cavity field $\mathbf{G}$ is in the following relationship with the external field: $\mathbf{G} = 3\varepsilon_0\mathbf{E}/(2\varepsilon_0 + n^2)$. Thus,to create a reactive field with the same strength as that of the cavity field, the applied external field should be $E = 2.2 \times 10^5$ e.s.u. ($= 6.6 \times 10^7$ V/cm) which would involve extreme technical difficulties. The non-linear dielectric behaviour is usually studied at fields of $2 \times 10^2 - 3.3 \times 10^2$ e.s.u. ($= 60 - 100$ kV/cm). Under such conditions the original water structure can be regarded unaltered. This fact, as a matter of course, is not in contradiction with the consequences of the above example.

The above data yield for water $W = -4.4$ kcal/mol. This means that the potential energy of a water molecule originating from dipolar interactions is approximately equal to the hydrogen bond energy. Thus it is not unlikely that a relatively small change of W under the effect of the electric field can alter the hydrogen-bonded structure of water and, as a consequence, change the value of the Kirkwood factor.

At present no information is available on the field-dependence of the Kirkwood factor, therefore, we can use a power series of E with constants unkown for the time being. Only even powers of E can occur in this series, since $g(E)$ must always be equal to $g(-E)$.

Let g_E denote the Kirkwood factor belonging to a field strength E, while g_0 be that in the limit of very weak fields. In first approximation we have:

$$g_E = g_0 + g_1 E^2 \tag{4}$$

where g_1 is a constant independent of the field. (We have to note here that the cavity field G would perhaps be more adequate in place of E. Considering, however, that — even in the limiting case of $\varepsilon_0 \to \infty$ — $G = 3E/2$, and this proportionality factor varies only between 1 and 1.5, the use of E in the power series is also acceptable.)

From the power series of the Booth—Onsager equation [5], the dielectric displacement can be obtained as:

$$D = n^2 E + 4\pi N\mu \left\{ \frac{1}{3}\left(\frac{3\mu E}{2kT}\right) - \frac{1}{45}\left(\frac{27\mu^3 E^3}{8(kT)^3}\right) + \dots \right\} \tag{5}$$

where N is the number of molecules in unit volume, μ the actual dipole moment of the molecules in liquid phase:

$$\mu = \frac{\mu_g g_E^{1/2}(n^2 + 2)}{3} \tag{6}$$

From Eqs (5) and (6), we get:

$$D = n^2 E + \frac{4\pi N_A \mu_g (n^2+2)\, g_E^{1/2}}{3V} \left\{ \frac{3\mu_g (n^2+2)\, g_E^{1/2} E}{3 \times 3 \times 2\, kT} - \frac{27\mu_g^3 (n^2+2)^3\, g_E E^3}{45 \cdot 3^3 \times 8 \times (kT)^3} \right\} \tag{7}$$

For the sake of simplification, let us introduce the following abbreviations:

$$A = \frac{4\pi N_A \mu_g (n^2+2)}{3V} \tag{8}$$

$$B = \frac{\mu_g (n^2+2)}{2kT} \tag{9}$$

With these, Eq (7) takes the from:

$$D = n^2E + \frac{AB}{3} g_E E - \frac{AB^3}{45} g_E^2 E^3 \tag{10}$$

Let us calculate the differential relative permittivity according to the definition:

$$\varepsilon_{\mathrm{d}} = \frac{\mathrm{d}D}{\mathrm{d}E} \tag{11}$$

Thus:

$$\varepsilon_{\mathrm{d}} = n^2 + \frac{AB}{3}\left(\frac{\mathrm{d}g_E}{\mathrm{d}E} E + g_E\right) - \frac{AB^3}{45}\left(2\frac{\mathrm{d}g_E}{\mathrm{d}E} E^3 + 3g_E^2E^2\right) \tag{12}$$

From Eqs (4) and (12) — neglecting the terms containing E at powers higher than two — we have:

$$\varepsilon_{\mathrm{d}} = n^2 + \frac{AB}{3} g_0 + AB\, g_1 E^2 - \frac{AB^3}{15} g_0^2 E^2 \tag{13}$$

Taking into account the abbreviations in Eqs (8) and (9), we can see that in Eq (13):

$$n^2 + \frac{AB}{3} g_0 = \varepsilon_0 \tag{14}$$

i.e. the differential relative permittivity is:

$$\varepsilon_{\mathrm{d}} = \varepsilon_0 - \left(\frac{AB^3}{15} g_0^2 - AB\, g_1\right) E^2 \tag{15}$$

and the usual quantity characterizing the non-linear dielectric behaviour in this approximation becomes:

$$\frac{\Delta\varepsilon}{E^2} = \frac{\varepsilon_{\mathrm{d}} - \varepsilon_0}{E^2} = AB\, g_1 - \frac{AB^3}{15} g_0^2 \tag{16}$$

Equation (16) predicts both the normal and the anomalous dielectric saturation effects. According to Eqs (8) and (9), $A > 0$ and $B > 0$. The KIRKWOOD factor is always positive. Thus, if $g_1 < 0$, Eq. (16) can lead only to normal dielectric saturation. If $0 < g_1 < B^2g_0^2/15$, the liquid will show normal dielectric saturation, while if $g_1 > B^2g_0^2/15$, the dielectric saturation will be anomalous. If $g_1 = B^2g_0^2/15$, then apparently no dielectric saturation would be observed up to the field strength where this approximation is valid. If $g_0 = 1$ and $g_1 = 0$, Eq. (16) will reduce to:

$$\frac{\Delta\varepsilon}{E^2} = -\frac{\pi N \mu_g^4 (n^2+2)^4}{90(kT)^3} \tag{17}$$

which is the special form the of THIÉBAUT equation [6, 7] in the case when $\varepsilon_0 \gg n^2$. Finally, if $g_1 = 0$ and $g_0 = g$, then Eq. (16) reduces to Eq. (14) of our previous paper [1]:

$$\frac{\Delta\varepsilon}{E^2} = -\frac{\pi N \mu_g^4 (n^2+2)^4 g^2}{90(kT)^3} \tag{18}$$

On the basis of Eq. (4) and with respect to the sign of g_1, one can draw conclusion on whether the high field has a structure-making or a structure-breaking effect on the liquid, increasing or decreasing, respectively, the number and/or size of the structured regions originally present. For liquids with no specific interactions between molecules ("gas-like liquids") g_0 is unity. If $g_0 < 1$ and $g_1 > 0$, then the external electric field decreases the number of ring-like units, whereas if $g_0 > 1$ and $g_1 < 0$, the number of chain-like units is decreased, *i.e.* in both of these cases the field is structure-breaking. On the other hand, if $g_0 < 1$ and $g_1 < 0$ or $g_0 > 1$ and $g_1 > 0$, the field has a structure-making effect.

Results and Discussion

The applicability of Eq. (16) has been tested on some examples. Most of the liquids chosen (water and normal alcohols) show normal dielectric saturation, while nitrobenzene is one with anomalous non-linear dielectric behaviour [8, 9]. The data used in the calculations are collected in Table I. Substituting these into Eq. (16), the values of g_1 could be determined. These data are shown in Table II.

Table I

Some properties of polar liquids at 298 K

Liquid	n_D^2	μ_g/D	V (cm^3 mol^{-1})	g_0	$\frac{\Delta\varepsilon}{E^2} \times 10^8$(e.s.u.)
Water	1.79	1.85	18.07	2.8	−90
Methanol	1.77	1.71	40.48	2.83	−54
Ethanol	1.85	1.70	58.37	3.1	−36
1-Propanol	1.92	1.69	75.13	3.1	−27
1-Butanol	1.96	1.67	91.52	3.1	−20
1-Pentanol	1.99	1.65*	108.69	3.1	−17
1-Hexanol	2.01	1.63	125.58	3.1	−15
Nitrobenzene	2.40	4.22	102.7	0.92	+27

* Estimated value

Table II

Data on the field-dependence of the Kirkwood factor

Liquid	$g_1 \times 10^8$ (e.s.u.)$^{-2}$	$E(g_E=1) \times 10^4$ (e.s.u.)
Water	-0.56	1.8
Methanol	-1.29	1.6
Ethanol	-1.15	1.4
1-Propanol	-1.05	1.4
1-Butanol	-0.91	1.5
1-Pentanol	-0.94	1.5
1-Hexanol	-1.00	1.5
Nitrobenzene	$+0.56$	0.4

One can draw two conclusions from the g_0 values in Table I and from the g_1's in Table II:

1. For water and normal alcohols, $g_0 > 1$ and $g_1 < 0$, *i.e.* the KIRKWOOD factor approaches unity with increasing field, the amount of chain-like structures decreases, which means that the field has a structure-breaking effect. The same can be said about nitrobenzene for which $g_0 < 1$ and $g_1 > 0$. The structure-breaking effect of the field in this case is manifested by the decrease of the number of pairs with antiparallel dipole orientation [12].

2. The g_1 values are rather low. If one takes into account that the $\Delta\varepsilon/E^2$ data in Table I have been determined in a field not higher than 200 e.s.u. (= 60 kV/cm), one can see that the KIRKWOOD factor is altered only in the fifth digit under such a field. The present experimental techniques allow the determination of g to two or three digits, thus it would be practically impossible to detect the change of the KIRKWOOD factor itself by measurements of ε as a function of the field, whereas this small change in g affects considerably the non-linear dielectric behaviour by increasing three-fold the $\Delta\varepsilon/E^2$ values.

The electric field has a structure-breaking effect in all the liquids studied. From Eq. (4) the field strength could be calculated at which g_E becomes 1, *i.e.* the original liquid structure is completely destroyed. [In reality, this state, as a matter of course, is approached asymptotically with the increase of the field. Assuming, however, that g_1 is always the dominating term in the power series approximated by Eq. (4), one can expect that the majority of the structured units of the liquid is already destroyed when the field-dependent KIRKWOOD factor becomes unity in Eq. (4).] These results are shown in the last columns of Table II. The field necessary for nearly complete structure-breaking is by two orders of magnitude higher than those applied in the experiments. This increases the difficulties in studying the effect. However, in electrolyte solutions, the field is significantly stronger in the vicinity of ions. Our results indicate that even the structured liquids behave as structureless ones around the ions dissolved in them. This observation is supported by earlier calculations on the solvation free enthalpy and entropy, too. The free enthalpy of solvation could be described by the same model both in aprotic and structured liquids (*e.g.* tetrahydrofuran and water) [13]. In the case of the entropy of solvation, however, a large positive contribution could not be accounted for by the model [14] which, by all means, originates from the structure-breaking effect of the electric field discussed above. Thus, the structure of the pure liquid is destroyed in the vicinity of ions, and this process is accompanied by an increase in entropy.

REFERENCES

[1] Liszi, J., Mészáros, L., Ruff, I.: Acta Chim. Acad. Sci. Hung., to be published
[2] Piekara, A., Kielich, S.: Phys. Rad., **18,** 490 (1957)
[3] Piekara, A.: J. Chem. Phys. **36,** 2145 (1962)
[4] Onsager, L.: J. Amer. Chem. Soc., **58,** 1486 (1936)
[5] Booth, F.: J. Chem. Phys., **19,** 39 (1951)
[6] Thiébaut, J. M.: Thesis, Nancy, 1968
[7] Thiébaut, J. M.,Weisbecker, A., Ginet, C.: Compte Rendu, **267,** 661 (1968)
[8] Piekara, A., Piekara, B.: Compte Rendu **203,** 852 (1936)
[9] Małecki, J.: Acta Physica Polon **XXI,** 13 (1962)
[10] Kołodziej, H. A., Parry Jones, G., Mansel Davies: J. C. S. Faraday II, **70,** 269 (1974)
[11] Brown, V. L., Parry Jones, G.: J. C. S. Faraday II, **70,** 1657 (1974)
[12] Liszi, J.: Acta Chim. (Budapest), **84,** 125 (1975)
[13] Abraham, M. H., Liszi, J.: J. C. S. Faraday I, **74,** 1604 (1978)
[14] Abraham, M. H., Liszi, J.: J. C. S. Faraday I, **74,** 2858 (1978)

János Liszi
Lajos Mészáros } H-8200 Veszprém, Schönherz Z. u. 12.

Imre Ruff H-1088 Budapest, Múzeum krt. 4/b.

Acta Chimica Academiae Scientiarum Hungaricae, Tomus 104 (3), pp. 287–294 (1980)

STEREOCHEMICAL STUDIES, XXXVI* STUDIES ON CYCLIC 2-HYDROXYCARBOXYLIC ACIDS, VII**

^{1}H NMR INVESTIGATIONS OF ETHYL *CIS*- AND *TRANS*-2-HYDROXY-1-CYCLOPENTANE-, -HEXANE-, -HEPTANE- AND OCTANECARBOXYLATES AND THEIR TRICHLOROACETYL CARBOXAMIDO DERIVATIVES BY Eu(fod)$_3$ SHIFT REAGENT***

Gy. Dombi, I. Pelczer, J. A. Szabó, Gy. Göndös and G. Bernáth****

(*Institute of Organic Chemistry József Attila University, Szeged, Hungary*)

Received March 29, 1979
Accepted for publication August 31, 1979

The ^{1}H NMR spectra of ethyl *cis*- and *trans*-2-hydroxy-1-cyclopentane carboxylate (1, 2), as well as their homologues with cyclohexane, cycloheptane and cyclooctane skeleton (3–8) and the changes occurring in the spectra on the effect of the reaction with trichloroacetyl isocyanate and Eu(fod)$_3$ shift reagent were investigated, with special attention to the possible effect of the shift reagent on the conformational equilibria. The dependence of the shifts on the molar ratio permit conclusions regarding the favoured conformation of the *cis* isomers, in which the carbethoxy group and the hydroxyl group are in *equatorial* and *axial* positions, respectively.

Introduction

In the course of our earlier stereochemical investigations of alicyclic 1,3-aminoalcohols [1] and saturated heterocyclic compounds with condensed skeleton [2], a reasonable procedure was developed for the preparation of alicyclic *cis*- and *trans*-2-hydroxy-1-carboxylic acids [3, 4]. Neighbouring group participation by the hydroxyl in the hydrolysis of homologous alicyclic ethyl *cis*- and *trans*-2-hydroxy-1-carboxylates was studied [5], as well as the IR, ^{1}H [5] and ^{13}C NMR spectra of these compounds were examined [6]. In the present work the conformation of the *cis* isomers was to be determined; for this purpose the ^{1}H NMR spectra of the starting materials (**1**–**8**) and the urethane (TAU) derivatives (**9**–**16**) prepared with trichloroacetyl isocyanate (TAI) were compared and evaluated, furthermore, the differences in changes occurring on the effect of the Eu(fod)$_3$ shift reagent in the spectra of the isomers and homologues were studied.

---

* Part XXXV, see Ref. [2].

** Part VI, see Ref. [5].

*** A preliminary announcement of this work was made in a lecture of Dombi, Gy., Pelczer, I., Szabó, J. A., Göndös, Gy. and Bernáth, G., presented at the Meeting organized by the Committee of Theoretical Organic Chemistry of the Hungarian Academy of Sciences, Visegrád, Hungary, March 29, 1979.

**** Present address: Institute of Pharmaceutical Chemistry, University Medical School, Szeged, Hungary.

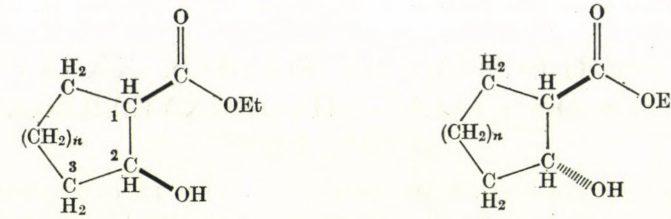

$n = 1$	**1**	**2**
$n = 2$	**3**	**4**
$n = 3$	**5**	**6**
$n = 4$	**7**	**8**

Fig. 1

Trichloroacetylurethane derivatives

Chemical shifts of the hydroxyl protons are dependent on the solvent, temperature and concentration, owing to rapid exchange processes. Alcohols can be investigated by the NMR technique in the form of their urethane derivatives prepared with TAI [7]. In the NMR sample tube primary, secondary and tertiary alcohols react with TAI rapidly and quantitatively (Fig. 2). In the NH signal appears at about 9 ppm, and the signal of the methine proton adjacent to the hydroxyl group of secondary alcohols appears at δ values 1.0—1.5 ppm higher than in the original alcohol [8]. The methylene signal of TAU derivatives of primary alcohols is shifted by 0.5—1.0 ppm.

Spectral data of compounds **1**—**8** and their TAU derivatives **9**—**16** (^{1}H NMR spectra) are shown in Table I. It can be seen that the H-2 values are always higher in the *cis* isomers (**1**, **3**, **5**, **7**) than in the *trans* isomers (**2**, **4**, **6**, **8**). The $\delta_{cis}-\delta_{trans}$ ($\Delta_{c,t}$) value is 0.16 and 0.15 ppm in the cyclopentane and and cyclohexane derivatives, respectively, while a lower value (0.07 and 0.06 ppm) was observed for the cycloheptane and cyclooctane derivatives. The TAU derivatives **9**—**16** and the corresponding hydroxy compounds (**1**—**8**) exhibited the following differences in the shift of the H-2 signal ($\Delta_{\mathrm{OH}}^{\mathrm{TAU}}$): for the **9**—**10** and **11**—**12** isomeric pairs the $\Delta_{\mathrm{OH}}^{\mathrm{TAU}}$*trans* $-\Delta_{\mathrm{OH}}^{\mathrm{TAU}}$ *cis* $= \Delta^{*}_{c,t}$ value was 0.09 and 0.08 ppm, respectively, while for the isomeric pairs **13**—**14** and **15**—**16** this value was 0.04 and 0.03 ppm, respectively.

In comparing the H-17 chemical shifts in 17-hydroxy- and 17-carbonyloxysteroids having fixed skeleton it was stated [8] that the $\Delta_{\mathrm{OH}}^{\mathrm{TAU}}$ value of *quasiaxial* α-protons was by about 0.1 ppm higher than that of the β-protons. Since the substituents in **4** and consequently in **12** are in *equatorial* position [6, 9], and the $\Delta_{\mathrm{OH}}^{\mathrm{TAU}}$ value is lower for the *cis* isomer **11** (1.37 ppm) than for the *trans* derivative **12** (1.45), it is probable that in the *cis* isomer **3** the

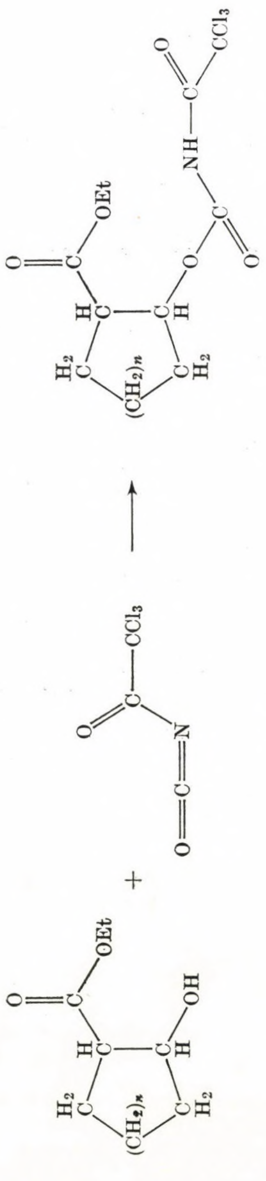

1—8

TAI

	cis	trans
$n = 1$	**9**	**10**
$n = 2$	**11**	**12**
$n = 3$	**13**	**14**
$n = 4$	**15**	**16**

Fig. 2

Table I

^1H NMR data of ethyl cis- and trans-2-hydroxy-1-cyclopentane, cyclohexane-, cycloheptane- and cyclooctanecarboxylates **(1—8)** *and of their trichloroacetyl isocyanate derivatives* **(9—16)**

No.	H-1				H-2				$CH_2CH^*_3$		δOH	δNH
	δ	$\delta_c - \delta_t$	Δ^{TAU}_{OH}	$\Delta^*_{c,t}$	δ	$\delta_c - \delta_t$	Δ^{TAU}_{OH}	$\Delta^*_{c,t}$	δ	Δ^{TAU}_{OH}		
1	2.54				4.38				4.12		3.46	
2	2.52	0.02			4.22	0.16			4.11		3.37	
9	2.86		0.32		5.53		1.15		4.13	0.01		9.58
10	2.92	0.06	0.40	0.08	5.46	0.07	1.24	0.09	4.16	0.05		8.94
3	2.26				3.99				4.11		3.25	
4	2.25	0.01			3.84	0.15			4.12		3.45	
11	2.55		0.29		5.36		1.37		4.11	0.00		9.20
12	2.60	0.05	0.35	0.06	5.29	0.07	1.45	0.08	4.16	0.04		9.10
5	2.40				4.08				4.12		2.95	
6	2.39	0.01			4.01	0.07			4.12		3.60	
13	2.69		0.29		5.42		1.34		4.12	0.00		9.03
14	2.72	0.03	0.33	0.04	5.39	0.03	1.38	0.04	4.16	0.04		8.90
7	2.50				4.01				4.12		3.90	
8	2.49	0.01			3.95	0.06			4.12		2.64	
15	2.80		0.30		5.34		1.33		4.12	0.00		9.02
16	2.82	0.02	0.33	0.03	5.31	0.03	1.36	0.03	4.15	0.03		8.72

$\delta_c = \delta_{cis}$ $\delta_t = \delta_{trans}$; Δ^{TAU}_{OH} = shift difference between the hydroxy and the trichloroacetyl isocyanate derivative in δ ppm

$\Delta^*_{c,t} = \Delta^{TAU}_{OH}$ *trans* — Δ^{TAU}_{OH} *cis*; $^*\delta CH_2CH_3$ (for all compounds) = 1.26 ppm

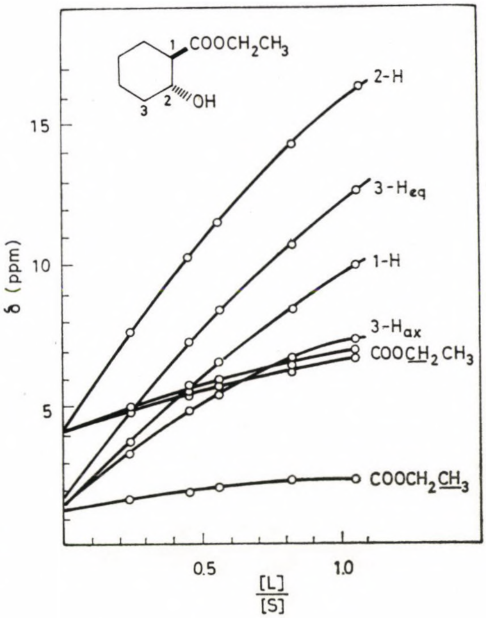

Fig. 3

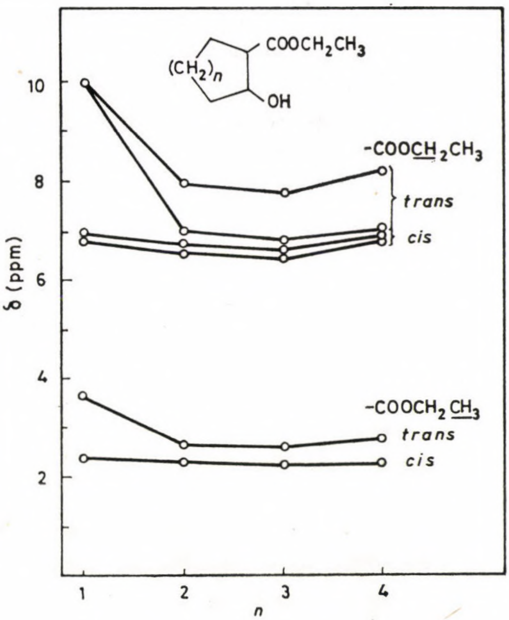

Fig. 4

C*H*—OH methine proton is in *equatorial* position. Consequently, the alcoholic hydroxyl group and the carbethoxy group must be in *axial* and *equatorial* positions, respectively. This is in accordance with earlier results [5, 9].

The TAU shift observed for the methylene protons of the ethyl group on the formation of the TAU derivatives **9**—**16** also is in agreement with the above statements. In the case of the *cis* isomers containing *axial* hydroxyl the methylene protons of the ethyl group are far from the urethane carbonyl group, thus the latter does not affect their chemical shifts. In the *diequatorial trans* isomers, however, a change in shift by about 0.03—0.05 ppm can be observed. For the methyl protons located farther, no change in shift can be observed in the *trans* isomers, either.

Measurements by the use of Eu(fod)$_3$ shift reagent

Further data regarding the conformational conditions in compounds **1**—**8** were to be obtained from the changes in shifts caused by the Eu(fod)$_3$ shift reagent and from the coupling constants becoming measurable in its presence.

The shift reagent was added in increasing amounts and the chemical shifts of the individual protons were plotted as a function of the molar ratio of the shift reagent. First a straight line was obtained; at higher molar ratios a saturated section appeared. The slope of the straight section (the extent of dependence on the molar ratio) was inversely proportional to the third power of the distance between the respective proton and the metal ion [10].

The changes in the shifts of the relevant protons of compound **4** as a function of the shift reagent concentration are shown in Fig. 3. The most important data obtained on the shifting of compounds **1**—**8** are shown in Table II.

Complex formation caused the most significant changes in the chemical shifts of the hydroxyl protons. These shift values, however, are not presented in the Table, since these are not characteristic as regards the present problem, owing to the chemical nature of hydroxyl protons.

As can be seen, the molar ratio function of the H-2 protons is the steepest one, proving that complex formation involves primarily the hydroxyl group. If it is assumed that the ester carbonyl is simultaneously also in complex bond, the molar ratio function of the H-1 protons would be the steeper, owing to the Θ-dependence of the shift. The slope of the H-2 protons is not characteristic of the conformation of the compounds, since the ring in the cyclopentane, cycloheptane and cyclooctane derivatives is flexible and thus the dihedral angle of the C-1 and C-2 substituents is not 60° but deviates from it to a variable extent, therefore the C-1 substituent affects complex formation at C-2 in different ways, through its space requirement. It can also be supposed that the angle-dependent factor in the McConnel equation cannot be neglected in the present case because of the steric effect of the substituent at C-1; however owing to the flexibility of the skeleton, its quantitative evaluation is much more difficult here than in compounds with fixed skeleton [12, 13].

Table II

^{1}H-NMR data of ethyl cis- and trans-2-hydroxy-1-cyclopentane-, cyclohexane-, cycloheptane- and cyclooctane carboxylate (**1**—**8**) *Eu(fod)$_3$ complexes*

No.	Slope				J(Hz)		
	H-1	H-2	H-3e	COOCH_2CH$_3$	$J_{1,2}$	$J^*_{2,3a}$	$J^*_{2,3e}$
1	6.9	14.1	11.6	7.5	4.5	4.5	1
2	8.65	10.6	8.5	10.5	9	9	9
3	9.7	15.9	12.2	6.8	44	7	3
4	11.8	15.8	6.0	7.2	10.5	12	7
5	10.8	17.2	13.1	6.2	4	7	3
6	14.8	18.2	6.8	7.6	8	7.5	4
7	12.8	17.3	10.6	6.8	4	7	**
8	13.2	19.0	6.9	7.4	8	8	3

* Values given by first order approximation
** It could not be determined

The ester carbonyl in the *trans* isomers also takes part in the complex formation, which can be confirmed by the more emphasized dependence of the proton of the ethyl groups on the ratio molar (Fig. 4).

The dependence of the H-1 value on the molar ratio is always higher in the *trans* isomers. This can easily be explained, since in these compounds the *axial* C-1 proton is near to the europium atom which forms a complex with the *equatorial* hydroxyl group, whereas in the complexes formed with the *axial* or *quasiaxial* proton is farther from the europium atom. This is further evidence for the conformations derived for the *cis* isomers, and also shows that the shift reagent does not alter the conformational equilibrium significantly in the given group of compounds.

It can be seen that when the number of ring members is increased, the difference in the dependence on the molar ratio between the complexes of the *cis* and *trans* pairs decreases, as a consequence of the increasing flexibility of the rings.

The changes in the chemical shift of the H-3*a* signal is entirely in accordance with the above statements, being evidently opposite to the case of H-1*a*, that is, the slope is steeper for the *cis* isomers. This also points to the fact that the hydroxyl group in *cis* isomers approaches the *equatorial* direction, thus its distance from the *equatorial* proton in the 3-position decreases.

In the Eu(fod)$_3$ complexes the $J_{1,2}$ coupling constant can easily be determined. Interestingly, in the *trans* cyclopentane derivatives the vicinal coupling constants of the C-2 proton agree, thus a quartet appears in the spectrum. The 2-H, 3-H$_e$ coupling constants decrease with the increasing number of ring members and approach each other for the *cis* and *trans* isomers, also indicating the distortion of rings mentioned above.

When the chemical shifts of the methyl and methylene protons of the carbethoxy groups obtained at 1 : 1 ratio of the shift reagent and substrate are plotted as a function of the number of ring members (Fig. 4). It can be seen that in all cases the higher chemical shift change is obtained for the *trans* isomers; this indicates the closer location of the ethyl group and the europium ion in the *trans* isomers. In the *cis* isomers (**1**, **3**, **5**, **7**) the chemical shifts observed at 1 : 1 molar ratio of the shift reagent and substrate are hardly altered with the number of ring members, whereas in the *trans* isomers the shift of both the methyl signal and methylene signal characteristically depends on the ring size. The very high shift of the Eu(fod)$_3$ complex of **2** is striking; thus the europium atom is here significantly closer to the methylene protons of the ethyl group than in other *trans* homologues.

The diastereotopic methylene protons form the AB part of an ABX$_3$ spin system in the spectrum. The $\Delta\delta$AB shift difference increases with the number of ring members in the *trans* isomers, while this value is low and practically constant in the *cis* isomers.

Experimental

The spectra were recorded with a JEOL C 60 HL 60 MHz high resolution NMR spektrophotometer at room temperature in $CDCl_3$ (BDH) solutions.

The shift reagent was tris-(1,1,1,2,2,3,3-heptafluoro-7,7-dimethyl-4,6-octanedionato)-europium (BDH); before use it was dried in a Fischer tube at 60 °C under reduced pressure 20.267 kPa over P_2O_5 for 24 h. The chemical shifts (δ) were referred to TMS internal standard.

In the shifting experiments, $20-30 \pm 0.1$ mg of the sample was dissolved in $CDCl_3$ (0.3 cm^3), then the shift reagent, weighed with an accuracy of 0.1 mg, was added to the solution in 5—6 portions until the 1 : 1 molar ratio had been reached. The spectra were recorded 10—15 minutes after completing the addition of the shift reagent. The small change in concentration due to the addition of the reagent was neglected.

REFERENCES

[1] Bernáth, G., Göndös, Gy., Láng, K. L.: Acta Chim. (Budapest) **86**, 187 (1975)

[2] Bernáth, G., Fülöp, F., Jerkovich, Gy., Sohár, P.: Acta Chim. Acad. Sci. Hung. **101**, 61 (1979)

[3] Bernáth, G., Göndös, Gy., Márai, P., Gera, L.: Acta Chim. (Budapest) **74**, 471 (1972)

[4] Bernáth, G., Göndös, Gy., Gera, L.: Acta Phys. et Chem. Szeged **20**, 139 (1974)

[5] Bernáth, G., Sohár, P., Láng, K. L., Göndös, Gy., Gera, L., Pál, A.: Acta Chim. (Budapest) **92**, 175 (1977)

[6] Jancke, H., Engelhardt, G., Bernáth, G., Göndös, Gy., Tichý, M.: J. prakt. Chem. **317**, 1005 (1975)

[7] Goodlett, V. W.: Anal. Chem. **37**, 431 (1965)

[8] Schönecker, B., Tresselt, D., Ponsold, K.: Tetrahedron **31**, 2845 (1975)

[9] Bernáth, G., Sohár, P., Láng, K. L., Tornyai, I., Kovács, Ö. K. J.: Acta Chim. Acad. Sci. Hung. **64**, 81 (1970)

[10] Cockerill, A. F., Davies, G. L. O., Harden, R. C., Rackham, D. M.: Chem. Revs. **73**, 553 (1973)

[11] Hawkes, G. E., Marzin, C., Leibnitz, D., Johns, S. R., Herwig, K., Cooper, R. A., Roberts, D. W., Roberts, J. D.: in Nuclear Magnetic Shift Reagents (Ed. Sievers, R. E.) pp. 129—142, Academic Press, New York 1973

[12] Davis, R. E., Willcott, R. M.: in Nuclear Magnetic Shift Reagents (Ed. Sievers, R. E.) pp. 143—157, Academic Press New York 1973

György Dombi
István Pelczer
József A. Szabó
György Göndös
H-6720 Szeged, Dóm tér 8.

Gábor Bernáth
H-6720 Szeged, Eötvös u. 6.

Acta Chimica Academiae Scientiarum Hungaricae, Tomus 104 (3), pp. 295—301 (1980)

EXCESS VOLUMES AND ISENTROPIC COMPRESSIBILITIES OF *n*-BUTYLAMINE WITH *n*-ALCOHOLS

A. Krishnaiah and P. R. Naidu*

(Chemical Laboratories Sri Venkateswara University College of Engineering, Tirupati India)

Received June 12, 1979

Accepted for publication August 31, 1979

Volumes of mixing and deviations in isentropic compressibility for binary mixtures of *n*-butylamine with *n*-propanol, *n*-butanol, *n*-pentanol and *n*-hexanol, were measured at 303.15 and 313.15 K. The excess volumes and deviations in isentropic compressibility are negative over the entire range of mole fractions in all the systems. The negative values suggest that strong hydrogen bonding exists between unlike molecules. The results also show that the chain length of alcohols does not influence the deviations to any significant extent. Both V^E and the deviation in isentropic compressibility decrease with increasing temperature.

Introduction

The thermodynamic properties of binary mixtures containings self-associated components exhibit significant deviations from ideality, arising not only from differences in molecular size but also from changes in hydrogen bonding between like and unlike molecules. A survey of the literature has shown that many binary mixtures containing associated liquids like water, alcohols, acids, and amines as one component have been studied. However, very few attempts have been made to study excess volumes and isentropic compressibilities of mixtures containing two associated components. Excess properties of these mixtures depend on (a) the degree of association of each component in pure state, (b) the structure breaking effect of the components and (c) the possible interaction between unlike molecules. Hence, excess volumes and isentropic compressibilities for mixtures of *n*-butylamine with *n*-propanol, *n*-butanol, *n*-pentanol and *n*-hexanol were determined at 303.15 and 313.15 K. The results were analyzed in terms of the relative strengths of structure breaking and structure making effects.

Experimental

n-Butylamine was dried over potassium hydroxide for 3 d, refluxed for 2 h and fractionally distilled [1]. *n*-Propanol, *n*-butanol, *n*-pentanol and *n*-hexanol were purified by the methods described Rao and Naidu]2]. The purity of the samples was checked by comparing the experimental density with those reported in the literature [1, 3]. The data are given in Table I.

---

* To whom correspondence should be addresed

Table I

Density of the pure component liquids

Component liquid	T (K)	Density (g cm^{-3})	
		Present work	Literature
n-Butylamine	298.15	0.73452	0.73460
n-Propanol	303.15	0.79564	0.79567
n-Butanol	303.15	0.80203	0.80206
n-Pentanol	303.15	0.80761	0.80764
n-Hexanol	303.15	0.81196	0.81201

Excess volumes were measured directly using a single composition per loading type dilatometer described by RAO and NADUI [2] at 303.15 and 313.15 K. The values of V^E were accurate to ± 0.003 cm^3 mol^{-1}. Four dilatometers with different capacities were used to cover the entire mole fraction range.

Isentropic compressibilities were computed from densities and sound velocities determined at 303.15 and 313.15 K. Densities of the mixtures were obtained from experimental excess volumes using the relation

$$\varrho = \frac{x_1 M_1 + x_2 M_2}{V + V^E} \tag{1}$$

where x_1, x_2 and M_1, M_2 stand for the mole fractions and molecular weights of amine and alcohol, respectively. V and V^E denote the molar volume and excess volume, respectively. This method is used to obtain the density if one of the components is volatile [4]. n-Butylamine is a volatile component and hence the indirect method has been employed. The density values obtained are accurate to $\pm 5 \times 10^{-5}$ g cm^{-3}.

Ultrasonic sound velocities were measured with a single crystal ultrasonic interferometer at a frequency of 2 MHz, and were accurate to $\pm 0.15\%$ [5]. The isentropic compressibilities were calculated from the relation [6]

$$k_S = u^{-2} \varrho^{-1} \tag{2}$$

where u and ϱ denote sound velocity and density, respectively. The values of k_S were accurate to ± 2 TPa^{-1} (Tera pascals^{-1}). The quantity K_S was computed employing the equation

$$K_S = k_S - \Phi_1 k_{S,1} - \Phi_2 k_{S,2} \tag{3}$$

where k_S, $k_{S,1}$ and $k_{S,2}$ are the isentropic compressibilities of the mixture and the pure components. Φ_1 and Φ_2 are the volume fractions of amine and alcohol. The isentropic compressibility for an ideal mixture is assumed to be additive with respect to volume fraction. K_S represents the deviation from ideal behaviour.

Results

The experimental values of V^E for the four binary liquid mixtures at 303.15 and 313.5 K are presented graphically in Figs 1—4. The V^E data may be represented by an empirical equation of the form

$$V^E/\text{cm}^3\,\text{mol}^{-1} = x_1 x_2[a_0 + a_1(x_1 - x_2) + a_2(x_1 - x_2)^2] \tag{4}$$

where a_0, a_1 and a_2 are parameters and x_1 and x_2 are the mole fractions of amine and alcohol, respectively. The values of the parameters, obtained by a least-squares procedure are shown in Table II along with the standard deviation $\sigma(V^E)$

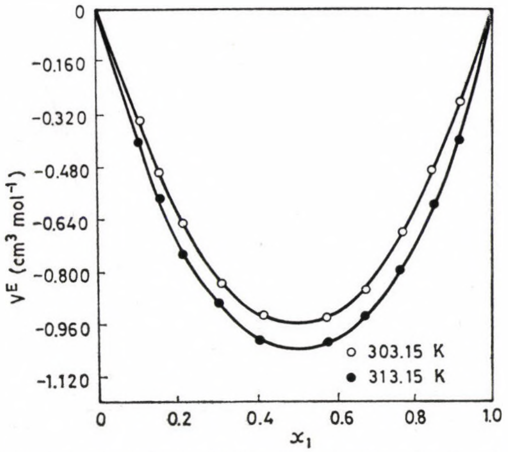

Fig. 1. Values of V^E plotted against the mole fraction of *n*-butylamine (x_1) for *n*-butylamine + *n*-propanol

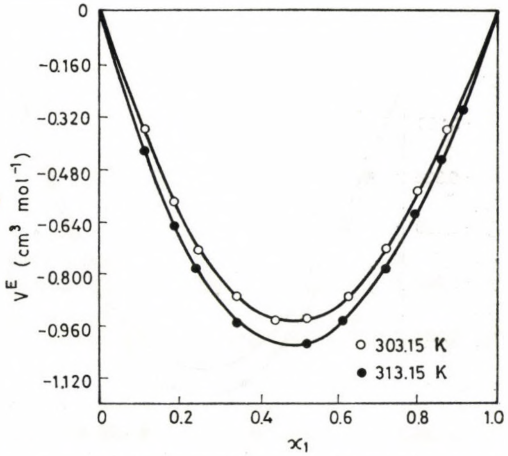

Fig. 2. Values of V^E plotted against the mole fraction of *n*-butylamine (x_1) for *n*-butylamine + *n*-butanol

Table II

Values of the constants a_0, a_1 and a_2 of equation (4) and the standard deviation $\sigma(V^E)$

System	T (K)	a^0 (cm^3 mol^{-1})	a_1 (cm^3 mol^{-1})	a_2 (cm^3 mol^{-1})	$\sigma(V^E)$ (cm^3 mol^{-1})
n-Butylamine + *n*-propanol	303.15	−3.908	0.065	0.195	0.004
n-Butylamine + *n*-butanol	303.15	−3.811	0.328	0.364	0.004
n-Butylamine + *n*-pentanol	303.15	−3.676	0.154	0.347	0.005
n-Butylamine + *n*-hexanol	303.15	−3.672	−0.024	0.469	0.006
n-Butylamine + *n*-propanol	313.15	−4.157	−0.177	−0.936	0.004
n-Butylamine + *n*-butanol	313.15	−4.090	0.411	0.162	0.007
n-Bytulamine + *n*-pentanol	313.15	−4.003	0.056	0.073	0.005
n-Butylamine + *n*-hexanol	313.15	−3.985	−0.046	0.345	0.008

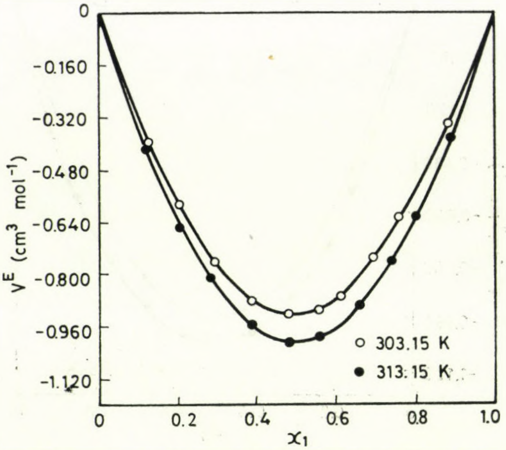

Fig. 3. Values of V^E plotted against the mole fraction of n-butylamine (x_1) for n-butylamine + n-pentanol

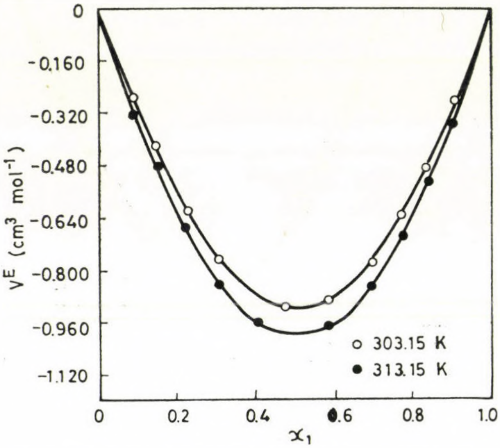

Fig. 4. Values of V^E plotted against the mole fraction of n-butylamine (x_1) for n-butylamine + n-hexanol

Values of K_S for the four mixtures at 303.15 and 313.5 K are graphically illustrated in Figs 1a—4a.

The values of K_S fit an empirical equation of the form

$$K_S/\mathrm{TPa}^{-1} = \Phi_1\Phi_2[b_0 + b_1(\Phi_1 - \Phi_2) + b_2(\Phi_1 - \Phi_2)^2] \tag{5}$$

where Φ_1 and Φ_2 are the volume fractions of amine and alcohol, and b_0, b_1 and b_2 are the parameters, obtained by the method of least-squares and are given in Table III along with the standard deviation $\sigma(K_S)$.

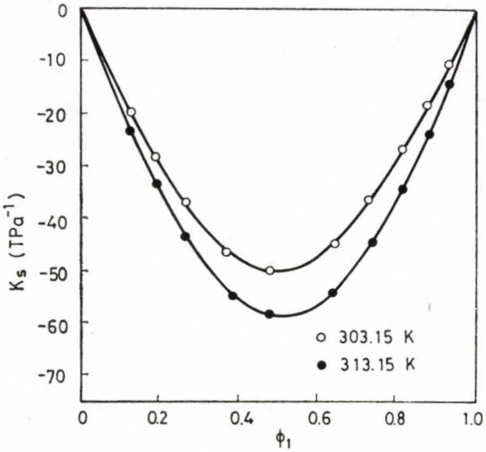

Fig. 1a. Values of K_S plotted against the volume fraction of *n*-butylamine (Φ_1) for *n*-butylamine + *n*-propanol

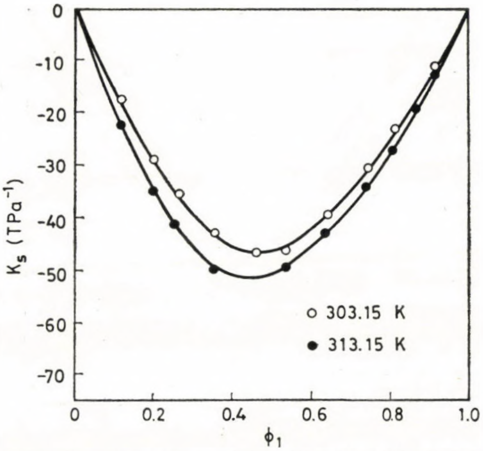

Fig. 2a. Values of K_S plotted against the volume fraction of *n*-butylamine (Φ_1) for *n*-butylamine + *n*-butanol

Table III

Values of the constants b_0, b_1 and b_2 of equation (5) and the standard deviation $\sigma(K_S)$

System	T (K)	b_0 (TPa^{-1})	b_1 (TPa^{-1})	b_2 (TPa^{-1})	$\sigma(K_s)$ (TPa^{-1})
n-Butylamine + *n*-propanol	303.15	—197	7	41	1
n-Butylamine + *n*-butanol	303.15	—187	43	84	1
n-Butylamine + *n*-pentanol	303.15	—155	— 6	40	1
n-Butylamine + *n*-hexanol	303.15	—136	17	49	1
n-Butylamine + *n*-propanol	313.15	—232	—10	20	2
n-Butylamine + *n*-butanol	313.15	—199	36	18	1
n-Butylamine + *n*-pentanol	313.15	—183	—19	29	1
n-Butylamine + *n*-hexanol	313.15	—177	23	33	1

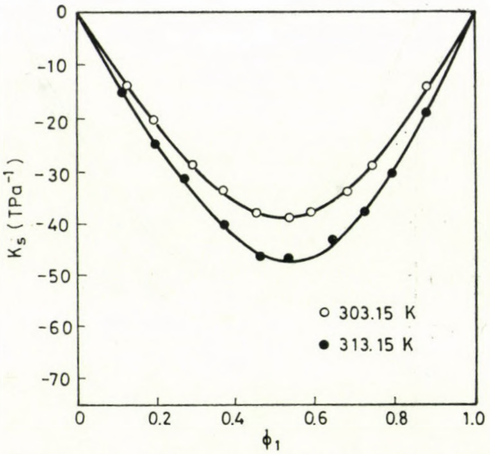

Fig. 3a. Values of K_s plotted against the volume fraction of *n*-butylamine (Φ_1) for *n*-butylamine + *n*-pentanol

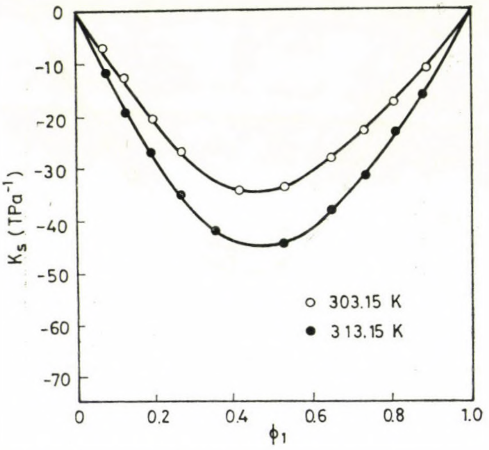

Fig. 4a. Values of K_s plotted against the volume fraction of *n*-butylamine (Φ_1) for *n*-butylamine + *n*-hexanol

Discussion

Excess volume *vs.* composition plots in Figs 1—4 show that V^E is negative over the entire range of composition at both temperatures in the four mixtures. The negative values of V^E are strikingly large. These large values may be ascribed to two opposing effects: (1) expansion due to depolymerization of the amine by the alcohol or the alcohol by the amine and size differences, (2) contraction due to hydrogen bonding between amine and alcohol. The actual value of V^E would depend upon the relative strengths of the two opposing effects. The experimental values of V^E suggest that the later effect is stronger than the former. There is spectroscopic evidence for hydrogen bonding between a primary amines and alcohols [7]. Hydrogen bond association between *n*-butylamine and *n*-alcohols has been reported in terms of heats of mixing and physical properties, dielectric constant and viscosity by RATKOVICS and co-workers [8, 9, 10]. The algebric values of V^E for the four systems are in the order *n*-propanol $<$ *n*-butanol $<$ *n*-pentanol $<$ *n*-hexanol. However, the differences in excess volumes from propanol to hexanol are not significant. This shows that interaction between unlike molecules is not very much influenced by the chain length of the alcohol. A similar observation has been made by RATKOVICS and LASZLO [8], who studied the heats of mixing of *n*-butylamine with methanol, ethanol, *n*-propanol, *n*-butanol and *n*-heptanol.

A comparison between V^E values determined at 303.15 and 313.15 K shows that V^E becomes more negative with increasing temperature. The temperature coefficient of V^E depends on : (a) the decrease in degree of self-association and association between unlike molecules with increasing temperature, (b) the decrease in molar volume of complex formation with increasing temperature. The sign of the actual temperature coefficient of V^E would be determined by the dominant factor. The results of the present investigation show that the second factor dominantes in the four mixtures. A negative temperature coefficient for V^E was also reported for complexes formed between chloroform and triethylamine [11].

The deviation in isentropic compressibility observed at 303.15 and 313.15 K is also negative over the whole range of compositions. K_s values become more negative with increasing temperature. Thus, the sign of K_s and the trend between temperature, and K_s support the postulates used to interpret the sign of excess volume and the effect of temperature on excess volume.

*

This works was supported by the financial assistance of University Granst Commission, New Delhi, India.

REFERENCES

[1] RIDDICK, J. A., BUNGER, W. B.: Organic Solvents. Wiley-Intersicence, New York 1970
[2] RAO, M. V. P., NAIDU, P. R.: Can. J. Chem., **52**, 788 (1974)
[3] TIMMERMANS, J.: Physico-chemical Constants of Organic Compounds. Elsevier, Amsterdam 1950
[4] MARSH, K. N.: Chemical Thermodynamics, **2**, 1 (1978)
[5] RAO, M. V. P., NAIDU, P. R.: J. Chem. Thermodyn., **6**, 1195 (1974)
[6] THEODOR, F. H., RICHARD, H. B.: Sonics. John Wiley, Sydney 1955
[7] SPRINGER, JR., L. S., MEEK, D. W., J. Phys. Chem., **70**, 481 (1966)
[8] RATKOVICS, F., LÁSZLÓ, M.: Acta Chim. (Budapest) **79**, 395 (1973)
[9] LISZI, J., SALAMON, T., RATKOVICS, F.: Acta Chim. (Budapest) **81**, 467 (1974)
[10] RATKOVICS, F., SALAMON, T., DOMONKOS, L.: Acta Chim. (Budapest) **83**, 53 (1974)
[11] CHAND, A., HANDA, Y. P., FENBY, D. V.: J. Chem. Thermodyn., **7**, 401 (1975)

A. KRISHNAIAK } College of Engineering, Sri Venkateswara University,
P. R. NAIDU } Tirupati 517 502 India

Acta Chimica Academiae Scientiarum Hungaricae, Tomus 104 (3), pp. 303—309 (1980)

INTERACTION BETWEEN ALUMINATE AND HYDROXIDE IONS

M. Pálfalvi-Rózsahegyi, Z. G. Szabó and L. Barcza

(Department of Inorganic and Analytical Chemistry of the Eötvös Loránd University, Budapest)

Received March 29, 1979
Accepted for publication September 12, 1979

It has been pointed out that conductivity data can be characteristic when the total cation (or anion) concentration is constant. Such measurements (together with viscosity and density data) show that special interaction exists in rather concentrated aluminate lyes, which is interesting also from industrial point of view.

It seems that a hydrogen bridged 1 : 1 chelate complex forms between tetrahydroxo aluminate and hydroxide ions: $Al(OH)_4^- \cdot OH^-$. The formation constants of this species have been measured at different total concentrations and at different temperatures.

In industrial processes rather concentrated aluminate solutions are produced. It is known [1] that these are true, however, supersaturated, unstable solutions and therefore they can be decomposed.

The most interesting questions concerning these solutions are:

i) which are the (main) species present;

ii) which equilibria ensure the stability of these solutions over long periods, and

iii) which is the first irreversible step resulting in the decomposition of the system.

Several methods were used to investigate the oversaturated aluminate solutions [1, 2], among them the conductivity measurements. Conductivity changes in function of the sodium hydroxide and aluminium concentrations, in function of their ratio, as well as in function of the temperature [3], *etc.* could give data characterizing the system under investigation.

As the aluminate ion in solutions exists only in presence of hydroxide excess, its equivalent conductivity can not be measured directly, but seems to be extremely sensitive against changes in concentration, ionic strength, temperature, *etc.* Further problem is that rather concentrated solutions have to be studied and it is well known [4], that activity coefficients, equivalent conductivities, *etc.* are changed more and more complex and individual ways in function of the increasing concentrations. It follows that the detailed analysis of conductivity data of aluminate solutions is rather complicated and its lack in the literature is well understandable.

We have thought to solve the problems through study of simple binary and ternary systems first [5] and the following conclusions could be drawn:

i) In simplest cases the law of conductivity additivities

$$\varkappa = \Sigma \lambda_i c_i \tag{1}$$

(where λ is the equivalent conductivity and c is the concentration of the components) is nearly valid even at high concentrations.

ii) The deviations depend on temperature and total concentration but they are not a function of ionic strength.

iii) Viscosity and density data can be explained with constants measured conductometrically.

iv) "Negative" conductivities can be caused by complex formations omitted from considerations.

After thorough preliminary studies we started to investigate systems with relatively low aluminate and high sodium hydroxide concentrations.

Experimental

In the course of investigations, the sodium ion, *i.e.* the alkaline concentrations were always kept constant. The sodium hydroxide and water were purified *to* eliminate any carbonate content. Aluminate solutions were prepared by dissolving aluminium metal of high purity in sodium hydroxide solutions. The volumes were adjusted at constant temperature equal with that of the measurements. Contaminations by silicates and carbonates were carefully avoided: the solutions were prepared and stored in polyethylene vessels and under carbon dioxide free nitrogen.

To find how the properties of solutions (first of all their conductivities) differ in function of their preparations, freshly prepared or aged; heated or/and mixed or/and diluted solutions of the same contents were studied. Disregarding extreme cases, we found that the final result is irrelevant to the method of the preparation up to the point where these obviously still are true solutions. We concluded that fast equilibria exist in aluminate — hydroxide system and they are reversible up to a given, easiliy discernible limit.

Most of the experiments were carried out at 25.00 ± 0.02 °C; but measurements were made also at 15.00 and 35.00 (±0.02) °C. Conductivity data were recorded with a Radiometer CDM — 2d type conductometer using CDC — 104 or some other, specially adapted electrodes. An *Ostwald* viscosimeter with capillaries of alkali-resistant glass of 0.8 mm in diameter were used; densities were obtained from pycnometric measurements.

Experimental data were evaluated by a rather simple computer programme.

Detailed studies were carried out at 1.00, 2.00, 4.00 and 6.00 M sodium ion concentrations and at mole rations, where

$$\frac{[\mathrm{OH}^-]_T}{[\mathrm{Al(OH)}_4^-]_T} \gg 6.$$

Results and Discussion

When, according to accepted interpretation we suppose that the formation of aluminate ions involves only a substitution of hydroxide ion by aluminate ion:

$$\underline{\mathrm{Al(OH)}_3} + \mathrm{OH}^- = \mathrm{Al(OH)}_4^- \tag{2}$$

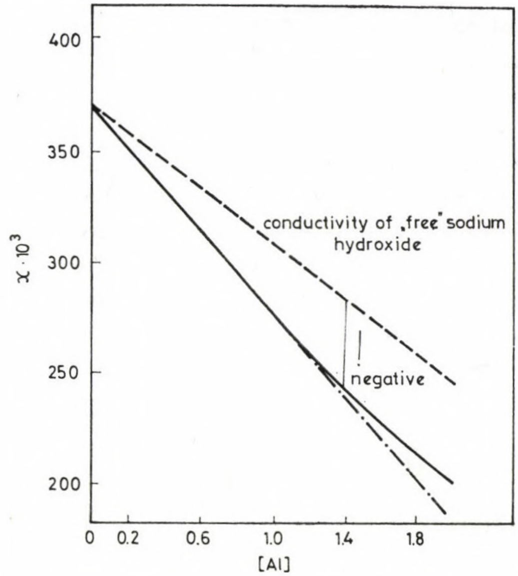

Fig. 1. Conductivity *vs* aluminate content in 6.00 M NaOH at 25 °C

and additionally we suppose that tetrahdyroxo aluminate ions form completely undissociated ion pairs with sodium ions, the observed phenomena (see Fig. 1) can not be explained.

Though there is no evidence at all of, or any reference to, that sodium aluminate is a non-dissociated ion pair (having this way no equivalent conductivity), even this supposition fails to explain the decrease of conductivities already at lowest concentrations of aluminium. This rather great anomaly could be formally interpreted as negative conductivity, but our recent studies [5], too, have proved that this phenomenon means always a complex species omitted from considerations. It has to be mentioned, that a number of references to this anomaly [1, 6] can be found in the literature together with some attempts for its interpretation or elimination.

When all the results considered, the working hypothesis follows that the phenomena can be explained only if association of one tetrahydroxo aluminate and one hydroxide ion is supposed. In the literature [1], the existence of pentahydroxo, even of hexahydroxo aluminate ions has been mentioned. Relevant studies in solid phases [7, and refs. therein] gave uncertain results; Raman spectroscopic studies refer only to tetrahedral symmetry in solutions [8] (even at dimeric aluminates) and make the existence of octahedral hydroxoaluminate complexes (in solution) very improbable.

The interaction of aluminate and hydroxide ions is not only supported by the data of conductivity but by the viscosity and density measurements, too. It should be noted that when the formation constants of tetrahydroxo aluminate ion and of the associate of this with hydroxide (*cf.* Eqs 2 and 5) are formally evaluated, we get

$$K_4 \gg K_5 \qquad (3)$$

In other words, the conductometric method registers tetrahydroxo aluminate as a basic unit and an unexpectedly great difference exists between the stabilities of tetrahydroxo and of supposed pentahydroxo aluminate ions.

On the basis of these results we assume that the new coming hydroxide ion does not form a dative bond with the central aluminium but a hydrogen bridged chelate complex of the structure below is formed:

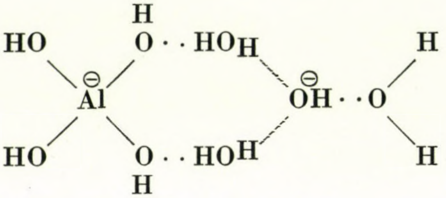

(4)

(The existence of this structure is probable because the six-membered ring thus formed may be relatively stable.)

Independently of structure 4, which may be proposed on the grounds of our studies (but it is not proven), the overall process:

$$\mathrm{Al(OH)_4^-} + \mathrm{OH^-} \rightleftharpoons \mathrm{Al(OH)_4^-} \cdot \mathrm{OH^-} \qquad (5)$$

seems to exist unambiguously and the association can be characterized by an equilibrium constant as

$$\beta_{11} = \frac{[\mathrm{Al(OH)_4^-} \cdot \mathrm{OH^-}]}{[\mathrm{Al(OH)_4^-}]\,[\mathrm{OH^-}]} \qquad (6)$$

Using this constant, all anomalies can be solved: in Fig. 1 the conductivity curve is recalculated with the computed equilibrium constant $\beta_{11} = 3.88 \pm 0.11$. (With this value, the data of viscosity and density measurements can be explained, too.) It is interesting, that the viscosity of aluminate solution seems to be more sensitive against associations, than its conductivity is. Therefore the β_{11} values for $\mathrm{Al(OH)_4^-} \cdot \mathrm{OH^-}$ were calculated for that concentration range, for which a direct proportionality prevails not only between aluminate concentration and conductivity but also between aluminium concentration and viscosity. However, the question arises whether (again at 25 °C) a similar effect is observable also at lower total concentrations (*i.e.* at 4.00, 2.00 and 1.00 *M*) of sodium hydroxide. Though the apparent negative conductivity decreases in function of decreasing total concentrations, too (see Fig. 2), the $\mathrm{Al(OH)_4^-} \cdot \mathrm{OH^-}$

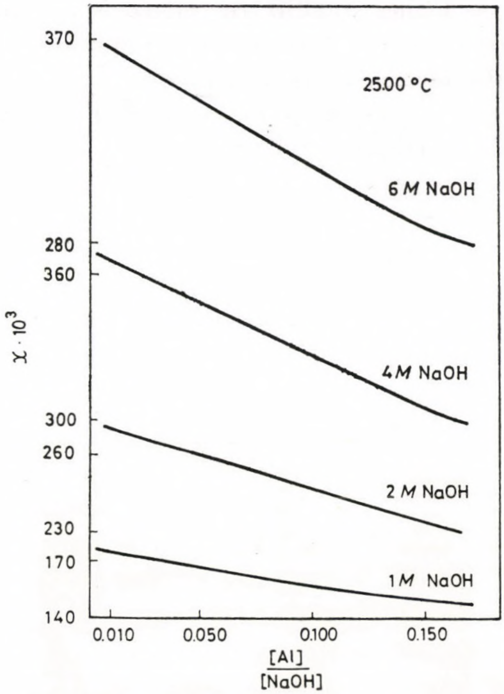

Fig. 2. **Conductivity changes in function of total and relative concentrations**

associate can be detected in every case and its formation constant can be calculated.

The values of conductivity found and calculated are practically identical with those shown in Fig. 1, thus, instead of details, the computed β_{11} values (measured conductometrically at 25.00 °C) are summarized in Table I.

Table I

Formation constants of $Al(OH)_4^- \cdot OH^-$ *associate at 25 °C*

Total concentration	$\beta_{11}(\pm 3\sigma)$
1.00 *M*	0.76 ± 0.09
2.00 *M*	0.90 ± 0.11
4.00 *M*	1.56 ± 0.12
6.00 *M*	3.88 ± 0.18

Based on these data, some conclusions can be drawn as

i) in more concentrated aluminate lyes there exists the $Al(OH)_4^- \cdot OH^-$ associate;

ii) which has the higher stability the higher is the total concentration. (This latter fact supports some earlier assumptions: the water concentration decreases with increasing total molarities, thus anionic hydrations through hydrogen bonds compete with each other and hydrogen bridged, direct anion–anion interactions can be realized.)

A similar or a more pronounced phenomenon is to be expected [5] also as the effect of a change in temperature. This is why conductivities (in several cases also viscosities and densities) have been measured also at 15 and 35 °C. These data (shown in Table II) together with those in Table I indicate the great temperature dependence of the association constants which is characteristic to hydrogen bonding.

Table II

Formation constants at 15 and 35 °C

Total concentration	$\beta_{11}(\pm 3\sigma)$	
	15 °C	35 °C
1.00 *M*	1.44 ± 0.15	0.52 ± 0.08
2.00 *M*	1.69 ± 0.18	0.55 ± 0.09
4.00 *M*	3.02 ± 0.18	0.75 ± 0.09
6.00 *M*	7.67 ± 0.32	1.61 ± 0.15

(It has to be mentioned that, during the evaluation of conductivity data measured in highest total concentration at the lowest temperature, a 1 : 2 aluminate—hydroxide interaction [6] can not be definitely neglected.)

The data available suggest that it is not only the change in total concentration but also a change in temperature that substantially influences the structure of the solutions. It means that the validity of the generally known correlation:

$$-RT \ln \beta_{11} = \Delta H - T\Delta S \tag{6}$$

might be questionable. We tried to evaluate the data in Tables I and II; and Eq. 6 was proved to be valid (within a limit of errors of 5—12%). The calculated values are summarized in Table III.

Table III

ΔH and ΔS values of $Al(OH)_4^- \cdot OH^-$ *associate*

Total concentration	ΔH kJ/mole	ΔS J/mole · degree
1.00 *M*	—37.5	—129
2.00 *M*	—40.8	—137
4.00 *M*	—50.4	—177
6.00 *M*	—57.5	—183

From these results the following conclusions can be drawn:

i) The ΔS and ΔH values (and their correlation) are characteristic for hydrogen bridged complexes.

ii) The relatively high ΔH and $T\Delta S$ values reflect contrary tendencies which give rise to the relatively low β_{11} formation constants.

iii) The dependence of ΔH and ΔS on the total concentration proves that water acts against the formation of hydrogen bridged complexes in competing reactions.

REFERENCES

[1] Kuznetsov, S. I., Dereogakin, V. A.: Physical Chemistry of Aluminium Production by the Bayer Method, Metallurgy Publishing House, Moscow 1964
[2] Eremin, N. I., Volkov, U. A., Miranov, V. E.: USp. Khim., **43**, 224 (1974)
[3] Klug, O., Dekovics, A., Wéber, J.: Bányászati és Kohászati Lapok, **111**, 139 (1978)
[4] Fuoss, R. M., Accascina, F.: Electrolytic Conductance Interscience, New York, 1959
[5] Pálfalvi-Rózsahegyi, M., Buvári, Á., Barcza, L., Szabó, Z. G.: Acta Chim. Acad. Sci. Hung. **102**, 401 (1979)
[6] Maksimova, I., Maschovets, V., Jushkevich, V.: Zh. Prikl., Khim., **40**, 2717 (1967)
[7] Gessner, W., Ködderitzsch, B.: Z. Chem., **18**, 370 (1978)
[8] Molenaar, R. J., Evans, J. O., McKeevar, L. D.: J. Phys. Chem., **74**, 3629 (1970)

Márta Pálfalvi-Rózsahegyi
Zoltán G. Szabó
Lajos Barcza
H-1443 Budapest, P.O.Box. 123.

Acta Chimica Academiae Scientiarum Hungaricae, Tomus 104 (3), pp. 311–316 (1980)

STUDY OF THE RATE OF CORROSION OF METALS BY A FARADAIC DISTORTION METHOD, II

EFFECT OF THE OHMIC RESISTANCE AND CAPACITY OF THE DOUBLE LAYER ON THE MEASUREMENT OF THE HARMONIC COMPONENTS OF THE FARADAIC CURRENT

J. Dévay and L. Mészáros

(Research Group for Electrochemistry of the Hungarian Academy of Sciences, Veszprém)*

Received March 5, 1979

Accepted for publication September 17, 1979

In our previous communication [1] the theory of a faradaic distortion method has been presented for the study of the rate of corrosion. In the present communication we investigated the applicability of this method to measuring cells employed in practice, namely the effect of the capacity of the double layer and the ohmic resistance of the solution have also been considered in addition to that of the faradaic impedance. The ohmic resistance of the solutions can readily be compensated by a potentiostat permitting the compensation of the total ohmic drop in the cell. The effect of the capacitive current flowing through the double layer can be eliminated by performing measurements at least at two different frequencies and by extrapolating the data to $\omega = 0$ frequency. The capacitive current appears in the fundamental harmonic component of the current only.

In our previous communication [1] a method has been presented for the determination of the rate of corrosion of metals by faradaic distortion assuming that the faradaic impedance only consisted of a resistance having characteristics corresponding to the charge transfer reaction of the anodic and cathodic partial processes. The method is based on the measurement of the harmonic components of the current flowing through the electrode under the effect of a potentiostatically controlled sinusoidal alternating voltage superimposed on the polarizing direct voltage.

The electrochemical parameters of the metal (such as corrosion current and the slopes of the Tafel's equations of the cathodic and anodic processes, respectively) have been calculated on the basis of the measurement of the first three harmonic components of the faradaic alternating current at two potentials, one is the anodic and the other is the cathodic Tafel range, respectively. The electrochemical parameters can also be calculated by the measurement of the harmonic component at the corrosion potential. In the calculation previously reported, the effect of the capacity of the double layer of the electrode and that of the solution resistance between the working electrode and the reference electrode have been left out of consideration.

---

* Present address: Hungarian Academy of Sciences, Research Laboratory for Inorganic Chemistry H-1112 Budapest, Budaörsi út 45

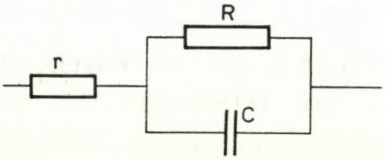

Fig. 1. Equivalent circuit of the electrode

Without these assumptions, the electrode behaviour or actually the cell impedance can be characterized by the equivalent circuit shown in Fig. 1, where r is the constant solution resistance mentioned above, while the electrode impedance consists of faradaic impedance R and capacity C of the double layer. In the present case the former is equal to a resistance corresponding to the charge transfer reaction wich depends on the potential but is independent of the frequency of the a.c. component, while the latter is the capacity of the double layer which, as a first approximation is assumed to be independent of the electrode potential, *i.e.* it is assumed to be a linear circuit element. This assumption is generally valid for small amplitudes of the alternating voltage.

In our earlier works [2—4], the effect of the ohmic resistance and that of the capacity of the double layer have been calculated in the case of a.c. polarography, *i.e.* diffusion polarization. The ohmic resistance and the capacity of the double layer have been found to modify the theoretical relationships to an extent depending on the frequency and the concentration of the solution.

This effect was found to be smaller when the frequency was low (the capacitive current was negligible as compared to the faradaic current) and/or concentration of the species determining the potential was low (*i.e.* the ohmic resistance is negligible as compared to the faradaic impedance). The above theoretical calculations have also been verified experimentally.

In the present communication, the application of the faradaic distortion method is studied for the case of an electrode impedance corresponding to the equivalent circuit of Fig. 1.

The impedance of the circuit shown in Fig. 1 is given by the following formula:

$$Z = \frac{1}{\frac{1}{R} + i\omega C} + r = \frac{(r + R) + i\omega rRC}{1 + i\omega RC}, \tag{1}$$

where ω is the angular frequency of the sinusoidal alternating voltage, and i is the imaginary unit. As the method is based on the study of the alternating current density proportional to the electrode admittance, the reciprocal of Eq. (1) has to be written

$$\frac{1}{Z}=\frac{1+i\omega RC}{(r+R)+i\omega rRC}=\frac{1}{r+R}\,\frac{1+i\omega RC}{1+i\omega\dfrac{rR}{r+R}C}=\frac{1}{r+R}\times$$

$$\times\frac{1+\omega^2R^2C^2\dfrac{r}{r+R}}{1+\omega^2R^2C^2\left(\dfrac{r}{r+R}\right)^2}+i\,\omega\frac{1}{r+R}\,\frac{RC\dfrac{R}{r+R}}{1+\omega^2R^2C^2\left(\dfrac{r}{r+R}\right)^2}\tag{2}$$

The discussion of Eq. (2) is rather cumbersome, therefore the admittance was studied three special cases.

1) When $\omega\to\infty$, the second term of Eq. (2) tends to zero and

$$\lim_{\omega\to\infty}\frac{1}{Z}=\frac{1}{r},\tag{3}$$

i.e. at very high frequencies the impedance of the double layer tends to zero and the admittance is determined by the ohmic resistance.

2) When $\omega\to 0$, the imaginary term of the admittance disappears again and

$$\lim_{\omega\to 0}\frac{1}{Z}=\frac{1}{r+R},\tag{4}$$

and thus the admittance is unaffected by the capacity of the double layer.

3) When ω is sufficiently small, the terms containing ω^2 are negligible as compared to unity and

$$\frac{1}{Z}=\frac{1}{r+R}+i\omega\frac{R^2C}{(R+r)^2}.\tag{5}$$

Writing the square of the absolute value of Eq. (5)

$$\left|\frac{1}{Z}\right|^2=\left(\frac{1}{r+R}\right)^2+\omega^2C^2\left(\frac{R}{R+r}\right)^4\tag{6}$$

it becomes evident that the square of the admittance is a function of the second power of the frequency, when ω is small.

The dependence of the square of the admittance on the frequency is shown in Fig. 2. Thus $\left|\frac{1}{Z}\right|^2$ assumes values between $\left(\frac{1}{r+R}\right)^2$ and $\left(\frac{1}{r}\right)^2$, depending on frequency ω.

In other words the ohmic resistance and the parellel *RC* circuit act as a voltage divider to a degree depending on the frequency and, consequently, only a fraction of the constant amplitude of the alternating voltage applied to the cell appears on the electrode impedance.

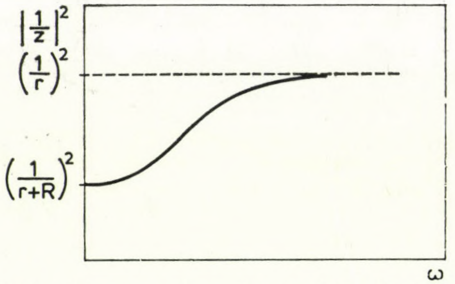

Fig. 2. The frequency dependence of the admittance

The fundamental harmonic component of frequency ω of the measured alternating current is proportional to the absolute value of the admittance given by the following expression

$$\left|\frac{1}{Z}\right| = \frac{1}{r+R}\sqrt{1+\omega^2R^2C^2\left(\frac{R}{r+R}\right)^2}\,. \tag{7}$$

It is apparent that the fundamental harmonic component of the current depends on the frequency, in contrast to the case when the electrode behaviour is only characterized by resistance R [1].

The frequency dependent voltage division between the ohmic resistance and the electrode impedance has a larger effect on the second and third harmonic components, which are functions of the second and third power, respectively, of the alternating voltage appearing across resistance R or across the electrode impedance in the present case [1].

The higher harmonic components generated on the faradaic impedance also flow through resistance r. As an undistorted sinusoidal alternating voltage was imposed on the cell impedance, the higher harmonic voltages appearing across resistance r also appear with opposite phase across the electrode impedance. The higher harmonic currents flowing under the effect of the above voltages decrease the intensity of the measured higher harmonic components on account of their phase relations and thus they cause an error in the evaluation of the experimental data.

Consequently, when the faradaic distortion method is employed in such cases when the ohmic resistance of the solution is considerable, it is advisable to impose the alternating voltage on the electrode by means of a potentiostat compensating the voltage drop on the above constant resistance in order to ensure that the voltage appearing on the faradaic impedance be undistorted and have the desired amplitude. In this case the electrode admittance is given by the following expression

$$\frac{1}{Z} = \frac{1}{R} + i\omega C\,. \tag{8}$$

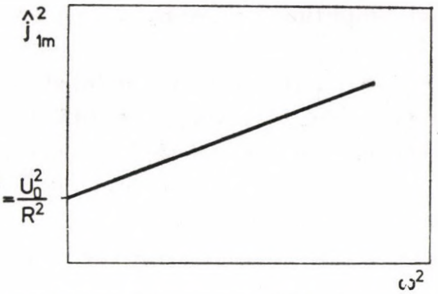

Fig. 3. Extrapolation of the measured first harmonic current

This equation still reflects the shunting effect of the capacity of the double layer on resistance R. However, the square of the amplitude of the experimentally measured fundamental harmonic current density ($\hat{\mathbf{j}}_{1m}$) is a linear function of ω^2, as it can be readily shown if the square of $\hat{\mathbf{j}}_{1m}$ is calculated using the square of the absolute value of the admittance. Then the following equation is obtained

$$\hat{\mathbf{j}}_{1m}^2 = \hat{\mathbf{j}}_1^2 + \omega^2 C^2 U_0^2 = \frac{U_0^2}{R^2} + \omega^2 C^2 U_0^2 , \tag{9}$$

where $\hat{\mathbf{j}}_1$ is the amplitude of the fundamental harmonic current density of the faradaic current and U_0 is the amplitude of the alternating voltage applied to the electrode (Fig. 3).

Thus $\hat{\mathbf{j}}_1$, *i.e.* the fundamental harmonic current component independent of double layer effects, can be obtained from measurements performed with alternating voltages at various frequencies and by linear extrapolation of $\hat{\mathbf{j}}_{1m}$ to $\omega = 0$.

This value can readily be employed to calculate the corrosion current density according to the method reported in our previous communication [1].

The capacity of the double layer can also be evaluated according to Eq. (9) and Fig. 3.

These data may also provide valuable information *e.g.* in the case of the adsorption of inhibitors.

The measured values of the second and third harmonic current components can be employed for the evaluation of the corrosion current density without further correction provided that the effect of r is eliminated by the use of an adequate potentiostat since the double layer capacity — being a linear circuit element — does not generate higher harmonic components and thus the source of the latter is only the faradaic impedance.

The above results lead to the conclusion that the effect of r should be compensated by using an adequate potentiostat and the measurements should be carried out applying at least two alternating voltages having different frequencies but equal amplitudes in order to permit extrapolation for the elimination of the effect of *C*.

The current densities of the second and third harmonic components are equal in the case of two applied voltages of different frequencies when the effect of *r* is properly compensated and the capacity of the double layer can really be assumed to be independent of the electrode potential in the potential range corresponding to the investigation.

The experimental results related to the above method will be published later.

REFERENCES

[1] DÉVAY, J., MÉSZÁROS, L.: Magy. Kém. Foly. **85**, 209 (1979) Acta Chim. Acad. Sci. Hung., **100**, 183 (1979)

[2] DÉVAY, J., MÉSZÁROS, L., GARAI T.: Magy. Kém. Foly., **74**, 491 (1968); Acta Chim. Acad. Sci. Hung., **60**, 67 (1969)

[3] DÉVAY, J., MÉSZÁROS, L., GARAI, T.: Magy. Kém. Foly., **75**, 219 (1969); Acta Chim. Acad. Sci Hung., **61**, 279 (1969)

[4] DÉVAY, J., GARAI, T., MÉSZÁROS, L., PALÁGYI-FÉNYES, B.: Magyar. Kém. Foly., **79**, 49 (1973); Acta Chim. Acad. Sci. Hung., **75**, 331 (1973)

József DÉVAY
Lajos MÉSZÁROS
H-1112 Budapest, Budaörsi út 45.

RECENSIONES

Structure and Bonding, Vol. **36**
Inorganic Chemistry and Spectroscopy

Springer-Verlag, Berlin—Heidelberg — New York, 1979

The most recent volume of the successful and popular series "Structure and Bonding" contains three reviews from the field of spectroscopy and inorganic chemistry.

The first one, "The Resonance Raman Effect. Review of the Theory and Application in Inorganic Chemistry", is by R. J. H. CLARK and B. STEWART. Raman spectroscopy is one of the spectroscopic methods which supply the richest structural information. Although the effect has been known for a relatively long time, its widespread application is due to the recent development in laser techniques, extremely sensitive phototubes and other technical novelties. A resonance Raman spectrum can be obtained by exciting the molecules of the sample by a laser radiation with a frequency coincident or very close to an allowed electronic transition of the molecules. In the resulting spectrum the bands corresponding to the totally symmetric vibrations of the molecule are extremely strong, and their overtones are enhanced, too. Consequently, certain compounds can also be investigated in very low concentrations (10^{-6} mol/l).

The authors review the theory and application of this new and very promising experimental technique. The first part of the review deals with the theory of the method at a high level but, in my opinion, too briefly, although it occupies 46 out of the total of 80 pages. It assumes the reader to be familiar with many basic principles, thereby barring interested non-experts from the complete understanding of the review. In this part normal and resonance Raman scattering are compared, the totally symmetric vibrational modes and Franck-Condon scattering as well as the not totally symmetric modes and Herzberg—Teller scattering are discussed. Chapter 3 gives a very brief account of experimental methods.

Chapter 4 shows the experimental results in a systematic way proceeding from diatomic molecules to more complicated ones, also including metal complexes and some biological systems. The results obtained for various types of molecules are summarized in tables which comprise all the literature data available. The review is complete with 110 references.

The oxides, peroxides and superoxides of alkali metals have been known for a long time. The existence of suboxides with low oxidation states was discovered in 1909, but their systematic investigation started only ten years ago. The results and literature of this ten-year period are reviewed by A. SIMON ("Structure and Bonding with Alkali Metal Suboxides").

The main concern of this work is to discuss the structures and physico-chemical properties of these compounds, but the review also deals briefly with their application and prospective applications. The detailed diagrams of Chapter II illustrate how many types of these compounds may exist. In addition to the binary systems Rb/Rb_2O and Cs/Cs_2Om the ternary Rb-Cs suboxides are also discussed.

Chapter III reviews the crystallographic investigations. The main emphasis is laid upon the structures of the two basic types, Rb_9O_2 and $Cs_{11}O_3$ clusters; the structures of the other suboxides can be understood on the basis of these two types. Chapter IV deals with bonding. The bond lengths of the compounds are compared, and conclusions are drawn on the ionic character of bonds in the clusters. Chapter V is concerned with the various physical properties, such as conductivity, colour, dielectric behaviour. PES and ESCA results are discussed in detail, which indicate that $Cs_{11}O_3$ is ready to emit photoelectrons when exposed to infrared radiation, and thus it can be applied as an IR sensitive photocathode. The 48-page review contains 89 references.

A special subject, of primary interest for specialists, is reviewed by C. Daul, C. W. Schläpfer and A. von Zelewsky ("The Electronic Structure of Cobalt(II) Complexes with Schiff Bases and Related Ligands").

This work is a complete and very detailed review of the spectroscopic and quantum chemical structure investigations performed on these complexes.

Owing to the planar tetragonal arrangement, the splitting of d orbitals produces a pattern in which four d orbitals are very close to one another and the fifth (d_{xy}) is destabilized by a strong σ interaction. The singly occupied d orbital of the ground state is in some cases d_{z^2} and in other cases d_{yz} ($\langle yz, {}^2A_2|$ or $\langle z^2, {}^2A_1|$ states, respectively). The spectroscopic and structural properties of complexes are determined by this state of affairs. The EPR spectra, which can be interpreted on the basis of four excited states (2 doublets and 2 quartets), are discussed in detail. These excited states are very close to the ground state. NMR and electron spectra as well as the results of magnetic susceptibility measurements are in agreement with the conclusions drawn from EPR. The review also contains a complete list of references on the quantum chemical investigations in this field, including simple AOM calculations, more advanced SCCC-MO approximations and *ab initio* methods. The results of calculations are presented in expressive diagrams. The review is concluded by a tabulated summary of the spectroscopic data of the 35 compounds investigated so far. 76 references are given.

J. Nagy

R. P. Houghton: *Metal Complexes in Organic Chemistry*

Cambridge University Press, Cambridge, 1979. pp. 308

Even organic chemists using complexes in their practical work may be surprised by their wide-ranging application in organic chemistry, as witnessed by this book. Thus among others "they may be used in the purification of organic compounds, in the resolution of racemic mixtures and for simplifying nuclear magnetic resonance spectra. In reactions they may be used as reactants or catalysts, they may be generated and function as reactive species, or they may be formed as products", as we can read in the preface of this very well written book. It is surprising indeed that "at the present time there does not appear to be a book devoted to those aspects of the chemistry of metal complexes that make this type of compound so important to modern organic chemistry".

The first chapter is devoted to the theoretical basis of organometallic complexes (σ-donor ligands and σ-donor strength, σ-donor/π-acceptor ligands, π-complexes of metals, σ-donor/π-donor ligands, chelation and macrocyclic ligands, steric hidrance in metal complexes).

The next chapter deals with the effects and uses of complex formation and in this chapter we can read about the implementation of the possibilities mentioned in the introductory part, with the exception of catalytic effects.

The last three chapters make the reader acquainted with the use of metal complex catalysts in substitution, addition, oxidative addition and insertion reactions.

Because of the breadth of the subject it is clear that every aspect could not be covered in a book of this size; one notable omission (with the exception of the Ziegler—Natta polymerizationof alkenes) is the metal-catalyzed polymerization of unsaturated organic compounds. The author's policy, therefore, has been to emphasize principles rather than facts and, generally speaking, detailed factual information is presented only in order to illustrate principles and not for its own sake.

This book is intended primarily for advanced undergraduates, graduates at the start of a research career in organic chemistry and practising organic chemists who wish to learn more about the chemistry of metal complexes. The author's expectation that the book will be of use to all chemists who are concerned with the interaction of metals with organic ligands, seems to be quite justified.

Gy. Deák

Topics in Current Chemistry, 80

In Memory of H. L. **Meerwein**
Springer Verlag, Berlin, Heidelberg, New York, 1979, 320 pages

The 80th volume of this popular series is devoted to the memory of Hans L. **Meerwein**.

Meerwein's paper published in 1922 on the investigation of the equilibrium between bornyl chloride, isobornyl chloride and camphene hydrochloride was of fundamental importance in respect of the development of theoretical organic chemistry. This paper was the first to suggest the existence of a carbocation intermediate in explaining the rearrangement. This paper also started the debate which has continued till today, whether carbocations represent an equilibrium mixture of classical structures rapidly transforming into each other or they exist as "non-classical" ions.

The dramatic character of the latter problem, and the Hamletian doubts it has raised, can be followed throughout the chapters of the book written by different authors.

Chapter *1* (18 pages), written by Herbert C. **Brown**, is entitled "Meerwein and Equilibrating Carbocations". The review aims at investigating the question, which way of description reflects better reality in the case of the 2-norbornyl cation. It is concluded that **Meerwein**'s original interpretation can be regarded as valid today, too.

The second chapter (61 pages), by George A. **Olah**, has the title "From Boron Trifluoride to Antimony Pentafluoride in Search of Stable Carbocations". After an introduction, the author discusses stable, long-lived carbocations, then proceeds to deal with five- and higher coordinated, non-classical carbocations. This very interesting chapter containing a great deal of information arrives, among others, at the conclusion that in the case of the norbornyl cation the non-classical description, maintaining **Winstein**'s original view, should be regarded as correct.

The third chapter (32 pages) is a paper by Hepke **Hogeveen** and Eugène M. G. A. **van Kruchten**: "Wagner—Meerwein Rearrangements in Long-lived Polymethyl Substituted Bicyclo [3.2.0] heptadienyl Cations"; it deals with the synthesis of precursors of carbocations, the generation of carbocations and their spectroscopic observation, and with the mechanism of rearrangements.

The last chapter (183 pages) was written by Wolfgang **Kirmse**; it is entitled "Rearrangements of Carbocations, Stereochemistry and Mechanism".

The author gives a survey of the following main topics: (a) Carbocations in the gas phase; (b) carbocations in superacids; (c) ion pairs; (d) micellar effects; (e) conformational control; (f) bridged ions, anchimeric assistance.

Every chapter is completed with a very comprehensive literature survey. The book affords very enjoyable reading not only to chemists advanced in the field, but practically to all interested in organic chemistry.

It would have been desirable if all authors had used the name carbocation, as also suggested by the IUPAC Nomenclature Committee, at least in this book of fundamental importance.

Cs. **Szántay**

INDEX

PHYSICAL AND INORGANIC CHEMISTRY

ORGANIC CHEMISTRY

ANALYTICAL CHEMISTRY

Printed in Hungary

A kiadásért felel az Akadémiai Kiadó igazgatója. Műszaki szerkesztő: Zacsik Annamária
A kézirat nyomdába érkezett: 1980 VII. 3. — Terjedelem: 10,85 (A/5) ív, 44 ábra

80.7855 Akadémiai Nyomda, Budapest — Felelős vezető: Bernát György

Les Acta Chimica paraissent en français, allemand, anglais et russe et publient des mémoires du domaine des sciences chimiques.

Les Acta Chimica sont publiés sous forme de fascicules. Quatre fascicules seront réunis en un volume (3 volumes par an).

On est prié d'envoyer les manuscrits destinés à la rédaction à l'adresse suivante:

Acta Chimica
Budapest, P.O. Box 67, H-1450, Hongrie

Toute correspondance doit être envoyée à cette même adresse.

La rédaction ne rend pas de manuscript.

Abonnement en Hongrie à l'Akadémiai Kiadó (1363 Budapest, P. O. B. 24, C. C. B. 215 11488), à l'étranger à l'Entreprise du Commerce Extérieur « Kultura » (H-1389 Budapest 62, P. O. B. 149 Compte-courant No. 218 10990) ou chez représentants à l'étranger.

Die Acta Chimica veröffentlichen Abhandlungen aus dem Bereich der chemischen Wissenschaften in deutscher, englischer, französischer und russischer Sprache.

Die Acta Chimica erscheinen in Heften wechselnden Umfanges. Vier Hefte bilden einen Band. Jährlich erscheinen 3 Bände.

Die zur Veröffentlichung bestimmten Manuskripte sind an folgende Adresse zu senden

Acta Chimica
Budapest, Postfach 67, H-1450, Ungarn

An die gleiche Anschrift ist jede für die Redaktion bestimmte Korrespondenz zu richten.

Manuskripte werden nicht zurückerstattet.

Bestellbar für das Inland bei Akadémiai Kiadó (1363 Budapest, Postfach 24, Bankkonto Nr. 215 11488), für das Ausland bei »Kultura« Außenhandelsunternehmen (H-1389 Budapest 62, P. O. B. 149. Bankkonto Nr. 218 10990) oder seinen Auslandsvertretungen.

«Acta Chimica» издают статьи по химии на русском, английском, французском и немецком языках.

«Acta Chimica» выходит отдельными выпусками разного объема, 4 выпуска составляют один том и за год выходят 3 тома.

Предназначенные для публикации рукописи следует направлять по адресу:

Acta Chimica
Budapest, P.O. Box 67, H-1450, ВНР

Всякую корреспонденцию в редакцию направляйте по этому же адресу.

Редакция рукописей не возвращает.

Отечественные подписчики направляйте свои заявки по адресу Издательства Академии Наук (1363 Budapest, P.O.B. 24, Текущий счет 215 11488), а иностранные подписчики через организацию по внешней торговле «Kultura» (H-1389 Budapest 62, P.O.B. 149. Текущий счет 218 10990) или через ее заграничные представительства и уполномоченных.

Reviews of the Hungarian Academy of Sciences are obtainable at the following addresses:

AUSTRALIA
C.B.D. LIBRARY AND SUBSCRIPTION SERVICE, Box 4886, G.P.O., *Sydney N.S.W. 2001*
COSMOS BOOKSHOP, 145 Ackland Street, *St. Kilda (Melbourne), Victoria 3182*

AUSTRIA
GLOBUS, Höchstädtplatz 3, *1200 Wien XX*

BELGIUM
OFFICE INTERNATIONAL DE LIBRAIRIE, 30 Avenue Marnix, *1050 Bruxelles*
LIBRAIRIE DU MONDE ENTIER, 162 Rue du Midi, *1000 Bruxelles*

BULGARIA
HEMUS, Bulvar Ruski 6, *Sofia*

CANADA
PANNONIA BOOKS, P.O. Box 1017, Postal Station "B", *Toronto, Ontario M5T 2T8*

CHINA
CNPICOR, Periodical Department, P.O Box 50, *Peking*

CZECHOSLOVAKIA
MAD'ARSKÁ KULTURA, Národni třida 22, *115 66 Praha*
PNS DOVOZ TISKU, Vinohradská 46, *Praha 2*
PNS DOVOZ TLAČE, *Bratislava 2*

DENMARK
EJNAR MUNKSGAARD, Norregade 6, *1165 Copenhagen*

FINLAND
AKATEEMINEN KIRJAKAUPPA, P.O. Box 128, *SF-00101 Helsinki 10*

FRANCE
EUROPERIODIQUES S. A., 31 Avenue de Versailles, *78170 La Celle St.-Cloud*
LIBRAIRIE LAVOISIER, 11 rue Lavoisier, *75008 Paris*
OFFICE INTERNATIONAL DE DOCUMENTATION ET LIBRAIRIE, 48 rue Gay-Lussac, *75240 Paris Cedex 05*

GERMAN DEMOCRATIC REPUBLIC
HAUS DER UNGARISCHEN KULTUR, Karl-Liebknecht-Strasse 9, *DDR-102 Berlin*
DEUTSCHE POST ZEITUNGSVERTRIEBSAMT, Strasse der Pariser Kommüne 3—4, *DDR-104 Berlin*

GERMAN FEDERAL REPUBLIC
KUNST UND WISSEN ERICH BIEBER, Postfach 46, *7000 Stuttgart 1*

GREAT BRITAIN
BLACKWELL'S PERIODICALS DIVISION, Hythe Bridge Street, *Oxford OX1 2ET*
BUMPUS, HALDANE AND MAXWELL LTD., Cowper Works, *Olney, Bucks MK46 4BN*
COLLET'S HOLDINGS LTD., Denington Estate, *Wellingborough, Northants NN8 2QT*
WM. DAWSON AND SONS LTD., Cannon House, *Folkestone, Kent CT19 5EE*
H. K. LEWIS AND CO., 136 Gower Street, *London, WC1E 6BS*

GREECE
KOSTARAKIS BROTHERS, International Booksellers, 2 Hippokratous Street, *Athens-143*

HOLLAND
MEULENHOFF-BRUNA B.V., Beulingstraat 2, *Amsterdam*
MARTINUS NIJHOFF B.V., Lange Voorhout 9—11, *Den Haag*
SWETS SUBSCRIPTION SERVICE, 347b Heereweg, *Lisse*

INDIA
ALLIED PUBLISHING PRIVATE LTD., 13/14 Asaf Ali Road, *New Delhi 110001*
150 B-6 Mount Road, *Madras 600002*
INTERNATIONAL BOOK HOUSE PVT. LTD., Madame Cama Road, *Bombay 400039*
THE STATE TRADING CORPORATION OF INDIA LTD., Books Import Division, Chandralok, 36 Janpath, *New Delhi 110001*

ITALY
EUGENIO CARLUCCI, P.O. Box 252, *70100 Bari*
INTERSCIENTIA, Via Mazzé 28, *10149 Torino*
LIBRERIA COMMISSIONARIA SANSONI, Via Lamarmora 45, *50121 Firenze*
SANTO VANASIA, Via M. Macchi 58, *20124 Milano*
D. E. A., Via Lima 28, *00198 Roma*

JAPAN
KINOKUNIYA BOOK-STORE CO. LTD., 17-7 Shinjuku-ku 3 chome, Shinjuku-ku, *Tokyo 160-91*
MARUZEN COMPANY LTD., Book Department, P.O. Box 5050 Tokyo International, *Tokyo 100-31*
NAUKA LTD. IMPORT DEPARTMENT, 2-30-19 Minami Ikebukuro, Toshima-ku, *Tokyo 171*

KOREA
CHULPANMUL, *Phenjan*

NORWAY
TANUM-CAMMERMEYER, Karl Johansgatan 41—43, *1000 Oslo*

POLAND
WĘGIERSKI INSTYTUT KULTURY, Marszalkowska 80, *Warszawa*
CKP 1 W ul. Towarowa 28 *00-958 Warszawa*

ROUMANIA
D. E. P., *Bucureşti*
ROMLIBRI, Str. Biserica Amzei 7, *Bucureşti*

SOVIET UNION
SOJUZPETCHATJ — IMPORT, *Moscow*
and the post offices in each town
MEZHDUNARODNAYA KNIGA, *Moscow G-200*

SPAIN
DIAZ DE SANTOS, Lagasca 95, *Madrid 6*

SWEDEN
ALMQVIST AND WIKSELL, Gamla Brogatan 26, *S-101 20 Stockholm*
GUMPERTS UNIVERSITETSBOKHANDEL AB, Box 346, *401 25 Göteborg 1*

SWITZERLAND
KARGER LIBRI AG, Petersgraben 31, *4011 Basel*

USA
EBSCO SUBSCRIPTION SERVICES, P.O. Box 1943, *Birmingham, Alabama 35201*
F. W. FAXON COMPANY, INC., 15 Southwest Park, *Westwood, Mass, 02090*
THE MOORE-COTTRELL SUBSCRIPTION AGENCIES, *North Cohocton, N. Y. 14868*
READ-MORE PUBLICATIONS, INC., 140 Cedar Street, *New York, N. Y. 10006*
STECHERT-MACMILLAN, INC., 7250 Westfield Avenue, *Pennsauken N. J. 08110*

VIETNAM
XUNHASABA, 32, Hai Ba Trung, *Hanoi*

YUGOSLAVIA
JUGOSLAVENSKA KNJIGA, Terazije 27, *Beograd*
FORUM, Vojvode Mišića 1, *21000 Novi Sad*

8. IX. 1980 HU ISSN 0001—5407 **Index: 26.007**

ACTA CHIMICA
ACADEMIAE SCIENTIARUM HUNGARICAE

TOMUS 104 FASCICULUS 4

AKADÉMIAI KIADÓ, BUDAPEST
1980

ACTA CHIM. ACAD. SCI. HUNG. ACASA2 104 (4) 321–424 (1980)

ACTA CHIMICA

A MAGYAR TUDOMÁNYOS AKADÉMIA KÉMIAI TUDOMÁNYOK OSZTÁLYÁNAK IDEGEN NYELVŰ KÖZLEMÉNYEI

Acta Chimica is a journal for the publication of papers on all aspects of chemistry in English, German, French and Russian.

Acta Chimica is published in 3 volumes per year. Each volume consists of 4 issues of varying size.

Manuscripts should be sent to

Acta Chimica
Budapest, P.O. Box 67, H-1450, Hungary

Correspondence with the editors should be sent to the same address. Manuscripts are not returned to the authors.

Hungarian subscribers should order from Akadémiai Kiadó, 1363 Budapest, P.O. Box 24. Account No. 215 11488.

Orders from other countries are to be sent to "Kultura" Foreign Trading Company (H-1389 Budapest 62, P.O. Box 149. Account No. 218 10990) or its representatives abroad.

Acta Chimica Academiae Scientiarum Hungaricae, Tomus 104 (4), pp. 321—328 (1980)

KINETICS AND MECHANISM OF THE REDUCTION OF COPPER(II) BY IRON(II) IN PRESENCE OF SODIUM FLUORIDE IN ACIDIC MEDIUM

R. K. SRIVASTAVA, K. K. SRIVASTAVA, M. N. SRIVASTAVA and B. B. L. SAXENA

(Chemical Laboratories, University of Allahabad, India)

Received September 18, 1977
In revised form October 13, 1978
Accepted for publication November 14, 1978*

The reduction of copper(II) by iron(II) in presence of sodium fluoride has been kinetically studied in acidic medium. The reaction rate is first order with respect to iron(II) but is independent of Cu(II) concentration. It is also directly proportional to fluoride concentration, but is inversely proportional to acid concentration. The rate constants decrease with increasing ionic strength as well as increasing dielectric constant of the medium. A suitable reaction mechanism has been proposed leading to a rate expression,

$$\frac{-\mathrm{d}\,\Sigma\,\mathrm{Fe(II)}}{\mathrm{d}t} = \frac{K_1 K K_a\,[\mathrm{Fe}^{++}]\,[\mathrm{HF}]}{[\mathrm{H}^+]}$$

where K represents the formation constant of the complex and K_a is the acid dissociation constant of hydrofluoric acid.

In alkaline medium copper(II) is well known to oxidise sugars [1—4] either alone or in the presence of some complexants as tartrate, citrate *etc.*, but in acidic medium, however, copper(II) has seldom been used as an oxidant. BELCHER and WEST [5] observed that copper(II) is reduced by iron(II) in presence of an appreciable excess of ammonium thiocyanate. With fluoride, the E_0 value of $\mathrm{Fe^{III}/Fe^{II}}$ system is suppressed from 0.77 volts in aqueous solution to $\sim$0.40 volts in presence of fluoride [6], and thus Fe(II) becomes a more potential reducing agent by adding fluoride. VERMA [7, 8] has employed it for the reduction of iodine and silver(I). The present paper describes the results on the kinetic study of the reduction of Cu(II) by Fe(II) in presence of sodium fluoride in low acidic medium.

Material Used

Copper sulphate (A.R.), ferrous ammonium sulphate (A.R.), sodium fluoride (B.A. quality A.C.S. reagent), perchloric acid (Riedel), sulphuric acid (A.R.), absolute ethyl alcohol, sodium perchlorate (Riedel), ceric sulphate (B.D.H.).

All the solutions were prepared in double distilled water, stored in Jena glass bottles, and were suitably standardized. Ceric sulphate solution was prepared by digesting it in *conc.* sulphuric acid and diluting it with distilled water, so that the final acid concentration was approximately 1 *N*. It was then standardized by titration against a standard ferrous ammonium sulphate solution using ferroin as an indicator. Further solutions were obtained by dilution but the acid concentration was maintained approximately 1 *N*.

---

* In final form accepted December 21, 1979

Procedure

The progress of the reaction was followed by estimating the amount of remaining Fe(II) at different intervals of time. The requisite quantities of the solutions of copper sulphate (containing a known concentration of sulphuric or perchloric acid) and sodium fluoride were taken in seperate well stoppered 100 ml flasks (coated with black Japan from outside) and were kept in an electrically operated thermostat at the desired temperature. Ferrous ammonium sulphate solution of desired concentration (containing also a known concentration of sulphuric acid or perchloric acid) was kept in a separate 100 ml flask in the same thermostat. After about half an hour, when the solutions had attained the temperature of the bath, the reaction was started by adding 5 ml of ferrous ammonium sulphate solution in each of the reaction bottles. At definite intervals of time the entire reaction mixture of each flask was poured into a beaker containing ice cubes made from distilled water to quench the reaction. The flasks were also washed three times with ice cold distilled water and washings were added to the main reaction mixture in the beaker. It was then filtered through a gravimetric filter paper (Whatman No. 42) and the cuprous precipitate was thoroughly washed with ice-cooled distilled water. In the filtrate ferrous ion was titrated with a standardized ceric sulphate solution using ferroin as an indicator. The blank reading with ferroin was substracted from the titre value. Thus the concentration of remaining Fe(II) was calculated at different intervals of time.

Results and Discussion

The stoichiometry of the reaction was first studied by leaving a reaction mixture over night, and it was observed that Fe(II) and Cu(II) react in the ratio of 1 : 1. Thus the precipitate appears to contain copper(I) and the reaction may be represented as:

$$Cu^{++} + Fe^{++} \rightarrow Fe^{3+} + Cu^{+}$$

The red cuprous precipitate was found to be soluble in both HCl and dil. HNO_3, further it also gave a positive test for fluoride and Fe^{3+} even after repeated through washings. On further analysis it was found to contain Fe^{3+} and Cu^{+} in the ratio 1 : 1 whereas the amount of fluoride varied, depending upon the amount of sodium fluoride used in the reaction mixture. Thus the precipitate may be represented by a general formula as $Cu^{I}M^{I}_{2}[Fe^{III}F_{6-n}(H_2O)_n]$, (where M^{I} represents a univalent cation as Na^+ or H^+); but for simplicity it will be referred simply as Cu(I).

Determination of Order with Respect to Fe(II)

The order of the reaction with respect to Fe(II) was determined by isolation method. The results are graphically represented in Fig. 1, containing plots of log $(a - x)$ *vs.* time, and hence it can be inferred that the reaction is of first order with respect to Fe(II). A notable feature of the curves is, however, that they show a break at about 45—60 minutes although they retain their lienar nature even after the break. This is generally the period at which the precipitates appear in conspicuous manner in the reaction mixtures. It is also to

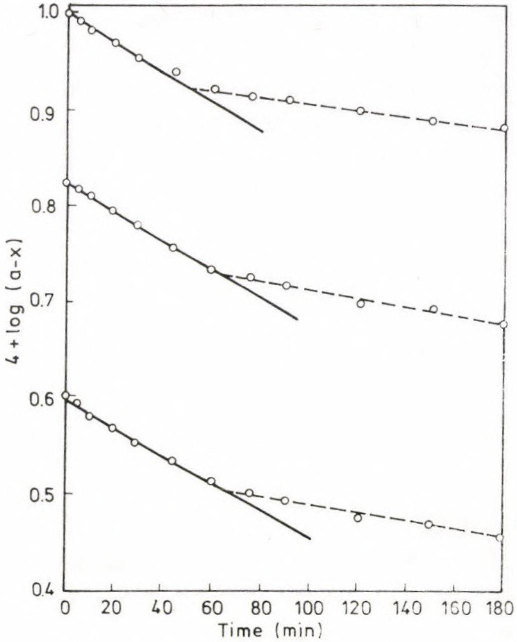

Fig. 1. First order rate plots for the $Cu^{II}-Fe^{II}$ reaction in the presence of fluoride. [Copper sulphate] = 0.02 *M*; [Sodium fluoride] = 0.1 *M*; [Sulphuric acid] = 0.2 *N*; [Ferrous ammonium sulphate] = 25, 20, 13×10^{-4} *M*

be noted that the reaction does not show any induction period which is generally observed in reduction reaction of Cu(II). It appears that in the reduction of Cu(II) by Fe(II) in presence of fluoride both homogeneous catalysis due to fluoride and heterogeneous catalysis due to particles of reduced Cu(I) have a cumulative effect. The induction period vanishes because of the prominent role of homogeneous catalysis due to fluoride. VERMA [7] obtained similar results in the reduction of Ag(I) by Fe(II) in presence of fluoride. KRISHNA and GHOSH [9] also observed a shortening of the induction period in the reduction of Ag(I) by Fe(II) in presence of acetate buffer, and ascribed this to homogeneous catalysis of acetate ion.

The breaks observed in the above curves may be explained in the following manner. In presence of fluoride Cu(II)is readily reduced by Fe(II) producing primary particles of reduced copper(I), which in turn themselves act as centres of heterogeneous catalysis. However, as the reaction proceeds, the primary particles slowly coalesce together to form bigger secondary particles, thus reducing their total surface area. In about 45—60 minutes the particles grow to such a size that a precipitate appears and the reaction rate suddenly falls, thus accounting for the observed breaks in Fig. 1. Probably after this break, the role of heterogeneous catalysis is reduced to minimum. Similar observations were made earlier in the reduction of selenium(IV) by iron(II) in presence of fluoride [10] and explained similarly.

A question may arise why this reaction does not show any phenomenon of autocatalysis with the accumulation of the product Cu(I) in the system. The reason for this may lie in the fact that actually these may be the primary reduced Cu(I) particles which may be responsible for the heterogenous catalysis The various equilibria in such system may be expressed as

$$\begin{array}{r} \mathrm{Cu^{II} + Fe^{II}} \text{ (in presence of } \mathrm{F^{I}}) \rightleftharpoons \mathrm{Fe^{III} + Cu(I)} \text{ (Primary particles)} \\ \downarrow \qquad\quad \\ \mathrm{Cu(I)} \text{ (Secondary particles)} \rightarrow \text{ppt.} \end{array}$$

i.e., as with the progress of the reaction primary reduced Cu(I) particles are being formed, they are being constantly converted into Cu(I) secondary particles, so that the concentration of primary Cu(I) particles actually responsible for heterogeneous catalysis may be assumed to be practically constant, and hence autocatalysis is not observed. Of course, when the particles grow to such a size that they result into a precipitate, heterogeneous catalysis due to Cu(I) particles is reduced to minimum as shown by a break in reaction rate curves.

Hence for evaluation of velocity constants, only the initial part of the reaction has been considered worthwhile. The constants were obtained both by taking the average of the constants in the initial part of the reaction before the breaks, and also from the initial slope of the curves (Fig. 1). It was noted that the first order constants obtained by both the methods were in good agreement. The results for different variations as of Fe(II), Cu(II), fluoride, acid and temperature are presented in summarized form in Table I.

A perusal of the Table I shows that the reaction is first order with respect to Fe(II), whereas it is independent of the Cu(II) concentration. It was also observed that a linear plot is obtained when k values are plotted against fluoride concentration showing that the reaction rate is directly proportional to fluoride concentration. Fluoride variation was done, at constant ionic strength and constant free acid concentration. This was achieved by adding equivalent amount of perchloric acid as the fluoride concentration was varied. The ionic strength was maintained constant by adding required amount of sodium perchlorate.

Similarly the effect of acid variation was studied at constant ionic strength by employing the various amounts of perchloric acid and sodium perchlorate. A plot of log k_1 against log [free $HClO_4$] gave a straight line with a slope of **—1.** The free perchloric acid concentration was calculated by substracting the concentration of sodium fluoride from total concentration of perchloric

Table I

Pseudo I order contants for the reduction of Cu(II) *by* Fe(II) *in presence of fluoride in acidic medium*

Temp. — 30 °C

$[\mathrm{Fe(II)}] \times 10^3$ *M*	[Cu(II)] *M*	[NaF] *M*	$[\mathrm{H_2SO_4}]$ *N*	$[\mathrm{HClO_4}]$ *N*	$[\mathrm{NaClO_4}]$ *N*	$k_1 \times 10^3$ min^{-1}
2.50	0.02	0.1	0.2	—	—	3.45
2.00	0.02	0.1	0.2	—	—	3.34
1.33	0.02	0.1	0.2	—	—	3.42
1.00	0.02	0.1	0.2	—	—	3.62
0.66	0.02	0.1	0.2	—	—	3.40
0.40	0.02	0.1	0.2	—	—	3.65
2.00	0.02	0.2	0.4	—	—	6.05
2.00	0.04	0.2	0.4	—	—	6.15
2.00	0.05	0.2	0.4	—	—	6.85
2.00	0.08	0.2	0.4	—	—	6.68
2.00	0.10	0.2	0.4	—	—	6.85
1.00	0.02	0.04	—	0.04	0.11	3.46
1.00	0.02	0.06	—	0.06	0.09	3.81
1.00	0.02	0.08	—	0.08	0.07	4.24
1.00	0.02	0.10	—	0.10	0.05	4.45
1.00	0.02	0.12	—	0.12	0.03	4.75
1.00	0.02	0.15	—	0.15	0.00	5.18
1.00	0.02	0.10	—	0.13	0.12	8.05
1.00	0.02	0.10	—	0.15	0.10	4.27
1.00	0.02	0.10	—	0.17	0.08	2.51
1.00	0.02	0.10	—	0.21	0.04	1.54
1.00	0.02	0.10	—	0.25	0.00	1.15

acid present in the reaction mixture. Sodium fluoride by reacting with perchloric acid gives the weak hydrofluoric acid [11] and this latter practically does not contribute the hydrogen ion concentration in presence of a strong acid. Theresults thus indicate that the reaction rate is inversely proportional to acid concentration.

The temperature coefficient of the reaction is found to be 2.33 in the range of 25—35 °C; 2.30 in the range of 30—40 °C and 2.08 in the range of 35—45 °C, *i.e.* an average value of 2.24 for every rise of 10 °C. The apparent energy of activation is calculated by graphical method as $E_a = 15.3$ K.cal mol^{-1}.

Variation of Ionic Strength and Dielectric Constant

Table II contains average k_1 values for a particular set of different ionic strengths and dielectric constants of the medium, which were achieved by using different amounts of sodium perchlorate and ethyl aclohol respectively. It is observed that the rate constants decrease with increasing ionic strength as well as increasing dielectric constant. A plot of log k against μ gave almost parallel straight lines with negative slopes and a plot of log k_1 at $\mu = 0$ (obtained by extrapolation) against $1/D$ exhibited linear relationship. Such a behaviour [12, 13] could be due to either

Table II

Effect of ionic strength and dielectric constant on rate constants

Temp. — 30 °C; $[CuSO_4] = 0.004$ *M*; $[NaF] = 0.02$ *M*; $[HClO_4] = 0.02$ *M*; Ferrous ammonium sulphate = 0.0002 *M*

$[NaClO_4] \times 10^2$ *M*	μ	$k \times 10^3$ min^{-1} Ethyl alcohol				
		5%	10%	20%	30%	40%
0	0.0574	6.55	10.9	24.4	47.8	67.7
5	0.1074	5.75	8.32	19.2	27.7	50.4
10	0.1574	5.29	6.90	15.7	25.1	35.5
20	0.2574	5.54	6.43	14.4	17.9	31.0
By extrapolation at $\mu = 0$		8.13	16.6	39.8	91.2	151.4

(i) a reaction between oppositely charged ions, or

(ii) a reaction between a positive ion and a neutral molecule, if a decrease in rate constant with increasing μ could be ascribed to a negative secondary salt effect.

Reaction Mechanism

Ferric ion forms stable complexes with fluoride [14], the stability of the ferrous ion with fluoride complex, however, is rather low. Nevertheless it may be assumed, that in the present reaction ferrous ion first combines with fluoride to form $[FeF^+]$ complex [15], which inspite of its law stability is present in appreciable concentration to initiate the reaction. That is why the reaction rate is directly proportional to fluoride concentration.

The concentration of $[FeF^+]$ is given by the reaction, $[FeF^+] = K.$ $[Fe^{++}]$ $[F^-]$, where K is the equilibrium constant for the formation of this complex. Further $[F^-] = K_a\,[HF]/[H^+]$, where K_a is the acid dissociation constant of hydrofluoric acid. Thus the concentration of $[FeF^+]$ or

$[FeF(H_2O)_5]^+$,if water of coordination is also considered, would be given

$$[FeF(H_2O)]^+ = K.K_a[Fe^{++}][HF]/[H^+]$$

Thus the reaction mechanism may be represented as,

$$HF \rightleftharpoons H^+ + F^- \qquad \text{(i)}$$

$$[FeH_2O)_6^{++}] + [F^-] \rightleftharpoons [Fe(H_2O)_5F^+] + H_2O \qquad \text{(ii)}$$

$$[Fe(H_2O)_5F]^+ \xrightarrow[k_{-1}]{k_1} [Fe(H_2O)_4F(OH)] + H^+ \qquad \text{(iii)}$$

$$[Fe(H_2O)_4F(OH)] + Cu^{++} \xrightarrow{k_2} [Fe(H_2O)_4F(OH) --- Cu^{++}]$$

$$[Fe(H_2O)_4F(OH) --- Cu]^{++} \xrightarrow{\text{fast}} [Fe^{III}(H_2O)_4F(OH)]^+ + Cu(I)$$

↓

(Product)
(precipitate)

If the complexes $[FeF(H_2O_5)^+]$ and $[Fe(H_2O)_4F(OH)]$ are represented by $[C]$ and $[C_1]$ respectively, by applying steady state treatment, it leads to a rate expression,

$$\frac{-d\sum[Fe^{II}]}{dt} = \frac{k_2 k_1 [C][Cu^{++}]}{k_{-1}[H^+] + k_2[(Cu^{++})]}$$

Now if $k_2 \gg k_{-1}$.

$$\frac{-d\sum(Fe^{II})}{dt} = k_1[C] = \frac{k_1 K_a K [Fe^{++}][HF]}{[H^+]}$$

Thus the rate expression is quite consistent with the observed facts that

(i) The reaction rate is first order with respect to Fe(II) but is independent of Cu^{++} concentration.

(ii) The reaction is catalysed by hydrofluroic acid.

(iii) The reaction is retarded by (H^+), the rate constants being inversely proportional to acid concentration.

(iv) The behaviour of dielectric constant and ionic strength can be explained if the reaction is assumed to be between positive ion and a neutral molecule provided there is negative secondary salt effect. Now it is quite clear that reaction step (iii) is just equivalent as

$$[FeF(H_2O)_n^+] + H_2O \rightleftharpoons [FeF(H_2O)_{n-1}] + H_3O^+$$

i.e., a hydrolysis reaction involving the reaction between a positive ion and a neutral water molecule. The behaviour of dielectric constant variation is thus explained.

As regards negative secondary salt effect, hydrofluoric acid being a weak acid, its dissociation increases with the increasing ionic strength of the medium. Therefore, with an increase in ionic strength there is a consequent increase in hydrogen ion concentration. But we know that in this reaction hydrogen ion has a retarding effect. That is why we observe a negative secondary salt effect. The ionic strength may also influence step (iii) in which also the H^+ is formed thus contributing the negative secondary salt effect.

The important role of fluoride in this reaction may also lie in the formation of the product, the stable ferric fluoride complex [15], so that in its presence the concentrations of free ferric ions is drastically reduced, and thus chance of back oxidation of Cu^I by Fe^{III} is eliminated. The reaction proceeds in the forward direction.

REFERENCES

[1] Urech, F.: Ber., **22**, 318 (1889)
[2] Singh, M. P., Krishna, B., Ghosh, S.: Z. Phys. Chem., **204**, 1 (1955); **205**, 285 (1956); **208**, 273 (1958)
[3] Marshall, B. A., Walters, J.: J. Chem. Soc. **1961**, 1579
[4] Singh, S. V., Saxena, O. C., Singh, M. P.: J. Am. Chem. Soc., **92**, 537 (1970)
[5] Belcher, R., West, T. S.: Anal. Chim. Acta, **5**, 364 (1951)
[6] Moeller, T.: "Inorganic Chemistry", Asia Edn., Asia Publishing House, p. 302 (1963)
[7] Verma, H. S.: D. Phil. Thesis, Allahabad University (1969)
[8] Verma, H. S., Srivastava, M. N., Saxena, B. B. L.: Indian J. Chem., **16-A**, 208 (1978)
[9] Krishna, B., Ghosh, S.: J. Phys. Coll. Chem., **55**, 1503 (1951)
[10] Srivastava, R. K., Srivastava, V. K., Srivastava, M. N., Saxena, B. B. L.: J. Chim. Phys., **70**, 918 (1973)
[11] Vogel, A. I.: "Qualitative Inorganic Analysis", Longmans, (1953), p. 27
[12] Frost, A. A., Pearson, R. G.: "Kinetics and Mechnism", 2nd Edn., John Wiley & Sons, (1961)
[13] Amis, E. S.: "Kinetics of Chemical Change in Solution", Macmillans (1949)
[14] Dodgen, H. W., Rollefson, G. K.: J. Am. Chem. Soc., **71**, 2600 (1949)
[15] Cotton, F. A., Wilkinson, G.: "Advanced Inorganic Chemistry", Wiley, Eastern, p. 859 (1969)

Rajni K. Srivastava
Kamala K. Srivastava
Manharan N. Srivastava
Balded B. L. Saxena
Allahabad-211 022, India

Acta Chimica Academiae Scientiarum Hungaricae, Tomus 104 (4), pp. 329—335 (1980)

ON THE MECHANISM OF THE SYNERGISTIC EXTRACTION OF LANTHANIDES WITH THENOYLTRIFLUOROACETONE AND ALIQUATE-336S

I. L. Dukov and L. Ch. Genov

(Department of Inorganic Chemistry, Higher Institute of Chemical Technology, Sofia)

Received May 18, 1979
Accepted for publication July 26, 1979

Extraction of trivalent lanthanides Pr, Eu and Yb with thenoyltrifluoroacetone and Aliquate-336S in benzene, carbon tetrachloride and cyclohexane has been investigated. It was found that the extracted adduct has the formula $M(TTA)_4^- Q^+$, Q^+ is a quaternary ammonium cation. Equilibrium constants for the synergistic reactions have been calculated. Some assumptions about the mechanism of the extraction process have been discussed.

Introduction

The use of quaternary ammonium salts in the synergistic extraction of metals is on increase in recent years. Several investigations are known in which quaternary ammonium salts are used as synergists in mixtures with chelating [1—7] and neutral organophosphorus [8—12] extractants. Synergistic effect is found even for the extraction of Zn with di-2-ethylexylphosphoric acid and tetraoctylammonium chloride [13]. However, the mechanism of the synergistic extraction with the participation of a chelating extractant and a quaternary ammonium salt is not quite clear.

The present work was undertaken in order to study the synergistic extraction with mixtures of these extractants.

Experimental

Reagents. Aliquate-336S (a long-chain quaternary ammonium chloride henceforth called QCl) was obtained from General Mills USA and thenoyltrifluoroacetone (HTTA) was a Merck analytical grade product. The quaternary ammonium salt was purified before use [14]. Pr_6O_{11}, Eu_2O_3 and Yb_2O_3 (99.9%) were used to prepare the stock solutions of the metals. Other reagents used were of A. R. quality.

Procedure. Partition experiments were carried out using 20 ml volumes of the aqueous and organic phases. The equilibrium was reached within 1 hour by mechanical shaking. After the separation of the phases the concentration of the metals was determined using Arsenazo III [15]. The acidity of the aqueous phase was measured by a pH meter with an accuracy of ± 0.01 pH unit.

In all experiments the concentration of the metals was 2.5×10^{-4} *M*. The ionic strength was maintained at 0.1 with (Na, H)Cl with the exception of one series of experiments where the chloride ion concentration was varied (Fig. 5).

The extraction of the metals with HTTA only was realized in the same manner.

Results and Discussion

Although, HTTA is one of the most widely used extractants [16] however, some data for the extraction of metals with HTTA are missing.

Extraction of trivalent lanthanides with HTTA can be represented by Eq. (1)

$$M^{3+}_{aq} + 3\ HTTA_{org} \rightleftharpoons M(TTA)_{3org} + 3\ H^{+}_{aq} \qquad (1)$$

The equilibrium constant K_T can be expressed as

$$K_T = \frac{[M(TTA)_3]_{org}\,[H^+]^3_{aq}}{[M^{3+}]_{aq}\,[HTTA]^3_{org}} = D_T\,\frac{[H^+]^3_{aq}}{[HTTA]^3_{org}} \qquad (2)$$

where D_T is the distribution coefficient.

Figure 1 shows the plots of log D_T *vs.* pH for the extraction of Pr, Eu and Yb with 0.1 *M* HTTA in benzene, carbon tetrachloride and cyclohexane. The dependences give straight lines of slope 3. The values of the equilibrium constants K_T, calculated from the experimental data are given in Table I.

Table I

Equilibrium constants of the synergistic extraction of Pr, Eu and Yb with HTTA and QCl

Metal	Solvent	log K_T	log K				log β
			From pH variation	From HTTA variation	From QCl variation	Mean log K	
Pr	C_6H_6	−9.05	−3.39	−3.47	−3.32	−3.39	5.66
	CCl_4	−9.98	−3.35	−3.45	−3.34	−3.38	6.60
	C_6H_{12}	−9.65	−2.91	−2.91	−3.00	−2.94	6.71
Eu	C_6H_6	−7.83	−2.19	−2.23	−2.20	−2.21	5.62
	CCl_4	−8.62	−2.27	−2.20	−2.22	−2.23	6.39
	C_6H_{12}	−8.20	−1.81	−1.69	−1.92	−1.81	6.39
Yb	C_6H_6	−6.68	−1.76	−1.74	−1.77	−1.76	4.92
	CCl_4	−7.45	−1.77	−1.77	−1.78	−1.77	5.68
	C_6H_{12}	−7.09	−1.39	−1.22	−1.46	−1.36	5.73

The plots of log *D* *vs.* pH; log *D* *vs.* log [HTTA] and log *D* *vs.* log [QCl] were determined by the investigation of the synergistic extraction of metals. These dependences are given in Figs 2—4 and they represent straight lines of. slopes 4,4 and 1, respectively. Since the quaternary ammonium salt exists as a monomer in the concentration range used [17] the synergistic extraction of the lanthanides can be described by the following reaction

$$M^{3+}_{aq} + 4\ HTTA_{org} + QCl_{org} \rightleftharpoons M(TTA)^{-}_{4}\ Q^{+}_{erg} + 4\ H^{+}_{aq} + Cl^{-}_{aq} \qquad (3)$$

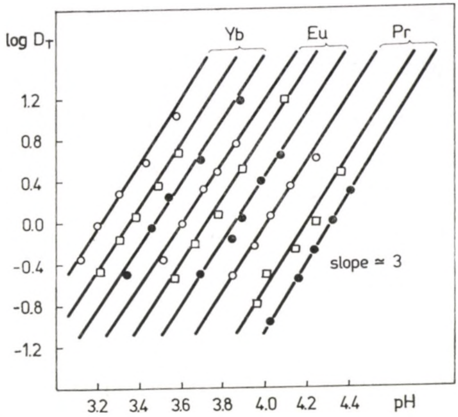

Fig. 1. log D_T *vs.* pH for Pr, Eu and Yb at [HTTA] = 0.1*M*. C_6H_6 (open circles); CCl_4 (closed circles); C_2H_{12} (squares)

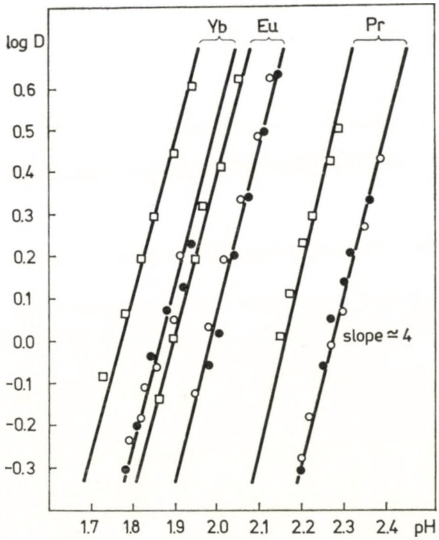

Fig. 2. log *D vs.* pH for Pr, Eu and Yb at [HTTA] = $8\times10^{-2}M$ and [QCl] = $4.9\times10^{-3}M$. C_6H_6 (open circles); CCl_4 (closed circles); C_6H_{12} (squares)

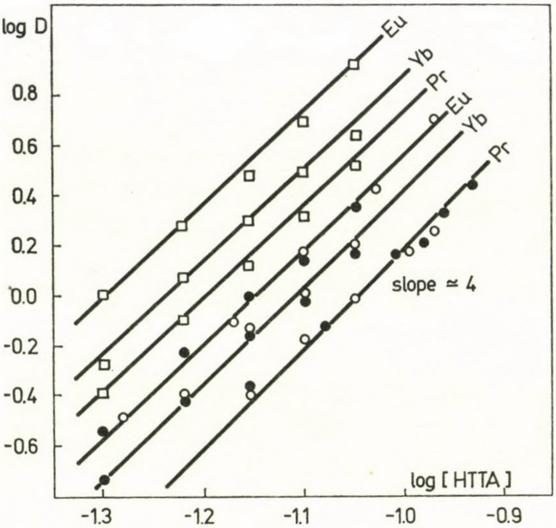

Fig. 3. log *D* *vs.* log [HTTA] for Pr(pH = 2.24), Eu(pH = 2.03) and Yb (pH = 1.87) at [QCl] = $4.9 \times 10^{-3}M$. C_6H_6 (open circles); CCl_4 (closed circles); C_6H_{12} (squares)

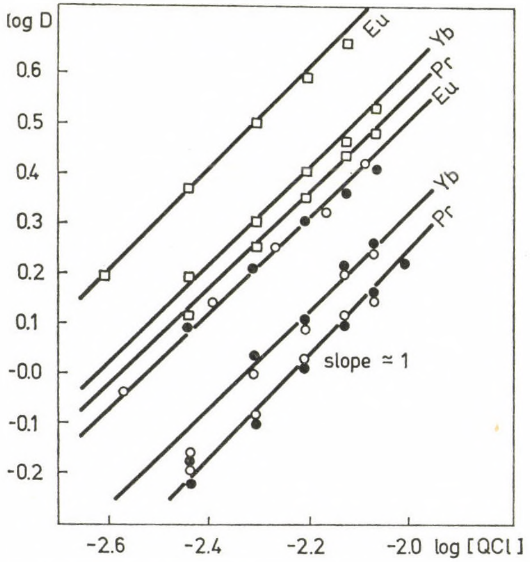

Fig. 4. log *D* *vs.* log [QCl] for Pr (pH = 2.24), Eu (pH = 2.03) and Yb (pH = 1.87) at [HTTA] = $8 \times 10^{-2}M$. C_6H_6 (open circles); CCl_4 (closed circles); C_6H_{12} (squares)

The equilibrium constant K can be expressed as

$$K = \frac{[\mathrm{M(TTA)_4^-\,Q^+}]_{\mathrm{org}}\,[\mathrm{H^+}]_{\mathrm{aq}}^4\,[\mathrm{Cl^-}]_{\mathrm{aq}}}{[\mathrm{M^{3+}}]_{\mathrm{aq}}\,[\mathrm{HTTA}]_{\mathrm{org}}^4\,[\mathrm{QCl}]_{\mathrm{org}}} = D\,\frac{[\mathrm{H^+}]_{\mathrm{aq}}^4\,[\mathrm{Cl^-}]_{\mathrm{aq}}}{[\mathrm{HTTA}]_{\mathrm{org}}^4\,[\mathrm{QCl}]_{\mathrm{org}}} \tag{4}$$

where D is the synergistic distribution coefficient. Taking logarithms on both sides of Eq. (4)

$$\log K = \log D + 4\log[\mathrm{H^+}] + \log[\mathrm{Cl^-}] - 4\log[\mathrm{HTTA}] - \log[\mathrm{QCl}] \tag{5}$$

The values of the equilibrium constant K can be calculated easily from (5). These values are given in Table I.

It can be noted that the mechanism of the synergistic extraction of lanthanides with HTTA and QCl is analogous to the mechanism described for the extraction of divalent metals with mixtures of chelating extractant and a quaternary ammonium salt [1—3].

It can be assumed that the following interaction takes place in the organic phase

$$\mathrm{M(TTA)_{3\,org}} + \mathrm{HTTA_{org}} + \mathrm{QCl_{org}} \rightleftharpoons \mathrm{M(TTA)_4^-\,Q_{org}^+} + \mathrm{H_{aq}^+} + \mathrm{Cl_{aq}^-} \tag{6}$$

Probably, appropriate condition for displacing the equilibrium to the right is created by the presence of the quaternary ammonium salt since its cation participates in the ion pair formation.

The equilibrium constant β for the organic phase synergistic extraction is given by equation (7)

$$\beta = \frac{[\mathrm{M(TTA)_4^-\,Q^+}]_{\mathrm{org}}\,[\mathrm{H^+}]_{\mathrm{aq}}\,[\mathrm{Cl^-}]_{\mathrm{aq}}}{[\mathrm{M(TTA)_3}]_{\mathrm{org}}\,[\mathrm{HTTA}]_{\mathrm{org}}\,[\mathrm{QCl}]_{\mathrm{org}}} = \frac{K}{K_{\mathrm{T}}} \tag{7}$$

The values of β are also given in Table I.

The mechanism described is supperted also by data obtained on the influence of chloride ion concentration on the extraction process. Figure 5 shows the dependences of log D *vs.* log $[\mathrm{Cl^-}]$. The slope of 1 obtained for the $[\mathrm{Cl^-}]$ variation plots is in agreement with the mechanism proposed by Eq. (2). Besides, these experiments prove that the mechanism of the synergistic extraction of Eu given in [6] is not quite correct. According to this mechanism the synergistically extracted adduct is $[\mathrm{Eu(TTA)_3Cl}]^-\mathrm{Q}^+$ and thus the distribution coefficient is not influenced by the concentration of chloride ions because these ions in such case, do not influence the extraction equilibria.

Unfortunately, for the present it is not clear why the mechanism proposed is realised only when a quaternary ammonium salt is used as a synergist. For example, high molecular weight amines resemble the quaternary ammonium

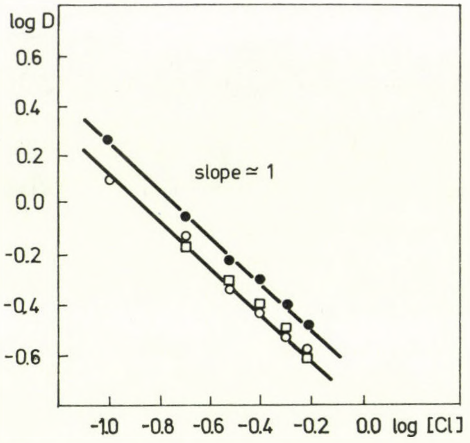

Fig. 5. log *D vs.* log $[Cl^-]$ for Pr (pH = 2.31, open circles), Eu (pH = 2.05, closed circles) and Yb (pH = 1.84, squares) at [HTTA] = $8 \times 10^{-2}M$ and [QCl] = $4.9 \times 10^{-3}M$. Solvent: C_6H_6

salts because amines take part in the extraction processes as amine salts. However, in mixtures with HTTA adduct of the type $M^{+n}(TTA)_nAmHX$ [18—21] is formed. (AmHX is an amine salt with a monobasic acid.) Therefore, the extraction mechanism is not the same.

It must be added that when a quaternary ammonium salt is used as a synergist the synergistic effect is higher than the effect obtained using aliphatic amines. This is noted also in [6]. The fact can be explained assuming that in the adduct $M(TTA)_4^-Q^+$ the four chelating ligands satisfy the coordination requirements of the metal. The two molecules of water in the metal chelate $M(TTA)_3 2\ H_2O$ [22] are not the components of the mixed adduct, however, one molecule of water probably is component of the adduct $M^{3+}(TTA)_3AmHX$.

REFERENCES

[1] Nishimura, M., Noriki, S., Muramoto, S.: Anal. Chim. Acta, **70**, 121 (1974)
[2] Noriki, S., Muramoto, M.: Anal. Chim. Acta, **72**, 339 (1974); **94**, 57 (1977)
[3] Noriki, S.: Anal. Chim. Acta, **76**, 215 (1975)
[4] Genov, L. Ch., Dukov, I. L., Kassabov, G. I.: Acta Chim. Acad. Sci. Hung., **95**, 361 (1977)
[5] Hiroshi, K., Hideo, K.: Jap. Anal., **23**, 495 (1974)
[6] Khopkar, P. K., Mathur, J. N.: J. Inorg. Nucl. Chem., **39**, 2063 (1977)
[7] Desreux, J. F., Massaux, J., Duyskaerts, G.: J. Inorg. Nucl. Chem., **40**, 1159 (1978)
[8] Khopkar, P. K. Narayanankutty, P.: J. Inorg. Nucl. Chem. **34**, 3233 (1974)
[9] Kolarik, Z., Puzić, R. G., Maksimović, Z. W.: J. Inorg. Nucl. Chem., **31**, 2485 (1969)
[10] Mihlin, E. B., Rozen, A. M., Norina, T. M., Nikonov, V. N., Afonina, T. A., Tumanov, A. V.: Radiokhimia, **19**, 294 (1977)
[11] Valkov, A. V., Kiznetsov, S. A., Makarenlo, M. K., Sergievski, V. V., Yagodin, G. A.: Izv. vuzov. Khim. i khim. tekhn., **21**, 542 (1978)
[12] Dukov, I., Kassabov, G., Genov, L.: Monatsh. Chem., **110**, 335 (1979)
[13] Tataribov, V. A., Ivanov, I. M., Gle, K., Mül, P., Fischer, K., Gindin, L.: Izv. Sib. Otd. Acad. Nauk SSSR, ser. khim. nauk, **9**, issue **4**, 96 (1978)
[14] Goto, T.: J. Inorg. Nucl. Chem., **31**, 1111 (1969)

[15] SAVVIN, S. B.: Arsenazo III, p. 177, Atomizdat, Moscow, 1966
[16] STARY, J., FREIZER, H.: Equilibrium Constants of Liquid—Liquid Distribution Reactions. Part IV: Chelating Extractants, p. 131, Pergamon Press, Oxford 1978
[17] GOOD, M. L., SRIVASTAVA, S. C.: J. Inorg. Nucl. Chem., **27**, 2429 (1965)
[18] NEWMAN, L., KLOTZ, P.: Inorg. Chem., **11**, 2150 (1972)
[19] GENOV, L., DUKOV, I.: Monatsh. Chem., **104**, 750 (1973); Z. Chem., **14**, 446 (1974)
[20] KE, C. H., LI, N. C.: J. Inorg. Nucl. Chem., **31**, 1383 (1969)
[21] ALY, H. F., RAIEH, M., MOHAMED, S., ABDEL-RASSOUL, A. A.: J. Inorg. Nucl. Chem., **40**, 567 (1978)
[22] KASSIERER, E. F., KERTES, A.S.: J. Inorg. Nucl. Chem., **34**, 778 (1972)

Ivan L. DUKOV
Limon Ch. GENOV
Department of Inorganic Chemistry, Higher Institute of Chemical Technology, 1156 Sofia, Bulgaria

Acta Chimica Academiae Scientiarum Hungaricae, Tomus 104 (4), pp. 337—343 (1980)

ELECTROCHEMICAL INVESTIGATION OF 5 wt% PLATINUM CATALYSTS ON CARBON SUPPORT

É. POLYÁNSZKY,[1] T. MALLÁT,[1] J. PETRÓ[1] and A. SÁRKÁNY[2]

([1] Department of Organic Chemical Technology of the Technical University, Budapest,
[2] Isotope Institute of the Hungarian Academy of Sciences, Budapest)

Received March, 30, 1979
Accepted for publication August 2, 1979

1. The dispersity of 5 wt% Pt/C catalysts, impregnated in the same way, depends very strongly on further treatment, particularly on the mode of reduction ($D = 0.29$—0.86).

2. The character of hydrogen sorption on the catalyst precipitated from a metal salt solution in the presence of support, is similar to that of platinum (2 kinds of hydrogen), while that of the catalysts reduced after previous impregnation of carbon is different (one kind of hydrogen).

In the shaping of the surface excess free energy of the catalysts, dispersity is the decisive factor; compared to it, the role of physical and chemical defects seems to be negligible.

Introduction

Platinum on carbon support has been extensively investigated by STONEHART [1] and KINOSHITA *et al.* [2—6] by electrochemical (potentiodynamic) methods. However, for catalysts of less than 5 wt% metal content the polarization curves could not be evaluated because of the interfering effect of the carbon double layer capacity, while at a metal content of 5 wt% or higher, the character of the curves was the same as that of platinum without support, only the height of the peaks corresponding to certain hydrogen forms changed, depending on the dispersity of the catalyst.

We found in our earlier investigations [7] for palladium catalysts on carbon support that the character of potentiodynamically determined hydrogen sorption strongly depends on the metal content: at low metal content the polarization curve is similar to that of the support, while at high metal content to that of the support-free metal.

In our present experiments, Pt/C catalysts of low metal content have been investigated by the method developed for supported palladium with the aim to clarify whether the character of hydrogen sorption is influenced by the support.

Another object was to investigate at identical metal content the effect of the mode of preparation of the catalyst on hydrogen sorption and on the surface excess free energy.

The relationship between the surface excess free energy of various noble metal and alloyed noble metal catalysts and their other properties has been studied [8, 9], and results obtained for the excess free energy of Pt/C and Rh/C catalysts of various metal contents are under publication [10]. The final object of these studies is to establish the effects of dispersity and the chemical and physical defects, on the excess free energy of catalysts.

As a supplement to the interpretation of our results, H_2 and CO chemisorption, and the liquid phase hydrogenating activity of the catalysts have been investigated.

Experimental

Preparation of 5 wt% Pt/C catalysts

With 105 cm^3 of an aqueous solution containing 1.036 g of $PtCl_4$, 11.4 g of active carbon (Carbo C-extra; surface area 954 m^2/g) was impregnated in 6 portions; it was dried after each wetting at 343 K in vacuum. The support thus impregnated was treated in portions of 2.4 g in five different ways.

1. Under stirring, the impregnated support was sprinkled into 100 cm^3 of 2 wt% $NaHCO_3$ solution at 333 K, and after 15 min of stirring reduced at room temperature in hydrogen atmosphere. The substance was filtered, washed with 3 dm^3 of distilled water for 3 hrs, and dried at room temperature in vacuum.

2. The impregnated support was sprinkled under stirring in 100 cm^3 of 2 wt% $NaBH_4$. After stirring for 15 min at room temperature the catalyst was filtered off, washed and dried as desrcibed above.

3. The impregnated support was sprinkled at room temperature into a solution of 18 g NaOH and 10 cm^3 of 35 wt% HCOH made up to a total volume of 100 cm^3. After stirring for 15 min, the catalyst was filtered off, washed and dried.

4. The impregnated support was reduced in a hydrogen stream at 373 K for 30 min, then flooded with distilled water. Filtration, washing, drying as above.

5. Five cm^3 of 10 wt% $NaHCO_3$ solution was deposited by evaporation in vacuum at 333 K on the impregnated support, which was then reduced in dry state in hydrogen at 373 K for 30 min, and flooded with distilled water. Filtration, washing, drying as above.

Further two catalysts were prepared by reduction with $NaBH_4$ in the following way:

6. 1.9 g Active carbon was shaken at 333 K in vacuum for 30 min, then impregnated under the same conditions with 10 cm^3 of 0.05 M H_2PtCl_6 solution for 3.5 hrs. The impregnated support and 150 cm^3 of 0.5 wt% $NaBH_4$ were fed in parallel into 50 cm^3 of 0.5 wt% $NaBH_4$ solution. After stirring for 30 min, the catalyst was filtered, washed and dried.

7. 1.9 g Active carbon was suspended in 100 cm^3 distilled water. Under stirring, 5 cm^3 0.1 M H_2PtCl_6 solution, then 20 cm^3 10 wt% $NaBH_4$ solution were added dropwise. After 15 min stirring, the catalyst was filtered, washed and dried.

Potentiodynamic measurements

During polarization the potential of the catalyst (measuring electrode) was changed at constant rate with respect to the platinized Pt/hydrogen reference electrode and the current passing through the measuring electrode was recorded. For the measurements a potentiostat AMEL 551/SU was used. The design of the three-electrode cell has been described in an earlier communication [7]. For the measurement 5 mg dry catalyst was placed on the measuring electrode, the cell was flushed with argon, then with hydrogen for 10 min, and with argon again for 4 min, to remove excess hydrogen. Next, still in argon atmosphere, the cell was filled up with 0.5 M sulfuric acid. After filling in the acid, the potential of the catalyst was 50—90 mV.

Measuring was started with cathodic polarization, and was continued on with anodic polarization from 30 mV up to 1000 mV, in each case at a rate of 10 mV/min.

The quantity of hydrogen can be determined from the area enclosed by the curve, under consideration of the current measured in the double layer region.

However, the double layer capacity of the active carbon of large surface area (954 m^2/g) was so high that this operation could not be performed with adequate accuracy, thus, the curves were evaluated only qualitatively.

Determination of apparent activity

The hydrogenating activity of the catalysts was investigated in the liquid phase reduction of cyclohexene and phenylacetylene.

20 mg dry catalyst and 10 cm^3 ethanol were weighed into a 50 cm^3 flask. Air above the mixture was exchanged for hydrogen and, under shaking (298 K, 1.013 bar, 330 vibrations/min), the catalyst was saturated with hydrogen. Without disconnecting the system, 2 cm^3 1 *M* cyclohexene or 0.5 *M* phenylacetylene solution in ethanol was injected, and the hydrogen consumption was measured with a gas burette while shaking.

The initial value of hydrogen consumption in unit time, referred to 1 g metal, was considered as the activity.

Measurement of surface excess free energy

The excess free energy of the catalyst was measured on the basis of the principle [8] according to which, in a metal ion solution, the potential difference (E) between the active metal (catalyst) and the metal at stable thermodynamic equilibrium is proportional to the excess free energy of the catalyst ($\Delta F'$):

$$\Delta F' = -zFE$$

where: z is the change in electron number,
F is Faraday's constant.

The measurement was performed in the apparatus described earlier [9].

About 50 mg catalyst was weighed on the glass filter. In 1 *M* hydrochloric acid solution and oxygen-free argon stream it was polarized to the value corresponding to the gas-free double layer region (400 mV), the electrolyte was then exchanged for 10^{-3} *M* H_2PtCl_6 solution, the chloride ion concentration of which was 1 *M*. Next, under magnetic stirring, the potential of the catalyst was measured in argon atmosphere until it became constant, or changed only very slowly. In the latter case, a value extrapolated to zero time was used for the calculation.

Investigation of chemisorption

The chemisorption of H_2 and CO was measured volumetrically in the pressure interval from 0.013 to 1.3 kPa at 298 K. From the catalyst reduced at 420 K hydrogen was removed in a dynamic vacuum of 1.3×10^{-4} Pa at 473—530 K (4—6 hrs). To eliminate the support effect, the points of the isotherm were extrapolated to zero pressure.

Dispersity [11] and surface of the catalyst were calculated from hydrogen chemisorption data under the assumption that 1 hydrogen atom is attached to 1 metal atom, and the density of the Pt atoms [12] is 1.3×10^{15} cm^{-2}. Dispersity is considered as the ratio of the surface metal atoms and the total metal atoms.

Experimental results and their evaluation

For the evaluation of the electrochemical investigations, the knowledge of the dispersity of the catalyst and of its surface is indispensable.

Table I shows the CO and H_2 chemisorption data for catalysts containing 5 wt% Pt on active carbon support, prepared by 7 different methods. The CO/H ratio increases with dispersity, its value in the dispersity interval from 0.21 to 0.86 ranges between 0.73 and 0.83.

With the exception of catalyst 5, dispersity values calculated from the hydrogen content vary between 0.21 and 0.43, and metal surface areas between 46 and 99 m^2/g. Catalyst 5, impregnated before reduction with hydrogen gas also with $NaHCO_3$, has outstandingly high dispersity (0.86) and metal surface area (192 m^2/g).

Table I

Dispersity and surface area of catalysts calculated from chemisorption

Symbol of catalyst	Chemisorbed CO (cm^3/g metal)	Chemisorbed H (cm^3/g metal)	Chemisorbed CO/H	Dispersity	Metal surface (m^2/g)
1	30.0	19.2	0.78	0.33	74
2	40.7	25.7	0.79	0.43	99
3	33.7	21.9	0.77	0.37	85
4	26.4	16.9	0.78	0.29	65
5	82.6	49.8	0.83	0.86	192
6	20.3	13.9	0.73	0.24	54
7	18.4	11.9	0.77	0.21	46

In the liquid phase reduction of the double and triple bonds (cyclohexene and phenylacetylene) the activity of the 7 catalysts shows virtually the same trend (Table II). Catalysts reduced with hydrogen gas are the most active (4, 5), the sample reduced with formaldehyde (3) has the lowest activity. No correlation was found between activity and dispersity, *e.g.* catalyst 4 of relatively small surface area revealed nearly the same activity as catalyst 5 of the highest dispersity. Thus, the different modes of preparation do not affect the activity only by changing the dispersity, but presumably the structure of the surface, the quantity and nature of impurities and sorption properties will also be different, and all this influences the activity.

The situation is just the opposite in the relationship of surface excess free energy and dispersity (Table II, Fig. 1). The surface excess free energy

Table II

Apparent activity and surface excess free energy of the catalysts

Symbol of catalysts	Activity: Cyclohexene $\left(\frac{cm^3\ H_2}{min\ g\ metal}\right)$	Activity: $-C{\equiv}C-$ bond of phenylacetylene $\left(\frac{cm^3\ H_2}{min\ g\ metal}\right)$	Surface excess free energy (kJ/mol)
1	230	200	17.3
2	435	320	35.7
3	160	80	—
4	870	1280	27.3
5	890	1020	39.3
6	215	200	21.7
7	460	620	28.5

increases with increasing dispersity, approaching a limiting value. Thus, of the factors [8] affecting excess free energy, dispersity plays in our case a decisive role, as compared to chemical defects. The effect of impregnation, of the nature of the reducing agent, can be practically neglected. The same results were obtained earlier in the investigation of alloy catalysts [9], where the surface excess free energy changed in parallel with dispersity, independently of the chemical composition.

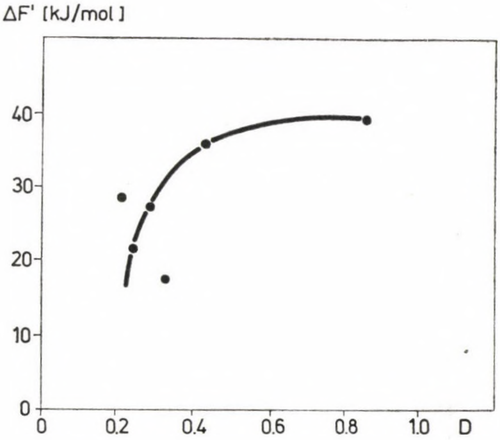

Fig. 1. Surface excess free energy of 5 wt% Pt/C catalysts as a function of dispersity

Table II does not contain the surface excess free energy of catalyst 3, because this catalyst did not yield reproducible results.

The potentiodynamic curves of the catalysts are shown in Figs 2 and 3. Figure 2 shows the curves of the catalysts reduced with $NaBH_4$, while Fig. 3 those of the catalysts impregnated in the same way, but reduced differently. With the exception of catalyst 7, a single (higher or lower) maximum appears in the hydrogen region (0—400 mV); catalyst 7 presents two maxima in this region.

Thus, the polarization curve of catalyst 7 of the lowest dispersity, precipitated from a metal salt solution in the presence of support, is similar to the curve of unsupported platinum shown in the same Figure, while the other curves differ basically from the latter.

It should be mentioned that STONEHART, KINOSHITA and BETT *et al.* [1—6] found in each case that the potentiodynamic curves of supported and unsupported platinum are of identical character: two characteristic maxima are present in the hydrogen region, and a smaller intermediate maximum, depending on dispersity.

Owing to reasons discussed in the experimental part, the hydrogen content has not been numerically determined, however, it is clear that the quan-

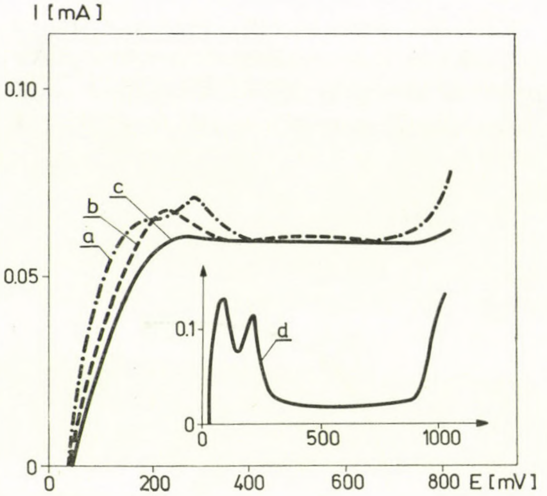

Fig. 2. Potentiodynamic curves of catalysts reduced with sodium borohydride in 0.5 *M* sulfuric acid. a) catalyst 7 ($m = 5$ mg); b) catalyst 6 ($m = 5$ g); c) catalyst 2 ($m = 5$ mg); d) unsupported platinum ($m = 4$ mg) BET surface area 9 m^2/g

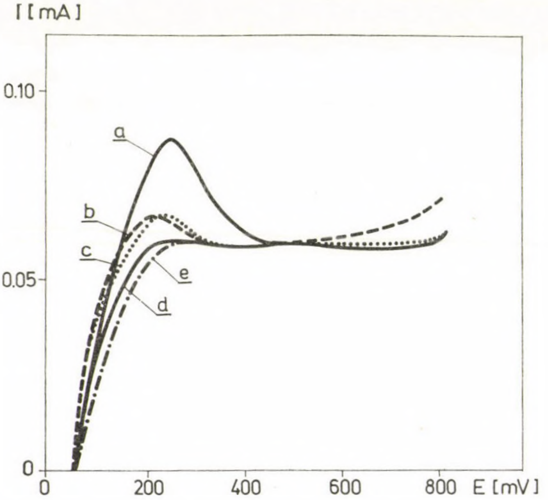

Fig. 3. Potentiodynamic curves in 0.5 *M* sulfuric acid of 5 wt% Pt/C catalysts impregnated at the same time and reduced differently ($m = 5$ mg). a) catalyst 5; b) catalyst 3; c) catalyst 4; d) catalyst 1; e) catalyst 2

tity of hydrogen (area enclosed by the curve) sorbed on catalyst 5 of outstanding dispersity (Fig. 3) is considerably higher, than in the case of the other four catalysts impregnated in the same way, but reduced differently. Apart from this quantitative difference, the character of the curves shown in Fig. 3 is similar, independently of the mode of preparation.

REFERENCES

[1] STONEHART, P.: Electrochim. Acta, **15**, 1853 (1970)
[2] KINOSHITA,(K., LUNDQUIST, J. T., STONEHART, P.: Electroanal. Chem. Interfacial Electrochem., **48**, 157 (1973)
[3] KINOSHITA, K., LUNDQUIST, J. T., STONEHART, P.: J. Catal., **31**, 325 (1973)
[4] BETT, J., KINOSHITA, K., ROUTSIS, K., STONEHART, P.: J. Catal., **29**, 160 (1973)
[5] STONEHART, P., KINOSHITA, K., BETT, J.: Proc. Symp. Electrocatal., 1974, p. 275
[6] KINOSHITA, K., STONEHART, P.: Electrochim. Acta, **20**, 101 (1975)
[7] POLYÁNSZKY, É., MALLÁT, T., PETRÓ, J.: Acta Chim. (Budapest) **92**, 147 (1977)
[8] PETRÓ, J., POLYÁNSZKY, É., CSÜRÖS, Z.: J. Catal., **35**, 289 (1974)
[9] MALLÁT, T., POLYÁNSZKY, É., PETRÓ, J.: Acta Chim. Acad. Sci. Hung. **96**, 245 (1978)
[10] To be published
[11] BRUNELLE, J., SUGIER, A., le PAGE, J.: J. Catal., **43**, 273 (1976).
[12] BRUMMER, S. B.: J. Phys. Chem., **69**, 562 (1965)

Éva POLYÁNSZKY
Tamás MALLÁT
József PETRÓ
H-1521 Budapest, Műegyetem

Antal SÁRKÁNY H-1525 Budapest, P.O.Box 77

Acta Chimica Academiae Scientiarum Hungaricae, Tomus 104 (4), pp. 345—361 (1980)

ELECTROCHEMICAL STUDIES ON CARBON SUPPORTED PLATINUM AND RHODIUM CATALYSTS

É. POLYÁNSZKY,[1] J. PETRÓ[1] and A. SÁRKÁNY[2]

([1] Department of Organic Chemical Technology, Technical University of Budapest, [2] Institute for Isotopes of the Hungarian Academy of Sciences, Budapest)

Received March 30, 1979
Accepted for publication September 18, 1979

Carbon supported Pt and Rh catalysts, containing 2, 5, 10, 20 and 100 wt.% of Pt and 1, 5, 10, 20 and 100 wt.% of Rh have been prepared.

The catalytic activity, the hydrogen content obtainable from electrochemical polarization measurements, the surface area and the excess surface free energy were investigated as a function of metal content and dispersity.

Introduction

The primary aim of our research was to study the activity of polycrystalline catalysts used in industry by experimental methods that presumably do not affect structural and catalytic properties, *i.e.* enable active catalysts to be investigated. Such methods are the determination of excess surface free energy of powdered noble metal catalysts by potential measurements [1], and the investigation of their sorption properties by potentiodynamic polarization [2, 3].

The relatively simple apparatus and potentiodynamic polarization technique elaborated during these measurements have also been used successfully in the investigation of supported Pd catalysts [4]. The potentiodynamic technique has now been extended to carbon supported Pt and Rh catalysts, investigating simultaneously whether the excess surface free energy of supported catalysts can be measured by the method previously elborated for unsupported, powdered metals [1].

In accordance with our primary aim stated above, thermal or vacuum pre-treatments and cyclic pre-polarization, applied *e.g.* by KINOSHITA *et al.* [5], were avoided, in order to prevent the structure of active catalyst from changing during the measurement.

These measurements aim at correlating the results obtained from electrochemical investigations (amount and nature of sorbed hydrogen, surface area) with dispersity obtained by chemisorption studies and hydrogenation activity, in order to have a more accurate picture on the behaviour of supported noble metal catalysts.

Experimental

Preparation of catalysts

For the preparation of Pt/C catalysts of 2, 5, 10, 20 wt.% and Rh/C catalysts of 1, 5, 10 and 20 wt.% metal content, active carbon (Carbo-C extra), previously heated in vacuum for 1/2 hr at 333 K, was impregnated for 3 hrs at 333 K under shaking with 0.1 *M* H_2PtCl_6 or 0.02 *M* H_3RhCl_6 solution, respectively. The solutions also contained hydrochloric acid. In all cases 2 g of catalyst was prepared. The amounts of carbon and noble metal solutions used in the experiments are given in Table I. With catalysts requiring less than 10 cm^3 of noble metal solution, the solution was made up to 10 cm^3 with distilled water. When more than 10 cm^3 of solution was used, the support was impregnated with portions of the solution, and the carbon-metal salt mixture was evaporated to dryness after each 10 cm^3 of the solution added.

Table I

Amounts of carbon and noble metal solutions used in the preparation of the catalysts

Pt/C catalysts			Rh/C catalysts		
Metal content (wt.%)	Carbon (g)	0.1 *M* H_2PtCl_6 (cm^3)	Metal content (wt.%)	Carbon (g)	0.02 *M* H_3RhCl_6 (cm^3)
2	1.96	2	1	1.98	10
5	1.9	5	5	1.9	50
10	1.8	10	10	1.8	100
20	1.6	20	20	1.6	200

Thereafter 1 g of $NaBH_4$ was dissolved in 200 cm^3 of distilled water. The dry, impregnated support and the remaining 150 cm^3 of sodium borohydride solution were added in portions to 50 cm^3 of this solution over 1/2 hr, under stirring. The mixture was stirred for further 1/2 hr, allowed to settle, filtered, and washed for 3 hrs with 3 dm^3 of distilled water. Finally, the catalysts were dried in a vacuum desiccator until constant weight at 298 K (the 2 and 5 wt.% Pt/C catalysts were dried at 370 K).

In the preparation of unsupported, 100 wt.% Pt and Rh catalysts the above procedure was applied with the difference that instead of the impregnated support the appropriate amount of noble metal solution was added in portions to the $NaBH_4$ solution.

Measurement of activity

The apparent activity of catalysts was measured in liquid phase hydrogenation using 100 mg of previously hydrogenated catalyst. 4 cm^3 of a cyclohexanone stock solution [4.9 g/100 cm^3 of 0.5 *M* H_2SO_4] in 10 cm^3 of 0.5 *M* H_2SO_4 or 2 cm^3 of phenylacetylene stock solution [5.11 g/100 cm^3 absolute alcohol] in 10 cm^3 of absolute alcohol, respectively, were hydrogenated at 298 Kat a pressure of 1.013 bar, under shaking at 330 r.p.m.

Activity was defined as the volume (cm^3) of hydrogen consumed in 1 min by 1 g of catalyst. In order to determine the selectivity of catalysts, in some experiments on the hydrogenation of phenylacetylene the reaction was stopped at half of the hydrogen consumption, a sample was taken, and the phenylacetylene, styrene and ethylbenzene content of the sample was determined by gas chromatographic analysis.

Electrochemical polarization measurements

The electrochemical measurements were performed in the three-electrode cell described previously [2]. 4 mg of catalyst was placed on a bright Pt sheet measuring electrode and the apparatus was filled with 0.5 *M* H_2SO_4. The potential of the catalyst was measured *vs.* a platinized Pt/H_2 electrode connected to the surface of the catalyst by a Luggin capillary. As polarization auxiliary electrode, a bright Pt sheet was applied.

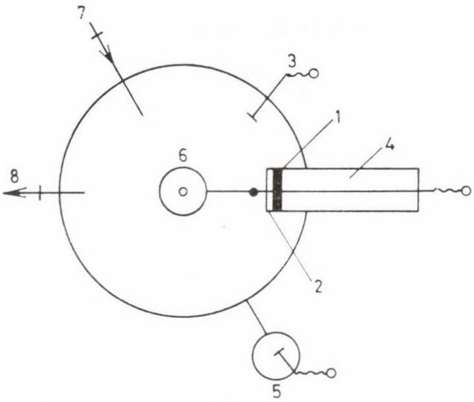

Fig. 1. Apparatus for the measurement of free energy. 1 — Pt sheet measuring electrode; 2 — Glass filter; 3 — Pt sheet polarization auxiliary electrode; 4 — Piston; 5 — Ag/AgCl/HCl reference electrode; 6 — Ar inlet and outlet; 7 — Inlet of oxygen-free electrolyte; 8 — Outlet of electrolyte

Since the catalysts exposed to air may contain oxygen on their surfaces, they were saturated with hydrogen by cathodic polarization prior to measuring the anodic galvanostatic and potentiodynamic curves from 40—60 mV to 800—1000 mV.

Galvanostatic polarization was carried out with a current of 0.1 mA. Under such conditions the curves can be regarded as equilibrium curves.

Potentiodynamic curves were recorded at a potential sweep rate of 2—50 mV/min. From the curves, after a correction for the double layer capacity of carbon and metal, the amount of sorbed hydrogen was determined graphically.

Determination of excess surface free energy

In the measuring cell shown in Fig. 1 *ca.* 40 mg of catalyst was placed onto glass filter 2. The Pt sheet measuring electrode of the piston was pressed to the catalyst, and the cell was filled with 1 *M* HCl. As reference electrode, an Ag/AgCl/HCl system (5) was applied. Using a bright Pt sheet polarizing electrode (3), the catalysts were polarized in oxygen-free Ar flow to a potential where they contain neither hydrogen nor oxygen (Rh — 350 mV, Pt — 400 mV). Thereafter the electrolyte was replaced under Ar flow by a 10^{-3} *M* H_2PtCl_6 or H_3RhCl_6 solution, having a Cl^- concentration of 1 *M*. (Before use, oxygen was removed from the electrolyte in Ar flow). The system was stirred with a magnetic stirrer, and the potential of the catalyst was measured until it became constant. The excess surface free energy was calculated from the measured values by a method described in one of our previous papers [1].

Determination of the dispersity and surface area of catalysts from chemisorption and potentiodynamic measurements

The chemisorption of H_2 and CO was measured volumetrically at 298 K by a Barocell pressure detector. To determine the chemisorbed amount, the points of the isotherm between 0.013 and 1.3 kPa were extrapolated linearly to zero pressure. The catalyst was reduced under hydrogen flow at 420 K, and then hydrogen chemisorbed on the sample was removed by slowly increasing the temperature of catalyst (to 470—570 K), and applying vacuum (a dynamic pressure of 1.3×10^{-4} Pa).

The dispersity (the raio of surface and bulk metal atoms) of the catalyst [14] was determined from the data of hydrogen chemisorption, since the CO/Me ratio varies with dispersity. In the calculation of metal surface area a stoichiometry of H/Me = 1 and a metal atom density of 1.3×10^{15} metal atoms/cm^2 [15] was assumed.

The surface area was also calculated, under the above two assumptions, from the hydrogen content obtained with potentiodynamic polarization.

The BET surfaces of the catalysts were measured by N_2 adsorption.

Results and Discussion

We have investigated the correlation of hydrogenation activity, hydrogen absorption measured by potentiodynamic and galvanostatic methods, surface area and excess surface free energy of supported platinum and rhodium catalysts with active metal content and dispersity.

Electrochemical polarization studies

All catalysts were studied by potentiodynamic and galvanostatic polarization at 298 K in 0.5 *M* H_2SO_4.

Potentiodynamic measurements

The potentiodynamic curves of Pt catalysts measured between 60 and 1000 mV at a potential rate of 20 mV/min show the two characteristic hydrogen peaks of platinum only in the case of pure Pt and of the supported catalyst containing 20 wt.% of Pt (Fig. 2) at 130—150 and 250—260 mV; the other catalysts have only one hydrogen maximum. At lower polarization rates [5—10 mV/min], however, weakly and strongly bonded hydrogen could be distinguished on the other catalysts, too. After correcting the curves for the double layer capacity, the amount of hydrogen sorbed on the catalyst was

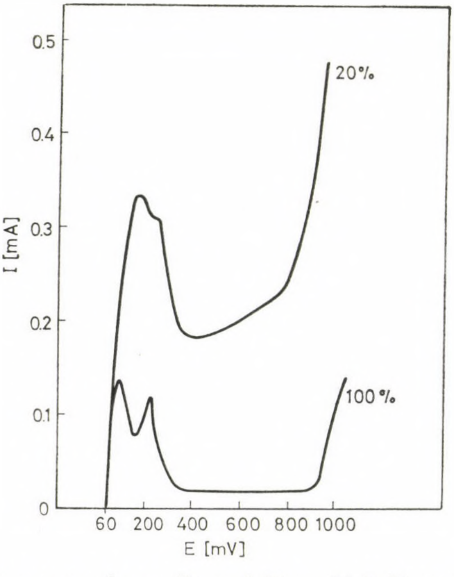

Fig. 2. Potentiodynamic curves of pure Pt and 20 wt.% Pt/C catalysts in 0.5 *M* H_2SO_4 at 298 K. Potential rate: 20 mV/min. Weight of catalyst: 4 mg

calculated, and referred to the weight of catalyst and the active metal content. The locations of peaks were also determined. The curve of the catalyst containing 2 wt.% of metal runs below that of carbon, and thus it cannot be taken into account owing to the experimental error. This phenomenon was also pointed out by BETT *et al.* [8].

Hydrogen contents obtained for the other catalysts, and the peak locations are listed in Table II.

Table II

Potentiodynamic results of carbon supported Pt catalysts

Metal content (wt.%)	Hydrogen content						Peak locations (mV)	
	(cm^3 H_2/g cat.)			(cm^3 H_2/g metal)				
	peak 1	peak 2	total	peak 1	peak 2	total	peak 1	peak 2
2	—	—	—	—	—	—	—	—
5	1.65	0.32	1.97	33.00	6.40	39.40	164	255
10	2.00	0.41	2.41	20.00	4.10	24.10	156	260
20	2.93	1.25	4.18	14.60	6.20	20.90	148	250
100	1.08	1.01	2.09	1.08	1.01	2.09	130	260

It can be seen from the table that the hydrogen content referred to unit weight of catalyst increases from 1.97 to 4.18 cm^3/g with an increase from 5 to 20 wt.% in metal content. The hydrogen content of pure Pt is half of that of the 20% catalyst [2.09 cm^3 H_2/g catalyst]. The amounts of weakly and strongly bonded hydrogen increase with increasing metal content (to 20%), but their ratio decreases (Table III).

Table III

Ratio of weakly and strongly bonded hydrogen on carbon supported platinum

Metal content (wt.% Pt)	$\frac{\text{Weakly bonded H}}{\text{Strongly bonded H}}$
5	5.20
10	5.02
20	2.35
100	1.06

Whereas on the 5 wt.% catalyst the amount of weakly bonded hydrogen is *ca.* five times higher than that of strongly bonded H_2, on the 20 wt% catalyst their ratio drops to 2.3, and hydrogen appears at lower potentials (Table II). With increasing metal content, the first hydrogen peak is gradually shifted to lower potentials (from 169 to 130 mV), whereas the location of the second maximum, corresponding to strongly bonded hydrogen, remains unchanged (250—260 mV). The shift in the first hydrogen peak (change in bond strength) and the increasingly larger deviation of the ratio of the two types of hydrogen from the ratio of 1 : 1 observed with pure platinum can be attributed to the effect of the carbon support, due partly to the dispersion of metal and partly to superstoichiometric adsorption (spill-over) [9].

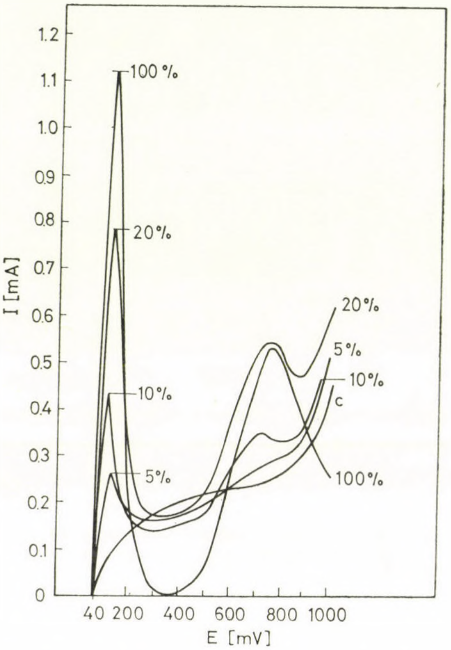

Fig. 3. Potentiodynamic curves of Rh/C catalysts of various concentrations in 0.5 M H_2SO at 298 K. Potential rate: 20 mV/min. Weight of catalyst: 4 mg

The hydrogen content of catalysts referred to the active metal content decreases monotonically from the 5 wt.% Pt/C catalyst to the pure metal.

According to the potentiodynamic polarization measurements on Rh-containing catalysts in the 40—1000 mV range, even at the lowest polarization rate possible, for all catalysts only one peak appears in the hydrogen region around 100 mV. This indicates that both supported and unsupported rhodium catalysts contain only one type of sorbed hydrogen. The peak height increases monotonically as a function of the active metal content (Fig. 3). A further maximum can be observed around 750 mV on the curves of catalysts containing more than 5 wt.% of Rh, which also increases monotonically as a function of metal content, and corresponds to the early oxidation of Rh.

The potentiodynamic curve of the 1 wt.% catalyst cannot be interpreted owing to the large experimental errors.

The integrals under the hydrogen regions of the curves indicate that with an increase in the metal content from 5 to 100 wt.%, the hydrogen content increases monotonically from 1.6 to 8.3 cm^3/g catalyst, whereas the specific hydrogen content decreases from 31.3 to 8.3 cm^3/g metal (Table IV).

Table IV

Potentiodynamic results for carbon supported Rh catalysts

Metal content (wt.%)	Hydrogen content		Peak location (mV)
	(cm^3 H_2/g cat.)	(cm^3 H_2/g metal)	
1	—	—	—
5	1.57	31.4	100
10	2.09	20.9	91
20	4.79	23.95	92
100	8.29	8.29	108

The determination of peak positions involved some difficulty since even at low polarization rates [5 mV/min] the data measured under anodic and cathodic polarization were different, indicating the non-equilibrium nature of the process. This was also pointed out by Woods [10] and McIntyre [11] in connection with measurements on Rh.

Peak potentials can be regarded as constant within the experimental error, *i.e.* the metal-hydrogen bond strength does not change.

Comparison of the results obtained for Pt and Rh shows that the metal content *vs.* hydrogen sorption relationships are different for the two metals. It can be observed in the region of 5—20% metal content that with rhodium the amount of hydrogen sorbed on 1 g of metal varies much less and the sorption energy of hydrogen is practically constant, whereas with the platinum catalysts of low metal content (5%), the hydrogen content strongly increases (primarily the weakly bonded form), as does its bond strength (Fig. 4).

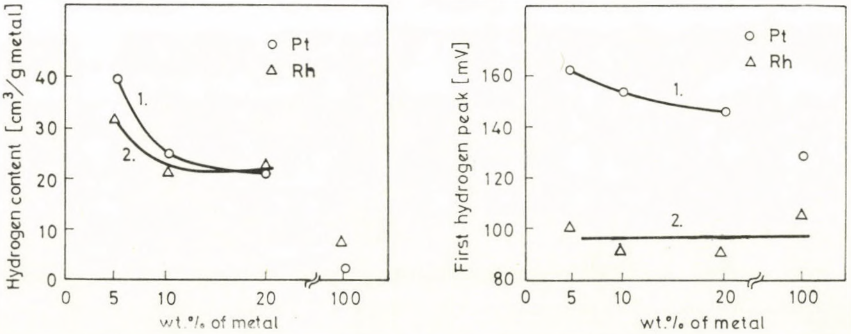

Fig. 4. **Amount of sorbed hydrogen on supported catalysts and the location of the first hydrogen peak as a function of metal content [1 — Pt/C, 2 — Rh/C]**

Galvanostatic measurements

Galvanostatic polarization was performed with a current of 0.1 mA on 4 mg catalyst in 0.5 *M* H_2SO_4. From the charge consumed up to the middle of the double layer region of the potential *vs.* charge curves obtained (Pt — 400 mV, Rh — 350 mV), the amount of hydrogen sorbed on the catalyst was calculated. The capacity of the double layer was taken into account as correction.

The curves of the catalysts with the lowest metal content [2 wt.% Pt/C and 1 wt.% Rh/C] could not be evaluated, since for these low metal contents the large double-layer capacity of carbon leads to false results.

The hydrogen contents of the other catalysts are shown in Table V.

Table V

Hydrogen contents of Pt/C and Rh/C catalysts from galvanostatic polarization

Metal content (wt.%)		Hydrogen content	
		(cm^3 H_2/g catalyst)	(cm^3 H_2/g metal)
	2	—	—
	5	1.8	36.2
Pt	10	2.5	25.0
	20	4.1	20.5
	100	2.6	2.6
	1	—	—
	5	1.4	28.0
Rh	10	1.9	19.0
	20	4.1	20.5
	100	7.6	7.6

Similarly to the hydrogen contents determined from the potentiodynamic curves, the results of galvanostatic polarization measurements show that in the Pt series the 20 wt.% catalyst has a maximum [4.1 cm^3 H_2/g of catalyst], whereas in the Rh series, the hydrogen content increases monotonically with increasing metal content.

The average differences between the hydrogen contents measured by galvanostatic and potentiodynamic methods are 8% for the Pt catalysts and 12% for the Rh catalysts. They can be attributed to experimental errors.

Investigation of hydrogenation activity

The activities of all carbon supported platinum [2, 5, 10, 20 and 100 wt.% Pt/C] and rhodium [1, 5, 10, 20 and 100 wt.% Rh/C] catalysts were determined in 0.5 *M* H_2SO_4 as solvent in the reduction of cyclohexanone, and in absolute alcohol in the hydrogenation of phenylacetylene.

The activities measured in the reduction of cyclohexanone are shown in Fig. 5 and 6.

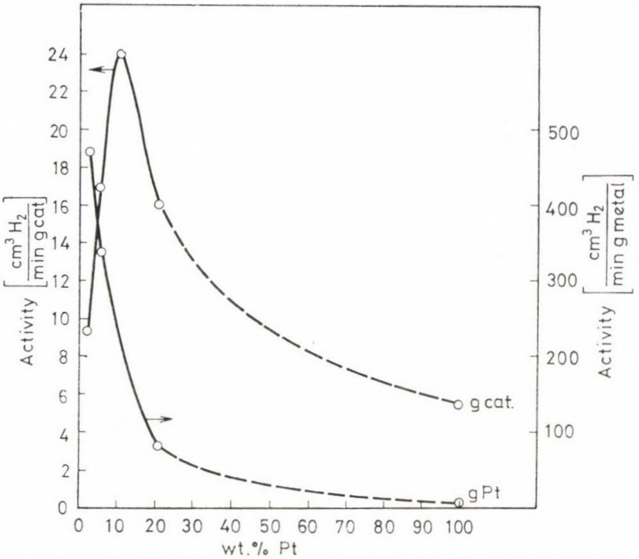

Fig. 5. Activity of Pt/C catalysts with various metal concentrations in the hydrogenation of cyclohexanone in 0.5 M H_2SO_4 at 298 K

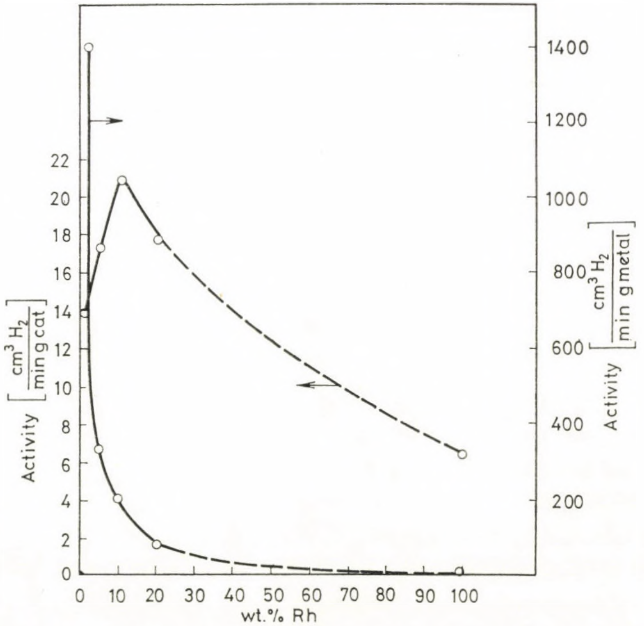

Fig. 6. Activity of Rh/C catalysts with various metal concentrations in the hydrogenation of cyclohexanone in 0.5 M H_2SO_4 at 298 K

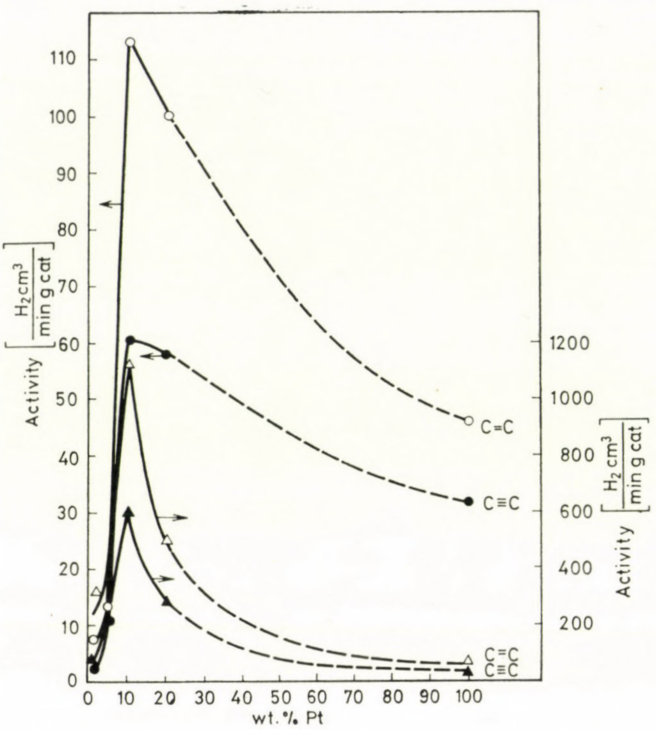

Fig. 7. **Activity of Pt/C catalysts with various metal concentrations in the hydrogenation of phenylacetylene in *abs.* alcohol at 298 K**

When investigating the activities referred to unit weight of the catalysts, it can be found that the activities of supported catalysts are always higher than those of pure metals. This specific activity has a maximum at 10 wt.% of active metal content; 24 cm^3 H_2/min g catalyst for Pt catalysts and 21 cm^3 H_2/min g catalyst for Rh catalysts. Consequently, the combination of Pt and Rh catalysts with carbon support ensures the most advantageous conditions for the hydrogenation of $-C=O$ bonds at a metal content of 10%. Above this metal content the effect of support rapidly decreases.

The activity referred to the active metal content also shows the same trend for the two metals, decreasing monotonically with increasing metal content, indicating that the surface area advantageous for the reaction decreases with decreasing amounts of support.

The activity curves measured in absolute alcohol with phenylacetylene have two sections for all catalysts: the activity is constant up to *ca.* half of the hydrogen consumption, then reaches a maximum, and finally decreases. In the first section presumably the triple bond is hydrogenated at a relatively low, steady rate, and when strongly sorbed phenylacetylene disappears from the reaction mixture, the hydrogenation of double bond starts at a much higher

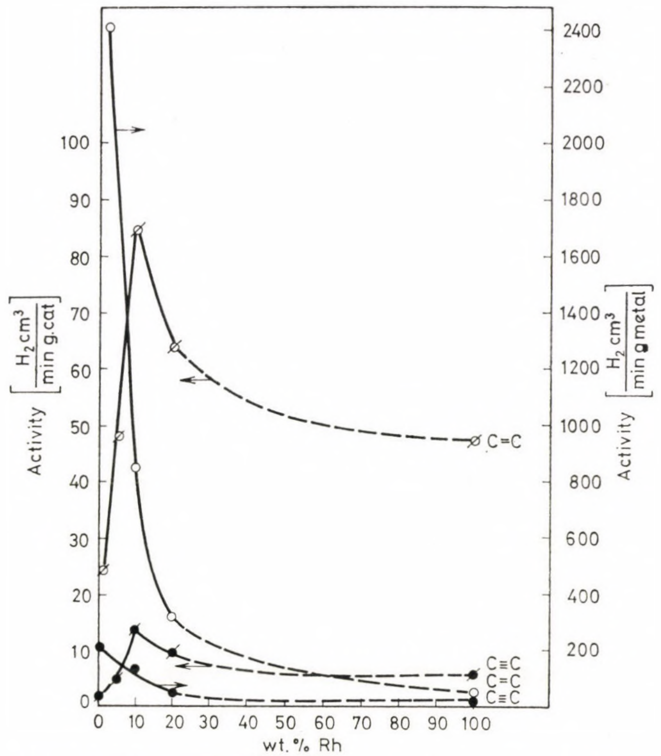

Fig. 8. **Activity of Rh/C catalysts with various metal concentrations in the hydrogenation of phenylacetylene in *abs.* alcohol at 298 K**

rate and passes through a maximum. The assumption concerning the consecutive character of the reaction has been proved by the gas chromatographic analysis of the reaction mixture.

The ratio of the activities of the maximum and the steady section is much higher for the catalysts with the lowest metal contents than for the other catalysts. This ratio is 4.6 for the 2 wt.% Pt/C catalyst, 1.2—1.8 for the other Pt catalysts; 11.4 for 1 wt.% Rh/C, and 6—9.6 for the other Rh catalysts. ZAKUMBAYEVA *et al.* [6] gave a ratio of 4 for Rh.

The fact that on catalysts with low metal content the hydrogenation of triple bond proceeds at a relatively much lower rate than the hydrogenation of double bond is due presumably to the blocking effect of strongly sorbed phenylacetylene on the few active centers present [7].

The activities of the catalysts in the hydrogenation of phenylacetylene are shown in Fig. 7 and 8.

With Rh, the activities referred to unit weight of metal decrease monotonically with increasing metal content, whereas those referred to the weight of the catalyst pass a maximum at 10 wt.% of metal.

Table VI

Dispersities and surface areas of Pt/C *and* Rh/C *catalysts*

Metal content (wt.%)		Chemisorption results			Metal surface area		BET surface area of catalyst (N_2 sorption) (m^2/g cat.)
		CO content (cm^3/g met.)	H content (cm^3/g met.)	Dispersity D_H	Chemisorption (m^2/g met.)	Potentiodynamic (m^2/g met.)	
	2	14.29	10.51	0.18	40.5	—	614
	5	25.98	18.04	0.31	69.5	162	903
Pt	10	32.99	22.59	0.39	87.0	99	558
	20	33.15	22.39	0.38	86	87.5	486
	100	4.52	3.32	0.057	12.8	8.6	9
	1	169.3	92.8	0.85	358	—	865
	5	191.7	100.5	0.92	387	128	705
Rh	10	91.7	55.2	0.50	213	86	425
	20	132.4	68.0	0.62	262	98.5	285
	100	10.48	6.71	0.061	26	34.1	12
Active carbon		—	—	—	—	—	994

With Pt, the activities referred to the weight of both the catalyst and the metal have a maximum at 10 wt.% The fact that this specific activity is not monotonically decreasing like in other cases, *i.e* 1 g of metal is less active in the 2 and 5 wt% catalysts than in the 10 wt.% catalyst, can be explained on the one hand by a maximum of dispersity at 10 wt.% of Pt (Table VI). On the other hand, it is conceivable that the large amount of relatively more strongly bonded hydrogen sorbed on the catalysts with lower Pt content suppresses the sorption of the reactant.

Dispersities and surface areas of the catalysts

The dispersities were calculated from the results of chemisorption measurements. The results of CO and H chemisorption are shown in Table VI. Their ratio has been found to increase very slightly with increasing dispersity [CO/H ratio is 0.78 ± 0.05 for Pt/C and 0.89 ± 0.08 for Rh/C]. The nearly constant value of this ratio indicates that under the conditions of chemisorption measurements, the phenomenon of hydrogen spill-over need not be considered.

The dispersities and surface areas calculated from hydrogen sorption have a maximum in the Pt series at the 10 and 20 wt.% catalysts, whereas in the Rh series they decrease monotonically with increasing metal content.

On comparing the metal surface area calculated from chemisorption with that calculated from the electrochemical measurements, large differences can be found. In the Pt/C series, for the sample with low Pt concentration, the results obtained by the potentiodynamic method are usually higher than the results of chemisorption measurements. The largest difference can be observed with the 5 wt.% catalyst [162 and 69.5 m^2/g of metal]. The smaller surface areas obtained from chemisorption can be explained by the fact that the catalysts heated to 470—520 K before measurement undergo structural changes, and their surface area decreases. In addition, the phenomenon of spill-over may also contribute to the larger surface area obtained by the potentiodynamic method. As known, favourable conditions for spill-over are created by the presence of water molecules. Therefore, the surface areas calculated from the potentiodynamic measurements are higher than the true value owing to the spill-over, whereas those calculated from chemisorption are lower owing to shrinking.

The specific surface area of the 2 wt.% Pt/C catalyst was also determined by small-angle X-ray diffraction. It was found that the surface area calculated from the distribution according to diameter is 20.7 m^2/g, which is about one half of the value calculated on the basis of chemisorption.

With all members of the Rh/C series, there is a 2—3-fold difference between the surfaces calculated from the electrochemical and chemisorption measurements, the latter being higher.

This may be interpreted as follows. In addition to sorbed atomic hydrogen, Rh may also contain large amounts of less strongly bonded molecular hydrogen [16], which cannot be detected by the potentiodynamic method, since at the potential corresponding to the start of measurement (40—60 mV) it has already been desorbed. It is measured, however, in chemisorption. The large difference between the results of the two measurements can also be attributed to the fact that the Rh/C samples are strongly diluted with carbon in the chemisorption measurement, and the carbon content may cause large errors. This problem should be solved by further investigations.

In addition to the surface area of metal, the total surface areas of catalysts were also determined by N_2 sorption, and, as expected, they were always found to be smaller than that of carbon. The surface area and dispersity of Rh containing catalysts decrease monotonically with increasing metal content; in the Pt series they have a maximum at 10 wt.% Pt/C, and then decrease monotonically.

Excess surface free energy

The excess surface free energies of Pt/C and Rh/C catalysts studied are shown in Table VII.

According to the data, the excess free energies of pure metals are the lowest in both series: 8.8 kJ/mol for Pt, in close agreement with the value given in our previous paper [1], and 65.3 kJ/mol for Rh, also in agreement with

Table VII

Excess surface free energy of Pt/C *and* Rh/C *catalysts*

Metal content (wt.%)		Excess surface free energy (kJ/mol)
	2	25.1
	5	25.9
Pt	10	31.4
	20	25.1
	100	8.8
	1	82.1
	5	77.8
Rh	10	73.7
	20	72.4
	100	65.3

the data reported previously [13]. The application of pure metals to a support increases the excess free energy: it is 31 kJ/mol for 10 wt.% Pt/C, and 82 kJ/mol for 1 wt.% Rh/C.

Excess free energy and dispersity decrease monotonically with increasing metal content in the Rh series, whereas in the Pt series both dispersity and excess free energy decrease after a maximum found at a metal content of 10 wt.%.

The parallel behaviour of dispersity and excess free energy indicates that under the present circumstances, of the four possible factors [1], excess surface free energy is determined primarily by dispersity. This is not surprising if it is considered that the members of both catalyst series were prepared under strictly identical conditions, and thus other factors which could affect the free energy (physical, chemical and phase dislocations) were similar within the Pt and Rh series, while the dispersity strongly varies with the metal content.

Conclusion

The dispersity, excess surface free energy and hydrogen sorption from electrochemical polarization, and the activity in liquid phase reduction have been determined for the catalyst series of 2—100 wt.% Pt/C and 1—100 wt.% Rh/C. The following results were obtained.

1. The hydrogen sorption of highly disperse supported catalysts can be studied at much lower potentiodynamic polarization rates than that of pure metals. Under such quasi-equilibrium conditions the nature of sorption is

always characteristic of the given metal: on rhodium only one type, on platinum two types of hydrogen may be bonded. The amount of hydrogen and the ratio of hydrogen types with different bond strengths are a function of dispersity.

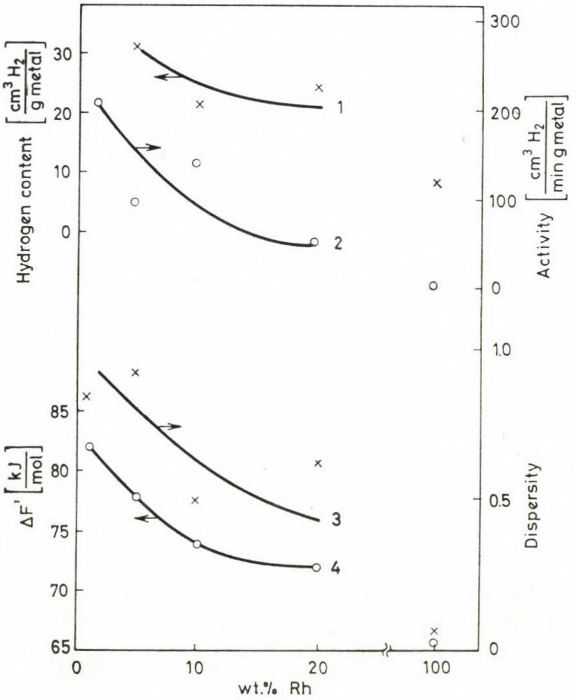

Fig. 9. Most important properties of carbon supported Rh catalysts as a function of Rh content. 1 — hydrogen content (from potentiodynamic measurement); 2 — activity in the hydrogenation of —C≡C— bonds; 3 — dispersity of catalyst; 4 — excess surface free energy

2. The application of metal onto a support substantially increases the excess free energy, the catalytic activity and the amount of sorbed hydrogen, through increasing the dispersity.

For the catalysts of the Rh series, the dispersity increases monotonically from the pure, unsupported metal to the 1 wt.% Rh/C catalyst, and the hydrogen sorption capacity, excess surface free energy and catalytic activity of the catalyst in the hydrogenation of triple bonds increases in the same sense (Fig. 9).

In the Pt series, the hydrogen sorption capacity and the metal-hydrogen bond strength increase monotonically in the direction of low metal content. Dispersity, excess surface free energy and the specific activity measured in the hydrogenation of the —C≡C— bond is a maximum at 10 wt.% metal

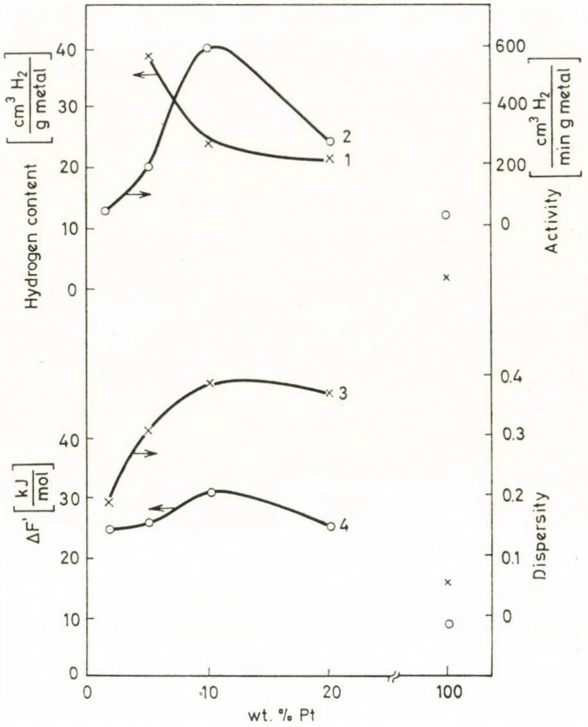

Fig. 10. **Most important properties of carbon supported Pt catalysts as a function of Pt content. 1 — hydrogen content (from potentiodynamic measurement); 2 — activity in the hydrogenation of —C≡C—bonds; 3 — dispersity of catalyst; 4 — excess surface free energy**

content (Fig. 10). The maximum of activity is due partly to the high dispersity, and partly to the different conditions of sorption (hydrogen sorption in smaller amounts with lower bond strength).

*

We are indebted to Dr. Géza Bodor for the small-angle X-ray measurements carried out in the Research Institute for Plastics.

REFERENCES

[1] Petró, J., Polyánszky, É., Csűrös, Z.: J. Catal., **35**, 289 (1974)
[2] Petró, J., Polyánszky, É.: Acta Chim. Acad. Sci. Hung., **87**, 385 (1975)
[3] Mallát, T., Polyánszky, É., Petró, J.: J. Catal., **44**, 345 (1976)
[4] Polyánszky, É., Mallát, T., Petró, J.: Acta Chim. Acad. Sci. Hung. **92**, 147 (1977)
[5] Kinoshita, K., Lundquist, J., Stonehart, P.: J. Catal., **31**, 325 (1973)
[6] Zakumbayeva, G. D., Beketayeva, L. A., Sokolskii, D. V.: Tr. Inst. Org. Katal. Elektrokhim. Akad. Nauk. Kaz. SSR, **5**, 138 (1973)
[7] Sokolskii, D. V.: Katalyticheskoe Gidrirovanie i Okislenie, **9**, 3 (1974)
[8] Bett, J., Kinoshita, K., Routsis, K., Stonehart, P.: J. Catal., **29**, 160 (1973)
[9] Bagotzkii, V. S., Kanevskii, L. S., Palanker, V. Sh.: Electrochim. Acta, **18**, 473 (1973)

[10] Woods, R.: J. Electroanal. Chem. Interfacial Electrochem., **49**, 217 (1974)
[11] McIntyre, J. D., Peck, W. F.: Proc. Symp. Electrocatal., **1974**, 212
[12] Sokolskii, D. V.: Gidrirovanie v rastvorakh, Izd. Akad. Nauk. Kaz. SSR, Alma-Ata 1962
[13] Polyánszky, É.: PhD Thesis (1971)
[14] Brunelle, J., Sugier, A., Page, J.: J. Catal., **43**, 273 (1976)
[15] Brummer, S. B.: J. Phys. Chem., **69**, 562 (1965)
[16] Zakumbayeva, G. D., Beketayeva, L. A., Levit, P. M.: React. Kinet. Katal. Lett., **4**, 207 (1976)

Éva Polyánszky
József Petró
H-1111 Budapest, Műegyetem rkp. 3.

Antal Sárkány
H-1525 Budapest, Konkoly Thege u. 29-33

Acta Chimica Academiae Scientiarum Hungaricae, Tomus 104 (4), pp. 363—368 (1980)

RAYLEIGH LIGHT SCATTERING AND INTERMOLECULAR ORIENTATION IN LIQUIDS

GY. BEKE and E. KESZEI

(*Institute of Physical Chemistry and Radiology, L. Eötvös University, Budapest*)

Received May 7, 1979
In revised form July 10, 1979
Accepted for publication September 19, 1979

Rayleigh scattering measurements provide information about the orientation of molecules in liquids. The present paper outlines some possibilities to develop SHAKHPARONOV's theory for interpreting the measured data. It is pointed out that if experimental data cannot be interpreted by the chaotic orientation of molecules, it is not necessary to suggest the presence of molecular associates. The parameters determining molecular orientation should always be considered as continuous probability variables.

The experimental study of molecular light scattering provides information regarding intermolecular orientation in pure liquids or in solutions. If the polarizability of molecules is anisotropic, the intensity of the scattered light has a contribution due to the fluctuation in intermolecular orientation, even if the molecules orientate randomly. This contribution in the latter case depends on some macroscopic parameters of the liquid and on the anisotropy of the polarizability of the molecules. If the experimentally determined anisotropic contribution is different from that calculated on the basis of random orientation, a usual explanation is that complexes are formed in the liquid [1—7].

In the present paper we show that light scattering data can be explained without assuming the existence of complex species, using continuous random variables for specifying intermolecular orientation. To calculate the anisotropic contribution to the light scattering we need the actual probability density of these variables. A rather convenient way of calculating the probability densities may be to consider the effect of orientating interaction between molecules on the "basic" probability density function characterizing a system of randomly orientating molecules.

Calculation of Anisotropic Rayleigh Scattering from Macroscopic and Molecular Data

When the Rayleigh factor (R) and the degree of depolarization (Δ) of the Rayleigh line are known from experimental data, the anisotropic component of the Rayleigh factor (R_a) can be expressed [8] as

$$R_a = R \frac{13}{6} \frac{\Delta}{1+\Delta}$$

R_a can be calculated also in a different way. For this calculation, one should know the wavelength of the incident light (λ), the refractive index of the scattering medium (n) and some molecular data like the main polarizability axes a_x, a_y, a_z of the molecules, and some intermolecular data like parameters describing mutual orientation.

Gans was the first to study the problem of anisotropic scattering. He related the anisotropy of the polarizability of molecules to the anisotropic scattering factor [9]. Later **Anselm** considered the effect of intermolecular orientation [10]. The same problem has been treated by different authors. Finally, the work of **Shakhparonov** made it possible to check ideas concerning the structure of liquids on the basis of experimental light scattering data. **Shakhparonov** has investigated the formulas for calculating the intensity of the scattered light and has corrected a mistake in the power of the term containing the refractive index; also he has simplified the model for anisotropic scattering so that his results can be used in practice. According to this, the anisotropic scattering factor is given by

$$R_a = QN \left(g^2 + \frac{z}{2} \sum_i \sum_j a_i a_j (3 \cos^2 \eta_{ij} - 1) \right), \quad i, j = x, y, z,$$

where

$$Q = \frac{104}{45} \frac{\pi^4}{\lambda^4} \left(\frac{n^2 + 2}{3} \right)$$

and

$$g^2 = \frac{1}{2} \left((a_x - a_y)^2 + (a_y - a_z)^2 + (a_z - a_x)^2 \right)$$

is the anisotropy of the polarizability; N denotes the number of molecules per unit volume and η_{ij} is the angle between the i axis of the polarizatiblity of one, and the j axis of that of the other molecule.

Shakhparonov has assumed that orientating interactions of a molecule exert an effect only on molecules included in its first coordination sphere. If the number of molecules in the first coordination sphere is z, the coefficient $z/2$ stands in the formula for the summation over all interacting molecules **Shakhparonov** has derived a similar formula for counting R_a in multicomponent solution, which has a separate term for each pair of component including the respective polarizability values.

Complex species?

If the anisotropic scattering factor is different from that calculated fos randomly orientated molecules with known optical anisotropy, **Shakhporonov** and his coworkers assume the formation of complex species in liquird [1—3]. They calculate data concerning the concentration of the complexes and the equilibrium of the association processes.

SHAKHPORONOV does not mention probability densities. When he does not suppose any order in orientation ("chaotic arrangement"), he uses the average of $\cos^2 \eta_{ij}$ and says: "We have to average over all possible arrangements". In the case of nonchaotic orientation he fixes one ore more angles for associated pairs of molecules (complexes) and "averages" according to this condition. The rest of the molecules (non-associated) are treated according to the chaotic arrangement. On the basis of experimental light scattering data he calculates the fraction of molecules forming the complexes assumed.

Perhaps it is justified to assume that the structure of liquids is not as simple as that. It is rarely correct to characterize liquid structures assuming that some fractions P_1 or P_2 of the pairs of molecules are arranged in a well defined position, while the others are arranged randomly. So we have only one possibility left, *viz.* to describe intermolecular orientation in terms of continuous random variables instead of treating the problem using discrete quantities. Experimental data are to be used for calculating the distribution function of the random variables.

Description of Anisotropic Scattering in Terms of Random Variables

Let us consider an arbitrary pair of molecules. The formula for calculating their anisotropic contribution to the Rayleigh factor is:

$$R_{\mathrm{a}}^{\mathrm{lk}} = K(n, \lambda)[g_{\mathrm{l}}^2 + g_{\mathrm{k}}^2 + a_{\mathrm{l}}\, \mathbf{O}_{\mathrm{lk}}\, a_{\mathrm{k}}']$$

The sub- and superscripts l and k symbolize the two molecules. The first two terms in brackets are directly associated with the optical anisotropy of the molecules; the last one depends on the intermolecular orientation. The matrix $\mathbf{O}_{\mathrm{lk}}$ can be represented in terms of the acute angles $\eta_{i_{\mathrm{l}} j_{\mathrm{k}}}$ $(i, j = x, y, z)$ between the respective main polarizability axes of molecules l and k:

$$\mathbf{O}_{\mathrm{lk}} = \begin{bmatrix} 3\cos^2 \eta_{x_1 x_1} - 1 & \ldots\ldots & 3\cos^2 \eta_{x_1 x_3} - 1 \\ \ldots & \ldots & \ldots \\ 3\cos^2 \eta_{x_3 x_1} - 1 & \ldots\ldots & 3\cos^2 \eta_{x_3 x_3} - 1 \end{bmatrix}$$

a_{l} denotes the row matrix $a_{x_{\mathrm{l}}}, a_{y_{\mathrm{l}}}, a_{z_{\mathrm{l}}}$,
containing the main polarizability values of molecule l; a_{k}' is the transposed of the similarly constructed row matrix $a_{\mathrm{k}} \cdot K(n, \lambda)$ is a function of macroscopic parameters having no molecular meaning.

The angles $\eta_{i_{\mathrm{l}} j_{\mathrm{k}}}$ are to be considered as random variables since the equations of motion for individual molecules are unknown. Because of the fact that the mutual position (of the polarizability ellipsoids) of two molecules can be specified by three independent parameters, all of the individual $\eta_{i_{\mathrm{l}} j_{\mathrm{k}}}$ angles cannot be independent of each other. Let us specify intermolecular orientation in terms of the parameters α, β and γ. Generally, these are independent; in our case they are considered as independent random variables. Each of the angles $\eta_{i_l} j_{\mathrm{k}}$ can be regarded as a function of the parameters; $\eta_{i_l j_{\mathrm{k}}} = \eta_{i_l j_{\mathrm{k}}}$ (α, β, γ). The sample space is the total domain of the parameters. The expected value of the angles $\eta_{i_l} j_{\mathrm{k}}$ or that of any function of the angles can be calculated if the probability density $\Psi_{\mathrm{lk}}(\alpha, \beta, \gamma)$ is known. Accordingly, we can calculate the expectation values of the functions occurring in the elements of the matrix $\mathbf{O}_{\mathrm{lk}}$. Let us symbole these expectation values by $\cos^2 \overline{\eta_{i_l j_{\mathrm{k}}}}$, and the matrix containing these values by $\overline{\mathbf{O}}_{\mathrm{lk}}$. If we omit the two first terms in the expression for $R_{\mathrm{a}}^{\mathrm{lk}}$ and denote the remainder by $R_{\mathrm{or}}^{\mathrm{lk}}$ (associated with orientation), it can be expressed using the "expectation value" of matrix $\mathbf{O}_{\mathrm{lk}}$:

$$R_{\mathrm{or}}^{\mathrm{lk}} = K(n, \lambda)(a_{\mathrm{l}}\, \mathbf{O}_{\mathrm{lk}}\, a_{\mathrm{k}}')$$

If there are N molecules per unit volume, the orientational scattering factor can be given as

$$R_{\mathrm{or}} = \sum_{k<1} \sum_{l=1}^{N} R_{\mathrm{or}}^{\mathrm{lk}}\,.$$

In terms of these considerations, we can write the actual probability density Ψ_{lk} for each pair of molecules. However, we do not have to distinguish between the same type (*i.e.* the same composition) of pairs. If the liquid is (macroscopically) isotropic, it is obvious that a unique $\Psi_{\mathrm{lk}} = \Psi$ is valid for each pair of molecules l, k, in which the intermolecular distance is much greater than the size of the molecules. Further it can be shown that this Ψ value, common for distant molecules, has the property that the $\overline{3 \cos^2 \eta_{i_l j_{\mathrm{k}}} - 1}$ values calculated from them are equal to zero for every $i_l j_{\mathrm{k}}$.

To show this, let us consider points on a surface of a sphere which are marked by lines starting from the center of the sphere and parallel to one of the main polarizability axes of either molecule. Let the points of intersection be denoted by x, y and z, respectively. The points can be specified in spherical polar coordinates by two angles, $0 \leq \vartheta \leq \pi$ and $0 \leq \psi \leq 2\pi$. Let the orientation of the molecules, *i.e.* the position of the points x, y, z be taken at random. The mutual orientation of molecules l and k is independent if ϑ_{i_l} and $\vartheta_{j_{\mathrm{k}}}$, ϑ_{i_l} and $\psi_{j_{\mathrm{k}}}$, ψ_{i_l} and $\vartheta_{j_{\mathrm{k}}}$ and, finally ψ_{i_l} and $\psi_{i_{\mathrm{k}}}$ are independent random variables, respectively. It can be shown that the probability density of the respective angle $\eta_{i_l j_{\mathrm{k}}}$ in this case is

$$f(\eta_{i_l j_{\mathrm{k}}}) = \sin \eta_{i_l j_{\mathrm{k}}} \quad (i, j = x, y, z)\,.$$

Upon integration we have $\cos^2 \eta_{i_l j_{\mathrm{k}}} = 1/3$ for independently orientating molecules, which means $R_{\mathrm{or}}^{\mathrm{lk}} = 0$.

We call chaotic orientation that case in which all pairs of molecules orientate randomly. Thus, for a liquid containing chaotically orientated molecules, $R_{\mathrm{or}} = 0$. In this case the correlation coefficient for the previous pairs of coordinates (ϑ_{i_l}, ϑ_{j_k}, *etc.*) equals zero. On the other hand, if the molecules are fixed together by rigid binding, the correlation coefficient becomes unity. The latter case can be considered as the highest degree of order between molecules.

It is reasonable to assume that liquids consist not only of either completely disordered or completely ordered molecules. In fact, various intermolecular effects hinder the molecules in arranging all possible positions with equal probability in the actual molecular environment. The higher the degree of order between neighbouring molecules, the greater is the probability of some given intermolecular orientations. There arises the question of what degree of order in orientation can be considered as a case of associated molecules. Let us regard this question in more detail.

Suppose that there is no correlation between the spatial positions of two neighbouring molecules. Thus, as we have seen, the probability density of the angle η between their pairs of axes is $f(\eta) = \sin \eta$. Let us introduce that transform of η for which the probability density for chaotic spatial orientation is uniform. This variable must be $K = -\cos \eta$. K can assume a continuum of values within the interval $(-1,\ 0]$ and is a monotonically increasing function of η. Thus, the probability density function for K can be obtained [11] as

$$g(K) = \mathrm{f}(K)\frac{\mathrm{d}\eta}{\mathrm{d}K} = \sin \operatorname{arc} \cos(-K)\frac{\mathrm{d}\eta}{\mathrm{d}(-\cos\eta)} = 1\,.$$

Though the one-variable function $g(K)$ represents orientation only in the case of one degree of (orientational) freedom (*e.g.* for one-dimensional molecules), considerations concerning the probability density of the function $g(K)$ (Fig. 1) are rather helpful for the explanation of the problem of molecular complexes.

Curve (a) shows the uniform distribution. Curve (b) indicates a kind of order in orientation; mutual positions close to K^* dominate. Curve (c) represents an orientation where positions close to K^* are more probable than in the previous case. Values around K^* can be further enhanced, but which is the first distribution, $g(K)$, that already indicates a really existing associate

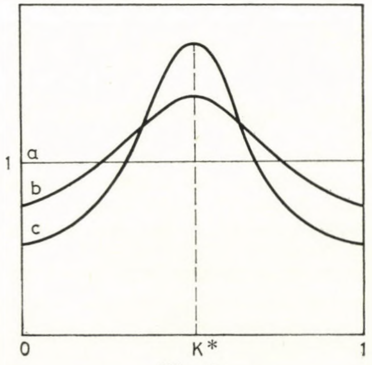

Fig. 1

or complex of molecules? Does it have any meaning in the case of a given order in orientation to speak about complexes?

Consider this problem in a different way; suppose that complexes exist in the liquid. However, we generally do not assume complexes either to be of everlasting life or to be rigid. Again, restricted to one angle η between two molecules, we can say that this angle assume values close to η^*; moreover, in some favourable conditions the molecules can move away from each other to join other molecules. As to the liquid structure, it can be completely characterized by the radial distribution and the distribution of parameters of intermolecular orientation. Whatever the cause of the order in orientation, we are interested in the actual structure rather than the reason for this structure. Furthermore, our instruments cannot see but some transformed consequences of the parameters concerning the structure. Experimental data — like anisotropic light scattering — do not provide evidence for complexes. On the contrary, we apparently limit ourselves trying to explain the situation originating from the random character of intermolecular orientation in terms of discrete concepts (*e.g.* complexes of a given shape).

According to the previous discussion, we restrict the problem of intermolecular orientation to the construction of the probability density function $\Psi(\alpha, \beta, \gamma)$. However, we do not deny the importance of the formation of different complexes or other effects yielding a given orientation in liquids. The only difference is that we never consider molecular associates to be rigid and we do not explain experimental data by giving the respective fractions of the complexes but by giving some properties of the function $\Psi(\alpha, \beta, \gamma)$.

Before doing this it is rather useful to select the parameters of intermolecular orientation (*i.e.* α, β, γ) carefully. This particular problem will be treated in a subsequent article.

REFERENCES

[1] Shakhparonov, M. I.: Methods of Studying the Thermal Motion of Molecules and the Structure of Liquids; (in Russian), Izd. MGU, Moscow 1963
[2] Shakhparonov, M. I. Merzhanov, I. A., Lanshina, L. V.: Vestnik Mosk. Univ., Ser. Khim., **2**, 24 (1968)
[3] Shakhparonov, M. I.: Modern Problems of Physical Chemistry Vol. **5** (in Russian), Izd. MGU, Moscow, 1970
[4] Shakhparonov, M. I.: Vestnik Mosk. Univ., Ser. Khim., **3**, 3 (1969)
[5] Shakhparonov, M. I.: Physics and Physical Chemistry of Liquids, 2nd Edition (in Russian Izd. MGU, Moscow 1973
[6] Durov, V. A.: Zh. Fiz. Khim., **50**, 2236 (1976)
[7] Durov, V. A.: in Physics and Physical Chemistry of Liquids, Izd. MGU, Moscow 1976
[8] Cabannes, J.: La Diffusion Moleculaire de la Lumiere, Les Presses Univ. de France, 1929
[9] Gans, P. J.: Ann. Physik, **37**, 881 (1912); **65**, 97 (1921)
[10] Anselm, A. I.: Zh. Eksp. Teor. Fiz., **17**, 489 (1947)
[11] Rényi, A.: Probability Theory (in Hungarian), Tankönyvkiadó, Budapest 1966

Gyula Beke
Ernő Keszei
H-1088 Budapest, Puskin u. 11–13.

Acta Chimica Academiae Scientiarum Hungaricae, Tomus 104 (4), pp. 369—374 (1980)

ULTRAVIOLET SPECTRAL PROPERTIES AND BASICITY OF (*E*)-3-BENZYLIDENEFLAVANONES

É. R. DÁVID, A. LÉVAI and G. B. SZABÓ

(*Institute of Organic Chemistry, Kossuth Lajos University, Debrecen*)

Received April 27, 1979
In revised form September 5, 1979
Accepted for publication October 9, 1979

The relationship between the thermodynamic pK_{BH^+} value and the electronic character of the substituent in the *para*-position of the benzylidene group of (*E*)-3-benzylideneflavanones (**I** — **X**) has been studied by means of UV spectroscopy. It has been found that this relationship is linear and the magnitude of the pK_{BH^+} values measured (-5.0 to -6.0) is quite similar to that of *s*-*Z*-(*E*)-chalcones, and Φ is between 0.02 and 0.09. Owing to certain differences in the structure and electron distribution, the UV spectra measured in sulfuric acid are somewhat different from those of *s*-*Z*-(*E*)-chalcones obtained under the same conditions.

Although (*E*)-3-benzylideneflavanones (termed flavindogenides) are known for a long time, relatively few data are available in the literature concerning their physico-chemical and spectral properties in relation to their stereochemistry and electronic structure. It is well established that the condensation of flavanones and benzaldehydes gives (*E*)-3-benzylideneflavanones [1, 2].

Since the structure of (*E*)-3-benzylideneflavanones is analogous to that of *s*-*Z*-(*E*)-chalcones, the double bond of these compounds can also transmit substituent effects to the carbonyl group. This feature has in fact been demonstrated in the course of a study of the IR spectroscopic properties of the (*E*)-3-benzylideneflavanones **I**—**X** [3]. In the present paper, the influence of substituent effects on the UV spectra and pK_{BH+} values is reported.

Experimental

The compounds under investigation (**I** — **X**) were synthesized as reported [2]. UV spectra were measured with a UNICAM SP 800 instrument in $5 \cdot 10^{-5}$ *M* ethanolic solution and in aqueous sulfuric acid solutions of various concentration, respectively, at room temperature.

For the calculation of the pK_{BH+} values, BUNNETT—OLSEN's linear free energy relationship [4] was used, according to which

$$\log \frac{C_{BH^+}}{C_B} + H_0 = \Phi(H_0 + \log C_{H^+}) + pK_{BH^+}$$

where $\frac{C_{BH^+}}{C_B}$ is the concentration ratio of the protonated and non-protonated molecules, H_0

is the Hammett acidity value of the aqueous sulfuric acid, and C_{H^+} is the hydrogen ion concentration (molarity) belonging to the given H_0.

The pK_{BH^+} value can be obtained by plotting $\log \frac{C_{BH^+}}{C_B} + H_0$ against $H_0 + \log C_{H^+}$ and then correlating this with infinite dilution in water. The Φ parameter, which refers to the shift of the equilibrium accompanying the change of acid concentration, is obtained from the slope of the straight line.

Results and Discussion

The UV spectra of the (*E*)-3-benzylideneflavanones **I** — **X** measured in ethanolic solutions exhibit one intense band between 290 and 422 nm (Fig. 1), which is characteristic of *s*-*Z*-(*E*)-chalcones, and the flavanone character is not manifested in the spectra (λ_{max} [nm] (log ε): chalcone 300 (4.25), 2'-benzyloxychalcone 307 (4.26) and flavanone 320 (3.56), 252 (3.98) [5, 6]. This band, maintaining the 'chalcone' character of the spectrum is shifted by the substituent of the benzylidene group to the longer wavelength region (Table I). This shift might be due to the inductive and resonance interaction of the substituents [7]. Substituents with $+I$ and $+M$ effects give rise to particularly large bathochromic shifts since their non-bonding electrons also participate in the electron delocalization of the conjugate system resulting in some 'charge transfer' contribution. The largest bathochromic shift (118 nm) was observed for the dimethylamino group, and the smallest for halogens. It is of interest that the electron-withdrawing nitro group did not influence considerably the spectrum of the unsubstituted compound (**I**) and only the cyano group caused a hypsochromic shift (14 nm). If the shift caused by the substituent was inter-

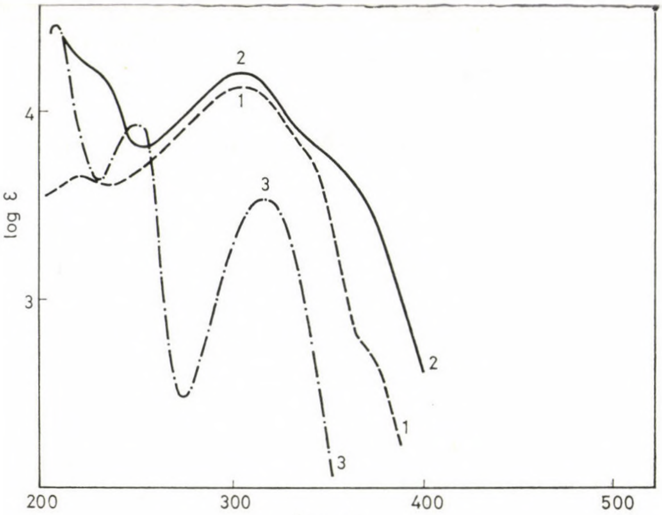

Fig. 1. UV spectrum of (*E*)-3-benzylideneflavanone (1), *s*-*Z*-(*E*)-chalcone (2) and flavanone (3)

Table I

UV spectra and band shifts of (E)-3-benzylideneflavanones, referred to the unsubstituted compound

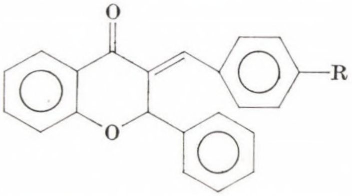

	R	λ_{max} [nm] (log ε)			$\Delta\lambda$ [nm]
I	H	350*	304 (4.24)	220*	—
II	$N(CH_3)_2$		422 (4.40)	275 (4.18)	+118
III	OH		351 (4.25)	220*	+ 47
IV	OCH_3		340 (4.23)	242*	+ 36
V	CH_3		320 (4.00)	240*	+ 16
VI	$C(CH_3)_2$		320 (4.11)	240*	+ 16
VII	Cl	350*	309 (4.22)	220*	+ 5
VIII	Br	350*	311 (4.17)	240*	+ 7
IX	CN	350*	290 (4.23)	240*	— 14
X	NO_2	350*	305 (4.33)	215 (4.48)	+ 1

* Inflexion

preted by means of the linear free energy relationship [7], two independent linearities were obtained (Fig. 2) using either σ or σ^*

$$\lambda^{R} - \lambda^{H} = \varrho\sigma(\text{or } \varrho\sigma^*)$$

where σ is the Hammett constant, σ^* is the Brown—Okamoto's constant and ϱ is the reaction constant, the value of which is obtained from the slope of the straight lines.

The slope of the straight line (1.013) is almost equal to those of 2'-hydroxychalcone (1.081) and 2'-benzyloxychalcone (1.096) [6], evidencing that the Ar—C=C—C=O part of all these molecules should be nearly coplanar.

As a result of the protonation of the carbonyl group, the spectra recorded in aqueous sulfuric acid solutions are considerably different from those measured in ethanol. Two new bands appear in the long wavelength region (380—520 nm) the intensity of which is somewhat altered by the substituent effects (Table II). The curves obtained in aqueous sulfuric acid solutions of different concentrations intersect at the isobestic point, which also proves an equilibrium between the non-protonated (B) and protonated (BH^+) forms.

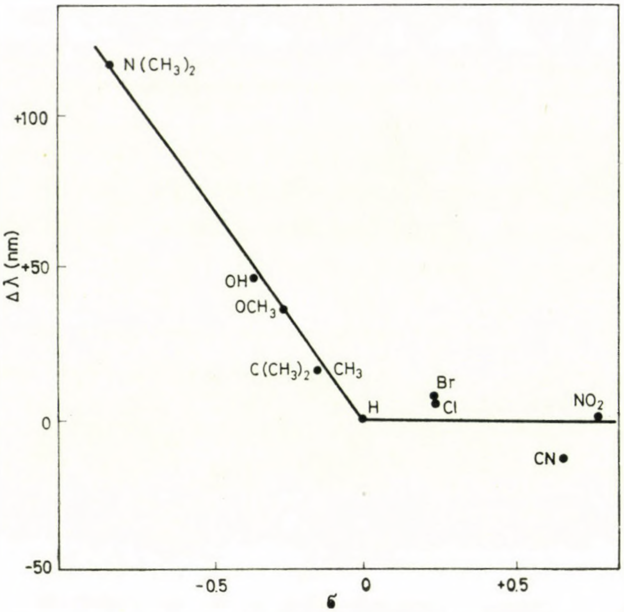

Fig. 2. **Relationship between the band shift and the Hammett σ constant**

Table II

UV spectra of (E)-3-benzylideneflavanones measured in concentrated sulfuric acid

	λ_{max} [nm] (log ε)	
I	460 (4.18)	400 (4.25)
II	470 (3.78)	380 (4.35)
III	502 (4.35)	412 (4.20)
IV	510 (4.41)	415 (4.15)**
V	475 (41.9)	400 (4.30)
VI	480 (4.19)	407 (4.28)
VII	470 (4.08)	400 (4.36)
VIII	470 (4.12)	406 (4.36)
IX	470 (3.88)	385 (4.33)
X	465 (4.04)	380 (4.33)

** In 80% sulfuric acid

For the calculation of the pK_{BH^+} values, the extinction data belonging to λ_{max} in the long wavelength region of the protonated form were used [8], since the non-protonated molecule shows practically no absorption in this area.

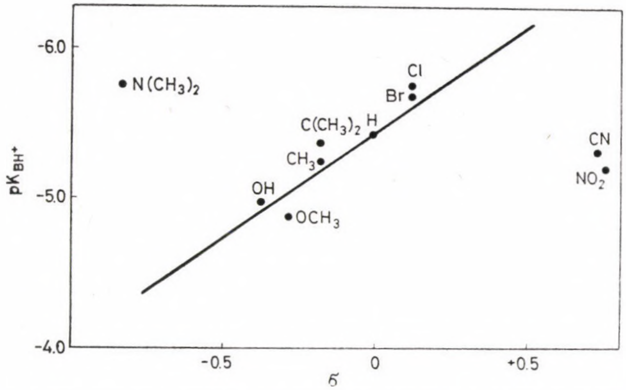

Fig. 3. Correlation between the basicity and the Hammett σ constant

Table III

Thermodynamic pK_{BH^+} *and* Φ *values of (E)-3-benzylideneflavanones*

	Φ	pK_{BH^+}
I	0.03	-5.42 ± 0.02
II	0.04	-5.76 ± 0.02
III	0.05	-4.98 ± 0.03
IV	0.03	-4.88 ± 0.02
V	0.02	-5.22 ± 0.03
VI	0.02	-5.38 ± 0.03
VII	0.00	-5.76 ± 0.02
VIII	0.00	-5.68 ± 0.02
IX	0.03	-5.37 ± 0.02
X	0.26	-5.22 ± 0.04

Change in the electron density of the carbonyl group is well reflected by the pK_{BH+} values (Table III, Fig. 3) of compounds having different substituents. However, since the dimethylamino group is protonated already in dilute sulfuric acid solution, its electron-releasing effect cannot alter considerably the protonation of the carbonyl group. An anomaly was found in the case of the nitro group, which decreased the electron density of the carbonyl group to a larger extent than expected. This is probably due to solvation effect, as shown by the Φ value differing from the others by one order of magnitude.

The Φ values for all compounds (0.00—0.05) but **X** prove that (*E*)-3-benzylideneflavanones represent a uniform class from the aspect of protonation [8, 9] and, therefore, behave as 'nearly' ideal Hammett bases, like *s*-*Z*-(*E*)-chalcones. Their thermodynamic pK_{BH^+} values (Table III) are similar to those of *s*-*Z*-(*E*)-chalcones (*s*-*Z*-(*E*)-chalcone: pK_{BH^+} -5.39, Φ -0.06) [6].

*

The authors' thanks are due to Professor R. BOGNÁR for valuable discussions.

REFERENCES

[1] KEANE, D. D., MARATHE, G. K., O'SULLIVAN, W. I., PHILBIN, E. M., SIMONS, R. M., TEAGUE, P. C.: J. Org. Chem., **35**, 2286 (1970)
[2] LÉVAI, A., HETEY, E. H.: Pharmazie, **33**, 378 (1978)
[3] DINYA, Z., SCHÁG, J. B., LÉVAI, A.: Acta Chim. Acad. Sci. Hung., **99**, 453 (1979)
[4] BUNNETT, J. F., OLSEN, P. F.: Canadian J. Chem., **44**, 1899 (1966)
[5] DÁVID, É. R., JANZSÓ, G., BÁLINT, J., BOGNÁR, R.: Acta Chim. Acad. Sci. Hung., **88**, 309 (1976)
[6] DÁVID, É. R., SZABÓ, G. B., RÁKOSI, M., LITKEI, GY.: Acta Chim. Acad. Sci. Hung., **94**, 57 (1977)
[7] BECKER, H. G. O.: Einführung in die Electronentheorie der organisch-chemischer Reaktionen. VEB Deutscher Verlag der Wissenschaften, Berlin, 1974
[8] SCORRANO, G.: Accounts Chem. Res., **6**, 132 (1973)
[9] LEVI, A., MODENA, G., SCORRANO, G.: J. Am. Chem. Soc., **96**, 6585 (1974)

Éva R. DÁVID
Albert LÉVAI
Gizella B. SZABÓ
H-4010 Debrecen, P.O. Box 20

Acta Chimica Academiae Scientiarum Hungaricae, Tomus 104 (4), pp. 375—383 (1980)

SYNTHESIS OF PEPTIDES CONTAINING D-GLUCOSAMINIC ACID, I

SYNTHETIC METHODS

Gy. Deák[1], K. Gáll-Istók[1], E. Zára-Kaczián[1] and L. Kisfaludy[2]

([1] *Research Institute of Experimental Medicine, Hungarian Academy of Sciences, Budapest, and* [2] *Gedeon Richter Chemical Works, Budapest)*

Received May 16, 1979
Accepted for publication October 9, 1979

The azide method has been found suitable for the preparation of peptides containing D-glucosaminic acid as the *N*-terminal amino acid, protected from lactonization in the form of the 4,6-*O*-benzylidene derivative. When acted upon by dicyclohexylcarbodiimide, even in the presence of pentachlorophenol, 4,6-*O*-benzylidene-D-glucosaminic acid is converted into 4,6-*O*-benzylidene-2-benzyloxycarbonylamino-2-deoxy-D-glucono-1,5-lactone. This reaction reveals that the strongly polarized carbonyl carbon atom of the *O*-acylisourea intermediate is attacked not by the phenolate anion but, probably owing to steric reasons, intermolecularly by the oxygen atom of the C-5 hydroxyl group, which is much less nucleophilic, but sterically more favoured.

D-Glucosaminic acid (2-amino-2-deoxy-D-gluconic acid), regarded as an analogue of serine, has been rarely employed as a non-natural amino acid in peptide chemistry. Bergmann *et al.* [1] synthesized 4,6-*O*-benzylidene [(*N*-Z-glycyl)amino]- and -2[(*N*-Z-L-phenylalanyl)amino]-2-deoxy-D-gluconic acids, among other peptides, by means of the acid chloride method; however, the yields were rather poor, hence the attempts at synthesizing other similar peptides were not continued. The lack of interest in glucosaminic acid derivatives can only partly be explained by the great proneness of D-glucosaminic acid to lactone formation, making necessary the preparation of the 4,6-*O*-benzylidene derivative, which is a rather complicated and time-consuming procedure. In spite of these difficulties, it appears interesting to elucidate the conditions for the application of glucosaminic acid as an amino acid component of peptides and to determine the suitable protecting groups and coupling methods. The incorporation of D-glucosaminic acid into the peptide chain is expected to increase the hydrophilic character of the molecule and a corresponding substitution by serine would allow to establish the function of the hydroxyl group. Another possibility is the preparation the polyamino acids by the polimerization of short-chain peptides containing glucosaminic acid, the sulfation of which would yield compounds with potential heparin activity. Therefore, in the first stage of the present work the preparation of such model tripeptides was aimed at in which the glucosaminic acid is located in the *N*-terminal, *C*-terminal and intermediate positions, respectively.

In the present paper the results of the first part of the work, the synthetic methods are discussed. In the following text and Figures D-glucosaminic acid and 4,6-*O*-benzylideneglucosaminic acid are represented by the symbols H—GA—OH and H—BEGA—OH, respectively, similarly to the symbols internationally accepted for amino acids.

The starting H—GA—OH was prepared from glucosamine by the method of Hope and Kent [2]; freshly prepared yellow mercury oxide was used for the oxidation. In accordance with the literature, the optimum yield (62%) was obtained, when 10 g of glucoseamine was processed; in a batch of 100 g starting material the yield was as low as 39%. On the basis of the IR spectrum, the product has a zwitterion structure.

The Hope and Kent method was also used for the preparation of H—BEGA—OH from H—GA—OH; an ethanolic solution containing the starting material and benzaldehyde was rapidly saturated with dry hydrogen chloride gas.

H—BEGA—OEt was to be prepared, too, by the Hope and Kent method [2]: the protected acid was to be esterified to obtain the corresponding ester. This reaction remained, however, unsuccessful, in spite of varying the parameters. In the IR spectrum of the product of esterification the νCO band characteristic of the ester group could be indentified yet it was weak, and the occurrence of some other reaction was evident. Since in the course of the esterification process benzaldehyde could be detected in all cases, it can be assumed that the water liberated in this step gave rise to a significant hydrolysis of the benzylidene protective group in the presence of hydrochlorid acid, yielding a reaction mixture difficult to process. Therefore we developed a one-step preparation of H—BEGA—OEt HCl, which finally resulted in the desired product: under carefully controlled experimental conditions H—BEGA—OEt HCl could be synthesized directly from H—GA—OH in a well reproducible process.

Z—BEGA—OEt was made in the well-known manner in the presence of MgO; the pure product was isolated in 64% yield.

Methods of coupling

In the next step, the model compound to be prepared was ethyl-4,6-*O*-benzylidene-2-[(*N*-Z-glycyl)-amino]-2-deoxy-D-gluconate. Acylation of H—BEGA—OEt HCl with Z—Gyl—OH was effected by both the DCC and the pentachlorophenyl ester techniques. In both cases the same product was obtained, but the yield was higher in the active ester method. In the latter case, pentachlorophenol had to be removed from the crude product after coupling by extraction with ether; omitting this step prevented the preparation of a pure end-product, in spite of repeated recrystallizations.

Ethyl 4,6-*O*-benzylidene-2-[(*N*-Z-glycyl)amino]-2-deoxy-D-gluconate was converted into the dipeptide acid by alkaline hydrolysis. The product was, probably owing to the presence of free hydroxyl groups, liable to hydrate formation.

As on the basis of theoretical considerations the coupling procedures were to be effected by the active ester method, it was examined whether the PCP ester of *N*-Z-4,6-*O*-benzylidene-D-glucosaminic acid could be prepared. In the reaction of Z—BEGA—OH, pentachlorophenol and DCC, the separation of DCU was observed, however, the product was not the expected one. Similarly, a product of unknown structure was obtained when *N*-(Z-glycyl)-4,6-*O*-benzylideneglucosaminic acid was treated in order to convert it into the activated ester. The product had an ester character, but the band at 1810 cm^{-1} characteristic of PCP esters was absent in the IR spectrum.

It is known that serine could not be converted into the p-NO_2-phenyl ester; the product was the p-NO_2-phenyl ester of seryl-serine [8]. Kovács *et al.* [3] applied a high excess of pentachlorophenol and a short reaction time, thus the activated ester of serine could be synthesized. The desired product, however, could not obtained in our experiments by this method either.

On the basis of the above results it seemed reasonable to suspect that DCC caused a change in the 4,6-*O*-benzylideneglucosaminic acid part, in both reactions. The experiments confirmed this hypothesis.

When *N*-Z-4,6-*O*-benzylideneglucosaminic acid was allowed to react in DMF solution with an equimolar amount of pentachlorophenol in the presence of one equivalent of DCC at room temperature for 24 hr, the urea derivative separated was filtered off and the filtrate processed, the resulting end-product contained no chlorine, and almost the entire amount of pentachlorophenol was found in the mother liquor of recrystallization. The experiment was then repeated in the absence of pentachlorophenol giving the same result: a white crystalline substance was obtained, which was not identical with the starting material and produced two spots in various developing solvent mixtures in TLC. Separation of the product on a preparative layer was attempted, while monitoring the extent of separation by IR spectroscopy. The substance was found to be very sensitive and to decompose rapidly under the conditions of TLC, as well as during recrystallization. (*N*-Z-4,6-*O*-Benzylideneglucosaminic acid could also be detected among the decomposition products.) Finally, the pure, homogeneous δ-lactone, *i.e.* 4,6-*O*-benzyilidene-2-benzyloxycarbonylamino-2-deoxy-D-glucono-1,5-lactone could be prepared without recrystallization in 90% yields.

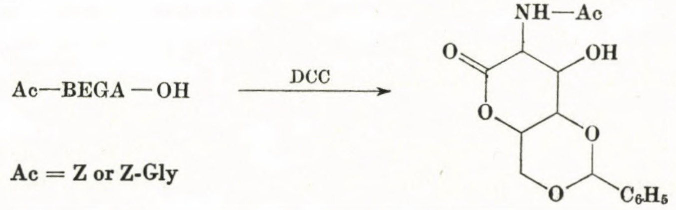

Ac = Z or Z-Gly

This result indicates that the strongly polarized carbonyl carbon atom of the intermediate *O*-acylisourea is attacked not by the phenolate anion, but, probably owing to steric reasons, in an intermolecular reaction, by the oxygen atom of the C-5 hydroxyl group, which is much less nucleophilic, yet sterically more favoured.

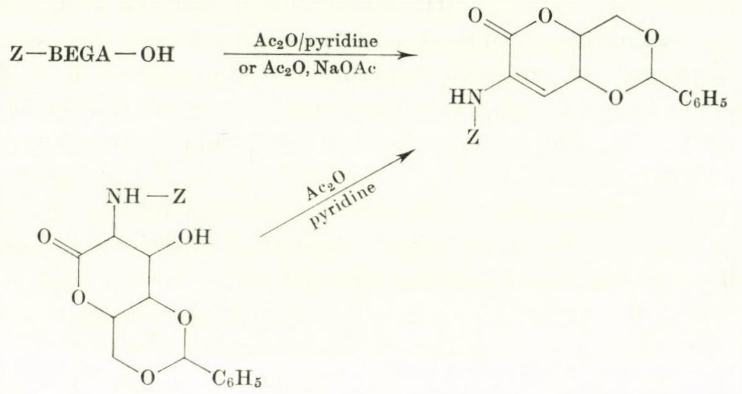

During TLC monitoring of the reaction using the IR technique for examining the samples taken at frequent intervals, only the starting material and the end-product could be detected. Still, the possibility of the formation of the PCP ester can not be excluded, which may transform rapidly and quantitatively in an intramolecular acylation reaction into the δ-lactone.

The experiments have unambiguously confirmed so far that the varioiu interfering actions of the hydroxyl groups in 4,6-*O*-benzylidene-D-glucosamincs acid (poor solubility in apolar solvents, impossibility of preparation of the active ester and use of the DCC technique) requires their temporary blocking. Hence in the following part of the work we aimed at finding suitable protective groups.

1. *Protective groups*

According to literature data, the *t*-butoxy group serves effectively for temporary protection of hydroxyl groups. We attempted the preparation of the 3,5-di-*t*-butyl ethers of *N*-Z-4,6-*O*-benzylidene-D-glucosaminic acid ethyl ester and ethyl 4,6-*O*-benzylidene-2-[(*N*-Z-glycyl)-amino]-2-deoxy-D-gluconate by allowing the starting esters to react with isobutylene in methylene chloride solution in the presence of sulfuric acid catalyst. During proccessing, the smell of benzaldehyde could be strongly felt, indicating decomposition caused by sulfuric acid. In the IR spectra of the non-crystallizing oily products obtained from the above ethyl esters the significant intensification of the $\nu_{as}CH_3$ band at 2980 cm^{-1} revealed the occurrence of ether formation (at least partly); at the same time the appearance of a new strong carbonyl band at 1975—

1800 cm^{-1} signalled a side-reaction, probably the formation of a cyclic compound.

Since the *t*-butoxy group thus could not be used for protection, temporary blocking of the hydroxyl groups was tried by means of acylation. As it has been reported [4], ethyl 4,6-*O*-benzylidene-2-[(*N*-Z-glycyl)amino]-2-deoxy-D-gluconate could be converted into the 3,5-diacyl derivative with acylating agents in anhydrous pyridine. However, acylation of *N*-Z-4,6-*O*-benzylidene-D-glucosaminic acid with acylating agents or acid anhydrides in the presence of the sodium salt of the acid, using anhydrous pyridine solvent, yielded 2-benzyloxycarbonylamino-4,6-benzylidene-2,3-dideoxy-D-*erythro*-hex-2-eno-1,5-lactone by β-elimination, instead of the expected diacetyl derivative. The same product was obtained by acylation of the δ-lactone described above with Ac$_2$O in pyridine.

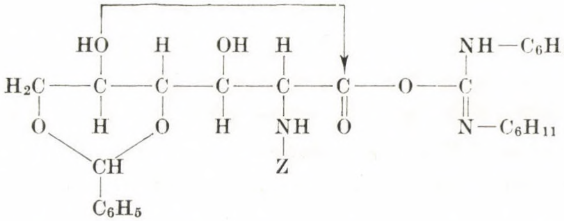

Since complete protection of glucosaminic acid could not be achieved, such a coupling method was to be found in which free hydroxyl groups do not interfere. For this purpose, the azide method was tried.

2. *Coupling with azide*

In the course of the adaptation of the azide coupling method to glucosaminic acid, it was found that the formation of hydrazide was significantly affected by the water content and the amount of hydrazine hydrate used. Ethyl 4,6-*O*-benzylidene-2-[(*N*-Z-gylcyl)-amino]-2-deoxy-D-gluconate could be transformed into the hydrazide by means of 98% N_2H_4 in 60% yield.

The next task was the effecting of coupling by means of the hydrazide prepared as described above, in order to establish the peptide bond. As a model compound methyl *N*-(*Z*-4,6-*O*-benzylideneglucosaminyl)-glycinate was prepared in 60% yield.

The next step was the hydrolysis of the dipeptide ester obtained in the azide coupling procedure. As reported earlier [5], alkaline hydrolysis was accompanied by the well-known decomposition of the benzyloxycarbonyl group and the respective hydantoin derivative was formed.

On varying the conditions of the reaction, finally pure 5-(2,4-*O*-benzylidene-1,2,3,4-tetrahydroxybutyl)-2,4-dihydroxy-3-imidazolidineacetic acid was obtained in 23% yield.

Owing to the well known sensitivity of peptides containing glycine, the methyl ester of *N*-(Z-4,6-*O*-benzylidene-D-glucosaminyl)alanine was prepared again by the azide method. During the alkaline hydrolysis of this compound no formation of hydantoin was observed, and the corresponding dipeptide acid could be synthesized without any difficulty.

The azide method was used in the preparation of the dipeptide from *N*-Z-glycyl azide and ethyl 4,6-*O*-benzylidene-2-amino-2-deoxy-D-gluconate, which had been synthesized earlier by us using the DCC and the activated ester methods. This dipeptide was obtained in 42% yield by the DCC method, while the yields of the activated ester procedure using the PCP ester and of the azide method were 60% and 73%, respectively.

Ethyl 4,6-*O*-benzylidene-2-[(*N*-Z-glycyl)-amino]-2-deoxy-D-gluconate could be hydrolyzed into the corresponding acid in alcoholic solution with aqueous NaOH at 0— —5 °C in 50 min in 80% yield. According to our observation, the alkaline hydrolysis of the dipeptide takes place surprisingly rapidly. The situation is similar with *N*-Z-4,6-benzylideneglucosaminic acid ethyl ester, which undergoes hydrolysis in 3 h, again at 0 — —5 °C. Interestingly, the ethyl ester of 4,6-benzylideneglucosaminic acid cannot be hydrolyzed under such conditions, whereas under more vigorous conditions side reactions also occur.

In summary, it can be stated that, in accordance with expectation, the incorporation of D-glucosaminic acid into the peptide chain allows several side-reactions to occur, which, however, can be eliminated by the application of suitable protective groups and coupling methods.

Experimental

M.p.'s were determined on a Büchi—Tottoli apparatus and are uncorrected. IR spectra were determined in KBr pellets (Perkin Elmer Model 457). The R_f values were determined using the ascending technique of thin layer chromatography in the following solvent systems: (1) BuOH : AcOH : H_2O = 80 : 20 : 5 (2) $CHCl_3$: MeOH = 95 : 5. For the detection of the spots ninhydrin and chlorotoluidine were used, respectively. All compounds were analyzed for C, H, N with results of a least 0.4% accuracy.

D-Glucosaminic acid

It was prepared according to the method of HOPE and KENT [2] and crystallized from aqueous methanol. $[\alpha]_D^{20}$—14.4° (in 2.5% aqueous hydrochloric acid); m.p. 250 °C (d.).

Ethyl 4,6-*O*-benzylidene-2-amino-2-deoxy-D-gluconate. HCl

Finely powdered D-glucosaminic acid (6.6 g; 34 mmoles) was suspended in anhydrous alcohol (45 ml), and freshly distilled benzaldehyde (9 ml; 89 mmoles) was added to the suspension vigorous. A stream of dry hydrochloric acid gas was introduced into the solution, without cooling, until a clear solution had formed. The period till dissolution was 6—8 min and the maximum temperature of the mixture 60 °C. The yellowish solution was allowed to stand at room temperature for 16—20 h, during which time it solidified. The crystalline mass obtained in this way was rubbed with some ether, filtered off and thoroughly washed with ether. After drying, white crystals decomposing at 168 °C were obtained (10.7 g; 91%). $[\alpha]^{20}_{D}$ —30° ($c = 1$, H_2O), in agreement with the literature data [2].

Ethyl 4,6-*O*-benzylidene-2[(*N*-Z)-amino]-2-deoxy-D-gluconate and 4,6-benzylidene-2[(*N*-Z)-amino]-2-deoxy-D-gluconic acid hydrazide were prepared as described earlier [5].

Hydrolysis of ethyl 4,6-*O*-benzylidene-2-[(*N*-Z)-amino]-2-deoxy-D-gluconate

The ester (5 mmoles) was suspended in methanol (20 ml), cooled to 0 °C and 1 *N* NaOH (5.5 mmoles) was added to the suspension. The solid was maintained at 0— +5 °C and stirred, whereupon it slowly dissolved. The solution was filtered, methanol was removed in vacuum at maximum 30 °C bath temperature, and the residual jelly was mixed with water (20 ml), acidified with 2 *N* hydrochloric acid (2.7 ml) with cooling, mixed with water again (20 ml) and rubbed. After refrigerating for a few hours the crystals which separated were washed with water until free from chloride. On drying, a product of m.p. 167—168 °C was obtained in 82% yield.

IR: νCO (acid) 1723; Amide I (Z) 1685; Amide II (Z) 1450 cm^{-1}.

4,6-*O*-Benzylidene-2-[(*N*-Z-glycyl)amino]-2-deoxy-D-gluconic acid

a *Dicyclohexylcarbodiimide method*

(1) Ethyl 4,6-*O*-benzylidene-2-[(*N*-Z-glycyl)-amino]-2-deoxy-D-gluconate

Ethyl 4,6-*O*-benzylidene-2-amino-2-deoxy-D-gluconate. HCl (3.5 g; 10 mmoles) was dissolved in anhydrous DMF (7 ml), the solution was cooled to 0 °C, and triethylamine (1.39 ml) was added. The mixture was stirred for 20 min, then Z-glycine (2.1 g; 10 mmoles) was added. After stirring for 5 min more, DCC (2.1 g; 10 mmoles) was added and the solution was allowed to warm to room temperature under stirring. The reaction mixture was processed after standing for 24 h. First, it was mixed with acetic acid (1 ml) and stirred for 5 min, then it was tered; the filtrate was evaporated to dryness in vacuum, the residual orange oil was dissolved in ethyl acetate (10 ml) and purified by washing in the usual manner. It was then dried, evaporated to dryness, in vacuum the residual sticky substance was rubbed with anhydrous ether (50 ml) and the solid was filtered off. In this way a substance melting at 125—128 °C was obtained (3.2 g). This was crystallized from a mixture of ethanol (15 ml) and water (13 ml). The pure ester (2.1 g; 42%) had m.p. 128—130°, and 130—132 °C after drying at 110 °C.

(2) 4-6-*O*-benzylidene-*N*-(Z-glycyl)-D-glucosaminic acid

The ester prepared as given under (1) (2.0 g; 4 mmoles) was dissolved in methanol (20 ml), cooled to 0 °C, and 1 *N* NaOH (4.4 ml) was added, with stirring. The solution was stirred at 0— +5 °C for 1 h. The solvent was evaporated, the remaning jelly diluted with water (20 ml) and the mixture was adjusted to pH 3 with 1 *N* HCl, under cooling. The mixture containing a white precipitate was refrigerated for 10—12 h, filtered off and washed with water until free from chloride. After drying it was crystallized from 90% ethanol to obtain a white crystalline substance (1.5 g; 80%); m.p. 162 °C (d.) $[\alpha]^{20}_{D}$—28° ($c = 2$, DMF).

b *Activated ester method*

Ethyl 4,6-*O*-benzylidene-2-amino-2-deoxy-*O*-gluconate. HCl (3.5 g; 10 mmoles) was dissolved in anhydrous DMF (10 ml) and cooled to 0 °C. Triethylamine (1.35 ml) was then added dropwise, the mixture was stirred for 20 min, the amino salt was filtered off and wa with DMF (1 ml); the washing liquor was added to the main solution. The combined DMF solution was then mixed with Z-glycinepentachlorophenyl ester [6] (4.6 g; 10 mmoles), stirred for 3 h, and after a 24-h reaction period at room temperature it was evaporated in vacuum to

dryness. The residual brownish yellow oil (9.1 g) was rubbed with anhydrous ether (100 ml) until it solidified. In order to remove pentachlorophenol, the mass was triturated with ether (3×50 ml) to obtain a beige-white crystalline substance (4.5 g), m.p. 120—127 °C. This was dissolved in ethyl acetate (150 ml), washed until neutral in the usual manner, dried and evaporated to dryness in vacuum. The residual yellowish white substance was rubbed with anhydrous ether (50 ml) and filtered off to give a white powder (3 g; 60%), m.p. 127—129 °C.

When the hydrolysis of the ester was affected as described before, a product melting at 160—162 °C (2.2 g) was obtained. Crystallization from ethyl acetate by the addition of petroleum ether gave a product identical in all respects with that described under a.

c *Azide method*

A solution of Z-glycine hydrazide [7] (2.2 g; 10 mmoles) in DMF (15 ml) was cooled to —10 °C, then 6 *N* HCl (31.9 mmoles; 5.38 ml) was added, followed by the dropwise addition of an aqueous solution (1.5 ml) of $NaNO_2$ (11.9 mmoles) at —10— —15 °C, under stirring, during 5 min. The azide separated as a white precipitate after stirring for 10 min. The solution was diluted with ethyl acetate (20 ml) and added at —10 °C to a solution which consisted of ethyl 4,6-*O*-benzylideneglusoaminate (8.2 mmoles), DMF (12 ml) and triethylamine (31.9 mmoles), and had been cooled to —20 °C; the addition was effected in 40 min. The mixture was stirred at —10 °C for 1 h and then refrigerated for 16 h. DMF was removed in vacuum in a bath of maximum 35 °C. The sticky crystalline residue was dissolved in a mixture of ethyl acetate (60 ml) and 20% NaCl solution (70 ml) cooled to 0 °C, the phases were separated, the aqueous phase was twice extracted with ethyl acetate, and the combined ethyl acetate solution was washed twice with 20% NaCl solution. The extraction and washing procedures were carried out at 0 °C. The ethyl acetate solution was dried over. Na_2SO_4, filtered, the solvent was removed in vacuum and the residue crystallized from a mixture of ethyl acetate and petroleum ether to give the product (3.0 g; 73%), m.p. 129 °C.

When the ester was hydrolyzed as described above and the product crystallized from 96% ethanol, the resulting substance was identical in all respects with the product prepared according to a, the yield being 80%.

4,6-*O*-Benzylidene-2-benzyloxycarbonylamino-2-deoxy-D-glucono-1,5-lactone

N-*Z*-4,6-*O*-Benzylideneglucosaminic acid (2.1 g; 5 mmoles) was dissolved in anhydrous DMF (12 ml), cooled to 0 °C, and a solution of dicyclohexylcarbodiimide (1.04 g; 5 mmoles), in anhydrous DMF (4 ml) was added to it. The clear solution was stirred at 0 °C for 1 h, and allowed to stand at room temperature for 24 h. The urea derivative which separated was filtered off and washed with anhydrous dioxan. The washing liquor was combined with the main solution, evaporated to dryness in vacuum on a bath of maximum 40 °C, and the somewhat sticky crystalline residue was thoroughly washed first with hot then with cold dry ether and dried over P_2O_5 and paraffin in a vacuum desiccator. A white crystalline substance (1.8 g; 90%) was obtained, m.p. 184 °C.

IR: CO (lactone) 1765; Amide I (Z) 1690; Amide II (Z) 1540 cm^{-1}. (δ-lactone).

2-Benzyloxycarbonylamino-4,6-*O*-benzylidene-2,3-dideoxy-D-*erythro*-hex-2-eno-1,5-lactone from 2-benzyloxycarbonylamino-4,6-*O*-benzylidene-2-deoxy-D-glucono-1,5-lactone (δ-lactone)

The δ-lactone (0.8 g; 2 mmoles) was dissolved in anhydrous pyridine (10 ml), cooled to 0 °C and acetic anhydride (0.45 g; 0.42 ml; 4.4 mmoles +10% excess) was added to it. The clear solution was kept at room temperature for 48 h, then poured onto ice, and acidified to pH 3 with conc. hydrochloric acid, whereupon a white powder separated. This was filtered off, thoroughly washed with water, dried and crystallized from ethyl acetate to obtain the 1.5-lactone (0.72 g; 96%), m.p. 190 °C.

N-(Z-4,6-*O*-Benzylideneglucosaminyl)alanine methyl ester

4,6-*O*-Benzylidene-2[(*N*-*Z*)-amino]-2-deoxy-D-gluconic acid hydrazide (1.5 g; 3.5 mmoles) was converted into the azide as described under **c**, and this was allowed to react with alanine methyl ester hydrochloride (1.4 g; 10.4 mmoles) in DMF (18 ml) in the presence of triethylamine (5.8 ml; 41.6 mmoles). The reaction mixture was processed as in **c**.

The crude product was crystallized from aqueous methanol to give the pure compound (1.05 g; 60%), m.p. 155 °C.

IR: νCO (ester) 1745; Amide I (Z) 1690; Amide I (peptide) 1660; Amide II 1540 cm^{-1}.

Ethyl 3,5-*O*-acetyl-4,6-*O*-benzylidene-2-[(*N*-Z)-amino]-2-deoxy-D-gluconate

Ethyl 4,6-benzylidene-2-[(*N*-*Z*)-amino]-2-deoxy-D-gluconate (1.5 g; 3.3 mmoles) was dissolved in anhydrous pyridine (10 ml) at 0 °C, and freshly distilled acetic anhydride (0.81 g; 8 mmoles) was added to the solution at 0 °C, with stirring and cooling. The solution was allowed to warm to room temperature, the stirring was stopped, and it was allowed to stand for 50 h. The mixture was then poured into ice-water, whereupon an oil separated which solidified on rubbing and changing the cold water. The solid was filtered off, washed with water (6 × 15 ml) until free from pyridine, dried and crystallized from a mixture of methanol (47 ml) and water (19 ml) to obtain (1.43 g 82%) of the product, m.p. 105 °C; R_f^2 0.942.

IR: νNH 3353; CO (ester) 1750; Amide II (Z) 1540 cm^{-1}.

Ethyl 3,5-*O*-benzyol-4,6-*O*-benzylidene-2-[(*N*-Z)-amino]-2-deoxy-D-gluconate

The compound was prepared as described above, using 5 mmoles of the starting material, with benzoyl chloride. On pouring into ice-water, an oil separated; the pH of the solution was adjusted to 3 with conc. hydrochloric acid, the viscous sticky substance was dissolved in methylene chloride and processed in the usual way. It was crystallized from a mixture of ethyl acetate and petroleum ether to obtain a product (2.0 g; 61.5%) m.p. 129 °C.

IR: νNH 3390; CO (ester) 1740; CO (benzoyl) 1730; Amide II 1530 cm^{-1}.

*

The authors gratefully adenowledge the support of this work by the Gedeon Richter Chemical Works, Budapest.

REFERENCES

[1] Bergmann, M., Zervas, L., Rinke,H., Scheich, H.: Z. physiol. Chem., **224**, 33 (1934)
[2] Hope, D. P., Kent, P. W.: J. Chem. Soc., **1955**, 1831
[3] Kovács, J., Ceprini, M. Q., Dupraz, C. A., Schmit, G. N.: J. Org. Chem., **32**, 3696 (1967)
[4] Deák, Gy., Gáll-Istók, K., Haskó-Breuer, J., Sohár, P.: Acta Chim. Acad. Sci., Hung., **92**, 421 (1977)
[5] Deák, Gy., Zára-Kaczián, E., Kisfaludy, L.: Acta Chim. (Budapest) **75**, 185 (1973)
[6] Kupryszewski, G., Formela, M.: Roczniki Chem., **35**, 1533 (1961); C.A. **57**, 7373a (1962)
[7] Erlanger, B. P., Brand, E.: J. Am. Chem. Soc., **73**, 3508 (1951)
[8] Bodanszky, M., Ondetti, M. A.: Chem. Ind. (London), **1966**, 26

Gyula Deák
Klára Gáll-Istók
Erzsébet Zára-Kaczián
H-1450 Budapest, P.O.Box 67

Lajos Kisfaludy
H-1475 Budapest, P.O. Box 27

Acta Chimica Academiae Scientiarum Hungaricae, Tomus 104 (4), pp. 385—387 (1980)

OXAZEPINES AND THIAZEPINES, IX*

THE SCHMIDT REACTION OF 1-THIOFLAVANONE

A. Lévai

(Institute of Organic Chemistry, Kossuth Lajos University, Debrecen)

Received July 11, 1979
In revised form September 19, 1979
Accepted for publication October 9, 1979

2,3-Dihydro-2-phenyl-1,4-benzothiazepin-5(4*H*)-one (**I**) and 2,3-dihydro-2-phenyl-1,5-benzothiazepin-4(5*H*)-one (**II**) were synthesized *via* the Schmidt reaction of 1-thioflavanone.

The Schmidt reaction of flavanone and its substituted derivatives has been studied by several research groups [2—6] and it was found that the reaction took place mainly with alkyl migration to give 2.3-dihydro-2-phenyl-1,4-benzoxazepin-5(4*H*)-ones. In some cases, as a result of aryl migration, a very small amount of the 1,5-isomer was also obtained[4, 5]. Under the same reaction conditions isoflavanone, however, reacted differently and besides the 2,3-dihydro-3-phenyl-1,4-benzoxazepin-5(4*H*)-one a considerable quantity of 2,3-dihydro-3-phenyl-1,5-benzoxazepin-4(5*H*)-one could also be isolated [7]. Evaluating the experimental results, Misiti and Rimatori [7] established that the ratio of products formed from flavanone by alkyl and aryl migration was about 30 : 1, whereas that found for isoflavanone was about 3 : 1. As an extension of our former investigations on the conversion of flavanones into benzoxazepinones [6], now we report on the Schmidt reaction of 1-thioflavanone. The aim of this study was to compare the reaction of flavanone and its sulfur-containing analogue and to work out a new synthesis of benzothiazepinones.

1-Thioflavanone was allowed to react with sodium azide in a mixture of concentrated sulfuric acid and acetic acid under the reaction conditions described for flavanones [2—6]. According to TLC analysis, 2,3-dihydro-2-phenyl—1,4-benzothiazepin-5(4*H*)-one (**I**) and 2,3-dihydro-2-phenyl-1,5-benzothiazepin-4(5*H*)-one (**II**) were obtained in 1 : 1 ratio. The two isomers could readily be separated on a silica gel column. The course of the reaction can be postulated as follows (Scheme 1):

The conjugate acid of the ketone produces a protonated azidohydrin with hydrazoic acid, which loses water to form an iminodiazonium ion. This ion can exist in the *Z* and *E* forms. The *Z*-isomer produces a carbonium ion through alkyl migration followed by nitrogen elimination which gives 2,3-

---

* For Part VIII, see Ref. [1].

dihydro-2-phenyl-1,4-benzothiazepin-5(4*H*)-one (**I**) on hydration. The *E*-isomer yields 2,3-dihydro-2-phenyl-1,5-benzothiazepin-4(5*H*)-one (**II**).

Thus it seems to be a reasonable assumption that the same mechanism is valid for the Schmidt reactions of flavanone, isoflavanone and 1-thioflavanone, and the ratio of alkyl and aryl migration is determined by the stereochemistry of the iminodiazonium ion. In case of flavanone the *Z*-isomer predominates [6], with isoflavanone a considerable amount of the *E*-isomer is also present [7], while in 1-thioflavanone the ratio of the two isomers should be about 1 : 1.

The Schmidt reaction of 1-thiochromanones, variously substituted in the aromatic ring, was studied by **Wünsch** *et al.* [8] and it was found that the ratio of 2,3-dihydro-1,4-benzothiazepin-5(4*H*)-one and 2,3-dihydro-1,5-

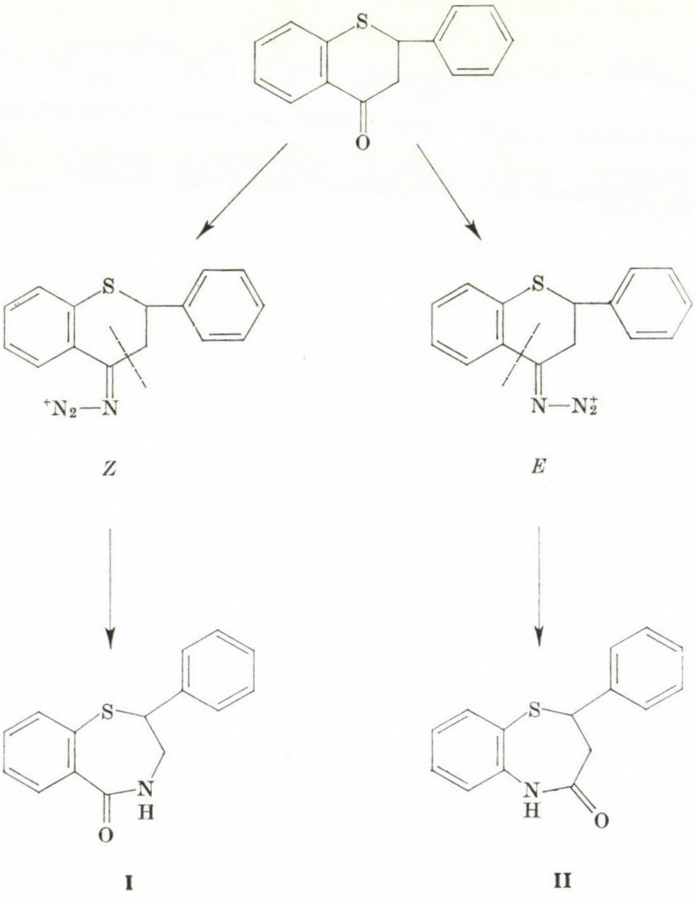

Scheme 1

benzothiazepin-4(5*H*)-one obtained was dependent on the electron character of the substituents. In our opinion, the course of the reaction is determined in this case also by the stereochemistry of the iminodiazonium ion which, in turn, can be influenced by the substituents.

Both 2,3-dihydro-2-phenyl-1,4-benzothiazepin-5(4*H*)-one (**I**) and 2,3-dihydro-2-phenyl-1,5-benzothiazepin-4(5*H*)-one (**II**) were previously synthesized by KRAPCHO *et al.* [9, 10] and the substances obtained in different ways are identical in every respect.

Experimental

M.p.'s are uncorrected.

The IR spectra were taken in KBr pellets on a Perkin-Elmer 283 instrument. The ^{1}H-NMR spectra were recorded with a Jeol MH 100 instrument in deuterochloroform (internal standard TMS, $\delta = 0$ ppm) at room temperature. TLC and column chromatography were performed on Kieselgel G (Merck) adsorbent using ethyl acetate — hexane 6 : 4 (*v*/*v*) eluent.

Concentrated sulfuric acid (4.0 ml) was added, in portions, to a stirred and cooled mixture of 1-thioflavanone (4.0 g), sodium azide (2.0 g) and glacial acetic acid (15.0 ml). The mixture was stirred for further 2 h at 45—50 °C and then poured into water. The precipitated material (3.4 g) was filtered off, washed free of acid, analyzed by means of TLC, and then separated by column chromatography.

Fractione one

2,3-Dihydro-2-phenyl-1,5-benzothiazepin-4(5*H*)-one (**II**), m.p. 180—181 °C, *lit.* [9] m.p. 176—177 °C.

IR: νC=O 1676 cm^{-1}.

^{1}H-NMR: NH (9.36 s); aromatic protons (7.34—7.92 m); CH (5.22 q); CH_2 (2.96 t).

$C_{15}H_{13}NOS$ (255.25). Calcd. N 5.49; S 12.54. Found N 5.33; S 12.73%.

Fraction two

2,3-Dihydro-2-phenyl-1,4-benzothiazepin-5(4*H*)-one (**I**), m.p. 186—187 °C, *lit.* [10] m.p. 186 —188 °C.

IR: νC=O 1664 cm^{-1}.

^{1}H-NMR: NH (8.57 t); aromatic protons (7.42—8.06 m); CH (4.74 q); CH_2 (3.53 m).

$C_{15}H_{13}NOS$ (255.25). Calcd. N 5.49; S 12.54. Found N 5.44; S 12.63%.

The NH signal is extinguished by D_2O.

The corresponding products obtained in this way and in those described by KRAPCHO *et al.* [9, 10] gave no m.p. depression in admixture.

*

The author's thanks are due to Drs. L. SZILÁGYI and Z. DINYA for the spectra and to Mrs. E. HAJNAL for her assistance in the experimental work. The present study was sponsored by the Hungarian Academy of Sciences for which our gratitude is expressed.

REFERENCES

[1] LÉVAI, A.: Pharmazie, **34**, 439 (1979)
[2] KRAPCHO, J., TURK, C. F.: J. Med. Chem., **9**, 191 (1966)
[3] LOCKHART, I. M.: Chem. Ind. (London), **1968**, 1844
[4] MISITI, D., RIMATORI, V.: Tetrahedron Letters, **1970**, 947
[5] MISITI, D., RIMATORI, V.: Ann. Ist. Super. Sanita, **9**, 150 (1973)
[6] LÉVAI, A., BOGNÁR, R.: Acta Chim. Acad. Sci. Hung., **97**, 77 (1978)
[7] MISITI, D., RIMATORI, V.: Gazz. Chim. Ital., **101**, 167 (1971)
[8] WÜNSCH, K. H., STAHNKE, K. H., EHLERS, A.: Chem. Ber., **103**, 2302 (1970)
[9] KRAPCHO, J., SPITZMILLER, E. R., TURK, C. F.: J. Med. Chem., **6**, 544 (1963)
[10] KRAPCHO, J., TURK, C. F., PIALA, J. J.: J. Med. Chem. **11**, 361 (1968)

Albert LÉVAI H-4010 Debrecen, P.O. Box 20

Acta Chimica Academiae Scientiarum Hungaricae, Tomus 104 (4), pp. 389—396 (1980)

SYNTHESIS OF 4,5-DIPHENYLISOXAZOLES AND THEIR INSECTICIDAL DERIVATIVES

J. Borda[1], V. Szabó[1], L. Németh[1] and Gy. Bokor[2]

([1] *Institute of Applied Chemistry, Kossuth Lajos University, Debrecen, and*
[2] *North-Hungarian Chemical Works, Sajóbábony, Hungary*)

Received April 20, 1979
In revised from July 21, 1979
Accepted for publication October 10, 1979

4,5-Diphenylisoxazoles (**IIIa—m**) have been prepared in very good yields by the reaction of substituted isoflavones (**Ia—m**) with hydroxylamine in boiling aqueous alcohol at pH 8. In the cases of the poorly reactive 2-methylisoflavones (**Ih, j, k**) and 7-hydroxyisoflavone, which did not react under the above conditions, the reaction was effected in dry methanol in the presence of sodium acetate.

The isoxazoles prepared can be readily converted into phenol carbamates (**IV, V, VIa—i**) by means of alkyl isocyanates, or to thiophosphoric acid ester derivatives (**VIIa—c**) with the help of diethyl phosphorochloridothionate. Both groups of compounds possess insecticidal properties and the activity of **VIIa** is as high as that of commercial phosphoric acid esters (Imidan, Dipterex).

As reported in our previous papers [1,2], the reaction of isoflavone with hydroxylamine, under various conditions affords almost exclusively 4-phenyl-5-(2-hydroxyphenyl)isoxazole (**IIIa**).

In the recent past several bactericidal and fungicidal hydroxyphenylisoxazole derivatives have been described, which were prepared from β-diketones and chalcones [3, 4].

In the present work we report on a study of substituent effects in the reaction of variously substituted isoflavones with hydroxylamine, and on the preparation of carbamic and phosphoric acid ester derivatives of the 4,5-diphenylisoxazoles obtained. Tests on the insecticidal effect of the latter derivatives are also reported.

Results and Discussion

Variously substituted derivatives (**Ib—n**) of isoflavone (**Ia**) were allowed to react with hydroxylamine. The reactions were conducted at pH 4—11 in aqueous alcohol; in the case of **In** dry methanol was used. Each isoflavone gave a 4,5-diphenylisoxazole (**III**) as the main product. In the case of isoflavones having no substituent at the C-2 position (**Ia—g**) a compound of presumably aldoxime structure (**II**) was also detected in the reaction mixture [5], which could be isolated in some cases by thin-layer chromatography. However, its ring closure to the corresponding isoxazole **III** was so rapid that, on alcoholic elution from the layer, only the isoxazole was obtained. The aldoxime character of **II** was concluded, besides its colour reaction, just from this rapid ring closure. Dioximes [6] were detected in the reaction mixture only in basic media.

The rate of the reaction **I**→**III** increases in proportion to the increase of pH. Nevertheless, the reactions effected in boiling aqueous ethanol at pH

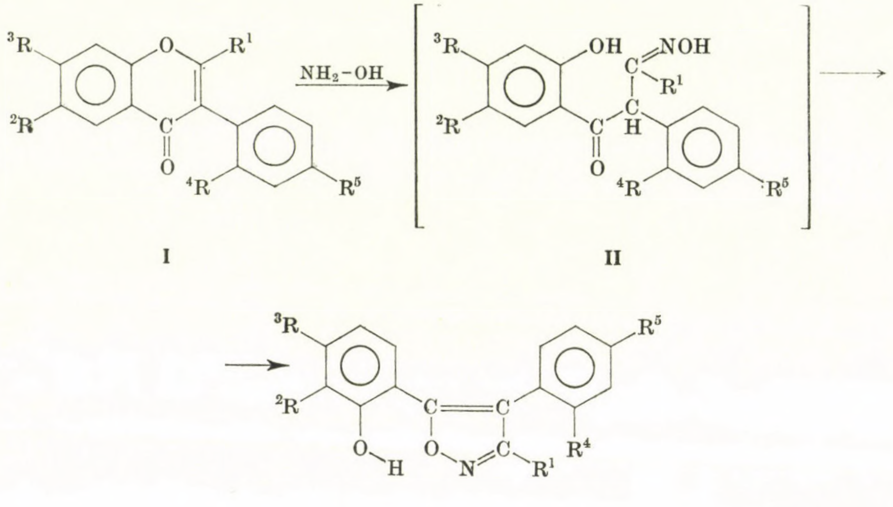

I II

III

I, II, III	R¹	R²	R³	R⁴	R⁵
a	H	H	H	H	H
b	H	CH_3	H	H	H
c	H	H	CH_3O	H	H
d	H	H	H	CH_3O	H
e	H	H	H	H	CH_3O
f	H	H	CH_3O	H	CH_3O
g	H	H	OH	H	NO_2
h	CH_3	H	H	H	H
i	CF_3	H	H	H	H
j	CH_3	CH_3	H	H	H
k	CH_3	H	CH_3O	H	H
l	CF_3	CH_3	H	H	H
m	CF_3	H	CH_3O	H	H
n	H	H	OH	H	H

Scheme 1

Table I

Characteristic parameters of the reaction **I** $\rightarrow$ **III** *and physical constants of the compounds formed*

Compound	Reaction time, h	Yield, %	M.p., °C	Analysis, N%		UV spectrum		IR spectrum cm^{-1}		NMR spectrum** (ppm)	
				Calcd.	Found	λ_{max} (nm)	log ε	C=N	OH	$\delta_{H(C\text{-}3)}$	δ_{OH}***
IIIa	3.0	92.8	163—4	5.90	5.84	263	4.03	1620	3420	9.12	10.17
b	6.0	77.7	171—2	5.57	5.58	265	4.09	1630	3210	9.06	9.84
c	8.5	71.2	163—4	5.24	5.35	276	3.90	1615	3150	9.07	10.19
d	2.0	82.4	127—9	5.24	5.24	291	3.83	1600	3160	8.86	10.00
e	4.0	82.0	155—7	5.24	5.20	279	3.96	1600	3170	9.06	10.15
f	7.5	70.5	184—6	4.71	4.81	279	3.96	1600	3170	8.93	10.09
g	0.5	87.2	331—2	9.39	9.20	257	4.05	1620	3150	9.14	6—9
h	>20	69.7	179—80	5.57	5.47	275	3.88	1630	3140	—	9.96
i	2.0	82.2	167—9	4.59	4.58	255	3.94	1625	3320	—	10.25
j	>20	82.0	191—3	5.28	5.25	257	3.96	1630	3140	—	9.66
k	>20	84.3	184—5	4.98	5.08	274	3.94	1625	3150	—	10
l	3.0	80.1	163—4	4.38	4.28	260	3.85	1625	3310	—	9.94
m	5.5	90.8	92—4	4.17	4.20	260	4.00	1615	3320	—	10.28
n*	7.0	71.1	185—6	5.53	5.39	280	3.84	1635	3310	8.98	9.91

* This compound was prepared in boiling *abs.* methanol in the presence of sodium acetate

** NMR spectra were measured in DMSO-d_6 solutions

*** These signals disappeared upon the addition of D_2O

8 were found the best and generally applicable, because at higher pH values the rate of undesirable reactions also increases [7, 1, 2].

The data in Table I show that substituents can greatly affect the rate of formation of **III**, but they do not alter the reaction course. At the same pH, the rate of reaction of isoflavones with hydroxylamine is determined by the stability of the γ-pyrone ring [8].

Owing to this effect, only 40—60% of the highly stable 2-methylisoflavones (**Ih, j, k**) could be converted into the corresponding isoxazoles (**IIIh, j, k**) even on boiling for 20 h at pH 8. These reactions were completed at pH 9, using an excess of the reagent.

The phenolic hydroxyl group in 7-hydroxyisoflavone stabilizes the molecule considerably [10]. As a consequence, under the described reaction conditions. We could not prepare the respective isoxazole from **In** with yield similar to other derivatives and without secondary products. This compound also failed to react in dry methanol, in the presence of hydrochloric acid catalyst [9].

However, when dry sodium acetate was added to the reaction mixture, the 4,5-diphenylisoxazole was obtained on boiling in a fairly good yield, corresponding to attack at the C-2 atom.

This latter method proved to be very efficient also for the conversion of the poorly reactive 2-methylisoflavones (**Ih, j, k**).

The NMR spectra of the isoxazoles (**IIIa—n**) supported not only the presence of the phenolic hydroxyl group but, with the exception of **IIIg**, the chemical shift value also showed the formation of a hydrogen-bonded chelate system.

The *O*-alkylcarbamoyl derivatives (**IV, V, VIa—i**) of the 4,5-diphenylisoxazoles **IIIa—c** and **IIIh—m** were prepared with a small excess of alkyl isocyanates (R^4 = methyl, ethyl, butyl) in benzene solution at room temperature, in the presence of a catalytic amount of triethylamine.

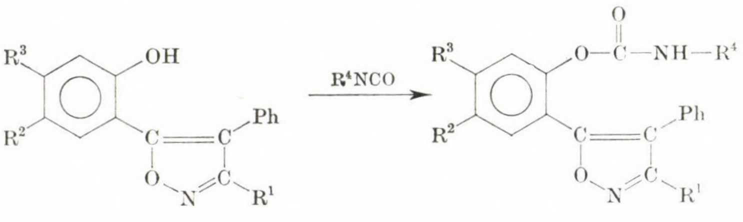

III a—c, h—m **IV, V, VI a—i**

Scheme 2

The results summarized in Table II show that under such circumstances the *O*-carbamates of the isoxazoles **IIIa—c, h—m** are formed generally in good yields. It can also be seen that the rate of carbamoylation is greatly influenced

Table II

Characteristic data of the carbamoylation reaction and of the compounds formed

	R^1	R^2	R^3	R^4	Reaction time, h	Yield %	M.p., °C	Analysis, N%	
								Calcd.	Found
IVa	H	H	H	CH_3	1.5	53	133—134	9.52	9.49
b	H	H	H	C_2H_5	6.0	77	81— 82	9.09	8.98
c	H	H	H	C_4H_9	12.0	47	109—111	8.33	8.25
d	CH_3	H	H	CH_3	2.0	75	140—142	9.09	9.13
e	CH_3	H	H	C_2H_5	10.0	83	113—115	8.69	8.71
f	CH_3	H	H	C_4H_9	20.0	89	83— 85	8.00	7.96
g	CF_3	H	H	CH_3	0.5	85	145—148	7.86	7.82
h	CF_3	H	H	C_2H_5	2.5	85	105—108	7.57	7.59
i	CF_3	H	H	C_4H_9	7.0	86	77— 78	7.03	7.11
Va	H	H	CH_3O	CH_3	2.0	82	125—127	8.72	8.64
b	H	H	CH_3O	C_2H_5	7.0	94	89— 90.5	8.35	8.38
c	H	H	CH_3O	C_4H_9	12.0	92	67— 68	7.71	7.65
d	CH_3	H	CH_3O	CH_3	16.0	83	144—145	8.35	8.41
e	CH_3	H	CH_3O	C_2H_5	48.0	69	133—135	8.02	8.11
f	CH_3	H	CH_3O	C_4H_9	71.0	67	57— 58	7.42	7.37
g	CF_3	H	CH_3O	CH_3	1.0	89	88— 90	7.31	7.26
h	CF_3	H	CH_3O	C_2H_5	5.0	97	60— 61	7.05	7.09
i	CF_3	H	CH_3O	C_4H_9	7.0	92	59— 60	6.58	6.46
VIa	H	CH_3	H	CH_3	1.0	89	128—129.5	9.09	9.13
b	H	CH_3	H	C_2H_5	1.5	83	115—116	8.33	8.26
c	H	CH_3	H	C_4H_9	2.5	73	94— 95	8.00	8.05
d	CH_3	CH_3	H	CH_3	12.0	82	151—153	8.69	8.61
e	CH_3	CH_3	H	C_2H_5	16.0	86	155—156	8.33	8.43
f	CH_3	CH_3	H	C_4H_9	24.0	83	73— 75	7.69	7.60
g	CF_3	CH_3	H	CH_3	0.25	85	74— 76	7.54	7.45
h	CF_3	CH_3	H	C_2H_5	1.0	87	109—110	7.27	7.30
i	CF_3	CH_3	H	C_4H_9	4.0	81	105—107	6.77	6.86

by the substituents R^1 and R^4. On the basis of the reaction times, the order of the reaction rates is $v_{CF_3} > v_H > v_{CH_3}$ for R^1, and $v_{Me} > v_{Et} > v_{Bu}$ for R^4.

Phosphoric acid ester derivatives of **IIIa, h, i** were synthesized with diethyl phosphorochloridothionate in chloroform at 40—50°, in the presence of pyridine.

Although the isoxazoles **III** reported herein do not possess considerable insecticidal effect, their phosphoric acid ester (**VII**) and some of the carbamoyl (**IV**) derivatives proved to be remarkable insecticides in the tests.

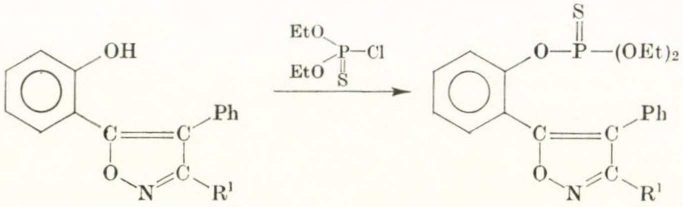

III a, h, i

VII a—c

Scheme 3

Table III

Characteristic data of the reaction **III** → **VII** *and of the compounds formed*

	R^1	Yield, %	M.p., °C	Analysis,			
				N%		P%	
				Calcd.	Found	Calcd.	Found
VIIa	H	74	151—153	3.60	3.50	7.96	7.86
b	CH_3	76	175—176	3.46	3.52	7.76	7.69
c	CF_3	54	155—157	3.09	3.14	6.85	6.92

Table IV

Mortality values for compounds **IV** *and* **VII** *in dried-bean beetle test*

Compound	Mortality, %		
	5 h	24 h	48 h
IVa	3	40	76
b	21	38	68
c	3	11	43
d	3	30	50
e	5	31	66
f	3	11	68
g	8	56	85
h	35	65	90
i	15	46	77
VII a	86	92	99
b	40	74	81
c	52	77	91
Imidan	98	98	100
Dipterex	60	89	98

The insecticidal activity of compounds **IVa–i** and **VIIa–c** was studied on dried-bean beetle *(Acanthoscelides obtectus)*, determining the mortality values at the ages of 5, 24 and 48 hours.

The data in Table IV show that most of the tested compounds had higher insecticidal activities than the acceptable 60% threshold value.

It is remarkable that in the group of the relatively less effective *O*-alkylcarbamates, the presence of a trifluoromethyl group enhances the activity. The *O*-diethylthiophosphoryl derivatives **VIIa–c** had outstanding activities. Compound **VIIa** and, in the 48-h test also **VIIc** and the *O*-carbamate **IVh**, had very good activity values, comparable with that of commercial phosphoric ester derivatives, such as Imidan (Safidon, *O,O*-dimethyl-*S*-phthalimidomethyl dithiophosphate) or Dipterex (*O,O*-dimethyl-2,2,2-trichloro-1-hydroxyethylphosphonate).

Experimental

The UV spectra were recorded on a UNICAM SP 800 spectrophotometer in ethanol solution, and the IR spectra on a PERKIN-ELMER 283 spectrophotometer in KBr pellets. ^{1}H-NMR spectra were obtained with a JEOL MH 100 spectrometer; chemical shifst are given in δ ppm (TMS internal reference).

Reactions were followed by TLC on Merck PF$_{254}$ DC-Alurolle. Reaction times were characterized by that moment when the starting material could no longer be detected by TLC.

M.p.'s are uncorrected.

Biological tests were conducted with 5 × 50 dried-bean beetles in Petri dishes, by the standard method.

General method for the preparation of 4,5-diphenylisoxazoles (IIIa–m)

Isoflavone or its derivative (**Ia–m**) (10 mmoles) was suspended in 80% aqueous ethanol (50 cm^3), then hydroxylamine hydrochloride (30 mmoles) and sodium acetate (30 mmoles) were added. The pH was adjusted to 8 (or to 9 in the case of **Ih, j, k**) with 2 *M* sodium hydroxide, and the mixture was refluxed until the spot of the starting material had disappeared in TLC. The solution was acidified (pH ~5) with hydrochloric acid, a part of ethanol was evaporated in vacuum, the precipitate was filtered off, washed with water until neutral and recrystallized from 80% ethanol.

The reaction conditions and physical constants are summarized in Table I.

Synthesis of 4-phenyl-5-(2,4-hydroxyphenyl)-isoxazole (IIIn)

A mixture of 7-hydroxyisoflavone (**In**) (0.476 g; 2.0 mmoles), dry sodium acetate (0.98 g), and dry methanol (20 ml) was refluxed for 7 h. The product was precipitated by the addition of water, filtered off, washed with water and recrystallized from 80% ethanol to yield 0.36 g of **IIIn** (71.1%), m.p. 185–186°.

UV: λ_{max}, nm: 280 (log ε 3.84), 299 (log ε 3.82).

IR: ν1635 (C=N), 3310 cm^{-1} (OH).

NMR (DMSO-d_6): δ 8.98 (s, 1 *H*, C^3–H); 9.91 (s, 2 H, 2 OH, disappearing on the addition of D$_2$O).

C$_{15}$H$_{11}$NO$_3$ (253.24). Calcd. N 5.53. Found N 5.39%.

General method of carbamoylation by means of isocyanates (IV, V, VIa–i)

The 4,5-diphenylisoxazole derivative (10 mmoles) was suspended in dry benzene (20 cm^3), then triethylamine (0.05 cm^3) and the appropriate alkyl isocyanate (11 mmoles) were added at room temperature, with stirring. After the completion of the reaction, the major part of the solvent was evaporated and the residue diluted with petroleum ether. The precipitated crystalline product was homogeneous. The reaction conditions and physical data of the products are listed in Table II.

General method of esterification by means of diethyl phosphorochloridothionate acid chloride (VIIa–c)

The 4,5-diphenylisoxazole derivative (10 mmoles) was dissolved in a mixture of chloroform (20 cm^3) and dry pyridine (11 mmoles), then diethyl phosphorochloridothionate (20 mmoles) was added, with continous stirring. At the end of the reaction the solution was extracted with water, the organic layer was dried (Na_2SO_4) and concentrated until crystallization of the product had started. The crystalline precipitate was removed by filtration and recrystallized from ethanol–petroleum ether mixture. Data of the products are summarized in Table III.

*

The authors are indebted to the North-Hungarian Chemical Works, personally to Mrs. J. Dudás and Mrs. J. Grega for making possible the biological test of the reported compounds. Thanks are due to Miss E. Theisz, Miss É. Vesza and Mrs. K. N. Vass for their valuable technical assistance and to Mr. J. Borbély for the recording and evaluation of the NMR spectra.

REFERENCES

[1] Szabó, V., Borda, J., Losonczi, L.: Magy. Kém. Folyóirat, **83**, 278 (1977)
[2] Szabó, V., Borda, J., Losonczi, L.: Acta Chim. Acad. Sci., Hung., **97**, 69 (1978)
[3] Murthy, A. K., Rao, K. S. R. K. M., Rao, N. V. S.: J. Ind. Chem. Soc., **50**, 213 (1973)
[4] Thakar, K. A., Muley, P. R.: Ind. J. Chem., Sect. B., **14**, 224 (1976)
[5] Szabó, V., Borda, J.: Acta Chim. Acad., Sci. Hung., **95**, 333 (1977)
[6] Szabó V., Borda, J., Végh, V.: Magy. Kém. Folyóirat, **83**, 434 (1977)
[7] Szabó, V., Zsuga, M.: Acta Chim. Acad. Sci. Hung., **85**, 179 (1975)
[8] Szabó, V., Zsuga, M.: Acta Chim. Acad. Sci. Hung., **97**, 451 (1978)
[9] Beugelmans, R., Morin, C.: Tetrahedron Lett., **1976**, 2145
[10] Szabó, V., Zsuga, M., Nemes, S.: Unpublished results

Jenő Borda
Vince Szabó
László Németh
H-4010, Debrecen 10.

György Bokor
North-Hungarian Chemical Works, Sajóbábony, Hungary

Acta Chimica Academiae Scientiarum Hungaricae, Tomus 104 (4), pp. 397—403 (1980)

A POSSIBILITY TO STUDY THE NONLINEAR BEHAVIOUR OF DIELECTRICS BY A.C. TECHNIQUE

L. MÉSZÁROS[1] and J. LISZI[2]*

([1] *Hungarian Academy of Sciences, Research Laboratory for Inorganic Chemistry, Budapest,* [2] *University of Veszprém Department of Analytical Chemistry, Veszprém*)

Received March 2, 1979
Accepted for publication October 12, 1979

A possibility is given to study the nonlinear dielectric behaviour by a.c. technique without the use of a high voltage impulse. Using an undistorted sinusoidal voltage with high amplitude, the nonlinear $E-\mathbf{D}$ characteristics of dielectrics result that the current passing through the measuring cell contains harmonic components, too. The third harmonic component seems to be useful to measure the nonlinear dielectric behaviour.

The nonlinear dielectric behaviour of liquids usually is studied by the pulse technique: a high field pulse is superimposed on a measuring cell which works as the frequency control capacity of an oscillator. The permittivity of the dielectrics changes because of the high field pulse and this change can be indicated by the frequency of the oscillator. The method was proposed by MALSCH [1] and GUNDERMANN [2]. Recently the measuring method developed by MAŁECKI [3] is used. BRADLEY and PARRY JONES [4], as well as BROWN, PARRY JONES and DAVIES [5] improved the technique, however, all these methods use the high field pulse.

In the present paper a measuring possibility without high field pulse is given, the nonlinear dielectric behaviour is indicated by alternating voltage.

The dielectric displacement in nonlinear dielectrics

The dielectric displacement vector (**D**) as a function of the field strength (E) is given by the modified [7] BOOTH-equation [6]:

$$\mathbf{D} = n^2E + A\sqrt{g}\left\{\operatorname{cth}\,(B\sqrt{g}\,E) - \frac{1}{B\sqrt{g}\,E}\right\}, \tag{1}$$

where g is the Kirkwood-factor. A and B contain the universal constants, the permanent dipole moment in gas phase (μ_g), the internal refractivity (n), the

---

* To whom correspondence should be addressed.

molar volume (V) and the temperature (T):

$$A = \frac{4\pi N_A \mu_g (n^2+2)}{3V}, \tag{2}$$

$$B = \frac{3\mu_g (n^2+2)}{6kT}, \tag{3}$$

where N_A is the Avogadro-number and k is the Boltzmann-constant.

Approximating the Langevin-function in eqn. (1) by its third order Taylor polynomial:

$$\mathbf{D} = n^2 E + \frac{AB}{3} gE - \frac{AB^3}{45} g^2 E^3. \tag{4}$$

Inserting the field dependent Kirkwood's g [7]

$$g = g_0 + g_1 E^2 \tag{5}$$

into eqn. (4):

$$\mathbf{D} = n^2 E + \frac{AB}{3} g_0 E + \left(\frac{AB}{3} g_1 - \frac{AB^3}{45} g_0^2\right) E^3. \tag{6}$$

The terms with higher order than three are neglected.

If a static and a superimposed sinusoidal field,

$$E = E_0 + E_1 \sin \omega t, \tag{7}$$

together act on the dielectrics where E_0 is the static field strength, E_1 is the amplitude of the alternating field, ω is the angular frequency, t is the time, then the dielectric displacement vector contains not only the stationary component ($\mathbf{D}_0$) and that of belonging to the ω angular frequency ($\mathbf{D}_1$), but as a result of the nonlinearity of the $\mathbf{D}-E$ characteristics the harmonic components corresponding to 2ω, 3ω also appear:

$$\mathbf{D} = \mathbf{D}_0 + \mathbf{D}_1 \sin \omega t + \mathbf{D}_2 \cos 2\omega t + \mathbf{D}_3 \sin 3\omega t, \tag{8}$$

where

$$\mathbf{D}_0 = \left(n^2 + \frac{AB}{3} g_0\right) E_0 + \left(\frac{AB}{3} g_1 - \frac{AB^3}{45} g_0^2\right)\left(E_0^3 + \frac{3}{2} E_0 E_1^2\right), \tag{9}$$

$$\mathbf{D}_1 = \left(n^2 + \frac{AB}{3} g_0\right) E_1 + \left(\frac{AB}{3} g_1 - \frac{AB^3}{45} g_0^2\right)\left(3E_0^2 E_1 + \frac{3}{4} E_1^3\right), \tag{10}$$

$$\mathbf{D}_2 = -\left(\frac{AB}{3} g_1 - \frac{AB^3}{45} g_0^2\right) 3E_0 E_1^2, \tag{11}$$

$$\mathbf{D}_3 = -\left(\frac{AB}{3} g_1 - \frac{AB^3}{45} g_0^2\right) \frac{E_1^3}{4}. \tag{12}$$

It can be seen that $\mathbf{D}_0$, $\mathbf{D}_1$ and $\mathbf{D}_2$ contain both E_0 and E_1, these components are determined by both the stationary and the alternating fields. $\mathbf{D}_3$ depends only on the alternating field, because in eqn. (6) we neglected the terms with higher order than three. Consequently, eqn. (12) is valid only if $E_0 = 0$, because using higher order Taylor polynomials, the terms containing E_0 also appear in the expression of $\mathbf{D}_3$. It is worthy to note that the nonlinearity is included in all the components of the dielectric displacement, even in the stationary and basic harmonic components. It is also interesting that the nonlinearity always is included in the terms containing $\left(\frac{AB}{3} g_1 - \frac{AB^3}{45} g_0^2\right)$.

Static and differential relative permittivity

The static relative permittivity, $\varepsilon = \mathbf{D}_0/E_0$, from eqn. (9) is

$$\varepsilon = n^2 + \frac{AB}{3} + \left(\frac{AB}{2} g_1 - \frac{AB^3}{45} g_0^2\right)\left(E_0^2 + \frac{3}{2} E_1^2\right) . \tag{13}$$

It is of some interest to see that the static and alternating field — except a factor of 3/2 — has analogous effect on the value of ε, that is the distortion in the nonlinear characteristics (like in the case of rectification) superimposes $3/2\, E_1^2$ on E_0^2, changes the work point of the dielectrics.

The differential relative permittivity at a given E_0 from eqn. (6) is

$$\varepsilon_{\mathrm{d}} = \frac{\partial D}{\partial E} = n^2 + \frac{AB}{3} g_0 + \left(\frac{AB}{3} g_1 - \frac{AB^3}{45} g_0^2\right) 3E_0^2. \tag{14}$$

Otherwise, using a.c. method with alternating field strength E_1, $\varepsilon_{\mathrm{dm}} = \mathbf{D}_1/E_1$, so from eqn. (10)

$$\varepsilon_{\mathrm{dm}} = n^2 + \frac{AB}{3} g_0 + \left(\frac{AB}{3} g_1 - \frac{AB^3}{45} g_0^2\right)\left(3E_0^2 + \frac{3}{4} E_1^2\right) . \tag{15}$$

It can be seen that using sufficiently high alternating field strength E_1, one should measure a value different from ε_{d}.

In limitation case

$$\varepsilon_{\mathrm{d}} = \lim_{E_1 \to 0} \varepsilon_{\mathrm{dm}}, \tag{16}$$

consequently, the differential relative permittivity can be measured only by small alternating measuring voltage. This experience gives a possibility for the experimental study of the nonlinear dielectric behaviour. Namely at constant E_0 from eqns. (14) and (15):

$$\varepsilon_{\mathrm{d}} - \varepsilon_{\mathrm{dm}} = \left(\frac{AB}{3} g_1 - \frac{AB^3}{45} g_0^2\right) \frac{3}{4} E_1^2 , \tag{17}$$

where ε_{d} and ε_{dm} are the relative permittivities measurable by small and high amplitude, respectively. For the application of eqn. (17) we note that

1. the effect is independent of the static field strength E_0, it arises even in the case of $E_0 = 0$, and depends only on the amplitude of the alternating field strength.

2. The measurement needs an oscillator which can supply oscillations of both small and high amplitudes. The change of capacity can be indicated by the change of the frequency as in the earlier measurements.

It is of some interest to note that measuring the change of relative permittivity in strong E_0 and weak ($E_0 = 0$) fields at constant E_1, eqn. (15) yields:

$$(\varepsilon_{\text{dm}})_{E_0} - (\varepsilon_{\text{dm}})_{E_0=0} = \left(\frac{AB}{3} g_1 - \frac{AB^3}{45} g_0^2\right) 3E_0^2 , \tag{18}$$

$$\frac{\Delta\varepsilon}{E_0^2} = ABg_1 - \frac{AB^3}{15} g_0^2 . \tag{19}$$

These eqns. show that if E_1 is constant when $\Delta\varepsilon/E_0^2$ is independent of E_1, so the alternating field may have any amplitude, consequently the earlier measuring methods are also valid in strong alternating fields.

Measuring possibilities by analysis of the harmonics of a.c.

The displacement current passing through the dielectrics under the effect of the alternating field is

$$\mathbf{j} = \frac{1}{4\pi} \frac{\partial \mathbf{D}}{\partial t} = \frac{1}{4\pi} (\mathbf{D}_1 \omega \cos \omega t - \mathbf{D}_2 2\omega \sin 2\omega t + \mathbf{D}_3 3\omega \cos 3t), \tag{20}$$

where t is the time. The displacement current density beside the basic harmonic contains the higher harmonics as well. The amplitude of the basic harmonic current density is

$$\hat{\mathbf{j}}_1 = \frac{\omega}{4\pi} |\mathbf{D}_1| = \frac{\omega}{4\pi} \left| \left(n^2 + \frac{AB}{3} g_0\right) E_1 + \left(\frac{AB}{3} g_1 - \frac{AB^3}{45} g_0^2\right) \times \right.$$

$$\left. \times \left(3E_0^2 E + \frac{3}{4} E_1^3\right) \right| = \frac{\omega}{4\pi} \varepsilon_{\text{dm}} \frac{U_1}{d} , \tag{21}$$

where U_1 is the amplitude of the alternating voltage on the measuring cell, d is the distance between the armatures of the measuring condensers. Eqn. (21) gives a possibility for the experimental study of the nonlinear dielectric behaviour, even in the case of $E_0 = 0$. One may measure selectively the amplitudes of the basic harmonics by small and high alternating voltage and from these two measurements the difference in $\frac{\hat{\mathbf{j}}}{E_1}$ is proportional with $\Delta\varepsilon$. However, this method is only a theoretical possibility, because the uncertain current measurements do not yield sufficiently correct results.

The amplitude of the second harmonics of the current density is:

$$\hat{\mathbf{j}}_2 = \frac{\omega}{2\pi}\,|\mathbf{D}_2| = \frac{3\omega}{2\pi}\left|\frac{AB}{3}g_1 - \frac{AB^3}{45}g_0^2\right| E_0 E_1^2 =$$

$$= \frac{3\omega}{2\pi}\left|\frac{AB}{3}g_1 - \frac{AB^3}{45}g_0^2\right| E_0 \frac{U_1^2}{d^2}\,. \tag{22}$$

The experimental study of the nonlinear dielectric behaviour on the basis of the second harmonics is only possible if $E_0 \neq 0$. It is a natural consequence of the fact that the $\mathbf{D} - E$ characteristics is an odd function. In the application of the second harmonics, like in the earlier methods, one has to use a pulse of high amplitude. The only difference is that one should measure the current instead of the change in frequency. Note, that this method does not need the measuring capacity built in the oscillator circuit, an independent supply can also be used.

The amplitude of the third harmonics of the current density is

$$\hat{\mathbf{j}}_3 = \frac{3\omega}{4\pi}\,|\mathbf{D}_3| = \frac{3\omega}{16\pi}\left|\frac{AB}{3}g_1 - \frac{AB^3}{45}g_0^2\right| E_1^3 =$$

$$= \frac{3\omega}{16\pi}\left|\frac{AB}{3}g_1 - \frac{AB^3}{45}g_0^2\right| \frac{U_1^3}{d^3}\,, \tag{23}$$

from which the term giving the nonlinearity:

$$\left|\frac{AB}{3}g_1 - \frac{AB^3}{45}g_0^2\right| = \frac{16\pi\, d^2\, \hat{\mathbf{j}}_3}{3\omega\, U_1^3}\,. \tag{24}$$

Comparing this last term with eqn. (19) we see that the left side of eqn. (24) is three times $\Delta\varepsilon/E_0^2$:

$$\left|\frac{\Delta\varepsilon}{E_0^2}\right| = \left|AB\,g_1 - \frac{AB^3}{15}g_0^2\right| = \frac{16\pi\, d^3\, \hat{\mathbf{j}}_3}{\omega\, U_1^3}\,. \tag{25}$$

Consequently, the experimental study of the nonlinear dielectric behaviour can be carried out by the selective measurement of the third harmonic component of the a.c. passing through the cell, moreover, this can be done by a simple measuring technique, without a high field pulse.

Eqns. (21)—(25) contain the amplitudes of the harmonic components of the current density, which are always positive quantities, therefore absolute values are used in the expressions cited above. However, in this way one can not distinguish between the normal and anomalous dielectric saturations. If the harmonic components of the alternating current are measured by a phase-sensitive instrument, then the angle of the phase should show the sign. Namely, in the case of

a, normal dielectric saturation:

$$\frac{\Delta\varepsilon}{E_0^2} = \left(AB\,g_1 - \frac{AB^3}{15}\,g_0^2\right) = -\frac{16\pi\,d^3}{\omega\,U_1^3}\,\hat{j}_3\,, \tag{26}$$

b, anomalous dielectric saturation:

$$\frac{\Delta\varepsilon}{E_0^2} = \left(AB\,g_1 - \frac{AB^3}{15}\,g_0^2\right) = \frac{16\pi\,d^3}{\omega\,U_1^3}\,\hat{j}_3\,. \tag{27}$$

Technical problems

As we have seen above the measurement of the third harmonic component of the current density gives a new experimental possibility for the study of the nonlinear dielectric behaviour. However, we note some technical problems, namely

1. the measurements require a sine wave generator of high output voltage and very low distortion, otherwise, the distortion of the generator (mainly its third harmonic distortion) can disturb the third harmonic component caused by nonlinear dielectric behaviour. This difficulty can be eliminated by the use of an intermodulation technique, what about we are going to report soon.

2. A further problem is caused by the impedance of the interface between the liquid and the electrodes of the measuring cell [8]. Namely, at the interface an electric double layer arises and so electrochemical reaction may take place. At a given frequency electrically the interface is equivalent with a parallel $R-C$ circuit. The electric equivalent circuit of the measuring cell is given in Fig. 1, where C_e and R_e with indices 1 and 2 refer to the interfaces, C and R belong to the dielectric liquid. It can be seen that a part of the measuring voltage drops on the two interfacial impedances. (In Fig. 1 U is voltage, the indices have the same meaning as earlier.) The double layer capacity and the current-voltage characteristics of the Faraday impedance of the electrode process are

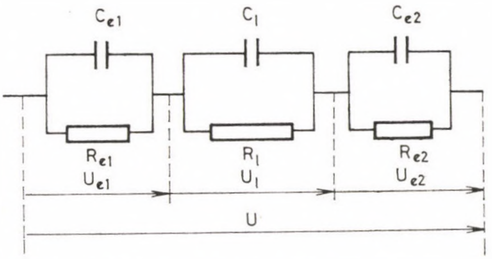

Fig. 1. The electric equivalent circuit of the measuring cell

nonlinear, thus these circuit elements cause a harmonic distortion which can disturb the effect of the nonlinear dielectric behaviour. This disturbing effect can be decreased by the decrease of the interfacial impedances. The increase of the effective electrode surfaces is a simple way of the decrease of the interfacial impedances. (A similar method is used in the conductivity cells via platinum black.)

3. Another problem may be caused by a possible nonlinearity of the ohmic conductivity of the dielectrics. This question requires further investigations.

We note that these last two disturbing effects can also take place in the earlier measuring methods.

REFERENCES

[1] Malsch, J.: Ann. Phys. (Leipzig), **84**, 841 (1927); Phys. Z., **29**, 770 (1928); **30**, **837** (1929)
[2] Gundermann, H.: Ann. Phys. (Leipzig), **6**, 545 (1930)
[3] Małecki, J.: Acta Phys. Polonica, **XXI**, **13** (1962), J. Chem. Phys., **36**, 2144 (1962)
[4] Bradley, P. A., Parry Jones, G.: J. Phys. E., **7**, 449 (1974)
[5] Brown, B. L., Parry Jones, G., Davies, M.: J. Phys. D, **7**, 1192 (1974)
[6] Booth, F.: J. Chem. Phys., **19**, 391 (1951)
[7] Liszi, J., Mészáros, L., Ruff, I.: Acta Chim. Acad. Sci. Hung. (In press)
[8] Yeager, E., Salind, A. J.: Techniques of Electrochemistry, V. 1. Wiley-Interscience, New York, 1972

Lajos Mészáros H-1112 Budapest, Budaörsi út 45.
János Liszi H-8201 Veszprém, P.O. Box 28.

Acta Chimica Academiae Scientiarum Hungaricae, Tomus 104 (4), pp. 405—415 (1980)

DIGITAL SIMULATION MODEL OF THE ROTATING RING-DISC ELECTRODE, I

J. Farkas[1], L. Kiss[1], A. Fóthi[2] and J. Házi[1]

([1] *Department of Physical Chemistry and Radiology, L. Eötvös University, Budapest and* [2]*Department of Numerical and Computer Mathematics, L. Eötvös University, Budapest*)

Received June 18, 1979
Accepted for publication October 12, 1979

A digital simulation model of the rotating ring-disc electrode has been developed. The model permits to take into consideration homogeneous chemical reactions, and the inhomogenities of the disc electrode.

The rotating ring-disc electrode is suitable also to study the mechanism of electrochemical reactions [1, 2, 3]. For the elucidation of quantitative relationships an as exact as possible description of the system is needed. In the case of the rotating ring-disc electrode this is considerably facilitated by the fact that hydrodynamical conditions are simple and their mathematical description is essentially known [4]. Nevertheless, there are still many problems, the theory of which is incomplete or had not been yet discussed (*e.g.* when chemical reactions take place in homogeneous solution when the surface of the disc electrode is inhomogeneous; *etc.*). The solutions of such problems, if they exist at all, are very complicated relationship difficult to handle, so that digital simulation systems find increasing application [2, 5, 6, 7, 8, 9, 10].

Digital simulation methods gained ground in chemical kinetics on the basis of the works of Feldberg [11, 12]. The digital simulation model of the rotating ring-disc electrode has been developed first by Prater and Bard [5, 6, 7]. In the formulation of the simulation system it has been accepted as initial condition that concentration distribution in the space below the disc electrode is independent of the radius [1, 2], so that no radial division was made in the space below the disc electrode. In order to reduce computation time, correction factors were introduced which are difficult to justify. Of the series expansion forms of the flow-rate factors used in the calculations only the first terms were taken into consideration, and thus calculated liquid volumes flowing into and out of the single cells are not identical (as if the liquid would not be incompressible).

In the following a digital simulation model will be described, which eliminates the above shortcomings without a substantial change in computation time. More fully:

a) the space below the disc electrode is not considered as a single cell here radial division is also applied (as different from [5, 6, 7]).

b) non-equidistant division is used,

c) algorithms are used, which provide even without correction factors at a relatively low number of steps satisfactory accuracy.

For the deriving of the simulation algorithm, the process investigated is divided into elementary parts considered homogeneous in space and time. Owing to the cylindrical symmetry, in the case of the rotating ring-disc electrode concentration distribution in space is a function of two variables (Y the distance measured from the surface, R the distance measured from the axis of rotation), so that the solution space is divided according to two variables (Fig. 1). With planes parallel to the surface the solution space is divided into layers. The thickness of the I-th layer from the surface is marked with $DY(I)$, the distance of the I-th plane from the surface with $Y(I)$. The layers obtained in this way are further divided by cylinders, the symmetry axis of which is the axis of rotation [the radius is marked with $R(J)$]. The cylindrical rings obtained in this way are called cells. The J-th ring calculated from the rotational axis of the I-th layer is the I, J-th cell of the solution space. Each cell is bordered by four surfaces (Fig. 2): the internal cylinder surface $F1$, the lower annulus $F2$, the external cylinder surface $F3$ and the upper annulus $F4$. The $F2$ and $F4$ surfaces of each cell are of identical magnitude. The $F1$ surface of the I, 1-th cell is zero. The heights $DY(I)$ and the widths $DR(J)$ of the various cells may by different (as contrary to [5]).

The concentration of a substance A in the I, J-th cell can be considered as homogeneous (if suitably small $DY(I)$ and $DR(J)$ values were selected), and is marked with $A(I, J)$. Thus, the concentration distribution in space of the substance A can be represented by a two-dimensional matrix. In the further, the geometrical data (surfaces, volume, *etc.*) of the single cells will be needed. The surfaces, volume, *etc.* of the I, J-th cell can be obtained in knowledge of $Y(I)$ and $R(J)$ values by elementary calculation:

$$F1(I, J) = DY(I)2\pi R(J-1) \tag{1}$$

$$F3(I, J) = DY(I)2\pi R(J) \tag{2}$$

$$F2(I, J) = F4(I, J) = \pi[R(J)^2 - R(J-1)^2] =$$

$$= \pi DR(J)[R(J-1) + R(J)] \tag{3}$$

and

$$V(I, J) = F2(I, J)DY(I). \tag{4}$$

After the clearing of geometrical conditions, processes proceeding in the system will be investigated. The single processes are divided into such small Δt time intervals, during which the concentrations do not substantially change. Concentration can change in a cell, because:

1. material passes through its surfaces,
2. chemical reaction (homogeneous) takes place in the cell.

From the aspect of material passage the surfaces limiting the space investigated (not of necessity the whole solution space) play a distinct role. Material can pass through the cell surfaces because of liquid flow (convection), molecular diffusion and migration. (In the further, migration will not be taken into consideration.*) Electrochemical reactions and heterogeneous reactions, which can also cause changes in concentration, proceed at the cell surfaces in contact with the electrode surfaces. Concentration changes caused by molecular diffusion can be taken into account by difference approximation analogous to Fick's first law. According to the approximation, moles passing in time Δt through the surfaces of the I, J-th cell:

$$DN1\,(I,J) = \frac{F1\,(I,J)\,D_{\mathrm{A}}[\mathrm{A}(I,J-1) - \mathrm{A}\,(I,J)]\;2\Delta t}{DR\,(J-1) + DR\,(J)} \tag{5}$$

$$DN2\,(I,J) = \frac{F2\,(I,J)\,D_{\mathrm{A}}[\mathrm{A}\,(I+1,J) - \mathrm{A}(I,J)]\,2\Delta t}{DY(I+1) + DY(I)} \tag{6}$$

$$DN3\,(I,J) = \frac{F3\,(I,J)\,D_{\mathrm{A}}[\mathrm{A}(I,J+1) - \mathrm{A}(I,J)]\,2\Delta t}{DR(J+1) + DR(J)} \tag{7}$$

$$DN4\,(I,J) = \frac{F4\,(I,J)\,D_{\mathrm{A}}[\mathrm{A}(I-1,J) - \mathrm{A}\,(I,J)]\,2\Delta t}{DY(I-1) + DY(I)} \tag{8}$$

where D_{A} is the diffusion coefficient of substance A. A $(I, 0)$ is according to definition A $(I, 1)$.

Change in concentration caused by diffusion is:

$$D\mathrm{A}\,(I,J) = \frac{DN1\,(I,J) + DN2\,(I,J) + DN3\,(I,J) + DN4(I,J)}{V\,(I,J)}\,. \tag{9}$$

When a too high Δt value is selected, difference approximation may result negative concentrations. This can be avoided if:

$$\Delta t < \frac{0.5\,\Delta^2}{D_{\mathrm{A}}} \tag{10}$$

where:

$$\Delta^2 = \min\,[DR(J) \cdot DY(I)]\,. \tag{11}$$

At the $F4(1, J)$ surface of the cells adhering to the electrode surface. relationship (8) can not be used for the calculations, since here direct material transfer takes place because of the electrochemical and other heterogeneous reaction. Let us investigate by way of example a single metal dissolution:

$$\mathrm{M} \underset{k_{\mathrm{k}}}{\overset{k_{\mathrm{a}}}{\rightleftharpoons}} \mathrm{M}^{z+} + z\mathrm{e}^- \tag{I}$$

---

* The high foreign ion concentration used in electrochemical kinetic investigations suppresses migration.

where let the ion M^{z+} be substance A, k_a and k_k are rate constants dependent also on the electrode potential (13) and z is the change in charge number. It can be written for Eq. (I):

$$DN4\,(1,J) = \left[F4\,(1,J)\frac{k_a}{zF} - F4\,(1,J)\frac{k_k}{zF}\,\mathrm{A}\,(1,J)\right]\Delta t \qquad (12)$$

where F is the Faraday number.

For cases more complicated than reaction (I), Eq. (12) becomes also more complicated (*e.g.* the concentrations of other dissolved components must be taken into account, *etc.*).

Current strength flowing through surface $F4$ of the $1, J$-th cell can also be calculated:

$$I_D\,(1,J) = zF\,\frac{DN4\,(1,J)}{\Delta t}\,. \qquad (13)$$

The current strength I_D of the disc electrode is obtained from (13) by summation for all those J values, for which (Fig. 1):

$$R(I,J) \geq R1 > R(I,J-1)\,. \qquad (14)$$

Since for each single cell different rate constants can be given, this permits also the simulation of inhomogeneous disc surfaces. It follows from this that it is sufficient to assume for the cells below the sealing ring that here each rate constant is zero [there is no material transfer at the surfaces $F4(1, J)$]. In the same way, discretional rate constants can be given at the ring electrode; if, *e.g.* the limiting current of the M^{z+} ions formed in reaction (I) is to be calculated, extra high k_k values are given. The current of the ring electrode can be calculated on the analogy of expression (13). In the measurement of limiting current a different mode of calculation can also be used (namely all the substance reaching the electrode undergoes reaction):

$$I_R(1,J) = zFV(1,J)\,\mathrm{A}\,(1,J)/\Delta t\,. \qquad (15)$$

The total current of the ring electrode can be calculated likewise by summation over the whole electrode surface.

Change in concentration caused by solution flow can be calculated when the flow velocity vector is known. The components of the velocity vector according to cylindrical coordinates are known (4) in series expansion form, the small Y values near the electrode in polynomial form, the large Y values, far from the electrode in the form of exponential series [1, 2].

For small Y values:

$$VY = -0.51\,\omega^{3/2}\,\nu^{-1/2}Y^2 + 1/3\omega^2\,\nu^{-1}Y^3 \ldots \qquad (16)$$

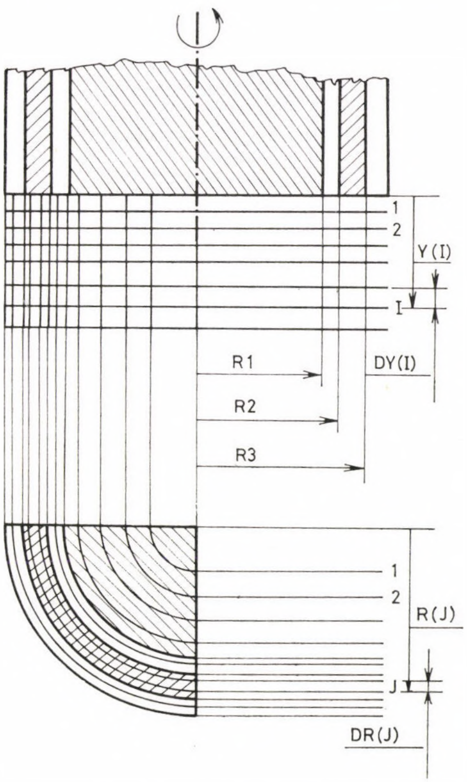

Fig. 1. **Division of the space below the rotating ring-disc electrode. *R*1: radius of the disc electrode; *R*2: internal radius of the ring electrode; *R*3: external radius of the ring electrode**

where ω is the angular velocity of the rotating electrode and ν the kinematic viscosity.

For large Y values:

$$VY = \omega^{1/2}\,\nu^{1/2}\Big[-\alpha + \frac{2a}{\alpha}\exp\left(-\alpha\,\omega^{1/2}\,\nu^{1/2}\,Y\right) - \\ - \frac{a^2+b^2}{2\alpha^3}\exp\left(-2\alpha\omega^{1/2}\nu^{-1/2}Y\right)\,\ldots\Big] \tag{17}$$

where α, a and b are constants [1].

In Fig. 3 the VY velocity component perpendicular to the electrode surface has been plotted. It will be noted that the first term of the polynomial expansion gives only up to very small Y values a good approximation. If only this first term is taken into consideration, a concentration distribution depending on the radius is obtained in the space below the disc electrode (Fig. 4). The consideration of two terms of the series expansion proved to be of suf-

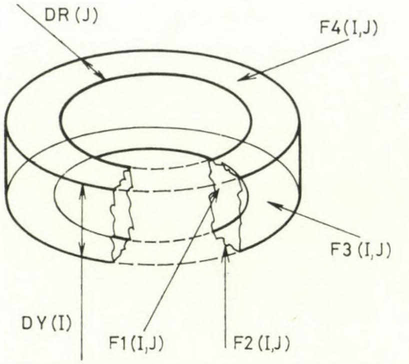

Fig. 2. Schematic diagram of a cell. $DR(J)$: width of the cell; $DY(I)$: height of the cell; $F1(I, J)$: internal cylinder surface; $F2(I, J)$: surface of the lower annulus; $F3(I, J)$: external cylinder surface; $F4(I, J)$: surface of the upper annulus

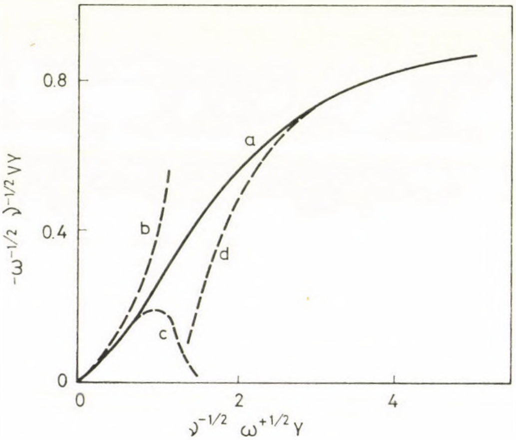

Fig. 3. The flow velocity component perpendicular to the surface as a function of the distance from the surface; a) theoretical curve [1, 2, 3, 4]; b) calculated on the basis of the first term of Eq. (16); c) calculated according to Eq. (16); d) calculated according to Eq. (17)

ficient accuracy, so that formula (16) was used for the calculations. The values of the velocity component VR were not needed, because considering the liquid as incompressible (presuming identical in- and outflowing volumes), volumes in- and outflowing at all four surfaces of the single cells can be calculated. The course of calculation is the following: the $F1$ surface of the I, 1-th cell is zero (Fig. 1), thus there is neither inflow nor outflow here. Inflow at surface $F2$ and outflow at surface $F4$ can be calculated in knowledge of VY.

$$DV2(I, 1) = F2(I, 1)\,VY(I)\,\Delta t\,. \tag{18}$$

This liquid volume brings from the cell below it $DN2\ (I, 1)$ mole of substance:

$$DN2(I, 1) = DV2(I, 1)\ \mathrm{A}\ (I + 1, 1)\,. \tag{19}$$

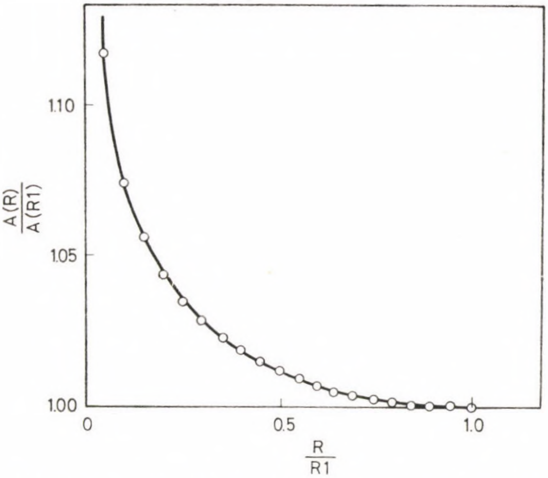

Fig. 4. Relative concentration distribution in the space below the disc electrode, when only the first term of Eq. (16) is taken into consideration

The liquid volume leaving the cell at surface $F4$ is:

$$DV4(I, 1) = F4(I, 1)\ VY(I-1)\ \Delta t\,. \tag{20}$$

The number of leaving moles is:

$$DN4(I, 1) = DV4\ (I, 1)\ \mathrm{A}\ (I, 1)\,. \tag{21}$$

The difference in volume entering at surface $F2$ and leaving at surface $F4$ leaves the cell at surface $F3$:

$$DV3(I, 1) = DV2(I, 1) - DV4(I, 1)\,. \tag{22}$$

The number of moles carried away is:

$$DN3(I, 1) = DV3(I, 1)\mathrm{A}(I, 1)\,. \tag{23}$$

Thus, the change in concentration caused by convection in the I, 1-th cell is:

$$D\mathrm{A}\,(I, 1) = \frac{DN2\,(I, 1) - DN3\,(I, 1) - DN4\,(I, 1)}{V\,(I, 1)}\,. \tag{24}$$

Calculations can be performed also in the next I, 2 cell, because the

$$F3\,(I, 1) = F1\,(I, 2) \tag{25}$$

surfaces are identical, and hence:

$$DV3(I, 1) = DV1(I, 2) \tag{26}$$

$$DN3(I, 1) = DN1(I, 2)\,. \tag{27}$$

In the further cells calculation is analogous to the above.

Changes in concentration caused by homogeneous chemical reactions will be discussed only for the cases of (quasi) first order and pure second order important in the anodic dissolution of metals (naturally, the model can be rewritten also for other cases).

In reactions of first and second order (similarly as in the case of molecular diffusion) a difference approach of the kinetic equations was used:

$$DA\ (I, J) = -k_1 A(I, J)\ \Delta t \tag{28}$$

and

$$DA\ (I, J) = -k_2 A(I, J)^2\ \Delta t \tag{29}$$

The difference approaches (28) and (29), particularly at high k_1 and k_2 rate constants, may result negative concentrations if the value selected for Δt is not very small. To reduce computation time, we started instead of expressions (28 and (29) from the integral form of the kinetic equations:

$$DA\ (I, J) = A\ (I, J)[1 - \exp\,(-k_1 \Delta t)] \tag{30}$$

$$DA\ (I, J) = \frac{A\,(I, J)}{1 + \dfrac{1}{A\,(I, J)\,k_2\,\Delta t}}\,. \tag{31}$$

The use of very small Δt values (and thus, of a very large number of steps) can be avoided in this way even in the case of high rate constants. (Eqs. (30) and (31) are not approximations!)

By the performance of the above algorithms, the total change in concentration in the single cells during the time Δt, during the time Δt, and the **A**(I, J) matrix modified with this value are obtained. On repeating L-times thw whole procedure, the matrix **A**(I, J) will represent already the concentration distribution at time

$$t = t_0 + L\Delta t\,. \tag{32}$$

If max $DR(J) \rightarrow 0$, max $DY(I) \rightarrow 0$ and $\Delta t \rightarrow 0$, the process is accurately described by the procedure (during a calculation process of infinite length). To reduce the computation time, PRATER and BARD [5] introduced so called correction factors. The justification of their use was the finding that in this way the results after 50 iteration steps are the same as those obtained in

1000 iteration steps without the use of the correction factors. The correction factors can be conceptualized as if the rate components *VR* and *VY* had been increased by 3% and 11%, respectively, however, this means an arbitrary changing of the physical system, upon which the model is based.

A reduction of computation time is essential, but incorrect results may be obtained, when a too large value is selected for Δt. This danger is particularly imminent, if the second derivative by time of some characteristics of the system is large.

Any characteristics of the system is an f(t) function of the time t. During simulation, the values of the f(t) function are generated. The method is analogous to Euler's method used in the numerical solution of differential equation [14], essentially the value

$$\mathrm{f}(t_0 + \Delta t) = \mathrm{f}(t_0) + \Delta t[\mathrm{f}'(t_0)] \tag{33}$$

is considered as the new value of function after time Δt. An improved form of the Euler method is also known [41]. Here, the formula

$$\mathrm{f}(t + \Delta t) = \mathrm{f}(t_0) + \mathrm{f}'\left(t_0 + \frac{\Delta t}{2}\right)\frac{\Delta t}{2} + \mathrm{f}'(t_0)\cdot\frac{\Delta t}{2} + \\ + \frac{1}{3} \times \left[\mathrm{f}'(t_0)\,\frac{\Delta t}{2} + \mathrm{f}'\left(t_0 + \frac{\Delta t}{2}\right)\frac{\Delta t}{2} - \mathrm{f}'(t_0)\,\Delta t\right] \tag{34}$$

is used for calculation. The error of formula (34) is proportional to $(\Delta t)^2$, while that of formula (33) to Δt. This modified process was used also in the simulation model. Fig. 5 shows for comparison the results obtained with the two methods

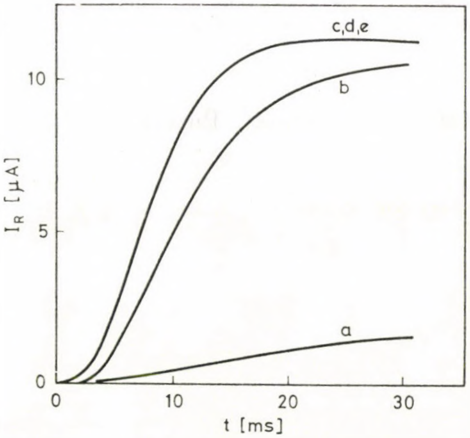

Fig. 5. Time-dependence of the limiting current calculated at the ring electrode, when the disc electrode is switched on galvanostatically, at various Δt values ($\omega = 100$/s; $k_a = 10^{-5}$ A cm^{-2}; $k_k = 0$; $k_1 = 500$/s). a) $t = 2 \cdot 10^{-3}$ s [according to Eq. (33)]; b) $t = 2 \cdot 10^{-4}$ s [according to Eq. (33)]; c) $t = 2 \cdot 10^{-5}$ s [according to Eq. (33)]; d) $t = 2 \cdot 10^{-6}$ s [according to Eq. (33)]; e) $t = 2 \cdot 10^{-4}$ s [according to Eq. (34)]

at various Δt values. As can be noted, when using the modified method a Δt step interval larger by about an order of magnitude can be selected.

It has been already mentioned in the discussion of geometrical division that the division used is not of necessity equidistanced.

Since changes in concentration are the greatest in the immediate vicinity of the electrode, when a sufficiently small thickness is selected for the surface cells DY (1), the other $DY(I)$ thicknesses can be already larger (thus, an adequate accuracy can be achieved with a small number of divisions). With the method used, 30—100 iteration steps furnish sufficiently accurate results. Thus, calculation time remained the same as in the method of PRATER and BARD [5], while the physical picture had not to be changed and the number of cells could also be reduced.

REFERENCES

[1] LEVICS, V. G.: Fiziko-himicheskaya gidrodinamika Fizmatgiz. Moscow 1959

[2] ALBERY, V. J., HITCHMAN, M. L.: Ring-disc Electrodes. Oxford University Press. London 1971

[3] PLESZKOV, JU. V., FILINOVSZKIJ, V. YU.: Vrasajusijsya diskovüy electrod. Izdatyelsztvo Nauka. Moscow 1972

[4] KÁRMÁN, T.: Z. angew. Mat. Mech., **1921**, 1244

[5] PRATER, K. B., BARD, A. J.: J. Am. Chem. Soc., **117**, 207 (1970)

[6] PRATER, K. B., BARD, A. J.: J. Am. Chem. Soc., **117**, 335 (1970)

[7] PRATER, K. B., BARD, A. J.: J. Am. Chem. Soc., **117**, 1515 (1970)

[8] MATTSON, J. S., MARK, H. B., MACDONALS, H. C.: Computers in Chemistry. Vol. **2**, Marcel Dekker, New York 1972

[9] MALOY, J. T., PRATER, K. B., BARD, A. J.: J. Am. Chem. Soc., **93**, 5959 (1971)

[10] MARGARIT, J., LEVY, M.: J. Electronal. Chem., **49**, 369 (1974)

[11] FELDBERG, S. W., AUERBACH, C.: Anal. Chem., **36**, 505 (1964)

[12] FELDBERG, S. W. Electroanalytical Chemistry Vol. **3**, Band **1**. Marcel Dekker, New York 1968

[13] KISS, L., FARKAS, J., FÓTHI, Á.: Acta Chim. Acad. Sci. Hung., **82**, 153 (1974)

[14] COLLATZ, L.: Közönséges differenciálegyenletek numerikus megoldása (Numerical solution of common differential equations), Akadémiai Kiadó 1960

József FARKAS
László KISS } H-1088 Budapest, Puskin u. 11—13.
Jenő HÁZI

Ákos FÓTHI H-1088 Budapest Múzeum krt. 6-8.

Acta Chimica Academiae Scientiarum Hungaricae, Tomus 104 (4), pp. 415–419 (1980)

ISOLATION AND IDENTIFICATION OF PARAFFINIC HYDROCARBONS FROM BULGARIAN OIL SHALES USING GAS CHROMATOGRAPHY AND MASS SPECTROMETRY

G. Kovachev

(Laboratory of Organic Geochemistry, Geological Institute, Bulgarian Academy of Science, Sofia)

Received June 28, 1979
Accepted for publication November 1, 1979

In connection with prospecting for oil shales in Bulgaria, we investigated the chemical composition of organic matter extracted from sediment samples. Using gas chromatography, a homologous series in the $C_{13}-C_{34}$ range-with maxima at C_{17} and C_{27} was obtained. With the combined method of gas chromatography and mass spectrometry, isoprenoid structures C_{15}, C_{16}, C_{18}, C_{19} and C_{20} were identified.

Introduction

The necessity of identification and investigation of paraffinic hydrocarbons isolated from the organic matter of sedimentary rocks, is determined by the fact that they refer to the so-called „biological features". When the "features" are known, the way of formation of the organic matter, its migration and conversion from one structure into another can be traced.

Besides that, paraffinic hydrocarbons are structures which have a very high chemical stability and have remained unchanged during the geological periods, carrying information inherited from the initial organic matter. On the basis of this information and comparison of the isolated hydrocarbon structures, one can form a more clear idea about the processes that occurred millions of years before. All these processes are connected with the formation and accumulation of organic matter on earth.

This paper presents an analysis of saturated hydrocarbons isolated from the organic matter of Bulgarian oil shales.

Results and Discussion

n-Alkanes

The chromatograms of the fractions treated with 5 Å molecular sieves show the homologous series of n-alkanes from C_{13} to C_{34} with two maxima, one at C_{17}, and the other at C_{27}. It is interesting to mention that the odd/even ratio calculated from the presentage of individual homologues shows a strong predominance of the odd homologues over the even ones (Fig. 1).

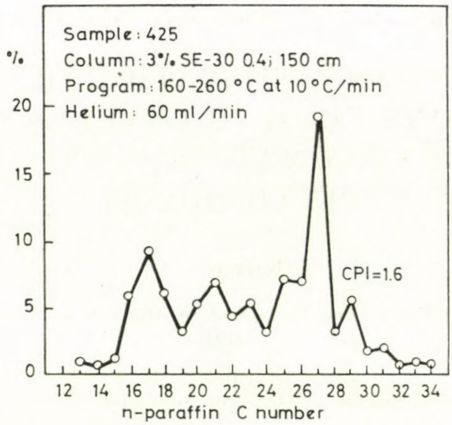

Fig. 1. Diagram of *n*-alkane distribution

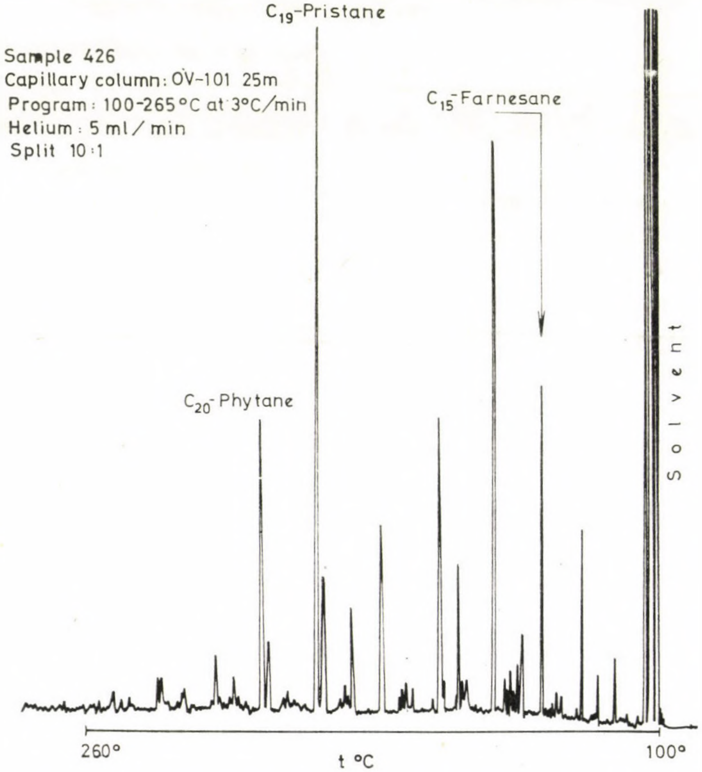

Fig. 2. Capillary chromatogram of the "non adduct" fraction

Isoprenoid alkanes

From the "non-adduct" fraction [7], using the combined methods of gas chromatography and mass spectrometry, the isoprenoid structures C_{15}, C_{16}, C_{18}, C_{19} and C_{20} were identified on the basis of the characteristic features of their spectra. The typical fragments $[C_8H_{17}]^+$ — 113, $[C_{13}H_{27}]^+$ — 183 and $[C_{18}H_{37}]^+$ — 253, present in the mass spectra, determine the structure of chains where the 2, 6, 10 and 2, 6, 10, 14 sites are replaced. The values of m/e 127, 141, 169, 183 and 197 correspond to the CH_3 group located at each fifth carbon atom [8]. On the basis of the mass spectra so obtained and their similarity to the isoprenoid spectra published earlier [3], the structures C_{15}, C_{16} and C_{18} were identified as 2,6,10-trimethyldodecane(farnesane), 2,6,10-trimethyltridecane and 2,6,10-trimethylpentadecane. The hydrocarbons C_{19} and C_{20} were

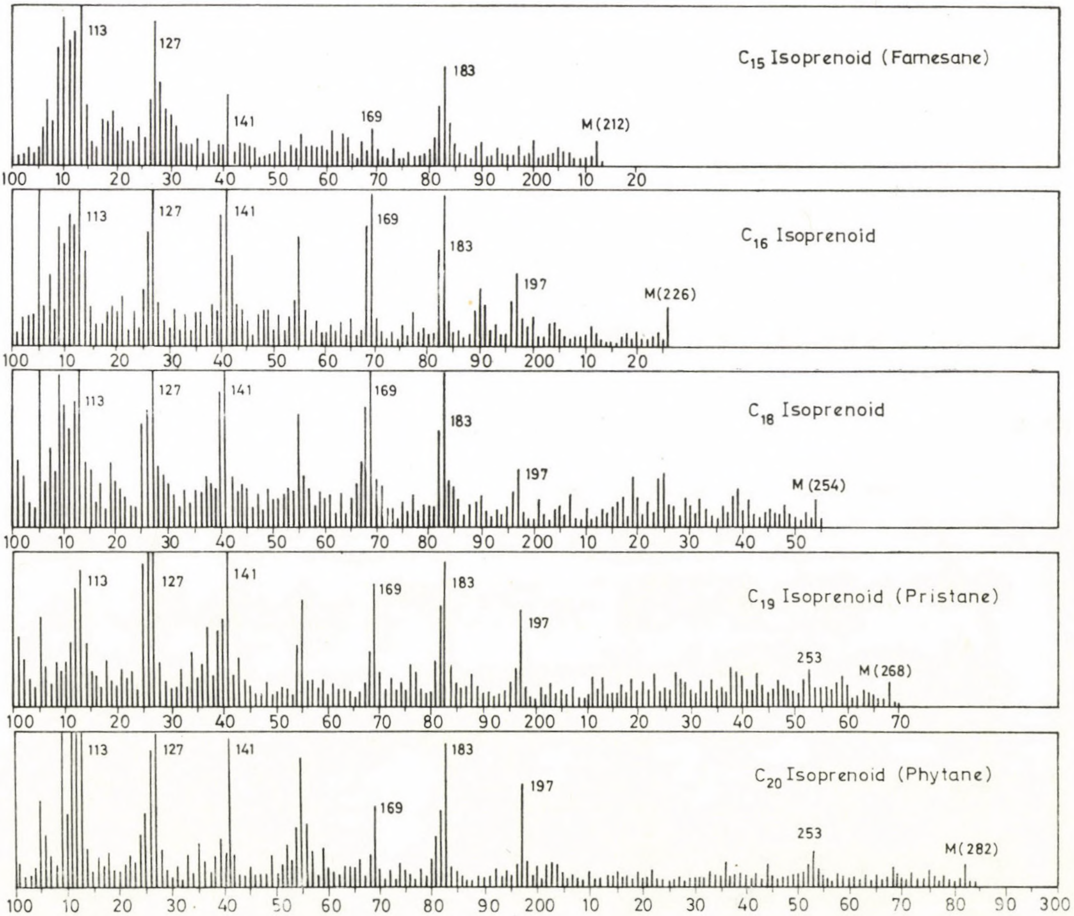

Fig. 3. Mass spectra of the isoprenoids isolated

identified as 2,6,10,14-tetramethylpentadecane (pristane) and 2,6,10,14-tetramethylhexadecane (phytane) (Fig. 3).

The high value of the pristance/phytane ratio (Fig. 2) is very characteristic of the organic matter isolated from comparatively recent geological formations, containing the oil shales. On the other hand, the high contents of pristane shows a humolite type of organic matter formed and accumulated on the bottom of a water basin [1]. The maximum at C_{17} in the distribution of n-alkanes (Fig. 1) indicates the existence of a rich submarine life of photosynthetic algae [2]. Having in mind the action of temperature, pressure, pH of the environment, the oxidizing action of sunlight, the living microorganisms and their selective enzymes, we assume that one of the ways to form the isoprenoid structures involves breaking of the long phytol chain of the "enormous" chlorophylls molecule, which is a product of the above photosynthetic algae, distributed in the water fauna of the Paleogen. The rich and manifold green vegetable life which existed during the Paleogen had turned into the basic raw material for the formation of organic matter [9, 11]. It is very likely that after sedimentation, the hydrocarbons contacted a layer enriched in microorganisms on the bottom of the water basin. The warm climate, warm water and high alkalinity (pH = 9) [5] were very favourable conditions for the life of these kinds of microorganisms during the Paleogen [4]. As a result of this selective action of the said microorganisms, there is a high value of Pristane. In all likelihood, the large amount of Pristane, a typical representative of green vegetation, can be explained by the fact that in the Paleogen the green vegetation was distributed in enormous quantities and different kinds [10].

Experimental

Samples from two oil shales were used as material for the analyses. The first one was taken from the gallery of Yaroslavtsy near the village of Krassava, from the following depths: No. 7308 — 29 m, No. 7309 — 32 m, No. 7314 — 40 m and No. 7315 — 46 m. The second collection contains three samples, which were taken from the borehole near the village of Mandra from the following depths: No. 425 — 85 m, No. 426 — 86 m and No. 427 — 87 m.

The samples were disintegrated and ground dry in a ball grinder (particle size 200 mesh) and extracted with benzene/ethanol in a 3 to 1 ratio in a Soxhlet apparatus for 50 hrs. After 15 hrs. sedimentation with light petroleum (b.p. 45—60 °C), insoluble asphaltens were eliminated. The residue was chromatographed on a glass column with Al_2O_3. Hexane elution gave the hydrocarbon fraction. The separation of hydrocarbons was carried out using the urea clathrate method and sorption on molecular sieves, following a procedure described earlier [6].

Gas chromatography was carried out on a Perkin Elmer, model F-17 chromatograph provided with flame ionization detectors and a dual column system (0.4×150 cm) 3% SE-30 on Chromosorb W-HP (100—120 mesh). A 50 m long capillary column containing OV-101 was used for running the isoprenoid hydrocarbons. Farnesane, pristane and phytane were used as standarts.

Mass spectrometry was carried out on an AEI MS-902 apparatus (70 eV, ion source temperature 150 °C) combined with a Pye Unicam chromatograph, series 104, model 64, provided with a dual column system, 3% SE-30 on Gas Chrom — Q (80—100 mesh), using helium as carier gas (60 ml/min). A Watson—Bieman separator was used as a coupling element between the gas chromatograph and the mass spectrometer.

REFERENCES

[1] Avigan, J., Blumer, M.: J. Lipid Research, **9,** 350 (1968)

[2] Brooks, J. D,. Gould, K., Smith, J. W.: Nature, **222,** 55 (1969)

[3] Eglinton, G., Murphy, M. T. J.: Organic Geochemistry p. 47—51, 1974

[4] Jons, R. B. Belsky, T., McCarthy, E. D., Burlingame, A. L., Haug, P., Schnoes, H. K., Richter, W., Calvin, M.: Geochimica et Cosmochimica Acta **30,** 1191 (1966)

[5] Konstantinova, V., Gnoeva, N., Chuneva, V., Jordanova, A., Popova, K.: Petroleum Coal Geology, **5,** 33 (1976)

[6] Kovachev, G., Delova, D., Stransky, K.: Collec. Czech. Chem. Commun., **37,** 4106 (1972)

[7] Kovachev, G., Ubik, K., Nikolov, R., Mincheva, T.: Collect, Czech. Chem. Commun., **40,** 3728 (1975)

[8] Kovjasin, V. E., Hala, S.: Collect. Czech. Chem. Commun., **38,** 2938 (1973)

[9] Meinschein, W. G., Barghorn, E. S., Schopf, L. S.: Science, **145,** 262 (1964)

[10] Murphy, M. E., Narayanan, S., Gould, G., Lawlar, S., Noonan, J., Prentice, D.: Short Papers on Research in 1971. Bull. **204,** Part **1,** 19—25 (1972)

[11] Oro, J., Nooner, D. W., Zlatkis, A., Wikström, S. A., Barghorn, E. S.: Science, **148,** 77 (1965)

Georgi Kovachev Sofia 1113, G. Bonchev str., II bl. Bulgaria

RECENSIONES

H. Drost: *Plasmachemie*

Akademie-Verlag, Berlin, 1978
91 Abb., 32 Tab., 420 Seiten

Die sich im Plasma abspielenden Reaktionen finden eine sich stets erweitemde Anwendung in der präparativen Chemie und erfreulicherweise erhöht sich auch auf dieses Gebiet die Zahl der Publikationen. Es gibt jedoch wenig zusammenfassende, die Frage allseitig behandelnde Monographien. Der Verfasser setzte sich das Ziel, eine umfassende, auch auf die neuesten theoretischen und praktischen Fragen eingehende Übersicht der Plasmachemie zu geben.

Der erste Abschnitt des Buches befasst sich mit den physikalischen Grundlagen der Plasmachemie. Schon seit langem sind die physikalischen Grundlagen des Zustandekommens des Plasmazustandes ausgearbeit und die zur Beschreibung des Plasmas nötigen Eigenarten interpretiert. Der Verfasser gibt eine gedrangte auch vom theoretischen Gesichtspunkt einwandfreie Zusammenfassung der sich im Plasma abspielenden Elementarvorgänge und ihr Zustandekommen bei elektrischer Entladung Die elektrischen Methoden der Plasmaherstellung sind vom anwendungstechnischen Gesichtspunkt aus sehr wichtig, sowohl was die eingehend behandelte Mikrowellenentladung betrifft, als auch hinsichtlich der in der Messtechnik grosse Rolle spielenden Hohlkathodenentladungen. Besondere Erwähnung verdient in diesem Teil die detaillierte Diskussion der plasmadiagnostischen Methoden, die das Messen der Plasmacharakteristika und besonders die mit der Temperatur zusammenhängenden Fragen behandelt.

Der zweite Hauptabschnitt der Monographie behandelt die im Plasma verlaufenden chemischen Stoffumwandlungen. Streng genommen bilden diese das Thema der Plasmenchemie. Bei diese Methoden werden die im Plasma herrschende hohe Temperatur, die hohe Energiekonzentration und die extrem hohe Konzentration der aktiven Teilchen (Ionen, angeregte Teilchen, Radikale) genutzt.

Sehr nützlich ist es, dass im Buch ausser den Kriterien der Herstellbarkeit auch die zur praktischen Realisierung verwendeten Geräte behandelt werden.

Der Kreis der plasmachemisch herstellbaren Stoffe ist sehr weit. Die Acetylensynthese, die Herstellung Stickstoff enthaltender, niedermolekularen Verbindungen (Stickstoffoxide, Cyanwasserstoff, Dicyan, Hydrazin usw.) werden eingehend diskutiert. Ein wichtiger Abschnitt ist die Zusammenfassung der plasmathermischen Halogenisierungen, zu denen z. B. auch die Herstellung des Teflon-Grundstoffes, des Fluoräthylens gehört. Weitere Anwendung finden plasmachemische Verfahren auf dem Gebiet der Metallurgie. Die gegenwärtig verwendbaren Verfahren sind: Reduktion von Metallchloriden und Metalloxiden sowie Herstellung von metallkeramischen Bindungen und auf dieser Basis arbeitende Plasmaschweissmethoden. Zu den im thermischen Plasma durchführbaren Reaktionen gehört auch die Herstellung gewisser Si-organischen Verbindungen, doch werden diese bedauerlicherweise nur sehr knapp in der Monographie behandelt.

Das nicht-thermische (bei elektrischer Entlandung entstehende) Plasma wird ebenfalls in der Plasmachemie weitgehend verwendet. Im Buch werden Dissoziations- und Krachreaktionen, Kondensationsreaktionen, an der Grenzfläche verlaufende Reaktionen bzw. thermodynamisch interessante, über instabile Produkte velaufende endotherme präparative Methoden diskutiert. Ein grosser Teil der im Plasma herstellbaren organischen und metallorganischen Verbindungen gehört hierher. Wir meinen, dass für diejenigen, die diese Methode anzuwenden gedenken, vielleicht dieser Teil am nützlichsten sein wird. Der Abschnitt enthält auch ein sehr reiches Literaturverzeichnis, was der Erweiterung der Kenntnisse förderlich ist.

Der dritte Hauptteil der Monographie befasst sich mit der physikalisch-chemischen Charakterisierung der plasmachemischen Reaktionen: Thermodynamik und reaktionskinetische Beziehungen der plasmachemischen Reaktionen werden beschrieben, und verhältnissmäßig kürzer werden die zu ihrer Untersuchung benötigten molekularspektroskopischen Methoden und die in letzterer Zeit in vermehrtem Masse angestellten theoretischen Überlegungen behandelt.

Der letzte Hauptteil des Buches befasst sich mit technischen Anwendungen. Dieses Gebiet wird, offensichtlich wegen des beschränkten Umfanges und wegen der Manigfaltigkeit der Anwendungen, nur sehr kurz überblickt: die gleichzeitige Darlegung der Kohlenwasserstoffsynthese und — beispielweise — der Entfernung des in der Mikroelektrik verwendeten Photolacks kann auch in Form einer Aufzählung erfolgen.

Was für Schlüsse können nach der theoretischen und praktisch-industriellen Betrachtung der Plasmachemie gezogen werden? Plasmachemische Methoden sind auf dem ganzen Gebiet der Chemie zur Herstellung von anorganischen, organischen und metallorganischen Verbindungen geeignet, und zwar sowohl im Laboratoriums- wie auch im Betriebsmassstab. Das theoretische Studium setzt eine interdisziplinare Methode voraus, die verschiedene Gebiete der Chemie und Physik- Thermodynamik, Reaktionskinetik, theoretische Methoden der Stoffstrukturuntersuchung-, aber zugleich auch eine ganze Reihe der technische Wissenschaften umfasst, Das Werk "Plasmachemie" von Prof. H. DROST ist eine moderne, niveauvolle und — was besonders hervorgehoben werden soll — auch vom praktischen Gesichstpunkt aus nützliche Zusammenfassung dieser komplexen Frage.

Als einleitendes Werk kann das Buch jenen theoretischen und praktischen Fachmännern empfohlen werden, die sich mit diesem Gebiet befassen wollen. Weiterhin kann das Buch für Spezialgebiete des Universitätsunterrichtes warm empfohlen werden, denn es eignet sich wegen seiner Klarheit, Verständlichkeit und strengen theoretischen Begründung ausgezeichnet zu diesem Zweck.

J. BOROSSAY

M. SITTIG: *Detergent Manufacture Including Zeolite Builders and Other New Materials*

Noyes Data Corporation, Park Ridge, New Jersey, USA 1979
Chemical Technology Review No. 128, 579 pages

The book published in 1979 in the series Chemical Technology Review can be regarded as a continuation of the same author's book entitled Detergent Manufacture, published in 1976. This new book proved to be necessary since in the period between the two publications the industry manufacturing tensides have greatly developed and an enormous amount of information has been obtained. This can be illustrated best by the fact that the earlier book consisted of 388 pages, while the present book comprising mainly the results of 3 years takes 579 pages. Favourable properties of the previous book have been retained in the second one, too: the branch of industry manufacturing tensides is treated on the basis of US patents to such an extent and with such thoroughness as to make possible for the reader to get sufficiently acquainted with the different procedures. Works of such type are rare except the earlier book of the author. Owing to its nature, it is useful primarily for engineers working in the industry, however, those dealing with theoretical principles of the field may also find it informative.

In construction, the book is similar to its predecessor. In the first chapters the starting materials of tenside production and their preparation are discussed. Linear paraffins and olefins, propylene trimers and tetramers, alcohols, alkyl halides, alkylaromatic and alkylcycloparaffin compounds, and alkylphenols are discussed with respect to their preparation. After the synthesis of raw materials, the actual procedures for preparation of tensides are discussed. Oxyalkylation, sulfation and sulfonation are examined in detail, including purification, neutralization of the products obtained in these ways; finally, the most important compounds are treated.

The other active additives, formation and examination methods are described in a separate chapter. After reviewing the builders, a new section comes which was absent in the former book, and these are the zeolite builders, gaining increasing importance. At the end of the book, other additives, shipping and final application, as well as predictable development tendencies in the given branch of industry are discussed using the available data.

The book includes Inventor and US Patent Number Indices, which, together with the very detailed contents, replace the Subject Index.

There are several (more than one hundred) clearly constructed process diagrams and schemes of apparatus. They can be utilized while reading the text and facilitate understanding.

Construction of the individual chapters is logical, the language is concise and clear. This high-level, valuable book is useful for chemists producing or using tensides.

J. MORGÓS

Metal Ions in Biological Systems, Vol. 8 Nucleotides and Derivatives: Their Ligating Ambivalency

SIEGEL, H. ed. Marcel Dekker, New York and Basel, 1979, XIX + 232 pp.

One of long-standing challenges to chemists active in the field of coordination chemistry is to understand the diversity in the complex-forming properties of low molecular weight ligands. Namely, some ligand can coordinate to the central atom through different donor atoms. Such qualities are referred to in the literature as "ambivalent" and they are also characteristic for nucleotides. With these compounds a metal ion may coordinate through the nucleic acid base moiety, the phosphate group or the sugar part.

In the first review written by R. W. GELLERT and R. BAU and entitled "X-ray structural studies of metal-nucleoside and metal-nucleotide complexes". The authors deal with the metal complexes of nucleosides and nucleotides — both purine and pyrimidine ones. They also discuss the dinucleotide salts and the metal complexes of transfer RNA. From this review article it is clear that the field of metal nucleotide and related complexes has undergone a period of extremely rapid growth since 1967, when the first structure (a Cu-adenine complex) was reported. 105 references are listed at the end of the review article.

The second paper, by R. B. MARTIN and Y. H. MARIAM, has the title "Interactions between metal ions and nucleic bases, nucleosides, and nucleotides in solution". The authors present overview of favoured metal ion binding sites in nucleic acids in solution. They discuss rather extensively the factors (*e.g.* basicity, pH, hydroxy complex formation, kinetic, base stacking) that influence metal ion binding sites. Then they deal with the metal ion bonding to nucleic bases, 1-alkylpyrimidines, 9-alkylpurines, nucleosides, and nucleotides. They touch upon also other problems, such ring carbons as binding sites, ribose metal ion binding, and NMR relaxation methods as a probe of binding sites.

240 references close the review.

The third review "The ambivalent properties of some base-modified nucleotides" is authored by H. SIEGEL. The modified nucleotides and nucleosides are not only biologically active compounds, but they are also of potential chemotherapeutic value. The author discusses the adenosine *N*(1)-oxide and inosine *N*(1)-oxide nucleotides, the potential ambivalent properties of nucleotides and the formation of mixed ligand complexes. The author concludes that base-modified nucleotides are expected to have properties different from natural nucleotides and to alter therefore biological processes.

88 references are listed.

The fourth article written by T. R. JACK is entitled "Heavy metal labeling of nucleotides and polynucleotides for electron microscopy studies". This article is an assessment of the feasibility of sequencing the polynucleotides DNA and RNA by electron microscopy using heavy atom labeling procedures. In the first part of the paper the author describes the electron microscope used in such studies, and then discusses the chemistry of the procedures (criteria for labeling schemes, potential labels, reaction types, selective modification of bases, incorporation of modified nucleotides), and finally the sequencing by electron microscopy. It is obvious from this article that a great progress has been made in developing both electron microscope techniques to image individual heavy atoms and the chemical reactions necessary to attach heavy atoms selectively and quantitatively to the nucleic acid bases.

44 references are given.

The last review in this volume "Macromolecules of biological interest in complex formation" is authored by S. L. DAVYDOVA. Here the author discusses the complex formation with macromolecules of nucleic acids and polypeptides — the possible sites of binding and cooperativity, the structure of coordination centers, pH dependence and conformational changeability, reversibility, and model compounds of macromolecules. The author deals also with the specificity of macromolecule — metal ion interactions. Finally she concludes that the conformation of biopolymers in greatly influenced by complex formation with metal ions, and that specific complex formation is affected also by hydrophobic interactions.

75 references are listed.

Volume **8** of this series dealing with the part played by metal ions in biological system provides the reader again with a wealth of novel informations. It can be highly recommended to biochemists, coordination chemists and biologists.

E. KŐRÖS

Metal Ions in Biological Systems. Vol. 9 Amino acids and derivatives as ambivalent ligands

Sigel, H. ed. Marcel Dekker, New York and Basel, 1979, XIX + 277 pp.

Amino acids with a suitable side chain donor atom, and their amino and carboxylate group can coordinate to metal ions. Depending on both the properties of the amino acid and the metal ion several structural possibilities exist for the resulting complex. These "ambivalent" qualities of amino acids and derivatives are in the center of Volume **9**.

The first chapter is written by R. B. **Martin** and entitled "Complexes of α-amino acids with chelatable side—chain donor atoms". The amino acids examined in this article include asparagine, glutamine, serine, threonine, methionine, *S*-methylcysteine, cystine, some α,ω-diaminocraboxylates (2,3-diaminopropanoate, 2,4-diaminobutanoate, ornithine and lysine) and histidine. The chapter concerns side—chain binding sites that are potentially chelatable to metal, and the author emphasizes on complexes that occur in neutral solutions. A brief discussion of the role of aromatic side chains in complex formation is also given. — 150 references.

The second chapter on "Metal complexes of aspartic acid and glutamic acid" is authored by C. A. **Evans**, R. **Guevremont** and D. L. **Rabenstein**. The authors review the coordination chemistry of the title compounds, which have three binding sites for metal ions. They outline the acid-base chemistry of the two amino acids, their complexes with main group metal ions (alkali and alkaline earth metals, zinc, cadmium, gallium, indium and lead), with transition metals [mainly Co(III), Co(II), Ni(II) and Fe(II)] and with lanthanides and actinides. 164 references.

The third chapter entitled "The coordination chemistry of L-cysteine and D-penicillamine" is written by A. **Gergely** and I. **Sóvágó**. The authors review the results of the researches directed to reveal the possible complex formation reactions of L-cysteine and D-penicillamine. First they describe the properties of the ligands and then deal with their complexes of main group metal ions, zinc group ions and some transition metals (Cr, Mo, Fe, Co, Ni, Pd, Pt, Cu). Also mixed ligand complexes are mentioned. On the basis of the data the authors group the metals according to their coordinating characteristics toward the title compounds. — 97 references.

In chapter *4* D. L. **Rabenstein**, R. **Guevremont** and C. A. **Evans** deal with "Glutathione and its metal complexes". They discuss the biological occurrence and functions of glutathione, its redox and acid-base chemistry, the coordination chemistry (with Zn, Cd, Pb, Hg, Ag, Ni, Cu, Co, Mo, Mn, Fe, Au, Cr, Ca, Mg, and lanthanides) of reduced glutathione and briefly the coordination chemistry of oxidized glutathione. — 122 references.

Chapter *5* is written by A. **Gergely** and T. **Kiss** and entitled "Coordination chemistry of L-DOPA and related ligands". L-DOPA and related compounds are of great biological significance, since they are used as neurotransmitters by the living organisms. The authors chemically characterize the title compounds and provide the reader with a wealth of informations on their metal complexes (equilibrium constants, thermodynamic data). They also describe mixed ligand complexes and close the article by discussing the part played by metal ions and their complexes in biological functions of catecholamines. — 54 references.

"Stereoselectivity in the metal complexes of amino acids and peptides" is the title of chapter 6, written by L. D. **Pettit** and R. J. W. **Hefford**. Many biological systems that involve metal ions are selective in the chirality of the ligand molecules with which they interact and many are even stereospecific. This review corvers some recent results in the field of thermodynamic stereoselectivity in the complexes of amino acids and dipeptides. The authors emphasize on α-amino acids important in the biological field and on dipeptides. They included also some synthetic-substituted amino acids. — 80 references.

The last chapter of this volume is written by K. **Burger** and entitled "Protonation and complexation of macromolecular polypeptides: corticotropin fragments and basic trypsin inhibitor (Kunitz base)". The author presents the systematic equilibrium study of corticotropin (ACTH) fragments and basic bovine pancreatic trypsin inhibitor. He deals with protonation equilibria of both polypeptides, and with complex formation equilibria between the title compounds and zinc and silver, respectively. These studies show the possibilities and restrictions of equilibrium methods in the characterization of macromolecular polyfunctional ligands. — 42 references.

Volume **9** of this excellent series of books on the role of metal ions in biosystems covers complexes with a number of amino acids with chelatable side chain donor atoms, the coordinating properties of aspartic and glutamic acids, cystein, penicillamine, L-DOPA, glutathion and some polypeptides and the stereoselectivity in metal complexes of amino acids and dipeptides.

E. Kőrös

INDEX

PHYSICAL AND INORGANIC CHEMISTRY

ORGANIC CHEMISTRY

Printed in Hungary

A kiadásért felel az Akadémiai Kiadó igazgatója. Műszaki szerkesztő: Zacsik Annamária
A kézirat nyomdába érkezett: 1980. II. 4. — Terjedelem: 9,45 (A/5) ív, 40 ábra

80.7971 Akadémiai Nyomda, Budapest — Felelős vezető: Bernát György